The influence of gas and liquid physical properties on entrainment inside a sieve tray column

by

Ehbenezer Chris Uys

Dissertation presented for the Degree

Of

DOCTOR OF PHILOSOPHY
(Chemical Engineering)

in the Faculty of Engineering
at Stellenbosch University

Supervisor
Prof J.H. Knoetze

Co-Supervisor
Prof A.J. Burger

December 2012

Stellenbosch University http://scholar.sun.ac.za

Declaration

By submitting this dissertation electronically, I declare that the entirety of the work contained therein is my own, original work, that I am the sole author thereof (save to the extent explicitly otherwise stated), that reproduction and publication thereof by Stellenbosch University will not infringe any third party rights and that I have not previously in its entirety or in part submitted it for obtaining any qualification.

Ehbenezer Chris Uys December 2012

Copyright © 2012 Stellenbosch University

All rights reserved

Stellenbosch University http://scholar.sun.ac.za

Abstract

Distillation column design and operation require understanding of both the hydrodynamic and thermodynamic behaviour and limitations. One of the hydrodynamic aspects that negatively influence separation efficiency in the distillation column is entrainment of the liquid with the rising vapour or gas. Inaccurate entrainment predictions will lead to poor separation efficiencies in the column and consequently over design of the column diameter and/or height has to be incorporated. This has a significant impact on the capital cost due to the size and scale of industrial columns. Therefore, small improvements in entrainment prediction will lead to large savings in capital investment.

Previous research published in the open literature focused primarily on the influence of gas and liquid flow rates and, tray geometry on entrainment for the air/water system. Consequently the non-air/water database is small and consists of data obtained from various tray and column geometries. As a result the accuracy of current entrainment prediction models is questionable for systems other than air/water. Therefore, the first objective of this work was to investigate whether current prediction models perform well for systems other than air/water. To prove this air/water, air/ethylene glycol and air/silicon oil data were measured and compared with current prediction correlations. It was found that current prediction models perform poorly for the air/ethylene glycol and air/silicone oil systems. At the same time a new observation was made with regard to froth development and behaviour inside the column. The observation shows that liquid flow rate has a non-monotonic influence on entrainment, caused by the short (475mm) tray flow path.

The second objective was to examine the influence of gas physical properties on entrainment. New entrainment data were measured by individually contacting air, CO_2 and SF_6 with water and ethylene glycol, while n-butanol was contacted with CO_2 and SF_6. The data was compared with current prediction models which performed poorly for SF_6 results. This shows the inability of these models to predict entrainment for gas systems with high densities. Modified Reynolds and Froude numbers were developed to show the influence of gas physical properties on entrainment. Low modified Reynolds numbers and large modified Froude numbers resulted in high entrainment.

Stellenbosch University http://scholar.sun.ac.za

The third objective was to determine the influence of liquid physical properties on entrainment. New entrainment data were measured using CO_2 with Isopar G, n-butanol, water, silicone oil and ethylene glycol. Current prediction models compared poorly to the data and did not include the influence of liquid viscosity on entrainment. It was found that viscosity had an intricate non-monotonic influence on entrainment.

The fourth and final objective was to correlate the influence of gas and liquid properties on entrainment as determined by the previous two objectives. To make the dataset more complete, entrainment was measured for four tray spacings using CO_2/Isopar, CO_2/n-butanol, air/ethylene glycol, CO_2/ethylene glycol, air/silicone oil and CO_2/silicone oil (over 1700 data points). Two new correlations are presented to predict the fraction of liquid entraining with the rising gas (L'/G with R^2 = 85%) and the fraction of liquid entering the tray that entrains (L'/L with R^2 = 92%). The performance of the L'/G correlation (R^2 = 85%) is vastly superior to two other prominent correlations (R^2 = 61% and 23%). This correlation can be implemented to predict entrainment successfully for different tray geometries by combining the predicted influence of tray geometry, by Kister and Haas (1988), with results from the newly developed correlation. All four objectives are presented as manuscripts for journal publication and serve as alone standing documents.

Stellenbosch University http://scholar.sun.ac.za

Opsomming

Distillasie kolom ontwerp en bedryf vereis begrip van beide die hidrodinamiese en termodinamiese gedrag en beperkings. Een van die hidrodinamiese aspekte wat skeiding doeltreffendheid negatief beïnvloed in die distillasie kolom is meesleuring van die vloeistof met die stygende dampe of gas. Onakkurate meesleuring voorspellings sal lei tot swak skeiding doeltreffendheid in die kolom en gevolglik word die ontwerp van die kolom deursnee en / of hoogte beinvloed. Dit het 'n beduidende impak op die kapitale koste as gevolg van die grootte en skaal van industriële kolomme. Klein verbeterings in meesleuring voorspelling sal dus lei tot groot besparings in kapitaal belegging.

Vorige navorsing gepubliseer in die oop literatuur het hoofsaaklik gefokus op die invloed van gas- en vloeistof vloeitempos en plaat geometrie op meesleuring vir die lug/water sisteem. Gevolglik is die nie-lug/water databasis klein en bestaan van die data wat verkry is uit verskeie plaat en kolom-geometrieë. As gevolg is die akkuraatheid van die huidige meesleuring voorspelling modelle vir stelsels anders as lug/water te betwyfel. Daarom is die eerste doel van hierdie werk om ondersoek in te stel of die huidige voorspelling modelle goed presteer vir stelsels anders as lug/water. Om dit te bewys was lug/water, lug/etileenglikol en lug/silikon olie data gemeet en vergelyk met die huidige voorspelling korrelasies. Daar is bevind dat die huidige voorspellings modelle swak presteer vir die lug/etileenglikol en lug/silikon olie. Op dieselfde tyd was 'n nuwe waarneming gemaak met betrekking tot dispersie ontwikkeling en gedrag binne die kolom. Die waarneming toon dat vloeistof vloeitempo 'n nie-monotoniese invloed op meesleuring het, veroorsaak deur die kort (475mm) plaat vloei pad lengte.

Die tweede doelwit was om die invloed van gas fisiese eienskappe op meesleuring te ondersoek. Nuwe meesleuring data was gemeet deur individuele kontak van lug, CO_2 en SF_6 met water en etileenglikol, terwyl n-butanol slegs met CO_2 en SF_6 inkontak gebring was. Die eksperimentele resultate word vergelyk met die huidige voorspellings modelle wat swak presteer invergelyking met SF_6 resultate. Dit toon die onvermoë van hierdie modelle om meesleuring vir gas stelsels met hoë digthede te voorspel. Gemodifiseerde Reynolds en Froude getalle was ontwikkel om die invloed van gas fisiese eienskappe op meesleuring aan te toon. Lae gemodifiseerde Reynolds getalle en groot gemodifiseerde Froude getalle lei na hoë meesleuring.

Stellenbosch University http://scholar.sun.ac.za

Die derde doelwit was om die invloed van vloeistof fisiese eienskappe op meesleuring te bepaal. Nuwe meesleuring data is gemeet deur gebruik te maak van CO_2 met Isopar G, n-butanol, water, silikon olie en etileenglikol. Huidige voorspellings modelle vergelyk swak met die data en sluit nie die invloed van vloeistof viskositeit op meesleuring in nie. Daar is gevind dat viskositeit 'n ingewikkelde nie-monotoniese invloed op meesleuring het.

Die vierde en finale doelwit was om die invloed van die gas en vloeistof eienskappe op meesleuring soos bepaal deur die vorige twee doelwitte te korreleer. Om die datastel meer volledig te maak, is meesleuring vir vier plaat spasiërings met CO_2/Isopar, CO_2/n-butanol, lug/etileenglikol, CO_2/ethylene glycol, lug/silikon olie en CO_2/silikon olie (meer as 1700 data punte gemeet). Twee nuwe korrelasies word aangebied om die fraksie vloeistof wat meegesleur word met die stygende gas (L'/G met R^2 = 85%) en die fraksie vloeistof wat die plaat binnetree wat meegesleur word (L'/L met R^2 = 92%) te voorspel. Die prestasie van die L'/G korrelasie (R^2 = 85%) is aansienlik beter as twee ander prominente korrelasies (R^2 = 61% en 23%). Hierdie korrelasie kan suksesvol geïmplementeer word om meesleuring vir verskillende plaat geometrieë te voorspel deur die voorspelde invloed van plaat geometrie deur Kister en Haas (1988), met die resultate van die nuut ontwikkelde korrelasie te kombineer. Al vier doelwitte word as manuskripte vir joernaal publikasie aangebied en dien as alleenstaande dokumente.

Stellenbosch University http://scholar.sun.ac.za

Preface

This dissertation is presented as a compilation of four manuscripts. Each manuscript is introduced separately and is written accordingly to reflect a stand alone representation for journal submission.

Stellenbosch University http://scholar.sun.ac.za

Dedication

to

Lize-Mari for your love, support and motivation

Dirk and Martie Uys for being great parents

To the Creator for everything large and small

Stellenbosch University http://scholar.sun.ac.za

Acknowledgements

I wish to thank my supervisors, Prof. J.H. Knoetze and A.J. Burger. Their guidance, motivation and insight were invaluable and kept me challenged. Thank you for spending those hours of reviewing numerous errors. It is because of your time and patience that I was able to succeed. To all who reviewed this work who are unknown to me, I thank you for taking the time and making the effort. To Dr. C.E. Schwarz, thank you for trying to teach me how to write. I am definitely not there yet, but a whole lot closer.

The financial assistance of Sasol Technology (Pty) Ltd, Koch-Glitsch LP, Inher SA, and the Department of Trade and Industry (DTI) of South Africa through the Technology and Human Resources for Industry Programme (THRIP) towards this research is hereby acknowledged. I gratefully acknowledge the inputs from Dr. A. Erasmus and Dr. I. Nieuwoudt regarding the equipment design.

A special thanks to John Burchell and Dr. J.P. Barnard who helped me after hours with the MATLAB tools and coding. The model developed in Manuscript 4 was only possible with the coding assistance of the MATLAB tools by Dr. Barnard.

Without the analytical expertise of Me. Hanlie Botha, the manufacturing and maintenance support from Mr. Jannie Barnard, Anton Cordier, Oliver Jooste and Vincent Carolis, this project would not have produce results.

Without love life would be empty and mediocre. Lize – Mari, I am forever grateful for your support, motivation, love and encouraging words. A warm heart helped a lot during long cold nights in the lab. I am really blessed to have you in my life and I am excited about our future together. Mom and Dad, you taught me through your lives how to endure, persevere and to stay positive. A *“we are proud of you”* just means so much more coming from you.

Sarel Lamprecht and Leander Steynberg require mentioning as they had to listen to many frustrating discussions about research and life. I thank you both for your camaraderie, friendship, hours on the mountain bike and in the gym. Thanks for always cracking a joke and creating laughing scenarios when times were tough. The adventures we had will be remembered and will definitely continue.

Stellenbosch University http://scholar.sun.ac.za

I have been very privileged to have a mentor, friend and partner during the last 12 months of this work. Charles Back, you placed me in an environment that helped me to re-connect to life and all my passions. Talent without passion is worth nothing. I gained so much from our long before daybreak rides in the mountain and surroundings. Your insight, experience and advice motivated me and made me realise what I want to achieve in the future. Thank you for making me part of a very dynamic team and project that created the much needed *"real life"* exposure.

To the Creator, I thank You for giving me the ability and opportunity to study. I sincerely hope that the knowledge gained can be used to benefit those around me.

Stellenbosch University http://scholar.sun.ac.za

Table of contents

Stellenbosch University http://scholar.sun.ac.za

Stellenbosch University http://scholar.sun.ac.za

Nomenclature

A_c	column area = 635x175mm	[m^2]
A_f	fractional hole area = A_h/A_p	[-]
A_h	hole area	[m^2]
A_p	perforated area or bubbling area	[m^2]
C_F	capacity flow factor = $U_s.(\rho_g/(\rho_L-\rho_g))^{0.5}$	[m/s]
D_c	column diameter	[m]
d_H, D_H	hole diameter	[mm, m]
FPL	tray flow path length, 475 mm in this work	[mm]
F_h	hole vapour factor = $U_h.\rho_g^{0.5}$	[$kg^{0.5}/m^{0.5}.s$]
F_s	superficial vapour factor = $U_s.\rho_g^{0.5}$	[$kg^{0.5}/m^{0.5}.s$]
g	gravitational constant = 9.81	[m/s^2]
G	gas mass flow rate	[kg/s]
h_w, H_w	outlet weir height	[mm, m]
h_f, H_F	froth height	[mm, m]
h_L, H_L	clear liquid height	[mm, m]
$h_{L,ct}$	clear liquid height at the regime transition	[mm]
L	mass flow of liquid entering the tray	[kg/s]
L'	entrained liquid mass flow	[kg/s]
L_{FPL}	tray flow path length, 0.475 m in this work	[m]
MSE	mean of the squared error	[-]
p	hole pitch	[mm]
Q_L	liquid flow rate per weir length	[$m^3/(h.m)$]
s, S	tray spacing	[mm, m]
SSE	sum of the squared error	[-]
us , Us	superficial gas velocity, based on tray perforated/bubbling area	[m/s]
V_g	gas volumetric flow rate	[m^3/s]
V_L	liquid volumetric flow rate	[m^3/s]

Greek Letters

ρ_v, ρ_g	gas density	[kg/m^3]
ρ_L	liquid density	[kg/m^3]
σ	surface tension	[mN/m]
μ_g	gas viscosity	[mPa.s]
μ_L	liquid viscosity	[mPa.s]

Stellenbosch University http://scholar.sun.ac.za

ζ	correction term for Eq. 17 on page 18.

Stellenbosch University http://scholar.sun.ac.za

Introduction

1. Background

One way to separate component mixtures with different volatilities is to use a method called distillation. This is a unit operation also characterised as a physical separation process. In distillation energy is used to boil a liquid mixture. When the component mixture reaches boiling point, a vapour consisting of a large fraction of the most volatile component/s will escape the liquid phase which consists of a large fraction of the less volatile component/s. Some applications for distillation are;

- separating ethanol from malted barley mash to produce whiskey
- to fractionate crude oil for electricity generation, transportation and, for heating and packaging (Seader and Henley, 1998)
- to separate carbon dioxide from other fermentation by products to carbonate soft drinks, ciders and beers for the beverage industry
- separate oxygen, nitrogen and argon from air to supply the construction industry

Distillation is conducted in a vessel called a distillation column or tower. Generally cylindrical in shape and vertically placed, various geometries are used based on throughput and separation efficiency requirements. One of the key parameters driving the separation efficiency is interfacial contact area between the vapour and liquid phases. This is achieved in a distillation column on contacting devices known as trays or packing. Various criteria are used to determine the suitable contacting device for each application (Kister, 1992). In this study the focus is on sieve trays (see Figure 1) which are the simplest in design of the tray family. Most tray related data in literature were obtained using sieve trays. This, and due to the simplicity of design, is the reason for choosing the sieve tray for this work as the focus is on gas and liquid physical property related influences and not tray geometry changes.

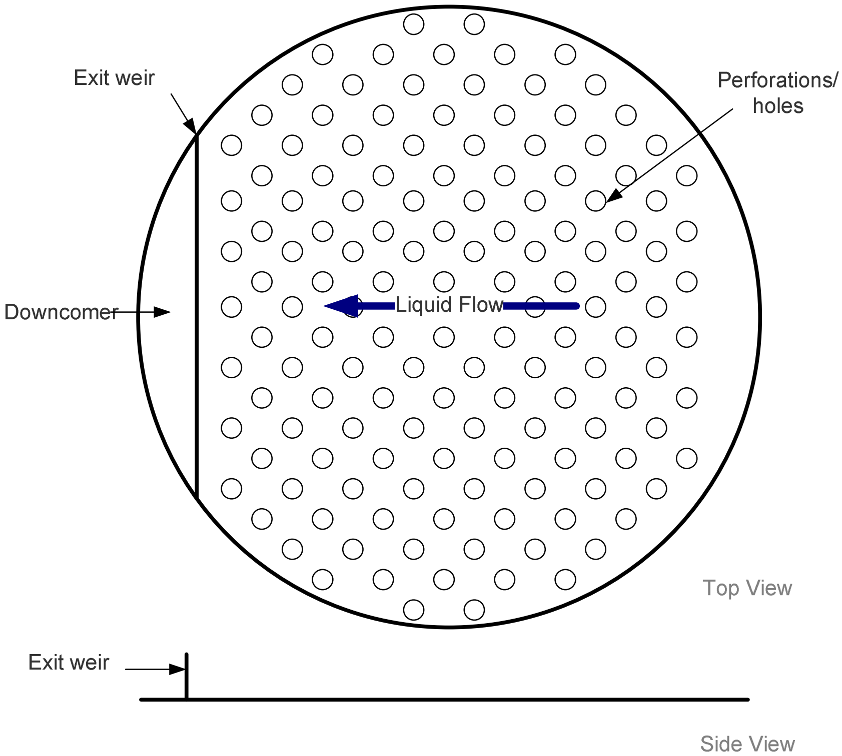

Figure 1. Basic sieve tray design.

In order to design a tray column the actual number of stages has to be calculated. By dividing the number of theoretical stages required for separation with the overall column efficiency the actual number of stages required can be determined (see figure 2). The number of theoretical stages can be determined with McCabe-Thiele method and the relative volatility and/or vapour liquid equilibrium data of the components. Column overall efficiency is calculated by starting with the tray point efficiency which depends on the gas and liquid film mass transfer resistance. By including the effect of gas and liquid mixing, the tray point efficiency is converted to a dry Murphree efficiency. Then entrainment and weeping are calculated. By adding the negative effect of entrainment and weeping to the dry Murphree efficiency the Murphree tray efficiency is determined. The overall column efficiency is a function of the Murphree efficiency. Therefore, entrainment and weeping has a negative effect on the overall column efficiency which will lead to more actual stages required to achieve the required separation. High levels of entrainment can lead to flooding which will also reduce gas-liquid mixing which will reduce the dry Murphree tray efficiency.

To summarise the number of theoretical stages depend on the thermodynamical driving force between the systems. The point efficiency depends on the mass transfer gradient and interfacial mass transfer resistance. Entrainment, weeping and mixing patterns can be grouped under hydrodynamics. This work will focus on the hydrodynamic aspect of distillation as these models form part of the overall column efficiency estimation.

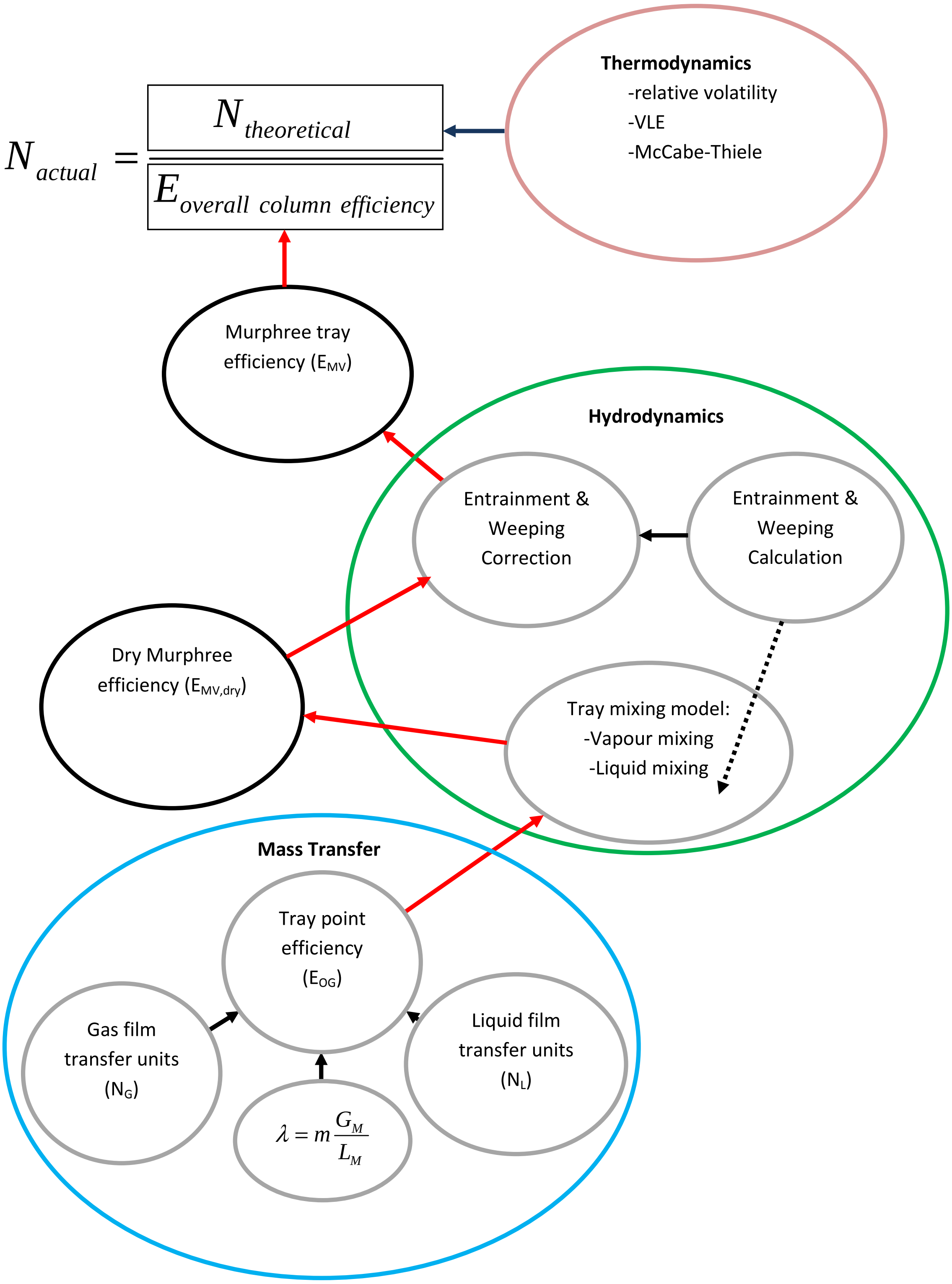

Figure 2. Sequence of steps for theoretical prediction of actual number of stages required for separation based on Figure 7.3 in Kister (1992).

Stellenbosch University http://scholar.sun.ac.za

2. Tray Column Hydrodynamics

Hydrodynamics is the scientific study of fluids in motion under the influence of internal or external forces. In tray columns, liquid flows down the column from tray to tray through isolated vertical sections called downcomers, see Figure 3. As the liquid reaches the bottom of the downcomer, it changes direction and passes through an opening called the downcomer escape area. As the liquid exits the downcomer it enters the tray where contact is made with the gas rising through the perforations. The area where contact is made between the gas and liquid is called the active area. In the active area, the rising gas disrupts the normal horizontal flow of clear liquid from the downcomer to form a dispersion commonly referred to as froth. The froth exits the tray over a weir into the next downcomer that feeds the tray below. This is a basic description of the classic tray hydrodynamic model as depicted in Figure 3. One important hydrodynamic parameter used in efficiency, flooding, pressure drop, downcomer backup, weeping and entrainment calculations is the liquid hold-up (h_L), also known as the clear liquid height (Kister, 1992). The clear liquid height indicates the height of liquid that will remain on the tray if the aerated froth would collapse in the absence of gas flow, assuming no liquid will fall through the holes.

Stellenbosch University http://scholar.sun.ac.za

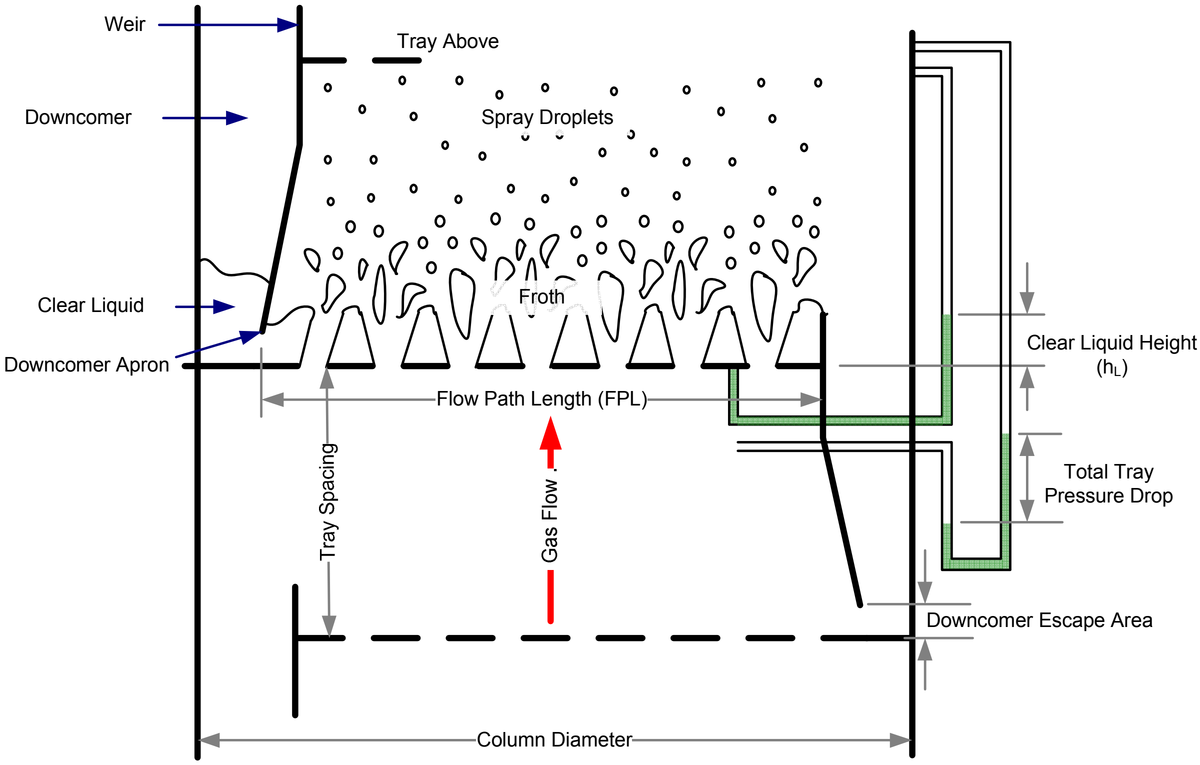

Figure 3. The classic tray hydrodynamic model with no entrainment, weeping or flooding.

Spray regime

During low liquid flow rate conditions (typically $Q_L < 12$ m^3/(h.m)) the liquid layer on the tray is thin. This thin layer is easily broken up into a spray of droplets, see Figure 4. The droplets are projected into the vapour space above the tray with an initial velocity close to that of the tray hole gas velocity. This regime, where most of the liquid is turned into droplets, is called the spray regime. Van Sinderen et al. (2003) refers to this regime as the two-layer regime.

Stellenbosch University http://scholar.sun.ac.za

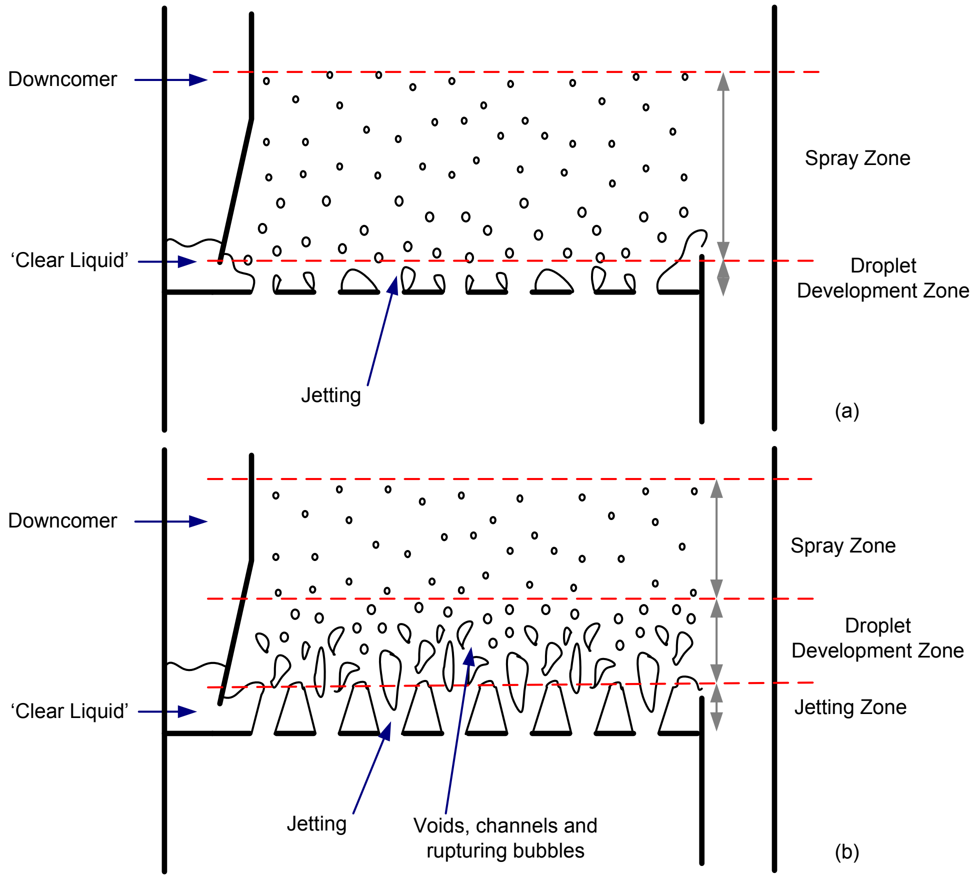

Figure 4. Depictions of the (a) spray and (b) froth regimes based on Van Sinderen et al. (2003).

<u>Froth regime</u>

With increasing liquid rate the liquid hold-up increases to the point where droplets are not formed at the tray perforations, but on top of the jetting zone in the droplet development zone (Kister and Haas, 1988 and Colwell, 1981). In this regime the gas creates multidirectional jets, channels and voids through the froth (jetting and droplet development zones). These channels and voids have a larger area than the tray perforations and therefore a lower gas velocity (Uys et al. 2012a). Consequently the ejection velocity of the droplets is lower than droplets ejecting from the holes. Due to their lower ejection velocity the droplets will travel a shorter vertical distance than in the spray regime. In these conditions three distinctive layers are formed (Van Sinderen et al., 2003). A froth layer on the tray deck followed by a droplet development layer in the middle, and a spray layer at the top. This regime is called the froth regime. For different gas and liquid flow rates and weir heights, the heights of these layers will differ (Van Sinderen et al., 2003). Generally an increase in liquid flow rate and weir height will increase the height of the jetting zone.

Stellenbosch University http://scholar.sun.ac.za

Regime identification

Various correlations and methods have been developed to characterise the transition from spray to froth regime. One such method, developed by Porter and Jenkins (1979), defines the transition as the point where minimum entrainment is measured for constant gas flow conditions with increasing liquid flow rate (see Figure 5). Therefore, entrainment will decrease with an increase in liquid flow rate in the spray regime. As soon as the minimum entrainment point is reached an increase in liquid flow rate will increase entrainment, caused by the further increase in liquid hold-up (Porter and Jenkins, 1979, Kister and Haas, 1988). This regime identification method is used throughout as it is simple to apply and not limited to the data used in the development of the other definitions. Therefore, this method will apply to a much larger scope of conditions.

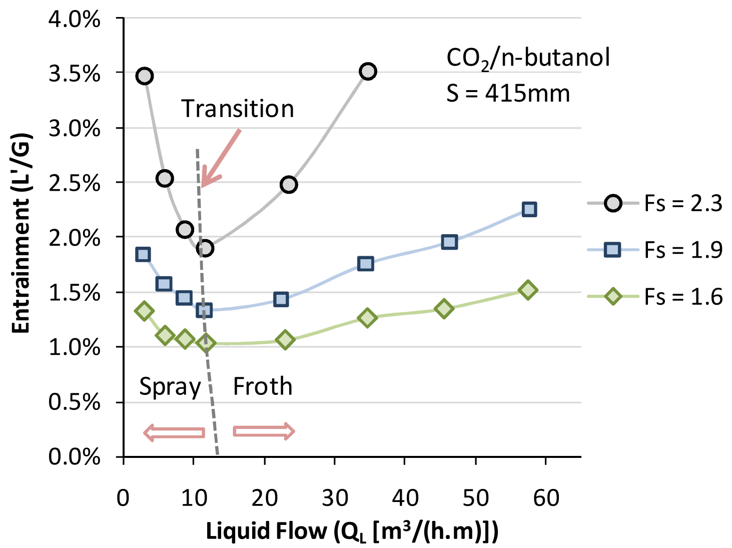

Figure 5. Entrainment with increasing gas flow factor ($F_s = u_s\rho_g^{0.5}$) and liquid flow rate for the CO_2/n-butanol system in a 415mm tray spacing.

There are a few hydrodynamic phenomena of importance to the operation, capacity and efficiency of a tray column. These phenomena are referred to as weeping, flooding, and entrainment.

Stellenbosch University http://scholar.sun.ac.za

Weeping

Weeping occurs when the static pressure of the liquid on the tray (or sections thereof) exceeds the pressure drop of the gas holding the liquid on the tray. Therefore, as the vapour rate decreases, weeping increases. Weeping will always take place to a certain extent in most tray columns for most systems (Kister, 1992). The liquid that weeps through the perforations short-circuits the intended flow path of the liquid across the tray and less contact is made with the rising vapour which reduces the tray efficiency.

Flooding

When a certain combination of gas and liquid flow rates exceeds the capacity of the column, flooding occurs. Flooding is characterised as a condition that restricts liquid from flowing down the column (Lockett, 1986). Therefore liquid will build up on the tray resulting in an excessive pressure drop across that section of the column. Kister (1992) defines four different flooding mechanisms: spray entrainment flooding, froth entrainment flooding, downcomer backup flooding and downcomer choke flooding. Spray- and froth entrainment flooding is also defined as jet flooding. Spray entrainment flooding occurs in the spray regime when most of the liquid on the tray is 'blown' to the tray above as the gas velocity is raised. The liquid then accumulates on the tray above instead of flowing down to the tray below. Froth entrainment flooding comes about in the froth regime at higher liquid flow rates. In this regime the froth layer (height) increases with an increase in gas velocity. For low tray spacings the envelope of the froth layer will move towards the tray above. The froth layer has a much higher density of liquid than the spray layer. Therefore, as this envelope moves closer to the tray above, entrainment rapidly starts to increase. This causes liquid to accumulate on the tray above. For larger tray spacings (> 457 to 610 mm) the top of the froth layer seldom reaches the tray above. As the gas velocity is raised the height of the droplet development layer and spray layer increases and flooding will take place by the spray regime flooding mechanism (Kister, 1992). Downcomer backup flooding occurs when the liquid enters the downcomer at a higher rate than the liquid exiting the downcomer. This phenomenon is influenced by tray pressure drop, clear liquid height, and the friction losses from the liquid flowing through the downcomer apron (Kister, 1992).

Stellenbosch University http://scholar.sun.ac.za

Entrainment

As the main focus of this work is on entrainment, this section will provide a background and introduction to entrainment. In section 3 (Entrainment Theory) entrainment is discussed in more detail. Liquid entrainment (will be referred to as entrainment throughout) is when the droplets ejecting from the spray or froth layer, reach the tray above. There are two definitions for measuring entrainment. The most common is to measure the mass flow rate of droplets entrained over the mass flow rate of the rising gas (L'/G). This definition is helpful to give an indication of the column capacity. High L'/G ratios will lead to jet flooding (spray – and froth entrainment flooding) of the column. The other definition is the mass flow rate of droplets entrained over the mass flow rate of the liquid entering the tray through the downcomer apron (L'/L). This definition relates the influence of entrainment on tray efficiency, where high L'/L ratios indicate a reduction in tray efficiency.

The aim in any separation column is to achieve a large fraction of the most volatile component in the top of the column (condenser) and less volatile component in the bottom of the column (re-boiler). Entrainment causes liquid with a larger fraction of less volatile component/s from the tray below to be transported to the tray above. This increases the fraction of less volatile component/s on the tray above which result in a reduction on separation efficiency. Lockett (1986) showed that this:

1. Reduces the driving force for mass transfer between the vapour and liquid
2. Increases the liquid to vapour ratio on each tray, which can cause instability and flooding
3. Increases the liquid load and point efficiency of the tray

The general result is that entrainment reduces tray and column efficiency. The allowable levels of entrainment in a column depend on the overall separation specifications required from the column. In some cases throughput might have priority over product purity and quality and then higher amounts of entrainment is acceptable. Various authors have developed correlations that show the negative influence of entrainment on efficiency (Colburn, 1936, Lockett et al., 1983, Bennett et al., 1995 and 1997). The influence of entrainment on separation efficiency does not form part of the scope of this work.

Stellenbosch University http://scholar.sun.ac.za

3. Entrainment Theory

Mechanisms of entrainment

In the literature there are two mechanisms for entrained droplet generation, see Figure 6**.** Some of the drops are created as the liquid sheet, or film that bridges the hole, is ruptured by the gas rushing through the liquid (Newitt et al., 1954). This mechanism also occurs when gas bubbles rise through the liquid to rupture at the surface. The other mechanism is the shearing action of a gas jet through the liquid which creates liquid jets or liquid sheets (Nielsen et al., 1965)**.** These liquid sheets are broken down into droplets that project into the vapour space above the froth. In general a combination of both these mechanisms occurs inside the column, depending on the flow regime (Lockett, 1986). These mechanisms have also been observed visually in the experiments conducted in this project. Entrainment will only occur if the droplets developed by these mechanisms have an ejection velocity large enough to be transported to the tray above.

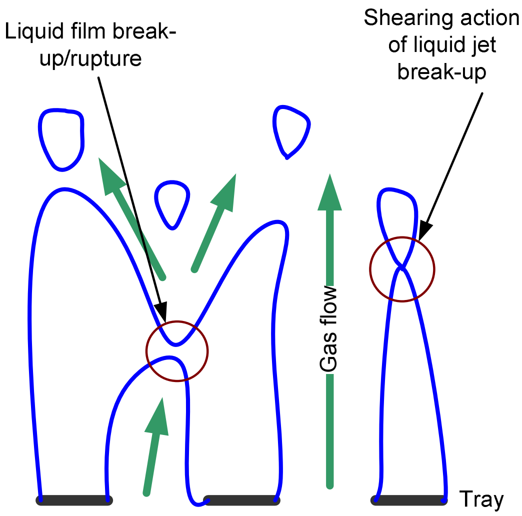

Figure 6. Droplet and entrainment generation mechanisms redrawn on Syeda et al. (2007).

Measuring Entrainment

There are four general methods for measuring entrainment (Lockett, 1986):

1. Free entrainment is measured by collecting drops in the vapour space above the froth, below the tray above.

Stellenbosch University http://scholar.sun.ac.za

2. Dry tray entrainment is a measurement technique where a special tray is placed above the operating tray. This tray has no downcomer feeding the tray and the liquid that collects on this tray is transported to a measuring device outside the column. This is the method used in this work.
3. In some cases a non-volatile tracer is introduced into the liquid on the tray. The liquid exiting the tray above is then sampled for the tracer. This technique is called wet tray entrainment.
4. Another method is to determine the reduction in tray efficiency caused by entrainment. This method is known as efficiency entrainment.

According to Lockett (1986), wet tray entrainment is preferred in industrial applications as well as laboratory experiments, the reason being that it is a direct method that does not influence the operating conditions, providing it does not change the surface tension. Very few users took advantage of this method (Lockett, 1986). The technique most used in literature is the dry tray entrainment capturing method (Lockett, 1986). There are two concerns regarding this technique. The one being that some of the liquid on the entrainment capturing tray can re-entrain and the other concern is that the liquid building up on this tray may influence the amount of entrainment it collects from the tray below (Lockett, 1986). This method is used in this work as it represents industrial operations where entrainment from the tray below influences the dynamics of the test tray (the tray above). To prevented liquid from re-entraining a demister pad was added above the entrainment collection tray to ensure no liquid droplets re-entrain from this section. This worked well as long as the de-entrainment tray is not flooded. Paper 1 will describe this modification and the effectiveness thereof in more detail. Efficiency entrainment determination is the most unreliable of the methods. This is due to the difficulty in measuring efficiency with high enough accuracy and then relating it to entrainment as many factor influences tray efficiency.

Parameters affecting entrainment

Various parameters affect entrainment. Tray and column geometry as well as gas and liquid physical properties play an important role in determining the hydrodynamic stability and entrainment inside the column. The influence of the following parameters on entrainment is

Stellenbosch University http://scholar.sun.ac.za

discussed based on findings made in literature (Lockett, 1986, Kister and Haas, 1988, and Kister, 1992):

1. *Column Diameter:* An increase in column diameter will decrease the velocity of the rising gas or vapour in the column. A reduction in gas velocity will reduce entrainment.
2. *Tray Spacing:* A decrease in tray spacing will always increase entrainment as the distance between the droplet development zone is decreased and more droplets will reach the tray above at lower tray spacings.
3. *Fractional Hole Area:* A reduction in fractional hole area will result in an increase in hole gas velocity. Thus increasing droplet ejection velocity which will increase entrainment.
4. *Hole diameter:* In general larger hole diameters will result in increasing entrainment. This effect is more prominent in the spray regime at low gas velocities than in the froth regime. Therefore, in the froth regime no significant difference in entrainment between hole diameters of 6.35 and 12.7mm has been noted by Kister and Haas (1988).
5. *Weir Height:* Kister and Haas (1988) showed three types of behaviour:
   a. Entrainment decrease with an increase in weir height in the spray regime. This behaviour is more prominent at low gas velocities.
   b. For high weirs at high gas and liquid flow rates, entrainment is less sensitive to weir height.
   c. For high liquid rates and low gas rates, an increase in weir height will increase entrainment.
6. *Liquid Flow Rate:* As shown in Figure 5, an increase in liquid rate will decrease entrainment in the spray regime. The opposite effect is true in the froth regime.
7. *Gas Flow Rate:* An increase in gas flow rate will always increase entrainment.
8. *Gas and liquid physical properties:* There is no clear evidence or mention of the influence of gas and liquid physical properties on entrainment. Most workers acknowledge the influence of gas and liquid density on entrainment. Some included surface tension as an important variable, others not. Gas viscosity has been included

Stellenbosch University http://scholar.sun.ac.za

in some of the spray regime entrainment prediction correlations. The general consensus in the literature is that liquid viscosity has no influence on entrainment.

The influence of these parameters on entrainment as depicted by current entrainment prediction models is discussed in the Entrainment Prediction Correlations section (section 4) to follow.

Stellenbosch University http://scholar.sun.ac.za

4. Entrainment Prediction Correlations

Various workers conducted research to gain understanding of the parameters that influence entrainment. In this section the focus is on the entrainment prediction correlations and their performance. Hunt et al. (1955), Thomas and Ogboja (1978), Zuiderweg (1982), Kister and Haas (1988), Koziol and Maćkowiak (1990), and Bennett et al. (1995) all developed entrainment prediction correlations based on various parameters. To understand their contributions and the limitations of their correlations a summarised review is conducted. Table 1 is a summary of the systems and, tray – and column geometries used by the different authors to develop their correlations.

Table 1. Summary of the column geometry, test ranges and systems used by the different authors to develop their correlations.

Author	Column Shape and Dimensions	Tray Spacing [m]	Gas Superficial Velocity [m/s]	Fractional Hole Area	Hole Diameter [mm]	Weir Height [mm]	Liquid Flow Rate [$m^3/(h.m)$]	Systems
Hunt *et al.* (1955)	0.152m Round	0.2 - 0.71	1.0 - 4.3 m/s	0.05 - 0.215	3.18 - 12.7	No Outlet Weir	0	Methane/Water, Freon 12/Water, Air/Kerosene, Air/Hexane, Air/CCl_4, Air/Water & Glycerine.
Thomas & Ogboja (1978)	0.3 x 0.91m Rectangular	0.3 - 0.457	1.9 - 3.2	0.124	25.4	76.2	4.5 - 40.3	Air/Water
	0.81m Round			0.118				
Kister & Haas (1988)	Data from various sources	0.3 - 1	0.3 - 3.5	0.04 – 0.2	1.5 – 25	0 - 80	2 - 130	Air/Water
Koziol and Maćkowiak (1990)	Data from various sources	0.15 - 0.6	0.9 – 3.2	0.03 – 0.34	6 - 15	0 - 80	1 - 14	Various
Bennet *et al.* (1995) (Air/Water)	Data from various sources	0.15 - 0.91	0.45 - 2.31	0.06 - 0.124	1.6 - 25.4	0 - 76.2	4.2 - 134	Air/Water

Stellenbosch University http://scholar.sun.ac.za

5. Review of current entrainment correlations

Hunt et al. (1955)

The first work on entrainment in sieve tray columns was conducted by Hunt et al. (1955) in a 0.152m round column with no liquid cross flow. They did not notice any flow regimes and Kister and Haas (1988) characterized their data to be related to the froth regime. Hunt et al. (1955) found entrainment to be a function of gas velocity, clear liquid height, tray spacing and liquid surface tension, but independent of gas density. Since they could not measure the froth height they assumed a constant froth density of 0.4 times the clear liquid density in order to develop their correlation, Equation 1. Their correlation does not account for the effects of cross flowing liquid and an outlet weir and is therefore not expected to be accurate at conditions commonly found in tray columns. Clear liquid height data or estimations are required to use Equation 1.

$$\frac{L'}{G} = 3.08\text{x}10^5\left(\frac{73}{\sigma}\right)\left(\frac{u_s}{s-2.5h_L}\right)^{3.2} \tag{1}$$

Thomas and Ogboja (1978)

Thomas and Ogboja (1978), like Hunt et al. (1955), noticed no change in the operating regime. They measured very low entrainment rates (L'/G = 0.001 - 0.1) in an air/water system for both a round and rectangular column using a catch-pot device filled with silica gel spheres. The accuracy of such a device is questionable (Uys, 2010). They based their correlation, Equation 2, on that of Hunt et al. (1955), excluding the surface tension dependency.

$$\frac{L'}{G} = 26.52\left(\frac{u_s}{s-h_f}\right)^{0.77} \tag{2}$$

Two froth height correlations were developed, one for their rectangular column, Equation 3 and the other for their round, Equation 4, column.

Stellenbosch University http://scholar.sun.ac.za

$$h_f = 0.0894Q_L + 1.279u_s\sqrt{\rho_v} + 3.52 \tag{3}$$

$$h_f = 0.0614Q_L + 1.77u_s\sqrt{\rho_v} + 4.83 \tag{4}$$

Zuiderweg (1982)

Zuiderweg (1982) developed his entrainment prediction correlation, Equation 5, for spray regime hydrocarbon systems based on data from Fractionation Research, Inc (FRI) and studies from Hofhuis and Zuiderweg (1979). The liquid hold-up (h_L) correlation, Equation 6, was developed by Hofhuis (1980).

$$\left(\frac{L'}{G}\right)_s = 1\times10^{-8} A_f \left(\frac{h_L}{S}\right)^3 \left(\frac{G}{L}\right)^2 \left\{1 + 265\left[\frac{u_s}{(gh_L)^{0.5}}\left(\frac{\rho_v}{\rho_l}\right)^{0.5}\right]^{1.7}\right\}^3 \tag{5}$$

$$h_L = 0.6\left(\frac{\psi p}{1000}\right)^{0.25}\left(\frac{h_w}{1000}\right)^{0.5} \tag{6}$$

$$\psi = \frac{Q_L}{3600u_s}\left(\frac{\rho_l}{\rho_g}\right)^{0.5} \tag{7}$$

Kister and Haas (1988)

Kister and Haas (1988) developed a prediction correlation for entrainment in the spray regime (Equation 8), froth regime (Equation 10) and for conditions where weeping occurs simultaneously (Equation 13). Their froth regime correlation is based on that of Hunt et al. (1955) with an empirically added hole diameter dependence and correction term for non-uniformity of the froth at low clear liquid heights. These correlations apply to the air/water system only and were correlated using data from various sources (Kister et al., 1981, Thomas and Ogboja, 1987, Bain and Van Winkle, 1961, Friend et al., 1960, Lemieux and Scotti, 1969, Brook et al., 1955, Benke, 1975, Calcaterra et al., 1968, and Nutter 1979). Kister

Stellenbosch University http://scholar.sun.ac.za

and Haas (1988) suggest that the correlation with the largest result (between Equation 8, 10 and 13) should be used to determine the rate of entrainment as well as indicate the active flow regime (spray, froth or weeping conditions). No correlation is given to calculate the froth height (h_f) and clear liquid height (h_L). The clear liquid height at the transition ($h_{L,t}$) from the froth to spray regime is calculated with Equation 12 developed by Jeronimo and Sawistowski (1973).

$$\left(\frac{L'}{G}\right)_s = 4.742^{(10/\sqrt{\sigma})^{1.64}}\left[872\left(\frac{u_s h_{L,ct}}{\sqrt{d_H s}}\right)^4\left(\frac{\rho_g}{Q_L \rho_l}\right)\left(\frac{\rho_l-\rho_g}{\sigma}\right)^{0.25}\right]^{(10/\sqrt{\sigma})} \quad (8)$$

$$h_{L,ct} = \frac{\left(\dfrac{0.4974 A_f^{-0.791} d_H^{0.833}}{1+0.013 Q_L^{-0.59} A_f^{-1.79}}\right)}{1+0.00262 h_w}\left(\frac{996}{\rho_l}\right)^{0.5\left(1-0.00091 d_H / A_f\right)} \quad (9)$$

$$\left(\frac{L'}{G}\right)_f = 111\left(\frac{u_s}{s-h_f}\right)^2 d_H^{0.5}(1+\zeta) \quad (10)$$

$$\zeta = \frac{0.00225}{A_f^3}\left(\frac{h_{L,t}}{h_L}-1\right) \quad \text{for } h_{L,t} > h_L$$
$$\zeta = 0 \quad \text{for } h_{L,t} \le h_L \quad (11)$$

$$h_{L,t} = \frac{0.4974 A_f^{-0.791} d_H^{0.833}}{1+0.013 Q_L^{-0.59} A_f^{-1.79}} \quad (12)$$

$$\left(\frac{L'}{G}\right)_w = \frac{0.3 d_H p^2}{h_L\left(s-h_f\right)^2} \quad (13)$$

$$\left(\frac{L'}{G}\right) = \left(\frac{L'}{G}\right)_s or \left(\frac{L'}{G}\right)_f or \left(\frac{L'}{G}\right)_w \text{ (whichever is largest)} \quad (14)$$

The air/water data used by Kister et al. (1981) showed that in the spray regime entrainment depends on gas velocity, liquid flow rate, tray spacing and tray geometry. The parameters influencing spray regime entrainment were expressed in the following dimensionless groups which represent the primary hydrodynamic phenomena on the tray;

1. a hole Weber to hole Reynolds number ratio

Stellenbosch University http://scholar.sun.ac.za

2. a dimensionless hole diameter to clear liquid height ratio
3. a dimensionless tray spacing to clear liquid height ratio
4. a dimensionless group they introduced which accounts for the effect of liquid cross flow
5. entrainment during weeping depend on hole diameter and hole pitch over the clear liquid height and effective tray spacing relationship

The correlations developed by Kister and Haas (1988) were the first to include both the spray and froth regimes. These correlations also included a large array of parameters, except gas - and liquid viscosity, and surface tension in the froth regime.

Koziol and Maćkowiak (1990)

They presented a correlation consisting of dimensionless numbers to predict entrainment in the spray regime. What makes this correlation unique is the fact that it can be used for all tray types such as sieve, valve, bubble cap, tunnel and cross-flow trays with downcomers. The correlation includes most of the column – and tray geometry parameters as well as most gas – and liquid physical properties. Liquid viscosity and weir height are not included in their correlation. In order to develop their correlation for systems other than air/water, Koziol and Maćkowiak (1990) used Equation 14 by Kister and Haas (1988) to generate data points.

$$\left(\frac{L'}{G}\right)_s = 0.37 Fr_G^{2/3} Fr_L^{-1/5} Fl^{-1/3} \left(\frac{\rho_g}{\rho_l}\right)\left(\frac{We}{Co}\right)^{133.7 Fl^{-1/6}} \quad (15)$$

$$Fr_G = \frac{F_h^2}{S\left(\rho_l - \rho_g\right) g} \quad (16)$$

$$Fr_L = \frac{V_L^2 \left(1 + e_L\right)^2}{g S^2 D_c^3} \quad \text{iterate from } e_L = 0 \quad (17)$$

$$Fl = \frac{\sigma^3 \rho_g^2}{\mu_g^4 \left(\rho_l - \rho_g\right) g} \quad (18)$$

Stellenbosch University http://scholar.sun.ac.za

$$We = \frac{F_s^2}{\left(\sigma g\left(\rho_l - \rho_g\right)\right)^{1/2}} \quad \textbf{(19)}$$

$$Co = \frac{A_f S}{D_c}\left(\frac{D_c}{D_h}\right)^{1/2} \quad \textbf{(20)}$$

$$e_L = \frac{V_g}{V_l}\left(\frac{L'}{G}\right)_s\left(\frac{\rho_g}{\rho_l}\right) \quad \textbf{(21)}$$

Bennett et al. (1995)

Bennett et al. (1995) developed entrainment correlations for both the froth and spray regime as well as for air/water and non-air/water systems using data from various sources (Thomas and Ogboja, 1978, Sakata and Yanagi, 1979, Lockett et al. 1976, Bain and Van Winkle, 1961, Friend et al., 1960, Lemieux and Scotti, 1969, Nutter, 1979, Pinczewski et al. 1975 and, Pupich and Goedecke, 1987). Their non-air/water entrainment correlations perform poorly (Uys, 2010) due to the small data base used during the development thereof. Therefore, the details of their non-air/water entrainment correlations will not be covered in this work. They suggest that entrainment should be correlated as a function of the ratio of tray spacing to froth height as shown in Equations 22 and 23. For low liquid hold-up ($h_L/d_H<2$) conditions the spray regime correlation applies and as the liquid hold-up increased ($h_L/d_H>2$) the froth regime correlation should be used. Entrainment in the froth regime was found to be independent of the average froth density while dependent on the average froth density in the spray regime. Droplet drag was assumed to be negligible for the air/water system at the conditions used by Bennett et al. (1995) to develop their correlation. Therefore, liquid surface tension was assumed to have no influence on entrainment. However, they did acknowledge that at high vapor velocities and for low surface tension liquid this assumption is not valid.

Entrainment in the spray – and froth regimes was found to have the following relationships:

$$\left(\frac{L'}{G}\right)_s = 0.0050\left(\frac{S}{H_f}\right)^{-1.26} f\left(\varepsilon\right)\left(\frac{\rho_L}{\rho_g}\right)^{0.5} \quad \textbf{(22)}$$

Stellenbosch University http://scholar.sun.ac.za

$$\left(\frac{L'}{G}\right)_f = 0.00164\left(\frac{S}{H_f}\right)^{-1.86}\left(\frac{\rho_L}{\rho_g}\right)^{0.5} \quad \textbf{(23)}$$

The expanded form of Equations 22 and 23 are as follows:

$$\left(\frac{L'}{G}\right)_s = 0.0050\left(\frac{K_s^2}{g\phi_e S}\right)^{1.26}\left[\frac{gH_L}{K_s^2}+\frac{9\sqrt{3}}{2A_f}\left(1+4.77\left\{\frac{D_H}{H_L}\right\}^{3.29}\right)\right]^{1.26}\varepsilon^{\beta}\left(\frac{\rho_L}{\rho_g}\right)^{0.5} \quad \textbf{(24)}$$

$$\left(\frac{L'}{G}\right)_f = 0.00164\left(\frac{K_s^2}{g\phi_e S}\right)^{1.86}\left[\frac{gH_L}{K_s^2}+\frac{9\sqrt{3}}{2A_f}\left(1+6.9\left\{\frac{D_H}{H_L}\right\}^{1.85}\right)\right]^{1.86}\left(\frac{\rho_L}{\rho_g}\right)^{0.5} \quad \textbf{(25)}$$

Bennett et al. (1995) developed their own set of liquid hold-up, froth height and froth density correlations as shown in Table 2.

Table 2. Relations developed by Bennett et al. (1995) to correlate froth height and froth density.

$H_L = \phi_e H_f$	$C = 0.501 + 0.439\exp[-137.8H_w]$	$K_s = u_s\sqrt{\frac{\rho_g}{\rho_l}}$
$H_f = H_w + C\left(\frac{Q_L}{3600\phi_e}\right)^{2/3}$	$\phi_e = \exp[-12.55K_s^{\ 0.91}]$	$Fr = \frac{u_{D0}^2}{gH_{Fe}}$
$u_{D0} = 3K_s\sqrt{\frac{\sqrt{3}}{A_f\phi_e}}$	$\beta = 0.5\left(1-\tanh\left[1.3\ln\left(\frac{H_L}{D_H}\right)-0.15\right]\right)$	$\varepsilon = \frac{H_L}{H_f}$

Stellenbosch University http://scholar.sun.ac.za

6. Critical Evaluation of Entrainment Prediction Correlations

In this section the prediction correlations discussed are compared in Figure 7 to Figure 16. The comparisons are made over a range of gas- and liquid flow rates, tray- and column geometries as well as for different gas- and liquid physical property ranges. The objective is to show where there is agreement, discrepancies and uncertainties between the correlations for each dependant variable. This will also show which authors assumed specific properties to have no influence on entrainment. For all comparisons air/water physical properties were *used* (ρ_l = 997kg/m^3, σ = 73mN/m, ρ_g = 1.18kg/m^3), *except* where any one of these properties were changed. The correlations by Hunt et al. (1955) and Kister and Haas (1988) require clear liquid height and froth height estimations. As these authors did not develop such correlations, the work of Colwell (1981) was used as recommended by Kister and Haas (1988). In the legend of each of the figures reference is made to the different authors. Thomas and Ogboja (1978) is shown as "*T & O*", Kister and Haas (1988) is "*K & H*" and, Koziol and Maćkowiak (1990) is indicated as "*M & K*". In the graphs to follow the correlations are plotted for conditions representing both the spray and froth regimes, although they are not necessarily valid for that specific regime. This is done to purposely show how the correlations perform over a large range of conditions.

It has to be noted that for most of the cases depicted in the graphs to follow, the correlations are compared at conditions beyond their recommended range of application. The reason for this is that most of the correlations were developed based on the air/water system, therefore, by changing the physical properties the correlation is extrapolated. The correlations of Zuiderweg (1982) and, Koziol and Maćkowiak (1990) are only valid in the spray regime and do not apply to the froth regime. Hunt et al. (1955) conducted their tests with a static liquid and industrial applications have cross flowing liquid. The correlations of Kister and Haas (1988) and Bennett et al. (1995) have the largest range of application for the air/water system and most industrial applications use non-air/water systems. The reason for comparing the different correlations over extended ranges is to show how much they deviate within and beyond their recommended range of application. The extended gas and liquid physical property ranges used in the comparisons do in most cases fall within industrial application ranges as shown by Uys (2010). It is also of great importance to the design engineer to know where the largest uncertainty in prediction of entrainment lies. In

Stellenbosch University http://scholar.sun.ac.za

this study the information is used to determine the experimental scope so that contributions can be made in the areas of greatest uncertainty.

The first comparison between the different correlations is made in Figure 7 where entrainment is shown as a function of gas velocity and liquid flow rate. In Figure 7 (a), for the low liquid rate, all the correlations predict a different result with the difference in prediction increasing with an increase in gas velocity. These conditions are typical to the spray regime. For the intermediate liquid rate, Figure 7 (b), most of the correlations show a similar trend with exception to Thomas and Ogboja (1978) and Bennett et al. (1995). It has to be noted that Bennett et al. (1995) specifies that their correlation is only valid up to a gas velocity of 2.3m/s. At the high liquid rate, Figure 7 (c), most of the correlations again show a similar influence of gas velocity on entrainment.

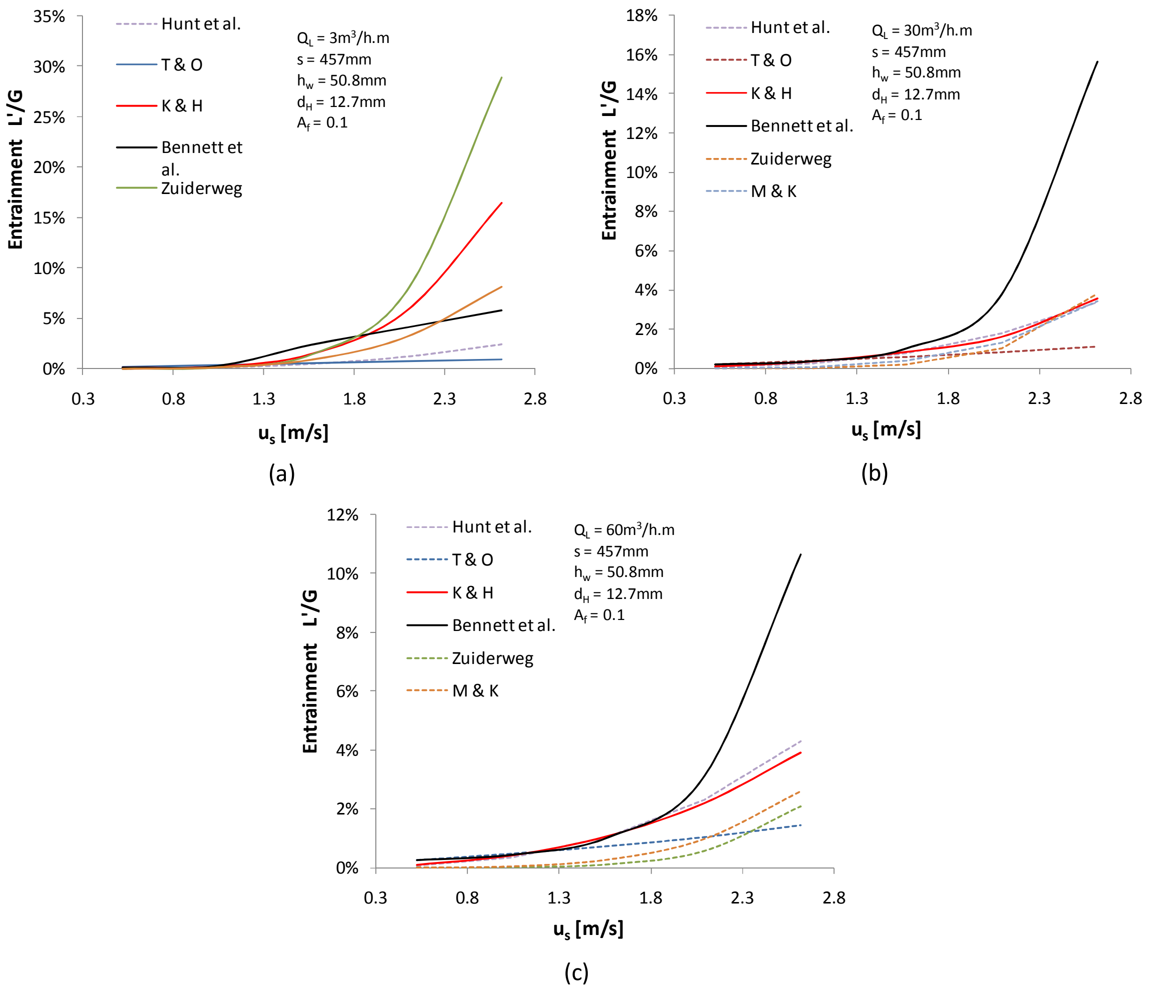

Figure 7. Variation between predictions for the influence of gas velocity on entrainment for three liquid rates. Broken lines indicate extrapolation beyond the recommended range of application.

Stellenbosch University http://scholar.sun.ac.za

Figure 8 shows the large discrepancy between the predictions with varying liquid flow rate. For the low gas velocity example typical to the froth regime, depicted in Figure 8 (a), most of the correlations show an increase in entrainment as liquid flow rate is increased. This is expected for froth regime conditions (Kister and Haas, 1988). The correlations developed by Zuiderweg (1982) and Koziol and Maćkowiak (1990) predict a decrease in entrainment with an increase in liquid rate. Their correlations are only valid in the spray regime, where an increase in liquid rate will cause entrainment to decrease. Figure 8 (b) and (c) show that the predicted entrainment varies significantly with an increase in gas velocity. The difference between the predictions is the smallest at the spray to froth regime transition, where the minimum entrainment is predicted. It is important to note that the correlations of Hunt et al. (1955) and Thomas and Ogboja (1978) have been developed for the froth regime (Kister and Haas, 1988). Therefore, according to their predictions, entrainment will always increase with an increase in liquid flow rate. The opposite is true for the predictions of Zuiderweg (1982) and Koziol and Maćkowiak (1990) that is valid in the spray regime only. Only the correlations of Kister and Haas (1988) and Bennett et al. (1995) have been developed to predict entrainment in both the spray – and froth regimes. The correlation of Bennett et al. (1995) shows an increase in entrainment in the spray regime. This becomes more prominent as the gas velocity is increased as shown in Figure 9.

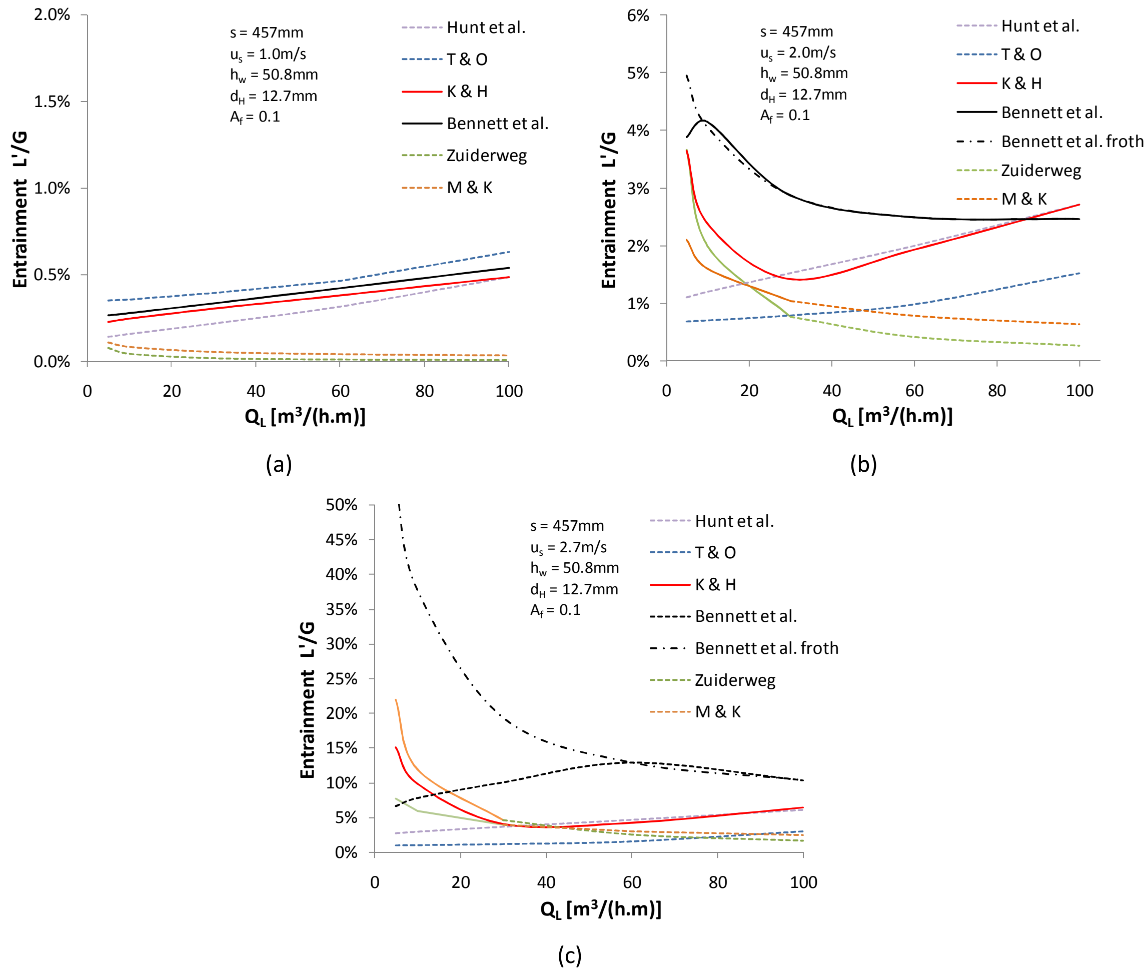

Figure 8. Predictions for the influence of liquid flow rate on entrainment for three gas velocities.

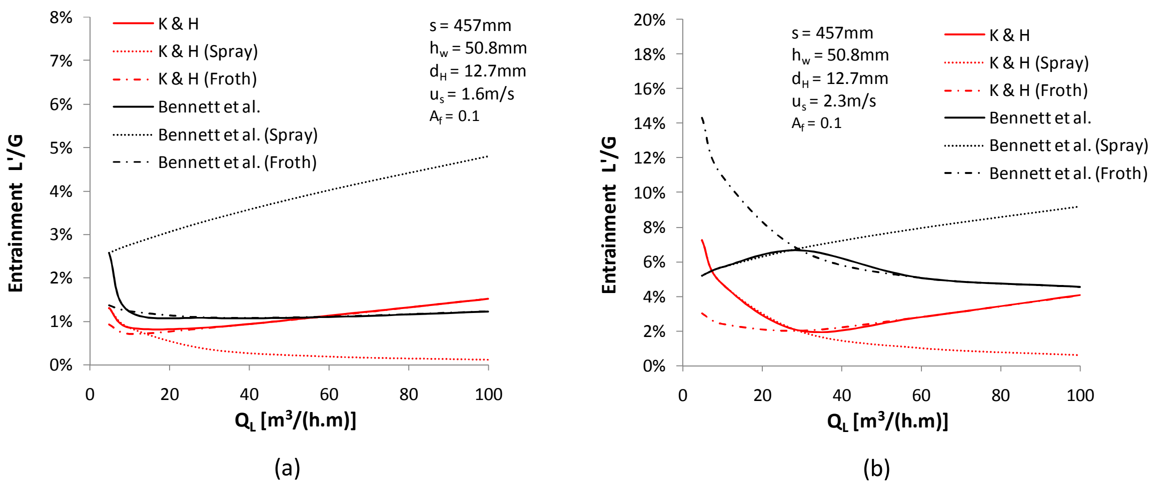

Figure 9. Difference in predictions between Kister and Haas (1988) and Bennett et al. (1995) for entrainment as a function of liquid rate for the spray and froth regime.

Stellenbosch University http://scholar.sun.ac.za

All the correlations indicate that an increase in tray spacing will result in a decrease in entrainment. The rate of decrease in entrainment with an increase in tray spacing varies at different liquid rates as shown in Figure 10. As tray spacing becomes smaller, the variation in entrainment prediction becomes larger.

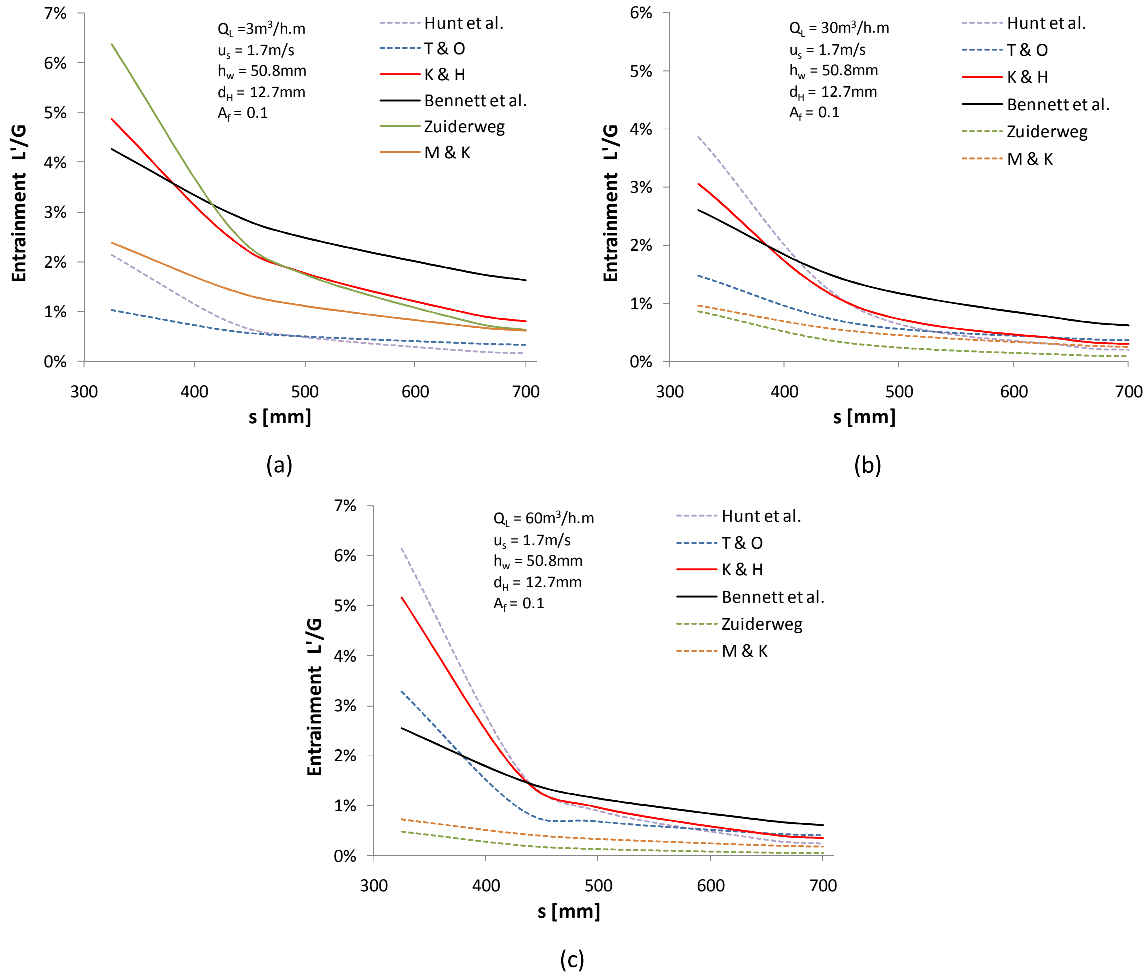

Figure 10. Predicted influence of tray spacing on entrainment for three liquid flow rates.

In Figure 11 the prediction by Thomas and Ogboja (1978) shows no influence of fractional hole area on entrainment. Only Hunt et al. (1955) shows an increase in entrainment with an increase in fractional hole area. Zuiderweg (1982), Kister and Haas (1988), Koziol and Maćkowiak (1990), and Bennett et al. (1995) all predict a decrease in entrainment with an increase in fractional hole area. Their predictions do, however, vary quite significantly from each other.

Stellenbosch University http://scholar.sun.ac.za

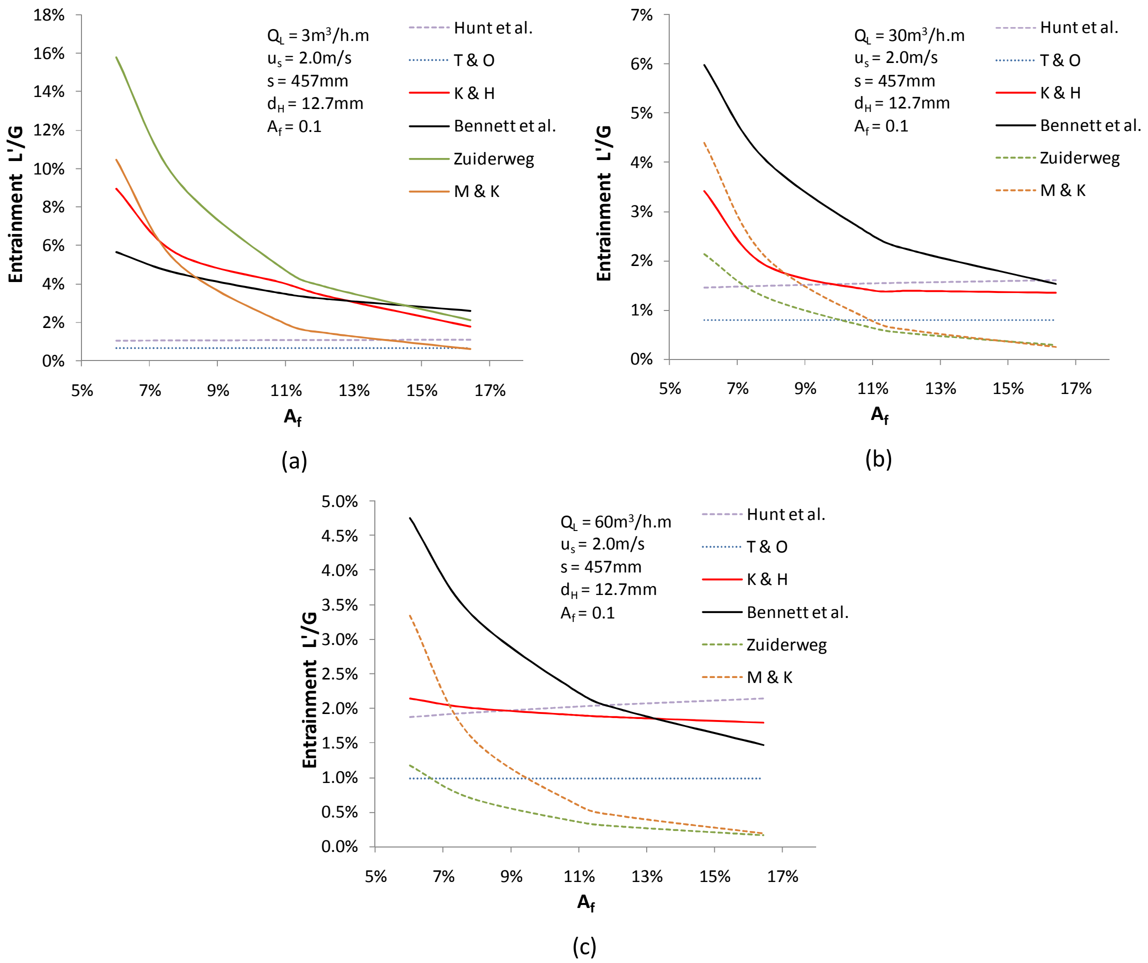

Figure 11. Predicted influence of fractional hole area on entrainment for three different liquid rates

Hunt et al. (1955), Thomas and Ogboja (1978) and Zuiderweg (1982) indicate that entrainment is independent of hole diameter. This is indicated in Figure 12. Koziol and Maćkowiak (1990) show a linear increase in entrainment with an increase in hole diameter. Kister and Haas (1988) show a non-linear increase in entrainment with increasing hole diameter. A non-monotonic relationship is shown by Bennet et al. (1995) between hole diameter and entrainment for the low and medium liquid flow rate illustrations (Figure 12 (a) and (b)).

Stellenbosch University http://scholar.sun.ac.za

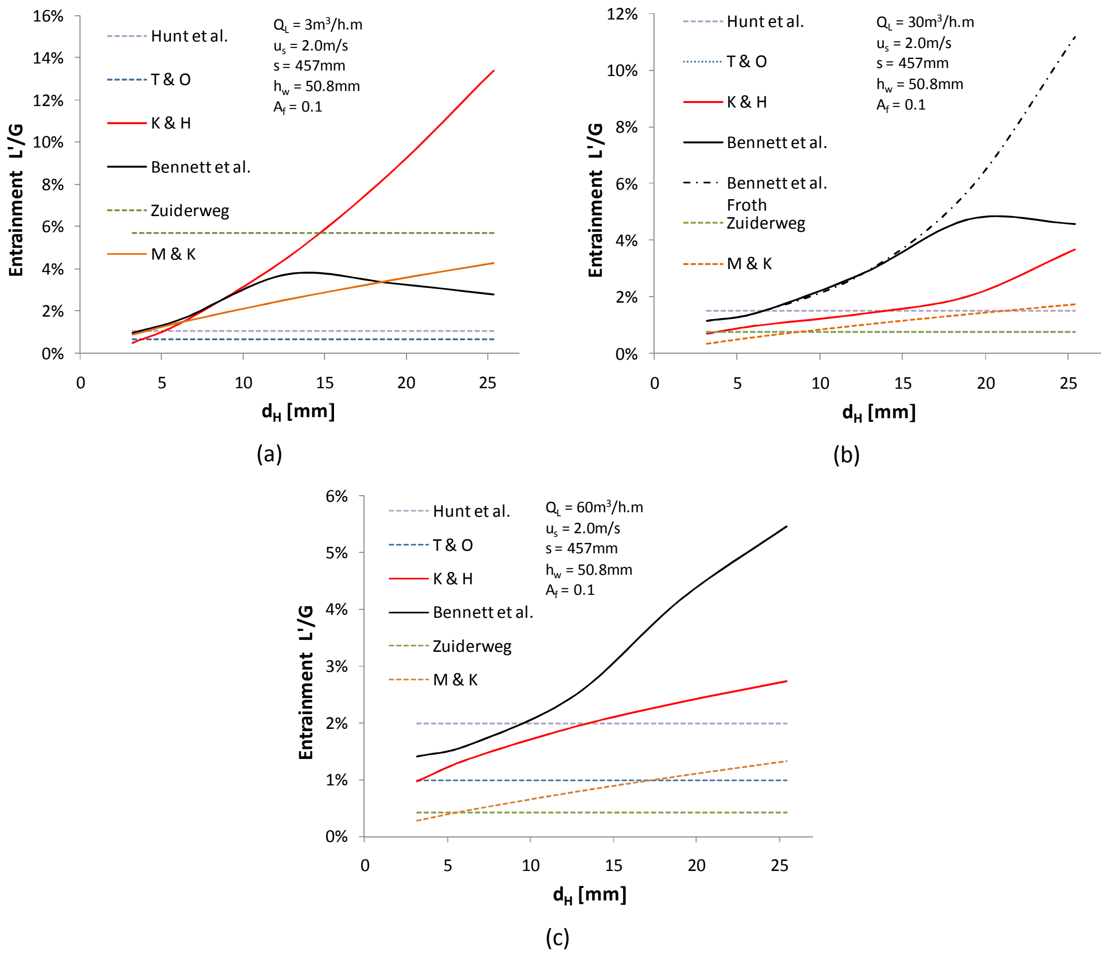

Figure 12. The predicted influence of hole diameter on entrainment for three different liquid rates.

Figure 13 is constructed to show how the correlations portray the influence of weir height on entrainment. Thomas and Ogboja (1978) and Koziol and Maćkowiak (1990) show that weir height has no influence on entrainment. For the low liquid rate example, Figure 13 (a), Zuiderweg (1982) indicates that entrainment will increase with an increase in weir height. Kister and Haas (1988) suggest the opposite effect, whereas Bennett et al. (1995) show an increase in entrainment for weir heights smaller than 55mm and a decrease in entrainment for weir heights lager than 55mm. There is very little agreement as to the influence of weir height on entrainment between the predictions.

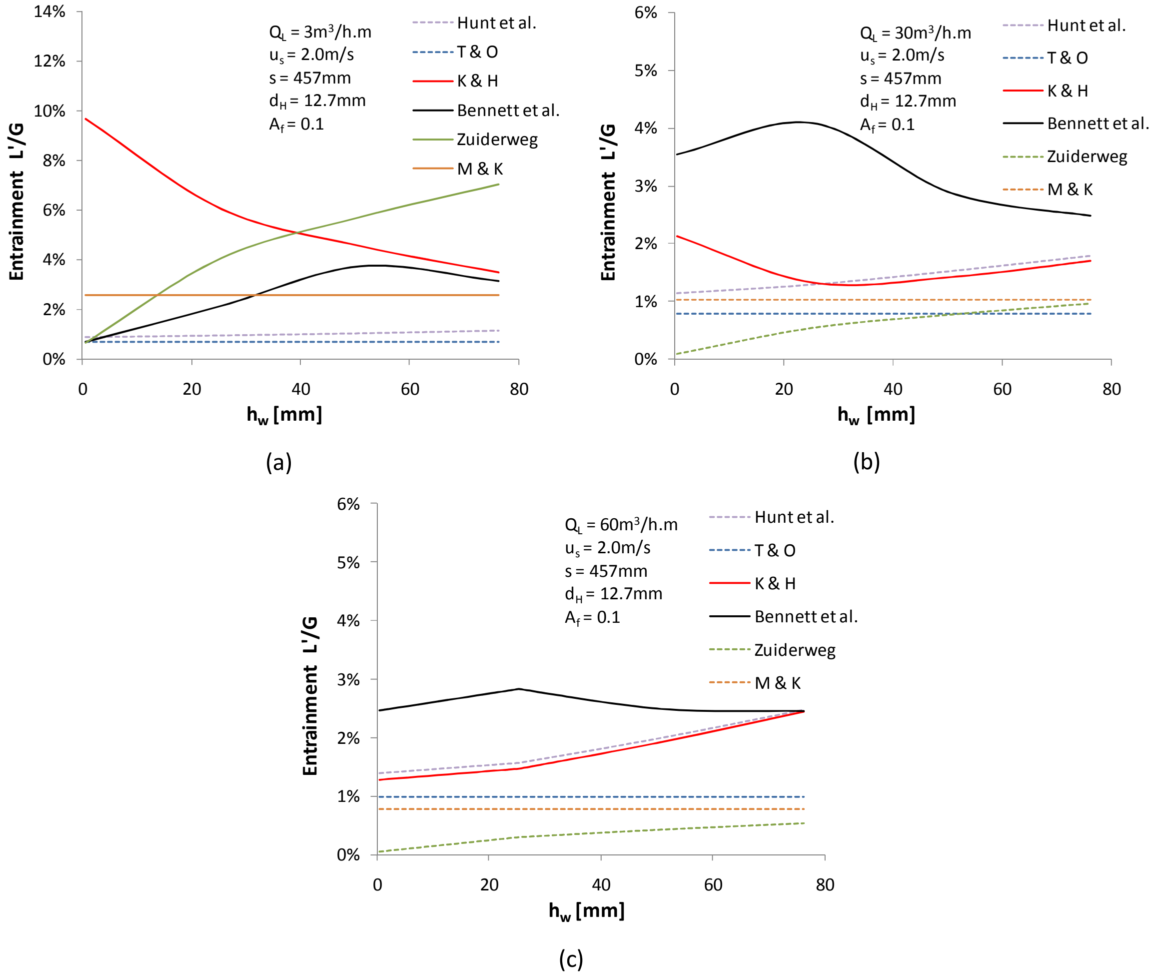

Figure 13. Variation between predictions for the influence weir height on entrainment for three liquid rates.

All the correlations show a non-linear decrease in entrainment with an increase in gas density at constant gas flow factor (F_S) conditions (see Figure 14). The gas flow factor is the square root of the gas kinetic energy.

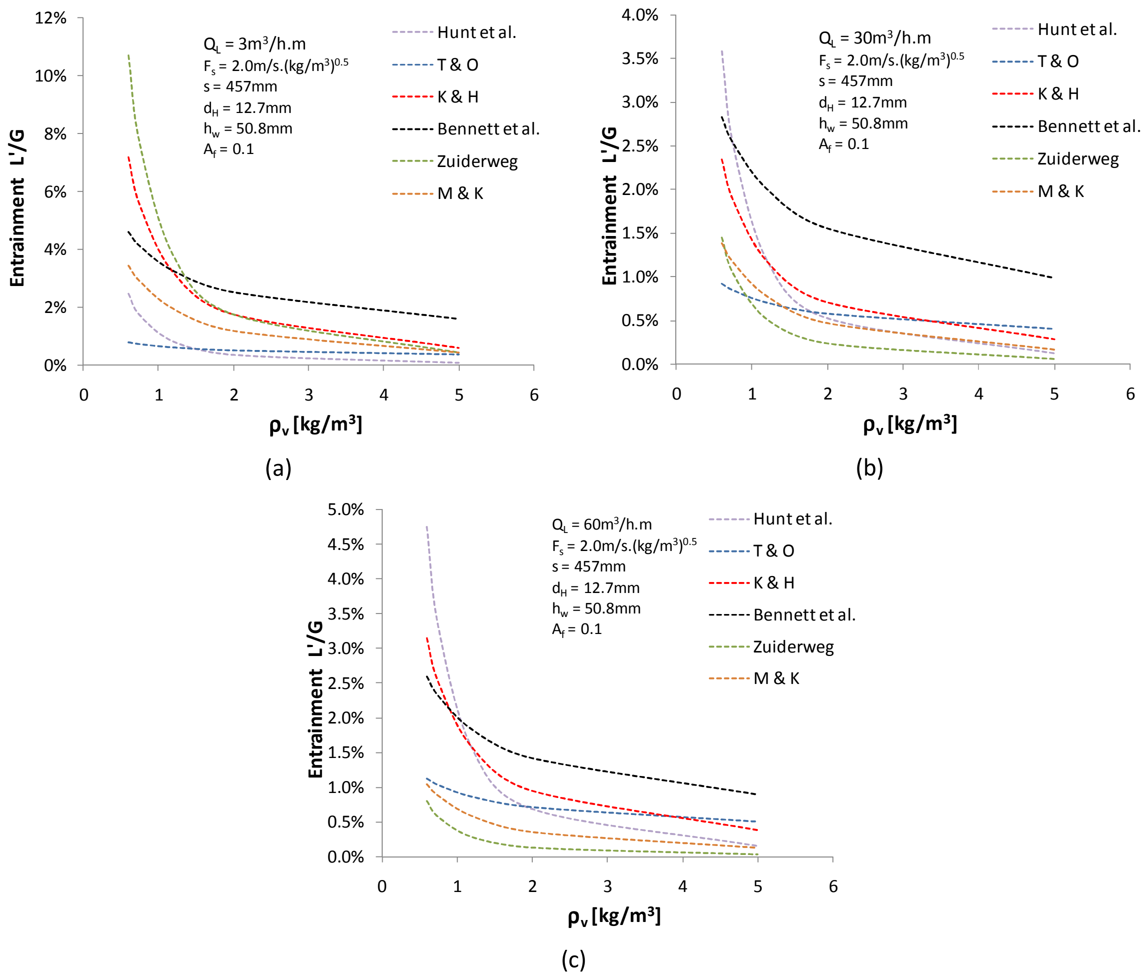

Figure 14. Predicted influence of gas density on entrainment for three liquid rates.

Kister and Haas (1988) and Koziol and Maćkowiak (1990) are the only workers who included surface tension in their spray regime entrainment prediction correlations. In the graphs depicted in Figure 15 the correlations are plotted for both regimes, although they are not necessarily valid for that specific regime. Therefore, although the correlation of Koziol and Maćkowiak (1990) is valid only in the spray regime, the result is still shown in Figure 15 (b) and (c), which are conditions typical to the froth regime. Hunt et al. (1955) also included a surface tension parameter in their correlation. Kister and Haas (1988) suggest that the experiments conducted by Hunt et al. (1955) represent froth regime conditions, although they had no liquid cross flow in the experiments.

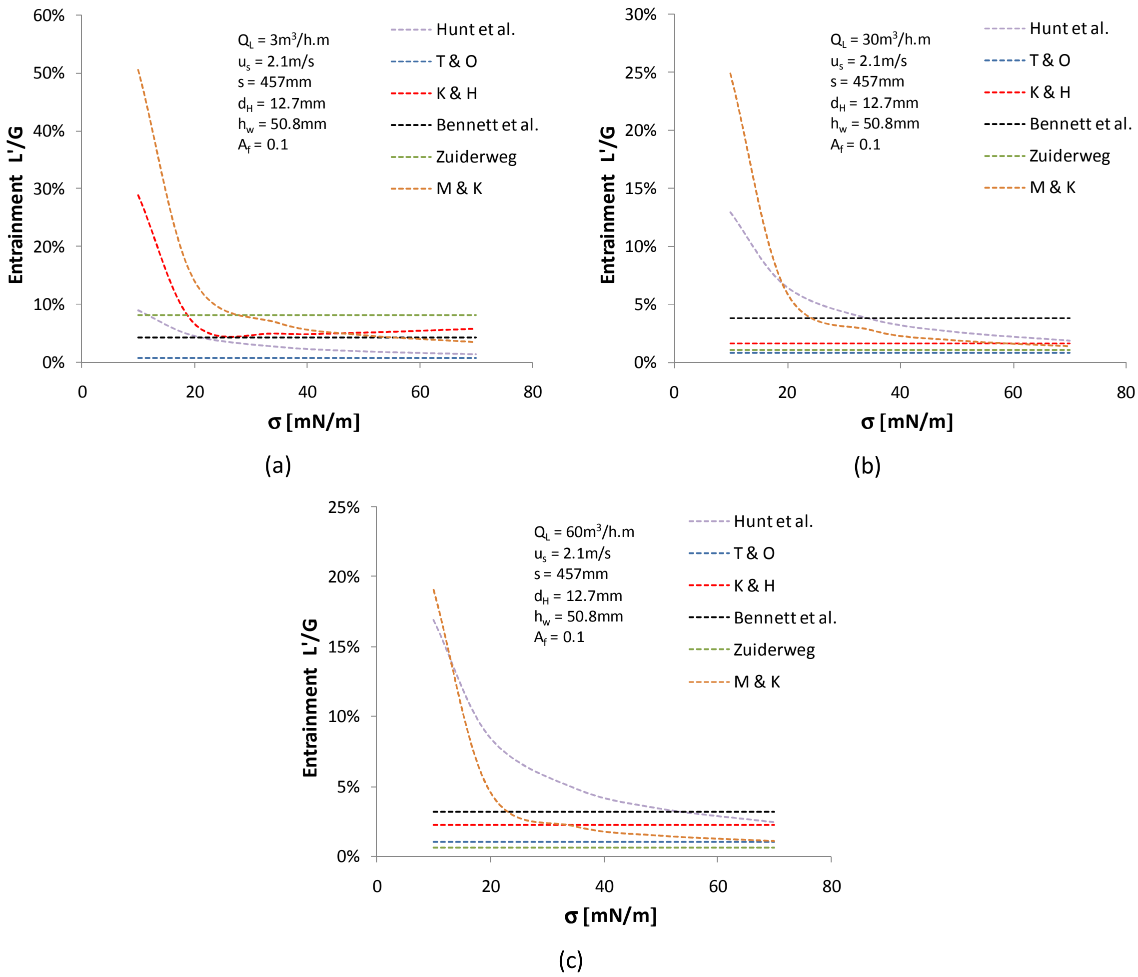

Figure 15. Predicted influence of surface tension on entrainment for three liquid rates.

Kister and Haas (1988) show very little influence of liquid density on entrainment in the froth regime. They do show significant decrease in entrainment in the spray regime with an increase in liquid density. Conversely, Bennett et al. (1995) show a very small variation in entrainment for a change in liquid density. Hunt et al. (1955) show a small increase in entrainment with increasing liquid density. A very small decrease in entrainment is suggested by Koziol and Maćkowiak (1990) for an increase in liquid density. The variation between the predictions is very significant especially at low liquid densities.

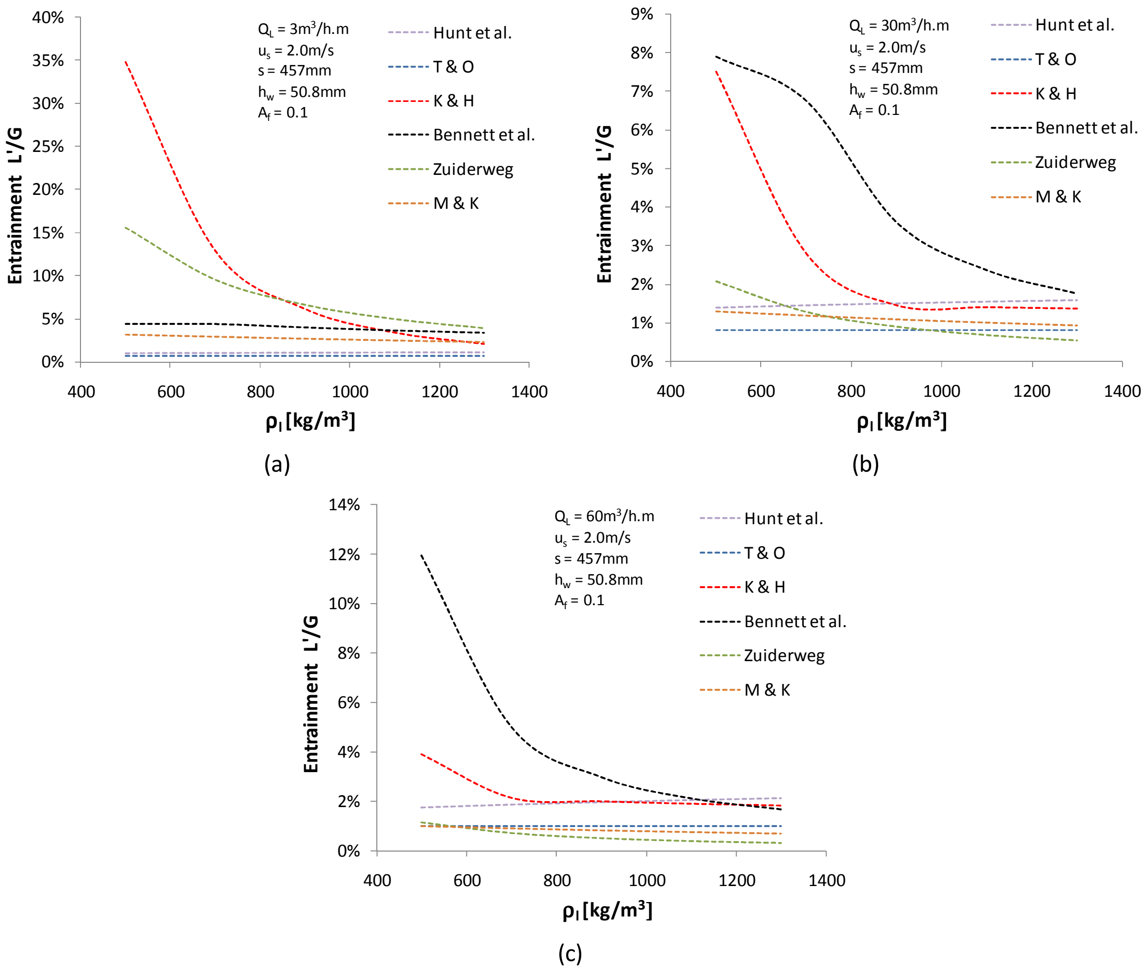

Figure 16. Variation in predictions made for the influence of liquid density on entrainment for three liquid rates.

The critical evaluation show that there is very little agreement between entrainment prediction correlations when each of the different variables is changed. These correlations were developed from a database consisting of a majority of air/water data, as very little non-air/water data were available. To conduct research with systems other than air/water is expensive and although industrial research is substantial, very few of the results are published (Bennett and Ludwig, 1994). Therefore, as stated by Bennett and Ludwig (1994), in some cases air/water results are better than no results at all, but not representative of actual industrial applications.

Stellenbosch University http://scholar.sun.ac.za

7. Thesis layout and objectives

As shown by the critical evaluation section, very little or no attention has been given to the influence of gas and liquid properties on entrainment, especially to liquid surface tension and viscosity. Single droplet formation and disintegration work by Decent et al. (2009), Pan and Hung (2010) and Fakhari and Rahimian (2011) suggest that surface tension and liquid viscosity do play a significant role in droplet development, deformation and disintegration. As entrainment is characterised by ejecting droplets, there is reason to believe that gas and liquid physical properties will influence entrainment to a larger extent than previously recognised. The objective of this project was to determine how gas and liquid physical properties influence entrainment over a range of gas and liquid flow rates, and tray spacings.

To achieve the project objective, the work was divided into four sub-sections followed by general conclusions, recommendations and appendixes with additional data and explanations as shown in Figure 17. The first section is an accepted paper and the remaining three sections are manuscripts written for journal publication. All four sections are alone standing documents. The objective of each section is as follows:

1. Paper One

   In this manuscript the assumption that the effect of liquid surface tension and liquid viscosity on entrainment is negligible, as assumed by others (Kister and Haas, 1988 and Bennett et al. 1995), is investigated. An experimental setup was designed and constructed to measure entrainment, weeping and tray pressure drop. Visual access to the froth in the column is incorporated to observe froth development and behaviour under different conditions. The experimental entrainment data for three systems, namely air/water, air/ethylene glycol and air/silicone oil, were compared to existing correlations. Entrainment data were generated for flow factors ranging from 1.6 $kg^{0.5}/(m^{0.5}.s)$, for a 415mm tray spacing to 4.0 $kg^{0.5}/(m^{0.5}.s)$ for a 615 mm tray spacing within a liquid flow range of 2.9 – 112 $m^3/(h.m)$. The results obtained were compared with entrainment correlations (Kister and Haas, 1988 and Bennett et al., 1995) to test if the assumption to neglect some of the physical properties is correct.

Stellenbosch University http://scholar.sun.ac.za

2. Manuscript Two

   In this work the objective was to investigate the influence of gas physical properties on entrainment. The influence of gas physical properties on both definitions of entrainment (L'/L and L'/G) is investigated. The objective was to find a correlation between entrainment, gas physical properties and gas-and-liquid flow rates. Therefore, new entrainment data were measured over a range of gas physical properties for three liquids. Air, CO_2 and SF_6 were passed through the column to cover a large gas density (1.2 – 5.8 kg/m^3) range. Water, ethylene glycol and n-butanol were used as liquids to provide liquid physical property variation. Liquid flow rates ranged from 2.9 – 80 m^3/(h.m) with gas flow factors ranging from 1.9 – 4.8 m/s.(kg/m^3)$^{0.5}$. The gas rates used in experiments were higher than the range covered by the Bennett et al. (1995) correlation. Extension of the gas flow rate test range will expand current knowledge found in the open literature. The data are compared with entrainment prediction correlations to investigate their scope and limitations.

3. Manuscript Three

   The objective of this manuscript was to investigate the influence of liquid physical properties on entrainment, with the main focus on surface tension and dynamic viscosity. One way of doing so is to determine whether findings related to single droplet development and disintegration have any correlation with sieve tray entrainment. Five liquids are used in an array of experiments to cover a large range of liquid density (739 - 1095 kg/m^3), surface tension (19.9 – 60 mN/m) and dynamic viscosity (0.9 – 48.8 mPa.s). These liquids were used with CO_2 to extend the current non-air/water database. Liquid flow rates ranged between 2.8 – 80m^3/(h.m) with gas flow factors ranged between 1.9 – 4.3 m/s.(kg/m^3)$^{0.5}$. Newly obtained data are compared with the entrainment prediction correlations of Kister and Haas (1988) and Bennett et al. (1995) to determine their shortcomings.

4. Manuscript Four

   Throughout the project a large databank has been built consisting of new entrainment data. This databank is larger than the databanks used by Kister and Haas (1988) and Bennett et al. (1995) combined. The objective of this manuscript was to develop simple, dimensionless entrainment prediction correlations for the

Stellenbosch University http://scholar.sun.ac.za

spray and froth regime that does not require clear liquid height or froth height estimations. These correlations include the influence of gas and liquid flow rates, gas and liquid physical properties and, tray spacing. The newly developed correlations are compared with entrainment data and other prediction correlations to show their scope and limitations. One limitation of the developed correlations is that they do not include the effect of tray geometry on entrainment. Therefore, the effect has to be determined using other correlations and added to the result of the new correlations.

5. Conclusions

   These general conclusions are made based on the findings and conclusions of the manuscripts.

6. Recommendations for future projects

   Recommendations for future projects are made based on the general conclusions.

7. Appendixes

   All the data measured in this work are published in this section. Pressure drop data were measured as it can be used extensively in future projects to determine flood points, pressure drop correlations and liquid hold-up correlations which did not form part of the focus of this project.

Stellenbosch University http://scholar.sun.ac.za

Introduction & Literature review

-Findings determined project scope and hypothesis
-Existing correlations limited to air/water system, do not include liquid dynamic viscosity and surface tension

Paper 1

-Initial experimental results prove hypothesis that liquid dynamic viscosity and surface tension influences entrainment and that current correlations are not able to predict this influence
-New froth behaviour theory established

Manuscript 2

-Measure new experimental data using three gasses and three liquids
-Investigate the influence of gas physical properties on entrainment
-Modified Reynolds and Froude numbers describe this influence

Manuscript 3

-Measure new data for five liquids
-Investigate the influence of liquid physical properties on entrainment
-Viscosity shows complex influence on froth behaviour and entrainment

Manuscript 4

-Measure new experimental data for various tray spacings
-Add data from Paper 1, Manuscript 2 and 3, compile
-Develop model for spray and froth regime entrainment
-Compare model with data and other correlations

Conclusions & Recommendations

-Based on the findings in Paper 1 and Manuscript 2 and 3 the conclusions are drawn
-Based on the conclusions in Paper 1 and Manuscript 2 and 3 the recommendations are drawn

Figure 17. Graphical representation of the thesis layout

Stellenbosch University http://scholar.sun.ac.za

8. References

Bain, J.F., Van Winkle, M., 1961. A study of entrainment, perforated plate column, air-water system, American Institute of Chemical Engineers, 7, (3), 363.

Bennett, D.L., Ludwig, K.A., 1994. Understand the limitations of air/water testing of distillation equipment. Chemical Engineering Progress, 72 – 79.

Bennett, D.L., Kao, A.S., Wong, L.W., 1995. A mechanistic analysis of sieve tray froth height and entrainment. American Institute of Chemical Engineers , 41 (9), 2067-2082.

Bennett, D.L., Watson, D.N., Wiescinski, M.A., 1997. New correlation for sieve-tray point efficiency, entrainment, and section efficiency. American Institute of Chemical Engineers, 43 (6), 1611 – 1626.

Benke, N.S.B.E, 1975. Thesis, School of Chemical Engineering. University of New South Wales.

Brook, W.E., Hannold, D.E., Cunningham, W.C., Huntington, R.L., 1955. Pet. Eng, 27, C-32.

Calcaterra, R.J, Nicholls, C.W., Weber, J.H., 1968. Free and capture entrainment and plate spacing in a perforated tray column. British Chemical Engineering, 13, (9), 1294.

Colburn, A.P., 1936. Effect of entrainment on plate efficiency in distillation. Industrial and Engineering Chemistry, 28, 526.

Colwell, C., 1981. Clear liquid height and froth density on sieve trays. Industrial and Engineering Chemistry Process Design and Development, 20 (2), 298-307.

Decent, S.P., King, A.C., Simmons, H.J.H., Părău, E.I., Wallwork, I.M., Gurney, C.J., Uddin, J., 2009. The trajectory and stability of a spiralling liquid jet: Viscous theory. Applied Mathematical Moddeling, 33, 4283-4302.

Fakhari, A., Rahimian, M.H., 2011. Investigation of deformation and breakup of a falling droplet using a multiple-relaxation-time lattice Boltzmann method. Computers & Fluids, 40, 156 – 171.

Friend, L., Lemieux, E.J., Schreiner, W.C., 1960. New data on entrainment from perforated trays at close spacings. Chemical Engineering., 67, 101.

Hofhuis, P.A.M., Zuiderweg, F.J., 1979. Sieve plates: dispersion density and flow regimes. Institution of Chemical Engineers Symposium Series. No 56 “Distillation 1979”, 2.2/1

Hofhuis (1980) from Zuiderweg 1982 or locket 1986

Stellenbosch University http://scholar.sun.ac.za

Hunt, C. d'A., Hanson, D.N., Wilke, C.R., 1955. Capacity factors in the performance of perforated plate columns. AIChE Journal. 1 (4), 441 – 451.

Jeronimo, M.A., Sawistowski, H., 1973. Phase inversion correlation for sieve trays. Transactions of the Institution of Chemical Engineers, 51, 265.

Kister, H.Z, Pinczewski, W.V., Fell, C.J.D., 1981. Entrainment from sieve trays operating in the spray regime. Industrial and Engineering Chemistry Process Design and Development , 20 (3), 528-532.

Kister, H.Z., Haas, J.R., 1988. Entrainment from sieve trays in the froth regime. Industrial and Engineering Chemistry Research , 27 (12), 2331-2341.

Kister, H.Z., 1992. Distillation design, McGraw-Hill.

Lemieux, E.H. and Scotti, L.H., (1969). Perforated tray performance. Chemical Engineering Progress, Vol 3, 65, 52.

Lockett, M.J., Spiller, G.T., Porter, K.E., 1976. The effect of the operating regime on entrainment from sieve trays. Transactions of the Institution of Chemical Engineers, 54, 202 – 205.

Lockett, M.J., 1986. Distillation tray fundamentals, Cambridge University Press, Cambridge.

Koziol, A., Mackowiak, J., 1990. Liquid entrainment in tray columns with downcomers. Chemical Engineering Process, 27, 145 – 153.

Newitt, D.M., Dombrowski, N., Knelman, F.H., 1954. Liquid entrainment 1. The mechanism of drop formation from gas or vapour bubbles. Transactions of the Institution of Chemical Engineers, 32, 244.

Nielsen, R.D., Trek, M.R., York, J.L., 1965. Mechanism of entrainment formation in distillation columns. Proceeding of the Symposium on Two-Phase Flow, 21-23 June, University of Exeter, United Kingdom, Vol 1, p. F201 – F225.

Nutter, D.E., 1979. Weeping and entrainment studies for sieve and v-grid trays in an air-oil system. Institution of Chemical Engineers Symposium Series No. 56 , 3.2/47 - 3.2/62.

Pinczewski, W.V., Benke, N.D. and Fell, C.J.D., (1975) AIChE Journal, 21, 1210

Pan, K.L., Hung, C.Y., 2010. Droplet impact upon a wet surface with varied fluid and surface properties. Journal of Colloid and Interface Science, 352, 186-193.

Porter, K.E., Jenkins, J.D., 1979. The interrelationship between industrial practice and academic research in distillation and absorption. Institution of Chemical Engineers Symposium Series No. 56 , 5.1/1-5.1/47.

Stellenbosch University http://scholar.sun.ac.za

Puppich, P., Goedecke, R., 1987. Investigation of entrainment in tray columns. Chemical Engineering and Technology , 10, 224-230.

Sakata. M., Yanagi, T., 1979. Performance of a commercial scale 14% hole area sieve tray. Institution of Chemical Engineers Symposium Series No. 56 , 5.1/1-5.1/47.

Seader, J.D. and Henley, E.J., 1998. Separation Process Principles, John Wiley & Sons, Inc.

Syeda, S.R., Afacan, A., Chuang, K.T., 2007. A fundamental model for prediction of sieve tray efficiency. Chemical Engineering Research and Design. Vol 85, 269-277.

Thomas, W. J. and Ogboja, O., 1978. Hydraulic studies in sieve tray columns. Industrial and Engineering Chemistry Process Design and Development , 17 (4), 429-443.

Uys, E.C., 2010. Entrainment in a sieve tray column, Masters Thesis. Stellenbosch University, South Africa. Uys,

Uys, E.C., Schwarz, C.E., Burger, A.J., Knoetze, J.H., 2012a. New froth behaviour observations and comparison of experimental sieve tray entrainment data with existing correlations. Chemical Engineering Research and Design (accepted for publication).

Van Sinderen, A.H., Wijn, E.F., Zanting, R.W., 2003. Entrainment and maximum vapour flow rate of trays. Transactions of the Institution of Chemical Engineers, Vol 81, 94 – 107.

Zuiderweg, F.J., 1982. A view on the state of the art. Chemical Engineering Science, 37 (10), 1441-1464.

Stellenbosch University http://scholar.sun.ac.za

Paper 1

New froth behaviour observations and comparison of experimental sieve tray entrainment data with existing correlations

Ehbenezer C. Uys[a], Cara E. Schwarz[a], Andries J. Burger[a], Johannes H. Knoetze[a,1]

[a]Department of Process Engineering, University of Stellenbosch, Private Bag X1, Matieland 7602, South Africa

Status: Accepted DOI 10.1016/j.cherd.2012.05.008

Journal: Chemical Engineering Research and Design

Keywords: Entrainment, sieve tray column, physical properties.

[1]Corresponding author. Tel.: +27 21 8084488; fax: +27 21 8082059.

E-mail address: jhk@sun.ac.za (Johannes H. Knoetze)

Stellenbosch University http://scholar.sun.ac.za

1. Abstract

A thorough understanding of the hydrodynamics in tray columns is required to optimise column and tray design for specific operating capacities and conditions. Liquid transported by the rising gas to the tray above, defined as entrainment, is one way of measuring the tray column capacity limit. Entrainment correlations available in the literature have been developed with predominantly air/water data, because of the limited availability of non-air/water data. In this work an experimental setup was constructed to measure entrainment, tray pressure drop and weeping for various gas and liquid systems. The experimental entrainment data for three systems, namely air/water, air/ethylene glycol and air/silicone oil, is compared to existing correlations. The effect of liquid physical properties on entrainment under flow factors ranging from 1.6 $kg^{0.5}/(m^{0.5}.s)$, for a 415mm tray spacing to 4.0 $kg^{0.5}/(m^{0.5}.s)$ for a 615 mm tray spacing within a liquid flow range of 2.9 – 112 $m^3/(h.m)$ was observed. The experimental results showed a somewhat complex dependency of entrainment on liquid physical properties. At gas flow factors of 2.2 $kg^{0.5}/(m^{0.5}.s)$ for the 415 mm tray spacing, entrainment reached a maximum in the froth regime and then decreased with increasing liquid rates. Notably, the liquid viscosity – not included in previously developed correlations – significantly influences the entrainment behaviour. Existing entrainment correlations agree better with the air/water data than with the air/ethylene glycol or air/silicone oil data.

Stellenbosch University http://scholar.sun.ac.za

2. Introduction

Distillation, absorption and stripping are the most widely used separation processes in the chemical industry. These separation methods rely on the contact between a gas or vapour, and a liquid in order to achieve the required separation. Contact between phases is established on column internals, typically packing or trays. In this paper the focus is on sieve trays, which is the most common and simplest of all tray types.

Significant contributions have been made (e.g. Lockett, 1986, Hofhuis and Zuiderweg, 1979, Kister et al., 1981, Zuiderweg, 1982, Kister and Haas, 1988, Bennett et al. 1995 and Van Sinderen et al., 2003) to add to the understanding and knowledge of the entrainment in tray distillation columns. The capacity of a tray column is limited by the occurrence of significant entrainment (L'/G) or jet flooding (Kister and Haas, 1990). Entrainment generally has two definitions with relation to tray capacity and efficiency. When tray capacity is of importance, entrainment is expressed as the mass of liquid that reaches the tray above per mass of rising gas (L'/G). When tray efficiency is of importance entrainment is measured as a percentage of the liquid entering the tray (L'/L) that is transported to the tray above.

The tray pressure drop, tray efficiency, entrainment, weeping and flow regime depend on the tray and column geometry, liquid and vapour loads, and liquid and vapour physical properties. By understanding how these variables influence entrainment, improvements can be made to the column and tray designs. Improved tray designs could potentially lead to higher column throughputs by retrofitting existing columns, or by reducing column height and therefore capital costs for new designs. The measurement and interpretation of entrainment profiles will provide the designer with an improved understanding of hydrodynamics in tray columns. Previous researchers considered the influence of gas and liquid flow rates, column geometry, and gas and liquid physical properties on entrainment, liquid hold-up, and tray pressure drop. However, a large portion of related measured data consists of air/water (A/W) data and the effect of physical properties is based on a much smaller non-air/water (NA/W) database (Bennett et al., 1995). However, most columns do not operate with an A/W system.

Bennett et al. (1995) assume that liquid surface tension is negligible in the spray regime as shown in Figure 1 (a). Both Bennett et al. (1995) and Kister and Haas (1988) assume that the effect of surface tension is negligible in the froth regime. The correlation from Kister and Haas (1988) suggests that liquid density does not have a significant influence on entrainment in the froth regime as shown in Figure 1 (b). Correlations developed by both Kister and Haas (1988) and Bennett et al. (1995) suggest that entrainment is independent of liquid viscosity. These correlations are based on data obtained from a variety of experimental setups and from various institutions. Apart from the assumptions related to liquid physical properties, most of the data and correlations found in literature focus on the onset of entrainment (L'/G << 5%) and the prediction of the flooding velocity (Kister and Haas, 1990). The question is how do the operating conditions and physical properties influence entrainment (L'/G) when entrainment is more than 5%?

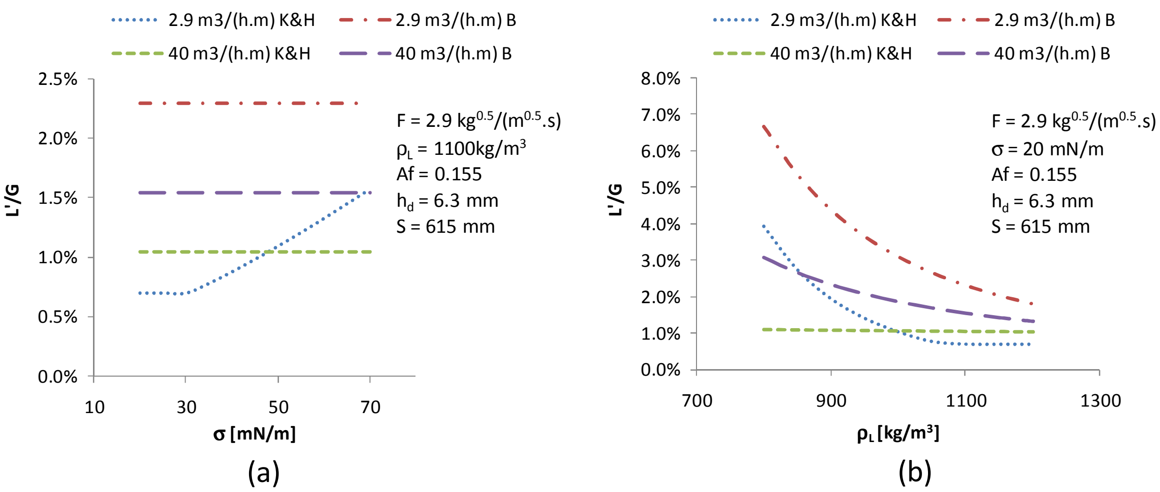

Figure 1. Predicted influence of liquid surface tension (a) and density (b) on entrainment for low, (Q_L = 2.9 m^3/(h.m) relating to spray regime conditions) and high liquid rate (Q_L = 40 m^3/(h.m) related to the froth regime) obtained using correlations from Kister and Haas (1988) (K&H) and Bennett et al. (1995) (B).

The objective is therefore to investigate whether the effect of surface tension and liquid viscosity on entrainment is negligible as assumed by others (Kister and Haas, 1988 and Bennett et al. 1995). To achieve this objective an experimental setup was designed and constructed to measure entrainment and tray pressure drop for a large range of gas and liquid physical properties, gas and liquid flow rates and tray spacings. It is important to have visual access to the froth in the column to observe froth development and behaviour under different conditions. These observations will aid to improve the understanding of froth hydrodynamics. To test if liquid surface tension and viscosity have an influence on entrainment different liquids were used in the experiments. The results were compared

Stellenbosch University http://scholar.sun.ac.za

with entrainment correlations (Kister and Haas, 1988 and Bennett et al., 1995) to test if the assumption to neglect some of the physical properties is correct. It is important to note that the objective of this study is not focused on the effect of gas and liquid physical properties on mass transfer. Only pure liquids were used to ensure no change in physical properties throughout the column.

3. Experimental

Experimental setup

Most of the experimental setups described in the literature are of rectangular or square shape with the exception of the larger diameter, 0.8m (Thomas and Ogboja, 1978) and 1.2m (Yanagi and Sakata, 1979), columns which were cylindrical. The experimental setup used in this work consists of a rectangular shaped sieve tray column, as shown in Figure 2. This geometry was chosen to reduce entrance and wall effects found at the inlet and outlet weirs of round columns as shown by Porter and Jenkins (1979). Another reason for this specific geometry is to represent a section of a multi-pass tray column with a tray flow path length of 475mm (measured from the start of the perforations at the downcomer outlet to the outlet weir).

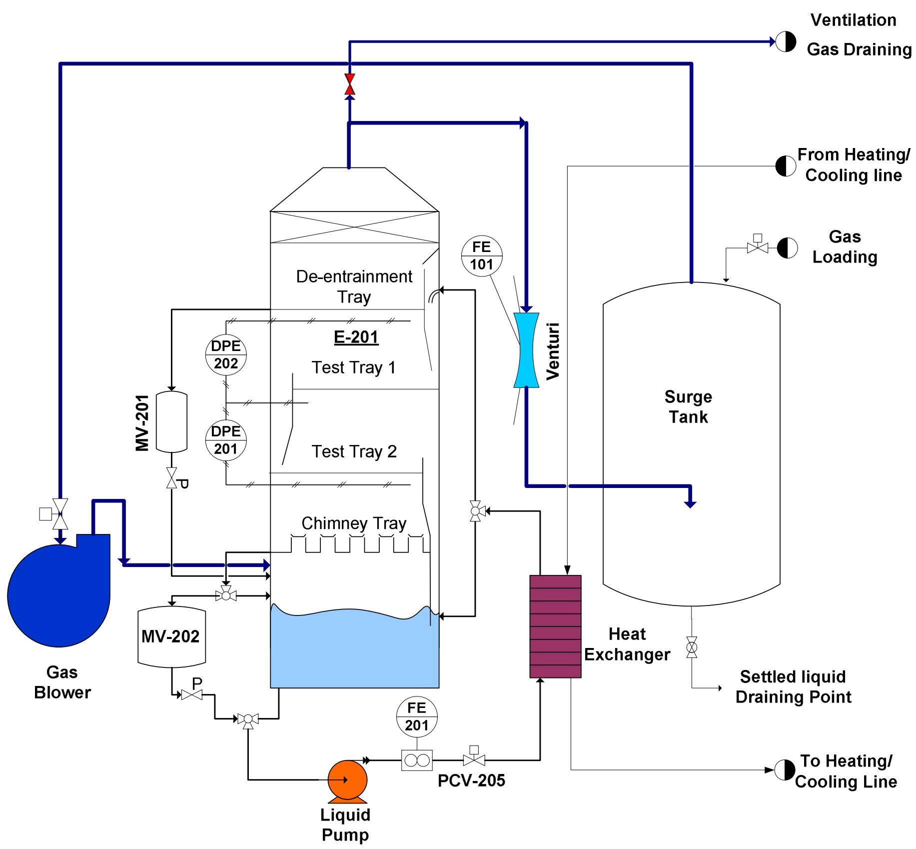

Figure 2. Process flow diagram of experimental setup.

The gas enters the column through a chimney distribution tray followed by two test trays. Two sieve test trays, with geometry as defined in Table 1, are used to represent column flow behaviour. A de-entrainment tray is positioned above test tray 1 (the top test tray) and is followed by a mist eliminator pad fitted at the top of the column. The de-entrainment tray is designed so that the liquid head on the tray does not influence the measurement accuracy under normal testing conditions. As soon as the de-entrainment section started to flood the efficiency of the de-entrainment tray decreased as liquid was carried over to the surge tank. No weeping was observed from the de-entrainment tray under flooding conditions. The de-entrainment tray was always stable and drained quickly during all the experiments. Polycarbonate view-ports are located on the downcomer side as well as on the front of the column to allow visual confirmation of a positive downcomer seal as well as observation of the flow path. The liquid that weeps through test tray 2 (the bottom test tray) is collected on the chimney tray and transferred to either the sump or the weeping hold-up tank (MV-202) through an isolated pipe-line. A closed downcomer is used to isolate the liquid transferred down to the sump from the bottom tray. The entrained liquid is separated from the gas in the de-entrainment section and transferred to the sump, or to the entrainment hold-up tank (MV-201) where the entrained liquid is measured as entrained liquid mass over time. The surge tank is used to settle any liquid droplets that manage to escape the entrainment collection section (also used to verify the efficiency of the entrainment collection section) and to reduce system oscillations.

Table 1. Tray and column geometry

Geometry		Unit
d_H	6.3	mm
No Holes	414	-
P	14.5	mm
A_h	0.0129	m^2
A_p	0.0830	m^2
A_f (A_h / A_p)	0.156	-
A_n	0.095	m^2
A_d	0.0158	m^2
A_c	0.1111	m^2
h_w	51	mm
S	415, 615	mm
FPL	475	mm

High accuracy (maximum specified error of 0.075% of the measurement range) Endress + Hauser digital differential pressure transmitters monitor the liquid levels and PT-100 temperature probes monitor the liquid temperatures in the two hold-up vessels. The tray pressure drop is measured using the same high accuracy digital differential pressure transmitters scaled to a range of 0 – 4 kPa. A venturi flow meter (verified by a Pitot tube) measures the gas flow rate while the liquid flow rate is measured using two positive displacement flow meters (one for low liquid rates, 0.5 – 2 m^3/h and another for high liquid rates, 2 – 20 m^3/h) in series with a venturi, which was used for verification purposes.

Gas is circulated through the column with a centrifugal blower. The gas flow rate is adjusted with a radial vane control valve placed at the blower inlet and by controlling the motor

Stellenbosch University http://scholar.sun.ac.za

rotational speed with an inverter. During sampling the radial control valve and inverter are kept at fixed settings. The liquid is circulated by means of a centrifugal pump and the flow rate is controlled by an inverter and control valve combination. The column is operated at 25 °C by controlling the liquid temperature using a plate heat exchanger. To ensure a positive downcomer seal (truncated downcomers were used) over a large range of liquid flow rates the downcomer escape area (apron area) can be varied. Changing the downcomer escape area affects the liquid escape velocity and a sensitivity analysis was therefore conducted to test the influence of downcomer escape area on entrainment.

To change the downcomer escape area the downcomers were modified with stainless steel slides that can extend the downcomer apron using a rack and pinion system. This enabled the downcomer escape area to be adjusted without opening the column. The liquid velocity was calculated by dividing the liquid rate (Q_L) with the downcomer escape area. For the sensitivity analysis two liquid (11.5 and 68.5 $m^3/(h.m)$) and gas flow factors (3.5 and 2.8 $kg^{0.5}/(m^{0.5}.s)$ were chosen respectively. The downcomer escape area was varied randomly and entrainment measured as shown in Figure 3. For the 11 $m^3/(h.m)$ test (Figure 3 (a)) entrainment stayed fairly constant for liquid velocities ranging from 0.2 to 0.6 m/s. Less entrainment was measured for a liquid velocity of 1.1 m/s and high entrainment was measured for a liquid velocity of 3.2 m/s. A similar observation was made for the 68.5 $m^3/(h.m)$ test. As the liquid velocity decreased below 0.5 m/s entrainment decreased as there was not enough liquid backed up in the downcomer to create a positive downcomer seal. As the liquid velocity increased past 0.8 m/s a decrease in entrainment was observed up to 1.4 m/s. High entrainment was observed at 1.7 m/s. The analysis showed that entrainment is reasonably stable for calculated liquid velocities between 0.3 and 0.6 m/s as prescribed by the tray manufacturer. This velocity range also ensured that sufficient backup of liquid is achieved in the downcomer without flooding at high liquid rates. Therefore to prevent liquid escape velocity from influencing the result, a dynamically sealed downcomer had to be used. At low weir loads (Q_L = 2.9 $m^3/(h.m)$) the downcomer apron clearance was set at 5mm to ensure a sealed downcomer. If this had to be the static opening, the liquid exit velocity would have been 4.4m/s for a weir load of 80 $m^3/(h.m)$. Such high velocities have a significant influence on entrainment as shown in Figure 3.

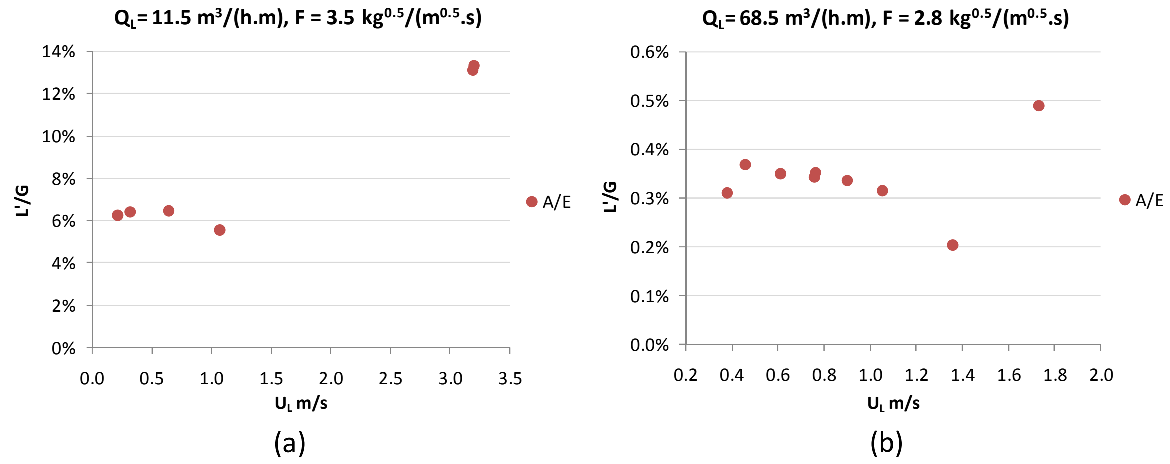

Figure 3. Air/ethylene glycol downcomer sensitivity analysis for a) a liquid rate of 11.5 m^3/(h.m) and gas velocity of 3.5 kg$^{0.5}$/(m$^{0.5}$.s) and b) a liquid rate of 68.5 m^3/(h.m) and gas velocity of 2.8 kg$^{0.5}$/(m$^{0.5}$.s). Tray spacing is 615 mm.

Experimental procedure

Gas and liquid was circulated through the column until the temperature stabilized at 25°C ± 1°C. The column was then flooded to ensure proper wetting of all the column internals, whereafter the flow rates were adjusted to test conditions. Once steady state was reached, entrainment or weeping was measured using a 4.5 litre and a 50 litre hold-up vessel (MV-201, MV-202) that measures liquid mass over time. Steady state was defined as when the column temperature, tray pressure drop and gas and liquid flow rates were stable for a minimum of 5 minutes. Samples were collected over a period of approximately 3 minutes or a minimum of 50 grams of liquid for low (< 1%) entrainment rates. To determine repeatability, sampling was repeated four times for each liquid rate. More details regarding calibration, verification and accuracy of the equipment can be found elsewhere (Uys, 2010, Uys et al., 2010). Figure 4 gives an indication of sampling repeatability. All the measured entrainment for this A/W system was within 2.5% of the average value of these measurements taken at each liquid rate.

Stellenbosch University http://scholar.sun.ac.za

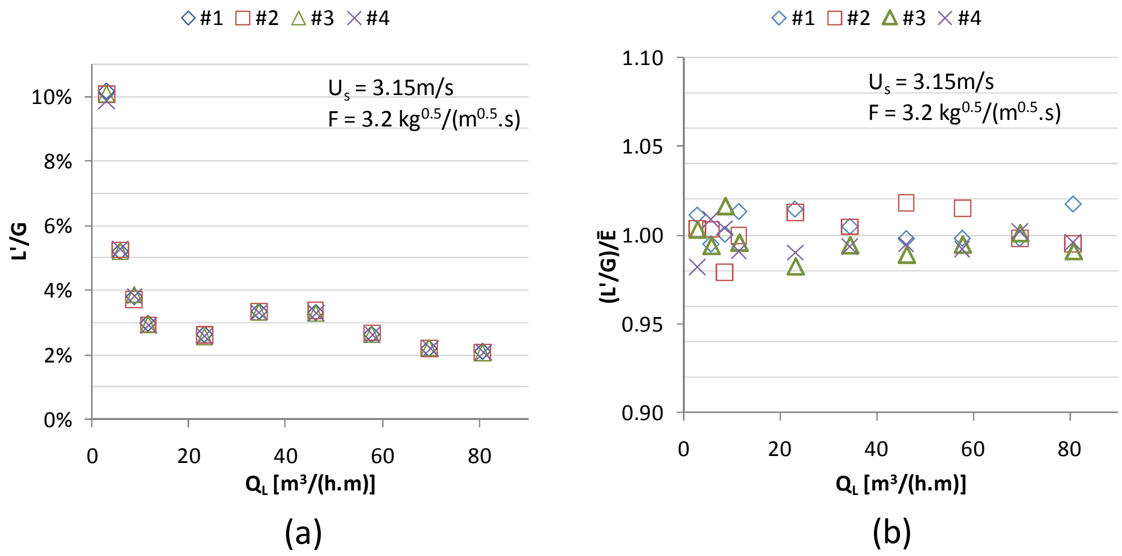

Figure 4. (a) Repeatability of air/water entrainment measurements at 615mm tray spacing. (b) Normalised entrainment results to quantify repeatability.

Tests were conducted for liquid rates ranging from 2.9 to 112 m^3/(h.m) for two tray spacings (415 and 615 mm) and four gas rates per liquid rate and tray spacing. Most of the available entrainment data is for liquid loads less than 50 m^3/(h.m). The liquid range was therefore chosen to be as large as possible to enable observation of the froth behaviour at higher liquid loads. Gas rates were chosen based on the minimum and maximum entrainment that the de-entrainment tray can accommodate. The maximum entrainment (L'/G) is limited by flooding of the de-entrainment tray or when liquid is carried over to the surge tank. The minimum entrainment is defined as when very little entrained liquid is visually observed on the de-entrainment tray. Entrainment correlations (Kister and Haas, 1988 and Bennett et al., 1995) include the dependence of liquid surface tension as well as gas-and-liquid density on entrainment based on limited NA/W system data. Therefore, three different liquids (water, ethylene glycol and silicone oil) were used in this work. These liquids differed in density, surface tension and viscosity, thereby allowing an evaluation of the influence of each of these properties (including viscosity) on entrainment. Note that liquid viscosity was not previously thought to have an effect (Kister and Haas, 1988 and Bennett et al. 1995).

Table 2 contains a summary of the gas and liquid physical properties as well as the gas and liquid flow rates used during the experiments.

Table 2. Gas and liquid physical properties and flow rate ranges used during experiments at 25°C and 99-100 kPa(abs).

Fluid	ρ [kg/m^3]	σ [mN/m]	μ [mPa.s]	F [kg$^{0.5}$/(m$^{0.5}$.s)]	Q_L [m^3/(h.m)]
Air	1.16 - 1.18	-	-	1.6 – 4.0	-
Water	997	60	0.9	-	2.9 - 112
Ethylene Glycol	1102	37	14.6	-	2.9 - 92
Silicone Oil	955	20	48.8	-	2.9 – 78.6

4. Results and discussion

Validation of experimental results

One of the methods to validate experimental results is to compare it with published data. To make a comparison between the data sets, the experimental conditions and setup must be similar. For the case at hand there was no published data which was obtained from experimental setups that used the same geometry and gas-and-liquid flow rates as this study. The experimental conditions and system (air/water) used by Nutter (1972) are similar to this study. However, the tray geometry varies the most. The hole diameters (12.7 mm) are larger, fractional hole area (0.079) is much lower, column diameter (1.2 m) is larger and the tray has a longer flow path length (806 mm). These geometrical differences are compared with the experimental setup in Table 3. The data of Nutter (1972) is compared with the experimental data in Figure 5 (a).

Table 3. Differences in tray geometry and flow ranges between the system of Nutter (1972) and of this work.

Data	Q_L [m^3/(h.m)]	F [m/s.(kg/m^3)$^{0.5}$]	A_f	d_H [mm]	S [mm]
Nutter (1972)	13.1	1.4 - 3.1	0.079	12.7	610
Exp Data	11.5	2.5 - 3.4	0.156	6.3	615

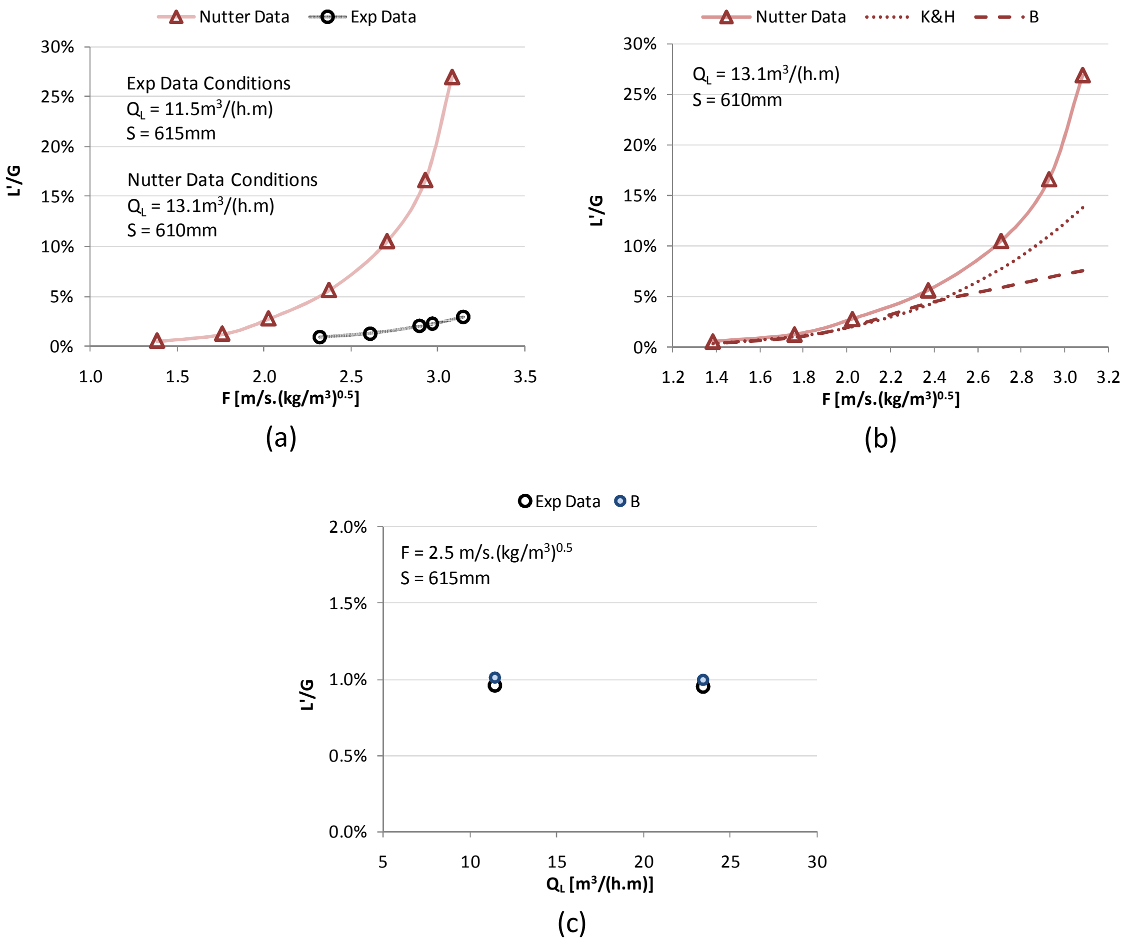

Figure 5. Comparison between a) the data of Nutter (1972) and experimental data b) the data of Nutter (1972) and predictions from the Kister and Haas (1988) and Bennett et al. (1995) correlations c) the experimental data and predictions from the Bennett et al. (1995) correlation.

In Figure 5 (a) the entrainment measured by Nutter (1972) is higher than the experimental data. This is to be expected due to the differences in tray geometry. Kister and Haas (1988) showed graphically that a reduction in fractional hole area and an increase in hole diameter will increase entrainment. Their findings correspond with that of Bennett et al. (1995). The exact amount with which entrainment will increase with decreasing fractional hole area and hole diameter depend on the gas and liquid flow rates. In Figure 5 (b) the correlations from Kister and Haas (1988) and Bennett et al. (1995) are compared with the data from Nutter (1972). The correlation from Bennett et al. (1995) performed better than that of Kister and Haas (1988) up to a flow factor of 2.5 $m/s(kg/m^3)^{0.5}$ whereafter it started to deviate. This deviation occurs due to the fact that the correlation of Bennett et al. (1995) is extrapolated beyond their recommended flow factor range ($\leq$ 2.5 $m/s(kg/m^3)^{0.5}$). Due to the good fit of

Stellenbosch University http://scholar.sun.ac.za

the Bennett et al. (1995) correlation to the Nutter (1972) data, their correlation is used to validate the experimental data at a flow factor of 2.5 m/s.(kg/m^3)$^{0.5}$. Nutter published data for only two liquid rates, 13.1 and 26.2 m^3/(h.m).

Figure 5 (c) was constructed to see how the experimental data of this work compare to the predictions of Bennet et al. (1995) at conditions similar to that of the Nutter (1972) data. The correlation of Bennett et al. (1995) predicts a similar result as that obtained by the experimental data. Based on these findings the authors are confident that the results are reliable.

Entrainment results related to capacity (L'/G)

Figure 6 show the entrainment (L'/G) results for the A/W, A/E and A/S systems for constant gas flow rates over a range of liquid rates. The first observation is that, irrespective of the liquid rate, an increase in gas velocity will result in an increase in entrainment. This phenomenon has also been observed by others (e.g. Lockett, 1986, Hofhuis and Zuiderweg, 1979, Kister et al., 1981, Zuiderweg, 1982, Kister and Haas, 1988, and Bennett et al. 1995). For liquid rates lower than approximately 9 m^3/(h.m), high entrainment was measured. This is typical of the spray regime which occurs at these low liquid flow rate conditions. As the liquid rate is increased above 12 m^3/(h.m) entrainment increases which, Kister and Haas (1988) suggests is due to the increase in liquid hold-up that occurs with increasing liquid flow rate. As the liquid rate exceeds 20 – 40 m^3/(h.m) for a 615mm tray spacing and 60 – 90 m^3/(h.m) for a 415 mm tray spacing, entrainment will decrease before it increases again at higher liquid rates. This local maxima and minima in the froth regime is a new observation which is discussed in detail in section 3.4.

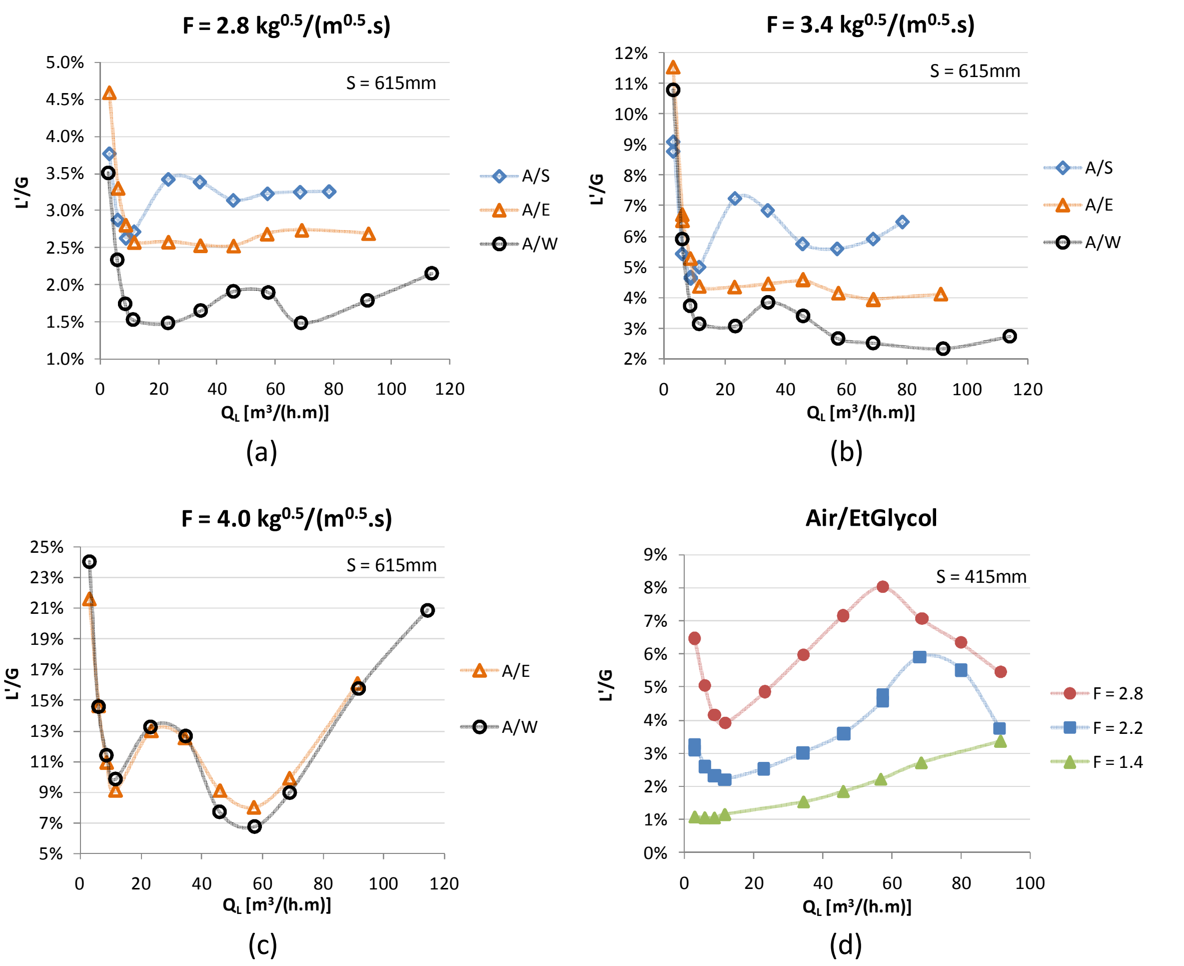

Figure 6. Influence of liquid flow rate on entrainment (L'/G) at 615mm tray spacing for A/S, A/E and A/W systems at (a) F = 2.8 kg$^{0.5}$/(m$^{0.5}$.s) (b) F = 3.4 kg$^{0.5}$/(m$^{0.5}$.s) (c) F = 4.0 kg$^{0.5}$/(m$^{0.5}$.s) only A/E and A/W since A/S flooded column (d) Influence of gas and liquid flow rate on A/E glycol at 415mm tray spacing.

When the entrainment results from the different liquids are compared, an observation related to the liquid physical properties is made. In the low liquid flow rate range (< 9 m^3/(h.m)) for low gas flow factors (F = 2.8 – 3.4 kg$^{0.5}$/(m$^{0.5}$.s)) ethylene glycol will entrain the most with water entraining the least. At the high gas flow factor (F = 4.0 kg$^{0.5}$/(m$^{0.5}$.s)) water entrained slightly more than ethylene glycol in the low liquid range. As the liquid rate is increased to above 12 m^3/(h.m) silicone oil will entrain the most with water still entraining the least for the lower gas flow factor (F = 2.8 – 3.4 kg$^{0.5}$/(m$^{0.5}$.s)). Approximately the same percentage entrainment is observed between water and ethylene glycol in high flow factor (F = 4.0 kg$^{0.5}$/(m$^{0.5}$.s)) conditions. The results show a very complex relationship between the liquid physical properties. The droplet size, mass, ejection velocity and froth height plays an integral role in the entrainment measured. The influence of

Stellenbosch University http://scholar.sun.ac.za

viscosity and surface tension can not be neglected as they contribute to the droplet size and the droplet ejection velocity from the froth into the vapour space.

These suggestions are consistent with recent work by Decent et al. (2009). They investigated the behaviour of a rotating liquid jet with varying liquid viscosity. Of interest to them was the size of the droplets formed as the liquid jet breaks-up, as well as the distance from the onset of the jet to the development of the droplet, called the break-up length. It was found that the droplet break-up length on a liquid jet is influenced by liquid viscosity. The break-up length and velocity of the jet have a non-monotonic relationship with changing viscosity. Decent et al. (2009) also found that droplet diameter has a non-monotonic dependence on viscosity. Fakhari and Rahimian (2011) found that drop viscosity is the principal factor in the mechanism for droplet disintegration. Pan and Hung (2010) found that upon impact with a wet surface, droplets of liquids with high viscosities are more stable and less susceptible to breaking-up than low viscosity liquids. However, reducing surface tension had the opposite effect.

Droplet diameter and liquid break-up lengths were not measured in this work. It is therefore difficult to make a quantitative comparison between the different liquids and more work is required to understand and predict the influence of surface tension and liquid viscosity on entrainment.

Entrainment results related to efficiency (L’/L)

When the results of Figure 6 are expressed as mass of liquid entrained per mass of liquid entering the tray (L’/L) in Figure 7, a completely different trend is noted than in Figure 6. In these cases the percentage liquid entrained will exponentially decrease with an increase in liquid rate. Thus, although entrainment (related to L’/G) is high at high liquid rates, the efficiency (related to L’/L) will tend to improve for increasing liquid rates. At low liquid rates (< 5.8 $m^3/(h.m)$) entrainment (L’/G) is high and the tray efficiency low. It is therefore undesirable to operate the column at these conditions.

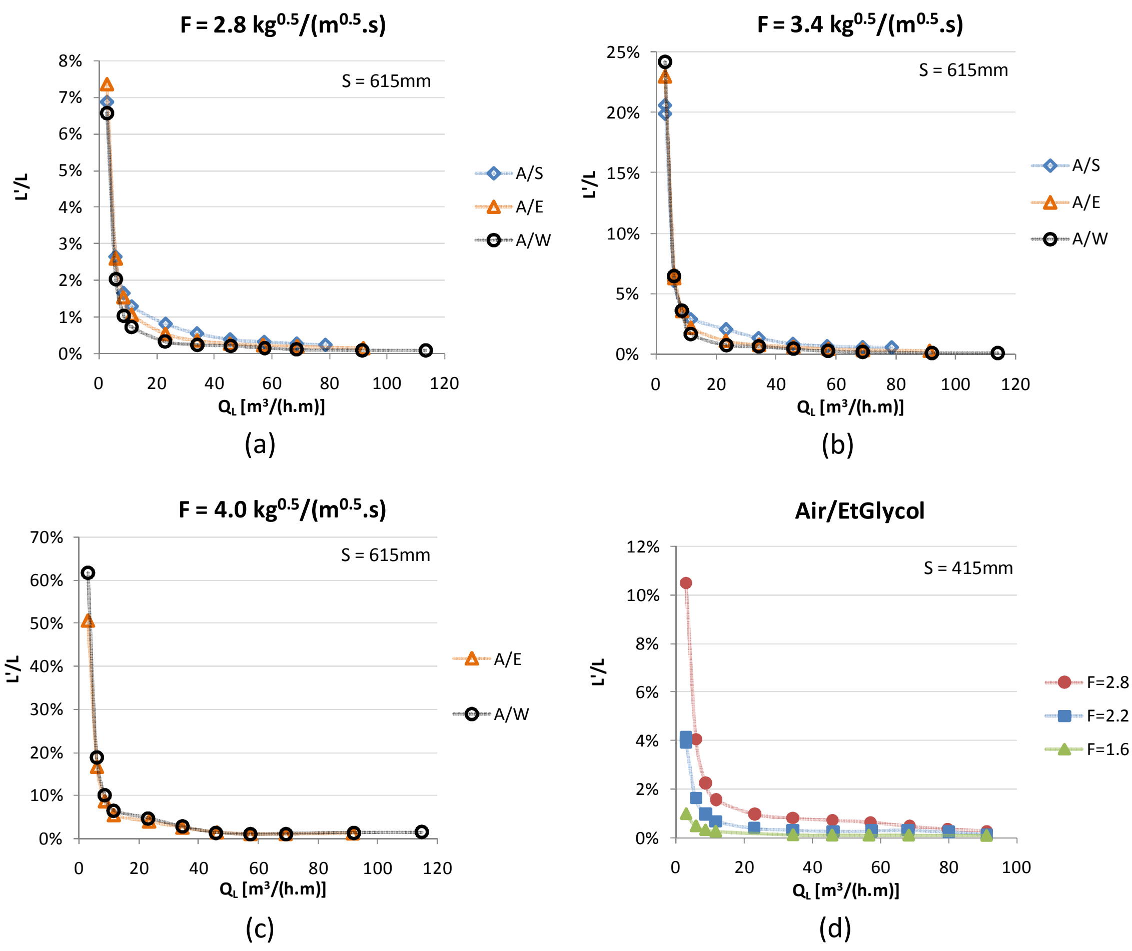

Figure 7. Influence of liquid flow rate on entrainment (L'/L) at 615mm tray spacing for A/S, A/E and A/W systems at (a) F = 2.8 kg$^{0.5}$/(m$^{0.5}$.s) (b) F = 3.4 kg$^{0.5}$/(m$^{0.5}$.s) (c) F = 4.0 kg$^{0.5}$/(m$^{0.5}$.s) only A/E and A/W since A/S flooded column (d) Influence of gas and liquid flow rate on A/E glycol at 415mm tray spacing.

New froth behaviour observation

Visual observation assisted by video and photos (shutter speed 1/500 s, aperture f3.8) showed non-monotonic froth shapes under medium to high gas flow factors (2.5 – 4.0 kg$^{0.5}$/(m$^{0.5}$.s)) and liquid rates (depending on the liquid and tray spacing) around 20 – 40 m^3/(h.m) for a 615mm tray spacing and around 60 – 90 m^3/(h.m) for a 415 mm tray spacing. This parabolic shape has also been observed by Nutter (1979), as well as Puppich and Goedecke (1987). They did not, however, relate this parabolic shape to entrainment (L'/G). In the present work maximum entrainment is measured in the froth regime when the froth has this parabolic shape. Figure 6 show that the maxima shifted to lower liquid rates as the

Stellenbosch University http://scholar.sun.ac.za

gas velocity was increased and is more prominent at lower tray spacings, as shown in Figure 6 (d). This behaviour will be explained further, while referring to Figure 8.

Figure 8 (a) is a schematic representation of the froth height with increasing liquid rates (with liquid rates increasing from profile 1 to 5) under constant gas flow factor. This phenomenon occurs in the froth regime and the explanation thereof is based on visual observations made during experiments, as shown in Figure 9. For the sake of this explanation it is assumed that the liquid exits the downcomer as a clear liquid. As the liquid enters the tray, it makes contact with gas passing through the perforations. This causes the clear liquid to expand into froth as it is penetrated by the gas by means of channels and voids that erupt at the surface to create ejecting droplets (Bennett et al., 1995). Depending on the liquid and gas rate, the froth requires a certain distance along the tray to expand to a maximum height. As the froth reaches the maximum expanded height, the voids and channels in the froth are at their largest, reducing the gas velocity that promotes froth expansion and the froth will contract or collapse as gravitational forces surpass the momentum and drag forces.

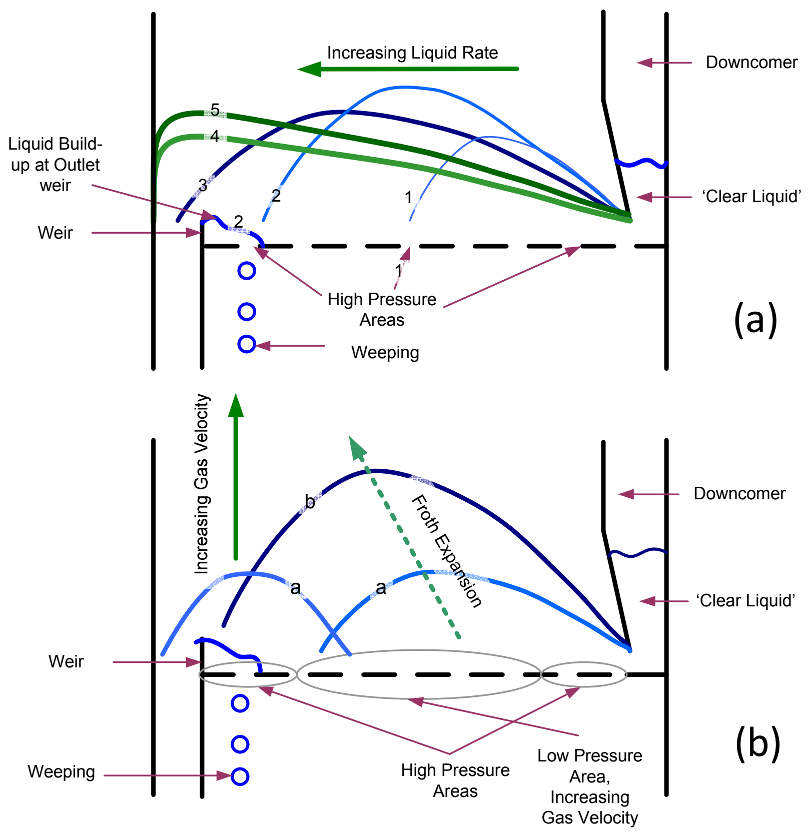

Figure 8. Graphical representation of the change in froth height with changes in (a) liquid rate, increasing from 1 to 5, under constant gas velocity and (b) gas velocity under constant liquid rate with 'a' representing low gas flow factor and 'b' high gas flow factor.

For liquid rates 1 and 2 in Figure 8 (a) the froth will go through the developing process once again after froth contraction. However, liquid rate 2 will cause a high pressure area at the exit weir caused by the collapsing froth, which reduces the available area for gas passage through the froth. The high pressure area promotes weeping at the outlet weir, while forcing the gas to move through the low pressure area, which is smaller than the tray active area, as shown in Figure 8 (b). Thus, the gas velocity that passes through the froth is increased, which ultimately increases the froth height and therefore entrainment. As the liquid rate is increased to 3 in Figure 8 (a), the high pressure area is moved to the downcomer and the area for gas passage is increased, which reduces the froth height and entrainment. A further increase in liquid rate to 4 will prevent the froth from reaching the maximum expansion point as the horizontal momentum of the liquid is too large. Based on visual observations, gas will predominantly jet through the liquid under these conditions. As the liquid rate is increased to 5 and above, the froth profile is lifted, caused by a

Stellenbosch University http://scholar.sun.ac.za

combination of the increased amount of liquid passing across the tray and downcomer choke flood. Downcomer choke flooding becomes more prominent at high liquid rates. For liquid rates just lower than 2, shown as “a” in Figure 8 (b), an increase in gas rate will expand the froth so that it eventually contracts or collapses at the exit weir as shown by profile “b”, consequently increasing froth height and entrainment. Therefore, as the gas rate is increased for each system from Figure 6 (a) to (b), (c) and (d) the maxima in entrainment is shifted to lower liquid flow rates.

The effect of the high pressure area at the outlet weir that promotes weeping is shown in Figure 10 for the air/silicone oil system. From Figure 10 weeping in the spray regime increases as the liquid rate is increased to the transition from spray to froth. This is caused by the increase in liquid hold-up. As the liquid rate is further increased past 23 $m^3/(h.m)$ in Figure 10 (a) and past 12 $m^3/(h.m)$ in Figure 10 (b) weeping continues to increase. As soon as the high pressure area shifts from in front of the weir to the downcomer, weeping and entrainment decreases. Weeping will continue to decrease until the amount of liquid passing over the tray, or downcomer choke flood, causes the liquid hold-up to increase which will cause weeping to increase.

Figure 9. Images showing influence of liquid rate on froth profile under a constant gas flow factor (F = 3.5 kg$^{0.5}$/(m$^{0.5}$.s)) and tray spacing (S=615mm) for the A/S system. The downcomer is situated on the right of the tray, with liquid flowing from right to left. (a) Q_L = 11.4 m^3/(h.m), (b) Q_L = 22.9 m^3/(h.m), (c) Q_L = 34.3 m^3/(h.m), (d) Q_L = 45.7 m^3/(h.m), (e) Q_L = 57.1 m^3/(h.m), (f) Q_L = 68.6 m^3/(h.m).

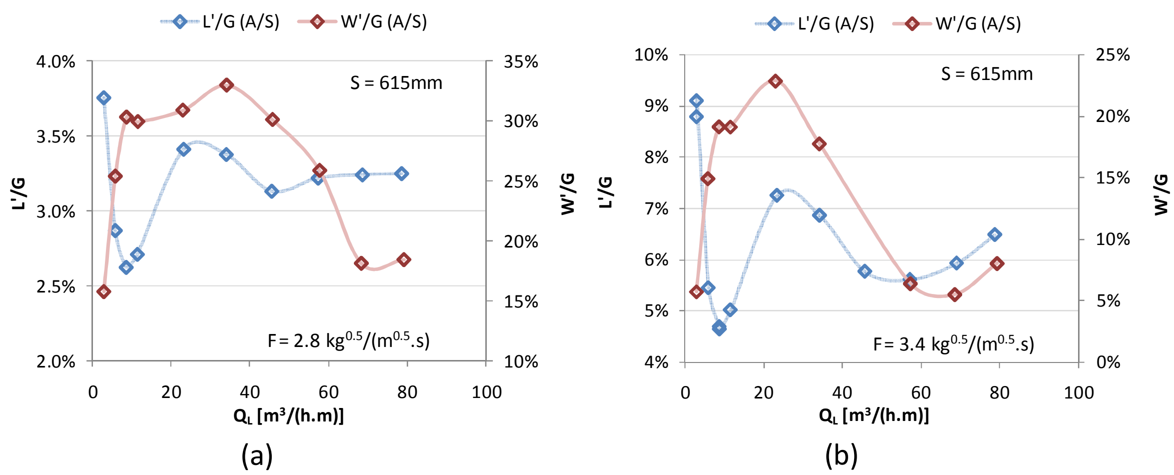

Figure 10. Entrainment and weeping results for the air/silicone oil system for a) F = 2.8 $kg^{0.5}/(m^{0.5}s)$ and b) F = 3.4 $kg^{0.5}/(m^{0.5}s)$. Tray spacing was 615 mm.

From this understanding of froth behaviour, it is clear that tray flow path length, that to date has not received much attention in the literature, will significantly influence entrainment. Tray flow path length is not varied in this work and the influence on entrainment can not be determined quantitatively.

Comparison between experimental data and correlations

An extensive literature study by Uys (2010) showed that the entrainment prediction correlations from Kister and Haas (1988) and Bennett et al. (1995), as given in Table 4, has the largest range of application. The work from these authors will therefore be compared with the experimental results.

In Figure 11 (a) and (b) entrainment results for the air water system under constant gas flow factor of 2.8 $kg^{0.5}/(m^{0.5}.s)$ is compared with the correlations of Kister and Haas (1988) and Bennett et al. (1995) over a range of liquid rates. Table 5 describes the range of application for the correlations provided by Kister and Haas (1988) and Bennett et al. (1995). Both authors suggest that their correlations are most suitable for the A/W system.

Stellenbosch University http://scholar.sun.ac.za

Table 4. Entrainment correlations developed by Kister and Haas (1988) and Bennett et al. (1995).

Author	Entrainment Correlations		L'/G
Kister & Haas (1988)	$\left(\frac{L'}{G}\right)_{froth} = 111\left(\frac{U_S}{s-h_F}\right)^2 d_H^{0.5}(1+\zeta)$	**(1)**	0.001 - 0.7
	$\left(\frac{L'}{G}\right)_{spray} = 4.742^{(10/\sqrt{\sigma})^{1.64}} X^{(10/\sqrt{\sigma})}$	**(2)**	
	$X = 872\left(\frac{u_b h_{L,ct}}{\sqrt{d_H s}}\right)^4 \left(\frac{\rho_g}{Q_L \rho_l}\right)\left(\frac{\rho_l - \rho_g}{\sigma}\right)^{0.25}$	**(3)**	
	$h_{L,ct} = \frac{\left(\frac{0.4974 A_f^{-0.791} d_H^{0.833}}{1+0.013 Q_L^{-0.59} A_f^{-1.79}}\right)}{1+0.00262 h_w}\left(\frac{996}{\rho_l}\right)^{0.5(1-0.00091 d_H / A_f)}$	**(4)**	
Bennet *et al.* (1995) (Air/Water)	$\left(\frac{L'}{G}\right)_{spray} = 0.0050\left(\frac{K_s^2}{g\phi_e S}\right)^{1.26}\left[\frac{gH_L}{K_s^2} + \frac{9\sqrt{3}}{2A_f}\left(1+4.77\left\{\frac{D_H}{H_L}\right\}^{3.29}\right)\right]^{1.26} \varepsilon^{\beta}\left(\frac{\rho_L}{\rho_g}\right)^{0.5}$	**(5)**	0.001 - 0.6
	$\left(\frac{L'}{G}\right)_{froth} = 0.00164\left(\frac{K_s^2}{g\phi_e S}\right)^{1.86}\left[\frac{gH_L}{K_s^2} + \frac{9\sqrt{3}}{2A_f}\left(1+6.9\left\{\frac{D_H}{H_L}\right\}^{1.85}\right)\right]^{1.86}\left(\frac{\rho_L}{\rho_g}\right)^{0.5}$	**(6)**	
	$K_s = u_s\sqrt{\frac{\rho_g}{\rho_l}}$	**(7)**	
	$H_L = \phi_e H_{Fe}$	**(8)**	
	$H_{Fe} = H_w + C\left(\frac{Q_L}{3600\phi_e}\right)^{2/3}$	**(9)**	
	$\phi_e = \exp[-12.55 K_s^{0.91}]$	**(10)**	
	$\varepsilon = \frac{H_L}{H_F}$	**(11)**	
	$\beta = 0.5\left(1-\tanh\left[1.3\ln\left(\frac{H_L}{D_H}\right)-0.15\right]\right)$	**(12)**	

Table 5. Recommended range of correlation application by Kister and Haas (1988) and Bennett et al. (1995).

Author	U_s [m/s]	Q_L [m^3/(h.m)]	S [m]	A_F	d_H [mm]
Kister and Haas, 1988	0.3 – 3.5	2-130	0.1-1	0.04 – 0.2	1.5-25
Bennett et al., 1995	0.4 - 2.3	4.2-134	0.15-0.91	0.06-0.124	1.6 – 25.4

Figure 11 (a), (c) and (e) represents the spray regime while Figure 11 (b), (d) and (f) focus on the froth regime. The criteria for regime selection was made based on the minimum entrainment region that Porter and Jenkins (1979) have used to distinguish between the two regimes. This method is not necessarily the most accurate, but for the sake of comparing the data and to improve the resolution of the data in the graphs under low liquid rates, this criterion was used. The deviation between the correlations and the data is shown in Table 6. The deviation is calculated as %Dev = ($L'/G_{predicted}$ – $L'/G_{measured}$)/ $L'/G_{measured}$ x 100.

Stellenbosch University http://scholar.sun.ac.za

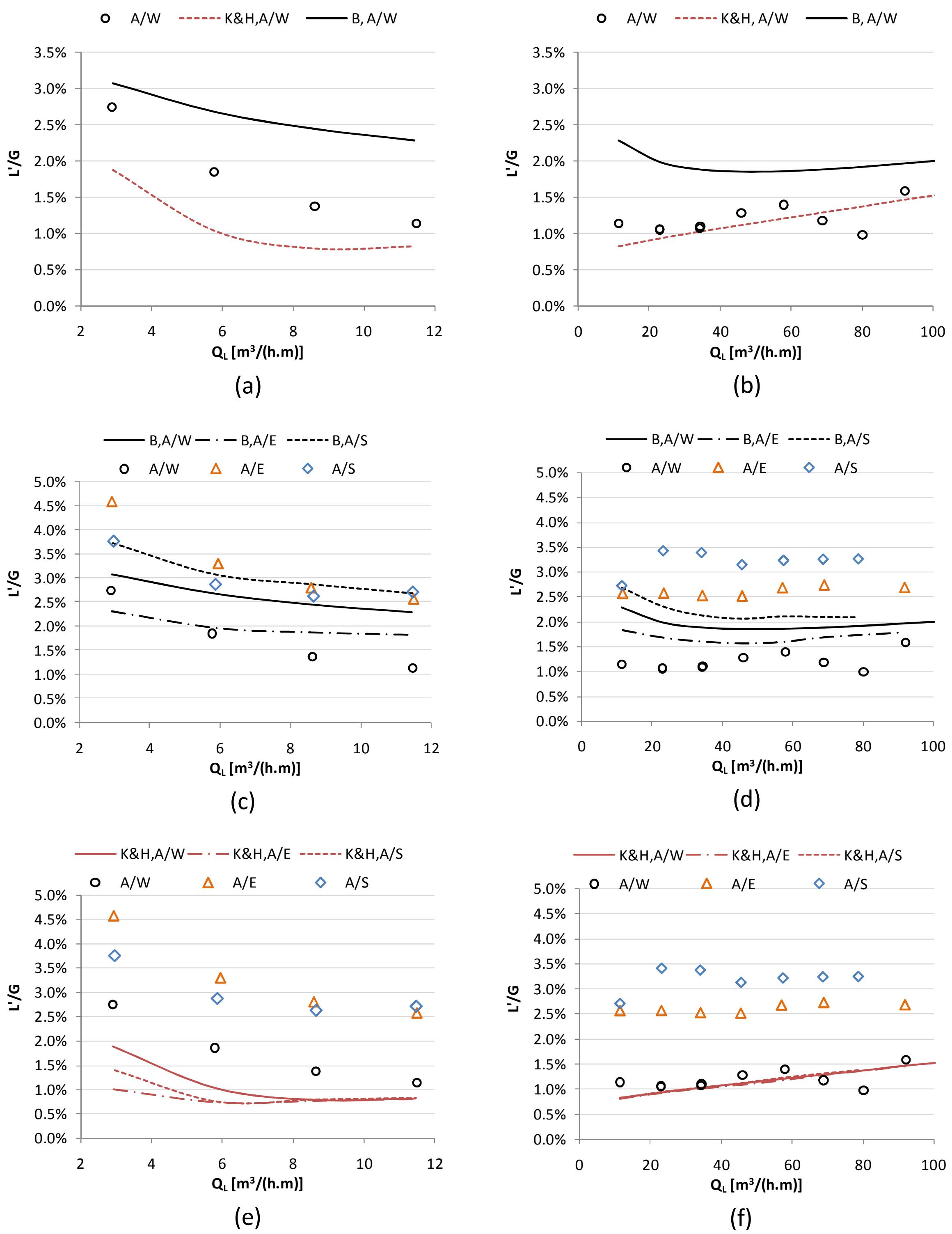

Figure 11. Comparing correlations from Kister and Haas [K&H] (1988) and Bennett et al. [B] (1995) with A/W entrainment data in the spray (a) and froth (b) regimes; Bennett et al. correlations in the spray (c) and froth (d) regimes with A/W, A/E and A/S; Kister and Haas correlations in the spray (e) and froth (f) regimes with A/W, A/E and A/S. Tray spacing = 615mm, F = 2.8 kg$^{0.5}$/(m$^{0.5}$.s) in all cases

Stellenbosch University http://scholar.sun.ac.za

Table 6. Deviations in predictions made by Kister and Haas (1988) and Bennett et al. (1995) from the experimental data.

Air/Water			Air/Silicone Oil			Air/Ethylene Glycol		
Q_L [m^3/(h.m)]	K&H (%Dev)	B (%Dev)	Q_L [m^3/(h.m)]	K&H (%Dev)	B (%Dev)	Q_L [m^3/(h.m)]	K&H (%Dev)	B (%Dev)
2.9	-31%	13%	3.0	-63%	-1%	2.9	-78%	-50%
5.8	-43%	49%	5.9	-74%	7%	5.9	-78%	-40%
8.7	-42%	78%	8.7	-70%	9%	8.6	-72%	-33%
11.4	-25%	108%	11.5	-69%	-1%	11.5	-68%	-29%
23.1	-9%	93%	23.2	-72%	-33%	23.2	-64%	-35%
34.4	-2%	80%	34.1	-69%	-37%	34.2	-60%	-37%
46.0	-8%	52%	45.6	-64%	-34%	45.6	-57%	-38%
57.4	-11%	37%	57.4	-62%	-35%	57.1	-56%	-41%
68.8	5%	54%	68.6	-60%	-36%	69.0	-53%	-38%
80.2	32%	85%	78.6	-58%	-36%	92.0	-46%	-34%
91.1	-10%	21%						

Figure 11 (c) show that the A/W system entrained the least in the spray regime, followed by A/S while A/E entrained the most. The A/S system showed a minimum in entrainment at lower liquid rates than the other two systems. A different observation is made in Figure 11 (d) where A/S entrained the most in the froth regime while A/W entrained the least. A comparison of the A/W data with correlations from Kister and Haas (1988) (K&H, A/W) and Bennett et al. (1995) (B,A/W) in Figure 11 (a) and (b) show that the former will under-predict entrainment and the latter will over-predict A/W entrainment in the spray regime. In the froth regime the experimental A/W data agrees well with the prediction made by the Kister and Haas (1988) correlation. The Bennett et al. correlation (1995) over-predicts entrainment in the froth regime. It has to be noted that their correlation was used slightly beyond their recommended gas flow factor range range of 2.5 kg$^{0.5}$/(m$^{0.5}$.s), as most of the experimental data was measured at gas flow factors of 2.8 kg$^{0.5}$/(m$^{0.5}$.s) and above. It was found that both correlations will under predict entrainment in both regimes when the gas rate is reduced from 2.8 to 2.5 kg$^{0.5}$/(m$^{0.5}$.s) for the A/S system. The correlations of Bennett et al. (1995), (Figure 11 (c) and (d)), predict that A/E will entrain the least and A/S the most. The A/W correlations of Bennett et al. (1995) (Table 4) were used for all the comparisons since their NA/W correlations performed poorly in relation to the data and their A/W correlations (Bennett et al., 1995 and Uys, 2010). A different result is obtained with the correlations of Kister and Haas (1988) in 11 (e) and (f). Their correlations predict that the

Stellenbosch University http://scholar.sun.ac.za

A/E system will entrain the least of the systems in Figure 11 (e) and A/W the most. For liquid rates above 9 $m^3/(h.m)$ as shown in Figure 11 (f) the froth regime correlation by Kister and Haas (1988) show very little difference between the systems. None of the correlations predict a maximum in entrainment in the froth regime, as shown by the data.

It is necessary to understand why differences are observed between the measured entrainment data and predictions made by the correlations. To gain more insight into the correlations they are now compared by considering potential changes in liquid density and surface tension. Figure 1 (a) and (b) show the dependency of these correlations on these two properties under specific hydrodynamic conditions.

The entrainment correlation developed by Kister and Haas (1988) for the spray regime is the only correlation that includes an empirical surface tension dependence on entrainment. Bennett et al. (1995) do not account for the effect of surface tension in any of their correlations. According to them, surface tension influences droplet diameter and therefore vapour drag on the droplet. They assumed that the effect of drag on froth height and entrainment can be neglected in the operating region used in their investigation. This assumption was qualified by Bennett et al. (1995) with the use of graphs where the effect of drag versus no-drag on froth height was compared over a range of Froude and Weber numbers. Their graphs indicated that the no-drag assumption will only hold true over a limited range of Froude and Weber numbers, and ratio of droplet ejection velocity to superficial vapour velocity.

Figure 1 (b) shows that these two correlations have a similar dependence on liquid density in the spray regime (Q_L = 2.9 $m^3/(h.m)$) for densities smaller than 1100 kg/m^3. In the higher liquid rate region (Q_L = 40 $m^3/(h.m)$), which relates to the froth regime, the Kister and Haas (1988) correlation shows little dependence on liquid density. For the froth regime, their correlation is only dependent on liquid density if it is assumed that the froth height term used in Equation 1, h_F, is dependent on liquid density, as suggested by Colwell (1981). The Colwell (1981) froth height correlation has therefore been used in Equation 1 in Table 4 as suggested. Bennett et al. (1995) suggest a much stronger dependence on liquid density in both regimes. They do, however, show that the dependency on liquid density in the froth regime is much less than in the spray regime, especially for lower liquid densities. For this

Stellenbosch University http://scholar.sun.ac.za

reason a small difference between the three liquids in the spray regime, and no significant deviation between the liquids in the froth regime, is expected when using the Kister and Haas (1988) entrainment prediction. Since Bennett et al. (1995) only considered the influence of liquid density as a physical property in the froth regime, it is expected that A/E will entrain the least with A/S the most. This is as a result of the high density of ethylene glycol and the low density of silicone oil. The liquid physical property that is clearly absent in any of the correlations is liquid viscosity.

Stellenbosch University http://scholar.sun.ac.za

5. Conclusions

An experimental setup that is capable of generating entrainment, tray pressure drop and weeping data for a range of gasses and liquids was successfully constructed. Tests were conducted over a large range of gas flow factors (1.6 $kg^{0.5}/(m^{0.5}.s)$ for the 415mm tray spacing up to 4.0 $kg^{0.5}/(m^{0.5}.s)$ for the 615mm tray spacing) and liquid flow rates (2.9 – 112 $m^3/(h.m)$) resulting in a large array of entrainment data (1.0 – 23% L'/G). The accuracy of the experimental data has been verified using air/water data from Nutter (1972) and the Bennett et al. (1995) correlation.

The results shows that ethylene glycol will entrain the most in the low liquid ($Q_L < 9$ $m^3/(h.m)$) and low gas factors ($F < 3.4$ $kg^{0.5}/(m^{0.5}.s)$) ranges with silicone oil that entrains the most in the high liquid range ($Q_L > 12$ $m^3/(h.m)$). Water entrained slightly more than ethylene glycol under the high ($F = 4.0$ $kg^{0.5}/(m^{0.5}.s)$) gas flow conditions.

The experimental entrainment data (L'/G) for air/water, air/ethylene glycol and air/silicone oil systems were compared with correlations from literature (Kister and Haas 1988, Bennett et al. 1995). It was found that the predictions deviated from the measured data for the non-air/water systems. This was to be expected, since these entrainment correlations have been developed using entrainment data that comprised of a very large percentage of air/water data and relatively little non-air/water data. To compensate for the influence of physical properties on entrainment, both correlations include gas and liquid density dependence. Kister and Haas (1988) included a surface tension term for entrainment in the spray regime.

The results from this work suggest that the influence of liquid physical properties on entrainment is more complex and regime-dependent than current correlations suggest. Consequently, more data is required to improve our understanding of froth behaviour. It follows from this study that viscosity cannot be neglected as a physical property affecting entrainment, especially for viscous systems (≥ 15 mPa.s). Also, the influence of gas and liquid density, and surface tension should be re-evaluated so that their fundamental influence on entrainment can be understood. This will only be possible after generating more entrainment data for additional systems and different tray spacings.

Entrainment (L'/G) results are compared with the percentage liquid entrained (L'/L). This comparison shows that high entrainment (L'/G) at increasing liquid rates (> 12 $m^3/(h.m)$)

Stellenbosch University http://scholar.sun.ac.za

results in an overall decrease in the percentage liquid entrained (L'/L). A decrease in the percentage liquid entrained will result in an increase in the Murphree tray efficiency. It is therefore preferable to operate the column at higher liquid loads as long as flooding does not occur.

The data and visual observations from this study, notably in the froth regime at increasing flow rates, suggest that the tray flow path length could play a prominent role in froth development and entrainment, especially at high gas velocities and lower tray spacings. Therefore, poor column performance could be the result of scale-up from small diameter columns, when using specific correlations developed in these small diameter columns. More research is required to quantify the influence of tray flow path length on froth behaviour. However, the data measured here is very relevant to multi-pass trays with similar geometry to that used in this study.

6. Acknowledgements

The financial assistance of Sasol Technology (Pty) Ltd, Koch-Glitsch LP, Inher SA, and the Department of Trade and Industry (DTI) of South Africa through the Technology and Human Resources for Industry Programme (THRIP) towards this research is hereby acknowledged. We gratefully acknowledge the inputs from Dr. A. Erasmus and Dr. I. Nieuwoudt regarding the equipment design. Opinions expressed and conclusions arrived at are those of the authors and are not necessarily to be attributed to the sponsors.

Stellenbosch University http://scholar.sun.ac.za

7. Nomenclature

A_c	column area = 635x175mm	[m^2]
A_d	downcomer inlet area	[m^2]
A_f	fractional hole area = A_h/A_p	
A_h	hole area	[m^2]
A_n	net column area = A_c-A_d	[m^2]
A_p	perforated area or bubbling area	[m^2]
d_H, D_H	hole diameter	[mm, m]
E	entrainment, L'/G	
$\bar{E}$	average entrainment for multiple samples	
FPL	tray flow path length	[mm]
F	superficial vapour factor = $U_s.\rho_g^{0.5}$	[$kg^{0.5}/m^{0.5}.s$]
g	gravitational constant = 9.81	[m/s^2]
G	gas mass flow rate	[kg/s]
h_L, H_L	clear liquid height	[mm, m]
h_F, H_F	froth height	[mm, m]
$h_{L,ct}$	clear liquid height at the regime transition	[mm]
h_w, H_w	outlet weir height	[mm, m]
L	mass flow of liquid entering the tray	[kg/s]
L'	entrained liquid mass flow	[kg/s]
P	hole pitch	[mm]
Q_L	liquid flow rate per weir length	[$m^3/(h.m)$]
s, S	tray spacing	[mm, m]
U_L	liquid velocity calculated as Q_L/downcomer escape area	[m/s]
U_s	superficial gas velocity, based on tray perforated/bubbling area	[m/s]
W'	weeping liquid mass flow	[kg/s]
Greek Letters		
ρ	density	[kg/m^3]
σ	surface tension	[mN/m]
μ	liquid viscosity	[mPa.s]

Stellenbosch University http://scholar.sun.ac.za

8. References

Bennett, D.L., Kao, A.S., Wong, L.W., 1995. A mechanistic analysis of sieve tray froth height and entrainment. AIChE , 41 (9), 2067-2082.

Colwell, C., 1981. Clear liquid height and froth density on sieve trays. Industrial and Engineering Chemistry Process Design and Development, 20 (2), 298-307.

Decent, S.P., King, A.C., Simmons, H.J.H., Părău, E.I., Wallwork, I.M., Gurney, C.J., Uddin, J., 2009. The trajectory and stability of a spiralling liquid jet: Viscous theory. Applied Mathematical Moddeling, 33, 4283-4302.

Fakhari, A., Rahimian, M.H., 2011. Investigation of deformation and breakup of a falling droplet using a multiple-relaxation-time lattice Boltzmann method. Computers & Fluids, 40, 156 – 171.

Hofhuis, P.A.M. and Zuiderweg, F.J., 1979. Sieve plates: dispersion density and flow regimes. Institution of Chemical Engineers Symposium Series, 1979, 56, 2.2/1-2.2/35.

Kister, H.Z, Pinczewski, W.V., Fell, C.J.D., 1981. Entrainment from sieve trays operating in the spray regime. Industrial and Engineering Chemistry Process Design and Development , 20 (3), 528-532.

Kister, H.Z., Haas, J.R., 1988. Entrainment from sieve trays in the froth regime. Industrial and Engineering Chemistry Research , 27 (12), 2331-2341.

Kister, H.Z., Haas, J.R., 1990. Predict entrainment flooding on sieve and valve trays. Chemical Engineering Progress , 63-69.

Lockett, M.J., 1986. Distillation tray fundamentals, Cambridge University Press, Cambridge.

Nutter, D.E., 1972. Amonia stripping efficiency studies. American Institute of Chemical Engineers Symposium Series No. 124, 68.

Nutter, D.E., 1979. Weeping and entrainment studies for sieve and v-grid trays in an air-oil system. Institution of Chemical Engineers Symposium Series No. 56 , 3.2/47 - 3.2/62.

Pan, K.L., Hung, C.Y., 2010. Droplet impact upon a wet surface with varied fluid and surface properties. Journal of Colloid and Interface Science, 352, 186-193.

Porter, K.E., Jenkins, J.D., 1979. The interrelationship between industrial practice and academic research in distillation and absorption. Institution of Chemical Engineers Symposium Series No. 56 , 5.1/1-5.1/47.

Puppich, P., Goedecke, R., 1987. Investigation of entrainment in tray columns. Chemical Engineering and Technology , 10, 224-230.

Thomas, W. J., Ogboja, O.,1978. Hydraulic studies in sieve tray columns. Industrial and Engineering Chemistry Process Design and Development , 17 (4), 429-443.

Uys, E.C., 2010. Entrainment in a sieve tray column, Masters Thesis. Stellenbosch University, South Africa.

Uys, E.C., Lamprecht, S.M., Schwarz, C.E., Burger, A.J., Nieuwoudt, I., Erasmus, A.B., Knoetze, J.H., 2010. Establishing a facility for the hydrodynamic characterisation of distillation column internals. Distillation Absorption conference proceedings, 659 – 664.

Van Sinderen, A.H., Wijn, E.F., Zanting, R.W., 2003. Entrainment and maximum vapour flow rate of trays. Transactions of the Institution of Chemical Engineers, Vol 81, 94 – 107.

Yanagi, T., Sakata. M., 1979. Performance of a commercial scale 14% hole area sieve tray. Institution of Chemical Engineers Symposium Series No. 56 , 5.1/1-5.1/47.

Zuiderweg, F.J., 1982. A view on the state of the art. Chemical Engineering Science, 37 (10), 1441-1464.

Stellenbosch University http://scholar.sun.ac.za

Manuscript 2

The influence of gas physical properties on entrainment inside a sieve tray column

Ehbenezer C. Uys[a], Andries J. Burger[a], Johannes H. Knoetze[a,2]

[a]Department of Process Engineering, University of Stellenbosch, Private Bag X1, Matieland 7602, South Africa

Status: Submitted

Journal: Chemical Engineering Research and Design

Keywords: Entrainment, sieve tray, physical properties, tray hydrodynamics.

[2]Corresponding author. Tel.: +27 21 8084488; fax: +27 21 8082059.

E-mail address: jhk@sun.ac.za (Johannes H. Knoetze)

Stellenbosch University http://scholar.sun.ac.za

1. Abstract

Existing entrainment prediction correlations, often used in the design of sieve tray distillation columns, were developed with limited non-air/water data. The aim of this work is to investigate the influence of gas physical properties on entrainment. Air, CO_2 and SF_6 are passed through a rectangular sieve tray column to cover a large gas density (1.2 – 5.8 kg/m^3) range. Water, ethylene glycol and n-butanol are used as liquids to provide liquid physical property variation. Liquid flow rates ranged from 2.9 – 80 m^3/(h.m) with gas flow factors ranging from 1.9 – 4.8 m/s.(kg/m^3)$^{0.5}$. The database consists of over 500 experimental data points. The objective is to use the data to describe the effect of gas physical properties and gas-and-liquid flow rates on entrainment. This data are also used to evaluate the scope and limitations of current prediction models. Prediction models compare well with air/water data, but poorly with the rest. A new variation of the Reynolds and Froude numbers together with a ratio of the gas to liquid density is used to describe the influence of the gas physical properties and, gas-and-liquid flow rates on entrainment.

Stellenbosch University http://scholar.sun.ac.za

2. Introduction

Distillation, stripping and absorption are the most important, based on capacity, separation processes used in the chemical industry. In these separation processes a gas or vapour is brought in contact with liquid in a column that is fitted with contacting devices. These devices are commonly referred to as packing or trays. Column design is based on the phase equilibria which determine the required number of theoretical stages. Mass transfer and hydrodynamic models then determine the size and number of plates or packing height of the column. These models predict efficiency based on the geometry of the contacting device, operating conditions, fluid properties and fluid flow rates. To improve these models it is important to understand how each of these parameters contribute to the mass transfer and hydrodynamic models. The focus of this work is on the hydrodynamic behaviour inside a sieve tray column, especially the entrainment. Entrainment influences both separation efficiency and column capacity.

Separation efficiency is reduced when a fraction of the liquid (L'/L) on the tray is transported with the rising gas to the tray above. The reduction in efficiency caused by entrainment (L'/L) is described by the Colburn equation (Colburn, 1936) and by the work of Mohan et al. (1983). Column capacity is reached when the mass fraction of liquid droplets suspended in the rising gas (L'/G) becomes too large. This will cause column operation to become unstable as flooding would occur (Kister, 1992). There are therefore two definitions of entrainment that has to be considered during column design and operation. The fraction of liquid entering the tray that is entrained (L'/L) as well as the fraction of droplets entrained (L'/G) in the rising gas. The preferred hydrodynamic operating conditions are when both definitions of entrainment are at a minimum for the required operating conditions. Uys et al. (2012a) show that this optimum generally occurs at liquid rates above 20 $m^3/(h.m)$, commonly referred to as the froth regime.

Uys et al. (2012a) suggest that there is scope for improving entrainment correlations for sieve tray columns. A considerable amount of research has been done with the air/water system to determine the influence of tray and column geometry and, gas – and liquid flow rates on entrainment. Far less research has been done with non-air/water systems. The current entrainment database in the open literature does not contain sufficient data to accurately model the influence of gas and liquid physical properties on entrainment. This is

Stellenbosch University http://scholar.sun.ac.za

largely due to the fact that the database consists of limited data from various institutions with different tray and column geometries. Thus, predictions made based on these limited data could be far from accurate for other systems (Schultes, 2010). By testing over a larger range of physical properties the influence of each property on entrainment can be investigated. An improved understanding will lead to more accurate predictions for systems other than air/water, relating more to what is common in industry.

The question is, how do gas physical properties influence entrainment and do the current correlations predict entrainment with sufficient accuracy? Some research has been done with systems other than air/water by Hunt et al. (1955) and Yanagi and Sakata (1979). They were the only workers to test for different systems using fixed tray- and column geometries. The work from both of these groups was used by others (Kister and Haas, 1988 and Bennett et al., 1995) to develop entrainment correlations.

Hunt et al. (1955) conducted experiments with methane, Freon 12 and air with physical properties shown in Table 1. For their experiments a static liquid height was used and the effect of liquid cross flow was therefore not considered. They stated that entrainment is independent of gas density as shown in their correlation (Equation 1 in Table 2). Since liquid hold-up was found to be dependent on gas density (Kister et al., 1981, Colwell, 1981, Bennett et al., 1995) Hunt et al. (1955) therefore unintentionally considered the effect of gas density to some degree. They did not correlate liquid hold-up, therefore, experimental or estimated liquid hold-up data has to be used to determine entrainment with their correlation. Kister and Haas (1988) used the data from Hunt et al. (1955) to develop their entrainment correlations shown in Table 2 (Equations 2 – 5). The recommended range of application for the correlations in Table 2 is shown in Table 3.

.

Stellenbosch University http://scholar.sun.ac.za

Table 1. Physical properties of the systems used by Hunt et al. (1955) and Yanagi and Sakata (1979).

Author	System	ρ_v [kg/m^3]	ρ_L [kg/m^3]	σ [mN/m]	μ_L [mPa.s]
Hunt et al. (1955)	CH_4/H_2O	0.6	993	73	±0.9*
	Freon 12/H_2O	5	993	73	±0.9*
	Air/H_2O	1.2	993	73	±0.9*
	Air/Kerosene	1.2	705	25	±1.6*
	Air/Hexane	1.6	673	18	±0.3*
	Air/CCl_4	1.9	1602	27	±0.9*
Yanagi and Sakata (1979)	Cyclohexane/n-heptane	1.1, 4.8	700, 641	18.5, 13.5	0.37, 0.23
	Isobutane/n-butane	28, 52, 78	493, 437, 391	5, 2.5, 1.1	0.09, 0.065, 0.05
*Values estimated					

Table 2. Entrainment correlations developed by Hunt et al. (1955), Kister and Haas (1988) and Bennett et al. (1995)

Author	Entrainment Correlations	
Hunt et al. (1955)	$\frac{L'}{G} = 3.08\text{x}10^5 \left(\frac{73}{\sigma}\right)\left(\frac{U_s}{s-2.5h_L}\right)^{3.2}$	(1)
Kister & Haas (1988)	$\left(\frac{L'}{G}\right)_{froth} = 111\left(\frac{U_s}{s-h_F}\right)^2 d_H{}^{0.5}(1+\zeta)$	(2)
	$\left(\frac{L'}{G}\right)_{spray} = 4.742^{(10/\sqrt{\sigma})^{1.64}} X^{(10/\sqrt{\sigma})}$	(3)
	$X = 872\left(\frac{U_s h_{L,ct}}{\sqrt{d_H s}}\right)^4 \left(\frac{\rho_g}{Q_L \rho_l}\right)\left(\frac{\rho_l-\rho_g}{\sigma}\right)^{0.25}$	(4)
	$h_{L,ct} = \frac{\left(\frac{0.4974 A_f{}^{-0.791} d_H{}^{0.833}}{1+0.013 Q_L{}^{-0.59} A_f{}^{-1.79}}\right)}{1+0.00262 h_w}\left(\frac{996}{\rho_l}\right)^{0.5(1-0.00091 d_H/A_f)}$	(5)
Bennet *et al.* (1995) (Air/Water)	$\left(\frac{L'}{G}\right)_{spray} = 0.0050\left(\frac{K_s^2}{g\phi_e S}\right)^{1.26}\left[\frac{gH_L}{K_s^2}+\frac{9\sqrt{3}}{2A_f}\left(1+4.77\left\{\frac{D_H}{H_L}\right\}^{3.29}\right)\right]^{1.26}\varepsilon^{\beta}\left(\frac{\rho_L}{\rho_g}\right)^{0.5}$	(6)
	$\left(\frac{L'}{G}\right)_{froth} = 0.00164\left(\frac{K_s^2}{g\phi_e S}\right)^{1.86}\left[\frac{gH_L}{K_s^2}+\frac{9\sqrt{3}}{2A_f}\left(1+6.9\left\{\frac{D_H}{H_L}\right\}^{1.85}\right)\right]^{1.86}\left(\frac{\rho_L}{\rho_g}\right)^{0.5}$	(7)
	$K_s = U_s\sqrt{\frac{\rho_g}{\rho_l}}$	(8)
	$H_L = \phi_e H_{Fe}$	(9)
	$H_{Fe} = H_w + 0.501 + 0.439\exp(-137.8H_w)\left(\frac{Q_L}{3600\phi_e}\right)^{2/3}$	(10)
	$\phi_e = \exp[-12.55 K_s{}^{0.91}]$	(11)
	$\varepsilon = \frac{H_L}{H_F}$	(12)
	$\beta = 0.5\left(1-\tanh\left[1.3\ln\left(\frac{H_L}{D_H}\right)-0.15\right]\right)$	(13)

Table 3. Recommended range of application for the Hunt et al. (1955), Kister and Haas (1988) and Bennett et al. (1995) correlations.

Author	U_s [m/s]	Q_L [m^3/(h.m)]	S [m]	A_F	d_H [mm]	System
Hunt et al. (1955)	1.0 – 4.3	0	0.2 – 0.71	0.05 – 0.22	3.2 – 12.7	Methane/Water, Freon 12/Water, Air/Kerosene, Air/Hexane, Air/CCl_4, Air/water, Air/glycerine
Kister and Haas (1988)	0.3 – 3.5	2-130	0.1-1	0.04 – 0.2	1.5-25	Air/water
Bennett et al. (1995)	0.4 - 2.3	4.2-134	0.15-0.91	0.06-0.124	1.6 – 25.4	Air/water

Yanagi and Sakata (1979 and 1982) conducted entrainment and efficiency experiments with cyclohexane/n-heptane and isobutane/n-butane systems under different pressures with physical properties as shown in Table 1. They found it difficult to predict entrainment and consequently did not develop a correlation to show the dependence of entrainment on gas and liquid properties. Bennett et al. (1995) used the data from Yanagi and Sakata (1979) to develop their own entrainment correlations shown in Table 2 (Equations 6 to 13).

Hunt et al. (1955) conducted tests with three different gasses and water at fixed liquid hold-up conditions. From these experiments it was possible to determine the effect of gas density on entrainment at a fixed liquid hold-up of 45.7 mm for water. However, it is not clear from their work how gas density influences entrainment over a range of liquid flow rates and liquid hold-up. Fixed hold-up conditions are seldom found in industrial applications as liquid hold-up will change with changing liquid flow rates, gas density, liquid density and gas velocity (Colwell, 1981). The systems used by Yanagi and Sakata (1979) covered a large gas density range but at the same time the liquid properties changed (as shown in Table 1). It is advantageous to use one liquid with three or more gasses covering a range of different densities without changing column and tray geometry. In doing this the effect of gas physical properties on entrainment is isolated from the effect of changing liquid physical properties.

It is therefore the aim of this work to generate new entrainment data over a range of gas physical properties for three liquids at gas rates higher than the range covered by the Bennett et al. (1995) correlation. By extending the gas flow rate test range past that found in the literature, new insight and knowledge will be gained. The data are compared with entrainment prediction correlations to investigate their reliability and limitations. The influence of gas physical properties on both definitions of entrainment (L'/L and L'/G) is investigated. The objective is to find a correlation between entrainment, gas physical properties and gas-and-liquid flow rates.

3. Experimental

Method

Two liquids (water and ethylene glycol) were individually contacted with three gasses (air, CO_2, SF_6). By adding n-butanol that was contacted with two gasses (CO_2 and SF_6) to the experimental range, the effect of liquid physical properties on entrainment could also be captured. The reason only three liquids were used in the tests is due to the high cost of SF_6. Liquid density was determined with hydrometers (0.5 kg/m^3 resolution) while the surface tension was measured using a Sigma 702 surface tensiometer (0.01 mN/m resolution). Liquid viscosity was measured with an Anton Paar Physica MCR501 2007 Rotaviscometer (0.01 mPa.s resolution).

The three gases used were selected primarily based on density, flammability, availability, cost and stability. These gases have a density range of 1.2 – 5.8 kg/m^3, which is representative of a large range of atmospheric distillation systems (Uys, 2010). The gas composition was determined using a HP 5890 GC (gas chromatograph) with a TCD detector and a Hayesep Q column (6ft x 1/8 in x 2.1 mm SS), supplied by Supelco. To convert the GC area plots to mole percentages, response factors were determined for each gas during the GC method development.

The physical properties of the systems and flow ranges used in the experiments are shown in Table 4. Water, ethylene glycol and n-butanol were chosen as they give a large spread of physical properties (density, viscosity and surface tension). As water and ethylene glycol are not flammable it was possible to safely conduct experiments with air. In Table 4 there are two different surface tension values for ethylene glycol. Initially ethylene glycol was used with air followed by air/silicone oil tests. With each change in liquid the system had to be evacuated and cleaned with an alcohol mixture. Upon reloading the system with CO_2 and ethylene glycol some of the remaining alcohol mixture contaminated the ethylene glycol and consequently slightly reduced the surface tension.

Table 4. Gas and liquid physical properties with flow ranges covered in experiments.

System	ρ_v [kg/m^3]	μ_G [mPa.s]	ρ_L [kg/m^3]	σ [mN/m]	μ_L [mPa.s]	s [mm]	Q_L [m^3/(h.m)]	F_s [m/s.(kg/m^3)$^{0.5}$]	U_s [m/s]
Air/water	1.2	0.0186	998	59	0.9	615	2.9 - 80	2.5 - 3.4	2.3 - 3.1
CO_2/water	1.8	0.0149	997	60	0.9	615	2.9 - 80	2.5 - 3.9	2.0 - 2.9
SF_6/water	5.8	0.0151	998	60	1.0	615	2.9 - 92	2.9 - 4.8	1.2 - 2.0
Air/ethylene glycol	1.2	0.0186	1102	37	15	615	2.9 - 69	2.5 - 4.0	2.3 - 3.7
CO_2/ethylene glycol	1.8	0.0149	1095	35	15	615	2.9 - 80	2.7 - 3.9	2.0 - 2.9
SF_6/ethylene glycol	5.8 - 5.9	0.0151	1097	35	15	615	2.9 - 69	2.9 - 4.8	1.2 - 2.0
CO_2/n-butanol	1.8	0.0149	806	23	2.6	615	2.9 - 69	1.9 - 3.1	1.4 - 2.3
SF_6/n-butanol	5.8	0.0151	819	23	2.6	615	2.9 - 57	2.4 - 3.4	1.0 - 1.4

The experimental setup, shown in Figure 1, was used to generate the experimental data. Detailed descriptions of the setup can be found in other publications (Uys, 2010 and Uys et al., 2012a). Tray spacing and weir height were set at 615 mm and 51mm while the liquid rate was varied from 2.9 – 80 m^3/(h.m) to cover both the froth and spray regimes. Two sieve test trays, with geometry as defined in Table 5 were installed in the column. A detailed drawing of the sieve tray is presented in Figure 1 of the Appendix.

Stellenbosch University http://scholar.sun.ac.za

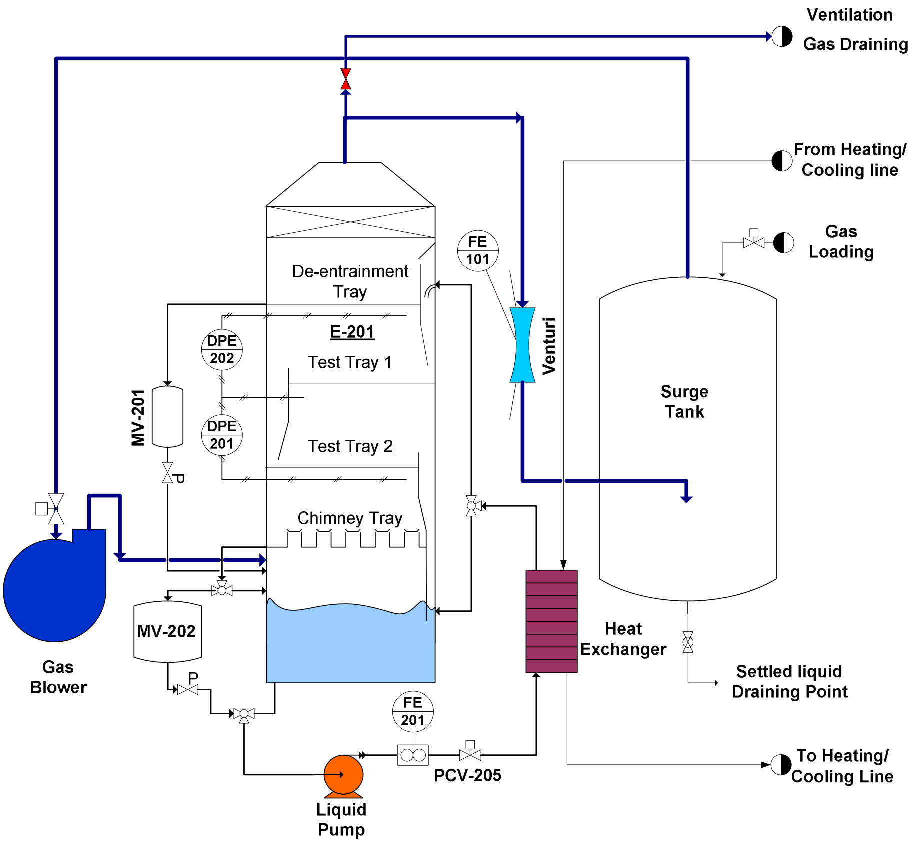

Figure 1. Process flow diagram of the experimental setup as shown in Uys et al. 2012a.

Table 5. Tray and column geometry

Geometry		Unit
d_H	6.3	mm
No Holes	414	-
P	14.5	mm
A_h	0.0129	m^2
A_p	0.0830	m^2
A_f (A_h / A_p)	0.156	-
A_n	0.095	m^2
A_d	0.0158	m^2
A_c	0.1111	m^2
h_w	51	mm
s	615	mm
L_w	175	mm
FPL	475	mm

Stellenbosch University http://scholar.sun.ac.za

Gas loading

Prior to loading CO_2 and SF_6 into the system, the surge tank was filled with water. The volume of the surge tank is 83% of the total system volume. By displacing the water in the surge tank with the test gas a 100% evacuation of the surge tank was achieved. The remaining 17% of air (or old gas) was replaced by purging the system with the required gas until the air (and CO_2 for the SF_6 tests) content was less than five mole percent. The gas composition was determined with a GC as mentioned in section 2.1.

Operation

During experiments the gas was circulated in a closed loop using a centrifugal blower. Although the blower intake and outlet were sealed from the environment, leakage can occur at the blower shaft seal. To prevent air from entering the system through the shaft seal, due to the low pressure created by the suction of the blower, the system pressure was elevated to 1.5 – 2 kPa above atmospheric pressure. This was achieved by connecting the gas (CO_2 or SF_6) cylinder to the system with a pressure regulator and a pneumatically operated pressure control valve. A water trap was connected to the surge tank to prevent the system from over pressure. The maximum system pressure was controlled by adjusting the water level in the water trap.

Gas samples were analysed every two hours throughout the experiments to determine any significant fluctuations in gas composition. It was found that the gas composition stabilised around three mole percent air over eight hours of testing. A venturi with temperature and pressure compensation measured the gas mass flow rate. To ensure accurate gas flow measurements the specific gas constant, used in the venturi mass flow algorithm, was updated if any change in gas composition occurred. Since the gas pressure (100.5 – 101.5 kPa, depending on atmospheric pressure) and liquid temperature (25°C ± 1°C) was controlled, the gas density never fluctuated with more than 1.0% for the air tests and 1.2% for the SF_6 tests.

The liquid surface tension, density and viscosity were determined at 25°C during each experimental run.

Stellenbosch University http://scholar.sun.ac.za

4. Results and discussion

Experimental data

Water and ethylene glycol were contacted individually with air, CO_2 and SF_6. n-Butanol was contacted only with CO_2 and SF_6 during the experiments. The results measured consist of 530 experimental data points. Water was contacted with air, CO_2 and SF_6 (Figure 2).

An increase in gas density led to a decrease in entrainment (L'/G) under constant gas flow factor (also known as the f-factor). The gas flow factor is the square root of the gas kinetic energy, calculated as the gas velocity (based on bubbling area) times the square root of the gas density (Kister, 1992). The results of all three liquids indicate a decrease in entrainment with an increase in gas density at constant flow factor conditions. Consequently the column can be operated at higher gas flow factors with increasing gas density (Figure 2 (a), (e) and (f)). The gas flow factor in Figure 2 (e) and (f) was too high for air experiments and caused the column to flood. Only SF_6 could be used for the high flow factor of 4.81 $m/s.(kg/m^3)^{0.5}$ in Figure 2 (f) without flooding the column. Inspection of the Kister and Haas (1988) and Bennett et al. (1995) correlations also showed a decrease in entrainment with an increase in gas density.

Stellenbosch University http://scholar.sun.ac.za

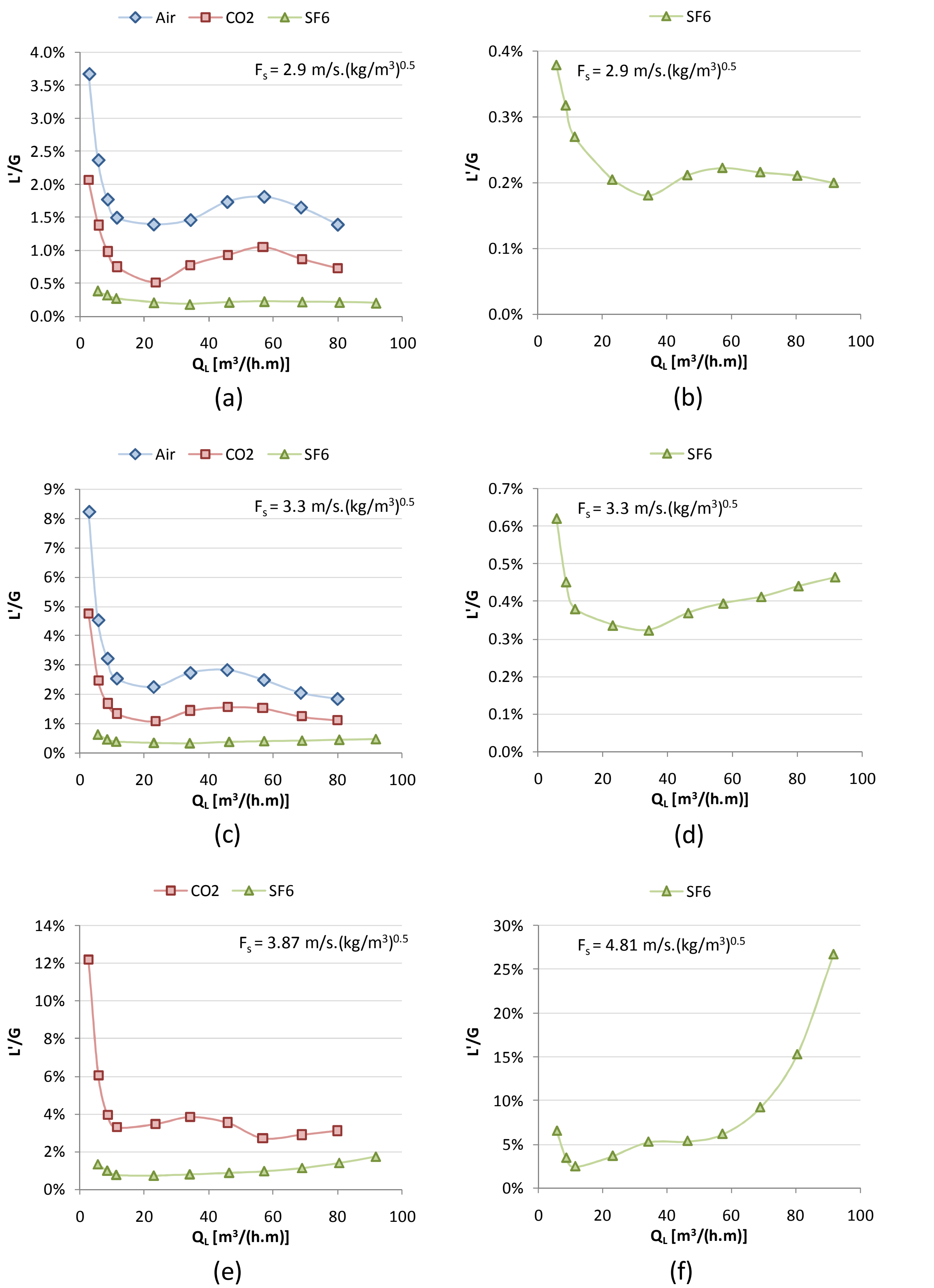

Figure 2. Experimental entrainment (L'/G) data for water with (a) air, CO_2 and SF_6 at F_s = 2.9 m/s.(kg/m^3)$^{0.5}$ (b) SF_6 at F_s = 2.9 m/s.(kg/m^3)$^{0.5}$ (c) air, CO_2 and SF_6 at F_s = 3.3 m/s.(kg/m^3)$^{0.5}$ (d) SF_6 at F_s = 3.3 m/s.(kg/m^3)$^{0.5}$ (e) CO_2 and SF_6 at F_s = 3.87 m/s.(kg/m^3)$^{0.5}$ and (f) SF_6 at F_s = 4.81 m/s.(kg/m^3)$^{0.5}$

Stellenbosch University http://scholar.sun.ac.za

Comparing experimental data with correlations

The correlations of Kister and Haas (1988) and Bennett et al. (1995) are compared to the data. These are not the only authors who developed entrainment correlations, but their correlations cover the spray and froth regimes as well as the largest array of operating conditions. Other correlations by Zuiderweg (1982) and Koziol and Mackowiak (1990) focus on the spray regime only and are therefore not considered for comparison with the data.

Entrainment predictions with the Kister and Haas (1988) and Bennett et al. (1995) correlations (Table 2) differ significantly. The Kister and Haas (1988) correlations generally predict lower entrainment than the Bennett et al. (1995) correlations. To investigate the differences in predictions of these correlations, they are compared with the data in Figure 3. The deviations between the experimental data and the correlations are shown in Table 6 with the percentage deviation calculated as:

$$\%Dev = (L'/G_{predicted} – L'/G_{measured})/(L'/G_{measured}) \times 100$$

Where the correlations are indicated as broken lines in the figures, they are extrapolated beyond the recommended range of application. All the details regarding data validation can be found in Uys et al. (2012a), where experimental air/water data are compared with published data from Nutter (1972). The data fall within the predictions made, with the Kister and Haas (1988) correlation under predicting, and Bennett et al. (1995) over predicting entrainment. This is also the case for the CO_2/water, CO_2/ethylene glycol, SF_6/ethylene glycol and CO_2/n-butanol predictions for the low (2.9 m/s.(kg/m^3)$^{0.5}$) flow factor conditions.

The Bennett et al. (1995) correlation performs poorly for the SF_6/water system (Figure 3 (b)), when compared to the Kister and Haas (1988) prediction. It is interesting to note that the Kister and Haas (1988) correlation does not show an increase in entrainment as the liquid rate drops below 20 m^3/(h.m)) for the SF_6/water system. At these low liquid rates, spray regime behaviour was noted during experiments and entrainment increased with decreasing liquid rate. Both correlations under-predict entrainment for the air/ethylene glycol (Figure 3 (c)) and SF_6/n-butanol (Figure 3 (e)) systems. As the flow factor is increased to 4.8 m/s.(kg/m^3)$^{0.5}$ for the SF_6/ethylene glycol system, the Bennett et al. (1995) correlation is extrapolated very far beyond the recommended range of application. Their prediction is poor and therefore not included (Figure 3 (d)). The maximum entrainment predicted by the

Stellenbosch University http://scholar.sun.ac.za

Bennett et al. (1995) correlation in Figure 3 (f) is a result of the transition from the spray to froth regime. At these conditions their correlations are extrapolated beyond the recommended range of application. The Kister and Haas (1988) correlation under-predicts the experimental result for this and most other conditions (Figure 3 (d), (e) and (f)). The results in Figure 3 demonstrate that the correlations by Kister and Haas (1988) and Bennett et al. (1995) have limited capability to accurately predict the influence of gas physical properties on entrainment.

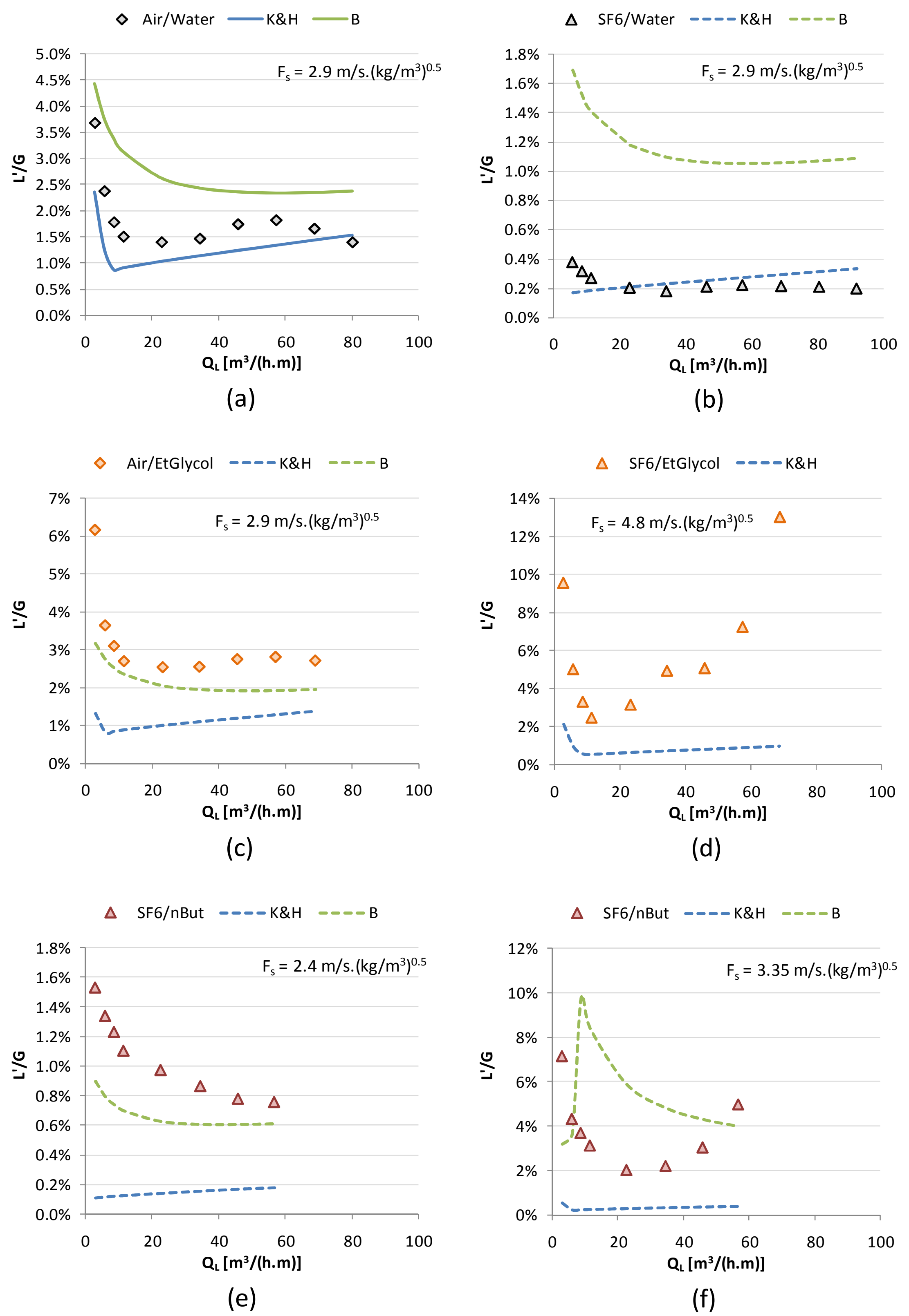

Figure 3. Comparing correlations from Kister and Haas [K&H] (1988) and Bennett et al. [B] (1995) with experimental data for the (a) air/water system at F_s = 2.9 m/s.(kg/m^3)$^{0.5}$ (b) SF_6/water system at F_s = 2.9 m/s.(kg/m^3)$^{0.5}$ (c) air/ethylene glycol system at F_s = 2.9 m/s.(kg/m^3)$^{0.5}$ (d) SF_6/ethylene glycol system at F_s = 4.8 m/s.(kg/m^3)$^{0.5}$ (e) SF_6/n-butanol at F_s = 2.4 m/s.(kg/m^3)$^{0.5}$ (f) SF_6/n-butanol at F_s = 3.35 m/s.(kg/m^3)$^{0.5}$

Table 6. Deviations between the experimental data and predictions made by Kister and Haas (1988) [K&H] and Bennett et al. (1995) [B].

	Air/Water F_s = 2.9 m/s.(kg/m^3)$^{0.5}$		SF_6/Water F_s = 2.9 m/s.(kg/m^3)$^{0.5}$		Air/EtGlycol F_s = 2.9 m/s.(kg/m^3)$^{0.5}$	
Q_L [m^3/(h.m)]	K&H (%Dev)	B (%Dev)	K&H (%Dev)	B (%Dev)	K&H (%Dev)	B (%Dev)
2.9	-36%	21%			-78%	-48%
5.7	-46%	59%	-56%	347%	-78%	-25%
8.6	-51%	91%	-45%	378%	-73%	-19%
11	-39%	109%	-32%	422%	-67%	-13%
23	-26%	89%	2%	476%	-61%	-20%
34	-22%	67%	2%	476%	-57%	-24%
46	-29%	36%	27%	507%	-56%	-31%
57	-26%	29%	19%	402%	-54%	-32%
69	-13%	43%	22%	374%	-49	-28
80	10%	71%	35%	390%	-	-
	SF_6/Etglycol F_s = 4.8 m/s.(kg/m^3)$^{0.5}$		SF_6/nBut F_s = 2.4 m/s.(kg/m^3)$^{0.5}$		SF_6/nBut F_s = 3.35 m/s.(kg/m^3)$^{0.5}$	
Q_L [m^3/(h.m)]	K&H (%Dev)	B (%Dev)	K&H (%Dev)	B (%Dev)	K&H (%Dev)	B (%Dev)
2.9	-78%	-59%	-93%	-42%	-92%	-56%
5.7	-81%	15%	-92%	-41%	-95%	-16%
8.6	-83%	116%	-90%	-40%	-93%	163%
11	-78%	232%	-89%	-37%	-92%	168%
23	-80%	1263%	-86%	-36%	-86%	190%
34	-85%	548%	-82%	-30%	-85%	118%
46	-84%	414%	-79%	-22%	-88%	41%
57	-88%	213%	-77%	-20%	-92%	-20%
69	-93%	58%	-	-	-	-

The influence of gas physical properties

Mass fraction of liquid droplets per mass rising gas (L'/G)

It is not clear from inspection of the data, how each of the gas physical properties influence entrainment over a range of gas- and liquid flow rates. A dimensionless number was developed using the Buckingham-π theorem with gas velocity, gas density, liquid flow rate, and gas viscosity as the physical variables. This was an attempt to find a relationship between entrainment and the system conditions in terms of a dimensionless group. Liquid physical properties were not considered as the influence of gas properties is investigated for one liquid at a time. The influence of liquid properties on entrainment is the focus of a subsequent study.

Stellenbosch University http://scholar.sun.ac.za

The dimensionless parameter that was developed from these variables showed that gas velocity was not required to render the group dimensionless (see Equation 14). Further inspection of the group shows that the dimensions of liquid flow rate, Q_L, are length squared over time (m^2/h) which is the same dimensions as for velocity times distance (VxL). Since the Reynolds number is the product of gas density (ρ_g), velocity (V) and a characteristic length (L) divided by the gas viscosity (μ_g), the dimensionless number is referred to as a modified Reynolds number (Re*).

$$\mathrm{Re}^* = \frac{\rho_g \frac{Q_L}{3600}}{\mu_g} \quad \textbf{(14)}$$

The mass fraction droplets suspended in the rising gas (L'/G) can therefore be expressed as a function of a modified Reynolds (Re*) number, shown in Equation 14 when more than one gas is used per liquid in the system. By adding the ratio of gas density divided by the difference between the liquid and gas density a better fit to the data was achieved. This group, Equation 15, was first introduced by Colwell (1981) when he created a modified version of the Froude number.

$$\left(\frac{\rho_g}{\rho_L - \rho_g}\right)^n \quad \textbf{(15)}$$

Following Colwell's approach the modified Reynolds number is combined with the density ratio group in Equation 15, to give the modified Reynolds number to describe entrainment, shown in Equation 16:

$$\mathrm{Re}^+ = \frac{\rho_g \frac{Q_L}{3600}}{\mu_g}\left(\frac{\rho_g}{\rho_L - \rho_g}\right)^n \quad \textbf{(16)}$$

The relationship shown in Figure 4 is separated between spray ($Q_L < 23m^3/(h.m)$) and froth regime ($Q_L > 23m^3/(h.m)$) conditions. The spray regime conditions are shown in Figure 4 (a) and (c) with the froth regime conditions shown in Figure 4 (b) and (d). These regimes are

Stellenbosch University http://scholar.sun.ac.za

defined using the method developed by Porter and Jenkins (1979). Their definition states that a regime change occurs when entrainment (L'/G) goes through a minimum with an increase in liquid rate, under constant gas flow conditions. This minimum occurs around 23 $m^3/(h.m)$ for the data shown in Figure 4.

Entrainment decreased with an increase in the expanded modified Reynolds number. Thus an increase in liquid flow rate and gas density will cause entrainment to decrease, given that the flow factor stays constant. An increase in gas viscosity will cause the expanded modified Reynolds number to decrease, therefore increasing entrainment. However, the gas viscosity range represented by the data is small compared to the other variables and the effect thereof was found to be negligible. By multiplying Equation 14 with the density ratio group in Equation 15, an increase in liquid density will decrease entrainment. This was, however, not the case as ethylene glycol with the highest density entrained more than water. This observation supports findings by Uys et al. (2012a). They showed that the dependence of entrainment on liquid properties is more complex than just liquid density and that liquid viscosity and surface tension also play an important role.

In al four cases (Figure 4) water entrained the least, with n-butanol the most over the range of modified Reynolds numbers. The n-butanol data is scattered more than the water and ethylene glycol data, especially at the high flow factor ($3.3 m/s.(kg/m^3)^{0.5}$) conditions. This could be attributed to the effects and interaction of liquid viscosity as explained by Uys et al. (2012a).

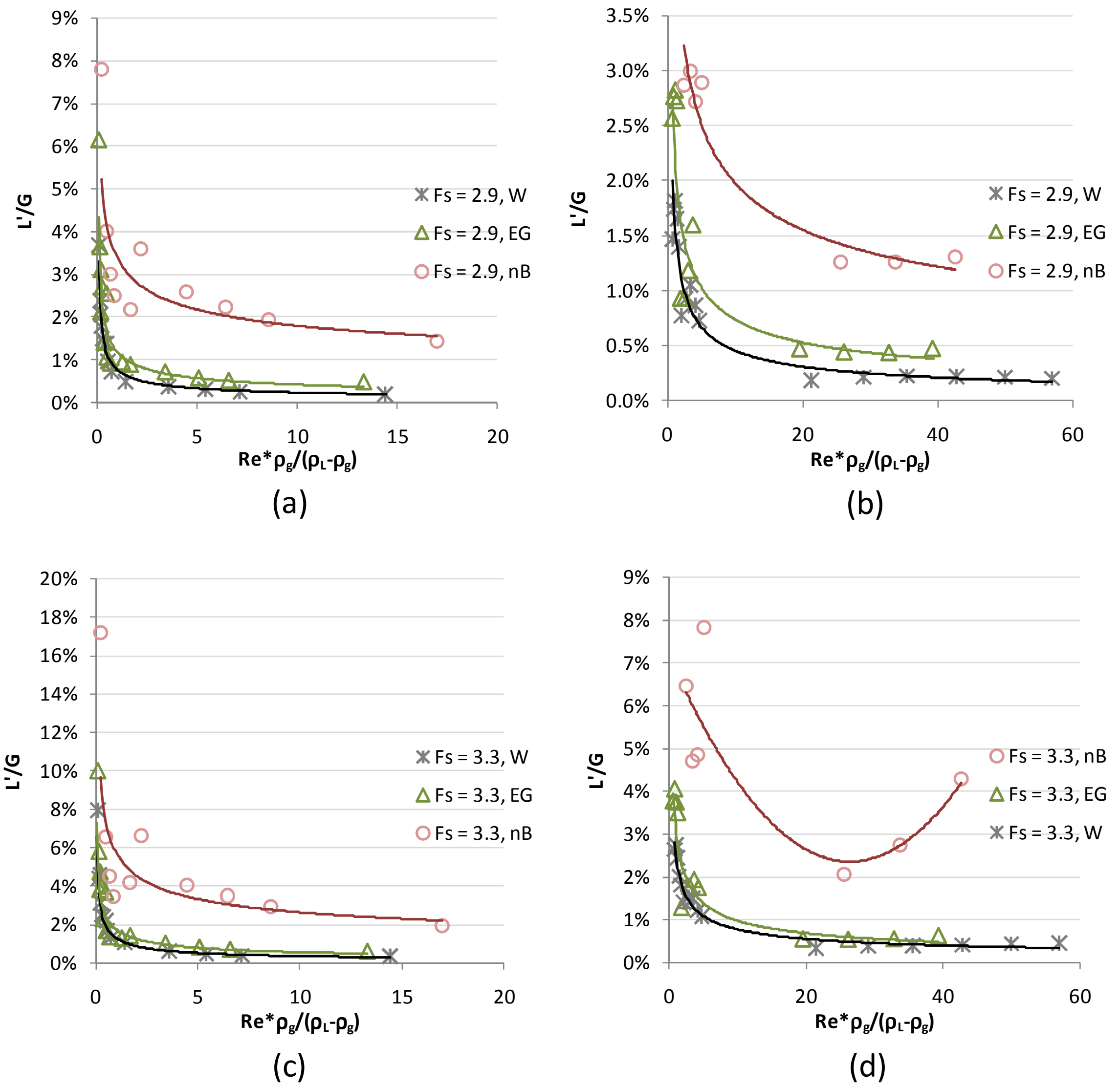

Figure 4. Experimental entrainment (L'/G) results for water [W], ethylene glycol [EG] and n-butanol [nB] as a function of the modified Reynolds (Re*) number for (a) Q_L < 23 $m^3/(h.m)$ at F_s = 2.9 $m/s.(kg/m^3)^{0.5}$ (b) Q_L > 23 $m^3/(h.m)$ at F_s = 2.9 $m/s.(kg/m^3)^{0.5}$ (c) Q_L < 23 $m^3/(h.m)$ at F_s = 3.3 $m/s.(kg/m^3)^{0.5}$ (d) Q_L > 23 $m^3/(h.m)$ at F_s = 3.3 $m/s.(kg/m^3)^{0.5}$

Mass fraction of liquid as droplets (L'/L)

Colwell (1981) used a modified version of the Froude number to describe the froth density. It was found that entrainment (L'/L) can also be described as a function of a modified and expanded Froude number. To achieve this, the length term in the Froude number (*L* in Equation 17) is changed to a ratio of the liquid rate per weir length over the gas velocity ((Q_L/U_s) in Equation 18). This is the same length parameter used in the modified Reynolds number.

Stellenbosch University http://scholar.sun.ac.za

$$\mathrm{Fr} = \frac{U_s^{\ 2}}{gL}$$

$$\mathrm{Fr}^* = \frac{U_s^{\ 2}}{g\dfrac{Q_L}{3600.U_s}} \tag{17}$$

$$\tag{18}$$

$$\mathrm{Fr}^* = \frac{3600U_s^{\ 3}}{gQ_L} \tag{19}$$

This modified Froude number times a ratio of the gas density over the difference between the liquid and gas density (see Equation 15) was a good indicator for the effects of the different gasses on entrainment for each liquid. This group is now referred to as the expanded modified Froude number as shown in Equation 20.

$$\mathrm{Fr}^+ = \frac{3600U_s^{\ 3}}{gQ_L}\left(\frac{\rho_g}{\rho_L - \rho_g}\right)^n \tag{20}$$

The advantage of using the expanded modified Froude number to characterise entrainment (L'/L) is that it is independent of the flow regime and therefore describes the data well over a large range of liquid rates and flow factors. Figure 5 indicates that the value of *n* in Equation 15 changes for the different liquids, showing that the density ratios between the gas and liquid play a varying role depending on the liquid.

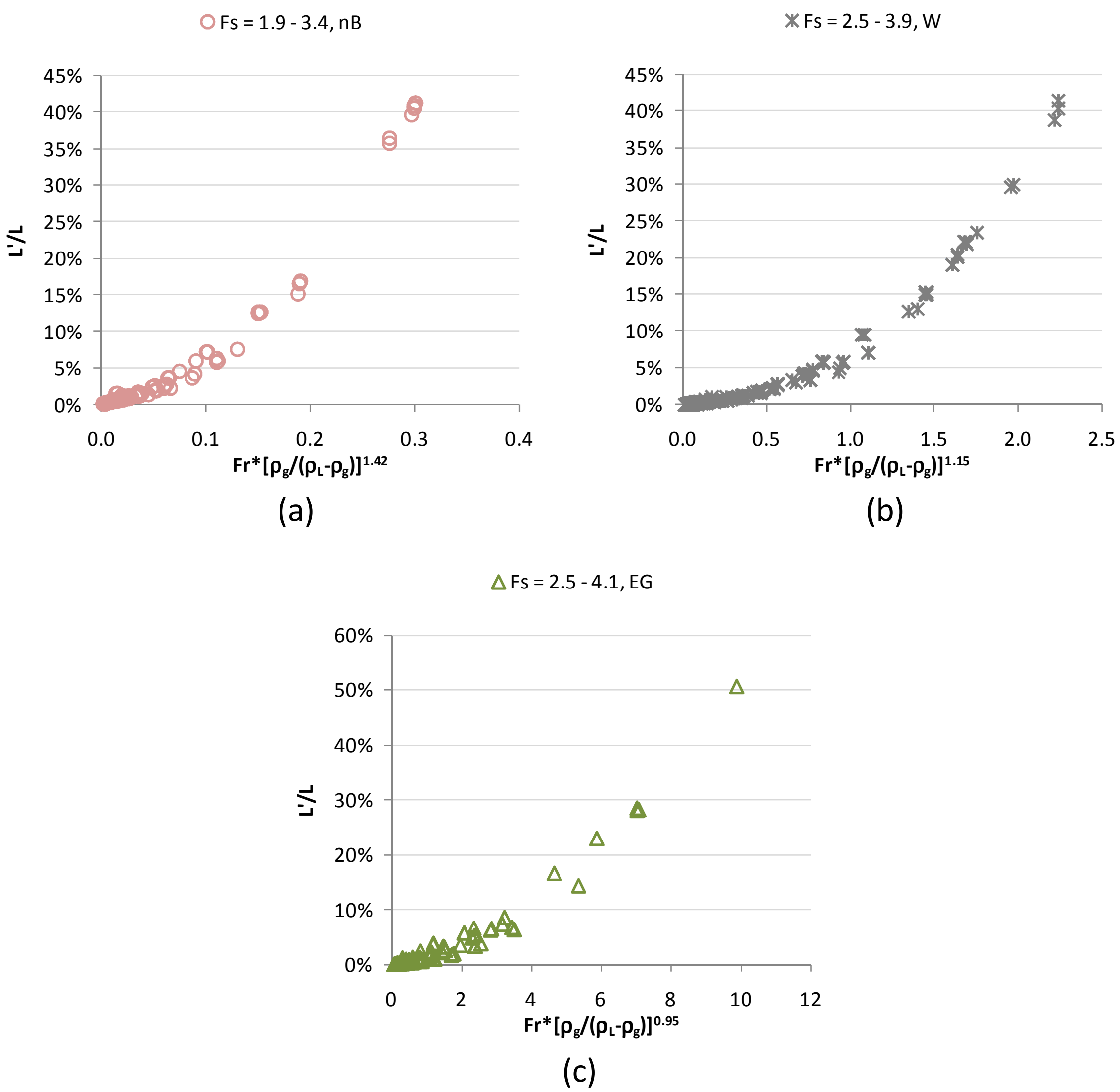

Figure 5. Experimental entrainment (L'/L) results as a function of the modified Froude number (Fr*) times the gas-to-liquid density ratio for (a) n-butanol [nB] (b) water [W] and (c) ethylene glycol [EG] systems over a larger range of flow factors

Stellenbosch University http://scholar.sun.ac.za

5. Conclusions

In this work entrainment was measured in air, CO_2 and SF_6 systems individually contacted with water, ethylene glycol and n-butanol (n-butanol was not contacted with air). The experimental database developed consists of over 500 data points, most of which were measured at gas rates higher than the range limit of the Bennett et al. (1995) correlation. It was found that under constant gas flow factor conditions, entrainment will decrease with an increase in gas density.

The air/water data compared well with predictions made with correlations by Kister and Haas (1988) and Bennett et al. (1995). It was found that the Kister and Haas (1988) correlation generally under-predict entrainment especially for systems other than water. The Bennett et al. (1995) correlations over-predicted most of the systems except air/ethylene glycol and SF_6/n-butanol for low (<2.9 m/s.$(kg/m^3)^{0.5}$) flow factor conditions. Their correlation was found to be very sensitive to extrapolation and performed poorly for the SF_6 system at high flow factor conditions.

To show the influence of gas physical properties on entrainment over a range of gas and liquid flow rates, two dimensionless groups were developed. These groups are modified versions of the Reynolds and Froude numbers together with a ratio of the gas to liquid density. The modified Reynolds number times a ratio of the gas density over the difference between the liquid and gas density show a good correlation between the mass of liquid entrained per mass of rising gas (L'/G) and gas physical properties. This relation is limited to constant flow factor conditions and, spray-and-froth regimes. For constant flow factor conditions, over a range of Reynolds numbers, n-butanol entrained the most, with water the least. This confirms the findings by Uys et al. (2012a) that liquid properties other than density also influence entrainment. Increasing gas density and liquid rate increase the modified Reynolds number. Increasing Reynolds number decreases entrainment (L'/G).

The modified Froude number together with a ratio of the gas to liquid density was developed to show the relationship between gas-and-liquid density, gas velocity, liquid flow rate and the fraction of liquid entering the tray that entrains (L'/L). The modified Froude number with the gas to liquid density ratio, showed a good relationship with entrainment data over a large range of flow factors and liquid rates for the different liquid systems. By

Stellenbosch University http://scholar.sun.ac.za

raising the gas velocity and gas density the modified Froude number increases while increasing liquid rate will decrease the modified Froude number. The fraction of liquid entering the tray that entrains (L'/L) increases with increasing Froude numbers.

Stellenbosch University http://scholar.sun.ac.za

6. Acknowledgements

The financial assistance of Sasol Technology (Pty) Ltd, Koch-Glitsch LP, Inher SA, and the Department of Trade and Industry (DTI) of South Africa through the Technology and Human Resources for Industry Programme (THRIP) towards this research is hereby acknowledged. We gratefully acknowledge the inputs from Dr. A. Erasmus and Dr. I. Nieuwoudt regarding the equipment design. Opinions expressed and conclusions arrived at are those of the authors and are not necessarily to be attributed to the sponsors.

Stellenbosch University http://scholar.sun.ac.za

7. Nomenclature

A_c	column area = 635x175mm	[m^2]
A_d	downcomer inlet area	[m^2]
A_f	fractional hole area = A_h/A_p	[-]
A_h	hole area	[m^2]
A_n	net column area = A_c-A_d	[m^2]
A_p	perforated area or bubbling area	[m^2]
d_H, D_H	hole diameter	[mm, m]
FPL	tray flow path length	[mm]
Fr*	modified Froude number	[-]
Fr^+	expanded modified Froude number	[-]
F_s	superficial vapour factor = $U_s.\rho_g^{0.5}$	[$kg^{0.5}/m^{0.5}.s$]
g	gravitational constant = 9.81	[m/s^2]
G	gas mass flow rate	[kg/s]
h_L, H_L	clear liquid height	[mm, m]
h_w, H_w	outlet weir height	[mm, m]
h_F, H_F	froth height	[mm, m]
$h_{L,ct}$	clear liquid height at the regime transition	[mm]
L	mass flow of liquid entering the tray	[kg/s]
L	length term in Equation 17	[m]
L’	entrained liquid mass flow	[kg/s]
L_w	weir length	[mm]
P	hole pitch	[mm]
Q_L	liquid flow rate per weir length	[$m^3/(h.m)$]
Re*	modified Reynolds number	[-]
Re^+	expanded modified Reynolds number	[-]
s, S	tray spacing	[mm, m]
U_s	superficial gas velocity, based on tray perforated/bubbling area	[m/s]

Greek Letters

ρ_g	gas density	[kg/m^3]
ρ_L	liquid density	[kg/m^3]
σ	surface tension	[mN/m]
μ_g	gas viscosity	[mPa.s]
μ_L	liquid viscosity	[mPa.s]

Stellenbosch University http://scholar.sun.ac.za

ζ	correction term for Equation 2

Stellenbosch University http://scholar.sun.ac.za

8. References

Bennett, D.L., Kao, A.S., Wong, L.W., 1995. A mechanistic analysis of sieve tray froth height and entrainment. AIChE , 41 (9), 2067-2082.

Colburn, A.P., 1936. Effect of entrainment on plate efficiency in distillation. Industrial and Engineering Chemistry, 28, 526.

Colwell, C., 1981. Clear liquid height and froth density on sieve trays. Industrial and Engineering Chemistry Process Design and Development, 20 (2), 298-307.

Hunt, C. d'A., Hanson, D.N., Wilke, C.R., 1955. Capacity factors in the performance of perforated plate columns. AIChE Journal. 1 (4), 441 – 451.

Kister, H.Z, Pinczewski, W.V., Fell, C.J.D., 1981. Entrainment from sieve trays operating in the spray regime. Industrial and Engineering Chemistry Process Design and Development , 20 (3), 528-532.

Kister, H.Z., Haas, J.R., 1988. Entrainment from sieve trays in the froth regime. Industrial and Engineering Chemistry Research , 27 (12), 2331-2341.

Kister, H.Z., 1992. Distillation design, McGraw-Hill.

Koziol, A., Mackowiak, J., 1990. Liquid entrainment in tray columns with downcomers. Chemical Engineering Process, 27, 145 – 153.

Mohan, T., Roa, K.K., Roa, D.P., 1983. Effect of vapour maldistribution and entrainment on tray efficiency. Industrial and Engineering Chemistry Process Design and Development, 22, 380 – 285.

Nutter, D.E., 1972. Amonia stripping efficiency studies. American Institute of Chemical Engineers Symposium Series No. 124, 68.

Porter, K.E., Jenkins, J.D., 1979. The interrelationship between industrial practice and academic research in distillation and absorption. Institution of Chemical Engineers Symposium Series No. 56 , 3.2/21-3.2/34.

Schultes, M., 2010. Research on mass transfer columns "old hat or still relevant?". Distillation and Absorption Conference Proceedings, 37 – 42.

Uys, E.C., 2010. Entrainment in a sieve tray column, Masters Thesis. Stellenbosch University, South Africa.

Uys, E.C., Schwarz, C.E., Burger, A.J., Knoetze, J.H., 2012a. New froth behaviour observations and comparison of experimental sieve tray entrainment data with existing

Stellenbosch University http://scholar.sun.ac.za

correlations. Submitted for review to Chemical Engineering Research and Design. DOI 10.1016/j.cherd.2012.05.008

Yanagi, T., Sakata. M., 1979. Performance of a commercial scale sieve tray. Institution of Chemical Engineers Symposium Series No. 56 , 5.1/1-5.1/47.

Yanagi, T., Sakata. M., 1982. Performance of a commercial scale 14% hole area sieve tray. Industrial and Engineering Chemistry Process Design and Development , 21 (4), 712-717.

Zuiderweg, F.J., 1982. A view on the state of the art. Chemical Engineering Science, 37 (10), 1441-1464.

Stellenbosch University http://scholar.sun.ac.za

Manuscript 3

The influence of liquid physical properties on entrainment inside a sieve tray column

Ehbenezer C. Uys[a], Andries J. Burger[a], Johannes H. Knoetze[a,3]

[a]Department of Process Engineering, University of Stellenbosch, Private Bag X1, Matieland 7602, South Africa

Status: To be submitted

Journal: Chemical Engineering Research and Design

Keywords: Entrainment, sieve tray, liquid physical properties, tray hydrodynamics.

[3]Corresponding author. Tel.: +27 21 8084488; fax: +27 21 8082059.

E-mail address: jhk@sun.ac.za (Johannes. H. Knoetze)

Stellenbosch University http://scholar.sun.ac.za

1. Abstract

To date only liquid density, and to a limited extent liquid surface tension, are used in correlations for the prediction of entrainment in sieve tray distillation columns. These correlations are often used in the design of sieve tray distillation columns and were developed with limited non-air/water data. The general assumption in previous studies of tray hydrodynamics is that liquid viscosity does not have an effect on entrainment. Recent work by Decent et al. (2009) showed that liquid viscosity and surface tension play a significant role in droplet size and development. The aim of this work is to investigate the influence of liquid physical properties on entrainment and whether findings related to liquid physical properties on single droplet formation and disintegration studies correspond with that of sieve tray entrainment. Non-air/water entrainment data were measured with Isopar G, n-butanol, silicone oil, water and ethylene glycol in a rectangular sieve tray column to cover large liquid density (739 - 1095 kg/m^3), surface tension (19.9 – 60 mN/m) and dynamic viscosity ranges (0.9 – 48.8 mPa.s). These liquids were used with CO_2 to extend the current non-air/water database. Liquid flow rates ranged between 2.8 – 80m^3/(h.m) with gas flow factors ranging between 1.9 – 4.3 m/s.(kg/m^3)$^{0.5}$. The database developed consists of 256 experimental data points. Experimental data are used to determine the effect of liquid physical properties on entrainment as well as to investigate the scope and limitations of current prediction models. The data prove that liquid dynamic viscosity significantly influences entrainment, contrary to what previous work on entrainment suggest. Rising liquid dynamic viscosity increases the froth height and decreases droplet break-up length and ejection velocity. The combined effect of these phenomena showed that viscosity has a complex non-monotonic effect on entrainment which corresponds with single droplet formation and disintegration studies. It is suspected that viscosity and surface tension have an interactive contribution on entrainment. An increase in surface tension will decrease entrainment. In general large deviations were observed between current prediction models and the non-air/water data.

Stellenbosch University http://scholar.sun.ac.za

2. Introduction

Absorption, stripping and distillation are the dominant separation processes used in the chemical industry. These separation processes make use of columns fitted with contacting devices, so that the rising gas or vapour can achieve equilibrium with the cross or counter flowing liquid. These contacting devices are commonly referred to as packing or trays. To design a distillation column for a required separation, estimations are made using mass transfer correlations, hydrodynamic models and thermodynamic data or models. These models use the contacting device geometry, operating conditions, fluid properties and fluid flow rates to predict the separation efficiency as well as the number of stages required as input parameters. To improve these models it is important to understand how each of these parameters contributes to the mass transfer and hydrodynamic models. The focus of this work is on the hydrodynamics inside a sieve tray column, especially entrainment. Entrainment affects both separation efficiency and column capacity. In this paper the focus is on the influence of liquid physical properties on entrainment related to capacity (L'/G), as existing prediction correlations are based on this definition.

When a fraction of the liquid (L'/L) on the tray is transported with the rising gas to the tray above, the separation efficiency is reduced. The negative influence of entrainment on efficiency has been shown by others (Colburn, 1936, Zuiderweg, 1982, Lockett, 1986, and Bennett et al. 1997). As the mass fraction of liquid droplets suspended in the rising gas (L'/G) becomes too large, column operation will become unstable and flooding can occur (Kister, 1992). Therefore both definitions (L'/L and L'/G) of entrainment have to be considered during the column design and operation.

According to the literature, a considerable amount of research has been done with the air/water system. The air/water results were then used to determine the influence of tray and column geometry and, gas-and-liquid flow rates on entrainment. In industrial applications, vapour-liquid systems separated by means of absorption, stripping or distillation cover a wide range of liquids. Consequently the liquid physical properties vary between the different industrial separation applications.

Currently the entrainment database does not contain sufficient non-air/water data to accurately model the influence of liquid density, surface tension and viscosity on

Stellenbosch University http://scholar.sun.ac.za

entrainment. Predictions made based on these data could be far from accurate for systems with physical properties that deviate from that of the air/water system (Schultes, 2010). This was confirmed by Uys et al. (2012a) who showed that entrainment correlations (Kister and Haas, 1988 and Bennett et al., 1995) are less accurate for liquids other than water.

Kister and Haas (1988) used the non-air/water data from Hunt et al. (1955) to develop their entrainment prediction correlations (Table 1). The recommended range of application for the correlations in Table 1 is shown in Table 2. Hunt et al. (1955) conducted experiments with water, kerosene, hexane and carbon tetrachloride with physical property ranges shown in Table 3. For their experiments static liquid at fixed liquid hold-up was used and the effect of liquid cross flow was therefore not considered. They concluded that liquid density and viscosity does not influence entrainment. This conclusion was based on the very small viscosity range (see Table 3) covered in their work. Hofhuis and Zuiderweg (1979), Kister et al. (1981), Zuiderweg (1982) and Kister (1992) showed that liquid density influences entrainment.

Table 1. Entrainment correlations developed by Hunt et al. (1955), Kister and Haas (1988) and Bennett et al. (1995).

Author	Entrainment Correlations	
Hunt et al. (1955)	$\frac{L'}{G} = 3.08\text{x}10^5 \left(\frac{73}{\sigma}\right)\left(\frac{U_s}{s-2.5h_L}\right)^{3.2}$	(1)
Kister & Haas (1988)	$\left(\frac{L'}{G}\right)_{froth} = 111\left(\frac{U_s}{s-h_F}\right)^2 d_H^{\,0.5}(1+\zeta)$	(2)
	$\left(\frac{L'}{G}\right)_{spray} = 4.742^{(10/\sqrt{\sigma})^{1.64}} X^{(10/\sqrt{\sigma})}$	(3)
	$X = 872\left(\frac{U_s h_{L,ct}}{\sqrt{d_H s}}\right)^4 \left(\frac{\rho_g}{Q_L \rho_l}\right)\left(\frac{\rho_l-\rho_g}{\sigma}\right)^{0.25}$	(4)
	$h_{L,ct} = \frac{\left(\frac{0.4974 A_f^{-0.791} d_H^{\,0.833}}{1+0.013 Q_L^{-0.59} A_f^{-1.79}}\right)}{1+0.00262 h_w}\left(\frac{996}{\rho_l}\right)^{0.5(1-0.00091 d_H/A_f)}$	(5)
Bennet *et al.* (1995) (Air/Water)	$\left(\frac{L'}{G}\right)_{spray} = 0.0050\left(\frac{K_s^2}{g\phi_e S}\right)^{1.26}\left[\frac{gH_L}{K_s^2}+\frac{9\sqrt{3}}{2A_f}\left(1+4.77\left\{\frac{D_H}{H_L}\right\}^{3.29}\right)\right]^{1.26} \varepsilon^{\beta}\left(\frac{\rho_L}{\rho_g}\right)^{0.5}$	(6)
	$\left(\frac{L'}{G}\right)_{froth} = 0.00164\left(\frac{K_s^2}{g\phi_e S}\right)^{1.86}\left[\frac{gH_L}{K_s^2}+\frac{9\sqrt{3}}{2A_f}\left(1+6.9\left\{\frac{D_H}{H_L}\right\}^{1.85}\right)\right]^{1.86}\left(\frac{\rho_L}{\rho_g}\right)^{0.5}$	(7)
	$K_s = U_s\sqrt{\frac{\rho_g}{\rho_l}}$	(8)
	$H_L = \phi_e H_{Fe}$	(9)
	$H_{Fe} = H_w + 0.501 + 0.439\exp(-137.8H_w)\left(\frac{Q_L}{3600\phi_e}\right)^{2/3}$	(10)
	$\phi_e = \exp[-12.55K_s^{\,0.91}]$	(11)
	$\varepsilon = \frac{H_L}{H_F}$	(12)
	$\beta = 0.5\left(1-\tanh\left[1.3\ln\left(\frac{H_L}{D_H}\right)-0.15\right]\right)$	(13)

Stellenbosch University http://scholar.sun.ac.za

Table 2. Recommended range of application of correlations by Hunt et al. (1955), Kister and Haas (1988) and Bennett et al. (1995).

Author	U_S [m/s]	Q_L [m^3/(h.m)]	S [m]	A_F	d_H [mm]
Hunt et al. (1955)	1.0 – 4.3	0	0.2 – 0.71	0.05 – 0.22	3.2 – 12.7
Kister and Haas (1988)	0.3 – 3.5	2-130	0.1-1	0.04 – 0.2	1.5-25
Bennett et al. (1995)	0.4 - 2.3	4.2-134	0.15-0.91	0.06-0.124	1.6 – 25.4

Table 3. Physical properties of the gas and liquid systems used by Hunt et al. (1955), Nutter (1979) and Yanagi and Sakata (1979).

Author	System	ρ_v [kg/m^3]	ρ_L [kg/m^3]	σ [mN/m]	μ_L [mPa.s]
Hunt et al. (1955)	CH_4/H_2O	0.6	993	73	±0.9*
	Freon 12/H_2O	5	993	73	±0.9*
	Air/H_2O	1.2	993	73	±0.9*
	Air/kerosene	1.2	705	25	±1.6*
	Air/hexane	1.6	673	18	±0.3*
	Air/CCl_4	1.9	1602	27	±0.9*
Nutter (1979)	Air/oil	1.2	770	24	2.3
Yanagi and Sakata (1979)	Cyclohexane/n-heptane	1.1, 4.8	700, 641	18.5, 13.5	0.37, 0.23
	Isobutane/n-butane	28, 52, 78	493, 437, 391	5, 2.5, 1.1	0.09, 0.065, 0.05

*Values estimated

Bennett et al. (1995) used the non-air/water data from Nutter (1979) and Yanagi and Sakata (1979) to develop an entrainment prediction correlation. The column and tray geometry differed between the data sets adding more uncertainty to the influence of the liquid physical properties on entrainment. Yanagi and Sakata (1979) conducted entrainment and efficiency experiments with cyclohexane/n-heptane and isobutane/n-butane systems under different pressures with physical properties as shown in Table 3. They found it difficult to predict entrainment and consequently did not develop a correlation to show the dependence of entrainment on gas and liquid properties. The systems used by Yanagi and Sakata (1979) covered a significant range of liquid properties, but as the liquid properties changed so did the gas properties. Thus it is impossible to isolate the effect of liquid physical properties on entrainment using their data.

Entrainment is characterised by droplets ejecting from the froth to the tray above (Bennett et al., 1995). Therefore droplet development, break-up and size influences entrainment. Decent et al. (2009) showed that viscosity has a non-monotonic influence on droplet size

Stellenbosch University http://scholar.sun.ac.za

and the break-up length of a liquid jet into a droplet. They investigated droplet formation from a viscous liquid jet emerging from a rapidly rotating orifice. The size of the droplets (which formed as the liquid jet disintegrates) was monitored, as well as the break-up length, which is the distance from the onset of the jet to the creation of the droplet. It was found that viscosity has a non-monotonic effect on the break-up length and velocity of the jet as well as on the droplet size. Fakhari and Rahimian (2011) investigated the deformation and fragmentation of droplets in free fall. They found that gas viscosity has no significant role in droplet break-up but that liquid viscosity is the principal factor in the mechanism of droplet disintegration. Pan and Hung (2010) studied the behaviour of a droplet upon impact with a wet surface. Their study shows that an increase in liquid viscosity inhibited disintegration into secondary droplets. However, reducing surface tension had the opposite effect. Therefore, the influence of viscosity on entrainment and tray hydrodynamics can not be neglected as previously assumed by Hunt et al. (1955), Kister and Haas (1988) and Bennett et al. (1995).

By testing over a larger range of liquid physical properties the influence of these properties on entrainment can be investigated. An improved understanding of the influence of liquid physical properties on entrainment will lead to more accurate predictions for systems other than air/water; closer to what is common in industry. With the wide variety of column geometries used in literature for different gas/liquid systems, it becomes increasingly difficult to determine the influence of liquid physical properties without considering the influence of tray-and-column geometry. No one has focused exclusively on the influence of liquid properties on entrainment without changing tray or column geometry.

Therefore the aim of this paper is to determine the influence of liquid physical properties on entrainment, with the focus on dynamic viscosity and surface tension. The strategy to accomplish this is to determine whether the findings related to single droplet studies for droplet development, formation and disintegration correlate to entrainment on sieve trays. To execute this strategy new entrainment data were measured using five liquids, one gas, one tray design and one tray spacing. In this way the influence of liquid physical properties were isolated from changing gas physical properties and tray-and-column geometry. The data are compared with entrainment prediction correlations from Kister and Haas (1988) and Bennett et al. (1995) to investigate their applicability and limitations.

Stellenbosch University http://scholar.sun.ac.za

3. Experimental

Selecting the liquids

The main objective in liquid selection was to choose liquids with a large range of surface tensions and viscosities that was not previously covered. Kister et al. (1981) did not include liquid viscosity in their correlation based on results from single hole studies, that showed no effect on entrainment for liquid viscosities in the range of 0.89 – 2.42 mPa.s. It was therefore decided to use liquids with viscosities ranging from 0.9 – 50 mPa.s to ensure that the effect of viscosity could be captured. Some work involving high viscosity applications has been done by Mahiout and Vogelpohl (1985), Böcker and Ronge (2005) and Li et al. (2008). Mahiout and Vogelpohl (1985) used glycerol solutions to investigate the influence of viscosity on mass transfer. They found that for viscosities smaller than 60 mPa.s, an increase in viscosity will lead to a large reduction in the mass transfer coefficient. They did not, however, investigate the influence of viscosity on the tray hydrodynamics. Böcker and Ronge (2005) suggested that the stripping of monomers from polymer solutions is an application of distillation of highly viscous liquids. An example of distillation of highly viscous mixtures is the separation of vinyl acetate from polyvinyl acetate with a viscosity of 50000 mPa.s reported by Li et al. (2008)

The motivation for the choice of liquids in this work was based on flash point and vapour pressure. High flash points and low vapour pressures will reduce the probability of evaporation. Another limitation that influenced the selection of liquids was cost. Based on these limitations it was decided to use Isopar G, n-butanol, silicone oil, water and ethylene glycol with properties shown in Table 4. To reduce the risk of potential fires or explosions, CO_2 was used as the gas. The liquid surface tension, density and dynamic viscosity were determined at 25°C for the liquid used in each experimental run. Liquid density was measured with hydrometers (0.5 kg/m^3 resolution) while the surface tension was measured using a Sigma 702 surface tensiometer (0.01mN/m resolution). Liquid viscosity was measured with an Anton Paar Physica MCR501 2007 Rotaviscometer (0.01 mPa.s resolution).

Table 4. Gas and liquid physical properties with flow ranges covered in experiments.

System	CO_2/Isopar G	CO_2/n-butanol	CO_2/silicone oil	CO_2/water	CO_2/ethylene glycol
F_s [m/s.(kg/m^3)$^{0.5}$]	1.9 - 3.1	1.9 - 3.2	2.7 - 4.2	2.7 - 4.3	2.7 - 3.9
ρ_v [kg/m^3]	1.8	1.8	1.8	1.8	1.8
U_s [m/s]	1.4 - 2.3	1.4 - 2.4	2.0 - 3.2	2.0 - 3.2	2.0 - 2.9
Q_L [m^3/(h.m)]	2.9 - 69.5	2.8 - 69.3	2.8 - 68.8	2.8 - 79.9	2.9 - 80.2
ρ_L [kg/m^3]	739	806	955	997	1095
σ [mN/m]	22.3	22.8	19.9	60	35.4
μ_L [mPa.s]	0.94	2.6	48.8	0.9	15
S [mm]	615	615	615	615	615
L'/G [%]	0.6 - 13.8	0.9 - 11.9	1.3 - 31.6	0.4 - 13.3	0.7 - 10.3
L'/L [%]	0.06 - 28.7	0.08 - 36.5	0.14 - 106*	0.06 - 41.3	0.09 - 28.5

Experimental setup

The experimental setup, shown in Figure 1, was used to generate the experimental data. Detailed descriptions of the setup can be found in Uys (2010) and Uys et al. (2012a and b). Tray spacing and weir height were set at 615mm and 51mm respectively, while the liquid rate was varied from 2.9 – 80m^3/(h.m) to cover both the froth and spray regimes. Two sieve test trays, with geometry as defined in Table 5 were installed in the column. A detailed drawing of the sieve tray is presented in Figure 1 of the Appendix. The downcomer escape area is changeable to ensure that the liquid velocity exiting the downcomer stayed between 0.3 – 0.6 m/s. A sensitivity analysis for downcomer escape velocity on entrainment was conducted during commissioning of the setup and more information is available in the work of Uys et al. (2012a). The analysis showed that entrainment will be influenced by the liquid escape velocity if the velocity is smaller or greater than this range.

There are generally four methods of measuring entrainment (Lockett, 1986):

1. Free entrainment – measuring the drops between the top of the froth and the tray above (Thomas and Ogboja, 1978).
2. Wet tray entrainment – using a non-volatile tracer (Lockett et al. 1976).
3. Efficiency entrainment – estimated from the reduction in tray efficiency caused by entrainment (Teller et al., 1963)

Stellenbosch University http://scholar.sun.ac.za

4. Dry tray entrainment – This is the most common technique and entrainment is measured using a special tray with no liquid entering from a downcomer. This tray collects the liquid that accumulates on it whereafter the liquid flows to a sampling vessel or hold-up tank where measurements take place (Hunt et al., 1955).

When using the dry tray measuring technique liquid on the tray can re-entrain. It was also important to ensure that the liquid level on the "dry tray" does not influence the entrainment it collects. In this experimental setup a specially designed collection (de-entrainment) tray was used with no liquid entering through a downcomer. The de-entrainment tray was designed so that the liquid head on the tray was collected on "blanked" areas and therefore did not influence the measurement accuracy under test conditions. The column area increases in the section above the de-entrainment tray and this section was fitted with a mist elimination pad. Thus small droplets that escaped the collecting tray were captured and measured. The efficiency of the de-entrainment section was verified by monitoring if any liquid accumulated in the surge tank which also acts as a settling tank. During normal testing conditions, no liquid accumulated in the surge tank. Only when the de-entrainment tray started to flood approximately 5 kg of liquid accumulated in the surge tank over 30 minutes. Verification of the experimental results, measurement accuracy and reliability were reported by Uys et al. (2012a).

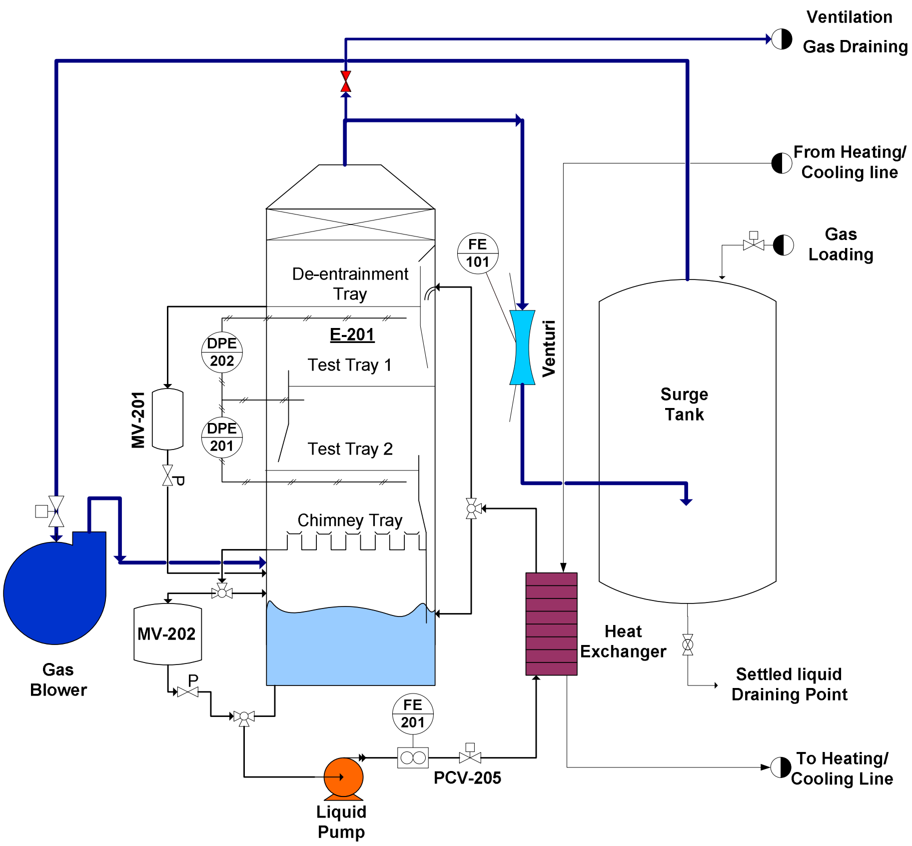

Figure 1. Process flow diagram of the experimental setup (Uys et al., 2012a).

Table 5. Tray and column geometry

Geometry		Unit
d_H	6.3	mm
No Holes	414	-
P	14.5	mm
A_h	0.0129	m^2
A_p	0.0830	m^2
A_f (A_h / A_p)	0.156	m^2
A_n	0.095	m^2
A_d	0.0158	m^2
A_c	0.1111	m^2
h_w	51	mm
s	615	mm
L_w	175	mm
FPL	475	mm

Stellenbosch University http://scholar.sun.ac.za

Liquid loading

The liquid testing sequence started with silicone oil, Isopar G, n-butanol, ethylene glycol and water. The order of this sequence was chosen based on the solubility of the liquids in each other although the column was cleaned between liquid changes. After each experimental run, the system was flushed with a mixture of alcohols and drained. During the column flushing and cleaning period the gas lines entering and exiting the column were closed to prevent CO_2 from exiting the system. A separate small blower was used to dry the column internals. Although great care was taken to remove the test liquid from the system, a very small amount (< 0.3%) of liquid remained in the system. This small amount tends to change the surface tension of the next liquid to be used slightly. Extra care has to be taken with cleaning when removing silicone oil. Even very small amounts of silicone oil will cause the Isopar G and n-butanol to foam.

Gas loading

Prior to loading CO_2 into the system, the surge tank was filled with water. The volume of the surge tank is 83% of the total system volume. By displacing the water in the surge tank with the test gas a 100% evacuation of the surge tank can be achieved. Most of the remaining 17% of air was removed by purging the system with CO_2 until the content was less than five mole percent. The gas composition was determined using a HP 5890 GC (gas chromatograph) with a TCD detector and a Hayesep Q column (6ft x 1/8 in x 2.1 mm SS), supplied by Supelco. To convert the GC area plots to mole percentages, response factors were determined for air and CO_2 during the GC method development.

Operation

Gas was circulated in a closed loop during experiments, using a centrifugal blower. Although the blower intake and outlet were sealed from the environment, leakage occurred at the blower shaft seal. The system pressure was elevated to 1.5 – 2kPa above atmospheric pressure to prevent air from entering the system through the shaft seal, due to the low pressure created by the suction of the blower. To control the system pressure a CO_2 cylinder was connected to the system through a pressure regulator and a pneumatically operated pressure control valve. A water trap was connected to the surge tank to prevent over pressure. The water level in the water trap determined the maximum pressure in the system.

Stellenbosch University http://scholar.sun.ac.za

Analysis of the gas samples was conducted approximately every two hours throughout experiments to determine any significant fluctuations in gas composition. It was found that the gas composition stabilised around three mole percent air over eight hours of testing. The gas mass flow rate was measured with a venturi meter and temperature and pressure compensation was used to ensure a high accuracy. The specific gas constant used in the venturi mass flow algorithm was updated if any change in gas composition occurred, to insure accurate gas flow measurements. The accuracy of the gas mass flow measurements were estimated to be within 2% (Uys, 2010). Since the gas pressure (100.5 – 101.5 kPa, depending on atmospheric pressure) and liquid temperature (25°C ± 1°C) were controlled, the gas density never fluctuated by more than 1.0% for the CO_2. The liquid surface tension, density and viscosity were determined at 25°C in the beginning and at the end of each experimental run.

Stellenbosch University http://scholar.sun.ac.za

4. Results and discussion

Experimental results

Isopar G, n-butanol, silicone oil, water and ethylene glycol was contacted individually with carbon dioxide. The results measured consist of 256 experimental data points. Isopar G and n-butanol showed the highest entrainment and consequently data were collected at much lower gas flow factors than for the other liquids, as shown in Figure 2 (a). The Isopar G and n-butanol data were collected at flow factors ranging from 1.9 – 3.1 m/s.$(kg/m^3)^{0.5}$. For ethylene glycol the data were collected at higher flow factors ranging from 2.7 – 3.9 m/s.$(kg/m^3)^{0.5}$ and for silicone oil and water at flow factors ranging from 2.7 – 4.3 m/s.$(kg/m^3)^{0.5}$.

A sharp increase in entrainment was observed for the CO_2/Isopar G system in Figure 2 (c) as the liquid rate increases from 46 - 69 m^3/(h.m). This sharp increase is caused by the froth building up against the column wall at the exit weir, similar to downcomer choke flooding. During these conditions the froth will start to reach the tray above (at the tray spacing of 615mm used for these experiments) and a sharp increase in entrainment is observed. The same observation is made in Figure 2 (d) for the CO_2/silicone oil system as the liquid rate increases from 46 - 69 m^3/(h.m). This phenomenon is explained in more detail in Uys et al. (2012a).

Stellenbosch University http://scholar.sun.ac.za

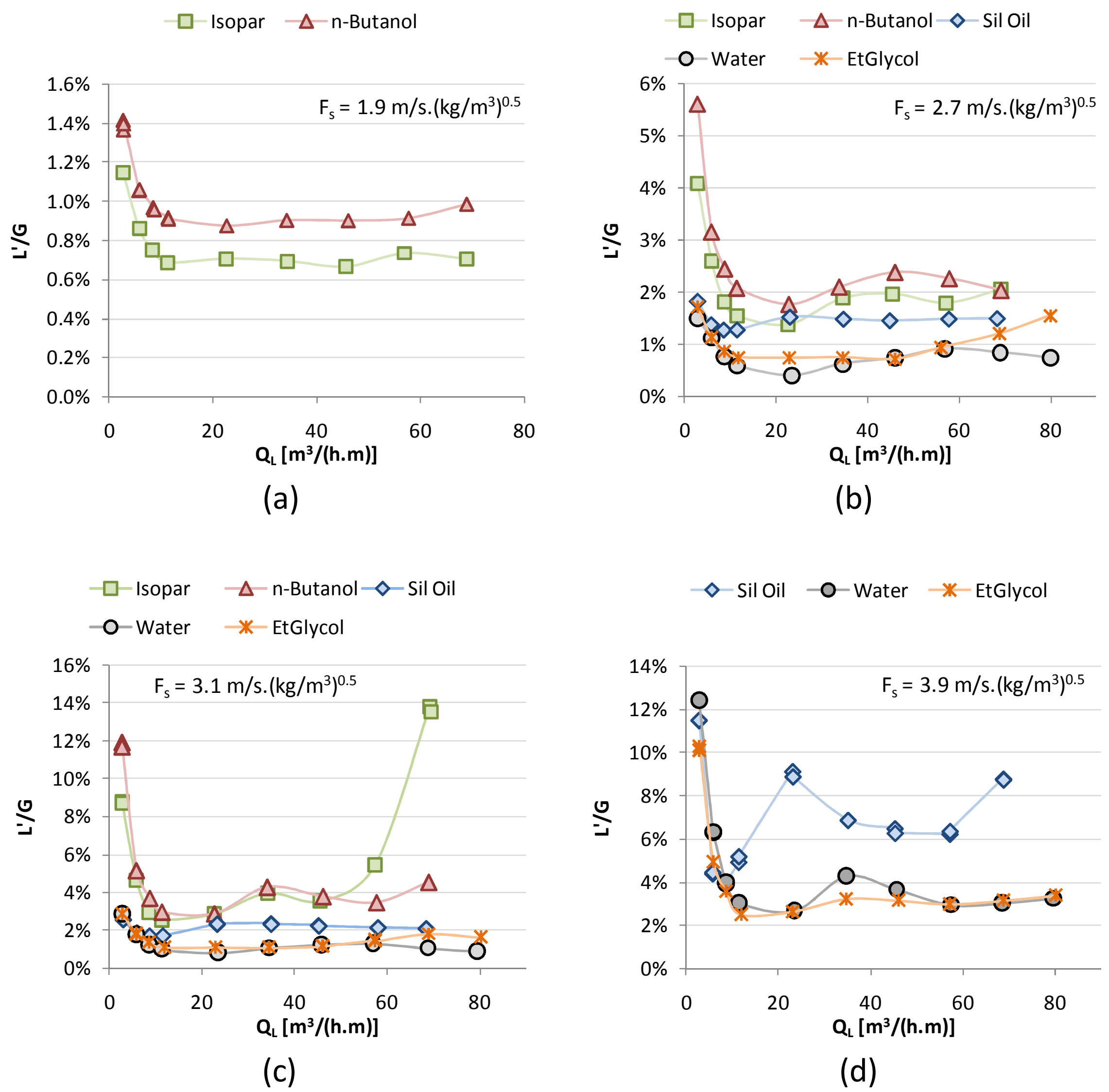

Figure 2. Experimental entrainment (L'/G) data for CO_2 with (a) Isopar G and n-butanol at F_s = 1.9 m/s.(kg/m^3)$^{0.5}$ (b) all five liquids at F_s = 2.7 m/s.(kg/m^3)$^{0.5}$ (c) all five liquids at F_s = 3.1 m/s.(kg/m^3)$^{0.5}$ and (d) silicone oil, water and ethylene glycol (EtGlycol) at F_s = 3.9 m/s.(kg/m^3)$^{0.5}$.

It was visually noted during the experiments that Isopar G formed a "low density sponge-like" froth with many very small droplets in the vapour continuous zone above the froth. The n-butanol froth tended to 'stick' together to form an intermediate (middle) layer between the froth and the droplet zone. This layer consisted of large droplets, liquid 'slugs' and liquid jets that projected high into the vapour space above the froth. The froth height for n-butanol also seemed higher than that of Isopar G, resulting in higher entrainment.

Stellenbosch University http://scholar.sun.ac.za

The froth height of the silicone oil system was higher than water and ethylene glycol (noted visually with the aid of a ruler fixed outside the column windows). Silicone oil also produced much smaller droplets than the water and ethylene glycol systems. It was increasingly difficult to distinguish between the froth heights and droplet sizes of water and ethylene glycol. Both liquid systems seemed to produce large droplets and slugs that did not project high into the vapour space above the froth.

Based on these observations high surface tension systems resulted in larger droplets. Due to the low viscosity the droplet ejection velocity is higher and more entrainment was measured than for systems with high viscosity and low surface tension. High viscosity, low surface tension liquids resulted in small droplets that did not eject with a high velocity and therefore less entrainment was measured.

Comparing experimental data with correlations

The data were compared to the entrainment predictions from the correlations of Kister and Haas (1988) and Bennett et al. (1995). These correlations were developed over the largest available entrainment database in the open literature and are applicable to the spray and froth regimes. Both authors suggest that their correlations are only applicable to the air/water system. Bennett et al. (1995) developed non-air/water correlations for the froth and spray regimes from a very small data base. These correlations performed very poorly and are therefore not included in this work. Uys (2010) showed that there is a significant difference between the predictions of the non-air/water and air/water correlations of Bennett et al. (1995). Although the correlations of Kister and Haas (1988) and Bennett et al. (1995) are only applicable to the air/water system, both authors included gas and liquid density in their correlations, which should account for some changes in the different systems. Kister and Haas (1988) also included surface tension in their spray regime correlation. They recommend that the froth height correlation of Colwell (1982) should be used in the calculation of their froth regime entrainment predictions. Uys et al. (2012a and b) compared their air/water entrainment results with predictions from Kister and Haas (1988) and Bennett et al. (1995). Bennett et al. (1995) over-predicted entrainment and Kister and Haas (1988) under-predicted entrainment for a flow factor of 2.9 m/s.$(kg/m^3)^{0.5}$.

Stellenbosch University http://scholar.sun.ac.za

Both correlations compare poorly with the Isopar G and n-butanol results shown in Figure 3 (a) and (b). The gas velocity for the comparisons, shown in Figure 4 (b), (c) and (d) exceeded the recommended application velocity (U_s = 2.3 m/s) of Bennett et al. (1995). Although both correlations predicted similar results, both under predicted entrainment. In general the Kister and Haas (1988) correlations under predicted entrainment. Their correlations did, however, compare well with the CO_2/water systems ranging from F_s = 2.7 to 3.9 m/s.(kg/m^3)$^{0.5}$. The correlations by Bennett et al. (1995) compared better than those of Kister and Haas (1988) with CO_2/Isopar G at F_s = 2.7 m/s.(kg/m^3)$^{0.5}$, CO_2/n-butanol at F_s = 2.7 m/s.(kg/m^3)$^{0.5}$, CO_2/silicone oil at F_s = 2.7 m/s.(kg/m^3)$^{0.5}$ and CO_2/ethylene glycol at F_s = 2.7 m/s.(kg/m^3)$^{0.5}$. The unexpected maxima at 5.9 m^3/(h.m) in the predictions made by Bennett et al. (1995) in Figure 4 (b), (c) and (d) is caused by the transition from their spray regime to froth regime correlation. Table 6 and Table 7 quantify the deviations in entrainment predictions between the correlations from Kister and Haas (1988) and Bennett et al. (1995), and the experimental data as shown in Figure 3 and Figure 4. The percentage deviation is calculated as:

$$\%Dev = (L'/G_{predicted} - L'/G_{measured}) / (L'/G_{measured}) \times 100.$$

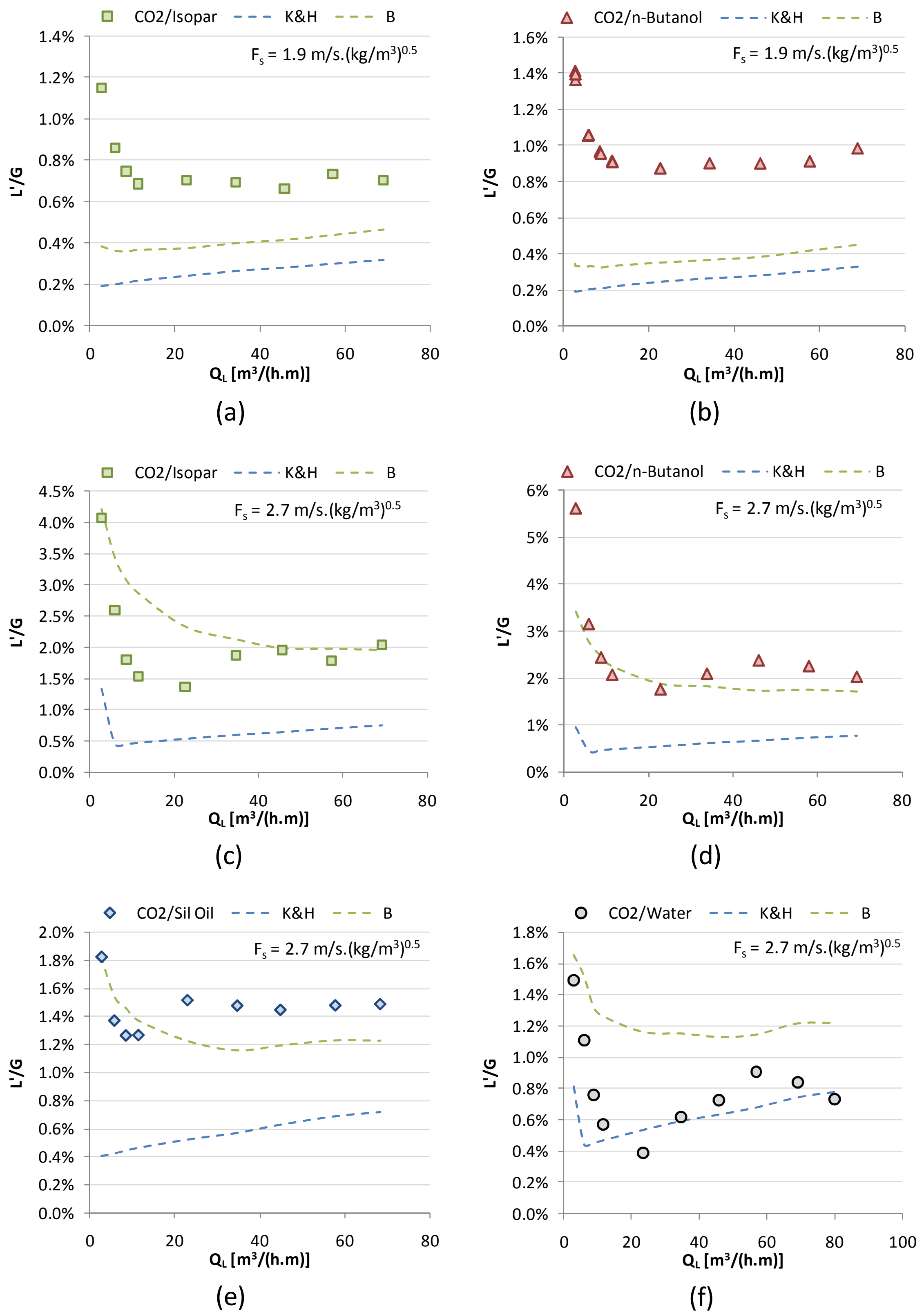

Figure 3. Comparison between experimental entrainment data and predictions made by the correlations of Kister and Haas (1988) [K&H], and Bennett et al. (1995) [B] for gas flow factors 1.9 and 2.7 m/s.(kg/m^3)$^{0.5}$. Broken lines are used for the predictions as the experimental conditions fall outside the recommended range of application.

Stellenbosch University http://scholar.sun.ac.za

Table 6. Deviations between the predictions made using the correlations of Kister and Haas (1988) [K&H]and Bennett et al. (1995) [B] compared to the experimental data shown in Figure 3.

CO_2/Isopar G			CO_2/n-butanol			CO_2/silicone oil		
F_s = 1.9 [m/s(kg/m^3)$^{0.5}$]			F_s = 1.9 [m/s(kg/m^3)$^{0.5}$]			F_s = 2.7 [m/s(kg/m^3)$^{0.5}$]		
Q_L [m^3/(h.m)]	K&H (%Dev)	B (%Dev)	Q_L [m^3/(h.m)]	K&H (%Dev)	B (%Dev)	Q_L [m^3/(h.m)]	K&H (%Dev)	B (%Dev)
2.9	-83%	-66%	2.9	-86%	1.35%	2.9	-78%	-1%
6.0	-77%	-57%	6.0	-81%	1.45%	5.9	-69%	12%
8.6	-72%	-51%	8.8	-78%	1.50%	8.6	-65%	16%
11.5	-68%	-46%	11.5	-76%	1.58%	11.5	-63%	8%
22.8	-66%	-46%	22.7	-72%	1.79%	23.0	-66%	-19%
34.3	-62%	-42%	34.2	-70%	1.95%	34.7	-61%	-21%
45.7	-57%	-37%	46.1	-69%	2.09%	44.9	-57%	-17%
57.0	-59%	-40%	57.7	-66%	2.26%	57.8	-53%	-17%
69.0	-54%	-34%	68.8	-66%	2.42%	68.4	-52%	-17%
CO_2/Isopar G			CO_2/n-butanol			CO_2/water		
F_s = 2.7 [m/s(kg/m^3)$^{0.5}$]			F_s = 2.7 [m/s(kg/m^3)$^{0.5}$]			F_s = 2.7 [m/s(kg/m^3)$^{0.5}$]		
Q_L [m^3/(h.m)]	K&H (%Dev)	B (%Dev)	Q_L [m^3/(h.m)]	K&H (%Dev)	B (%Dev)	Q_L [m^3/(h.m)]	K&H (%Dev)	B (%Dev)
6.0	-82%	33%	5.9	-86%	-12%	5.8	-60%	37%
8.7	-75%	70%	8.8	-81%	1%	8.7	-41%	74%
11.5	-69%	86%	11.5	-77%	9%	11.6	-19%	119%
22.7	-61%	70%	22.9	-69%	7%	23.5	37%	196%
34.6	-68%	14%	33.9	-71%	-12%	34.5	-5%	86%
45.7	-67%	2%	46.1	-72%	-27%	45.9	-13%	55%
57.4	-61%	11%	58.0	-68%	-22%	56.8	-25%	26%
69.3	-63%	-4%	69.3	-62%	-15%	68.9	-12%	45%
-	-	-	-	-	-	79.9	6%	65%

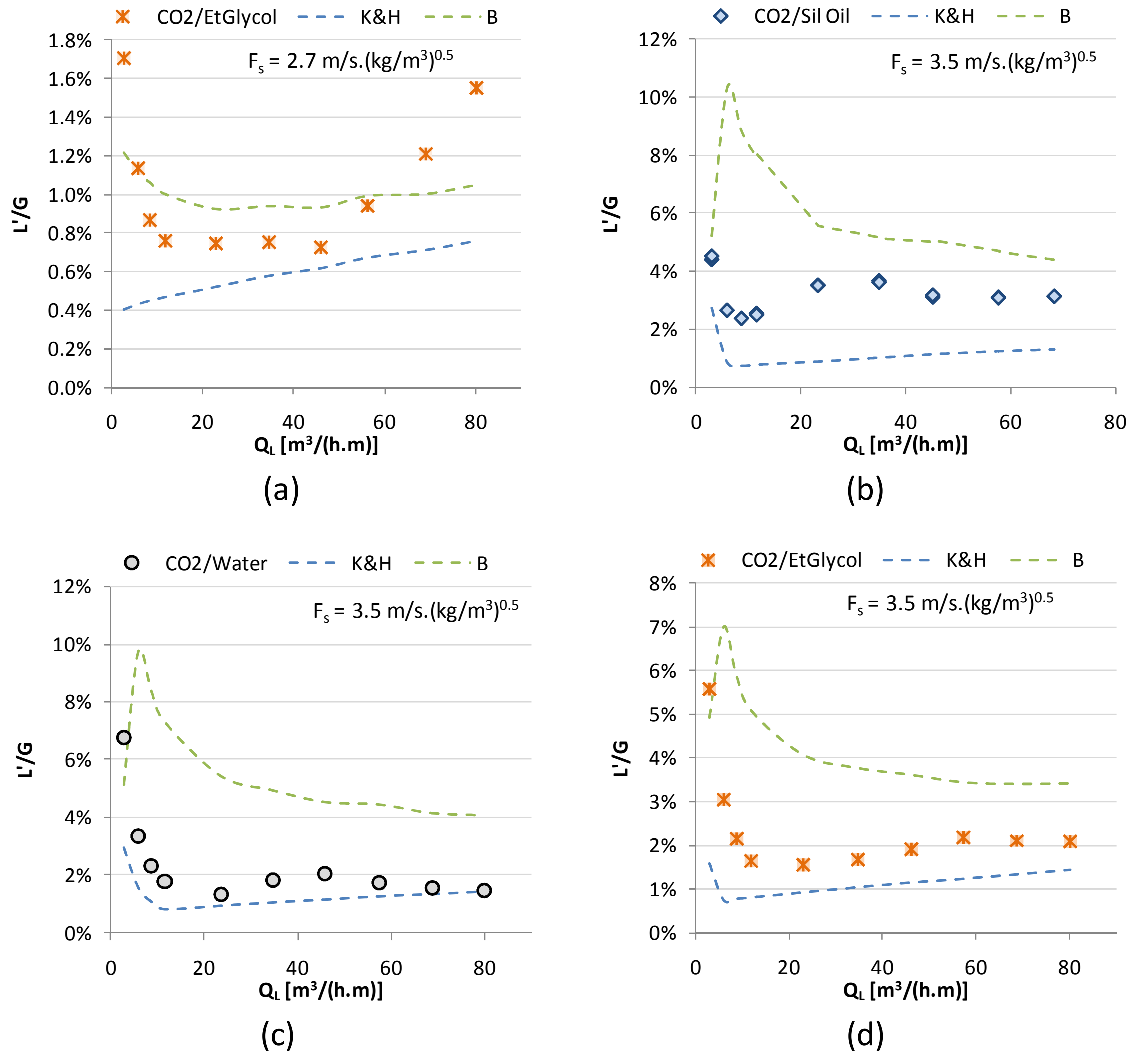

Figure 4. Comparison between experimental entrainment data and predictions made by the correlations of Kister and Haas (1988) [K&H], and Bennett et al. (1995) [B] for gas flow factors 2.7 and 3.5 m/s.(kg/m^3)$^{0.5}$.

Stellenbosch University http://scholar.sun.ac.za

Table 7. Deviations between the predictions made using the correlations of Kister and Haas (1988) and Bennett et al. (1995) compared to the experimental data shown in Figure 4.

CO_2/ethylene glycol			CO_2/silicone oil		
F_s = 2.7 [m/s(kg/m^3)$^{0.5}$]			F_s = 3.5 [m/s(kg/m^3)$^{0.5}$]		
Q_L [m^3/(h.m)]	K&H (%Dev)	B (%Dev)	Q_L [m^3/(h.m)]	K&H (%Dev)	B (%Dev)
2.9	-76%	-29%	3.0	-40%	16%
5.9	-62%	-1%	5.9	-67%	291%
8.6	-48%	23%	8.6	-68%	273%
11.9	-38%	33%	11.6	-68%	224%
23.0	-30%	24%	23.3	-74%	60%
34.5	-23%	25%	35.0	-71%	43%
46.1	-15%	29%	45.2	-63%	62%
56.2	-29%	5%	57.8	-59%	53%
68.9	-41%	-17%	68.5	-58%	42%
CO_2/water			CO_2/ethylene glycol		
F_s = 3.5 [m/s(kg/m^3)$^{0.5}$]			F_s = 3.5 [m/s(kg/m^3)$^{0.5}$]		
Q_L [m^3/(h.m)]	K&H (%Dev)	B (%Dev)	Q_L [m^3/(h.m)]	K&H (%Dev)	B (%Dev)
2.8	-56%	-24%	2.9	-72%	-12%
5.9	-53%	189%	5.9	-76%	129%
8.7	-54%	261%	8.6	-64%	174%
11.6	-55%	306%	11.9	-51%	209%
23.5	-31%	302%	23.1	-41%	161%
34.7	-42%	170%	34.8	-38%	126%
45.7	-45%	118%	46.1	-40%	89%
57.2	-27%	156%	57.3	-44%	57%
68.6	-14%	164%	68.8	-37%	61%
79.8	-4%	171%	80.2	-32%	62%

Stellenbosch University http://scholar.sun.ac.za

The influence of liquid physical properties

The correlations from Kister and Haas (1988) and Bennet et al. (1995) predict that an increase in liquid density will result in a decrease in entrainment (Uys et al., 2012a). From these correlations it is, however, not clear how surface tension and viscosity influence entrainment.

Based on the experimental data and visual observations it is evident that the influence of the different liquid physical properties on entrainment is of a complex nature. Silicone oil has the lowest surface tension (19.9 mN/m) and the highest viscosity (48.8 mPa.s) and it produced intermediate entrainment results. Isopar G has a fairly low surface tension (22.3 mN/m), the lowest density (739 kg/m^3) and the lowest viscosity (0.9 mPa.s) and it did not produce the highest entrainment, except where downcomer choke flooding occurred at very high vapour and liquid rates (see Figure 5 (c)). Generally the highest entrainment was measured with n-butanol, which has a low surface tension (22.8 mN/m), intermediate density (806 kg/m^3) and low viscosity (2.6 mPa.s), see Figure 5 (a) and (c). Increased entrainment for these liquids is therefore clearly caused by a intricate interaction between liquid density, surface tension and viscosity.

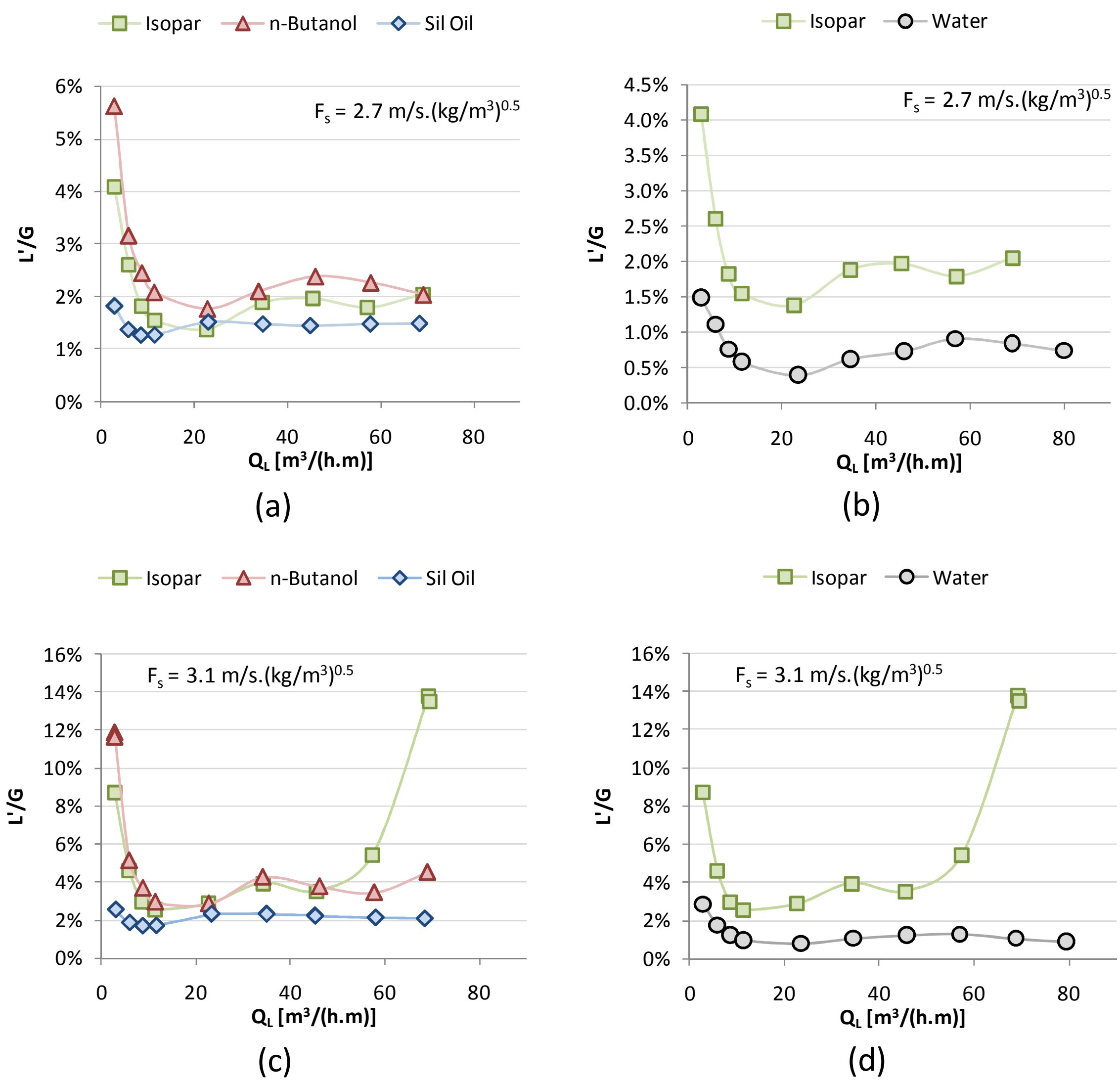

Figure 5. Entrainment results for (a) liquids with similar surface tension and ranging viscosity at F_s = 2.7 m/s.(kg/m^3)$^{0.5}$ (b) liquids with similar viscosity and ranging surface tension at F_s = 2.7 m/s.(kg/m^3)$^{0.5}$ (c) liquids with similar surface tension and ranging viscosity at F_s = 3.1 m/s.(kg/m^3)$^{0.5}$ (d) liquids with similar viscosity and ranging surface tension at F_s = 3.1 m/s.(kg/m^3)$^{0.5}$

This paper does not focus on developing a correlation based on the fundamentals that characterise entrainment. It is rather an attempt to offer a better understanding of how the liquid properties influence entrainment on a phenomenological basis.

The following observations of the influence of liquid physical properties on entrainment is based on the observations made by Decent et al. (2009), as well as the experimental data and the visual observations during experiments:

Stellenbosch University http://scholar.sun.ac.za

- An increase in liquid dynamic viscosity at constant surface tension (around 19 – 23 mN/m) will increase the froth height in the froth regime resulting in an increase in entrainment as shown by the n-butanol results. Increasing liquid viscosity inhibit gas passage through the liquid layer. Therefore the “bubbles” that are created as the gas starts to penetrate the liquid are pushed higher before the liquid film ruptures to form a channel. At the same time the liquid film (liquid jet) will stretch longer before the droplet breaks free to protrude into the vapour space. Therefore the froth height increases with an increase in viscosity. The froth height in this work is defined as the distinct boundary between the liquid continuous zone and the droplet/spray zone. The boundary of the froth is also defined as the region where the droplets are created and ejected into the spray and vapour space (see Figure 6). As the dynamic viscosity increases further (see silicone oil results in Figure 5 (a) and (c)) the viscosity will start to resist the formation (break up of the liquids jets/froth into droplets) of droplets and reduce the droplet ejection velocity. Thus, the froth height will still be higher than that of the lower viscosity liquids but the droplets will eject with a lower velocity into the vapour space. As a result silicone oil will entrain less than n-butanol.

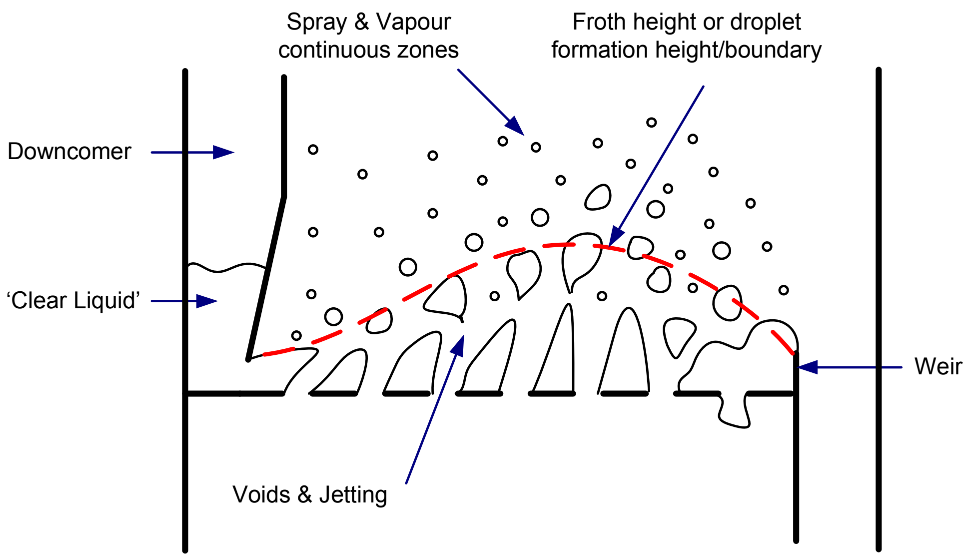

Figure 6. Graphical illustration of the froth height. The region below the froth height boundary is the liquid continuous zone and the region above the froth height boundary is the spray & vapour continuous zones.

- In the spray regime (Q_L < 12 $m^3/(h.m)$) there is no froth and the droplets are generated as the cross flowing liquid bridge the holes. Thus the influence of viscosity in the spray regime is solely related to droplet creation and ejection since there is no significant froth. The spray regime results highlight the resistance to droplet ejection from the holes for the high viscosity silicone oil. From this theory it is evident that liquid viscosity influences droplet size, droplet ejection velocity and froth height. Increasing liquid viscosity will increase froth height to a certain limit and also reduce droplet ejection velocity which will reduce entrainment. At the same time viscosity has a non-monotonic effect on droplet size (Decent et al., 2009) and could, under different conditions, create smaller or larger droplets.

- For the n-butanol system the viscosity is not high enough to reduce droplet ejection, but larger and more stable droplets, which are of greater mass than the Isopar G droplets, generate higher entrainment in the spray regime. Droplet diameter was not measured in this study and is based on visual observations. To get a holistic understanding of the dynamics related to the n-butanol system, compared to the other liquids, one has to consider the dynamic liquid head (hold-up) results for the different liquids shown in Figure 7. In this case liquid hold-up is calculated as the total pressure drop across the tray (measured from below test tray 1 to below the de-entrainment tray) minus the dry tray pressure drop. The pressure value is divided by the product of the liquid density and gravitational constant to give the liquid hold-up as a length parameter (see Lockett, 1986).

In the spray regime (Q_L < 12 m^3/(h.m) (identified using the Porter and Jenkins (1979) approach) of Figure 7 (a) and (b), n-butanol has the highest liquid hold-up of all the liquids. Therefore there is more interaction between the CO_2/n-butanol on the tray than the other liquids, resulting in higher entrainment.

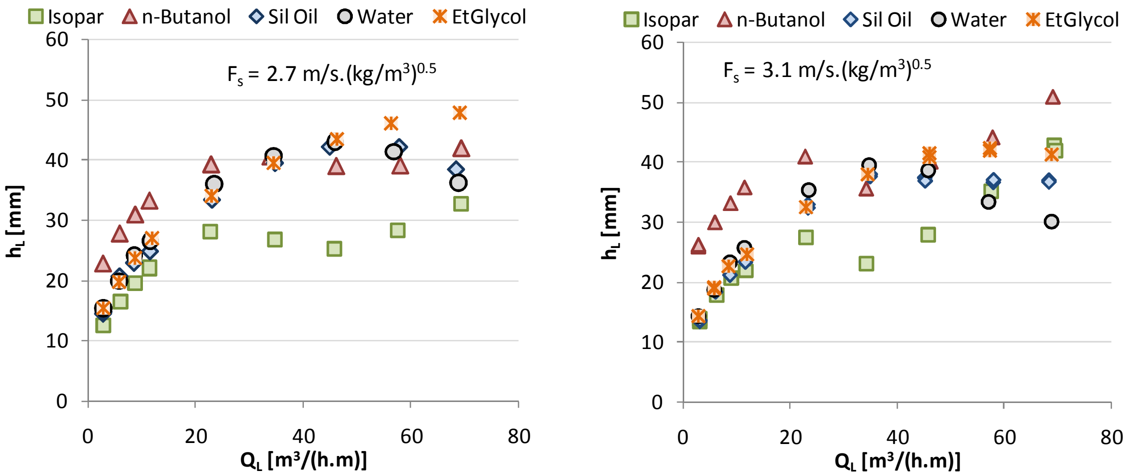

(a) (b)

Figure 7. Dynamic liquid hold-up results for all the liquids at a) F_s = 2.7 m/s.(kg/m^3)$^{0.5}$ and b) F_s = 3.1 m/s.(kg/m^3)$^{0.5}$.

To obtain some understanding of the influence of surface tension on entrainment it is important to refer to the results in Figure 5 (b) and (d). Since there are only two liquids, no conclusion can be drawn whether surface tension has a linear or non-linear effect on entrainment. However, in Figure 5 (b) and (d) water with the highest surface tension entrained less than Isopar G with the low surface tension. Water has a higher liquid density than Isopar G which will also reduce entrainment (Kister and Haas, 1988 and Bennett et al., 1995). There is consensus (Hunt et al., 1955 and Kister and Haas, 1988) that a reduction in surface tension will increase entrainment in the spray regime, which is consistent with the results of this study. However, this study shows that surface tension also increases entrainment in the froth regime.

In Figure 8, air, CO_2 and SF_6 data are used to determine if the same effects for liquid physical properties on entrainment are observed in different gases. The data were obtained in similar gas flow factor conditions ranging between 2.7 – 2.9 m/s.(kg/m^3)$^{0.5}$. In all the graphs water entrains the least and n-butanol the most. No air/n-butanol results were measured as n-butanol is highly flammable and poses the risk of fire and/or explosion. There are slight changes in the curvature of the trends when the CO_2 entrainment results are compared with the air and SF_6 results. This can be attributed to the change in gas viscosity and density. Information regarding the systems used in Figure 8 can be found in Uys et al. (2012b).

Stellenbosch University http://scholar.sun.ac.za

Therefore, from this data it is clear that a change in gas physical properties will change the effects liquid physical properties have on entrainment.

The results show that liquid viscosity greatly influences entrainment in three different areas. Increasing viscosity will lead to increasing froth height, decreasing droplet break-up length and decreasing droplet ejection velocity. More research is required to understand how the influence of each of these areas on entrainment are promoted by viscosity, liquid flow rate and gas velocity. Increasing froth height will increase entrainment, while decreasing break-up length- and droplet ejection velocity will decrease entrainment. At this moment the conditions for which the increasing effect of froth height dominates the decreasing effect of droplet ejection velocity- and break-up length on entrainment as viscosity is changed, have not been determined.

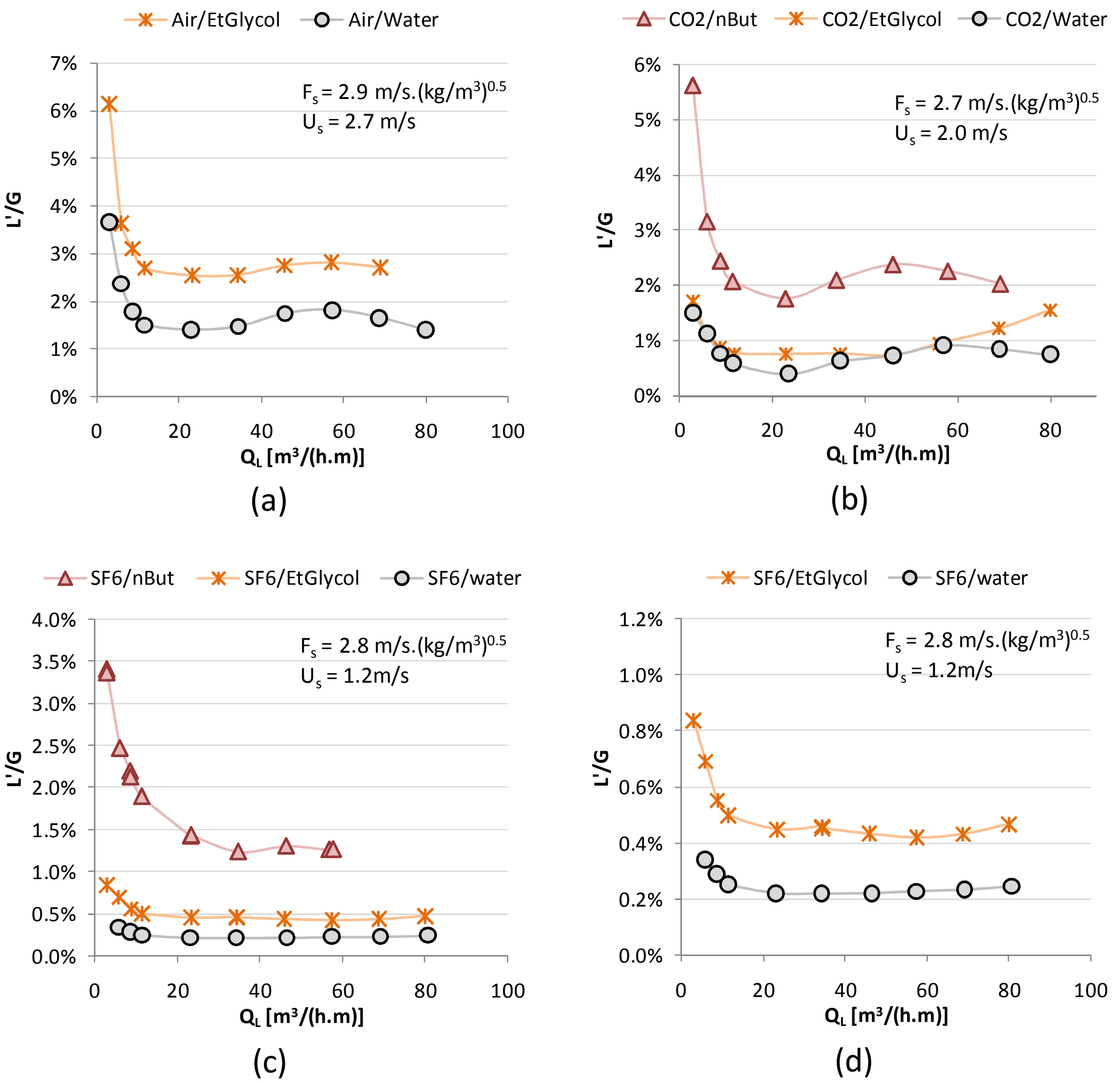

Figure 8. Entrainment results for (a) air/ethylene glycol and air/water at F_s = 2.9 m/s.(kg/m^3)$^{0.5}$ (b) CO_2/n-butanol, CO_2/ethylene glycol and CO_2/water at F_s = 2.7 m/s.(kg/m^3)$^{0.5}$ (c) SF_6/n-butanol, SF_6/ethylene glycol and SF_6/water at F_s = 2.8 m/s.(kg/m^3)$^{0.5}$ and (d) SF_6/ethylene glycol and SF_6/water at F_s = 2.8 m/s.(kg/m^3)$^{0.5}$ to show similarity to the air results in (a). A 615mm tray spacing was used.

Figure 9 is constructed to show the data depicted in Fig. 2 (b) and (d) as the percentage liquid that entrains (L'/L) for similar capacity flow factors. This gives an indication of how entrainment (L'/L) affects the separation efficiency. Low entrainment (L'/L) will result in higher separation efficiency than high entrainment (L'/L).

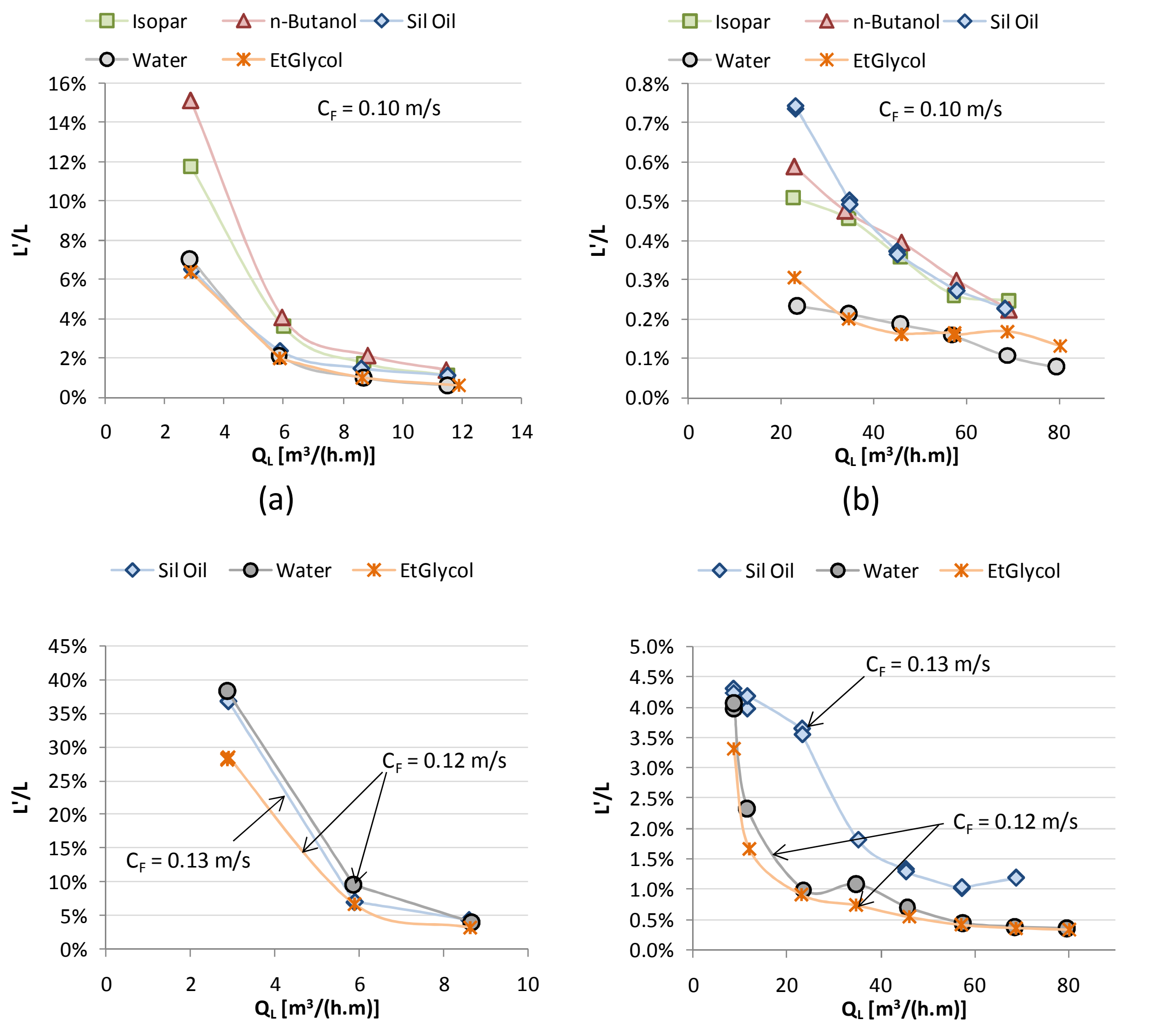

Figure 9. Fractional liquid entrainment data for (a) $Q_L < 12\ m^3/(h.m)$ and $C_F = 0.10$ m/s (except EtGlycol $C_F = 0.09$ m/s), (b) $Q_L > 20\ m^3/(h.m)$ and $C_F = 0.10$ m/s (except EtGlycol $C_F = 0.09$ m/s), (c) $Q_L < 12\ m^3/(h.m)$ and $C_F = 0.12$ m/s (except Silicone oil $C_F = 0.13$ m/s) and (d) $Q_L > 20\ m^3/(h.m)$ and $C_F = 0.12$ m/s (except Silicone oil $C_F = 0.13$ m/s).

Stellenbosch University http://scholar.sun.ac.za

5. Conclusions

Entrainment was measured for Isopar G, n-butanol, silicone oil, water and ethylene glycol contacted with CO_2. The experimental database developed consists of 256 data points and is completely unique to the data available in the literature. It was established that liquid dynamic viscosity significantly influences entrainment. This is contrary to what previous research on entrainment suggests. In this study it was found that surface tension and viscosity influences entrainment in both the froth and spray regimes. Entrainment is characterised by the mass of droplets ejecting at a certain velocity from the droplet formation height (measured from the tray) into the vapour space. It was found that dynamic viscosity influences the droplet size, ejection velocity as well as the droplet formation height. The summation of the effects of droplet creation (mass), ejection velocity and froth height (droplet formation height) will determine the percentage entrainment. Both dynamic viscosity and surface tension will influence the size of the droplet. Liquid density and size will determine the mass of the droplets. Therefore, a large mass of droplets ejecting into the vapour space with high velocities, close to the tray above, will cause high entrainment.

The results showed that increasing liquid viscosity both increased and decreased entrainment. The froth height, droplet ejection velocity and droplet formation height were influenced by the liquid viscosity. An increase in viscosity from 0.9 to 2.6 mPa.s increased entrainment. This result suggests that the increase in viscosity increased the froth height which increased entrainment. As the viscosity further increased to 48.8 mPa.s entrainment decreased. This showed that as viscosity increased past a certain point, the droplet ejection velocity and droplet formation height were reduced more than the effect of increasing froth height, resulting in a reduction in entrainment. An increase in surface tension decreases entrainment for the CO_2/water and CO_2/Isopar G systems. These findings agree with those of single droplet development, disintegration and size studies.

The results are compared to current entrainment prediction models from Kister and Haas (1988) and Bennett et al. (1995) to highlight their scope and limitations. None of these correlations include a liquid viscosity parameter. The correlation developed by Kister and Haas (1988) includes a surface tension parameter for the spray regime correlation. In general, the Kister and Haas (1988) correlation under-predicted entrainment and the correlation of Bennett et al. (1995) over-predicted entrainment at gas rates equal and

Stellenbosch University http://scholar.sun.ac.za

higher than 2.7 m/s.(kg/m^3)$^{0.5}$ for the different liquids. It has to be noted that the flow factors used during experiments were beyond the recommended range of application for the Bennett et al. (1995) correlations.

From the findings made in this study it is evident that the influence of viscosity and surface tension on entrainment can not be neglected. Both these parameters play a significant role in tray hydrodynamics and will influence liquid hold-up and entrainment.

Stellenbosch University http://scholar.sun.ac.za

6. Acknowledgements

The financial assistance of Sasol Technology (Pty) Ltd, Koch-Glitsch LP, Inher SA, and the Department of Trade and Industry (DTI) of South Africa through the Technology and Human Resources for Industry Programme (THRIP) towards this research is hereby acknowledged. We gratefully acknowledge the inputs from Dr. A. Erasmus and Dr. I. Nieuwoudt regarding the equipment design. Opinions expressed and conclusions arrived at are those of the authors and are not necessarily to be attributed to the sponsors.

Stellenbosch University http://scholar.sun.ac.za

7. Nomenclature

A_c	column area = 635x175mm	[m^2]
A_d	downcomer inlet area	[m^2]
A_f	fractional hole area = A_h/A_p	[-]
A_h	hole area	[m^2]
A_n	net column area = A_c-A_d	[m^2]
A_p	perforated area or bubbling area	[m^2]
C_F	capacity flow factor = $U_s.(\rho_g/(\rho_L-\rho_g))^{0.5}$	[m/s]
d_H, D_H	hole diameter	[mm, m]
FPL	tray flow path length	[mm]
F_s	superficial vapour factor = $U_s.\rho_g^{0.5}$	[$kg^{0.5}/m^{0.5}.s$]
g	gravitational constant = 9.81	[m/s^2]
G	gas mass flow rate	[kg/s]
h_w, H_w	outlet weir height	[mm, m]
h_F, H_F	froth height	[mm, m]
$h_{L,ct}$	clear liquid height at the regime transition	[mm]
h_w	weir height	[mm]
L	mass flow of liquid entering the tray	[kg/s]
L'	entrained liquid mass flow	[kg/s]
L_w	weir length	[mm]
P	hole pitch	[mm]
Q_L	liquid flow rate per weir length	[$m^3/(h.m)$]
s, S	tray spacing	[mm, m]
U_s	superficial gas velocity, based on tray perforated/bubbling area	[m/s]
Greek Letters		
ρ_g	gas density	[kg/m^3]
ρ_L	liquid density	[kg/m^3]
σ	surface tension	[mN/m]
μ_g	gas viscosity	[mPa.s]
μ_L	liquid viscosity	[mPa.s]
ζ	correction term for Eq. 1	

Stellenbosch University http://scholar.sun.ac.za

8. References

Bennett, D.L., Kao, A.S., Wong, L.W., 1995. A mechanistic analysis of sieve tray froth height and entrainment. AIChE , 41 (9), 2067-2082.

Bennett, D.L., Watson, D.N., Wiescinski, M.A., 1997. New correlation for sieve-tray point efficiency, entrainment, and section efficiency. AIChE, 43 (6), 1611 – 1626.

Böcker, S. and Ronge, G., 2005. Distillation of viscous systems. Chemical Engineering Technology, 28, 25-28.

Decent, S.P., King, A.C., Simmons, H.J.H., Părău, E.I., Wallwork, I.M., Gurney, C.J., Uddin, J., 2009. The trajectory and stability of a spiralling liquid jet: Viscous theory. Applied Mathematical Moddeling, 33, 4283-4302.

Colburn, A.P., 1936. Effect of entrainment on plate efficiency in distillation. Industrial and Engineering Chemistry, 28, 526.

Colwell, C., 1981. Clear liquid height and froth density on sieve trays. Industrial and Engineering Chemistry Process Design and Development, 20 (2), 298-307.

Fakhari, A., Rahimian, M.H., 2011. Investigation of deformation and breakup of a falling droplet using a multiple-relaxation-time lattice Boltzmann method. Computers & Fluids, 40, 156 – 171.

Hofhuis, P.A.M. and Zuiderweg, F.J., 1979. Sieve plates: dispersion density and flow regimes. Institution of Chemical Engineers Symposium Series, 1979, 56, 2.2/1-2.2/35.

Hunt, C. d'A., Hanson, D.N., Wilke, C.R., 1955. Capacity factors in the performance of perforated plate columns. AIChE Journal. 1 (4), 441 – 451.

Lockett, M.J., 1986. Distillation tray fundamentals, Cambridge University Press, Cambridge.

Li, Q.S., Song, C.Y., Wu, H.L., Liu, H., Qian, Y.Q., 2008. Performance and applications of flow-guided sieve trays for distillation of highly viscous mixtures. Korean Journal of Chemical Engineering, 25, 1509-1513.

Kister, H.Z, Pinczewski, W.V., Fell, C.J.D., 1981. Entrainment from sieve trays operating in the spray regime. Industrial and Engineering Chemistry Process Design and Development , 20 (3), 528-532.

Kister, H.Z., Haas, J.R., 1988. Entrainment from sieve trays in the froth regime. Industrial and Engineering Chemistry Research , 27 (12), 2331-2341.

Kister, H.Z., 1992. Distillation design, McGraw-Hill.

Stellenbosch University http://scholar.sun.ac.za

Mahiout, S. and Vogelpohl, A., 1985. Absorption of oxygen by aqueous glycerol solutions of squalane. Chemical Engineering Processes, 19, 221-226.

Nutter, D.E., 1979. Weeping and entrainment studies for sieve and v-grid trays in an air-oil system. Institution of Chemical Engineers Symposium Series No. 56, 3.2/47-3.2/62.

Pan, K.L., Hung, C.Y., 2010. Droplet impact upon a wet surface with varied fluid and surface properties. Journal of Colloid and Interface Science, 352, 186-193.

Porter, K.E., Jenkins, J.D., 1979. The interrelationship between industrial practice and academic research in distillation and absorption. Institution of Chemical Engineers Symposium Series No. 56 , 3.2/21-3.2/34.

Teller, A.J., Cheng, S.I., Davies, H.A., 1963. Protruded sieve tray performance. American Institute of Chemical Engineers. 9 (3), 407.

Thomas, W. J. and Ogboja, O., 1987. Hydraulic studies in sieve tray columns. Industrial and Engineering Chemistry Process Design and Development , 17 (4), 429-443.

Schultes, M., 2010. Research on mass transfer columns “old hat or still relevant?”. Distillation and Absorption Conference Proceedings, 37 – 42.

Uys, E.C., 2010. Entrainment in a sieve tray column, Masters Thesis. Stellenbosch University, South Africa.

Uys, E.C., Schwarz, C.E., Burger, A.J., Knoetze, J.H., 2012a. New froth behaviour observations and comparison of experimental sieve tray entrainment data with existing correlations. Submitted for review to Chemical Engineering Research and Design. DOI 10.1016/j.cherd.2012.05.008

Yanagi, T., Sakata. M., 1979. Performance of a commercial scale sieve tray. Institution of Chemical Engineers Symposium Series No. 56 , 5.1/1-5.1/47.

Zuiderweg, F.J., 1982. Sieve trays, a view on the state of the art. Chemical Engineering Science, 37 (10) 1441 – 1464.

Stellenbosch University http://scholar.sun.ac.za

Manuscript 4

A new simplified correlation to predict the influence of tray spacing and gas and liquid physical properties on entrainment inside a sieve tray column

Ehbenezer C. Uys[a], Andries J. Burger[a], Johannes H. Knoetze[a,4]

[a]Department of Process Engineering, University of Stellenbosch, Private Bag X1, Matieland 7602, South Africa

Status: To be submitted

Journal: Chemical Engineering Research and Design

Keywords: Entrainment correlation, sieve tray data, liquid physical properties, tray spacing.

.

[4]Corresponding author. Tel.: +27 21 8084488; fax: +27 21 8082059.

E-mail address: jhk@sun.ac.za (Johannes. H. Knoetze)

Stellenbosch University http://scholar.sun.ac.za

1. Abstract

Current entrainment prediction correlations were developed based on databases with a majority of air/water data. They therefore fail to accurately predict the influence of gas and liquid physical properties on entrainment. The reason for the limited non-air/water data available in the literature is related to the cost of obtaining such data. Generally these entrainment prediction correlations are complex and depend on estimations of clear liquid height and froth density if the data are not available. The aim of this work is therefore to develop a correlation that predicts the influence of gas and liquid physical properties on entrainment inside a sieve tray column. To achieve the objective, a large entrainment databank has been developed using five liquids, three gasses and four tray spacings. Liquid flow rates ranged from 2.9 to 91 $m^3/(h.m)$ with gas flow factor ranging from 1.5 to 4.8 $m/s.(kg/m^3)^{0.5}$. The physical property ranges include: liquid density 739 – 1102 kg/m^3, liquid dynamic viscosity 0.9 – 48.8 mPa.s, surface tension 20 – 61 mN/m, gas density 1.2 – 5.9 kg/m^3, gas viscosity $1.49x10^{-2}$ – $1.86x10^{-2}$ mPa.s, tray spacing 315 – 615 mm. The column has a constant flow path length of 475 mm. Newly measured entrainment data for CO_2/Isopar, CO_2/n-butanol, air/ethylene glycol, CO_2/ethylene glycol, air/silicone oil and CO_2/silicone oil are reported in this work. A new dimensionless correlation with much improved accuracy (R^2 = 85%) over existing predictions (R^2 = 61% for Kister and Haas (1988) and R^2 = 23% for Bennett et al. (1995)) is presented here. This correlation can also be used to successfully (R^2 = 92%) predict the fraction of liquid entering the tray that entrains.

Stellenbosch University http://scholar.sun.ac.za

2. Introduction

Distillation is a unit operation of significant importance to the chemical industry. To lower operating cost, separation efficiency and throughput has to be increased. One way of achieving this is to improve the understanding of the hydrodynamics inside distillation columns so that the appropriate design and operating strategies can be utilised. Column capacity and design is determined by entrainment prediction correlations. Uys (2010) and Uys et al. (2012a, b and c) showed that current prediction correlations, based mainly on air/water data obtained from various experimental setups and institutions, can not accurately predict entrainment for systems other than air/water. There is uncertainty in how the difference between air/water physical properties and the physical properties of distillation systems will affect entrainment (Bennett and Ludwig, 1994). Consequently columns have to be over designed. This could lead to an increase in energy consumption to ensure the column operates in the designed flow ranges. As the cost of energy is continuously escalating, small improvements in tray and column design could lead to large savings in operating costs.

Various researchers developed entrainment correlations as shown in Table 1 to 3. The first work was done by Hunt et al. (1955) who did not identify the regime applicable to their correlation. Kister and Haas (1988) later specified that the correlation of Hunt et al. (1955) relates to the froth regime. Thomas and Ogboja (1978) also developed a correlation for entrainment related to the froth regime. Through a series of papers Uys et al. (2012a, b and c) demonstrated the limitations of current entrainment prediction correlations. The main limitation is the inability of the correlations to include the effect of liquid viscosity on entrainment. Apart from that, all the correlations, except that of Koziol and Mackowiak (1990) in Table 2, make use of either the clear liquid height (h_L) or froth height (h_F). The use of the clear liquid height and froth height is a fundamental approach to correlate entrainment to the difference in height between the top of the froth and the tray above. The smaller this difference, the more entrainment is expected (Kister and Haas, 1988). Not all researchers developed methods to estimate clear liquid height and froth height. Alternatively clear liquid height data must be used if that is available, which is normally not the case. Froth height data are very difficult to measure as the froth does not have a distinguishable upper surface (Lockett, 1986).

Stellenbosch University http://scholar.sun.ac.za

Table 1. Entrainment correlations developed by Hunt et al. (1955) and Thomas and Ogboja (1978) for froth regime (Kister and Haas, 1988) conditions.

Author	Entrainment Correlations	
Hunt et al. (1955)	$$\frac{L'}{G} = 3.08\text{x}10^{5}\left(\frac{73}{\sigma}\right)\left(\frac{U_s}{s-2.5h_L}\right)^{3.2}$$	**(1)**
Thomas and Ogboja (1978)	$$\frac{L'}{G} = 26.52\left(\frac{U_s}{s-h_f}\right)^{0.77}$$	**(2)**
	$$h_f = 0.0894Q_L + 1.279u_s\sqrt{\rho_g} + 3.52 \quad \text{for rectangular column}$$	**(3)**
	$$h_f = 0.0614Q_L + 1.77u_s\sqrt{\rho_g} + 4.83 \quad \text{for round column}$$	**(4)**

Stellenbosch University http://scholar.sun.ac.za

Table 2. Spray regime correlations by Zuiderweg (1982) and Koziol and Mackowiak (1990).

Author	Entrainment Correlations
Zuiderweg (1982)	$\left(\frac{L'}{G}\right)_s = 1\times10^{-8} A_f \left(\frac{h_L}{S}\right)^3 \left(\frac{G}{L}\right)^2 \left\{1+265\left[\frac{U_s}{(gh_L)^{0.5}}\left(\frac{\rho_g}{\rho_l}\right)^{0.5}\right]^{1.7}\right\}^3$ **(5)**
	$h_L = 0.6\left(\frac{\psi p}{1000}\right)^{0.25}\left(\frac{h_w}{1000}\right)^{0.5}$ **(6)** $\psi = \frac{Q_L}{3600 u_s}\left(\frac{\rho_l}{\rho_g}\right)^{0.5}$ **(7)**
Koziol and Mackowiak (1990)	$\left(\frac{L'}{G}\right)_s = 0.37 Fr_G^{2/3} Fr_L^{-1/5} Fl^{-1/3}\left(\frac{\rho_g}{\rho_l}\right)\left(\frac{We}{Co}\right)^{133.7 Fl^{-1/6}}$ **(8)** $Fr_G = \frac{F_h^2}{S(\rho_l-\rho_g)g}$ **(9)** $Fl = \frac{\sigma^3\rho_g^2}{\mu_g^4(\rho_l-\rho_g)g}$ **(10)** $We = \frac{F_s^2}{\left(\sigma g(\rho_l-\rho_g)\right)^{1/2}}$ **(11)** $Fr_L = \frac{V_L^2(1+e_L)^2}{gS^2D_c^3}$ itterate from $e_L = 0$ **(12)** $Co = \frac{A_f S}{D_c}\left(\frac{D_c}{D_h}\right)^{1/2}$ **(13)** $e_L = \frac{V_g}{V_L}\left(\frac{L'}{G}\right)_s\left(\frac{\rho_g}{\rho_l}\right)$ **(14)**

Table 3. Correlations for prediction of entrainment in both regimes by Kister and Haas (1988) and Bennett et al. (1995).

Author	Entrainment Correlations	
Kister & Haas (1988)	$\left(\frac{L'}{G}\right)=\left(\frac{L'}{G}\right)_s \; or \left(\frac{L'}{G}\right)_f \; or \left(\frac{L'}{G}\right)_w$ (whichever is largest)	**(15)**
	$\left(\frac{L'}{G}\right)_w=\frac{0.3d_H p^2}{h_L\left(s-h_f\right)^2}$	**(16)**
	$\left(\frac{L'}{G}\right)_{froth}=111\left(\frac{U_s}{s-h_F}\right)^2 d_H^{\;0.5}\left(1+\zeta\right)$	**(17)**
	$\zeta=\frac{0.00225}{A_f^{\;3}}\left(\frac{h_{L,t}}{h_L}-1\right)$ for $h_{L,t}>h_L$ $\zeta=0$ for $h_{L,t}\le h_L$	**(18)**
	$\left(\frac{L'}{G}\right)_{spray}=4.742^{(10/\sqrt{\sigma})^{1.64}}\left(872\left(\frac{U_s h_{L,ct}}{\sqrt{d_H s}}\right)^4\left(\frac{\rho_g}{Q_L\rho_l}\right)\left(\frac{\rho_l-\rho_g}{\sigma}\right)^{0.25}\right)^{\left(10/\sqrt{\sigma}\right)}$	**(19)**
	$h_{L,ct}=\frac{\left(\frac{0.4974A_f^{\;-0.791}d_H^{\;0.833}}{1+0.013Q_L^{\;-0.59}A_f^{\;-1.79}}\right)}{1+0.00262h_w}\left(\frac{996}{\rho_l}\right)^{0.5\left(1-0.00091d_H/A_f\right)}$	**(20)**
Bennett *et al.* (1995) (Air/Water)	$\left(\frac{L'}{G}\right)_{spray}=0.0050\left(\frac{K_s^2}{g\phi_e S}\right)^{1.26}\left[\frac{gH_L}{K_s^2}+\frac{9\sqrt{3}}{2A_f}\left(1+4.77\left\{\frac{D_H}{H_L}\right\}^{3.29}\right)\right]^{1.26}\varepsilon^{\beta}\left(\frac{\rho_L}{\rho_g}\right)^{0.5}$	**(21)**
	$\left(\frac{L'}{G}\right)_{froth}=0.00164\left(\frac{K_s^2}{g\phi_e S}\right)^{1.86}\left[\frac{gH_L}{K_s^2}+\frac{9\sqrt{3}}{2A_f}\left(1+6.9\left\{\frac{D_H}{H_L}\right\}^{1.85}\right)\right]^{1.86}\left(\frac{\rho_L}{\rho_g}\right)^{0.5}$	**(22)**
	$K_s=U_s\sqrt{\frac{\rho_g}{\rho_l}}$ **(23)** $H_L=\phi_e H_{Fe}$	**(24)**
	$\phi_e=\exp[-12.55K_s^{\;0.91}]$ **(25)** $\varepsilon=\frac{H_L}{H_F}$	**(26)**
	$H_{Fe}=H_w+0.501+0.439\exp\left(-137.8H_w\right)\left(\frac{Q_L}{3600\phi_e}\right)^{2/3}$	**(27)**
	$\beta=0.5\left(1-\tanh\left[1.3\ln\left(\frac{H_L}{D_H}\right)-0.15\right]\right)$	**(28)**

Stellenbosch University http://scholar.sun.ac.za

Bennett and Ludwig (1994) showed that additional non-air/water data are required to develop more accurate entrainment prediction correlations than the existing correlations. One reason for the limited non-air/water data is attributed to the cost of establishing facilities which are capable of conducting tests over a large range of conditions that can represent industrial distillation hydrodynamics. The other reason for the limited non-air/water entrainment data is due to restricted publication of industrial research (Bennett and Ludwig, 1994). Uys (2010) and Uys et al. (2012a) developed a facility to conduct tray hydrodynamic experiments. New non-air/water data were measured in this facility shortly afterwards by Uys et al. (2012b and c) who investigated the influence of gas and liquid physical properties on entrainment.

This work is a continuation of the work done by Uys et al. (2012a, b and c) and serves to correlate the influence of gas and liquid physical properties on entrainment. In this manuscript the aim is to develop a correlation that is capable of predicting the influence of gas and liquid physical properties on entrainment without using clear liquid height or froth height. As neither liquid height nor froth height is used, the influence of tray spacing is incorporated to make the correlation more versatile. Part of the aim is to make the correlation as simple as possible, yet accurate. Future projects will investigate the influence of tray geometry for systems other than air/water so that a more general prediction correlation can be developed.

Stellenbosch University http://scholar.sun.ac.za

3. Composite database

In order to develop the correlation that focuses on the influence of gas and liquid physical properties, a comprehensive database is required. Uys (2010) established a facility capable of conducting entrainment, pressure drop and weeping tests for a range of gas and liquid flow rates, tray spacings, tray designs and, gas and liquid physical properties. Slight modifications were made to the experimental setup by Uys et al. (2012a). After that tests were conducted to graphically show the influence of gas physical properties (Uys et al. (2012b)) as well as the influence of liquid physical properties on entrainment (Uys et al., 2012c).

In this work the database of Uys et al. (2012a, b and c) is extended by test data at different tray spacings for CO_2 and water, ethylene glycol, silicone oil, n-butanol and Isopar G. Tests were also conducted with air and ethylene glycol, and silicone oil. These tests were conducted for three tray spacings, 315 mm, 415 mm and 515 mm. The cumulative database consists of more than 1700 data points. A summary of the test systems and ranges is presented in Table 4. The reason for the difference in surface tension between air/ethylene glycol and CO_2/ethylene glycol is explained in Uys et al. (2012c). More information regarding the experimental setup, experimental methods and analysis can be found in Uys (2010) and Uys et al. (2012a, b and c). The database was categorised into spray regime data and froth regime data. Regime determination occurred using the method of Porter and Jenkins (1979). This method is not necessarily the most accurate but in this case it was the most practical approach. Porter and Jenkins (1979) identified regime transition at the point of minimum entrainment when the liquid rate is increased during constant gas flow conditions. Their technique is graphically explained in Figure 1. It has to be noted that the transition from spray to froth regime is gradual and in actual fact a transition zone. However, for the purpose of this work and the sake of simplicity, the minima will act as the transition line between the regimes.

Table 4. Systems and variable ranges covered during experimental runs.

Range / System	U_s [m/s]	Q_L [m^3/(h.m)]	s [mm]	ρ_v [kg/m^3]	ρ_L [kg/m^3]	σ [mN/m]	μ_L [mPa.s]	μ_G [mPa.s]
air/water	2.3 - 3.1	2.9 - 81	615	1.2	997 - 998	58	0.9	0.0186
air/ethylene glycol	1.4 - 4.0	2.9 - 92	315 - 615	1.2	1102	37	15	0.0186
air/silicon oil	1.4 - 3.1	2.9 - 80	315 - 615	1.2	955	20	49	0.0186
CO_2/water	1.4 - 2.9	2.9 - 80	315 - 615	1.8	997	60	0.9	0.0149
CO_2/ethylene glycol	1.2 - 2.9	2.9 - 80	315 - 615	1.8	1095	35	15	0.0149
CO_2/Silicon oil	1.4 - 2.9	2.9 - 69	315 - 615	1.8	955	20	49	0.0149
CO_2/n-butanol	1.2 - 2.3	2.9 - 69	315 - 615	1.8	806	23	2.6	0.0149
CO_2/Isopar G	1.2 - 2.3	2.9 - 70	315 - 615	1.8	739	22	0.9	0.0149
SF_6/water	1.2 - 2.0	2.9 - 92	615	5.7 - 5.8	998	60	1.0	0.0151
SF_6/ethylene glycol	1.2 - 2.0	2.9 - 80	615	5.7 - 5.8	1097	35	15	0.0151
SF_6/n-butanol	1.0 - 1.4	2.9 - 58	615	5.7 - 5.8	819	23	2.6	0.0151

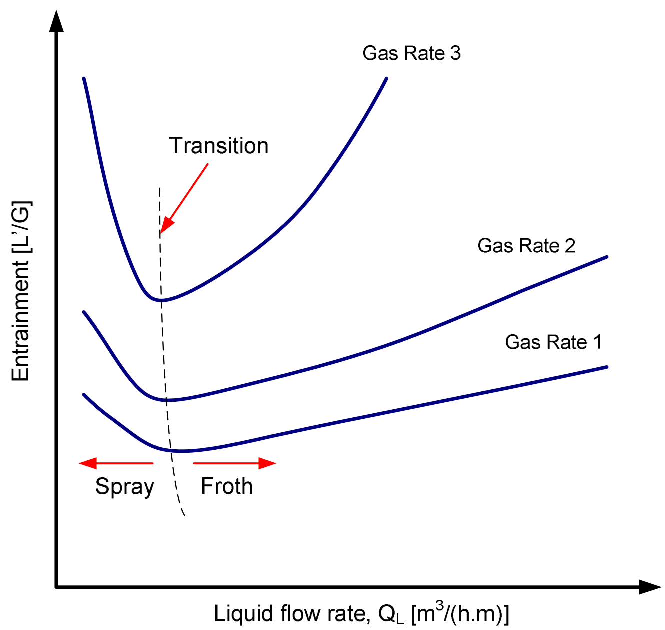

Figure 1. Regime identification method from Porter and Jenkins (1979).

Stellenbosch University http://scholar.sun.ac.za

4. Model development

The parameters that influence entrainment based on the scope of this work are shown in Equation (29). Dimensionless groups (shown in Equation (30)) were then developed using dimensional analysis, based on the Buckingham π-theorem. Most of the correlations in Tables 1 to 3 were developed from dimensionless groups where some of the parameters were expanded to capture the effects of certain variables and phenomena. The ratio of Q_L/U_s has the dimension of length (L). Therefore Equation (30) can be seen as modified versions of existing dimensionless numbers as shown in Equation (31).

$$\frac{L'}{G} = f\left(U_s^{\,a}, \rho_g^{\,b}, Q_L^{\,c}, \rho_l^{\,d}, \sigma^e, \mu_l^{\,f}, g^g, \mu_g^{\,h}, s^i\right) \quad \textbf{(29)}$$

Applying the Buckingham π-theorem (see method in section 6 in the Appendix) this leads to:

$$\begin{aligned}\frac{L'}{G} &= f\left(\left(\frac{\rho_l}{\rho_g}\right)^{a_1}, \left(\frac{\sigma}{\rho_g U_s Q_L}\right)^{a_2}, \left(\frac{\mu_L}{\rho_g Q_L}\right)^{a_3}, \left(\frac{gQ_L}{U_s^{\,3}}\right)^{a_4}, \left(\frac{\mu_G}{\rho_g Q_L}\right)^{a_5}, \left(\frac{U_s s}{Q_L}\right)^{a_6}\right) \\ &= k\left(\frac{\rho_l}{\rho_g}\right)^{a_1}\left(\frac{\sigma}{\rho_g U_s Q_L}\right)^{a_2}\left(\frac{\mu_L}{\rho_g Q_L}\right)^{a_3}\left(\frac{gQ_L}{U_s^{\,3}}\right)^{a_4}\left(\frac{\mu_G}{\rho_g Q_L}\right)^{a_5}\left(\frac{U_s s}{Q_L}\right)^{a_6}\end{aligned} \quad \textbf{(30)}$$

In Equation (30) the following well-known dimensionless groups can be identified:

$$\left(\frac{\sigma}{\rho_g U_s Q_L}\right) \Leftrightarrow \frac{1}{We^*}, \left(\frac{\mu_L}{\rho_g Q_L}\right) \Leftrightarrow \frac{1}{\mathrm{Re}_L^{\;*}}, \left(\frac{gQ_L}{U_s^{\,3}}\right) \Leftrightarrow \frac{1}{Fr^*}, \left(\frac{\mu_G}{\rho_g Q_L}\right) \Leftrightarrow \frac{1}{\mathrm{Re}_g^{\;*}} \quad \textbf{(31)}$$

To ensure that the contribution of each group is unaffected by scale, all groups were normalised (using constants N_1 to N_6 in Equation (32)) to a range between 0 and 1 before linear regression or optimisation took place. In the first attempt a simple linear regression, using the least squares method, was used for the spray and froth regime data after linearization of Equation (30) as shown in Equation (32). This did not yield great results. A non-linear model structure, as shown in equation (33), was then used, which improved results.

$$\log\left(\frac{L'}{G}\right) = \log k + a_1 \log\left(\frac{\rho_l}{N_1\rho_g}\right) + a_2 \log\left(\frac{\sigma}{N_2\rho_g U_s Q_L}\right) + a_3 \log\left(\frac{\mu_L}{N_3\rho_g Q_L}\right) + \ldots$$
$$a_4 \log\left(\frac{gQ_L}{N_4 {U_s}^3}\right) + a_5 \log\left(\frac{\mu_G}{N_5\rho_g Q_L}\right) + a_6 \log\left(\frac{U_s s}{N_6 Q_L}\right) \quad \textbf{(32)}$$

$$\frac{L'}{G} = k_0 \left(\left(\frac{\rho_l}{N_1\rho_g}\right)^{b_1} + k_1\right)^{a_1} \left(\left(\frac{\sigma}{N_2\rho_g U_s Q_L}\right)^{b_2} + k_2\right)^{a_2} \left(\left(\frac{\mu_L}{N_3\rho_g Q_L}\right)^{b_3} + k_3\right)^{a_3} \ldots.$$
$$\left(\left(\frac{gQ_L}{N_4 {U_s}^3}\right)^{b_4} + k_4\right)^{a_4} \left(\left(\frac{\mu_G}{N_5\rho_g Q_L}\right)^{b_5} + k_5\right)^{a_5} \left(\left(\frac{U_s s}{N_6 Q_L}\right)^{b_6} + k_6\right)^{a_6} \quad \textbf{(33)}$$

To determine the constants and coefficients in Equation (33), the MATLAB Global Optimisation Toolbox was used to find a global optimum in terms of the regression parameter set on the regression error surface. Due to sensitivity to initial conditions of the solution, a multi start function was selected from the toolbox. The initial parameter values, limited to pre-defined parameter bounds, were randomly selected at each restart. Local optimisation was conducted by the MATLAB function, *fmincon*, as a constrained minimisation. Constrained optimality used a Lagrange multiplier structure, subject to Karush-Kuhn-Tucker conditions. The local optimisation algorithm computes a quasi-Newton approximation to the Hessian of the Lagrangian, and can take large integration steps, so as to reduce convergence time. A sum-squared error objective function, point-wise scaled by the measured entrainment values, was defined to ensure a global optimum for low and high entrainment values, and avoid a minimisation of errors dominated by high entrainment values.

Spray regime entrainment

By replacing the last group of equation (30) with a Froude number that incorporates tray spacing as the length parameter (equation (34)), improved results were obtained for the spray regime correlation. Equation (35) shows the final spray regime correlation. The quality of the fit indicated by "Uys" is compared with the performance of the correlations of Kister and Haas (1988) (K & H), Bennett et al. (1995) (Bennett), Zuiderweg (1982) (Zuiderweg) and Koziol and Mackowiak (1990) (K & M) in Table 5.

$$\left(\frac{U_s s}{Q_L}\right)^{a_6} \Leftrightarrow \left(\frac{U_s^{\ 2}}{gs}\right)^{a_6} \tag{34}$$

$$\left(\frac{L'}{G}\right)_s = 817\left(\left(\frac{\rho_l}{945\rho_g}\right)^{-1.98} + 4.27\right)^{1.33}\left(\frac{\sigma}{9.7Q_L\rho_g U_s}\right)^{-0.673}\left(\left(\frac{\mu_l}{15.9Q_L\rho_g}\right)^{0.9} + 6\right)^{-6} \ldots$$
$$\left(\frac{U_s^{\ 3}}{1.86Q_L g}\right)^{-0.171}\left(\frac{\mu_g}{6\text{x}10^{-3}Q_L\rho_g}\right)^{1.347}\left(\frac{U_s^{\ 2}}{3.44\times10^{-3}gs}\right)^{1.53} \tag{35}$$

Table 5. Performance of the different correlations when compared to the measured entrainment for the spray regime with Q_L < 12 $m^3/(h.m)$ and within the ranges specified in Table 8.

Statistics	Uys	K & H	Bennett	Zuiderweg	K & M
Mean squared error	6.9E-05	5.7E-04	7.2E-04	5.6E-04	5.9E-04
Sum squared error	0.04	0.30	0.39	0.30	0.32
Pearson R^2	88.2%	54.9%	37.0%	75.3%	55.0%

Froth regime entrainment

Uys et al. (2012a) showed that the tray flow path length (L_{FPL} = 0.475 m in this work) influences the dispersion profile in the froth regime and therefore entrainment. To capture this effect to some extent, another dimensionless group, shown in equation (36), was added to the list of groups in equation (30). The final froth regime correlation is presented in equation (37). The quality of the fit (Uys) is compared with the performance of the correlations of Kister and Haas (1988) (K & H) and Bennett et al. (1995) (Bennett) in Table 6.

$$\left(\frac{Q_L}{U_s L_{FPL}}\right) \tag{36}$$

$$\left(\frac{L'}{G}\right)_f = 547\left(\left(\frac{\rho_l}{949\rho_g}\right)^{0.08} + 2.19\right)^{-3.72}\left(\left(\frac{\sigma}{9.55Q_L\rho_g U_s}\right)^{0.39} + 0.94\right)^{-5.12}\left(\left(\frac{\mu_l}{9.35Q_L\rho_g}\right)^{2.69} + 2.18\right)^{-4.81} \ldots$$

$$\left(\left(\frac{U_s^3}{0.433Q_L g}\right)^{0.41} + 0.28\right)^{5.81}\left(\left(\frac{\mu_g}{2.96\times10^{-3}Q_L\rho_g}\right)^{-3.38} + 1.47\right)^{-0.27} \ldots \quad \textbf{(37)}$$

$$\left(\left(\frac{U_s s}{223Q_L}\right)^{-1.68} + 0.97\right)^{1.63}\left(\left(\frac{Q_L}{162U_s L_{FPL}}\right) + 1.41\right)^{-3.44}$$

Table 6. Performance of the different correlations when compared to the measured entrainment for the froth regime with $Q_L > 23$ $m^3/(h.m)$ and within the ranges specified in Table 8.

Statistics	Uys	K & H	Bennett
Mean squared error	1.07E-04	5.76E-04	7.00E-04
Sum squared error	0.06	0.35	0.42
Pearson R^2	84.0%	66.9%	15.3%

Entrainment correlation

No regime identification correlation was developed in this study. However, the entrainment prediction correlation was developed so that the correlation, spray or froth regime, which ever yields the largest result, should be used as shown in equation (38). This approach was also used by Kister and Haas (1988). Table 7 compares the performance of the proposed correlation and those of Kister and Haas (1988) and Bennett et al. (1995) for all the data within the ranges shown in Table 8, 9 and 10.

$$\left(\frac{L'}{G}\right) = \left(\frac{L'}{G}\right)_s \; or \left(\frac{L'}{G}\right)_f \text{ (whichever is largest)} \quad \textbf{(38)}$$

Table 7. Performance of the entrainment correlation (Uys) compared to that of Kister and Haas (1988) and Bennett et al. (1995) compared to all date within the range of Table 8.

Statistics	Uys	K & H	Bennett
Mean squared error	8.91E-05	5.73E-04	7.11E-04
Sum squared error	0.10	0.65	0.81
Pearson R^2	85.4%	61.4%	23.3%

5. Applications and comparisons

The experimental data measured in this and previous works (Uys et al., 2012a, b and c) covers a large range of phenomena and regimes. At low tray spacing (315 mm) very high entrainment was observed for high liquid rates (> 46 $m^3/(h.m)$). No significant spray regime entrainment was observed for this low spacing. Figure 2 shows the high entrainment measured at high liquid rates for CO_2/Isopar G and CO_2/n-butanol at 315 mm tray spacing. This phenomenon is not limited to these two systems and was also observed for the other systems at these conditions. The correlations from Kister and Haas (1988) (K & H), Bennett et al. (1995) (B), Zuiderweg (1982) (Z), Koziol and Mackwiak (1990) (K & M), as well as the correlation developed in this work, fail to accurately predict entrainment at liquid rates exceeding 46 $m^3/(h.m)$. As Kister and Haas (1988) did not develop a froth height correlation, the Colwell (1981) correlation is used to calculate the predicted entrainment as recommended by Kister and Haas (1988). The correlations of Hunt et al. (1955) and Thomas and Ogboja (1978) is not compared to the data, due to its inferior performance.

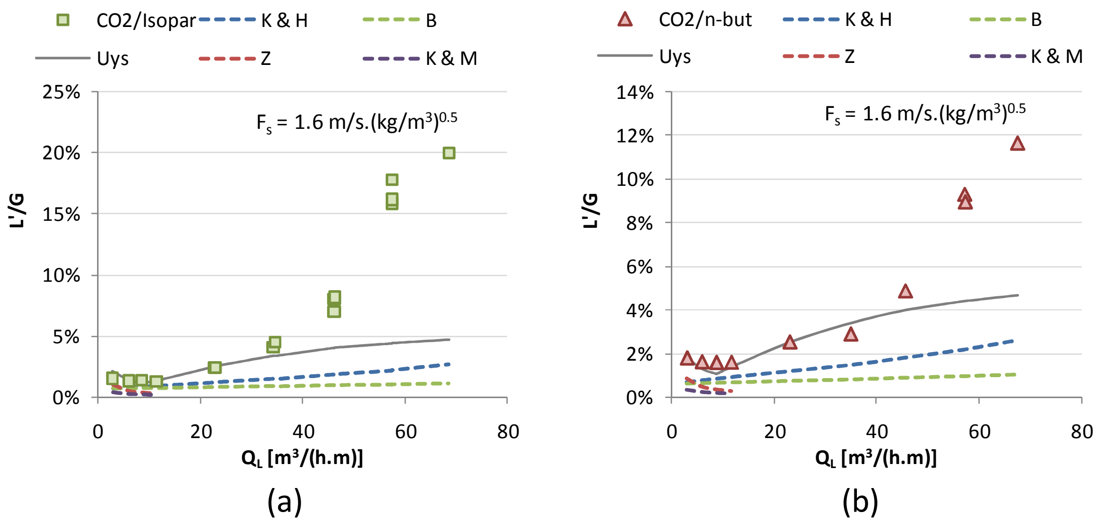

Figure 2. High entrainment observed at 315 mm tray spacing for CO_2/Isopar and CO_2/n-butanol at a flow factor of 1.6 $m/s.(kg/m^3)^{0.5}$ compared with predictions from Kister and Haas (1988) (K & H), Bennett et al. (1995) (B), the model developed in this work (Uys), Zuiderweg (1982) (Z) and, Koziol and Mackowiak (1990) (K & M).

Range of application

As with all correlations, the applicability of the correlation developed in this study (Uys) is limited to a certain range. This range of application is given in Table 8. Table 9 and 10 present the application ranges for the spray and froth regimes in terms of the dimensionless groups of the spray and froth regime correlations developed in this paper. The application ranges of the correlations (Exp data) are also compared to C1 – C12 alkane atmospheric distillation conditions in Table 9 and 10 for the dimensionless groups. This shows how the experimental ranges compare to C1 – C12 alkane ranges. The experimental ranges cover all the C1 – C12 alkane ranges in both regimes except for G3 where the experimental range is smaller. The G3 ranges for the alkanes are much lower than that of the experimental range. This is due to the very low viscosity (0.12 - 0.21 mPa.s) of the alkanes at atmospheric distillation conditions compared to the high viscosity (0.9 – 48 mPa.s) of the liquids used in this work.

Figure 3 and 4 show the distribution of the number of measurements made over the ranges shown in Table 9 and 10 in terms of the dimensionless groups. The y-axis ("Value Interval Frequency") represents the number of points within the interval denoted by the x-axis. It was not possible to find gas/liquid systems with physical properties that enable a factorial design. Therefore the data space is not uniformly distributed as shown in Figure 3 and 4. Manual inspection was executed to investigate the performance of the Uys correlation for the areas with limited data (shown in Figure 4 (b)). It was found that the correlation performed far within the average deviation of the predicted results for all the data.

At low tray spacings (315 and 415 mm) the application ranges of gas and liquid flow rates are much smaller than at higher tray spacings (515 and 615 mm). The data points within the ranges specified in Table 8 amount to 1139 data points.

Table 8. Range of application for the proposed correlation based on these experimental data ranges.

System	s [mm]	Q_L [$m^3/(h.m)$]	F_s [$m/s.(kg/m^3)^{0.5}$]	System	s [mm]	Q_L [$m^3/(h.m)$]	F_s [$m/s.(kg/m^3)^{0.5}$]
CO_2/Isopar G	315	2.9 - 23	1.6 - 2.3	CO_2/n-butanol	315	2.9 - 23 2.9 - 12	1.6 - 1.9 1.6 - 2.3
	415	2.9 - 68	1.9 - 2.3		415	2.9 - 68	1.9 - 2.3
	515	2.9 - 68	1.9 - 2.3		515	2.9 - 78	1.9 - 2.7
	615	2.9 - 68	1.9 - 2.7		615	6 - 68	1.9 - 3.1
Air/silicone oil	315	2.9 - 80 2.9 - 45 2.9 - 34	1.5 1.9 2.2	CO_2/silicone oil	315	2.9 - 56 2.9 - 34	1.8 - 1.9 2.3
	415	2.9 - 68 2.9 - 57	2.2 2.8		415	2.9 - 67 2.9 - 11	2.3 - 2.7 3.1
	515	2.9 - 79	2.2 - 3.1		515	2.9 - 68	2.3 - 3.1
	615	2.9 - 79	2.2 - 3.4		615	2.9 - 68	2.7 - 3.5
Air/water	615	2.9 - 92 2.9 - 60	2.5 - 2.8 3.2 - 3.4	CO_2/water	315	2.9 - 46 2.9 - 12	1.6 - 1.9 2.3 - 2.7
					415	2.9 - 91	1.9 - 3.1
					515	2.9 - 80	2.3 - 3.1
					615	2.9 - 69 5.9 - 80	2.7 - 3.1 3.5 - 3.9
Air/ethylene glycol	315	2.9 - 69 2.9 - 46 2.9 - 23	1.5 2.2 2.8	CO_2/ethylene glycol	315	2.9 - 58 2.9 - 46 2.9 - 12	1.6 - 1.9 2.2 2.7
	415	2.9 - 80 2.9 - 68 5.8 - 91	1.5 - 2.2 2.8 3.4		415	2.9 - 69	2.3 - 3.1
	515	2.9 - 92	2.2 - 3.4		515	2.9 - 80	3.5
	615	2.9 - 92 2.9 - 57	2.8 - 3.4 4.0		615	2.9 - 80	2.7 - 3.9
SF_6/n-butanol					615	2.9 - 35	2.4 - 3.4
SF_6/water					615	5.7 - 92	2.9 - 4.1
SF_6/ethylene glycol					615	2.9 - 46 2.9 - 68	3.3 4.1

Table 9. Dimensionless group distribution for the experimental- and C1-C12 alkane ranges for the spray regime correlation

	G1	G2	G3	G4	G5	G6
	$\frac{\rho_l}{945\rho_g}$	$\frac{\sigma}{9.7Q_L\rho_g U_s}$	$\frac{\mu_l}{15.9Q_L\rho_g}$	$\frac{U_s^3}{1.86Q_L g}$	$\frac{\mu_g}{6x10^{-3}Q_L\rho_g}$	$\frac{U_s^2}{3.44\times10^{-3}gs}$
Exp Min	1.49E-01	5.28E-03	3.67E-03	2.61E-03	4.74E-03	4.67E-02
Exp Max	9.99E-01	9.85E-01	8.84E-01	5.96E-01	9.66E-01	6.99E-01
C1-C12Min	1.33E-01	3.15E-03	1.15E-04	-	1.19E-02	-
C1-C12Max	2.74E-01	2.56E-01	1.74E-03	-	1.60E-01	-

Table 10. Dimensionless group distribution for the experimental- and C1-C12 alkane ranges for the froth regime correlation

	G1	G2	G3	G4	G5	G6	G7
	$\frac{\rho_l}{949\rho_g}$	$\frac{\sigma}{9.55Q_L\rho_g U_s}$	$\frac{\mu_l}{9.35Q_L\rho_g}$	$\frac{U_s^3}{0.433Q_L g}$	$\frac{\mu_g}{2.96\times10^{-3}Q_L\rho_g}$	$\frac{U_s s}{223Q_L}$	$\frac{Q_L}{162U_s L_{FPL}}$
Exp Min	1.81E-01	6.51E-03	2.05E-04	4.37E-03	9.58E-03	2.86E-02	1.05E-02
Exp Max	1.00E+00	5.93E-01	4.62E-01	4.23E+00	1.90E+00	3.56E+00	3.28E-02
C1-C12 Min	1.33E-01	8.79E-04	5.37E-05	-	6.63E-03	-	-
C1-C12 Max	2.74E-01	7.54E-02	8.58E-04	-	9.40E-02	-	-

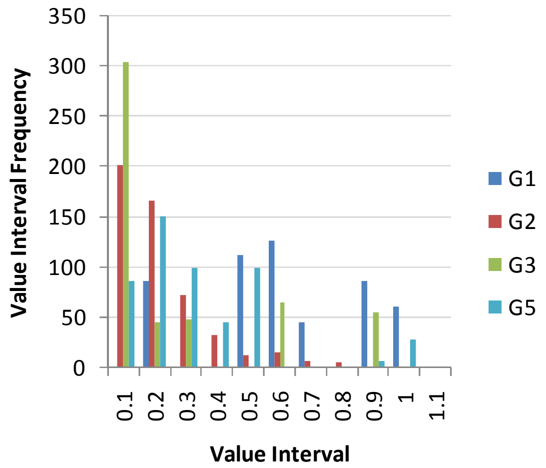

(a)

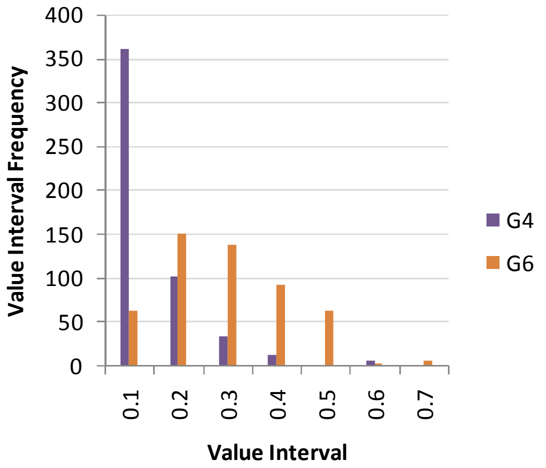

(b)

Figure 3. Frequency plots to indicate the distribution of the dimensionless groups (see Table 5 and Equation (35)) for the spray regime correlation presented in this work.

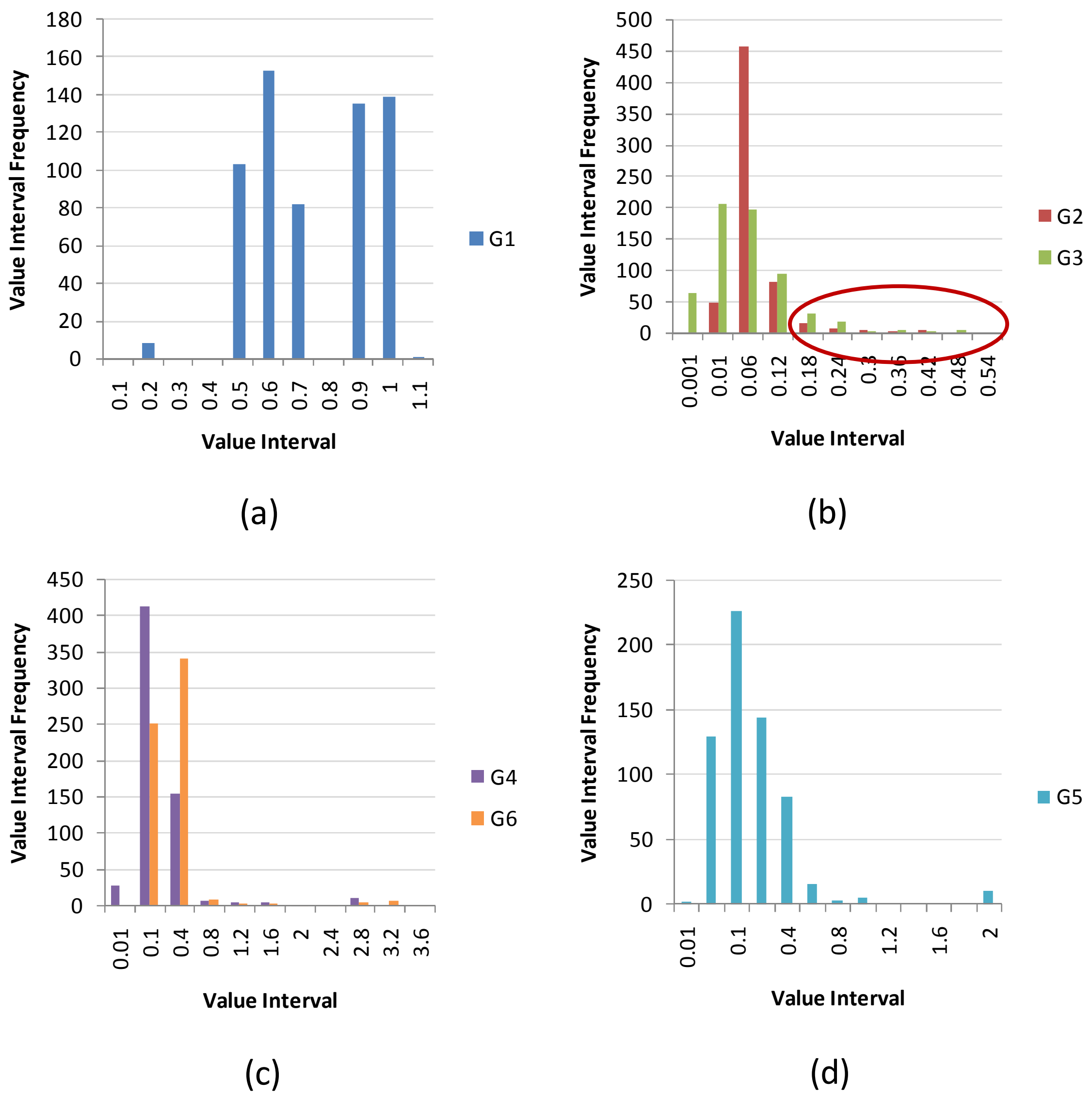

Figure 4. Frequency plots to indicate the distribution of the dimensionless groups (see Table 6 and Equation (37)) for the spray regime correlation presented in this work.

<u>**Comparison with experimental data and other correlations**</u>

In this work, new data were measured for different tray spacings. These data together with previously published data (Uys et al., 2012a, b and c) are compared with the different prediction correlations in Figure 5 and Figure 6. It has to be noted that all the correlations, except the one developed in this work, are extrapolated beyond their recommended range of application. The aim of these comparisons is to identify the scope and limitations of the different correlations. Kister and Haas (1988) (K & H) and Koziol and Mackowiak (1990) (M & K) tend to under predict entrainment while Zuiderweg (1982) (Z) and Bennett et al. (1995) (B) either under-predict and over-predict entrainment, depending on the gas-liquid system.

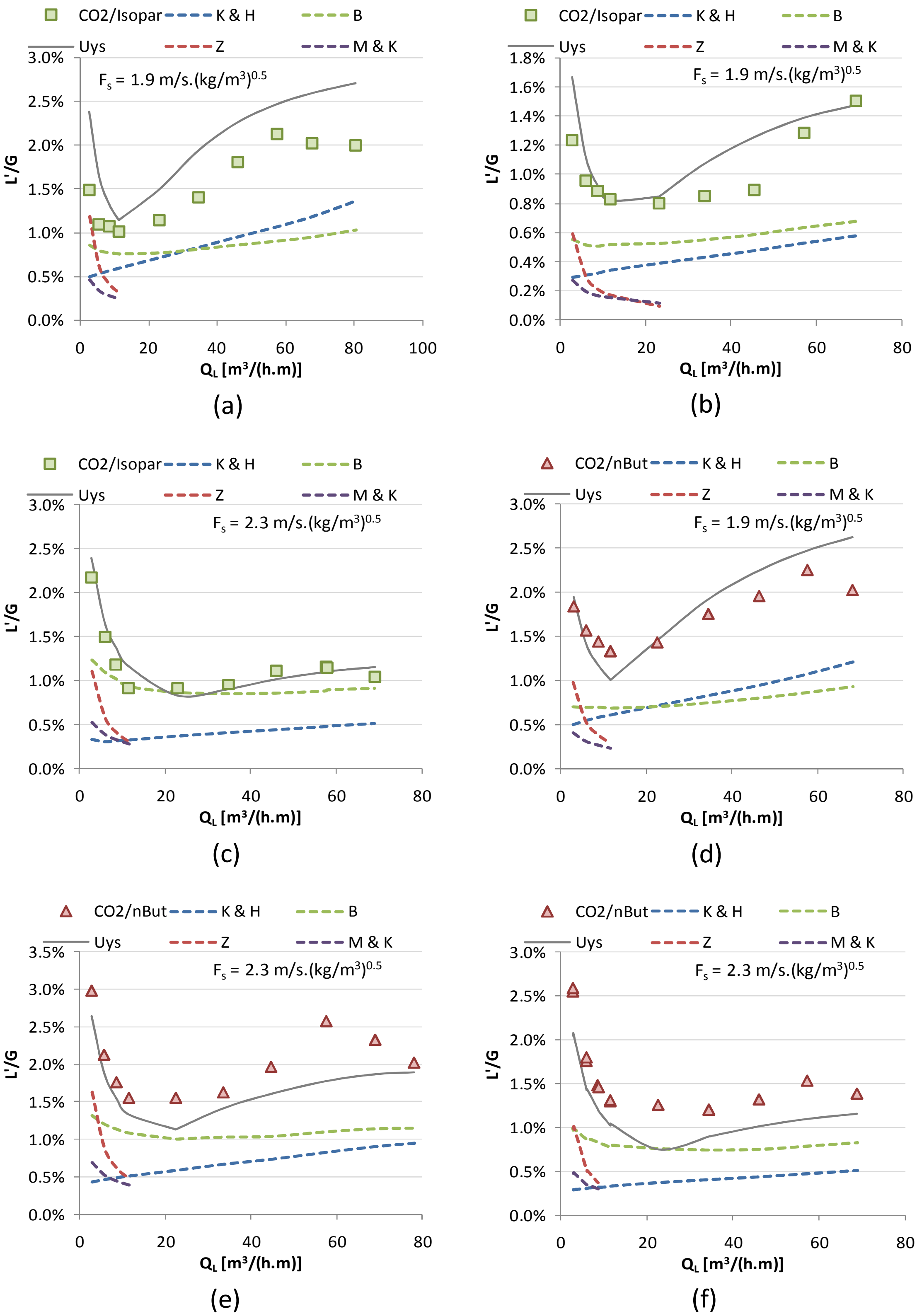

Figure 5. Comparing prediction correlations with data from (a) CO_2/Isopar G at S = 415mm and F_s = 1.9 m/s.(kg/m^3)$^{0.5}$, (b) CO_2/Isopar G at S = 515mm and F_s = 1.9 m/s.(kg/m^3)$^{0.5}$, (c) CO_2/Isopar G at S = 615mm and F_s = 2.3 m/s.(kg/m^3)$^{0.5}$, (d) CO_2/n-butanol at S = 415mm and F_s = 1.9 m/s.(kg/m^3)$^{0.5}$, (e) CO_2/n-butanol at S = 515mm and F_s = 2.3 m/s.(kg/m^3)$^{0.5}$ and (f) CO_2/n-butanol at S = 615mm and F_s = 2.3 m/s.(kg/m^3)$^{0.5}$.

Stellenbosch University http://scholar.sun.ac.za

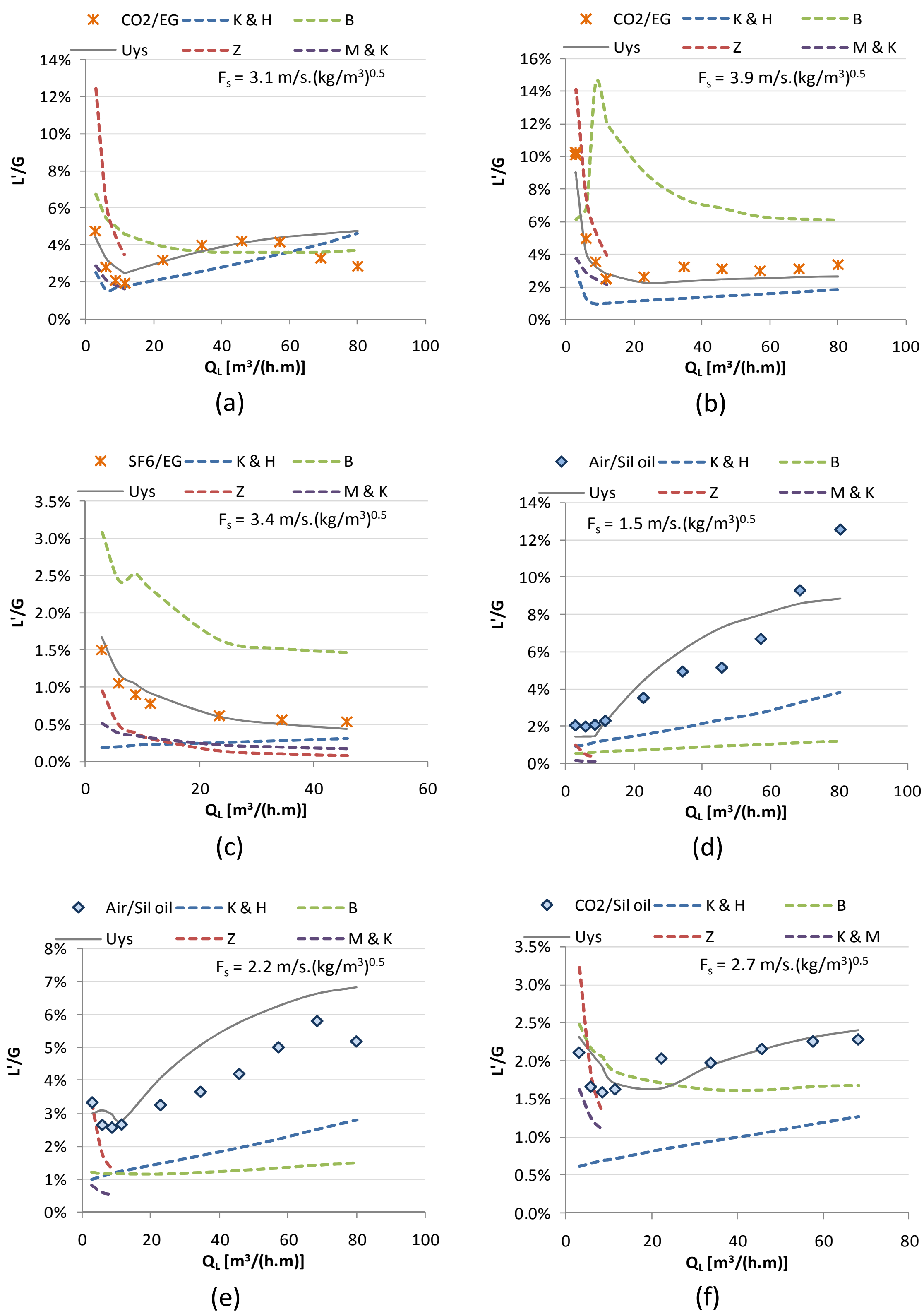

Figure 6. Comparing prediction correlations with data from (a) CO_2/ethylene glycol at s = 415mm and F_s = 3.1 m/s.(kg/m^3)$^{0.5}$, (b) CO_2/ethylene glycol s = 615mm and F_s = 3.9 m/s.(kg/m^3)$^{0.5}$, (c) SF_6/ethylene glycol at s = 615 mm and F_s = 3.4 m/s.(kg/m^3)$^{0.5}$, (d) air/silicone oil at S = 315mm and F_s = 1.5 m/s.(kg/m^3)$^{0.5}$, (e) air/silicone oil at S = 415mm and F_s = 2.2 m/s.(kg/m^3)$^{0.5}$ and (f) CO_2/silicone oil at S = 515mm and F_s = 2.7 m/s.(kg/m^3)$^{0.5}$.

Stellenbosch University http://scholar.sun.ac.za

The predictions for the model developed in this work (Uys) and the correlations of Kister and Haas (1988) and Bennett et al. (1995) are compared to the measured data in Figure 7 for the ranges shown in Table 8. To the knowledge of the authors, these are the correlations that cover the largest range of variables, thus the reason for comparison with the experimental data. The percentage deviations from a perfect fit (parity line) of the measured data are shown as + 30% and - 30%, and + 80% and -80% in Figure 7.

It is important to note that both Kister and Haas (1988) and Bennett et al. (1995) developed their correlations for air/water systems only, and their correlations are therefore extrapolated beyond the recommended range of application. It should also be noted that Bennett et al. (1995) developed non-air/water correlations for the froth and spray regimes from a small data base. These correlations performed very poorly when assessed for this work and are therefore not included here. Uys (2010) showed that there is a significant difference between the predictions of the non-air/water and air/water correlations of Bennett et al. (1995).

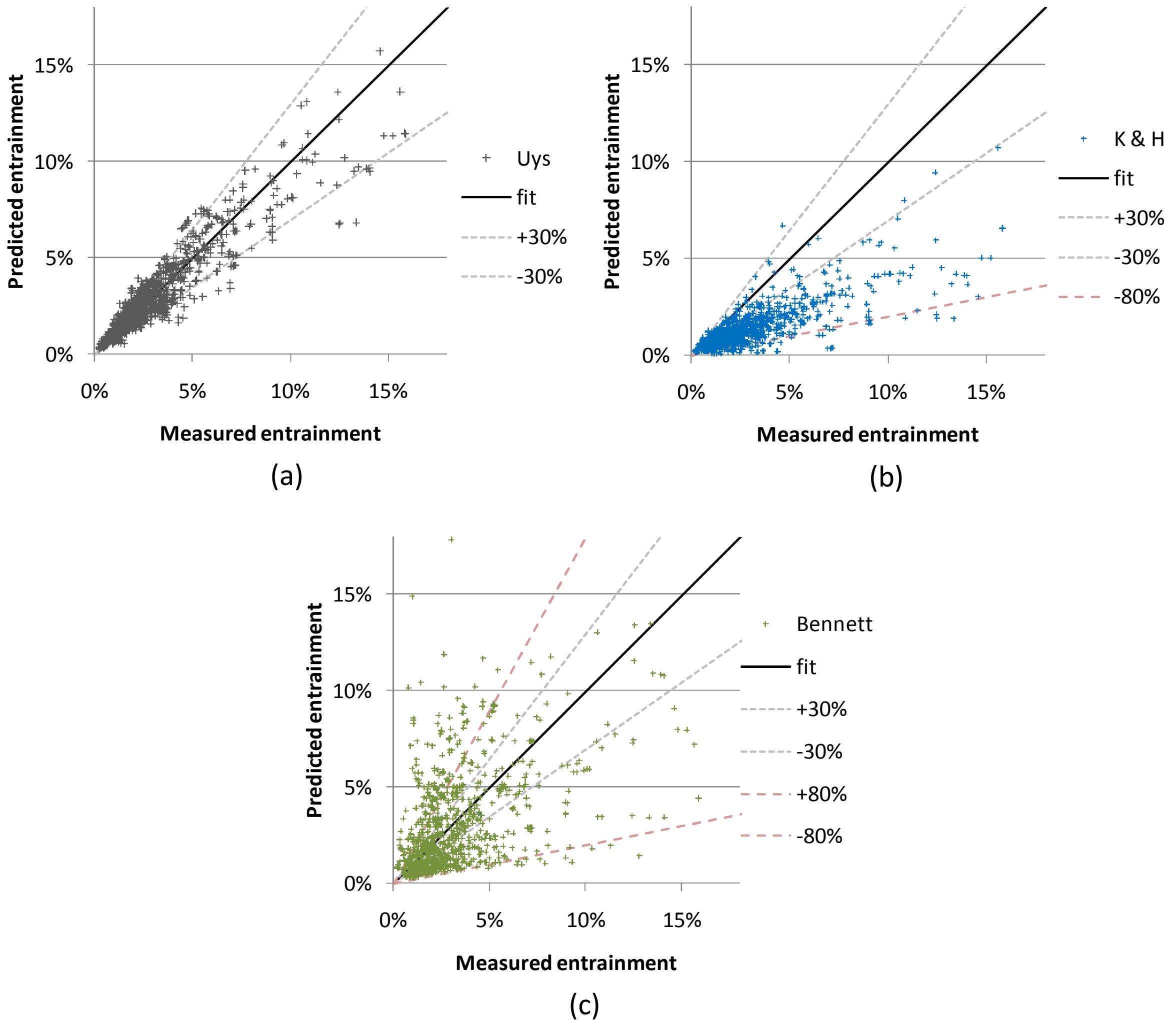

Figure 7. Predicted accuracies versus to measured entrainment for (a) the proposed correlation (Uys), (b) the Kister and Haas (1988) (K & H) correlation and (c) the Bennett et al. (1995) (Bennett) correlation.

The correlations developed by Zuiderweg (1982) and, Koziol and Mackowiak (1990) are limited to the spray regime. Figure 8 is constructed to show how all the correlations performed for conditions stipulated in Table 8 limited to liquid rates below 12 $m^3/(h.m)$. The proposed correlation fit the data for liquid rates lower than 12 $m^3/(h.m)$ with a higher accuracy than for the total range of liquid rates shown in Table 8. This is associated with the froth development behaviour of short flow path trays as shown by Uys et al. (2012a). The influence of tray flow path length on entrainment could not be quantified as there are no data available to the author and the generation of data for this was not part of the scope of this work. The model developed in this work is also the most accurate of all the correlations for the low liquid rate conditions of the ranges shown in Table 8. The correlation developed by Zuiderweg (1982) generally over predicted entrainment, while Koziol and Mackowiak (1990) (K & M) and Kister and Haas (1988) under predicted entrainment.

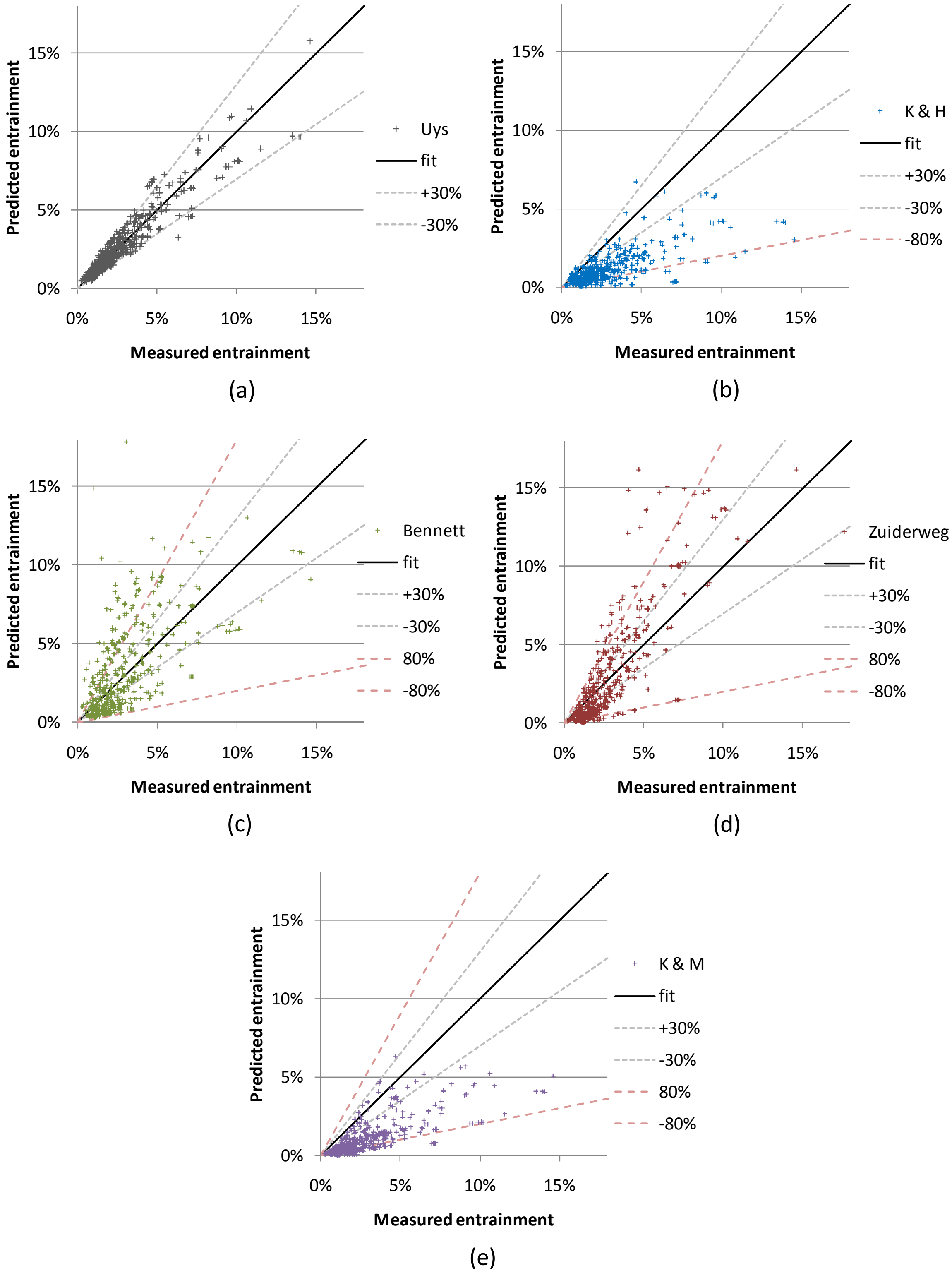

Figure 8. The predictions accuracies made by (a) the proposed correlation (Uys) (b) Kister and Haas (1988) (K & H) (c) Bennett et al. (1995) (Bennett) (d) Zuiderweg (1982) (Zuiderweg) and (e) Koziol and Mackowiak (1990) (K & M) are compared to the data for low liquid rates (Q_L < 12 m^3/(h.m)).

Stellenbosch University http://scholar.sun.ac.za

Methodology for extension of application range

The correlation developed in this work does not include the influence of tray geometry on entrainment. However, both Kister and Haas (1988) and Bennett et al. (1995) included tray geometry parameters in their correlations. They developed their correlations on entrainment data obtained from an extensive range of tray geometries. It is, therefore, possible to use these correlations to determine the contribution of tray geometry on entrainment and to add that contribution to the result of the correlation developed in this work. To do this, the tray geometry used in this work (see Table 11) acts as the reference. The correlation of Kister and Haas (1988) proved to predict the influence of tray geometry on entrainment with the highest accuracy, which will be shown in the following section.

Table 11. Differences between tray geometry used in this work and that of Nutter (1972).

	This work	Nutter (1972)
A_f	0.156	0.079
d_H [mm]	6.3	12.7

To use the Uys correlation for applications where tray geometry differs from that used in this work, two calculations are required. In the first calculation entrainment is calculated using the correlation of Kister and Haas (1988) and the tray geometry (including weir height) of this work. The second calculation also uses the Kister and Haas (1988) correlation and the same system conditions as the first calculation, but the tray geometry is changed to that of the tray in question. The difference between the result of the second and first calculation is then added to the result of the Uys correlation as shown in Equation (39) to give the extended Uys correlation.

$$\left(\frac{L'}{G}\right)_{\text{application in question}} = \left(\frac{L'}{G}\right)_{Uys} + \left[\left(\frac{L'}{G}\right)_{K\&H\,(\text{application in question geometry})} - \left(\frac{L'}{G}\right)_{K\&H\,(\text{Uys geometry})}\right] \quad \textbf{(39)}$$

Comparison of extended new correlation with previously published data

The data of Nutter (1972) are used to test the extended Uys correlation and to show the difference in tray geometry predictions made by Kister and Haas (1988) and Bennett et al.

Stellenbosch University http://scholar.sun.ac.za

(1995). The tray geometry used by Nutter (1972) differs significantly from that of the tray used in this work as shown in Table 11. To compare the extended Uys correlation with the data from Nutter (1972) the correlations of Kister and Haas (1988) and Bennett et al. (1995) are used. First entrainment is determined with these correlations for the Nutter (1972) conditions but with the geometry used in this work (A_f = 0.156 and d_H = 6.3 mm). These predictions are indicated in Figure 9 as K&H(Uys) and Bennett(Uys). Then entrainment is calculated using the conditions and tray geometry (A_f = 0.079 and d_H = 12.7 mm) from Nutter (1972), indicated as K&H(Nutter) and Bennett(Nutter) in Figure 9. The difference between these results, K&H(Nutter) – K&H(Uys) (shown as step 1 minus step 2), are then added to the result of the Uys correlation for the Nutter (1972) conditions shown as "Uys+K&H" in Figure 9 and Figure 10 (similar to Equation 39). The predictions made by the Uys correlation combined with the influence of tray geometry as described by Kister and Haas (1988) and Bennett et al. (1995) are shown in Figure 10 as Uys+K&H and Uys+Bennett.

The prediction by Bennett et al. (1995) for the Nutter (1972) conditions is less accurate than that of Kister and Haas (1988). Based on the results of Figure 10, the Uys correlation combined with the predicted influence of tray geometry by Kister and Haas (1988) can be used to predict entrainment for a large array of systems and operating conditions. The performance of the extended Uys correlation compared with the predictions from Kister and Haas (1988) and Bennett et al. (1995) for the Nutter (1972) conditions are shown in Table 12 and Table 13. The difference between K&H(Nutter) and K&H(Uys) are indicated as ΔK&H in Table 12 and 13. The same applies to ΔBennett which is calculated as Bennett(Nutter) minus Bennett(Uys).

For additional validation the extended correlation is compared to a single data point published by Sakata and Yanagi (1979) for the cyclo-hexane/n-heptane system (shown in Table 14). The extended correlation performed remarkably well even thought the viscosity, surface tension and liquid density of this system are beyond the range of application of the proposed correlation. The vapour viscosity of n-heptane was used for calculation purposes as Sakata and Yanagi (1979) did not publish this data. These comparisons show that the extended correlation developed in this work performs well for columns with tray geometries different to that used in this work. The correlation developed in this work can therefore be used over a larger range of systems, conditions and tray geometries than previously possible.

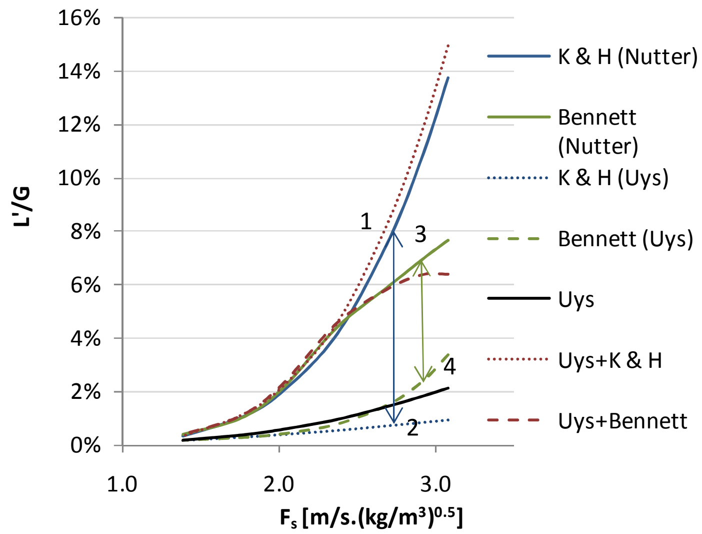

Figure 9. Method for predicting entrainment for systems with different geometries, using the Kister and Haas (1988), and Bennett et al. (1995) correlations as well as the conditions and tray geometry from Nutter (1972).

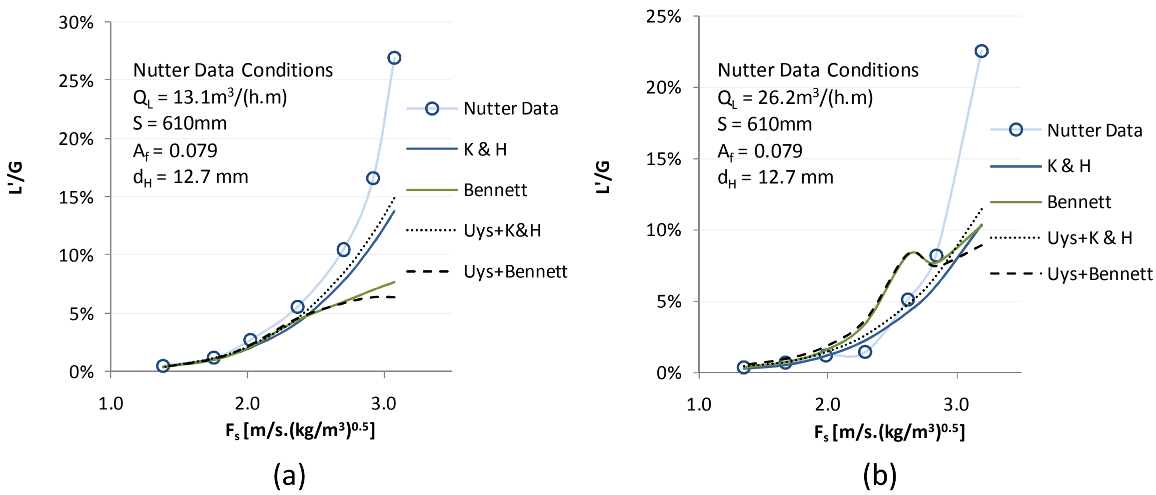

Figure 10. Comparing predictions with the data from Nutter (1972) for a liquid rate of (a) 13.1 m^3/(h.m) and (b) 26.2 m^3/(h.m).

Stellenbosch University http://scholar.sun.ac.za

Table 12. Comparison of performance of extended correlation with that of Kister and Haas (1988) and Bennett et al. (1995) for conditions shown in Figure 10 (a).

Statistics	Uys+ΔK&H	K&H	Uys+ΔBennett	Bennett
Mean squared error	2.4E-03	3.1E-03	7.8E-03	7.0E-03
Sum squared error	0.017	0.021	0.055	0.049
Pearson R^2	0.96	0.96	0.71	0.83

Table 13. Comparison of performance of extended correlation with that of Kister and Haas (1988) and Bennett et al. (1995) for conditions shown in Figure 10 (b).

Statistics	Uys+ΔK&H	K&H	Uys+ΔBennett	Bennett
Mean squared error	1.8E-03	2.2E-03	2.9E-03	2.4E-03
Sum squared error	0.013	0.015	0.020	0.017
Pearson R^2	0.93	0.93	0.60	0.70

Table 14. Comparing the predicted value of the extended correlation (Equation 39) with the single tabulated data point of Sakata and Yanagi (1979).

Sakata datam [L'/G]	Uys+ ΔK&H	Uys+ΔBennett	Kister	Bennett
5.94%	6.30%	2.42%	5.59%	3.95%

Extending correlation for fractional liquid entrainment (L'/L)

The prediction correlation (Equation 38) can be converted to determine the fraction of liquid entering the tray that entrains, shown in Equation (40) below:

$$\frac{L'}{L} = \frac{L'}{G} \times \frac{U_s A_p \rho_g 3600}{Q_L L_w \rho_L} \tag{40}$$

Performance of fractional liquid entrainment correlation

The fractional liquid entrainment (L'/L) correlation (Equation 40) is compared with experimental data in Figure 11 and performs with accuracy similar to Equation 38 as shown in Figure 12. Table 15 indicates that the prediction for L'/G and L'/L is of similar accuracy with the L'/L prediction giving a better R^2. The weir length (L_W) used in this work is 0.175m.

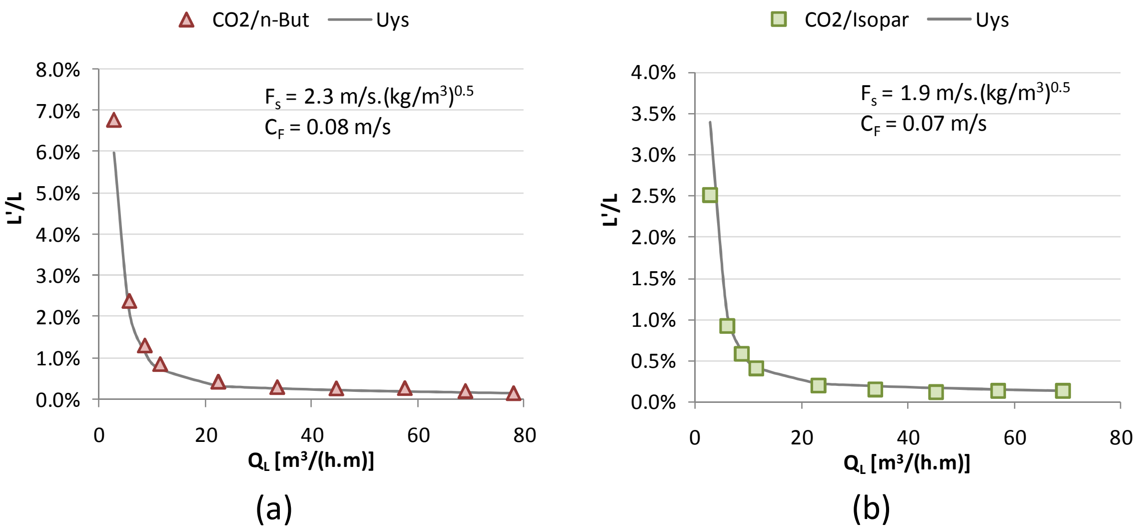

Figure 11. Comparison of fractional liquid entrainment (L'/L) prediction with (a) CO_2/n-butanol experimental data for 515mm tray spacing and (b) CO_2/Isopar experimental data for 515mm tray spacing.

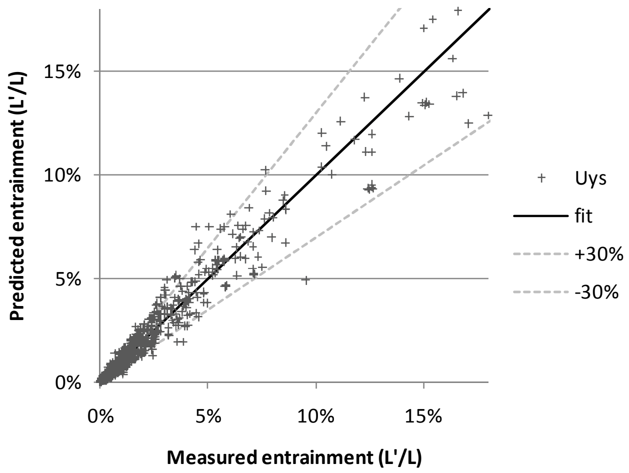

Figure 12. Overall performance of Equation 40 when compared to the experimental entrainment (L'/L) data measured within the ranges specified in Table 8.

Table 15. Comparing the prediction capability of Equation 38 (L'/G) and Equation 40 (L'/L).

Statistics	Uys (L'/G)	Uys (L'/L)
Mean squared error	8.91E-05	1.78E-04
Sum squared error	1.02E-01	2.03E-01
Pearson R^2	85.4%	92.4%

Stellenbosch University http://scholar.sun.ac.za

6. Conclusions

A new extended entrainment database was compiled consisting of over 1700 data points for CO_2/Isopar, CO_2/n-butanol, SF_6/n-butanol, air/ethylene glycol, CO_2/ethylene glycol, SF_6/ethylene glycol, air/silicone oil, CO_2/silicone oil, SF_6/silicone oil, air/water, CO_2/water and SF_6/water. Tray spacing ranged from 315 – 615mm, liquid rates from 2.9 – 91 $m^3/(h.m)$ and gas flow factors ranged from 1.5 – 4.8 $m/s.(kg/m^3)^{0.5}$. Of these data points, 1139 fell within the capable range of the new presented correlation. This new database is significantly larger than any other database in the open literature. The new correlation can predict entrainment for a range of different systems and, gas and liquid flow rates with higher accuracy (R^2 = 85%) than existing correlations (R^2 = 61% for Kister and Haas (1988) and R^2 = 23% for Bennett et al. (1995)). This correlation can be converted to predict fractional liquid entrainment (L'/L) with satisfactory accuracy (R^2 = 92%). Liquid viscosity, neglected by all other workers, is included in the Uys correlation. No froth height or froth density data or estimations thereof are required to use this model. However, tray geometry has not been varied and consequently the new correlation does not include tray design parameters. To extend the use of the model developed in this work to columns with different sieve tray geometry, the correlation developed by Kister and Haas (1988) can be used successfully.

The range of application for the Uys correlation was compared to atmospheric distillation conditions of C1 – C12 alkanes. All the parameter ranges compared very well except for the one that included liquid viscosity. Therefore, the Uys correlation can be used for industrial atmospheric distillation systems with greater accuracy and reliability than current entrainment prediction correlations. This work forms part of the first step towards developing of a new general correlation for predicting entrainment in tray columns, and future work will include an investigation of the effect of tray geometry.

Stellenbosch University http://scholar.sun.ac.za

7. Acknowledgements

The financial assistance of Sasol Technology (Pty) Ltd, Koch-Glitsch LP, Inher SA, and the Department of Trade and Industry (DTI) of South Africa through the Technology and Human Resources for Industry Programme (THRIP) towards this research is hereby acknowledged. We gratefully acknowledge the inputs from Dr. A. Erasmus and Dr. I. Nieuwoudt regarding the equipment design. The assistance of Dr. JP Barnard with regard to the MATLAB code development is greatly appreciated. Opinions expressed and conclusions arrived at are those of the authors and are not necessarily to be attributed to the sponsors.

Stellenbosch University http://scholar.sun.ac.za

8. Nomenclature

A_c	column area = 635x175mm	[m^2]
A_f	fractional hole area = A_h/A_p	[-]
A_h	hole area	[m^2]
A_p	perforated area or bubbling area	[m^2]
C_F	capacity flow factor = $U_s.(\rho_g/(\rho_L-\rho_g))^{0.5}$	[m/s]
D_c	column diameter	[m]
d_H, D_H	hole diameter	[mm, m]
FPL	tray flow path length, 475 mm in this work	[mm]
F_h	hole vapour factor = $U_h.\rho_g^{0.5}$	[$kg^{0.5}/m^{0.5}.s$]
F_s	superficial vapour factor = $U_s.\rho_g^{0.5}$	[$kg^{0.5}/m^{0.5}.s$]
g	gravitational constant = 9.81	[m/s^2]
G	gas mass flow rate	[kg/s]
h_w, H_w	outlet weir height	[mm, m]
h_f, H_F	froth height	[mm, m]
h_L, H_L	clear liquid height	[mm, m]
$h_{L,ct}$	clear liquid height at the regime transition	[mm]
L	mass flow of liquid entering the tray	[kg/s]
L’	entrained liquid mass flow	[kg/s]
L_W	weir length = 0.175m in this work	[m]
L_{FPL}	tray flow path length, 0.475 m in this work	[m]
MSE	mean of the squared error	[-]
p	hole pitch	[mm]
QL	liquid flow rate per weir length	[m3/(h.m)]
s, S	tray spacing	[mm, m]
SSE	sum of the squared error	[-]
us , Us	superficial gas velocity, based on tray perforated/bubbling area	[m/s]
V_g	gas volumetric flow rate	[m^3/s]
V_L	liquid volumetric flow rate	[m^3/s]
Greek Letters		
ρ_v	gas density	[kg/m^3]
ρ_L	liquid density	[kg/m^3]
σ	surface tension	[mN/m]
μ_g	gas viscosity	[mPa.s]

Stellenbosch University http://scholar.sun.ac.za

μ_L	liquid viscosity	[mPa.s]
ζ	correction term for Eq. 17	

Stellenbosch University http://scholar.sun.ac.za

9. References

Bennett, D.L., Ludwig, K.A., 1994. Understand the limitations of air/water testing of distillation equipment. Chemical Engineering Progress, 72 – 79.

Bennett, D.L., Kao, A.S., Wong, L.W., 1995. A mechanistic analysis of sieve tray froth height and entrainment. AIChE , 41 (9), 2067-2082.

Colwell, C., 1981. Clear liquid height and froth density on sieve trays. Industrial and Engineering Chemistry Process Design and Development, 20 (2), 298-307.

Hunt, C. d'A., Hanson, D.N., Wilke, C.R., 1955. Capacity factors in the performance of perforated plate columns. AIChE Journal. 1 (4), 441 – 451.

Kister, H.Z., Haas, J.R., 1988. Entrainment from sieve trays in the froth regime. Industrial and Engineering Chemistry Research , 27 (12), 2331-2341.

Koziol, A., Mackowiak, J., 1990. Liquid entrainment in tray columns with downcomers. Chemical Engineering Process, 27, 145 – 153.

Lockett, M.J., 1986. Distillation tray fundamentals, Cambridge University Press, Cambridge.

Nutter, D.E., 1972. Amonia stripping efficiency studies. American Institute of Chemical Engineers Symposium Series No. 124, 68.

Porter, K.E., Jenkins, J.D., 1979. The interrelationship between industrial practice and academic research in distillation and absorption. Institution of Chemical Engineers Symposium Series No. 56 , 5.1/1-5.1/47.

Sakata. M., Yanagi, T., 1979. Performance of a commercial scale 14% hole area sieve tray. Institution of Chemical Engineers Symposium Series No. 56 , 5.1/1-5.1/47.

Thomas, W. J., Ogboja, O., 1978. Hydraulic studies in sieve tray columns. Industrial and Engineering Chemistry Process Design and Development , 17 (4), 429-443.

Uys, E.C., 2010. Entrainment in a sieve tray column, Masters Thesis. Stellenbosch University, South Africa.

Uys, E.C., Schwarz, C.E., Burger, A.J., Knoetze, J.H., 2012a. New froth behaviour observations and comparison of experimental sieve tray entrainment data with existing correlations. Chemical Engineering Research and Design. DOI 10.1016/j.cherd.2012.05.008

Uys, E.C., Burger, A.J., Knoetze, J.H., 2012b. The influence of gas physical properties on entrainment inside a sieve tray column. To be submitted to Chemical Engineering Research and Design.

Stellenbosch University http://scholar.sun.ac.za

Uys, E.C., Burger, A.J., Knoetze, J.H., 2012c. The influence of liquid physical properties on entrainment inside a sieve tray column. To be submitted to Chemical Engineering Research and Design.

Zuiderweg, F.J., 1982. A view on the state of the art. Chemical Engineering Science, 37 (10), 1441-1464

Stellenbosch University http://scholar.sun.ac.za

Conclusions

A literature survey showed that existing entrainment prediction models give very little attention to the influence of gas and liquid physical properties on entrainment, especially with regards to liquid surface tension and viscosity. To improve the understanding of the influence of gas and liquid physical properties on entrainment, the project was divided into four sections, written in paper format.

In paper 1, experiments were conducted for air/water, air/ethylene glycol and air/silicone oil to test if surface tension and viscosity have an influence on entrainment. Experimental conditions were varied over a range of gas flow factors (1.6 $kg^{0.5}/(m^{0.5}.s)$ for the 415mm tray spacing up to 4.0 $kg^{0.5}/(m^{0.5}.s)$ for the 615mm tray spacing) and liquid flow rates (2.9 – 112 $m^3/(h.m)$) resulting in a large array of entrainment data (1.0 – 23% L'/G). The generated entrainment data (L'/G) were compared with correlations from Kister and Haas (1988) and Bennett et al. (1995). The air/water entrainment data gave similar results as these prediction correlations. However, predictions deviated considerably from the measured data for the non-air/water systems and showed that the influence of surface tension and viscosity on entrainment can not be neglected. Ethylene glycol entrained the most in the low liquid ($Q_L < 9$ $m^3/(h.m)$) and low gas factors ($F_s < 3.4$ $kg^{0.5}/(m^{0.5}.s)$) ranges with silicone oil entraining the most in the high liquid range ($Q_L > 12$ $m^3/(h.m)$). Water entrained slightly more than ethylene glycol under the high ($F_s = 4.0$ $kg^{0.5}/(m^{0.5}.s)$) gas flow conditions. The results from this work suggested that the influence of liquid physical properties on entrainment is greater than current correlations suggest. Consequently, more data were required to improve the understanding of froth behaviour. A new observation was made with regards to how the froth develops as liquid exit the downcomer. It was noted that in the froth regime at high gas rates, an increase in liquid flow rate will increase entrainment to a maximum before entrainment decreases. Literature suggests that entrainment should only increase with increasing liquid rate in the froth regime. In this case it was caused by the relatively short, 475 mm, flow path length and the effect of decreasing entrainment with increasing liquid flow is more prominent at lower tray spacings (< 415 mm). This observation

Stellenbosch University http://scholar.sun.ac.za

can be used to understand possible deviations from the predicted performance of shorter or multi-pass trays under high vapour and liquid capacities.

In manuscript 2, the influence of gas physical properties on entrainment was determined using air, CO_2 and SF_6 systems individually contacted with water, ethylene glycol and n-butanol (n-butanol was not contacted with air). Most of the data were measured at gas rates higher than the range limit (U_s = 2.3 m/s) of the Bennett et al. (1995) correlation to expand the database. Entrainment decreased with an increase in gas density for constant gas flow factors. The data was compared to the correlations of Kister and Haas (1988) and Bennett et al. (1995). Entrainment was generally under-predicted by the Kister and Haas (1988) correlation especially for systems other than water. The correlation by Bennett et al. (1995) over-predicted most of the systems except air/ethylene glycol and SF_6/n-butanol for low (<2.9 $m/s.(kg/m^3)^{0.5}$) flow factor conditions. Their correlation performed poorly when extrapolated beyond the recommended application range for the SF_6 system at high flow factor conditions, indicating the inability to predict entrainment for high gas density systems.

Modified versions of the Reynolds and Froude numbers, together with a ratio of the gas to liquid density were developed to show the influence of gas physical properties on entrainment. A good relationship was shown between the modified Reynolds and the mass of liquid entrained per mass of rising gas (L'/G). This comparison is limited to constant flow factor conditions and, spray-and-froth regimes separately. n-Butanol entrained the most with water the least over a range of modified Reynolds numbers at constant flow factor conditions. An increase in the modified Reynolds number resulted in a decrease in entrainment for constant gas flow factor conditions. Therefore, an increase in liquid flow rate and gas density will decrease entrainment. A modified Froude number was developed to show the relationship between gas-and-liquid density, gas velocity, liquid flow rate and the fraction of liquid entering the tray that entrains (L'/L). Increasing gas density and gas velocity will increase the modified Froude number which will increase the fraction of the liquid entering the tray that entrains. By increasing the liquid flow rate, the modified Froude number is decreased which resulted in a decrease in entrainment. Good correlation was shown between the modified Froude number and entrainment (L'/L) data over a large range of flow factors and liquid rates for the different liquid systems.

Stellenbosch University http://scholar.sun.ac.za

In manuscript 3 the influence of liquid physical properties on entrainment was determined. Isopar G, n-butanol, silicone oil, water and ethylene glycol were contacted with CO_2 with a tray spacing of 615 mm. The entrainment results were compared with prediction correlations from Kister and Haas (1988) and Bennett et al. (1995) to show their scope and limitations. The Kister and Haas (1988) correlation under predicted entrainment and the correlation of Bennett et al. (1995) over predicted entrainment for gas rates equal and higher than 2.7 m/s.(kg/m^3)$^{0.5}$ for the different liquids. The flow factors used during experiments were beyond the recommended range of application for the Bennett et al. (1995) correlations. The results proved that liquid viscosity influenced entrainment and can not be neglected as previously suggested. Liquid dynamic viscosity and surface tension played a significant role in droplet formation, ejection velocity and froth height. The end result was that viscosity had a non-monotonic effect on entrainment. Increasing viscosity (from 0.9 to 2.6 mPa.s) will initially increase the froth height, which will increase entrainment. A further increase in viscosity (48 mPa.s) will reduce liquid film break-up and droplet ejection velocity, which will reduce entrainment. For the two comparisons between Isopar and water, an increase in surface tension resulted in a decrease in entrainment. These findings agree with single droplet development, disintegration and droplet size studies (Decent et al., 2009).

In manuscript 4, a new dimensionless correlation (Uys) was developed to predict the influence of tray spacing, gas and liquid flow rates and, gas and liquid physical properties on entrainment. New entrainment data were measured for 315, 415 and 515mm tray spacings and combined with the data from papers 1 to manuscript 3 to form a database of over 1700 data points. Of these data points, 1139 fell within the application range of the presented correlation. Liquid flow rates ranged from 2.9 – 91 m^3/(h.m) and gas flow factors ranged from 1.5 – 4.8 m/s.(kg/m^3)$^{0.5}$. The systems used were CO_2/Isopar, CO_2/n-butanol, SF_6/n-butanol, air/ethylene glycol, CO_2/ethylene glycol, SF_6/ethylene glycol, air/silicone oil, CO_2/silicone oil, SF_6/silicone oil, air/water, CO_2/water and SF_6/water. The application ranges of the newly developed parameters cover most of the C1 – C12 alkane ranges common to atmospheric distillation conditions. Therefore this correlation can be extended to industrial distillation applications with higher reliability than existing entrainment correlations.

Stellenbosch University http://scholar.sun.ac.za

Further improvement can be made to the Uys correlation by generating entrainment data for low viscosity (< 0.9 mPa.s) liquids to expand the new range.

Some of the advantages of the new correlation are that liquid hold-up, or froth height data, or estimations are not required. The correlation is also relatively simple when compared to the correlation of Kister and Haas (1988) and Bennett et al. (1995) as they both required liquid hold-up and froth height estimations. The correlation (L'/G) fitted the experimental data with a R^2 of 84% compared to R^2 of 61% for Kister and Haas (1988) and 23% Bennett et al. (1995) respectively. The new correlation can also be converted to predict fractional liquid entrainment (L'/L) with an R^2 of 92%. One of the main limitations of the new correlation is that it does not include the effect of tray geometry. However, this correlation can predict entrainment successfully for different tray geometries by combining the predicted influence of tray geometry, by Kister and Haas (1988), with results from the Uys correlation. This method proved to be accurate when compared to data published in the literature.

Stellenbosch University http://scholar.sun.ac.za

Recommendations

A large database was developed in this work with regards to gas and liquid physical properties, tray spacing and, gas and liquid flow rates. Tray geometry and design were not changed and the influence thereof on entrainment for different gas and liquid physical properties is unknown. The data clearly showed that viscosity influences the froth height, droplet ejection velocity and droplet formation height. It is uncertain how viscosity influences each of these areas individually as entrainment measurements are a result of the combined effect of all three phenomena.

The correlation developed in this work is not capable of predicting entrainment over the complete range of measure data. One of the reasons is that froth behaviour at high capacities in short flow path trays is not properly understood. This is due to a lack of data with varying tray flow path length. In the literature the operating range has been divided into flow regimes as an attempt to simplify the understanding of the fundamentals that determine the froth behaviour. Much less attention has been given to describe the difference in froth composition and behaviour at gas and liquid capacities close to the onset of flooding. As a result, the transition to the different flooding conditions is not defined. Flooding velocity calculations are common but nothing is mentioned on how the flooding velocity was characterised or defined in terms of entrainment. One argument is that it is not ideal to operate columns at capacities close to the onset of flooding as separation efficiency is heavily compromised. However, from a tray design and operating perspective it is valuable to know which parameters will influence entrainment and flooding the most.

Until recently it was well known that gas flow factor influences entrainment the most and that column diameter should be increase. This work showed that tray flow path length also plays a major role. Clever downcomer apron and outlet weir designs could improve the capacity of short flow path trays. Therefore, based on the results, findings and conclusions of this work the following recommendations are made:

1. Measure entrainment for different fractional hole areas and hole diameters. By changing the distances between holes the liquid film between the jetting zones of surrounding holes is reduced. This will increase the area to volume ratio of the liquid

Stellenbosch University http://scholar.sun.ac.za

jet which should influence the froth height and droplet ejection velocity depending on the surface tension to dynamic viscosity ratio of the liquid. Larger fractional hole areas reduce the difference between the superficial vapour velocity and the hole velocity resulting in lower droplet ejection velocities (Bennett et al., 1995). At the same time increasing fractional area will increase the weeping rate.

2. Investigate the possibility of a regime change or fundamental change in froth behaviour at high gas flow rates up to the flood point. To do this the flood point has to be defined and characterised. Tray and/or dynamic pressure drop might be used to see if a sudden change in pressure drop relates to the onset of flooding. Liquid hold-up data were collected during experiments for future use and can be found in the Appendix as this did not form part of the scope of this work. A versatile monitoring tool for industrial tray columns can be developed by combining the tray pressure drop with gas and liquid flow rates if tray pressure drop can be used to indicate regime change or the onset of flooding.
3. Use different tray flow path length configurations to gain a better understanding of how the clear liquid develop into a froth as it exits the downcomer as well as how the froth expands and collapses due to the difference in gas superficial and hole velocities. In this work a tray flow path length of 475 mm was used. A shorter tray flow path length will show what the minimum liquid flow rate and gas velocity needs to be for the froth to collapse after the outlet weir. Tray flow path lengths longer that 475 mm will show what the minimum required tray flow length is to prevent the froth of collapsing in front of the outlet weir after on expansion cycle. One expansion cycle is when the clear liquid exits the downcomer, make contact with the rising gas, expands to the maximum froth height and minimum froth density and then collapses or "contracts" due to gravitation force exceeding the drag and buoyancy forces and, momentum of the ejecting droplets.
4. After the influence of tray flow path length on entrainment has been determined, new downcomer apron, inlet weir and out weir designs can be investigated to improve the capacity of existing columns. These designs should not be tray specific and could aid in increasing the capacity of a large range of tray types. It might be advantageous to start this investigation with the aid of computational fluid dynamics

Stellenbosch University http://scholar.sun.ac.za

(CFD). The best designs based on the CFD results could then be implemented for verification tests.

Once the above mentioned points have been addressed a new model for entrainment that includes the influence of gas/liquid physical properties, tray geometry, tray spacing, weir design, tray flow path length can be developed. To develop such a correlation it is important to understand and define the different regimes including transition into flooding.

Stellenbosch University http://scholar.sun.ac.za

Appendix

In this section the tray geometry (Table 1), entrainment (Table 2 – 10), liquid hold-up (Table 2 – 10), weeping (Table 11 – 13) and dry tray pressure drop (Table 14 – 16) data are presented. Liquid hold-up data were not use extensively in this work, but can be used for future projects beyond the scope of this project. Data presented in figures in the dissertation is enlarged for better viewing.

Table 17 acts as a reference for future users to ensure the proposed correlation is implemented correctly. The last two sections of this chapter, section 1.5 and 1.6, contain the MATLAB code for the data acquisition and data fitting tools.

Table 1. Column and tray geometry used in this work

Geometry		Unit
d_H	6.3	mm
No Holes	414	-
P	14.5	mm
A_h	0.0129	m^2
A_p	0.08295	m^2
A_f (A_h / A_p)	0.156	-
A_n	0.095	m^2
A_d	0.0158	m^2
A_c	0.1111	m^2
h_w	51	mm
S	315, 415, 515, 615	mm
FPL	475	mm
L_w	175	mm

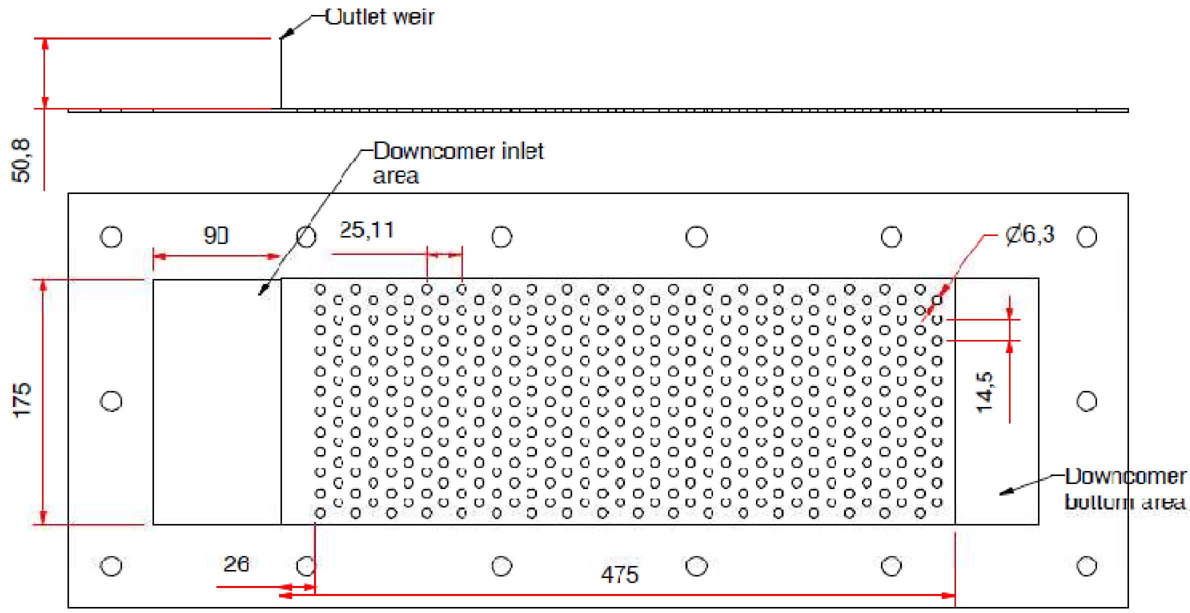

Figure 1. Detailed drawing of the tray used in experiments.

1. Entrainment and liquid hold-up data

Table 2. CO_2/Isopar G data for 315, 415, 515 and 615mm tray spacings.

A_p [m^2]	s [mm]	ρ_L [kg/m^3]	σ [mN/m]	μ_L [mPa.s]	ρ_V [kg/m^3]	μ_g [Pa.s]	U_s [m/s]	Q_L [m^3/(h.m)]	L'/L	L'/G	Holdup [Pa]	Holdup [mm liq]
0.08295	315	739	22.3	0.94	1.77	1.493E-05	1.21	2.8	2.68%	1.52%	115.6	15.9
0.08295	315	739	22.3	0.94	1.77	1.493E-05	1.20	6.0	1.08%	1.32%	148.2	20.4
0.08295	315	739	22.3	0.94	1.78	1.493E-05	1.21	8.5	0.78%	1.34%	163.9	22.6
0.08295	315	739	22.3	0.94	1.78	1.493E-05	1.20	11.4	0.56%	1.28%	180.7	24.9
0.08295	315	739	22.3	0.94	1.78	1.493E-05	1.20	11.4	0.56%	1.28%	180.7	24.9
0.08295	315	739	22.3	0.94	1.79	1.493E-05	1.21	22.8	0.52%	2.39%	222.0	30.6
0.08295	315	739	22.3	0.94	1.79	1.493E-05	1.21	22.9	0.53%	2.40%	222.9	30.8
0.08295	315	739	22.3	0.94	1.79	1.493E-05	1.21	34.2	0.59%	4.05%	255.8	35.3
0.08295	315	739	22.3	0.94	1.79	1.493E-05	1.20	34.6	0.64%	4.48%	259.7	35.8
0.08295	315	739	22.3	0.94	1.80	1.493E-05	1.21	46.1	0.87%	8.03%	286.4	39.5
0.08295	315	739	22.3	0.94	1.79	1.493E-05	1.20	46.1	0.75%	6.96%	289.3	39.9
0.08295	315	739	22.3	0.94	1.79	1.493E-05	1.21	46.2	0.89%	8.16%	285.6	39.4
0.08295	315	739	22.3	0.94	1.80	1.493E-05	1.19	57.4	1.53%	17.76%	311.1	42.9
0.08295	315	739	22.3	0.94	1.79	1.493E-05	1.21	57.4	1.37%	15.82%	307.7	42.4
0.08295	315	739	22.3	0.94	1.80	1.493E-05	1.20	57.4	1.40%	16.16%	306.5	42.3
0.08295	315	739	22.3	0.94	1.79	1.493E-05	1.21	68.5	1.45%	19.91%	299.7	41.3
0.08295	315	739	22.3	0.94	1.80	1.493E-05	1.21	68.7	1.47%	20.19%	297.4	41.0
0.08295	315	739	22.3	0.94	1.80	1.493E-05	1.20	68.9	1.71%	23.68%	297.8	41.1
0.08295	315	739	22.3	0.94	1.79	1.493E-05	1.20	69.0	1.69%	23.45%	291.2	40.2
0.08295	315	739	22.3	0.94	1.76	1.493E-05	1.43	2.8	5.07%	2.46%	102.9	14.2
0.08295	315	739	22.3	0.94	1.78	1.493E-05	1.41	6.0	1.81%	1.88%	137.5	19.0
0.08295	315	739	22.3	0.94	1.78	1.493E-05	1.41	8.5	1.24%	1.82%	155.7	21.5

A_p [m^2]	s [mm]	ρ_L [kg/m$_3$]	σ [mN/m]	μ_L [mPa.s]	ρ_v [kg/m^3]	μ_g [Pa.s]	U_s [m/s]	Q_L [m^3/(h.m)]	L'/L	L'/G	Holdup [Pa]	Holdup [mm liq]
0.08295	315	739	22.3	0.94	1.78	1.493E-05	1.41	11.4	0.94%	1.83%	169.0	23.3
0.08295	315	739	22.3	0.94	1.78	1.493E-05	1.41	11.4	0.94%	1.83%	169.0	23.3
0.08295	315	739	22.3	0.94	1.79	1.493E-05	1.41	22.7	0.96%	3.73%	210.8	29.1
0.08295	315	739	22.3	0.94	1.79	1.493E-05	1.40	34.1	1.30%	7.67%	244.0	33.7
0.08295	315	739	22.3	0.94	1.80	1.493E-05	1.40	45.9	1.93%	15.24%	278.6	38.4
0.08295	315	739	22.3	0.94	1.80	1.493E-05	1.39	46.0	1.96%	15.58%	276.8	38.2
0.08295	315	739	22.3	0.94	1.79	1.493E-05	1.41	57.5	2.22%	21.97%	290.6	40.1
0.08295	315	739	22.3	0.94	1.79	1.493E-05	1.41	57.6	2.33%	23.07%	286.1	39.5
0.08295	315	739	22.3	0.94	1.79	1.493E-05	1.40	68.4	1.48%	17.38%	264.1	36.4
0.08295	315	739	22.3	0.94	1.80	1.493E-05	1.41	68.4	1.56%	18.21%	261.9	36.1
0.08295	315	739	22.3	0.94	1.76	1.493E-05	1.74	2.8	13.93%	5.56%	83.3	11.5
0.08295	315	739	22.3	0.94	1.73	1.493E-05	1.77	2.9	14.70%	5.92%	80.6	11.1
0.08295	315	739	22.3	0.94	1.79	1.493E-05	1.71	6.2	4.04%	3.54%	130.5	18.0
0.08295	315	739	22.3	0.94	1.78	1.493E-05	1.72	8.6	2.82%	3.43%	140.6	19.4
0.08295	315	739	22.3	0.94	1.78	1.493E-05	1.72	8.6	2.82%	3.43%	140.6	19.4
0.08295	315	739	22.3	0.94	1.79	1.493E-05	1.72	11.4	2.31%	3.71%	158.7	21.9
0.08295	315	739	22.3	0.94	1.78	1.493E-05	1.72	11.4	2.26%	3.65%	156.7	21.6
0.08295	315	739	22.3	0.94	1.79	1.493E-05	1.71	22.7	3.79%	12.17%	200.2	27.6
0.08295	315	739	22.3	0.94	1.79	1.493E-05	1.71	22.7	3.55%	11.41%	198.1	27.3
0.08295	315	739	22.3	0.94	1.79	1.493E-05	1.71	34.4	5.61%	27.42%	242.7	33.5
0.08295	315	739	22.3	0.94	1.79	1.493E-05	1.72	34.4	5.20%	25.21%	236.3	32.6
0.08295	315	739	22.3	0.94	1.79	1.493E-05	1.71	45.9	7.41%	48.17%	292.7	40.4
0.08295	315	739	22.3	0.94	1.79	1.493E-05	1.70	45.9	6.70%	43.75%	284.8	39.3
0.08295	315	739	22.3	0.94	1.79	1.493E-05	1.71	46.0	7.41%	48.29%	290.3	40.0
0.08295	315	739	22.3	0.94	1.79	1.493E-05	1.71	57.2	13.59%	109.6%	343.0	47.3
0.08295	315	739	22.3	0.94	1.79	1.493E-05	1.71	57.3	14.19%	115.3%	326.7	45.1
0.08295	315	739	22.3	0.94	1.79	1.493E-05	1.72	57.4	12.13%	98.10%	334.3	46.1

A_p [m^2]	s [mm]	ρ_L [kg/m_3]	σ [mN/m]	μ_L [mPa.s]	ρ_v [kg/m^3]	μ_g [Pa.s]	U_s [m/s]	Q_L [$m^3/(h.m)$]	L'/L	L'/G	Holdup [Pa]	Holdup [mm liq]
0.08295	315	739	22.3	0.94	1.79	1.493E-05	1.71	57.6	13.67%	111.4%	338.7	46.7
0.08295	415	739	22.3	0.94	1.80	1.493E-05	1.42	2.8	3.10%	1.49%		
0.08295	415	739	22.3	0.94	1.80	1.493E-05	1.41	5.7	1.12%	1.10%		
0.08295	415	739	22.3	0.94	1.80	1.493E-05	1.40	8.7	0.73%	1.08%		
0.08295	415	739	22.3	0.94	1.80	1.493E-05	1.40	11.4	0.52%	1.02%		
0.08295	415	739	22.3	0.94	1.80	1.493E-05	1.40	11.4	0.52%	1.02%		
0.08295	415	739	22.3	0.94	1.80	1.493E-05	1.40	23.4	0.29%	1.15%		
0.08295	415	739	22.3	0.94	1.80	1.493E-05	1.40	34.6	0.24%	1.41%	251.1	34.6
0.08295	415	739	22.3	0.94	1.79	1.493E-05	1.40	46.2	0.23%	1.81%	272.4	37.6
0.08295	415	739	22.3	0.94	1.80	1.493E-05	1.40	57.5	0.21%	2.13%	272.1	37.5
0.08295	415	739	22.3	0.94	1.80	1.493E-05	1.40	67.8	0.17%	2.02%	242.9	33.5
0.08295	415	739	22.3	0.94	1.80	1.493E-05	1.40	80.5	0.14%	2.00%	228.1	31.5
0.08295	415	739	22.3	0.94	1.79	1.493E-05	1.70	2.9	7.67%	3.13%		
0.08295	415	739	22.3	0.94	1.79	1.493E-05	1.71	5.7	2.62%	2.13%		
0.08295	415	739	22.3	0.94	1.80	1.493E-05	1.72	8.6	1.44%	1.73%		
0.08295	415	739	22.3	0.94	1.80	1.493E-05	1.70	11.4	0.93%	1.51%		
0.08295	415	739	22.3	0.94	1.80	1.493E-05	1.70	11.4	0.93%	1.51%		
0.08295	415	739	22.3	0.94	1.80	1.493E-05	1.70	23.2	0.67%	2.22%	205.7	28.4
0.08295	415	739	22.3	0.94	1.80	1.493E-05	1.70	23.4	0.69%	2.28%	206.2	28.4
0.08295	415	739	22.3	0.94	1.80	1.493E-05	1.70	34.6	0.72%	3.53%	236.7	32.6
0.08295	415	739	22.3	0.94	1.79	1.493E-05	1.71	46.3	0.68%	4.48%	251.3	34.7
0.08295	415	739	22.3	0.94	1.79	1.493E-05	1.71	57.5	0.33%	2.71%	196.1	27.0
0.08295	415	739	22.3	0.94	1.79	1.493E-05	1.71	68.4	0.29%	2.79%	204.4	28.2
0.08295	415	739	22.3	0.94	1.79	1.493E-05	1.71	68.4	0.31%	3.03%	204.1	28.2
0.08295	415	739	22.3	0.94	1.78	1.493E-05	2.04	2.9	22.45%	7.65%		

A_p [m^2]	s [mm]	ρ_L [kg/m$_3$]	σ [mN/m]	μ_L [mPa.s]	ρ_v [kg/m^3]	μ_g [Pa.s]	U_s [m/s]	Q_L [m^3/(h.m)]	L'/L	L'/G	Holdup [Pa]	Holdup [mm liq]
0.08295	415	739	22.3	0.94	1.78	1.493E-05	2.04	2.9	23.27%	7.95%		
0.08295	415	739	22.3	0.94	1.79	1.493E-05	2.01	2.9	17.79%	6.25%	85.1	11.7
0.08295	415	739	22.3	0.94	1.80	1.493E-05	2.03	6.0	5.66%	4.06%	116.1	16.0
0.08295	415	739	22.3	0.94	1.80	1.493E-05	2.02	8.7	3.10%	3.22%	139.1	19.2
0.08295	415	739	22.3	0.94	1.80	1.493E-05	2.02	11.4	2.28%	3.11%	152.9	21.1
0.08295	415	739	22.3	0.94	1.80	1.493E-05	2.00	11.5	2.24%	3.10%	158.4	21.9
0.08295	415	739	22.3	0.94	1.80	1.493E-05	2.01	11.5	2.15%	2.97%	155.8	21.5
0.08295	415	739	22.3	0.94	1.80	1.493E-05	2.01	11.5	2.15%	2.97%	155.8	21.5
0.08295	415	739	22.3	0.94	1.79	1.493E-05	2.02	23.2	2.54%	7.05%	204.8	28.2
0.08295	415	739	22.3	0.94	1.79	1.493E-05	2.02	34.1	3.23%	13.15%	222.3	30.7
0.08295	415	739	22.3	0.94	1.80	1.493E-05	2.02	34.2	3.30%	13.46%	219.4	30.3
0.08295	415	739	22.3	0.94	1.80	1.493E-05	2.02	45.9	1.09%	6.00%	199.1	27.5
0.08295	415	739	22.3	0.94	1.79	1.493E-05	2.02	46.0	1.16%	6.38%	200.0	27.6
0.08295	415	739	22.3	0.94	1.79	1.493E-05	2.02	57.3	1.35%	9.26%	231.8	32.0
0.08295	415	739	22.3	0.94	1.79	1.493E-05	2.01	57.4	1.27%	8.74%	232.4	32.1
0.08295	415	739	22.3	0.94	1.79	1.493E-05	2.04	68.2	5.99%	48.51%	321.6	44.4
0.08295	415	739	22.3	0.94	1.79	1.493E-05	2.04	68.4	6.80%	55.07%	317.1	43.7
0.08295	415	739	22.3	0.94	1.79	1.493E-05	2.04	68.5	6.54%	53.23%	314.3	43.4
0.08295	415	739	22.3	0.94	1.79	1.493E-05	2.02	68.6	8.17%	66.90%	340.1	46.9
0.08295	415	739	22.3	0.94	1.80	1.493E-05	2.00	80.1	9.50%	91.49%	374.4	51.6
0.08295	415	739	22.3	0.94	1.80	1.493E-05	2.00	80.2	10.72%	103.5%	400.2	55.2
0.08295	415	739	22.3	0.94	1.78	1.493E-05	2.33	2.9	54.38%	16.62%	91.6	12.6
0.08295	415	739	22.3	0.94	1.78	1.493E-05	2.33	3.0	54.44%	16.78%	93.0	12.8
0.08295	415	739	22.3	0.94	1.79	1.493E-05	2.31	6.0	17.52%	10.97%	114.9	15.8
0.08295	415	739	22.3	0.94	1.79	1.493E-05	2.31	6.0	16.57%	10.42%	116.9	16.1
0.08295	415	739	22.3	0.94	1.79	1.493E-05	2.31	6.0	16.57%	10.42%	116.9	16.1
0.08295	415	739	22.3	0.94	1.79	1.493E-05	2.31	8.7	11.43%	10.36%	142.2	19.6

A_p [m^2]	s [mm]	ρ_L [kg/m3]	σ [mN/m]	μ_L [mPa.s]	ρ_v [kg/m^3]	μ_g [Pa.s]	U_s [m/s]	Q_L [m^3/(h.m)]	L'/L	L'/G	Holdup [Pa]	Holdup [mm liq]
0.08295	415	739	22.3	0.94	1.79	1.493E-05	2.32	8.7	12.39%	11.25%	133.3	18.4
0.08295	415	739	22.3	0.94	1.80	1.493E-05	2.31	11.3	12.81%	15.07%	151.0	20.8
0.08295	415	739	22.3	0.94	1.80	1.493E-05	2.31	11.5	12.19%	14.61%	155.5	21.5
0.08295	415	739	22.3	0.94	1.80	1.493E-05	2.31	11.5	12.53%	15.02%	152.2	21.0
0.08295	415	739	22.3	0.94	1.80	1.493E-05	2.31	11.6	11.93%	14.43%	157.6	21.7
0.08295	515	739	22.3	0.94	1.78	1.493E-05	1.41	2.9	2.52%	1.24%	100.9	13.9
0.08295	515	739	22.3	0.94	1.79	1.493E-05	1.40	6.0	0.92%	0.95%	133.6	18.4
0.08295	515	739	22.3	0.94	1.80	1.493E-05	1.40	8.7	0.59%	0.88%	154.4	21.3
0.08295	515	739	22.3	0.94	1.79	1.493E-05	1.41	11.7	0.41%	0.82%	167.3	23.1
0.08295	515	739	22.3	0.94	1.78	1.493E-05	1.41	23.2	0.20%	0.80%	208.7	28.8
0.08295	515	739	22.3	0.94	1.78	1.493E-05	1.41	23.2	0.20%	0.80%	208.7	28.8
0.08295	515	739	22.3	0.94	1.79	1.493E-05	1.41	33.9	0.14%	0.85%	240.1	33.1
0.08295	515	739	22.3	0.94	1.79	1.493E-05	1.41	45.4	0.11%	0.89%	264.4	36.5
0.08295	515	739	22.3	0.94	1.79	1.493E-05	1.42	57.0	0.13%	1.29%	278.9	38.5
0.08295	515	739	22.3	0.94	1.79	1.493E-05	1.42	69.2	0.13%	1.51%	261.4	36.1
0.08295	515	739	22.3	0.94	1.78	1.493E-05	1.72	2.9	6.43%	2.63%	86.8	12.0
0.08295	515	739	22.3	0.94	1.79	1.493E-05	1.71	6.0	2.08%	1.76%	120.0	16.6
0.08295	515	739	22.3	0.94	1.79	1.493E-05	1.71	8.7	1.18%	1.45%	140.1	19.3
0.08295	515	739	22.3	0.94	1.79	1.493E-05	1.71	11.6	0.72%	1.19%	155.6	21.5
0.08295	515	739	22.3	0.94	1.79	1.493E-05	1.71	11.6	0.72%	1.19%	155.6	21.5
0.08295	515	739	22.3	0.94	1.78	1.493E-05	1.72	22.7	0.39%	1.25%	194.7	26.9
0.08295	515	739	22.3	0.94	1.79	1.493E-05	1.71	34.1	0.30%	1.45%	226.4	31.2
0.08295	515	739	22.3	0.94	1.79	1.493E-05	1.72	45.4	0.25%	1.59%	234.4	32.3
0.08295	515	739	22.3	0.94	1.79	1.493E-05	1.71	57.5	0.24%	1.93%	232.5	32.1
0.08295	515	739	22.3	0.94	1.79	1.493E-05	1.71	69.2	0.23%	2.22%	217.4	30.0

A_p [m^2]	s [mm]	ρ_L [kg/m$_3$]	σ [mN/m]	μ_L [mPa.s]	ρ_v [kg/m^3]	μ_g [Pa.s]	U_s [m/s]	Q_L [m^3/(h.m)]	L'/L	L'/G	Holdup [Pa]	Holdup [mm liq]
0.08295	515	739	22.3	0.94	1.77	1.493E-05	2.04	2.9	16.35%	5.65%	72.2	10.0
0.08295	515	739	22.3	0.94	1.79	1.493E-05	2.02	5.9	4.59%	3.24%	115.7	16.0
0.08295	515	739	22.3	0.94	1.79	1.493E-05	2.03	8.6	2.48%	2.53%	126.4	17.4
0.08295	515	739	22.3	0.94	1.79	1.493E-05	2.03	11.4	1.45%	1.97%	146.6	20.2
0.08295	515	739	22.3	0.94	1.79	1.493E-05	2.03	11.4	1.45%	1.97%	146.6	20.2
0.08295	515	739	22.3	0.94	1.79	1.493E-05	2.02	23.2	0.81%	2.25%	188.2	26.0
0.08295	515	739	22.3	0.94	1.79	1.493E-05	2.02	33.9	0.82%	3.31%	190.6	26.3
0.08295	515	739	22.3	0.94	1.79	1.493E-05	2.02	45.4	0.56%	3.06%	177.3	24.5
0.08295	515	739	22.3	0.94	1.79	1.493E-05	2.02	58.3	0.53%	3.73%	214.5	29.6
0.08295	515	739	22.3	0.94	1.79	1.493E-05	2.03	69.0	0.55%	4.57%	237.1	32.7
0.08295	515	739	22.3	0.94	1.78	1.493E-05	2.34	2.9	41.67%	12.51%	82.6	11.4
0.08295	515	739	22.3	0.94	1.77	1.493E-05	2.34	2.9	42.06%	12.75%	83.0	11.5
0.08295	515	739	22.3	0.94	1.79	1.493E-05	2.33	5.9	11.14%	6.82%	109.4	15.1
0.08295	515	739	22.3	0.94	1.79	1.493E-05	2.32	8.6	5.18%	4.61%	129.2	17.8
0.08295	515	739	22.3	0.94	1.80	1.493E-05	2.32	11.4	3.53%	4.18%	147.7	20.4
0.08295	515	739	22.3	0.94	1.80	1.493E-05	2.32	11.4	3.53%	4.18%	147.7	20.4
0.08295	515	739	22.3	0.94	1.79	1.493E-05	2.31	23.2	3.32%	8.08%	172.7	23.8
0.08295	515	739	22.3	0.94	1.79	1.493E-05	2.32	34.1	2.43%	8.65%	157.7	21.8
0.08295	515	739	22.3	0.94	1.79	1.493E-05	2.31	45.6	2.18%	10.38%	198.7	27.4
0.08295	515	739	22.3	0.94	1.79	1.493E-05	2.32	45.7	2.14%	10.20%	194.6	26.8
0.08295	515	739	22.3	0.94	1.79	1.493E-05	2.32	54.8	2.63%	15.00%	227.6	31.4
0.08295	515	739	22.3	0.94	1.79	1.493E-05	2.31	57.8	2.84%	17.16%	240.6	33.2
0.08295	515	739	22.3	0.94	1.79	1.493E-05	2.32	58.1	2.84%	17.23%	234.4	32.3
0.08295	515	739	22.3	0.94	1.79	1.493E-05	2.31	69.2	5.69%	41.08%	282.3	38.9
0.08295	515	739	22.3	0.94	1.79	1.493E-05	2.31	69.7	5.81%	42.35%	286.0	39.4
0.08295	515	739	22.3	0.94	1.79	1.493E-05	2.31	70.0	5.56%	40.68%	285.3	39.4

A_p [m^2]	s [mm]	ρ_L [kg/m3]	σ [mN/m]	μ_L [mPa.s]	ρ_V [kg/m^3]	μ_g [Pa.s]	U_s [m/s]	Q_L [m^3/(h.m)]	L'/L	L'/G	Holdup [Pa]	Holdup [mm liq]
0.08295	615	739	22.3	0.94	1.80	1.493E-05	1.40	2.9	2.33%	1.15%	109.9	15.2
0.08295	615	739	22.3	0.94	1.80	1.493E-05	1.39	6.0	0.83%	0.86%	141.3	19.5
0.08295	615	739	22.3	0.94	1.80	1.493E-05	1.39	8.6	0.50%	0.75%	160.8	22.2
0.08295	615	739	22.3	0.94	1.79	1.493E-05	1.40	11.5	0.35%	0.68%	174.3	24.0
0.08295	615	739	22.3	0.94	1.80	1.493E-05	1.40	57.0	0.07%	0.73%	229.7	31.7
0.08295	615	739	22.3	0.94	1.80	1.493E-05	1.40	69.0	0.06%	0.70%	207.5	28.6
0.08295	615	739	22.3	0.94	1.79	1.493E-05	1.72	2.9	5.37%	2.18%	101.1	13.9
0.08295	615	739	22.3	0.94	1.80	1.493E-05	1.71	6.0	1.78%	1.50%	129.5	17.9
0.08295	615	739	22.3	0.94	1.80	1.493E-05	1.71	8.7	0.96%	1.18%	147.6	20.4
0.08295	615	739	22.3	0.94	1.80	1.493E-05	1.70	11.5	0.56%	0.91%	166.7	23.0
0.08295	615	739	22.3	0.94	1.79	1.493E-05	1.70	23.0	0.28%	0.92%	206.4	28.5
0.08295	615	739	22.3	0.94	1.79	1.493E-05	1.70	34.8	0.19%	0.95%	230.4	31.8
0.08295	615	739	22.3	0.94	1.79	1.493E-05	1.70	45.9	0.17%	1.11%	214.5	29.6
0.08295	615	739	22.3	0.94	1.79	1.493E-05	1.70	57.7	0.14%	1.16%	187.5	25.9
0.08295	615	739	22.3	0.94	1.80	1.493E-05	1.71	58.0	0.14%	1.15%	188.2	26.0
0.08295	615	739	22.3	0.94	1.80	1.493E-05	1.71	69.0	0.11%	1.04%	200.8	27.7
0.08295	615	739	22.3	0.94	1.79	1.493E-05	2.02	2.9	11.81%	4.07%	91.4	12.6
0.08295	615	739	22.3	0.94	1.79	1.493E-05	2.02	6.0	3.63%	2.60%	119.2	16.4
0.08295	615	739	22.3	0.94	1.80	1.493E-05	2.02	8.7	1.75%	1.81%	141.6	19.5
0.08295	615	739	22.3	0.94	1.80	1.493E-05	2.02	11.5	1.13%	1.54%	160.1	22.1
0.08295	615	739	22.3	0.94	1.79	1.493E-05	2.02	22.7	0.51%	1.38%	203.1	28.0
0.08295	615	739	22.3	0.94	1.79	1.493E-05	2.02	22.7	0.51%	1.38%	203.1	28.0
0.08295	615	739	22.3	0.94	1.80	1.493E-05	2.02	34.6	0.46%	1.88%	194.1	26.8
0.08295	615	739	22.3	0.94	1.79	1.493E-05	2.02	45.7	0.36%	1.96%	183.4	25.3
0.08295	615	739	22.3	0.94	1.80	1.493E-05	2.02	57.4	0.26%	1.79%	206.0	28.4
0.08295	615	739	22.3	0.94	1.80	1.493E-05	2.02	69.3	0.25%	2.05%	236.8	32.7

A_p [m^2]	s [mm]	ρ_L [kg/m$_3$]	σ [mN/m]	μ_L [mPa.s]	ρ_v [kg/m^3]	μ_g [Pa.s]	U_s [m/s]	Q_L [m^3/(h.m)]	L'/L	L'/G	Holdup [Pa]	Holdup [mm liq]
0.08295	615	739	22.3	0.94	1.78	1.493E-05	2.32	2.9	28.70%	8.74%	96.4	13.3
0.08295	615	739	22.3	0.94	1.79	1.493E-05	2.32	2.9	28.54%	8.69%	99.1	13.7
0.08295	615	739	22.3	0.94	1.79	1.493E-05	2.32	6.0	7.38%	4.61%	128.5	17.7
0.08295	615	739	22.3	0.94	1.79	1.493E-05	2.32	8.7	3.25%	2.96%	149.1	20.6
0.08295	615	739	22.3	0.94	1.79	1.493E-05	2.31	11.5	2.12%	2.54%	157.8	21.8
0.08295	615	739	22.3	0.94	1.79	1.493E-05	2.31	11.5	2.12%	2.54%	157.8	21.8
0.08295	615	739	22.3	0.94	1.79	1.493E-05	2.32	22.9	1.20%	2.86%	198.4	27.4
0.08295	615	739	22.3	0.94	1.80	1.493E-05	2.32	34.2	1.11%	3.94%	166.2	22.9
0.08295	615	739	22.3	0.94	1.79	1.493E-05	2.31	45.7	0.74%	3.52%	201.5	27.8
0.08295	615	739	22.3	0.94	1.80	1.493E-05	2.30	57.5	0.91%	5.44%	253.6	35.0
0.08295	615	739	22.3	0.94	1.80	1.493E-05	2.31	69.2	1.91%	13.79%	310.1	42.8
0.08295	615	739	22.3	0.94	1.80	1.493E-05	2.31	69.5	1.87%	13.54%	304.3	42.0

Table 1. CO_2/n-butanol data for 315, 415, 515 and 615mm tray spacings.

A_p [m^2]	s [mm]	ρ_L [kg/m$_3$]	σ [mN/m]	μ_L [mPa.s]	ρ_v [kg/m^3]	μ_g [Pa.s]	U_s [m/s]	Q_L [m^3/(h.m)]	L'/L	L'/G	Holdup [Pa]	Holdup [mm liq]
0.08295	315	806	22.8	2.6	1.77	1.493E-05	1.21	2.9	2.82%	1.80%	177.2	22.4
0.08295	315	806	22.8	2.6	1.78	1.493E-05	1.21	5.8	1.26%	1.62%	215.2	27.2
0.08295	315	806	22.8	2.6	1.78	1.493E-05	1.21	8.7	0.84%	1.59%	237.3	30.0
0.08295	315	806	22.8	2.6	1.78	1.493E-05	1.21	8.7	0.84%	1.59%	237.3	30.0
0.08295	315	806	22.8	2.6	1.78	1.493E-05	1.21	11.6	0.63%	1.60%	251.3	31.8
0.08295	315	806	22.8	2.6	1.78	1.493E-05	1.21	23.0	0.50%	2.53%	300.5	38.0
0.08295	315	806	22.8	2.6	1.77	1.493E-05	1.20	34.9	0.37%	2.89%	333.5	42.2
0.08295	315	806	22.8	2.6	1.77	1.493E-05	1.21	45.6	0.48%	4.86%	357.4	45.2
0.08295	315	806	22.8	2.6	1.78	1.493E-05	1.21	57.2	0.74%	9.28%	379.8	48.0

A_p [m^2]	s [mm]	ρ_L [kg/m_3]	σ [mN/m]	μ_L [mPa.s]	ρ_v [kg/m^3]	μ_g [Pa.s]	U_s [m/s]	Q_L [$m^3/(h.m)$]	L'/L	L'/G	Holdup [Pa]	Holdup [mm liq]
0.08295	315	806	22.8	2.6	1.78	1.493E-05	1.21	57.3	0.71%	8.93%	378.9	47.9
0.08295	315	806	22.8	2.6	1.77	1.493E-05	1.21	67.5	0.78%	11.63%	368.5	46.6
0.08295	315	806	22.8	2.6	1.78	1.493E-05	1.41	2.9	4.95%	2.70%	177.6	22.5
0.08295	315	806	22.8	2.6	1.78	1.493E-05	1.42	5.8	2.09%	2.28%	213.0	26.9
0.08295	315	806	22.8	2.6	1.78	1.493E-05	1.41	8.6	1.35%	2.20%	237.3	30.0
0.08295	315	806	22.8	2.6	1.78	1.493E-05	1.41	8.6	1.35%	2.20%	237.3	30.0
0.08295	315	806	22.8	2.6	1.78	1.493E-05	1.41	11.5	1.02%	2.21%	250.9	31.7
0.08295	315	806	22.8	2.6	1.77	1.493E-05	1.42	22.6	0.96%	4.08%	296.5	37.5
0.08295	315	806	22.8	2.6	1.78	1.493E-05	1.42	34.9	0.93%	6.08%	332.1	42.0
0.08295	315	806	22.8	2.6	1.77	1.493E-05	1.42	45.6	1.67%	14.21%	363.3	46.0
0.08295	315	806	22.8	2.6	1.78	1.493E-05	1.42	45.7	1.58%	13.48%	363.3	45.9
0.08295	315	806	22.8	2.6	1.77	1.493E-05	1.42	57.3	1.62%	17.31%	375.9	47.5
0.08295	315	806	22.8	2.6	1.78	1.493E-05	1.40	68.0	0.98%	12.69%	358.2	45.3
0.08295	315	806	22.8	2.6	1.78	1.493E-05	1.70	2.9	10.29%	4.64%	184.2	23.3
0.08295	315	806	22.8	2.6	1.77	1.493E-05	1.71	5.8	4.14%	3.77%	217.6	27.5
0.08295	315	806	22.8	2.6	1.78	1.493E-05	1.71	8.6	2.60%	3.48%	242.9	30.7
0.08295	315	806	22.8	2.6	1.78	1.493E-05	1.71	8.6	2.60%	3.48%	242.9	30.7
0.08295	315	806	22.8	2.6	1.78	1.493E-05	1.71	11.5	2.18%	3.89%	255.6	32.3
0.08295	315	806	22.8	2.6	1.77	1.493E-05	1.72	22.8	3.75%	13.27%	299.7	37.9
0.08295	315	806	22.8	2.6	1.77	1.493E-05	1.73	34.8	4.79%	25.75%	345.4	43.7
0.08295	315	806	22.8	2.6	1.77	1.493E-05	1.73	34.9	5.05%	27.22%	344.5	43.6
0.08295	315	806	22.8	2.6	1.78	1.493E-05	1.71	45.7	5.36%	38.02%	377.1	47.7
0.08295	315	806	22.8	2.6	1.78	1.493E-05	1.70	45.7	5.08%	36.18%	371.7	47.0
0.08295	315	806	22.8	2.6	1.78	1.493E-05	1.71	45.7	5.70%	40.46%	373.5	47.2
0.08295	415	806	22.8	2.6	1.78	1.493E-05	1.21	2.9	2.08%	1.32%	177.0	22.4

A_p [m^2]	s [mm]	ρ_L [kg/m$_3$]	σ [mN/m]	μ_L [mPa.s]	ρ_v [kg/m^3]	μ_g [Pa.s]	U_s [m/s]	Q_L [m^3/(h.m)]	L'/L	L'/G	Holdup [Pa]	Holdup [mm liq]
0.08295	415	806	22.8	2.6	1.78	1.493E-05	1.21	5.9	0.86%	1.10%	212.4	26.9
0.08295	415	806	22.8	2.6	1.78	1.493E-05	1.21	8.7	0.56%	1.07%	234.5	29.7
0.08295	415	806	22.8	2.6	1.78	1.493E-05	1.20	11.7	0.40%	1.04%	252.8	32.0
0.08295	415	806	22.8	2.6	1.78	1.493E-05	1.20	11.7	0.40%	1.04%	252.8	32.0
0.08295	415	806	22.8	2.6	1.78	1.493E-05	1.20	22.9	0.21%	1.06%	304.2	38.5
0.08295	415	806	22.8	2.6	1.78	1.493E-05	1.20	34.6	0.16%	1.26%	338.5	42.8
0.08295	415	806	22.8	2.6	1.78	1.493E-05	1.20	45.5	0.13%	1.35%	360.5	45.6
0.08295	415	806	22.8	2.6	1.78	1.493E-05	1.21	57.4	0.12%	1.52%	374.3	47.3
0.08295	415	806	22.8	2.6	1.78	1.493E-05	1.21	69.2	0.11%	1.73%	358.3	45.3
0.08295	415	806	22.8	2.6	1.78	1.493E-05	1.41	2.9	3.34%	1.84%	178.3	22.5
0.08295	415	806	22.8	2.6	1.78	1.493E-05	1.42	5.8	1.43%	1.57%	215.2	27.2
0.08295	415	806	22.8	2.6	1.78	1.493E-05	1.42	8.7	0.88%	1.44%	241.4	30.5
0.08295	415	806	22.8	2.6	1.78	1.493E-05	1.41	11.5	0.61%	1.33%	256.9	32.5
0.08295	415	806	22.8	2.6	1.78	1.493E-05	1.41	11.5	0.61%	1.33%	256.9	32.5
0.08295	415	806	22.8	2.6	1.78	1.493E-05	1.41	22.5	0.34%	1.43%	302.0	38.2
0.08295	415	806	22.8	2.6	1.78	1.493E-05	1.41	34.5	0.27%	1.76%	336.6	42.6
0.08295	415	806	22.8	2.6	1.78	1.493E-05	1.41	46.4	0.22%	1.96%	359.5	45.5
0.08295	415	806	22.8	2.6	1.78	1.493E-05	1.41	57.6	0.21%	2.26%	362.9	45.9
0.08295	415	806	22.8	2.6	1.78	1.493E-05	1.42	68.2	0.16%	2.03%	323.6	40.9
0.08295	415	806	22.8	2.6	1.78	1.493E-05	1.71	2.9	7.65%	3.49%	185.2	23.4
0.08295	415	806	22.8	2.6	1.78	1.493E-05	1.72	5.9	2.80%	2.54%	220.8	27.9
0.08295	415	806	22.8	2.6	1.78	1.493E-05	1.71	8.7	1.53%	2.08%	243.7	30.8
0.08295	415	806	22.8	2.6	1.78	1.493E-05	1.71	11.6	1.06%	1.91%	258.5	32.7
0.08295	415	806	22.8	2.6	1.78	1.493E-05	1.71	11.6	1.06%	1.91%	258.5	32.7
0.08295	415	806	22.8	2.6	1.78	1.493E-05	1.71	23.4	0.69%	2.48%	307.6	38.9
0.08295	415	806	22.8	2.6	1.78	1.493E-05	1.71	34.6	0.66%	3.52%	339.0	42.9

A_p [m^2]	s [mm]	ρ_L [kg/m^3]	σ [mN/m]	μ_L [mPa.s]	ρ_v [kg/m^3]	μ_g [Pa.s]	U_s [m/s]	Q_L [m^3/(h.m)]	L'/L	L'/G	Holdup [Pa]	Holdup [mm liq]
0.08295	415	806	22.8	2.6	1.77	1.493E-05	1.72	46.4	0.49%	3.53%	345.3	43.7
0.08295	415	806	22.8	2.6	1.78	1.493E-05	2.04	5.9	6.59%	5.05%	213.8	27.0
0.08295	415	806	22.8	2.6	1.78	1.493E-05	2.03	8.7	3.22%	3.64%	236.0	29.9
0.08295	415	806	22.8	2.6	1.78	1.493E-05	2.04	11.4	2.33%	3.45%	260.5	32.9
0.08295	415	806	22.8	2.6	1.78	1.493E-05	2.04	11.4	2.33%	3.45%	260.5	32.9
0.08295	415	806	22.8	2.6	1.78	1.493E-05	2.05	23.2	2.24%	6.74%	317.0	40.1
0.08295	415	806	22.8	2.6	1.77	1.493E-05	2.04	34.6	1.92%	8.66%	330.7	41.8
0.08295	415	806	22.8	2.6	1.78	1.493E-05	2.05	45.6		6.09%	315.4	39.9
0.08295	415	806	22.8	2.6	1.77	1.493E-05	2.04	57.5	0.80%	6.00%	331.9	42.0
0.08295	415	806	22.8	2.6	1.78	1.493E-05	2.03	68.4	0.82%	7.29%	358.4	45.3
0.08295	515	806	22.8	2.6	1.78	1.493E-05	1.42	2.9	3.19%	1.71%	173.9	22.0
0.08295	515	806	22.8	2.6	1.78	1.493E-05	1.40	5.8	1.20%	1.32%	206.1	26.1
0.08295	515	806	22.8	2.6	1.78	1.493E-05	1.41	8.6	0.72%	1.16%	233.6	29.5
0.08295	515	806	22.8	2.6	1.78	1.493E-05	1.42	11.5	0.52%	1.11%	252.2	31.9
0.08295	515	806	22.8	2.6	1.78	1.493E-05	1.41	22.2	0.27%	1.12%	302.5	38.3
0.08295	515	806	22.8	2.6	1.78	1.493E-05	1.41	34.5	0.17%	1.11%	340.5	43.1
0.08295	515	806	22.8	2.6	1.78	1.493E-05	1.41	34.5	0.17%	1.11%	340.5	43.1
0.08295	515	806	22.8	2.6	1.78	1.493E-05	1.41	46.2	0.13%	1.12%	370.3	46.8
0.08295	515	806	22.8	2.6	1.77	1.493E-05	1.42	57.5	0.12%	1.28%	376.8	47.7
0.08295	515	806	22.8	2.6	1.78	1.493E-05	1.42	69.0	0.11%	1.47%	371.6	47.0
0.08295	515	806	22.8	2.6	1.78	1.493E-05	1.41	79.3	0.10%	1.54%	349.9	44.3
0.08295	515	806	22.8	2.6	1.78	1.493E-05	1.71	2.9	6.76%	2.99%	185.3	23.4
0.08295	515	806	22.8	2.6	1.78	1.493E-05	1.71	5.8	2.39%	2.13%	216.3	27.4
0.08295	515	806	22.8	2.6	1.78	1.493E-05	1.71	8.7	1.32%	1.77%	244.2	30.9
0.08295	515	806	22.8	2.6	1.78	1.493E-05	1.71	11.6	0.87%	1.56%	258.0	32.6

A_p [m^2]	s [mm]	ρ_L [kg/m$_3$]	σ [mN/m]	μ_L [mPa.s]	ρ_v [kg/m^3]	μ_g [Pa.s]	U_s [m/s]	Q_L [m^3/(h.m)]	L'/L	L'/G	Holdup [Pa]	Holdup [mm liq]
0.08295	515	806	22.8	2.6	1.77	1.493E-05	1.70	22.5	0.44%	1.56%	304.2	38.5
0.08295	515	806	22.8	2.6	1.77	1.493E-05	1.70	22.5	0.44%	1.56%	304.2	38.5
0.08295	515	806	22.8	2.6	1.77	1.493E-05	1.71	33.6	0.31%	1.63%	339.3	42.9
0.08295	515	806	22.8	2.6	1.78	1.493E-05	1.71	44.8	0.28%	1.97%	358.2	45.3
0.08295	515	806	22.8	2.6	1.78	1.493E-05	1.72	57.7	0.29%	2.58%	363.1	45.9
0.08295	515	806	22.8	2.6	1.77	1.493E-05	1.72	69.1	0.22%	2.33%	337.7	42.7
0.08295	515	806	22.8	2.6	1.78	1.493E-05	1.71	78.1	0.17%	2.03%	310.0	39.2
0.08295	515	806	22.8	2.6	1.78	1.493E-05	2.05	2.9	17.09%	6.38%	190.4	24.1
0.08295	515	806	22.8	2.6	1.78	1.493E-05	2.03	5.8	4.83%	3.65%	223.3	28.2
0.08295	515	806	22.8	2.6	1.78	1.493E-05	2.04	8.7	2.50%	2.83%	245.8	31.1
0.08295	515	806	22.8	2.6	1.78	1.493E-05	2.03	11.6	1.61%	2.43%	263.8	33.4
0.08295	515	806	22.8	2.6	1.78	1.493E-05	2.03	11.6	1.61%	2.43%	263.8	33.4
0.08295	515	806	22.8	2.6	1.78	1.493E-05	2.03	22.4	0.85%	2.50%	314.6	39.8
0.08295	515	806	22.8	2.6	1.78	1.493E-05	2.05	22.7	0.86%	2.54%	319.8	40.4
0.08295	515	806	22.8	2.6	1.78	1.493E-05	2.05	34.3	0.69%	3.07%	328.1	41.5
0.08295	515	806	22.8	2.6	1.77	1.493E-05	2.03	34.6	0.65%	2.93%	321.6	40.7
0.08295	515	806	22.8	2.6	1.78	1.493E-05	2.04	45.7	0.58%	3.43%	322.5	40.8
0.08295	515	806	22.8	2.6	1.78	1.493E-05	2.04	46.2	0.60%	3.61%	329.6	41.7
0.08295	515	806	22.8	2.6	1.78	1.493E-05	2.04	57.3	0.44%	3.29%	316.4	40.0
0.08295	515	806	22.8	2.6	1.77	1.493E-05	2.04	57.8	0.43%	3.26%	311.2	39.4
0.08295	515	806	22.8	2.6	1.78	1.493E-05	2.04	68.5	0.35%	3.11%	330.2	41.8
0.08295	515	806	22.8	2.6	1.78	1.493E-05	2.04	68.7	0.36%	3.24%	329.6	41.7
0.08295	515	806	22.8	2.6	1.78	1.493E-05	2.04	79.7	0.29%	3.02%	345.6	43.7
0.08295	515	806	22.8	2.6	1.78	1.493E-05	2.32	2.9	41.48%	13.74%	215.7	27.3
0.08295	515	806	22.8	2.6	1.77	1.493E-05	2.32	2.9	41.50%	13.86%	217.5	27.5
0.08295	515	806	22.8	2.6	1.78	1.493E-05	2.31	5.8	10.00%	6.65%	240.3	30.4

A_p [m^2]	s [mm]	ρ_L [kg/m$_3$]	σ [mN/m]	μ_L [mPa.s]	ρ_v [kg/m^3]	μ_g [Pa.s]	U_s [m/s]	Q_L [m^3/(h.m)]	L'/L	L'/G	Holdup [Pa]	Holdup [mm liq]
0.08295	515	806	22.8	2.6	1.77	1.493E-05	2.32	8.7	4.66%	4.66%	262.3	33.2
0.08295	515	806	22.8	2.6	1.78	1.493E-05	2.31	11.6	2.82%	3.77%	287.8	36.4
0.08295	515	806	22.8	2.6	1.78	1.493E-05	2.31	11.6	2.82%	3.77%	287.8	36.4
0.08295	515	806	22.8	2.6	1.78	1.493E-05	2.32	22.7	2.15%	5.59%	325.1	41.1
0.08295	515	806	22.8	2.6	1.78	1.493E-05	2.32	34.3	1.55%	6.10%	291.6	36.9
0.08295	515	806	22.8	2.6	1.78	1.493E-05	2.33	46.4	1.19%	6.32%	327.9	41.5
0.08295	515	806	22.8	2.6	1.78	1.493E-05	2.33	57.2	1.06%	6.91%	352.8	44.6
0.08295	515	806	22.8	2.6	1.77	1.493E-05	2.32	68.7	1.21%	9.53%	390.4	49.4
0.08295	515	806	22.8	2.6	1.77	1.493E-05	2.32	79.8	1.60%	14.58%	416.8	52.7
0.08295	515	806	22.8	2.6	1.77	1.493E-05	2.32	79.8	1.68%	15.39%	419.5	53.0
0.08295	515	806	22.8	2.6	1.77	1.493E-05	2.60	5.8	31.28%	18.69%	280.7	35.5
0.08295	515	806	22.8	2.6	1.77	1.493E-05	2.61	5.8	30.95%	18.31%	272.6	34.5
0.08295	515	806	22.8	2.6	1.77	1.493E-05	2.61	5.8	29.22%	17.34%	267.4	33.8
0.08295	515	806	22.8	2.6	1.77	1.493E-05	2.62	8.7	23.11%	20.36%	287.6	36.4
0.08295	515	806	22.8	2.6	1.77	1.493E-05	2.62	8.7	20.20%	17.86%	289.0	36.6
0.08295	515	806	22.8	2.6	1.77	1.493E-05	2.63	8.7	21.19%	18.68%	284.7	36.0
0.08295	515	806	22.8	2.6	1.77	1.493E-05	2.62	8.7	23.11%	20.36%	287.6	36.4
0.08295	515	806	22.8	2.6	1.77	1.493E-05	2.63	8.7	21.19%	18.68%	284.7	36.0
0.08295	515	806	22.8	2.6	1.77	1.493E-05	2.62	8.7	20.20%	17.86%	289.0	36.6
0.08295	515	806	22.8	2.6	1.78	1.493E-05	2.62	11.5	26.95%	31.57%	304.0	38.4
0.08295	515	806	22.8	2.6	1.77	1.493E-05	2.62	11.6	27.19%	31.96%	295.4	37.4
0.08295	515	806	22.8	2.6	1.78	1.493E-05	2.62	11.6	26.43%	31.10%	303.9	38.4
0.08295	515	806	22.8	2.6	1.77	1.493E-05	2.63	23.0	21.31%	49.85%	340.5	43.1
0.08295	515	806	22.8	2.6	1.77	1.493E-05	2.63	23.1	21.69%	50.75%	330.9	41.8
0.08295	515	806	22.8	2.6	1.77	1.493E-05	2.63	23.1	20.82%	48.64%	345.2	43.7
0.08295	615	806	22.8	2.6	1.77	1.493E-05	1.72	2.9	5.80%	2.56%	179.9	22.8

Stellenbosch University http://scholar.sun.ac.za

A_p [m^2]	s [mm]	ρ_L [kg/m$_3$]	σ [mN/m]	μ_L [mPa.s]	ρ_v [kg/m^3]	μ_g [Pa.s]	U_s [m/s]	Q_L [m^3/(h.m)]	L'/L	L'/G	Holdup [Pa]	Holdup [mm liq]
0.08295	615	806	22.8	2.6	1.76	1.493E-05	1.74	2.9	5.86%	2.60%	180.0	22.8
0.08295	615	806	22.8	2.6	1.77	1.493E-05	1.72	5.9	1.91%	1.76%	215.5	27.3
0.08295	615	806	22.8	2.6	1.76	1.493E-05	1.73	6.0	1.94%	1.81%	212.4	26.9
0.08295	615	806	22.8	2.6	1.77	1.493E-05	1.72	8.6	1.12%	1.49%	236.6	29.9
0.08295	615	806	22.8	2.6	1.78	1.493E-05	1.72	8.8	1.08%	1.47%	238.1	30.1
0.08295	615	806	22.8	2.6	1.78	1.493E-05	1.71	11.5	0.73%	1.30%	253.8	32.1
0.08295	615	806	22.8	2.6	1.77	1.493E-05	1.72	11.5	0.74%	1.32%	252.5	31.9
0.08295	615	806	22.8	2.6	1.78	1.493E-05	1.72	22.6	0.36%	1.26%	299.2	37.8
0.08295	615	806	22.8	2.6	1.78	1.493E-05	1.71	34.4	0.23%	1.21%	333.0	42.1
0.08295	615	806	22.8	2.6	1.78	1.493E-05	1.71	34.4	0.23%	1.21%	333.0	42.1
0.08295	615	806	22.8	2.6	1.78	1.493E-05	1.71	46.1	0.18%	1.32%	344.6	43.6
0.08295	615	806	22.8	2.6	1.78	1.493E-05	1.72	57.3	0.17%	1.54%	320.1	40.5
0.08295	615	806	22.8	2.6	1.78	1.493E-05	1.72	68.8	0.13%	1.39%	280.8	35.5
0.08295	615	806	22.8	2.6	1.77	1.493E-05	1.42	2.8	2.69%	1.42%	173.7	22.0
0.08295	615	806	22.8	2.6	1.77	1.493E-05	1.41	2.9	2.52%	1.37%	174.2	22.0
0.08295	615	806	22.8	2.6	1.77	1.493E-05	1.41	2.9	2.57%	1.40%	175.9	22.2
0.08295	615	806	22.8	2.6	1.78	1.493E-05	1.41	5.8	0.96%	1.05%	208.2	26.3
0.08295	615	806	22.8	2.6	1.77	1.493E-05	1.42	6.0	0.94%	1.06%	211.5	26.7
0.08295	615	806	22.8	2.6	1.77	1.493E-05	1.42	8.6	0.60%	0.97%	232.6	29.4
0.08295	615	806	22.8	2.6	1.78	1.493E-05	1.41	8.8	0.58%	0.96%	235.7	29.8
0.08295	615	806	22.8	2.6	1.78	1.493E-05	1.42	11.5	0.43%	0.91%	251.5	31.8
0.08295	615	806	22.8	2.6	1.77	1.493E-05	1.42	11.5	0.42%	0.91%	250.9	31.7
0.08295	615	806	22.8	2.6	1.78	1.493E-05	1.41	46.1	0.10%	0.90%	357.2	45.2
0.08295	615	806	22.8	2.6	1.78	1.493E-05	1.42	57.7	0.08%	0.91%	356.3	45.1
0.08295	615	806	22.8	2.6	1.78	1.493E-05	1.43	68.8	0.08%	0.98%	312.3	39.5
0.08295	615	806	22.8	2.6	1.77	1.493E-05	2.06	2.9	15.15%	5.61%	180.6	22.8

A_p [m^2]	s [mm]	ρ_L [kg/m$_3$]	σ [mN/m]	μ_L [mPa.s]	ρ_v [kg/m^3]	μ_g [Pa.s]	U_s [m/s]	Q_L [m^3/(h.m)]	L'/L	L'/G	Holdup [Pa]	Holdup [mm liq]
0.08295	615	806	22.8	2.6	1.78	1.493E-05	2.05	5.9	4.08%	3.15%	219.7	27.8
0.08295	615	806	22.8	2.6	1.78	1.493E-05	2.04	8.8	2.13%	2.44%	244.4	30.9
0.08295	615	806	22.8	2.6	1.78	1.493E-05	2.04	11.5	1.39%	2.07%	262.5	33.2
0.08295	615	806	22.8	2.6	1.78	1.493E-05	2.03	22.9	0.59%	1.76%	309.7	39.2
0.08295	615	806	22.8	2.6	1.78	1.493E-05	2.03	22.9	0.59%	1.76%	309.7	39.2
0.08295	615	806	22.8	2.6	1.78	1.493E-05	2.05	33.9	0.48%	2.09%	319.8	40.4
0.08295	615	806	22.8	2.6	1.77	1.493E-05	2.05	46.1	0.40%	2.37%	307.6	38.9
0.08295	615	806	22.8	2.6	1.77	1.493E-05	2.06	58.0	0.30%	2.25%	308.4	39.0
0.08295	615	806	22.8	2.6	1.77	1.493E-05	2.04	69.3	0.22%	2.03%	330.7	41.8
0.08295	615	806	22.8	2.6	1.76	1.493E-05	2.34	2.8	36.47%	11.89%	204.2	25.8
0.08295	615	806	22.8	2.6	1.76	1.493E-05	2.34	2.9	35.72%	11.66%	206.5	26.1
0.08295	615	806	22.8	2.6	1.77	1.493E-05	2.32	5.9	7.54%	5.13%	235.9	29.8
0.08295	615	806	22.8	2.6	1.77	1.493E-05	2.32	8.8	3.62%	3.67%	261.2	33.0
0.08295	615	806	22.8	2.6	1.78	1.493E-05	2.31	11.5	2.24%	2.94%	282.0	35.7
0.08295	615	806	22.8	2.6	1.78	1.493E-05	2.31	22.8	1.09%	2.85%	322.7	40.8
0.08295	615	806	22.8	2.6	1.78	1.493E-05	2.31	22.8	1.09%	2.85%	322.7	40.8
0.08295	615	806	22.8	2.6	1.77	1.493E-05	2.33	34.2	1.09%	4.26%	280.6	35.5
0.08295	615	806	22.8	2.6	1.78	1.493E-05	2.32	46.2	0.71%	3.76%	315.9	40.0
0.08295	615	806	22.8	2.6	1.77	1.493E-05	2.32	57.8	0.52%	3.44%	348.0	44.0
0.08295	615	806	22.8	2.6	1.77	1.493E-05	2.32	69.0	0.57%	4.51%	401.5	50.8

Table 2. SF_6/n-butanol for 615 mm tray spacing.

A_p [m^2]	s [mm]	ρ_L [kg/m_3]	σ [mN/m]	μ_L [mPa.s]	ρ_V [kg/m^3]	μ_g [Pa.s]	U_s [m/s]	Q_L [$m^3/(h.m)$]	L'/L	L'/G	Holdup [Pa]	Holdup [mm liq]
0.08295	615	818.5	23.1	2.64	5.76	1.51E-05	1.00	2.9	6.33%	1.53%	168.3	21.0
0.08295	615	818.5	23.1	2.64	5.77	1.51E-05	0.99	6.1	2.57%	1.31%	204.5	25.5
0.08295	615	818.5	23.1	2.64	5.78	1.51E-05	0.99	6.1	2.57%	1.31%	206.2	25.7
0.08295	615	818.5	23.1	2.64	5.76	1.51E-05	0.99	8.6	1.64%	1.19%	224.7	28.0
0.08295	615	818.5	23.1	2.64	5.74	1.51E-05	0.98	8.7	1.63%	1.20%	225.5	28.1
0.08295	615	818.5	23.1	2.64	5.77	1.51E-05	0.99	8.7	1.66%	1.21%	225.1	28.0
0.08295	615	818.5	23.1	2.64	5.76	1.51E-05	0.99	11.4	1.13%	1.08%	239.2	29.8
0.08295	615	818.5	23.1	2.64	5.75	1.51E-05	1.20	2.9	16.82%	3.41%	149.1	18.6
0.08295	615	818.5	23.1	2.64	5.74	1.51E-05	1.20	2.9	16.53%	3.37%	148.8	18.5
0.08295	615	818.5	23.1	2.64	5.76	1.51E-05	1.20	6.1	5.84%	2.47%	192.9	24.0
0.08295	615	818.5	23.1	2.64	5.77	1.51E-05	1.19	6.1	5.84%	2.47%	192.6	24.0
0.08295	615	818.5	23.1	2.64	5.75	1.51E-05	1.20	8.6	3.68%	2.20%	209.7	26.1
0.08295	615	818.5	23.1	2.64	5.76	1.51E-05	1.20	8.7	3.53%	2.13%	210.9	26.3
0.08295	615	818.5	23.1	2.64	5.77	1.51E-05	1.20	11.4	2.40%	1.90%	225.6	28.1
0.08295	615	818.5	23.1	2.64	5.78	1.51E-05	1.39	2.9	41.24%	7.20%	150.7	18.8
0.08295	615	818.5	23.1	2.64	5.79	1.51E-05	1.39	2.9	40.94%	7.16%	150.3	18.7
0.08295	615	818.5	23.1	2.64	5.79	1.51E-05	1.39	2.9	40.54%	7.10%	148.7	18.5
0.08295	615	818.5	23.1	2.64	5.80	1.51E-05	1.39	2.9	39.68%	6.97%	149.2	18.6
0.08295	615	818.5	23.1	2.64	5.78	1.51E-05	1.40	5.9	12.61%	4.42%	183.6	22.9
0.08295	615	818.5	23.1	2.64	5.76	1.51E-05	1.40	5.9	12.43%	4.38%	181.5	22.6
0.08295	615	818.5	23.1	2.64	5.78	1.51E-05	1.40	5.9	12.59%	4.43%	185.5	23.1
0.08295	615	818.5	23.1	2.64	5.75	1.51E-05	1.39	8.6	7.16%	3.69%	210.4	26.2
0.08295	615	818.5	23.1	2.64	5.76	1.51E-05	1.39	8.6	7.15%	3.70%	203.5	25.3
0.08295	615	818.5	23.1	2.64	5.76	1.51E-05	1.40	8.7	7.14%	3.68%	200.7	25.0

A_p [m^2]	s [mm]	ρ_L [kg/m_3]	σ [mN/m]	μ_L [mPa.s]	ρ_v [kg/m^3]	μ_g [Pa.s]	U_s [m/s]	Q_L [m^3/(h.m)]	L'/L	L'/G	Holdup [Pa]	Holdup [mm liq]
0.08295	615	818.5	23.1	2.64	5.77	1.51E-05	1.39	11.5	4.46%	3.08%	221.4	27.6
0.08295	615	818.5	23.1	2.64	5.77	1.51E-05	1.40	22.5	1.53%	2.05%	280.3	34.9
0.08295	615	818.5	23.1	2.64	5.73	1.51E-05	1.41	24.1	1.43%	2.05%	284.9	35.5
0.08295	615	818.5	23.1	2.64	5.72	1.51E-05	1.41	24.1	1.43%	2.05%	278.4	34.7
0.08295	615	818.5	23.1	2.64	5.77	1.51E-05	1.40	22.5	1.53%	2.05%	280.3	34.9
0.08295	615	818.5	23.1	2.64	5.73	1.51E-05	1.41	24.1	1.43%	2.05%	284.9	35.5
0.08295	615	818.5	23.1	2.64	5.72	1.51E-05	1.41	24.1	1.43%	2.05%	278.4	34.7
0.08295	615	818.5	23.1	2.64	5.73	1.51E-05	1.42	34.5	1.13%	2.31%	302.2	37.6
0.08295	615	818.5	23.1	2.64	5.73	1.51E-05	1.41	35.3	1.11%	2.33%	306.5	38.2
0.08295	615	818.5	23.1	2.64	5.71	1.51E-05	1.41	45.7	1.14%	3.09%	332.3	41.4
0.08295	615	818.5	23.1	2.64	5.72	1.51E-05	1.41	45.8	1.21%	3.29%	332.3	41.4
0.08295	615	818.5	23.1	2.64	5.73	1.51E-05	1.41	46.0	1.21%	3.29%	333.6	41.5
0.08295	615	818.5	23.1	2.64	5.75	1.51E-05	1.40	56.8	1.49%	5.06%	403.1	50.2
0.08295	615	818.5	23.1	2.64	5.75	1.51E-05	1.40	56.9	1.50%	5.10%	408.7	50.9
0.08295	615	818.5	23.1	2.64	5.76	1.51E-05	1.40	56.9	1.45%	4.92%	400.5	49.9
0.08295	615	818.5	23.1	2.64	5.74	1.51E-05	1.41	56.9	1.58%	5.34%	405.8	50.5

Table 3. Air/silicone oil data for 315, 415, 515 and 615 mm tray spacings

A_p [m^2]	s [mm]	ρ_L [kg/m_3]	σ [mN/m]	μ_L [mPa.s]	ρ_v [kg/m^3]	μ_g [Pa.s]	U_s [m/s]	Q_L [m^3/(h.m)]	L'/L	L'/G	Holdup [Pa]	Holdup [mm liq]
0.08295	315	955	19.9	48.8	1.17	1.86E-05	1.41	2.9	2.11%	2.04%	208.4	22.2
0.08295	315	955	19.9	48.8	1.17	1.86E-05	1.40	5.9	0.98%	1.98%	256.9	27.4
0.08295	315	955	19.9	48.8	1.17	1.86E-05	1.43	8.6	0.72%	2.07%	284.9	30.4
0.08295	315	955	19.9	48.8	1.17	1.86E-05	1.43	8.6	0.72%	2.07%	284.9	30.4
0.08295	315	955	19.9	48.8	1.18	1.86E-05	1.43	11.6	0.59%	2.29%	311.2	33.2
0.08295	315	955	19.9	48.8	1.18	1.86E-05	1.42	22.8	0.46%	3.52%	415.3	44.3

Stellenbosch University http://scholar.sun.ac.za

A_p [m^2]	s [mm]	ρ_L [kg/m_3]	σ [mN/m]	μ_L [mPa.s]	ρ_V [kg/m^3]	μ_g [Pa.s]	U_s [m/s]	Q_L [m^3/(h.m)]	L'/L	L'/G	Holdup [Pa]	Holdup [mm liq]
0.08295	315	955	19.9	48.8	1.18	1.86E-05	1.43	34.3	0.43%	4.93%	475.8	50.8
0.08295	315	955	19.9	48.8	1.18	1.86E-05	1.44	45.7	0.34%	5.15%	504.0	53.8
0.08295	315	955	19.9	48.8	1.18	1.86E-05	1.42	57.1	0.35%	6.69%	533.8	57.0
0.08295	315	955	19.9	48.8	1.17	1.86E-05	1.43	68.6	0.41%	9.30%	554.0	59.1
0.08295	315	955	19.9	48.8	1.18	1.86E-05	1.42	80.4	0.47%	12.57%	578.3	61.7
0.08295	315	955	19.9	48.8	1.18	1.86E-05	1.69	22.7	0.83%	5.31%	399.1	42.6
0.08295	315	955	19.9	48.8	1.18	1.86E-05	1.71	34.2	0.80%	7.61%	445.6	47.6
0.08295	315	955	19.9	48.8	1.18	1.86E-05	1.71	34.3	0.72%	6.90%	446.0	47.6
0.08295	315	955	19.9	48.8	1.18	1.86E-05	1.70	45.6	0.70%	8.96%	480.0	51.2
0.08295	315	955	19.9	48.8	1.18	1.86E-05	1.70	57.2	0.80%	12.78%	511.3	54.6
0.08295	315	955	19.9	48.8	1.18	1.86E-05	1.71	68.7	0.88%	16.89%	524.9	56.0
0.08295	315	955	19.9	48.8	1.18	1.86E-05	1.70	80.3	0.79%	17.75%	528.2	56.4
0.08295	315	955	19.9	48.8	1.17	1.86E-05	2.00	2.9	7.10%	4.88%	178.6	19.1
0.08295	315	955	19.9	48.8	1.17	1.86E-05	2.00	5.9	3.00%	4.26%	230.2	24.6
0.08295	315	955	19.9	48.8	1.17	1.86E-05	2.00	5.9	3.00%	4.26%	230.2	24.6
0.08295	315	955	19.9	48.8	1.17	1.86E-05	2.00	8.6	2.15%	4.41%	264.2	28.2
0.08295	315	955	19.9	48.8	1.18	1.86E-05	1.99	11.6	1.90%	5.28%	288.6	30.8
0.08295	315	955	19.9	48.8	1.18	1.86E-05	1.99	22.8	1.68%	9.16%	374.9	40.0
0.08295	315	955	19.9	48.8	1.18	1.86E-05	1.99	34.2	1.38%	11.28%	424.6	45.3
0.08295	315	955	19.9	48.8	1.18	1.86E-05	2.00	45.7	1.76%	19.14%	458.6	49.0
0.08295	315	955	19.9	48.8	1.18	1.86E-05	1.99	57.2	2.04%	27.86%	496.8	53.0
0.08295	315	955	19.9	48.8	1.18	1.86E-05	2.00	57.2	1.94%	26.34%	496.1	53.0
0.08295	315	955	19.9	48.8	1.18	1.86E-05	1.99	68.6	1.62%	26.52%	498.5	53.2
0.08295	315	955	19.9	48.8	1.18	1.86E-05	1.98	68.8	1.77%	29.17%	504.3	53.8
0.08295	315	955	19.9	48.8	1.18	1.86E-05	1.98	80.2	0.95%	18.23%	486.6	51.9

A_p [m^2]	s [mm]	ρ_L [kg/m$_3$]	σ [mN/m]	μ_L [mPa.s]	ρ_v [kg/m^3]	μ_g [Pa.s]	U_s [m/s]	Q_L [m^3/(h.m)]	L'/L	L'/G	Holdup [Pa]	Holdup [mm liq]
0.08295	315	955	19.9	48.8	1.17	1.86E-05	2.27	2.8	9.44%	5.64%	156.8	16.7
0.08295	315	955	19.9	48.8	1.18	1.86E-05	2.29	5.9	4.60%	5.62%	214.3	22.9
0.08295	315	955	19.9	48.8	1.18	1.86E-05	2.29	5.9	4.60%	5.62%	214.3	22.9
0.08295	315	955	19.9	48.8	1.18	1.86E-05	2.28	8.6	3.58%	6.43%	249.4	26.6
0.08295	315	955	19.9	48.8	1.18	1.86E-05	2.29	11.5	3.53%	8.45%	274.2	29.3
0.08295	315	955	19.9	48.8	1.18	1.86E-05	2.27	23.1	3.86%	18.68%	358.7	38.3
0.08295	315	955	19.9	48.8	1.18	1.86E-05	2.27	23.1	4.01%	19.41%	360.8	38.5
0.08295	315	955	19.9	48.8	1.18	1.86E-05	2.28	34.4	3.86%	27.78%	413.7	44.2
0.08295	315	955	19.9	48.8	1.18	1.86E-05	2.27	34.5	3.74%	27.05%	419.7	44.8
0.08295	315	955	19.9	48.8	1.18	1.86E-05	2.26	45.6	4.79%	46.00%	476.3	50.8
0.08295	315	955	19.9	48.8	1.18	1.86E-05	2.26	45.7	4.96%	47.51%	478.6	51.1
0.08295	315	955	19.9	48.8	1.18	1.86E-05	2.26	45.7	4.58%	44.04%	461.0	49.2
0.08295	315	955	19.9	48.8	1.18	1.86E-05	2.29	57.2	4.54%	53.88%	478.5	51.1
0.08295	315	955	19.9	48.8	1.18	1.86E-05	2.28	57.3	4.79%	57.20%	488.7	52.2
0.08295	315	955	19.9	48.8	1.18	1.86E-05	2.29	57.4	5.20%	62.15%	482.7	51.5
0.08295	315	955	19.9	48.8	1.18	1.86E-05	2.27	68.5	2.97%	42.65%	506.3	54.0
0.08295	315	955	19.9	48.8	1.18	1.86E-05	2.28	68.9	3.00%	43.15%	495.1	52.9
0.08295	315	955	19.9	48.8	1.18	1.86E-05	2.27	68.9	2.89%	41.61%	490.2	52.3
0.08295	315	955	19.9	48.8	1.18	1.86E-05	2.26	80.1	2.91%	49.24%	575.5	61.4
0.08295	315	955	19.9	48.8	1.18	1.86E-05	2.27	80.2	2.55%	42.94%	553.5	59.1
0.08295	315	955	19.9	48.8	1.18	1.86E-05	2.26	80.2	2.98%	50.21%	562.2	60.0
0.08295	315	955	19.9	48.8	1.17	1.86E-05	2.56	2.9	16.83%	9.17%	172.7	18.4
0.08295	315	955	19.9	48.8	1.17	1.86E-05	2.57	6.0	7.90%	8.78%	216.1	23.1
0.08295	315	955	19.9	48.8	1.17	1.86E-05	2.57	6.0	7.90%	8.78%	216.1	23.1
0.08295	315	955	19.9	48.8	1.17	1.86E-05	2.57	8.6	6.00%	9.64%	241.7	25.8
0.08295	315	955	19.9	48.8	1.18	1.86E-05	2.55	11.6	6.59%	14.20%	265.8	28.4
0.08295	315	955	19.9	48.8	1.18	1.86E-05	2.54	11.6	6.57%	14.28%	265.7	28.4

A_p [m^2]	s [mm]	ρ_L [kg/m_3]	σ [mN/m]	μ_L [mPa.s]	ρ_v [kg/m^3]	μ_g [Pa.s]	U_s [m/s]	Q_L [m^3/(h.m)]	L'/L	L'/G	Holdup [Pa]	Holdup [mm liq]
0.08295	315	955	19.9	48.8	1.18	1.86E-05	2.57	22.5	13.33%	55.45%	334.4	35.7
0.08295	315	955	19.9	48.8	1.18	1.86E-05	2.54	22.7	12.92%	54.60%	369.6	39.5
0.08295	315	955	19.9	48.8	1.18	1.86E-05	2.56	22.7	12.31%	51.89%	350.0	37.4
0.08295	315	955	19.9	48.8	1.18	1.86E-05	2.57	34.1	12.03%	75.55%	409.7	43.7
0.08295	315	955	19.9	48.8	1.18	1.86E-05	2.56	34.1	12.67%	80.11%	427.8	45.7
0.08295	315	955	19.9	48.8	1.18	1.86E-05	2.57	34.3	11.66%	73.87%	424.8	45.3
0.08295	315	955	19.9	48.8	1.18	1.86E-05	2.55	45.6	11.46%	97.05%	466.4	49.8
0.08295	315	955	19.9	48.8	1.18	1.86E-05	2.55	45.6	10.80%	91.65%	475.1	50.7
0.08295	315	955	19.9	48.8	1.18	1.86E-05	2.57	45.8	10.87%	92.14%	460.9	49.2
0.08295	315	955	19.9	48.8	1.17	1.86E-05	2.87	2.9	36.28%	17.73%	174.3	18.6
0.08295	315	955	19.9	48.8	1.17	1.86E-05	2.86	2.9	33.67%	16.54%	174.3	18.6
0.08295	315	955	19.9	48.8	1.17	1.86E-05	2.86	6.0	14.37%	14.46%	209.3	22.3
0.08295	315	955	19.9	48.8	1.17	1.86E-05	2.86	6.0	14.37%	14.46%	209.3	22.3
0.08295	315	955	19.9	48.8	1.17	1.86E-05	2.85	8.6	12.22%	17.61%	230.4	24.6
0.08295	315	955	19.9	48.8	1.17	1.86E-05	2.86	8.6	12.40%	17.87%	233.6	24.9
0.08295	315	955	19.9	48.8	1.18	1.86E-05	2.83	11.6	14.40%	28.03%	252.2	26.9
0.08295	315	955	19.9	48.8	1.18	1.86E-05	2.83	11.6	14.46%	28.12%	255.8	27.3
0.08295	315	955	19.9	48.8	1.18	1.86E-05	2.83	11.6	14.67%	28.63%	254.3	27.1
0.08295	315	955	19.9	48.8	1.18	1.86E-05	2.83	22.7	19.63%	74.60%	338.6	36.1
0.08295	315	955	19.9	48.8	1.18	1.86E-05	2.84	22.8	25.78%	98.20%	351.3	37.5
0.08295	315	955	19.9	48.8	1.18	1.86E-05	2.84	22.9	31.22%	119.1%	335.7	35.8
0.08295	415	955	19.9	48.8	1.16	1.86E-05	1.43	2.9	1.43%	1.43%	200.7	20.8
0.08295	415	955	19.9	48.8	1.16	1.86E-05	1.42	5.8	0.65%	1.28%	250.0	26.7
0.08295	415	955	19.9	48.8	1.16	1.86E-05	1.44	8.6	0.45%	1.29%	279.7	29.9
0.08295	415	955	19.9	48.8	1.16	1.86E-05	1.44	11.4	0.33%	1.28%	307.0	32.8
0.08295	415	955	19.9	48.8	1.16	1.86E-05	1.44	11.4	0.33%	1.28%	307.0	32.8

A_p [m^2]	s [mm]	ρ_L [kg/m$_3$]	σ [mN/m]	μ_L [mPa.s]	ρ_v [kg/m^3]	μ_g [Pa.s]	U_s [m/s]	Q_L [m^3/(h.m)]	L'/L	L'/G	Holdup [Pa]	Holdup [mm liq]
0.08295	415	955	19.9	48.8	1.16	1.86E-05	1.42	22.5	0.19%	1.44%	415.6	44.4
0.08295	415	955	19.9	48.8	1.16	1.86E-05	1.45	34.3	0.15%	1.67%	461.8	49.3
0.08295	415	955	19.9	48.8	1.16	1.86E-05	1.45	46.0	0.12%	1.90%	496.3	53.0
0.08295	415	955	19.9	48.8	1.16	1.86E-05	1.43	46.2	0.12%	1.87%	497.4	53.1
0.08295	415	955	19.9	48.8	1.16	1.86E-05	1.42	57.1	0.11%	2.20%	530.1	56.6
0.08295	415	955	19.9	48.8	1.16	1.86E-05	1.42	68.6	0.11%	2.56%	553.5	59.1
0.08295	415	955	19.9	48.8	1.16	1.86E-05	1.42	79.8	0.11%	2.94%	571.2	61.0
0.08295	415	955	19.9	48.8	1.16	1.86E-05	2.01	2.9	4.85%	3.33%	171.6	18.3
0.08295	415	955	19.9	48.8	1.16	1.86E-05	2.01	5.8	1.91%	2.66%	218.9	23.4
0.08295	415	955	19.9	48.8	1.16	1.86E-05	2.02	8.6	1.25%	2.58%	257.6	27.5
0.08295	415	955	19.9	48.8	1.16	1.86E-05	2.02	8.6	1.25%	2.58%	257.6	27.5
0.08295	415	955	19.9	48.8	1.16	1.86E-05	2.02	11.4	0.98%	2.67%	282.1	30.1
0.08295	415	955	19.9	48.8	1.16	1.86E-05	2.01	22.8	0.60%	3.26%	364.0	38.9
0.08295	415	955	19.9	48.8	1.16	1.86E-05	2.00	34.4	0.44%	3.66%	415.5	44.4
0.08295	415	955	19.9	48.8	1.16	1.86E-05	2.00	45.7	0.38%	4.20%	451.3	48.2
0.08295	415	955	19.9	48.8	1.16	1.86E-05	2.00	57.1	0.36%	5.00%	477.4	51.0
0.08295	415	955	19.9	48.8	1.16	1.86E-05	2.01	68.4	0.35%	5.79%	471.2	50.3
0.08295	415	955	19.9	48.8	1.16	1.86E-05	2.01	79.9	0.27%	5.18%	432.9	46.2
0.08295	415	955	19.9	48.8	1.16	1.86E-05	2.58	2.9	11.17%	5.97%	158.8	16.9
0.08295	415	955	19.9	48.8	1.16	1.86E-05	2.58	5.8	4.40%	4.79%	196.2	20.9
0.08295	415	955	19.9	48.8	1.16	1.86E-05	2.58	8.6	2.80%	4.52%	225.8	24.1
0.08295	415	955	19.9	48.8	1.16	1.86E-05	2.58	8.6	2.80%	4.52%	225.8	24.1
0.08295	415	955	19.9	48.8	1.16	1.86E-05	2.58	11.4	2.42%	5.15%	251.3	26.8
0.08295	415	955	19.9	48.8	1.16	1.86E-05	2.57	22.9	2.09%	8.95%	338.3	36.1
0.08295	415	955	19.9	48.8	1.16	1.86E-05	2.57	22.9	2.08%	8.96%	335.5	35.8
0.08295	415	955	19.9	48.8	1.16	1.86E-05	2.58	34.7	1.91%	12.40%	399.5	42.6

A_p [m^2]	s [mm]	ρ_L [kg/m$_3$]	σ [mN/m]	μ_L [mPa.s]	ρ_v [kg/m^3]	μ_g [Pa.s]	U_s [m/s]	Q_L [m^3/(h.m)]	L'/L	L'/G	Holdup [Pa]	Holdup [mm liq]
0.08295	415	955	19.9	48.8	1.16	1.86E-05	2.57	45.8	1.64%	14.09%	418.2	44.6
0.08295	415	955	19.9	48.8	1.16	1.86E-05	2.57	45.9	1.54%	13.27%	419.9	44.8
0.08295	415	955	19.9	48.8	1.16	1.86E-05	2.58	57.1	0.99%	10.63%	407.0	43.4
0.08295	415	955	19.9	48.8	1.16	1.86E-05	2.57	57.2	1.01%	10.83%	399.7	42.7
0.08295	415	955	19.9	48.8	1.16	1.86E-05	2.58	68.6	0.59%	7.61%	337.9	36.1
0.08295	415	955	19.9	48.8	1.16	1.86E-05	2.58	68.6	0.59%	7.54%	333.5	35.6
0.08295	415	955	19.9	48.8	1.16	1.86E-05	2.59	79.7	0.49%	7.31%	349.9	37.3
0.08295	415	955	19.9	48.8	1.17	1.86E-05	2.86	2.9	17.71%	8.51%	155.8	16.6
0.08295	415	955	19.9	48.8	1.17	1.86E-05	2.86	2.9	17.61%	8.49%	164.9	17.6
0.08295	415	955	19.9	48.8	1.17	1.86E-05	2.86	6.0	6.93%	6.98%	200.6	21.4
0.08295	415	955	19.9	48.8	1.17	1.86E-05	2.87	8.7	4.74%	6.86%	222.3	23.7
0.08295	415	955	19.9	48.8	1.17	1.86E-05	2.87	8.7	4.74%	6.86%	222.3	23.7
0.08295	415	955	19.9	48.8	1.17	1.86E-05	2.86	11.4	3.99%	7.63%	244.3	26.1
0.08295	415	955	19.9	48.8	1.16	1.86E-05	2.89	23.3	6.96%	27.05%	335.6	35.8
0.08295	415	955	19.9	48.8	1.16	1.86E-05	2.89	23.4	6.88%	26.85%	335.0	35.8
0.08295	415	955	19.9	48.8	1.16	1.86E-05	2.86	34.6	4.75%	27.63%	384.7	41.1
0.08295	415	955	19.9	48.8	1.16	1.86E-05	2.86	34.6	4.74%	27.62%	380.0	40.6
0.08295	415	955	19.9	48.8	1.16	1.86E-05	2.85	34.7	4.75%	27.84%	382.9	40.9
0.08295	415	955	19.9	48.8	1.16	1.86E-05	2.85	46.4	2.55%	19.96%	393.5	42.0
0.08295	415	955	19.9	48.8	1.16	1.86E-05	2.85	46.8	2.56%	20.31%	394.4	42.1
0.08295	415	955	19.9	48.8	1.16	1.86E-05	2.86	57.6	1.23%	11.96%	348.4	37.2
0.08295	415	955	19.9	48.8	1.16	1.86E-05	2.87	69.0	1.05%	12.21%	367.5	39.2
0.08295	415	955	19.9	48.8	1.16	1.86E-05	2.87	79.8	1.34%	18.05%	435.4	46.5
0.08295	415	955	19.9	48.8	1.16	1.86E-05	2.87	79.9	1.40%	18.83%	433.3	46.2
0.08295	415	955	19.9	48.8	1.15	1.86E-05	3.17	2.8	40.68%	17.76%	175.5	18.7
0.08295	415	955	19.9	48.8	1.15	1.86E-05	3.17	2.9	37.25%	16.37%	174.5	18.6

A_p [m^2]	s [mm]	ρ_L [kg/m_3]	σ [mN/m]	μ_L [mPa.s]	ρ_v [kg/m^3]	μ_g [Pa.s]	U_s [m/s]	Q_L [m^3/(h.m)]	L'/L	L'/G	Holdup [Pa]	Holdup [mm liq]
0.08295	415	955	19.9	48.8	1.16	1.86E-05	3.16	5.8	13.02%	11.60%	192.5	20.5
0.08295	415	955	19.9	48.8	1.16	1.86E-05	3.16	5.8	12.53%	11.23%	196.1	20.9
0.08295	415	955	19.9	48.8	1.16	1.86E-05	3.15	8.6	8.34%	11.00%	220.8	23.6
0.08295	415	955	19.9	48.8	1.16	1.86E-05	3.15	8.6	8.54%	11.31%	225.2	24.0
0.08295	415	955	19.9	48.8	1.16	1.86E-05	3.15	8.7	8.05%	10.73%	218.2	23.3
0.08295	415	955	19.9	48.8	1.16	1.86E-05	3.15	8.6	8.34%	11.00%	220.8	23.6
0.08295	415	955	19.9	48.8	1.16	1.86E-05	3.15	8.6	8.54%	11.31%	225.2	24.0
0.08295	415	955	19.9	48.8	1.16	1.86E-05	3.15	8.7	8.05%	10.73%	218.2	23.3
0.08295	415	955	19.9	48.8	1.16	1.86E-05	3.15	11.4	8.00%	13.93%	241.4	25.8
0.08295	415	955	19.9	48.8	1.16	1.86E-05	3.15	11.4	8.45%	14.76%	243.8	26.0
0.08295	415	955	19.9	48.8	1.15	1.86E-05	3.19	11.5	10.55%	18.45%	243.1	25.9
0.08295	415	955	19.9	48.8	1.15	1.86E-05	3.19	11.5	10.46%	18.33%	235.4	25.1
0.08295	415	955	19.9	48.8	1.15	1.86E-05	3.19	11.5	10.67%	18.74%	248.5	26.5
0.08295	415	955	19.9	48.8	1.16	1.86E-05	3.15	22.9	18.22%	63.84%	339.2	36.2
0.08295	415	955	19.9	48.8	1.16	1.86E-05	3.15	23.0	17.59%	62.03%	336.6	35.9
0.08295	415	955	19.9	48.8	1.16	1.86E-05	3.14	23.2	16.32%	57.98%	333.3	35.6
0.08295	415	955	19.9	48.8	1.16	1.86E-05	3.15	34.6	9.09%	48.06%	377.8	40.3
0.08295	415	955	19.9	48.8	1.16	1.86E-05	3.16	34.6	9.13%	48.15%	394.5	42.1
0.08295	415	955	19.9	48.8	1.16	1.86E-05	3.15	34.7	8.57%	45.45%	385.7	41.2
0.08295	415	955	19.9	48.8	1.16	1.86E-05	3.12	45.9	5.29%	37.29%	411.6	43.9
0.08295	415	955	19.9	48.8	1.17	1.86E-05	3.14	45.9	5.29%	37.20%	391.8	41.8
0.08295	415	955	19.9	48.8	1.16	1.86E-05	3.14	45.9	5.34%	37.56%	397.4	42.4
0.08295	415	955	19.9	48.8	1.16	1.86E-05	3.16	57.0	5.29%	46.01%	403.4	43.1
0.08295	415	955	19.9	48.8	1.16	1.86E-05	3.16	57.1	5.34%	46.44%	405.4	43.3
0.08295	415	955	19.9	48.8	1.16	1.86E-05	3.15	57.4	4.97%	43.59%	409.9	43.7
0.08295	415	955	19.9	48.8	1.16	1.86E-05	3.14	57.4	5.62%	49.44%	412.1	44.0
0.08295	415	955	19.9	48.8	1.16	1.86E-05	3.16	67.8	8.34%	86.21%	492.4	52.6
0.08295	415	955	19.9	48.8	1.16	1.86E-05	3.16	68.1	8.46%	87.89%	478.4	51.1

A_p [m^2]	s [mm]	ρ_L [kg/m$_3$]	σ [mN/m]	μ_L [mPa.s]	ρ_V [kg/m^3]	μ_g [Pa.s]	U_s [m/s]	Q_L [m^3/(h.m)]	L'/L	L'/G	Holdup [Pa]	Holdup [mm liq]
0.08295	415	955	19.9	48.8	1.16	1.86E-05	3.16	68.6	8.02%	83.85%	483.7	51.6
0.08295	415	955	19.9	48.8	1.16	1.86E-05	3.16	68.7	8.67%	90.78%	490.0	52.3
0.08295	415	955	19.9	48.8	1.16	1.86E-05	3.15	68.7	8.61%	90.26%	488.8	52.2
0.08295	515	955	19.9	48.8	1.17	1.86E-05	2.00	2.9	3.70%	2.54%	165.8	17.7
0.08295	515	955	19.9	48.8	1.16	1.86E-05	1.99	6.3	1.36%	2.06%	219.4	23.4
0.08295	515	955	19.9	48.8	1.17	1.86E-05	2.00	8.6	0.95%	1.97%	252.9	27.0
0.08295	515	955	19.9	48.8	1.17	1.86E-05	1.99	11.7	0.70%	1.97%	283.1	30.2
0.08295	515	955	19.9	48.8	1.17	1.86E-05	1.99	11.7	0.70%	1.97%	283.1	30.2
0.08295	515	955	19.9	48.8	1.16	1.86E-05	2.00	22.3	0.45%	2.43%	354.5	37.8
0.08295	515	955	19.9	48.8	1.17	1.86E-05	2.01	33.8	0.29%	2.30%	404.3	43.2
0.08295	515	955	19.9	48.8	1.17	1.86E-05	2.00	45.8	0.21%	2.27%	445.7	47.6
0.08295	515	955	19.9	48.8	1.17	1.86E-05	2.00	57.5	0.17%	2.32%	464.2	49.6
0.08295	515	955	19.9	48.8	1.17	1.86E-05	1.99	68.3	0.16%	2.61%	472.0	50.4
0.08295	515	955	19.9	48.8	1.17	1.86E-05	1.99	79.3	0.15%	2.81%	457.2	48.8
0.08295	515	955	19.9	48.8	1.16	1.86E-05	2.56	2.9	8.50%	4.58%	154.1	16.4
0.08295	515	955	19.9	48.8	1.17	1.86E-05	2.57	6.3	3.06%	3.57%	200.9	21.4
0.08295	515	955	19.9	48.8	1.17	1.86E-05	2.56	8.7	2.05%	3.32%	224.4	24.0
0.08295	515	955	19.9	48.8	1.17	1.86E-05	2.56	8.7	2.05%	3.32%	224.4	24.0
0.08295	515	955	19.9	48.8	1.17	1.86E-05	2.57	11.7	1.65%	3.60%	246.3	26.3
0.08295	515	955	19.9	48.8	1.17	1.86E-05	2.57	22.4	1.27%	5.32%	318.8	34.0
0.08295	515	955	19.9	48.8	1.17	1.86E-05	2.56	34.0	0.83%	5.29%	376.2	40.2
0.08295	515	955	19.9	48.8	1.17	1.86E-05	2.58	45.8	0.60%	5.06%	401.4	42.8
0.08295	515	955	19.9	48.8	1.18	1.86E-05	2.57	57.4	0.45%	4.76%	388.2	41.4
0.08295	515	955	19.9	48.8	1.18	1.86E-05	2.55	68.2	0.36%	4.61%	370.1	39.5
0.08295	515	955	19.9	48.8	1.17	1.86E-05	2.56	79.2	0.31%	4.50%	350.7	37.4

A_p [m^2]	s [mm]	ρ_L [kg/m$_3$]	σ [mN/m]	μ_L [mPa.s]	ρ_V [kg/m^3]	μ_g [Pa.s]	U_s [m/s]	Q_L [m^3/(h.m)]	L'/L	L'/G	Holdup [Pa]	Holdup [mm liq]
0.08295	515	955	19.9	48.8	1.16	1.86E-05	2.88	2.8	13.90%	6.47%	147.7	15.8
0.08295	515	955	19.9	48.8	1.17	1.86E-05	2.86	6.2	4.57%	4.74%	189.4	20.2
0.08295	515	955	19.9	48.8	1.17	1.86E-05	2.85	8.7	3.02%	4.41%	212.7	22.7
0.08295	515	955	19.9	48.8	1.17	1.86E-05	2.85	8.7	3.02%	4.41%	212.7	22.7
0.08295	515	955	19.9	48.8	1.17	1.86E-05	2.86	11.7	2.42%	4.75%	237.2	25.3
0.08295	515	955	19.9	48.8	1.17	1.86E-05	2.87	22.4	2.43%	9.11%	310.7	33.2
0.08295	515	955	19.9	48.8	1.18	1.86E-05	2.85	34.1	1.59%	9.05%	367.0	39.2
0.08295	515	955	19.9	48.8	1.18	1.86E-05	2.85	34.1	1.57%	8.94%	355.8	38.0
0.08295	515	955	19.9	48.8	1.18	1.86E-05	2.85	46.0	0.92%	7.07%	354.5	37.8
0.08295	515	955	19.9	48.8	1.18	1.86E-05	2.85	57.4	0.65%	6.24%	339.1	36.2
0.08295	515	955	19.9	48.8	1.18	1.86E-05	2.84	68.0	0.55%	6.23%	354.2	37.8
0.08295	515	955	19.9	48.8	1.18	1.86E-05	2.85	68.0	0.54%	6.18%	351.9	37.6
0.08295	515	955	19.9	48.8	1.18	1.86E-05	2.87	79.2	0.53%	6.93%	386.5	41.3
0.08295	515	955	19.9	48.8	1.16	1.86E-05	3.15	2.8	26.18%	11.37%	155.2	16.6
0.08295	515	955	19.9	48.8	1.16	1.86E-05	3.15	2.8	26.71%	11.64%	160.1	17.1
0.08295	515	955	19.9	48.8	1.17	1.86E-05	3.15	6.3	7.23%	6.94%	186.8	19.9
0.08295	515	955	19.9	48.8	1.17	1.86E-05	3.13	8.7	4.61%	6.12%	209.7	22.4
0.08295	515	955	19.9	48.8	1.17	1.86E-05	3.13	8.7	4.61%	6.12%	209.7	22.4
0.08295	515	955	19.9	48.8	1.17	1.86E-05	3.14	11.7	3.77%	6.75%	236.0	25.2
0.08295	515	955	19.9	48.8	1.17	1.86E-05	3.14	22.4	4.50%	15.39%	290.6	31.0
0.08295	515	955	19.9	48.8	1.17	1.86E-05	3.14	22.5	4.11%	14.15%	300.0	32.0
0.08295	515	955	19.9	48.8	1.17	1.86E-05	3.16	22.6	4.73%	16.22%	280.7	30.0
0.08295	515	955	19.9	48.8	1.17	1.86E-05	3.17	22.9	4.82%	16.67%	292.4	31.2
0.08295	515	955	19.9	48.8	1.18	1.86E-05	3.13	33.9	2.69%	13.88%	319.3	34.1
0.08295	515	955	19.9	48.8	1.18	1.86E-05	3.14	34.1	2.84%	14.69%	320.2	34.2
0.08295	515	955	19.9	48.8	1.18	1.86E-05	3.15	45.9	1.34%	9.25%	298.8	31.9
0.08295	515	955	19.9	48.8	1.18	1.86E-05	3.13	45.9	1.44%	10.04%	311.5	33.3

A_p [m^2]	s [mm]	ρ_L [kg/m3]	σ [mN/m]	μ_L [mPa.s]	ρ_v [kg/m^3]	μ_g [Pa.s]	U_s [m/s]	Q_L [m^3/(h.m)]	L'/L	L'/G	Holdup [Pa]	Holdup [mm liq]
0.08295	515	955	19.9	48.8	1.18	1.86E-05	3.15	46.0	1.34%	9.35%	292.3	31.2
0.08295	515	955	19.9	48.8	1.18	1.86E-05	3.13	57.4	1.16%	10.06%	348.1	37.2
0.08295	515	955	19.9	48.8	1.18	1.86E-05	3.12	68.0	1.06%	10.95%	392.5	41.9
0.08295	515	955	19.9	48.8	1.18	1.86E-05	3.11	68.0	1.06%	11.03%	392.2	41.9
0.08295	515	955	19.9	48.8	1.18	1.86E-05	3.12	78.9	1.19%	14.33%	437.5	46.7
0.08295	515	955	19.9	48.8	1.18	1.86E-05	3.13	79.0	1.22%	14.65%	442.5	47.2
0.08295	615	955	19.9	48.8	1.17	1.86E-05	2.01	2.8	3.04%	2.04%	162.7	17.4
0.08295	615	955	19.9	48.8	1.17	1.86E-05	2.00	6.0	1.23%	1.76%	208.0	22.2
0.08295	615	955	19.9	48.8	1.17	1.86E-05	2.00	8.6	0.76%	1.56%	247.2	26.4
0.08295	615	955	19.9	48.8	1.17	1.86E-05	1.99	11.5	0.55%	1.53%	274.5	29.3
0.08295	615	955	19.9	48.8	1.17	1.86E-05	1.99	11.5	0.55%	1.53%	274.5	29.3
0.08295	615	955	19.9	48.8	1.17	1.86E-05	2.02	23.1	0.32%	1.72%	355.1	37.9
0.08295	615	955	19.9	48.8	1.17	1.86E-05	2.02	23.2	0.32%	1.74%	353.8	37.8
0.08295	615	955	19.9	48.8	1.17	1.86E-05	2.00	34.1	0.22%	1.78%	404.6	43.2
0.08295	615	955	19.9	48.8	1.17	1.86E-05	2.01	45.4	0.16%	1.73%	442.7	47.3
0.08295	615	955	19.9	48.8	1.17	1.86E-05	2.00	57.3	0.13%	1.78%	459.5	49.0
0.08295	615	955	19.9	48.8	1.16	1.86E-05	2.01	67.4	0.12%	1.89%	463.4	49.5
0.08295	615	955	19.9	48.8	1.17	1.86E-05	2.00	68.7	0.12%	1.91%	456.9	48.8
0.08295	615	955	19.9	48.8	1.17	1.86E-05	2.01	78.7	0.11%	1.96%	414.0	44.2
0.08295	615	955	19.9	48.8	1.17	1.86E-05	2.29	2.9	4.51%	2.76%	155.6	16.6
0.08295	615	955	19.9	48.8	1.17	1.86E-05	2.29	5.9	1.84%	2.27%	197.8	21.1
0.08295	615	955	19.9	48.8	1.17	1.86E-05	2.29	8.6	1.14%	2.06%	231.4	24.7
0.08295	615	955	19.9	48.8	1.17	1.86E-05	2.29	8.6	1.14%	2.06%	231.4	24.7
0.08295	615	955	19.9	48.8	1.17	1.86E-05	2.30	11.5	0.88%	2.10%	257.7	27.5
0.08295	615	955	19.9	48.8	1.17	1.86E-05	2.30	34.0	0.35%	2.47%	383.5	40.9
0.08295	615	955	19.9	48.8	1.17	1.86E-05	2.29	45.3	0.25%	2.32%	424.1	45.3

A_p [m^2]	s [mm]	ρ_L [kg/m$_3$]	σ [mN/m]	μ_L [mPa.s]	ρ_v [kg/m^3]	μ_g [Pa.s]	U_s [m/s]	Q_L [m^3/(h.m)]	L'/L	L'/G	Holdup [Pa]	Holdup [mm liq]
0.08295	615	955	19.9	48.8	1.17	1.86E-05	2.28	57.3	0.20%	2.40%	430.0	45.9
0.08295	615	955	19.9	48.8	1.17	1.86E-05	2.29	68.7	0.18%	2.58%	388.9	41.5
0.08295	615	955	19.9	48.8	1.17	1.86E-05	2.28	78.5	0.16%	2.57%	349.9	37.3
0.08295	615	955	19.9	48.8	1.17	1.86E-05	2.58	3.0	6.86%	3.76%	149.7	16.0
0.08295	615	955	19.9	48.8	1.17	1.86E-05	2.56	5.9	2.63%	2.87%	189.3	20.2
0.08295	615	955	19.9	48.8	1.17	1.86E-05	2.57	8.7	1.64%	2.63%	216.4	23.1
0.08295	615	955	19.9	48.8	1.17	1.86E-05	2.57	8.7	1.64%	2.63%	216.4	23.1
0.08295	615	955	19.9	48.8	1.17	1.86E-05	2.58	11.5	1.28%	2.71%	236.1	25.2
0.08295	615	955	19.9	48.8	1.17	1.86E-05	2.56	22.9	0.77%	3.30%	320.4	34.2
0.08295	615	955	19.9	48.8	1.17	1.86E-05	2.58	23.2	0.79%	3.42%	319.3	34.1
0.08295	615	955	19.9	48.8	1.17	1.86E-05	2.57	34.1	0.52%	3.31%	372.8	39.8
0.08295	615	955	19.9	48.8	1.17	1.86E-05	2.57	34.1	0.53%	3.38%	376.0	40.1
0.08295	615	955	19.9	48.8	1.17	1.86E-05	2.57	45.6	0.37%	3.13%	389.2	41.5
0.08295	615	955	19.9	48.8	1.17	1.86E-05	2.58	57.4	0.30%	3.22%	369.5	39.4
0.08295	615	955	19.9	48.8	1.16	1.86E-05	2.60	68.3	0.26%	3.26%	334.2	35.7
0.08295	615	955	19.9	48.8	1.17	1.86E-05	2.57	68.6	0.25%	3.25%	336.9	36.0
0.08295	615	955	19.9	48.8	1.17	1.86E-05	2.56	78.6	0.22%	3.25%	346.5	37.0
0.08295	615	955	19.9	48.8	1.16	1.86E-05	2.60	79.0	0.22%	3.25%	346.6	37.0
0.08295	615	955	19.9	48.8	1.17	1.86E-05	3.15	2.9	19.93%	8.78%	143.2	15.3
0.08295	615	955	19.9	48.8	1.17	1.86E-05	3.16	2.9	20.64%	9.09%	142.5	15.2
0.08295	615	955	19.9	48.8	1.17	1.86E-05	3.15	5.9	6.08%	5.44%	177.2	18.9
0.08295	615	955	19.9	48.8	1.17	1.86E-05	3.15	8.7	3.55%	4.68%	200.1	21.4
0.08295	615	955	19.9	48.8	1.17	1.86E-05	3.13	8.7	3.49%	4.63%	203.3	21.7
0.08295	615	955	19.9	48.8	1.17	1.86E-05	3.15	8.7	3.55%	4.68%	200.1	21.4
0.08295	615	955	19.9	48.8	1.17	1.86E-05	3.13	8.7	3.49%	4.63%	203.3	21.7
0.08295	615	955	19.9	48.8	1.17	1.86E-05	3.16	11.5	2.88%	5.01%	225.1	24.0

A_p [m²]	s [mm]	ρ_L [kg/m₃]	σ [mN/m]	μ_L [mPa.s]	ρ_V [kg/m³]	μ_g [Pa.s]	U_s [m/s]	Q_L [m³/(h.m)]	L'/L	L'/G	Holdup [Pa]	Holdup [mm liq]
0.08295	615	955	19.9	48.8	1.17	1.86E-05	3.13	23.0	2.01%	7.08%	298.5	31.9
0.08295	615	955	19.9	48.8	1.17	1.86E-05	3.14	23.3	2.05%	7.24%	279.6	29.8
0.08295	615	955	19.9	48.8	1.17	1.86E-05	3.15	34.1	1.33%	6.91%	308.9	33.0
0.08295	615	955	19.9	48.8	1.17	1.86E-05	3.14	34.2	1.32%	6.85%	298.4	31.9
0.08295	615	955	19.9	48.8	1.17	1.86E-05	3.14	45.7	0.83%	5.76%	285.6	30.5
0.08295	615	955	19.9	48.8	1.17	1.86E-05	3.13	57.1	0.64%	5.60%	334.5	35.7
0.08295	615	955	19.9	48.8	1.17	1.86E-05	3.15	57.3	0.64%	5.62%	337.4	36.0
0.08295	615	955	19.9	48.8	1.16	1.86E-05	3.16	57.5	0.63%	5.57%	338.8	36.2
0.08295	615	955	19.9	48.8	1.16	1.86E-05	3.17	68.7	0.58%	6.03%	388.9	41.5
0.08295	615	955	19.9	48.8	1.17	1.86E-05	3.13	69.0	0.56%	5.92%	389.9	41.6
0.08295	615	955	19.9	48.8	1.18	1.86E-05	3.13	78.7	0.54%	6.48%	437.2	46.7
0.08295	615	955	19.9	48.8	1.16	1.86E-05	3.16	79.4	0.54%	6.57%	430.3	45.9

Table 4. CO_2/silicone oil data for 315, 415, 515 and 615 mm tray spacings

A_p [m²]	s [mm]	ρ_L [kg/m₃]	σ [mN/m]	μ_L [mPa.s]	ρ_V [kg/m³]	μ_g [Pa.s]	U_s [m/s]	Q_L [m³/(h.m)]	L'/L	L'/G	Holdup [Pa]	Holdup [mm liq]
0.08295	315	955	19.9	48.8	1.78	1.493E-05	1.35	2.9	2.21%	1.50%	186.0	19.9
0.08295	315	955	19.9	48.8	1.78	1.493E-05	1.35	6.0	1.12%	1.56%	231.1	24.7
0.08295	315	955	19.9	48.8	1.80	1.493E-05	1.34	34.6	0.42%	3.39%	436.5	46.6
0.08295	315	955	19.9	48.8	1.80	1.493E-05	1.34	45.8	0.37%	3.98%	473.7	50.6
0.08295	315	955	19.9	48.8	1.79	1.493E-05	1.34	56.5	0.42%	5.55%	496.8	53.0
0.08295	315	955	19.9	48.8	1.79	1.493E-05	1.33	68.5	0.56%	8.93%	521.2	55.6
0.08295	315	955	19.9	48.8	1.78	1.493E-05	1.40	3.0	2.55%	1.72%	181.5	19.4
0.08295	315	955	19.9	48.8	1.79	1.493E-05	1.40	5.9	1.26%	1.67%	229.1	24.5
0.08295	315	955	19.9	48.8	1.79	1.493E-05	1.40	8.6	0.91%	1.73%	259.1	27.7
0.08295	315	955	19.9	48.8	1.78	1.493E-05	1.41	8.7	0.91%	1.76%	257.4	27.5

Stellenbosch University http://scholar.sun.ac.za

A_p [m^2]	s [mm]	ρ_L [kg/m_3]	σ [mN/m]	μ_L [mPa.s]	ρ_v [kg/m^3]	μ_g [Pa.s]	U_s [m/s]	Q_L [$m^3/(h.m)$]	L'/L	L'/G	Holdup [Pa]	Holdup [mm liq]
0.08295	315	955	19.9	48.8	1.78	1.493E-05	1.41	11.7	0.75%	1.95%	283.7	30.3
0.08295	315	955	19.9	48.8	1.82	1.493E-05	1.38	22.6	0.56%	2.82%	377.5	40.3
0.08295	315	955	19.9	48.8	1.80	1.493E-05	1.40	22.8	0.59%	2.99%	377.5	40.3
0.08295	315	955	19.9	48.8	1.80	1.493E-05	1.39	22.9	0.58%	2.97%	379.5	40.5
0.08295	315	955	19.9	48.8	1.79	1.493E-05	1.39	34.6	0.49%	3.83%	437.7	46.7
0.08295	315	955	19.9	48.8	1.80	1.493E-05	1.39	45.7	0.44%	4.51%	470.0	50.2
0.08295	315	955	19.9	48.8	1.79	1.493E-05	1.39	56.7	0.51%	6.48%	499.4	53.3
0.08295	315	955	19.9	48.8	1.79	1.493E-05	1.40	67.5	0.66%	9.92%	503.7	53.8
0.08295	315	955	19.9	48.8	1.79	1.493E-05	1.39	67.6	0.64%	9.68%	509.8	54.4
0.08295	315	955	19.9	48.8	1.78	1.493E-05	1.72	2.9	5.44%	2.89%	159.2	17.0
0.08295	315	955	19.9	48.8	1.78	1.493E-05	1.71	6.0	2.42%	2.67%	202.1	21.6
0.08295	315	955	19.9	48.8	1.78	1.493E-05	1.71	6.0	2.42%	2.67%	202.1	21.6
0.08295	315	955	19.9	48.8	1.78	1.493E-05	1.71	8.8	1.80%	2.88%	239.4	25.6
0.08295	315	955	19.9	48.8	1.77	1.493E-05	1.73	11.7	1.66%	3.53%	258.2	27.6
0.08295	315	955	19.9	48.8	1.80	1.493E-05	1.70	22.6	1.50%	6.19%	349.0	37.2
0.08295	315	955	19.9	48.8	1.80	1.493E-05	1.71	34.2	1.28%	8.03%	402.0	42.9
0.08295	315	955	19.9	48.8	1.80	1.493E-05	1.71	45.7	1.49%	12.38%	443.5	47.3
0.08295	315	955	19.9	48.8	1.80	1.493E-05	1.70	45.7	1.47%	12.30%	443.0	47.3
0.08295	315	955	19.9	48.8	1.79	1.493E-05	1.72	56.9	2.09%	21.62%	470.3	50.2
0.08295	315	955	19.9	48.8	1.79	1.493E-05	1.70	57.1	1.96%	20.59%	475.8	50.8
0.08295	315	955	19.9	48.8	1.79	1.493E-05	1.72	57.1	1.95%	20.27%	472.1	50.4
0.08295	315	955	19.9	48.8	1.79	1.493E-05	1.72	68.5	1.74%	21.73%	477.8	51.0
0.08295	315	955	19.9	48.8	1.79	1.493E-05	1.72	68.7	1.69%	21.10%	469.2	50.1
0.08295	315	955	19.9	48.8	1.79	1.493E-05	1.72	68.8	1.86%	23.32%	478.8	51.1
0.08295	315	955	19.9	48.8	1.76	1.493E-05	2.04	2.9	9.98%	4.53%	142.4	15.2
0.08295	315	955	19.9	48.8	1.78	1.493E-05	2.04	6.0	4.36%	4.07%	192.6	20.6

A_p [m^2]	s [mm]	ρ_L [kg/m$_3$]	σ [mN/m]	μ_L [mPa.s]	ρ_V [kg/m^3]	μ_g [Pa.s]	U_s [m/s]	Q_L [m^3/(h.m)]	L'/L	L'/G	Holdup [Pa]	Holdup [mm liq]
0.08295	315	955	19.9	48.8	1.78	1.493E-05	2.04	6.0	4.36%	4.07%	192.6	20.6
0.08295	315	955	19.9	48.8	1.78	1.493E-05	2.04	8.7	3.52%	4.75%	215.1	23.0
0.08295	315	955	19.9	48.8	1.77	1.493E-05	2.03	11.7	3.86%	7.00%	238.9	25.5
0.08295	315	955	19.9	48.8	1.79	1.493E-05	2.00	22.8	5.71%	20.25%	328.3	35.0
0.08295	315	955	19.9	48.8	1.79	1.493E-05	2.01	22.8	5.84%	20.63%	326.9	34.9
0.08295	315	955	19.9	48.8	1.79	1.493E-05	2.01	22.9	6.02%	21.35%	330.1	35.2
0.08295	315	955	19.9	48.8	1.79	1.493E-05	2.01	34.4	5.89%	31.55%	407.2	43.5
0.08295	315	955	19.9	48.8	1.79	1.493E-05	2.01	34.4	6.14%	32.91%	395.1	42.2
0.08295	315	955	19.9	48.8	1.80	1.493E-05	2.01	34.4	6.22%	33.29%	400.3	42.7
0.08295	315	955	19.9	48.8	1.79	1.493E-05	2.00	45.7	6.67%	47.49%	458.9	49.0
0.08295	315	955	19.9	48.8	1.79	1.493E-05	2.02	45.7	6.42%	45.56%	447.4	47.8
0.08295	315	955	19.9	48.8	1.79	1.493E-05	2.02	45.7	6.43%	45.53%	445.9	47.6
0.08295	315	955	19.9	48.8	1.79	1.493E-05	2.00	45.7	6.67%	47.68%	438.2	46.8
0.08295	315	955	19.9	48.8	1.79	1.493E-05	2.01	57.4	6.00%	53.35%	503.8	53.8
0.08295	315	955	19.9	48.8	1.79	1.493E-05	2.01	57.5	5.74%	51.20%	500.6	53.4
0.08295	315	955	19.9	48.8	1.79	1.493E-05	2.03	57.5	5.80%	51.32%	484.3	51.7
0.08295	315	955	19.9	48.8	1.79	1.493E-05	2.01	57.6	5.99%	53.42%	493.4	52.7
0.08295	315	955	19.9	48.8	1.79	1.493E-05	2.02	68.6	6.19%	65.62%	579.9	61.9
0.08295	315	955	19.9	48.8	1.79	1.493E-05	2.02	68.8	4.95%	52.73%	546.6	58.3
0.08295	315	955	19.9	48.8	1.79	1.493E-05	2.03	69.3	5.31%	56.73%	548.7	58.6
0.08295	315	955	19.9	48.8	1.79	1.493E-05	2.01	69.8	5.49%	59.47%	550.4	58.8
0.08295	315	955	19.9	48.8	1.73	1.493E-05	2.39	3.1	21.25%	8.83%	135.7	14.5
0.08295	315	955	19.9	48.8	1.75	1.493E-05	2.35	6.0	9.66%	7.83%	179.1	19.1
0.08295	315	955	19.9	48.8	1.75	1.493E-05	2.35	6.0	9.66%	7.83%	179.1	19.1
0.08295	315	955	19.9	48.8	1.76	1.493E-05	2.34	8.6	8.07%	9.39%	208.9	22.3
0.08295	315	955	19.9	48.8	1.77	1.493E-05	2.34	8.6	7.99%	9.28%	205.3	21.9
0.08295	315	955	19.9	48.8	1.77	1.493E-05	2.33	11.6	11.28%	17.82%	230.5	24.6

A_p [m^2]	s [mm]	ρ_L [kg/m3]	σ [mN/m]	μ_L [mPa.s]	ρ_v [kg/m^3]	μ_g [Pa.s]	U_s [m/s]	Q_L [m^3/(h.m)]	L'/L	L'/G	Holdup [Pa]	Holdup [mm liq]
0.08295	315	955	19.9	48.8	1.77	1.493E-05	2.33	11.7	11.43%	18.09%	229.6	24.5
0.08295	415	955	19.9	48.8	1.76	1.493E-05	1.74	2.9	4.03%	2.15%	160.4	17.1
0.08295	415	955	19.9	48.8	1.76	1.493E-05	1.74	2.9	3.88%	2.07%	159.8	17.1
0.08295	415	955	19.9	48.8	1.77	1.493E-05	1.72	5.9	1.64%	1.77%	209.2	22.3
0.08295	415	955	19.9	48.8	1.78	1.493E-05	1.72	8.6	1.07%	1.70%	242.5	25.9
0.08295	415	955	19.9	48.8	1.78	1.493E-05	1.72	8.6	1.07%	1.70%	242.5	25.9
0.08295	415	955	19.9	48.8	1.78	1.493E-05	1.71	11.6	0.83%	1.76%	266.3	28.4
0.08295	415	955	19.9	48.8	1.80	1.493E-05	1.70	22.9	0.50%	2.10%	352.2	37.6
0.08295	415	955	19.9	48.8	1.79	1.493E-05	1.72	33.4	0.36%	2.22%	398.2	42.5
0.08295	415	955	19.9	48.8	1.78	1.493E-05	1.71	45.8	0.32%	2.72%	437.8	46.7
0.08295	415	955	19.9	48.8	1.79	1.493E-05	1.72	57.4	0.30%	3.12%	461.3	49.2
0.08295	415	955	19.9	48.8	1.77	1.493E-05	1.74	66.8	0.30%	3.60%	446.9	47.7
0.08295	415	955	19.9	48.8	1.77	1.493E-05	2.05	2.8	6.78%	2.97%	152.6	16.3
0.08295	415	955	19.9	48.8	1.78	1.493E-05	2.01	5.9	2.56%	2.35%	195.9	20.9
0.08295	415	955	19.9	48.8	1.78	1.493E-05	2.01	5.9	2.56%	2.35%	195.9	20.9
0.08295	415	955	19.9	48.8	1.77	1.493E-05	2.04	8.6	1.87%	2.50%	222.0	23.7
0.08295	415	955	19.9	48.8	1.77	1.493E-05	2.06	11.6	1.62%	2.89%	240.8	25.7
0.08295	415	955	19.9	48.8	1.77	1.493E-05	2.05	11.6	1.58%	2.84%	243.3	26.0
0.08295	415	955	19.9	48.8	1.80	1.493E-05	2.02	23.0	1.23%	4.36%	329.7	35.2
0.08295	415	955	19.9	48.8	1.79	1.493E-05	2.03	34.0	0.92%	4.83%	380.4	40.6
0.08295	415	955	19.9	48.8	1.78	1.493E-05	2.02	46.2	0.80%	5.72%	416.7	44.5
0.08295	415	955	19.9	48.8	1.78	1.493E-05	2.04	57.4	0.71%	6.24%	427.4	45.6
0.08295	415	955	19.9	48.8	1.76	1.493E-05	2.05	66.8	0.47%	4.87%	381.7	40.7
0.08295	415	955	19.9	48.8	1.77	1.493E-05	2.36	2.8	12.29%	4.68%	147.5	15.7
0.08295	415	955	19.9	48.8	1.78	1.493E-05	2.33	5.9	4.57%	3.66%	189.7	20.3

Stellenbosch University http://scholar.sun.ac.za

A_p [m^2]	s [mm]	ρ_L [kg/m3]	σ [mN/m]	μ_L [mPa.s]	ρ_v [kg/m^3]	μ_g [Pa.s]	U_s [m/s]	Q_L [m^3/(h.m)]	L'/L	L'/G	Holdup [Pa]	Holdup [mm liq]
0.08295	415	955	19.9	48.8	1.78	1.493E-05	2.34	5.9	4.66%	3.72%	192.0	20.5
0.08295	415	955	19.9	48.8	1.78	1.493E-05	2.34	8.7	3.11%	3.65%	214.5	22.9
0.08295	415	955	19.9	48.8	1.78	1.493E-05	2.34	8.7	3.11%	3.65%	214.5	22.9
0.08295	415	955	19.9	48.8	1.78	1.493E-05	2.35	11.7	2.82%	4.43%	235.2	25.1
0.08295	415	955	19.9	48.8	1.79	1.493E-05	2.33	23.0	3.68%	11.41%	330.6	35.3
0.08295	415	955	19.9	48.8	1.79	1.493E-05	2.32	23.1	3.55%	11.09%	342.6	36.6
0.08295	415	955	19.9	48.8	1.78	1.493E-05	2.33	34.3	3.13%	14.49%	386.0	41.2
0.08295	415	955	19.9	48.8	1.78	1.493E-05	2.31	34.4	2.90%	13.55%	385.8	41.2
0.08295	415	955	19.9	48.8	1.78	1.493E-05	2.31	34.4	2.95%	13.84%	387.7	41.4
0.08295	415	955	19.9	48.8	1.78	1.493E-05	2.35	46.3	2.03%	12.59%	399.3	42.6
0.08295	415	955	19.9	48.8	1.78	1.493E-05	2.35	46.3	2.03%	12.62%	396.8	42.4
0.08295	415	955	19.9	48.8	1.78	1.493E-05	2.35	57.7	1.15%	8.88%	378.4	40.4
0.08295	415	955	19.9	48.8	1.77	1.493E-05	2.35	57.9	1.20%	9.37%	378.6	40.4
0.08295	415	955	19.9	48.8	1.77	1.493E-05	2.34	67.3	0.87%	7.88%	365.2	39.0
0.08295	415	955	19.9	48.8	1.77	1.493E-05	2.34	67.4	0.86%	7.84%	364.0	38.8
0.08295	515	955	19.9	48.8	1.79	1.493E-05	1.70	3.1	2.63%	1.48%	157.1	16.8
0.08295	515	955	19.9	48.8	1.80	1.493E-05	1.69	5.8	1.11%	1.18%	200.0	21.4
0.08295	515	955	19.9	48.8	1.79	1.493E-05	1.71	8.5	0.75%	1.17%	234.5	25.0
0.08295	515	955	19.9	48.8	1.79	1.493E-05	1.68	11.6	0.52%	1.12%	259.7	27.7
0.08295	515	955	19.9	48.8	1.79	1.493E-05	1.68	11.6	0.52%	1.12%	259.7	27.7
0.08295	515	955	19.9	48.8	1.80	1.493E-05	1.69	22.3	0.31%	1.27%	335.9	35.9
0.08295	515	955	19.9	48.8	1.80	1.493E-05	1.68	33.8	0.21%	1.29%	385.3	41.1
0.08295	515	955	19.9	48.8	1.81	1.493E-05	1.69	45.5	0.16%	1.31%	434.2	46.3
0.08295	515	955	19.9	48.8	1.81	1.493E-05	1.69	57.5	0.12%	1.29%	459.6	49.1
0.08295	515	955	19.9	48.8	1.80	1.493E-05	1.71	68.0	0.12%	1.43%	459.0	49.0
0.08295	515	955	19.9	48.8	1.79	1.493E-05	2.03	3.1	4.44%	2.11%	145.3	15.5

A_p [m^2]	s [mm]	ρ_L [kg/m$_3$]	σ [mN/m]	μ_L [mPa.s]	ρ_V [kg/m^3]	μ_g [Pa.s]	U_s [m/s]	Q_L [m^3/(h.m)]	L'/L	L'/G	Holdup [Pa]	Holdup [mm liq]
0.08295	515	955	19.9	48.8	1.79	1.493E-05	2.02	5.8	1.84%	1.66%	180.6	19.3
0.08295	515	955	19.9	48.8	1.79	1.493E-05	2.02	8.5	1.21%	1.58%	213.1	22.7
0.08295	515	955	19.9	48.8	1.79	1.493E-05	2.02	8.5	1.21%	1.58%	213.1	22.7
0.08295	515	955	19.9	48.8	1.80	1.493E-05	2.01	11.5	0.91%	1.62%	231.6	24.7
0.08295	515	955	19.9	48.8	1.80	1.493E-05	2.01	22.3	0.59%	2.03%	307.8	32.9
0.08295	515	955	19.9	48.8	1.80	1.493E-05	2.01	33.8	0.38%	1.97%	362.2	38.7
0.08295	515	955	19.9	48.8	1.81	1.493E-05	2.01	45.7	0.30%	2.15%	414.3	44.2
0.08295	515	955	19.9	48.8	1.81	1.493E-05	2.01	57.7	0.25%	2.25%	431.0	46.0
0.08295	515	955	19.9	48.8	1.80	1.493E-05	2.01	68.2	0.22%	2.28%	415.9	44.4
0.08295	515	955	19.9	48.8	1.79	1.493E-05	2.31	2.8	7.72%	2.96%	137.3	14.7
0.08295	515	955	19.9	48.8	1.79	1.493E-05	2.32	3.2	6.92%	2.96%	137.2	14.6
0.08295	515	955	19.9	48.8	1.80	1.493E-05	2.32	5.8	3.02%	2.36%	174.3	18.6
0.08295	515	955	19.9	48.8	1.80	1.493E-05	2.32	8.5	1.87%	2.15%	198.7	21.2
0.08295	515	955	19.9	48.8	1.80	1.493E-05	2.32	8.5	1.87%	2.15%	198.7	21.2
0.08295	515	955	19.9	48.8	1.80	1.493E-05	2.32	11.5	1.52%	2.35%	214.5	22.9
0.08295	515	955	19.9	48.8	1.80	1.493E-05	2.31	22.2	1.13%	3.39%	303.2	32.4
0.08295	515	955	19.9	48.8	1.80	1.493E-05	2.31	22.7	1.10%	3.36%	306.0	32.7
0.08295	515	955	19.9	48.8	1.80	1.493E-05	2.32	33.7	0.72%	3.26%	346.6	37.0
0.08295	515	955	19.9	48.8	1.80	1.493E-05	2.30	34.3	0.67%	3.12%	349.0	37.3
0.08295	515	955	19.9	48.8	1.81	1.493E-05	2.30	45.6	0.63%	3.89%	383.2	40.9
0.08295	515	955	19.9	48.8	1.81	1.493E-05	2.31	45.9	0.64%	3.92%	381.7	40.7
0.08295	515	955	19.9	48.8	1.81	1.493E-05	2.29	57.4	0.47%	3.67%	392.9	41.9
0.08295	515	955	19.9	48.8	1.81	1.493E-05	2.30	57.6	0.47%	3.63%	388.0	41.4
0.08295	515	955	19.9	48.8	1.80	1.493E-05	2.30	68.1	0.37%	3.37%	365.8	39.0
0.08295	515	955	19.9	48.8	1.80	1.493E-05	2.30	68.1	0.36%	3.33%	369.4	39.4
0.08295	515	955	19.9	48.8	1.79	1.493E-05	2.60	2.8	15.63%	5.31%	138.3	14.8

A_p [m^2]	s [mm]	ρ_L [kg/m$_3$]	σ [mN/m]	μ_L [mPa.s]	ρ_v [kg/m^3]	μ_g [Pa.s]	U_s [m/s]	Q_L [m^3/(h.m)]	L'/L	L'/G	Holdup [Pa]	Holdup [mm liq]
0.08295	515	955	19.9	48.8	1.79	1.493E-05	2.60	3.1	13.31%	5.01%	139.3	14.9
0.08295	515	955	19.9	48.8	1.79	1.493E-05	2.61	5.8	5.21%	3.64%	173.6	18.5
0.08295	515	955	19.9	48.8	1.79	1.493E-05	2.59	8.6	3.02%	3.13%	196.1	20.9
0.08295	515	955	19.9	48.8	1.79	1.493E-05	2.59	8.6	3.02%	3.13%	196.1	20.9
0.08295	515	955	19.9	48.8	1.79	1.493E-05	2.59	11.5	2.58%	3.57%	218.5	23.3
0.08295	515	955	19.9	48.8	1.79	1.493E-05	2.60	11.5	2.64%	3.64%	217.1	23.2
0.08295	515	955	19.9	48.8	1.80	1.493E-05	2.58	22.4	2.97%	8.00%	290.0	31.0
0.08295	515	955	19.9	48.8	1.80	1.493E-05	2.58	22.5	3.11%	8.43%	294.4	31.4
0.08295	515	955	19.9	48.8	1.80	1.493E-05	2.58	22.9	2.74%	7.52%	304.0	32.5
0.08295	515	955	19.9	48.8	1.81	1.493E-05	2.57	34.0	1.48%	6.02%	323.1	34.5
0.08295	515	955	19.9	48.8	1.81	1.493E-05	2.56	46.1	1.18%	6.59%	342.5	36.6
0.08295	515	955	19.9	48.8	1.81	1.493E-05	2.57	46.2	1.10%	6.14%	341.8	36.5
0.08295	515	955	19.9	48.8	1.81	1.493E-05	2.59	57.7	0.82%	5.64%	349.0	37.3
0.08295	515	955	19.9	48.8	1.81	1.493E-05	2.59	57.7	0.82%	5.68%	346.6	37.0
0.08295	515	955	19.9	48.8	1.80	1.493E-05	2.59	68.3	0.81%	6.61%	377.7	40.3
0.08295	515	955	19.9	48.8	1.80	1.493E-05	2.59	68.3	0.80%	6.54%	379.6	40.5
0.08295	615	955	19.9	48.8	1.79	1.493E-05	2.03	2.8	4.19%	1.82%	134.6	14.4
0.08295	615	955	19.9	48.8	1.79	1.493E-05	2.02	2.9	4.06%	1.82%	137.7	14.7
0.08295	615	955	19.9	48.8	1.80	1.493E-05	2.01	5.9	1.51%	1.37%	192.8	20.6
0.08295	615	955	19.9	48.8	1.80	1.493E-05	2.01	8.6	0.96%	1.26%	213.9	22.8
0.08295	615	955	19.9	48.8	1.80	1.493E-05	2.02	11.5	0.71%	1.27%	231.7	24.7
0.08295	615	955	19.9	48.8	1.80	1.493E-05	2.02	11.5	0.71%	1.27%	231.7	24.7
0.08295	615	955	19.9	48.8	1.80	1.493E-05	2.01	23.0	0.43%	1.52%	312.1	33.3
0.08295	615	955	19.9	48.8	1.80	1.493E-05	2.00	34.7	0.27%	1.48%	369.2	39.4
0.08295	615	955	19.9	48.8	1.78	1.493E-05	2.03	44.9	0.21%	1.45%	394.5	42.1
0.08295	615	955	19.9	48.8	1.78	1.493E-05	2.04	57.8	0.17%	1.48%	394.1	42.1
0.08295	615	955	19.9	48.8	1.80	1.493E-05	2.02	68.4	0.14%	1.49%	359.4	38.4

A_p [m^2]	s [mm]	ρ_L [kg/m$_3$]	σ [mN/m]	μ_L [mPa.s]	ρ_V [kg/m^3]	μ_g [Pa.s]	U_s [m/s]	Q_L [m^3/(h.m)]	L'/L	L'/G	Holdup [Pa]	Holdup [mm liq]
0.08295	615	955	19.9	48.8	1.79	1.493E-05	2.33	2.9	6.54%	2.57%	125.0	13.3
0.08295	615	955	19.9	48.8	1.79	1.493E-05	2.33	2.9	6.49%	2.56%	126.8	13.5
0.08295	615	955	19.9	48.8	1.81	1.493E-05	2.30	5.9	2.36%	1.86%	171.0	18.3
0.08295	615	955	19.9	48.8	1.80	1.493E-05	2.31	8.6	1.46%	1.69%	197.2	21.0
0.08295	615	955	19.9	48.8	1.80	1.493E-05	2.31	8.6	1.46%	1.69%	197.2	21.0
0.08295	615	955	19.9	48.8	1.80	1.493E-05	2.31	11.5	1.10%	1.70%	217.8	23.2
0.08295	615	955	19.9	48.8	1.79	1.493E-05	2.31	23.2	0.74%	2.31%	302.2	32.3
0.08295	615	955	19.9	48.8	1.79	1.493E-05	2.31	23.2	0.75%	2.34%	307.4	32.8
0.08295	615	955	19.9	48.8	1.79	1.493E-05	2.33	34.8	0.50%	2.35%	351.1	37.5
0.08295	615	955	19.9	48.8	1.79	1.493E-05	2.33	34.9	0.49%	2.32%	354.5	37.8
0.08295	615	955	19.9	48.8	1.78	1.493E-05	2.35	45.1	0.37%	2.26%	349.2	37.3
0.08295	615	955	19.9	48.8	1.77	1.493E-05	2.35	45.2	0.37%	2.22%	344.3	36.8
0.08295	615	955	19.9	48.8	1.78	1.493E-05	2.34	57.9	0.27%	2.13%	341.9	36.5
0.08295	615	955	19.9	48.8	1.78	1.493E-05	2.34	57.9	0.27%	2.14%	345.8	36.9
0.08295	615	955	19.9	48.8	1.80	1.493E-05	2.32	68.3	0.23%	2.09%	345.2	36.8
0.08295	615	955	19.9	48.8	1.80	1.493E-05	2.32	68.3	0.23%	2.08%	342.7	36.6
0.08295	615	955	19.9	48.8	1.78	1.493E-05	2.61	3.0	12.33%	4.39%	129.9	13.9
0.08295	615	955	19.9	48.8	1.78	1.493E-05	2.61	3.0	12.62%	4.51%	127.1	13.6
0.08295	615	955	19.9	48.8	1.81	1.493E-05	2.57	5.9	3.73%	2.64%	175.0	18.7
0.08295	615	955	19.9	48.8	1.80	1.493E-05	2.58	8.6	2.27%	2.37%	198.6	21.2
0.08295	615	955	19.9	48.8	1.80	1.493E-05	2.58	8.6	2.27%	2.37%	198.6	21.2
0.08295	615	955	19.9	48.8	1.80	1.493E-05	2.58	11.5	1.83%	2.53%	220.0	23.5
0.08295	615	955	19.9	48.8	1.80	1.493E-05	2.59	11.6	1.79%	2.49%	220.5	23.5
0.08295	615	955	19.9	48.8	1.80	1.493E-05	2.57	23.3	1.24%	3.51%	305.6	32.6
0.08295	615	955	19.9	48.8	1.80	1.493E-05	2.56	23.3	1.24%	3.50%	309.7	33.1
0.08295	615	955	19.9	48.8	1.79	1.493E-05	2.60	34.9	0.87%	3.66%	314.9	33.6

A_p [m^2]	s [mm]	ρ_L [kg/m_3]	σ [mN/m]	μ_L [mPa.s]	ρ_v [kg/m^3]	μ_g [Pa.s]	U_s [m/s]	Q_L [m^3/(h.m)]	L'/L	L'/G	Holdup [Pa]	Holdup [mm liq]
0.08295	615	955	19.9	48.8	1.78	1.493E-05	2.60	35.0	0.85%	3.60%	307.8	32.9
0.08295	615	955	19.9	48.8	1.77	1.493E-05	2.63	45.2	0.57%	3.10%	317.0	33.8
0.08295	615	955	19.9	48.8	1.78	1.493E-05	2.63	45.2	0.58%	3.16%	304.4	32.5
0.08295	615	955	19.9	48.8	1.78	1.493E-05	2.62	57.8	0.45%	3.09%	340.9	36.4
0.08295	615	955	19.9	48.8	1.78	1.493E-05	2.62	57.8	0.44%	3.07%	343.7	36.7
0.08295	615	955	19.9	48.8	1.80	1.493E-05	2.59	68.4	0.38%	3.12%	393.3	42.0
0.08295	615	955	19.9	48.8	1.80	1.493E-05	2.59	68.5	0.38%	3.13%	394.6	42.1
0.08295	615	955	19.9	48.8	1.80	1.493E-05	2.90	2.9	36.74%	11.48%	172.9	18.5
0.08295	615	955	19.9	48.8	1.79	1.493E-05	2.90	2.9	36.70%	11.50%	169.0	18.0
0.08295	615	955	19.9	48.8	1.81	1.493E-05	2.88	5.9	6.93%	4.39%	199.0	21.2
0.08295	615	955	19.9	48.8	1.81	1.493E-05	2.88	5.9	7.00%	4.44%	194.1	20.7
0.08295	615	955	19.9	48.8	1.80	1.493E-05	2.89	8.6	4.31%	3.99%	221.4	23.6
0.08295	615	955	19.9	48.8	1.80	1.493E-05	2.89	8.6	4.24%	3.93%	215.9	23.0
0.08295	615	955	19.9	48.8	1.80	1.493E-05	2.89	8.6	4.31%	3.99%	221.4	23.6
0.08295	615	955	19.9	48.8	1.80	1.493E-05	2.89	8.6	4.24%	3.93%	215.9	23.0
0.08295	615	955	19.9	48.8	1.80	1.493E-05	2.90	11.5	3.98%	4.92%	228.2	24.4
0.08295	615	955	19.9	48.8	1.80	1.493E-05	2.90	11.5	4.19%	5.18%	226.8	24.2
0.08295	615	955	19.9	48.8	1.81	1.493E-05	2.88	23.2	3.65%	9.12%	298.9	31.9
0.08295	615	955	19.9	48.8	1.81	1.493E-05	2.89	23.3	3.56%	8.88%	282.9	30.2
0.08295	615	955	19.9	48.8	1.78	1.493E-05	2.92	35.2	1.94%	7.33%	299.9	32.0
0.08295	615	955	19.9	48.8	1.78	1.493E-05	2.93	35.2	1.69%	6.39%	278.2	29.7
0.08295	615	955	19.9	48.8	1.78	1.493E-05	2.94	45.3	1.33%	6.47%	319.6	34.1
0.08295	615	955	19.9	48.8	1.78	1.493E-05	2.94	45.4	1.29%	6.26%	319.8	34.1
0.08295	615	955	19.9	48.8	1.80	1.493E-05	2.89	57.2	1.01%	6.22%	392.8	41.9
0.08295	615	955	19.9	48.8	1.81	1.493E-05	2.89	57.3	1.03%	6.35%	391.9	41.8
0.08295	615	955	19.9	48.8	1.80	1.493E-05	2.90	68.8	1.19%	8.78%	453.8	48.4
0.08295	615	955	19.9	48.8	1.80	1.493E-05	2.90	68.8	1.18%	8.73%	451.8	48.2

Table 5. CO_2/water data for 315, 415, 515 and 615 mm tray spacings.

A_p [m^2]	s [mm]	ρ_L [kg/m3]	σ [mN/m]	μ_L [mPa.s]	ρ_V [kg/m^3]	μ_g [Pa.s]	U_s [m/s]	Q_L [m^3/(h.m)]	L'/L	L'/G	Holdup [Pa]	Holdup [mm liq]
0.08295	315	997	60	0.9	1.77	1.493E-05	1.22	2.9	1.06%	0.82%	227.5	23.3
0.08295	315	997	60	0.9	1.78	1.493E-05	1.23	5.8	0.58%	0.89%	272.3	27.8
0.08295	315	997	60	0.9	1.78	1.493E-05	1.22	8.6	0.38%	0.89%	308.4	31.5
0.08295	315	997	60	0.9	1.78	1.493E-05	1.21	11.6	0.30%	0.93%	332.9	34.0
0.08295	315	997	60	0.9	1.77	1.493E-05	1.21	23.3	0.29%	1.86%	425.5	43.5
0.08295	315	997	60	0.9	1.77	1.493E-05	1.21	34.7	0.28%	2.63%	474.0	48.5
0.08295	315	997	60	0.9	1.78	1.493E-05	1.20	45.9	0.26%	3.28%	503.0	51.4
0.08295	315	997	60	0.9	1.78	1.493E-05	1.21	57.8	0.32%	4.96%	527.0	53.9
0.08295	315	997	60	0.9	1.78	1.493E-05	1.20	68.9	0.43%	8.09%	561.4	57.4
0.08295	315	997	60	0.9	1.77	1.493E-05	1.20	80.3	0.55%	12.20%	579.5	59.3
0.08295	315	997	60	0.9	1.78	1.493E-05	1.20	91.6	0.54%	13.69%	573.6	58.7
0.08295	315	997	60	0.9	1.78	1.493E-05	1.42	8.5	0.53%	1.05%	286.2	29.3
0.08295	315	997	60	0.9	1.78	1.493E-05	1.40	11.6	0.46%	1.26%	317.9	32.5
0.08295	315	997	60	0.9	1.78	1.493E-05	1.42	22.9	0.45%	2.39%	384.6	39.3
0.08295	315	997	60	0.9	1.78	1.493E-05	1.42	34.7	0.49%	3.91%	439.7	45.0
0.08295	315	997	60	0.9	1.78	1.493E-05	1.41	46.0	0.45%	4.84%	486.4	49.7
0.08295	315	997	60	0.9	1.77	1.493E-05	1.41	57.9	0.60%	8.12%	518.5	53.0
0.08295	315	997	60	0.9	1.78	1.493E-05	1.42	68.8	0.78%	12.39%	542.7	55.5
0.08295	315	997	60	0.9	1.77	1.493E-05	1.42	68.8	0.82%	13.13%	541.0	55.3
0.08295	315	997	60	0.9	1.78	1.493E-05	1.41	80.1	0.83%	15.47%	557.5	57.0
0.08295	315	997	60	0.9	1.78	1.493E-05	1.42	80.2	0.89%	16.62%	551.8	56.4
0.08295	315	997	60	0.9	1.77	1.493E-05	1.41	92.0	0.72%	15.49%	530.4	54.2
0.08295	315	997	65	0.9	1.78	1.493E-05	1.72	2.9	3.69%	2.05%	184.6	18.9
0.08295	315	997	65	0.9	1.78	1.493E-05	1.72	5.8	1.51%	1.67%	231.7	23.7

A_p [m^2]	s [mm]	ρ_L [kg/m_3]	σ [mN/m]	μ_L [mPa.s]	ρ_v [kg/m^3]	μ_g [Pa.s]	U_s [m/s]	Q_L [m^3/(h.m)]	L'/L	L'/G	Holdup [Pa]	Holdup [mm liq]
0.08295	315	997	60	0.9	1.78	1.493E-05	1.72	5.8	1.51%	1.67%	231.7	23.7
0.08295	315	997	60	0.9	1.78	1.493E-05	1.72	8.5	1.29%	2.10%	272.1	27.8
0.08295	315	997	60	0.9	1.78	1.493E-05	1.72	11.6	1.02%	2.25%	297.6	30.4
0.08295	315	997	60	0.9	1.77	1.493E-05	1.72	23.0	0.89%	3.93%	356.6	36.5
0.08295	315	997	60	0.9	1.78	1.493E-05	1.72	34.7	1.05%	6.98%	407.8	41.7
0.08295	315	997	60	0.9	1.77	1.493E-05	1.72	45.6	1.22%	10.62%	461.1	47.1
0.08295	315	997	60	0.9	1.78	1.493E-05	1.71	57.9	1.37%	15.25%	484.5	49.5
0.08295	315	997	60	0.9	1.78	1.493E-05	1.70	57.9	1.37%	15.28%	494.8	50.6
0.08295	315	997	60	0.9	1.78	1.493E-05	1.72	68.8	1.67%	21.91%	512.1	52.4
0.08295	315	997	60	0.9	1.78	1.493E-05	1.72	68.9	1.62%	21.29%	516.7	52.8
0.08295	315	997	60	0.9	1.78	1.493E-05	1.72	68.9	1.61%	21.22%	508.2	52.0
0.08295	315	997	60	0.9	1.78	1.493E-05	1.72	68.9	1.72%	22.70%	516.4	52.8
0.08295	315	997	65	0.9	1.78	1.493E-05	2.05	2.9	8.63%	4.03%	168.9	17.3
0.08295	315	997	65	0.9	1.78	1.493E-05	2.04	5.8	3.67%	3.44%	217.4	22.2
0.08295	315	997	65	0.9	1.78	1.493E-05	2.03	8.5	2.42%	3.33%	245.1	25.1
0.08295	315	997	60	0.9	1.78	1.493E-05	2.03	8.5	2.42%	3.33%	245.1	25.1
0.08295	315	997	60	0.9	1.78	1.493E-05	2.04	11.6	1.94%	3.63%	276.1	28.2
0.08295	315	997	60	0.9	1.78	1.493E-05	2.04	23.1	2.29%	8.51%	341.2	34.9
0.08295	315	997	60	0.9	1.77	1.493E-05	2.04	34.7	3.11%	17.38%	397.2	40.6
0.08295	315	997	60	0.9	1.78	1.493E-05	2.05	34.8	3.16%	17.62%	391.3	40.0
0.08295	315	997	60	0.9	1.78	1.493E-05	2.05	34.8	3.10%	17.32%	387.8	39.6
0.08295	315	997	60	0.9	1.78	1.493E-05	2.03	45.6	3.44%	25.43%	423.9	43.3
0.08295	315	997	60	0.9	1.77	1.493E-05	2.04	45.6	3.44%	25.44%	422.5	43.2
0.08295	315	997	60	0.9	1.78	1.493E-05	2.03	45.7	3.25%	23.97%	438.7	44.9
0.08295	315	997	60	0.9	1.77	1.493E-05	2.04	57.6	3.10%	28.79%	469.5	48.0
0.08295	315	997	60	0.9	1.77	1.493E-05	2.04	57.7	3.32%	30.84%	471.3	48.2
0.08295	315	997	60	0.9	1.78	1.493E-05	2.04	57.7	3.35%	31.22%	461.5	47.2

Stellenbosch University http://scholar.sun.ac.za

A_p [m^2]	s [mm]	ρ_L [kg/m$_3$]	σ [mN/m]	μ_L [mPa.s]	ρ_v [kg/m^3]	μ_g [Pa.s]	U_s [m/s]	Q_L [m^3/(h.m)]	L'/L	L'/G	Holdup [Pa]	Holdup [mm liq]
0.08295	315	997	60	0.9	1.77	1.493E-05	2.03	57.8	3.21%	30.07%	468.7	47.9
0.08295	315	997	60	0.9	1.78	1.493E-05	2.05	68.9	3.13%	34.57%	459.6	47.0
0.08295	315	997	60	0.9	1.78	1.493E-05	2.06	68.9	3.26%	35.94%	458.0	46.8
0.08295	315	997	60	0.9	1.78	1.493E-05	2.06	69.0	2.99%	33.00%	458.9	46.9
0.08295	315	997	60	0.9	1.78	1.493E-05	2.04	69.0	3.13%	34.86%	465.7	47.6
0.08295	315	997	65	0.9	1.77	1.493E-05	2.32	2.9	18.28%	7.60%	154.2	15.8
0.08295	315	997	65	0.9	1.76	1.493E-05	2.33	5.8	7.35%	6.04%	194.2	19.9
0.08295	315	997	65	0.9	1.78	1.493E-05	2.31	8.5	4.71%	5.68%	241.4	24.7
0.08295	315	997	60	0.9	1.78	1.493E-05	2.31	8.5	4.71%	5.68%	241.4	24.7
0.08295	315	997	60	0.9	1.78	1.493E-05	2.31	11.6	3.89%	6.41%	260.2	26.6
0.08295	315	997	60	0.9	1.77	1.493E-05	2.32	23.2	6.29%	20.72%	327.0	33.4
0.08295	315	997	60	0.9	1.77	1.493E-05	2.32	23.1	6.18%	20.31%	338.1	34.6
0.08295	315	997	60	0.9	1.77	1.493E-05	2.32	23.2	6.40%	21.05%	333.1	34.1
0.08295	415	997	65	0.9	1.78	1.493E-05	1.41	2.9	1.00%	0.68%	199.6	20.4
0.08295	415	997	65	0.9	1.78	1.493E-05	1.44	5.8	0.46%	0.61%	238.3	24.4
0.08295	415	997	65	0.9	1.78	1.493E-05	1.42	8.6	0.30%	0.59%	279.3	28.6
0.08295	415	997	60	0.9	1.78	1.493E-05	1.42	8.6	0.30%	0.59%	279.3	28.6
0.08295	415	997	60	0.9	1.78	1.493E-05	1.42	11.5	0.23%	0.61%	301.4	30.8
0.08295	415	997	60	0.9	1.77	1.493E-05	1.41	23.1	0.13%	0.69%	393.9	40.3
0.08295	415	997	60	0.9	1.77	1.493E-05	1.40	34.6	0.11%	0.88%	451.6	46.2
0.08295	415	997	60	0.9	1.78	1.493E-05	1.40	46.1	0.10%	1.12%	483.5	49.4
0.08295	415	997	60	0.9	1.78	1.493E-05	1.41	57.5	0.13%	1.78%	507.2	51.9
0.08295	415	997	60	0.9	1.77	1.493E-05	1.41	69.2	0.15%	2.38%	515.8	52.7
0.08295	415	997	60	0.9	1.78	1.493E-05	1.41	80.1	0.13%	2.42%	490.3	50.1
0.08295	415	997	60	0.9	1.77	1.493E-05	1.41	91.7	0.09%	1.85%	422.8	43.2

Stellenbosch University http://scholar.sun.ac.za

A_p [m^2]	s [mm]	ρ_L [kg/m_3]	σ [mN/m]	μ_L [mPa.s]	ρ_v [kg/m^3]	μ_g [Pa.s]	U_s [m/s]	Q_L [$m^3/(h.m)$]	L'/L	L'/G	Holdup [Pa]	Holdup [mm liq]
0.08295	415	997	65	0.9	1.78	1.493E-05	1.71	2.9	2.17%	1.21%	176.7	18.1
0.08295	415	997	65	0.9	1.78	1.493E-05	1.70	5.8	0.86%	0.96%	224.4	22.9
0.08295	415	997	65	0.9	1.78	1.493E-05	1.71	8.6	0.55%	0.90%	259.0	26.5
0.08295	415	997	65	0.9	1.78	1.493E-05	1.71	8.6	0.54%	0.90%	260.3	26.6
0.08295	415	997	65	0.9	1.78	1.493E-05	1.71	11.5	0.38%	0.84%	289.5	29.6
0.08295	415	997	60	0.9	1.78	1.493E-05	1.71	11.5	0.38%	0.84%	289.5	29.6
0.08295	415	997	60	0.9	1.78	1.493E-05	1.71	23.3	0.23%	1.02%	368.9	37.7
0.08295	415	997	60	0.9	1.77	1.493E-05	1.70	34.5	0.22%	1.46%	418.1	42.7
0.08295	415	997	60	0.9	1.78	1.493E-05	1.71	46.3	0.25%	2.22%	449.2	45.9
0.08295	415	997	60	0.9	1.77	1.493E-05	1.71	57.1	0.29%	3.18%	471.3	48.2
0.08295	415	997	60	0.9	1.78	1.493E-05	1.72	69.0	0.26%	3.38%	454.2	46.4
0.08295	415	997	60	0.9	1.78	1.493E-05	1.71	80.3	0.19%	2.95%	390.7	39.9
0.08295	415	997	60	0.9	1.77	1.493E-05	1.70	80.3	0.19%	2.93%	393.8	40.3
0.08295	415	997	60	0.9	1.78	1.493E-05	1.73	91.3	0.13%	2.28%	359.2	36.7
0.08295	415	997	65	0.9	1.78	1.493E-05	2.03	2.9	5.05%	2.35%	163.1	16.7
0.08295	415	997	65	0.9	1.78	1.493E-05	2.04	5.8	1.96%	1.83%	209.4	21.4
0.08295	415	997	65	0.9	1.78	1.493E-05	2.02	8.6	1.07%	1.50%	244.4	25.0
0.08295	415	997	65	0.9	1.78	1.493E-05	2.04	11.5	0.75%	1.39%	272.1	27.8
0.08295	415	997	60	0.9	1.78	1.493E-05	2.04	11.5	0.75%	1.39%	272.1	27.8
0.08295	415	997	60	0.9	1.78	1.493E-05	2.04	23.3	0.52%	1.95%	351.1	35.9
0.08295	415	997	60	0.9	1.77	1.493E-05	2.03	34.6	0.51%	2.85%	394.2	40.3
0.08295	415	997	60	0.9	1.78	1.493E-05	2.04	46.3	0.57%	4.23%	422.7	43.2
0.08295	415	997	60	0.9	1.78	1.493E-05	2.04	57.3	0.55%	5.05%	421.3	43.1
0.08295	415	997	60	0.9	1.78	1.493E-05	2.04	68.8	0.36%	3.95%	363.7	37.2
0.08295	415	997	60	0.9	1.78	1.493E-05	2.04	80.3	0.24%	3.10%	330.9	33.8
0.08295	415	997	65	0.9	1.78	1.493E-05	2.33	2.9	12.68%	5.21%	137.5	14.1

A_p [m^2]	s [mm]	ρ_L [kg/m_3]	σ [mN/m]	μ_L [mPa.s]	ρ_V [kg/m^3]	μ_g [Pa.s]	U_s [m/s]	Q_L [$m^3/(h.m)$]	L'/L	L'/G	Holdup [Pa]	Holdup [mm liq]
0.08295	415	997	65	0.9	1.78	1.493E-05	2.32	2.9	12.48%	5.14%	143.0	14.6
0.08295	415	997	65	0.9	1.78	1.493E-05	2.32	5.8	4.21%	3.45%	192.0	19.6
0.08295	415	997	65	0.9	1.78	1.493E-05	2.32	8.6	2.10%	2.56%	232.5	23.8
0.08295	415	997	65	0.9	1.78	1.493E-05	2.31	11.5	1.31%	2.14%	259.6	26.5
0.08295	415	997	60	0.9	1.78	1.493E-05	2.31	11.5	1.31%	2.14%	259.6	26.5
0.08295	415	997	60	0.9	1.77	1.493E-05	2.31	23.4	1.07%	3.57%	340.3	34.8
0.08295	415	997	60	0.9	1.78	1.493E-05	2.31	34.7	1.12%	5.52%	373.5	38.2
0.08295	415	997	60	0.9	1.77	1.493E-05	2.32	46.2	1.06%	6.92%	388.2	39.7
0.08295	415	997	60	0.9	1.78	1.493E-05	2.33	57.3	0.85%	6.90%	362.6	37.1
0.08295	415	997	60	0.9	1.77	1.493E-05	2.33	68.8	0.44%	4.26%	308.1	31.5
0.08295	415	997	60	0.9	1.77	1.493E-05	2.32	80.7	0.34%	3.96%	323.1	33.0
0.08295	515	997	65	0.9	1.78	1.493E-05	1.73	2.9	1.53%	0.85%	170.8	17.5
0.08295	515	997	65	0.9	1.78	1.493E-05	1.72	5.6	0.60%	0.65%	210.5	21.5
0.08295	515	997	65	0.9	1.78	1.493E-05	1.71	8.8	0.32%	0.55%	251.9	25.8
0.08295	515	997	65	0.9	1.78	1.493E-05	1.72	11.7	0.21%	0.48%	281.4	28.8
0.08295	515	997	65	0.9	1.78	1.493E-05	1.72	22.6	0.11%	0.46%	359.1	36.7
0.08295	515	997	60	0.9	1.78	1.493E-05	1.72	22.6	0.11%	0.46%	359.1	36.7
0.08295	515	997	60	0.9	1.78	1.493E-05	1.71	34.7	0.09%	0.58%	423.4	43.3
0.08295	515	997	60	0.9	1.78	1.493E-05	1.71	46.7	0.10%	0.92%	457.6	46.8
0.08295	515	997	60	0.9	1.78	1.493E-05	1.70	56.8	0.12%	1.35%	483.2	49.4
0.08295	515	997	60	0.9	1.78	1.493E-05	1.71	69.0	0.13%	1.72%	475.7	48.6
0.08295	515	997	60	0.9	1.78	1.493E-05	1.73	79.8	0.11%	1.68%	426.9	43.7
0.08295	515	997	65	0.9	1.77	1.493E-05	2.04	2.9	3.40%	1.62%	157.5	16.1
0.08295	515	997	65	0.9	1.78	1.493E-05	2.04	5.7	1.29%	1.17%	197.8	20.2
0.08295	515	997	65	0.9	1.78	1.493E-05	2.03	8.8	0.63%	0.90%	231.6	23.7
0.08295	515	997	65	0.9	1.78	1.493E-05	2.05	11.8	0.42%	0.78%	261.6	26.7

Stellenbosch University http://scholar.sun.ac.za

A_p [m^2]	s [mm]	ρ_L [kg/m$_3$]	σ [mN/m]	μ_L [mPa.s]	ρ_V [kg/m^3]	μ_g [Pa.s]	U_s [m/s]	Q_L [m^3/(h.m)]	L'/L	L'/G	Holdup [Pa]	Holdup [mm liq]
0.08295	515	997	60	0.9	1.78	1.493E-05	2.05	11.8	0.42%	0.78%	261.6	26.7
0.08295	515	997	60	0.9	1.78	1.493E-05	2.03	22.7	0.23%	0.83%	341.2	34.9
0.08295	515	997	60	0.9	1.78	1.493E-05	2.03	34.8	0.21%	1.19%	396.3	40.5
0.08295	515	997	60	0.9	1.78	1.493E-05	2.03	46.2	0.26%	1.91%	432.0	44.2
0.08295	515	997	60	0.9	1.77	1.493E-05	2.03	57.0	0.31%	2.85%	445.8	45.6
0.08295	515	997	60	0.9	1.78	1.493E-05	2.03	68.8	0.21%	2.31%	392.6	40.1
0.08295	515	997	60	0.9	1.77	1.493E-05	2.04	79.9	0.14%	1.86%	350.8	35.9
0.08295	515	997	60	0.9	1.78	1.493E-05	2.04	80.1	0.15%	1.93%	353.6	36.2
0.08295	515	997	65	0.9	1.77	1.493E-05	2.34	2.9	8.62%	3.57%	137.5	14.1
0.08295	515	997	65	0.9	1.78	1.493E-05	2.33	5.6	2.71%	2.15%	182.7	18.7
0.08295	515	997	65	0.9	1.78	1.493E-05	2.33	8.8	1.29%	1.60%	217.9	22.3
0.08295	515	997	65	0.9	1.78	1.493E-05	2.31	11.7	0.72%	1.20%	255.2	26.1
0.08295	515	997	60	0.9	1.78	1.493E-05	2.31	11.7	0.72%	1.20%	255.2	26.1
0.08295	515	997	60	0.9	1.78	1.493E-05	2.32	22.7	0.45%	1.46%	328.1	33.5
0.08295	515	997	60	0.9	1.78	1.493E-05	2.32	34.9	0.45%	2.24%	371.0	37.9
0.08295	515	997	60	0.9	1.78	1.493E-05	2.33	46.3	0.54%	3.55%	393.3	40.2
0.08295	515	997	60	0.9	1.77	1.493E-05	2.32	46.4	0.54%	3.57%	391.9	40.1
0.08295	515	997	60	0.9	1.78	1.493E-05	2.32	57.1	0.46%	3.69%	375.9	38.4
0.08295	515	997	60	0.9	1.78	1.493E-05	2.33	68.6	0.23%	2.26%	311.8	31.9
0.08295	515	997	60	0.9	1.77	1.493E-05	2.32	80.3	0.19%	2.19%	337.9	34.5
0.08295	515	997	65	0.9	1.77	1.493E-05	2.62	3.0	22.54%	8.35%	130.9	13.4
0.08295	515	997	65	0.9	1.77	1.493E-05	2.62	5.7	6.24%	4.45%	171.1	17.5
0.08295	515	997	65	0.9	1.78	1.493E-05	2.63	8.8	2.70%	2.98%	206.5	21.1
0.08295	515	997	65	0.9	1.78	1.493E-05	2.61	11.8	1.40%	2.07%	244.7	25.0
0.08295	515	997	60	0.9	1.78	1.493E-05	2.61	11.8	1.40%	2.07%	244.7	25.0
0.08295	515	997	60	0.9	1.78	1.493E-05	2.62	22.7	0.92%	2.64%	319.4	32.7

A_p [m^2]	s [mm]	ρ_L [kg/m_3]	σ [mN/m]	μ_L [mPa.s]	ρ_V [kg/m^3]	μ_g [Pa.s]	U_s [m/s]	Q_L [m^3/(h.m)]	L'/L	L'/G	Holdup [Pa]	Holdup [mm liq]
0.08295	515	997	60	0.9	1.77	1.493E-05	2.62	34.9	1.06%	4.67%	352.9	36.1
0.08295	515	997	60	0.9	1.78	1.493E-05	2.62	35.0	1.01%	4.45%	338.8	34.6
0.08295	515	997	60	0.9	1.78	1.493E-05	2.63	46.3	1.11%	6.40%	322.6	33.0
0.08295	515	997	60	0.9	1.78	1.493E-05	2.63	57.0	0.49%	3.52%	293.0	30.0
0.08295	515	997	60	0.9	1.78	1.493E-05	2.62	68.5	0.40%	3.45%	323.4	33.1
0.08295	515	997	60	0.9	1.78	1.493E-05	2.63	80.6	0.40%	4.01%	368.2	37.6
0.08295	615	997	60	0.9	1.77	1.493E-05	2.04	2.8	3.29%	1.49%	149.3	15.3
0.08295	615	997	60	0.9	1.78	1.493E-05	2.05	5.8	1.19%	1.11%	193.9	19.8
0.08295	615	997	60	0.9	1.78	1.493E-05	2.03	8.7	0.54%	0.76%	235.6	24.1
0.08295	615	997	60	0.9	1.78	1.493E-05	2.03	11.6	0.31%	0.58%	259.3	26.5
0.08295	615	997	60	0.9	1.78	1.493E-05	2.04	23.5	0.10%	0.39%	351.2	35.9
0.08295	615	997	60	0.9	1.78	1.493E-05	2.04	23.5	0.10%	0.39%	351.2	35.9
0.08295	615	997	60	0.9	1.78	1.493E-05	2.05	34.5	0.11%	0.62%	397.1	40.6
0.08295	615	997	60	0.9	1.78	1.493E-05	2.04	45.9	0.10%	0.73%	420.0	42.9
0.08295	615	997	60	0.9	1.78	1.493E-05	2.04	56.8	0.10%	0.91%	403.5	41.3
0.08295	615	997	60	0.9	1.78	1.493E-05	2.05	68.9	0.08%	0.84%	352.9	36.1
0.08295	615	997	60	0.9	1.78	1.493E-05	2.04	79.9	0.06%	0.74%	316.2	32.3
0.08295	615	997	60	0.9	1.78	1.493E-05	2.32	2.8	7.08%	2.85%	138.9	14.2
0.08295	615	997	60	0.9	1.77	1.493E-05	2.33	5.8	2.14%	1.77%	182.2	18.6
0.08295	615	997	60	0.9	1.78	1.493E-05	2.31	8.7	0.98%	1.22%	226.5	23.2
0.08295	615	997	60	0.9	1.78	1.493E-05	2.31	11.5	0.59%	0.96%	249.3	25.5
0.08295	615	997	60	0.9	1.77	1.493E-05	2.31	23.5	0.24%	0.79%	343.5	35.1
0.08295	615	997	60	0.9	1.77	1.493E-05	2.31	23.5	0.24%	0.79%	343.5	35.1
0.08295	615	997	60	0.9	1.78	1.493E-05	2.33	34.6	0.21%	1.05%	385.0	39.4
0.08295	615	997	60	0.9	1.77	1.493E-05	2.33	45.7	0.19%	1.21%	375.8	38.4
0.08295	615	997	60	0.9	1.78	1.493E-05	2.34	56.9	0.16%	1.28%	324.6	33.2

A_p [m^2]	s [mm]	ρ_L [kg/m3]	σ [mN/m]	μ_L [mPa.s]	ρ_V [kg/m^3]	μ_g [Pa.s]	U_s [m/s]	Q_L [m^3/(h.m)]	L'/L	L'/G	Holdup [Pa]	Holdup [mm liq]
0.08295	615	997	60	0.9	1.77	1.493E-05	2.34	68.8	0.11%	1.03%	293.5	30.0
0.08295	615	997	60	0.9	1.78	1.493E-05	2.32	79.4	0.08%	0.87%	300.0	30.7
0.08295	615	997	60	0.9	1.77	1.493E-05	2.62	2.8	18.94%	6.75%	129.6	13.3
0.08295	615	997	60	0.9	1.77	1.493E-05	2.63	5.9	4.58%	3.36%	179.0	18.3
0.08295	615	997	60	0.9	1.78	1.493E-05	2.63	8.7	2.13%	2.32%	212.2	21.7
0.08295	615	997	60	0.9	1.78	1.493E-05	2.62	11.6	1.24%	1.80%	239.3	24.5
0.08295	615	997	60	0.9	1.78	1.493E-05	2.62	23.5	0.46%	1.35%	336.6	34.4
0.08295	615	997	60	0.9	1.78	1.493E-05	2.62	23.5	0.46%	1.35%	336.6	34.4
0.08295	615	997	60	0.9	1.78	1.493E-05	2.63	34.7	0.42%	1.83%	343.1	35.1
0.08295	615	997	60	0.9	1.77	1.493E-05	2.63	45.7	0.36%	2.07%	312.6	32.0
0.08295	615	997	60	0.9	1.77	1.493E-05	2.64	57.2	0.24%	1.73%	295.5	30.2
0.08295	615	997	60	0.9	1.77	1.493E-05	2.63	68.6	0.18%	1.57%	319.4	32.7
0.08295	615	997	60	0.9	1.78	1.493E-05	2.62	79.8	0.15%	1.50%	346.5	35.4
0.08295	615	997	60	0.9	1.77	1.493E-05	2.94	2.9	41.34%	13.26%	149.0	15.2
0.08295	615	997	60	0.9	1.77	1.493E-05	2.94	2.9	40.21%	12.93%	138.6	14.2
0.08295	615	997	60	0.9	1.77	1.493E-05	2.94	2.9	38.76%	12.55%	140.9	14.4
0.08295	615	997	60	0.9	1.77	1.493E-05	2.92	5.9	9.55%	6.31%	190.6	19.5
0.08295	615	997	60	0.9	1.77	1.493E-05	2.91	8.7	3.97%	3.90%	212.2	21.7
0.08295	615	997	60	0.9	1.78	1.493E-05	2.92	8.7	4.07%	3.99%	218.9	22.4
0.08295	615	997	60	0.9	1.77	1.493E-05	2.92	11.5	2.34%	3.04%	247.1	25.3
0.08295	615	997	60	0.9	1.77	1.493E-05	2.91	23.5	1.00%	2.66%	320.9	32.8
0.08295	615	997	60	0.9	1.77	1.493E-05	2.91	23.5	1.00%	2.66%	320.9	32.8
0.08295	615	997	60	0.9	1.78	1.493E-05	2.92	34.8	1.09%	4.27%	287.7	29.4
0.08295	615	997	60	0.9	1.77	1.493E-05	2.93	45.6	0.71%	3.65%	282.9	28.9
0.08295	615	997	60	0.9	1.77	1.493E-05	2.93	57.4	0.45%	2.93%	317.1	32.4
0.08295	615	997	60	0.9	1.77	1.493E-05	2.92	68.4	0.39%	3.01%	355.7	36.4

A_p [m^2]	s [mm]	ρ_L [kg/m_3]	σ [mN/m]	μ_L [mPa.s]	ρ_v [kg/m^3]	μ_g [Pa.s]	U_s [m/s]	Q_L [$m^3/(h.m)$]	L'/L	L'/G	Holdup [Pa]	Holdup [mm liq]
0.08295	615	997	60	0.9	1.78	1.493E-05	2.91	79.6	0.36%	3.24%	395.9	40.5

Table 6. Air/water data for 615 mm tray spacing.

A_p [m^2]	s [mm]	ρ_L [kg/m_3]	σ [mN/m]	μ_L [mPa.s]	ρ_v [kg/m^3]	μ_g [Pa.s]	U_s [m/s]	Q_L [$m^3/(h.m)$]	L'/L	L'/G	Holdup [Pa]	Holdup [mm liq]
0.08295	615	998	59	0.9	1.17	1.86E-05	2.32	2.9	3.01%	1.87%	185.2	18.9
0.08295	615	998	59	0.9	1.17	1.86E-05	2.32	5.9	1.07%	1.36%	234.6	24.0
0.08295	615	998	59	0.9	1.17	1.86E-05	2.32	8.9	0.56%	1.06%	274.3	28.0
0.08295	615	998	59	0.9	1.17	1.86E-05	2.34	23.4	0.19%	0.95%	385.3	39.4
0.08295	615	998	59	0.9	1.17	1.86E-05	2.33	34.8	0.12%	0.91%	451.3	46.1
0.08295	615	998	59	0.9	1.17	1.86E-05	2.33	34.8	0.12%	0.91%	451.3	46.1
0.08295	615	998	59	0.9	1.16	1.86E-05	2.34	46.2	0.12%	1.20%	459.9	47.0
0.08295	615	998	59	0.9	1.16	1.86E-05	2.32	57.8	0.10%	1.29%	459.8	47.0
0.08295	615	998	59	0.9	1.16	1.86E-05	2.33	68.9	0.09%	1.37%	433.3	44.3
0.08295	615	998	59	0.9	1.16	1.86E-05	2.32	79.9	0.07%	1.16%	400.9	40.9
0.08295	615	998	59	0.9	1.16	1.86E-05	2.31	92.3	0.09%	1.71%	398.9	40.7
0.08295	615	998	59	0.9	1.17	1.86E-05	2.61	2.9	5.79%	3.19%	172.2	17.6
0.08295	615	998	59	0.9	1.17	1.86E-05	2.61	2.9	5.61%	3.12%	173.3	17.7
0.08295	615	998	59	0.9	1.17	1.86E-05	2.60	5.9	1.80%	2.04%	221.8	22.7
0.08295	615	998	59	0.9	1.17	1.86E-05	2.60	8.8	0.92%	1.56%	257.2	26.3
0.08295	615	998	59	0.9	1.16	1.86E-05	2.61	11.5	0.60%	1.34%	280.8	28.7
0.08295	615	998	59	0.9	1.17	1.86E-05	2.60	23.5	0.28%	1.26%	373.3	38.1
0.08295	615	998	59	0.9	1.17	1.86E-05	2.60	23.5	0.28%	1.26%	373.3	38.1
0.08295	615	998	59	0.9	1.17	1.86E-05	2.61	34.8	0.20%	1.34%	432.2	44.1
0.08295	615	998	59	0.9	1.17	1.86E-05	2.61	45.8	0.18%	1.55%	447.4	45.7

A_p [m^2]	s [mm]	ρ_L [kg/m_3]	σ [mN/m]	μ_L [mPa.s]	ρ_v [kg/m^3]	μ_g [Pa.s]	U_s [m/s]	Q_L [$m^3/(h.m)$]	L'/L	L'/G	Holdup [Pa]	Holdup [mm liq]
0.08295	615	998	59	0.9	1.16	1.86E-05	2.61	57.9	0.16%	1.77%	404.7	41.3
0.08295	615	998	59	0.9	1.16	1.86E-05	2.62	69.0	0.13%	1.66%	361.0	36.9
0.08295	615	998	59	0.9	1.16	1.86E-05	2.62	80.1	0.08%	1.26%	333.8	34.1
0.08295	615	998	59	0.9	1.16	1.86E-05	2.62	92.3	0.09%	1.56%	350.1	35.8
0.08295	615	998	59	0.9	1.17	1.86E-05	2.92	2.9	12.62%	6.23%	156.6	16.0
0.08295	615	998	59	0.9	1.17	1.86E-05	2.91	5.9	3.45%	3.49%	209.3	21.4
0.08295	615	998	59	0.9	1.17	1.86E-05	2.93	8.8	1.70%	2.56%	234.2	23.9
0.08295	615	998	59	0.9	1.18	1.86E-05	2.90	11.5	1.03%	2.03%	272.2	27.8
0.08295	615	998	59	0.9	1.17	1.86E-05	2.93	24.0	0.46%	1.90%	364.1	37.2
0.08295	615	998	59	0.9	1.17	1.86E-05	2.93	24.0	0.46%	1.90%	364.1	37.2
0.08295	615	998	57.7	0.9	1.18	1.86E-05	2.95	34.4	0.38%	2.18%	401.5	41.0
0.08295	615	998	57.7	0.9	1.18	1.86E-05	2.94	34.4	0.38%	2.18%	405.2	41.4
0.08295	615	998	57.7	0.9	1.18	1.86E-05	2.95	34.4	0.38%	2.18%	399.6	40.8
0.08295	615	998	57.7	0.9	1.18	1.86E-05	2.94	34.4	0.38%	2.22%	401.5	41.0
0.08295	615	998	59	0.9	1.17	1.86E-05	2.94	34.9	0.35%	2.10%	403.7	41.2
0.08295	615	998	59	0.9	1.17	1.86E-05	2.94	45.8	0.30%	2.34%	392.7	40.1
0.08295	615	998	59	0.9	1.16	1.86E-05	2.93	58.0	0.24%	2.35%	326.9	33.4
0.08295	615	998	59	0.9	1.17	1.86E-05	2.93	58.0	0.23%	2.32%	324.9	33.2
0.08295	615	998	59	0.9	1.16	1.86E-05	2.93	69.0	0.16%	1.92%	328.2	33.5
0.08295	615	998	59	0.9	1.16	1.86E-05	2.93	80.3	0.13%	1.73%	358.9	36.7
0.08295	615	998	59	0.9	1.16	1.86E-05	2.93	92.0	0.10%	1.50%	368.4	37.6
0.08295	615	998	57.7	0.9	1.18	1.86E-05	2.97	2.8	14.94%	7.09%	151.7	15.5
0.08295	615	998	57.7	0.9	1.18	1.86E-05	2.97	2.9	15.12%	7.18%	150.5	15.4
0.08295	615	998	57.7	0.9	1.18	1.86E-05	2.97	2.9	15.06%	7.17%	151.5	15.5
0.08295	615	998	57.7	0.9	1.18	1.86E-05	2.97	2.9	15.27%	7.27%	150.6	15.4
0.08295	615	998	57.7	0.9	1.18	1.86E-05	2.98	5.7	4.32%	4.11%	200.8	20.5

A_p [m^2]	s [mm]	ρ_L [kg/m_3]	σ [mN/m]	μ_L [mPa.s]	ρ_V [kg/m^3]	μ_g [Pa.s]	U_s [m/s]	Q_L [$m^3/(h.m)$]	L'/L	L'/G	Holdup [Pa]	Holdup [mm liq]
0.08295	615	998	57.7	0.9	1.18	1.86E-05	2.98	5.7	4.24%	4.04%	204.0	20.8
0.08295	615	998	57.7	0.9	1.18	1.86E-05	2.98	5.7	4.26%	4.06%	197.3	20.2
0.08295	615	998	57.7	0.9	1.18	1.86E-05	2.98	5.7	4.25%	4.06%	198.8	20.3
0.08295	615	998	57.7	0.9	1.18	1.86E-05	2.97	8.6	1.98%	2.85%	233.7	23.9
0.08295	615	998	57.7	0.9	1.18	1.86E-05	2.97	8.6	1.98%	2.86%	236.9	24.2
0.08295	615	998	57.7	0.9	1.18	1.86E-05	2.97	8.6	1.99%	2.86%	232.4	23.7
0.08295	615	998	57.7	0.9	1.18	1.86E-05	2.97	8.7	1.98%	2.86%	237.0	24.2
0.08295	615	998	57.7	0.9	1.18	1.86E-05	2.97	11.5	1.18%	2.27%	261.2	26.7
0.08295	615	998	57.7	0.9	1.18	1.86E-05	2.98	11.5	1.19%	2.27%	258.8	26.4
0.08295	615	998	57.7	0.9	1.18	1.86E-05	2.97	11.5	1.20%	2.30%	270.6	27.6
0.08295	615	998	57.7	0.9	1.18	1.86E-05	2.97	11.5	1.18%	2.27%	264.6	27.0
0.08295	615	998	57.7	0.9	1.18	1.86E-05	2.98	11.5	1.20%	2.29%	265.9	27.2
0.08295	615	998	57.7	0.9	1.18	1.86E-05	2.98	23.0	0.53%	2.03%	363.7	37.1
0.08295	615	998	57.7	0.9	1.18	1.86E-05	2.98	23.0	0.52%	1.99%	356.6	36.4
0.08295	615	998	57.7	0.9	1.18	1.86E-05	2.98	23.0	0.53%	2.03%	356.9	36.5
0.08295	615	998	57.7	0.9	1.18	1.86E-05	2.98	23.0	0.54%	2.07%	356.4	36.4
0.08295	615	998	57.7	0.9	1.18	1.86E-05	2.98	23.0	0.53%	2.03%	363.7	37.1
0.08295	615	998	57.7	0.9	1.18	1.86E-05	2.98	23.0	0.52%	1.99%	356.6	36.4
0.08295	615	998	57.7	0.9	1.18	1.86E-05	2.98	23.0	0.53%	2.03%	356.9	36.5
0.08295	615	998	57.7	0.9	1.18	1.86E-05	2.98	23.0	0.54%	2.07%	356.4	36.4
0.08295	615	998	57.7	0.9	1.18	1.86E-05	2.98	46.1	0.33%	2.54%	376.5	38.5
0.08295	615	998	57.7	0.9	1.18	1.86E-05	2.98	46.1	0.33%	2.53%	380.2	38.8
0.08295	615	998	57.7	0.9	1.18	1.86E-05	2.98	46.1	0.33%	2.53%	380.4	38.9
0.08295	615	998	57.7	0.9	1.18	1.86E-05	2.98	46.1	0.33%	2.52%	384.3	39.3
0.08295	615	998	57.7	0.9	1.18	1.86E-05	2.98	57.8	0.24%	2.35%	347.4	35.5
0.08295	615	998	57.7	0.9	1.18	1.86E-05	2.99	57.8	0.25%	2.37%	350.5	35.8
0.08295	615	998	57.7	0.9	1.18	1.86E-05	2.99	57.8	0.25%	2.38%	346.5	35.4
0.08295	615	998	57.7	0.9	1.18	1.86E-05	2.99	57.8	0.25%	2.36%	346.5	35.4

A_p [m^2]	s [mm]	ρ_L [kg/m_3]	σ [mN/m]	μ_L [mPa.s]	ρ_v [kg/m^3]	μ_g [Pa.s]	U_s [m/s]	Q_L [m^3/(h.m)]	L'/L	L'/G	Holdup [Pa]	Holdup [mm liq]
0.08295	615	998	57.7	0.9	1.18	1.86E-05	2.97	69.2	0.16%	1.87%	337.9	34.5
0.08295	615	998	57.7	0.9	1.18	1.86E-05	2.97	69.3	0.16%	1.87%	338.7	34.6
0.08295	615	998	57.7	0.9	1.18	1.86E-05	2.97	69.4	0.16%	1.89%	341.9	34.9
0.08295	615	998	57.7	0.9	1.18	1.86E-05	3.00	80.8	0.13%	1.69%	367.9	37.6
0.08295	615	998	57.7	0.9	1.18	1.86E-05	3.00	80.8	0.13%	1.70%	367.1	37.5
0.08295	615	998	57.7	0.9	1.18	1.86E-05	3.00	80.9	0.13%	1.67%	367.9	37.6
0.08295	615	998	57.7	0.9	1.18	1.86E-05	3.00	80.9	0.12%	1.66%	368.8	37.7
0.08295	615	998	57.7	0.9	1.18	1.86E-05	3.13	2.9	21.83%	9.87%	148.6	15.2
0.08295	615	998	58.7	0.9	1.15	1.86E-05	3.13	2.9	20.07%	9.34%	142.3	14.5
0.08295	615	998	58.7	0.9	1.15	1.86E-05	3.13	2.9	20.46%	9.54%	140.7	14.4
0.08295	615	998	57.7	0.9	1.18	1.86E-05	3.14	2.9	22.13%	10.09%	146.8	15.0
0.08295	615	998	57.7	0.9	1.18	1.86E-05	3.14	2.9	22.11%	10.09%	150.3	15.4
0.08295	615	998	57.7	0.9	1.18	1.86E-05	3.14	2.9	22.13%	10.17%	148.4	15.2
0.08295	615	998	57.7	0.9	1.18	1.86E-05	3.13	5.7	5.77%	5.24%	196.5	20.1
0.08295	615	998	57.7	0.9	1.18	1.86E-05	3.12	5.8	5.77%	5.25%	191.6	19.6
0.08295	615	998	57.7	0.9	1.18	1.86E-05	3.12	5.8	5.70%	5.20%	194.3	19.8
0.08295	615	998	57.7	0.9	1.18	1.86E-05	3.12	5.8	5.70%	5.20%	192.4	19.7
0.08295	615	998	57.7	0.9	1.18	1.86E-05	3.13	5.8	5.70%	5.20%	192.9	19.7
0.08295	615	998	57.7	0.9	1.18	1.86E-05	3.13	5.8	5.77%	5.28%	191.6	19.6
0.08295	615	998	58.7	0.9	1.15	1.86E-05	3.13	6.0	4.86%	4.74%	195.7	20.0
0.08295	615	998	57.7	0.9	1.18	1.86E-05	3.15	8.6	2.81%	3.81%	227.8	23.3
0.08295	615	998	57.7	0.9	1.18	1.86E-05	3.14	8.6	2.73%	3.72%	226.7	23.2
0.08295	615	998	57.7	0.9	1.18	1.86E-05	3.15	8.6	2.84%	3.86%	224.4	22.9
0.08295	615	998	58.7	0.9	1.15	1.86E-05	3.12	8.6	2.39%	3.35%	222.8	22.8
0.08295	615	998	57.7	0.9	1.18	1.86E-05	3.15	8.7	2.79%	3.80%	226.4	23.1
0.08295	615	998	57.7	0.9	1.18	1.86E-05	3.15	11.5	1.64%	2.97%	255.4	26.1
0.08295	615	998	57.7	0.9	1.18	1.86E-05	3.15	11.5	1.61%	2.92%	260.8	26.6

A_p [m^2]	s [mm]	ρ_L [kg/m$_3$]	σ [mN/m]	μ_L [mPa.s]	ρ_v [kg/m^3]	μ_g [Pa.s]	U_s [m/s]	Q_L [m^3/(h.m)]	L'/L	L'/G	Holdup [Pa]	Holdup [mm liq]
0.08295	615	998	57.7	0.9	1.18	1.86E-05	3.14	11.5	1.60%	2.91%	258.4	26.4
0.08295	615	998	57.7	0.9	1.18	1.86E-05	3.15	11.5	1.62%	2.93%	257.6	26.3
0.08295	615	998	58.7	0.9	1.15	1.86E-05	3.13	23.0	0.50%	1.87%	366.8	37.5
0.08295	615	998	57.7	0.9	1.18	1.86E-05	3.15	23.1	0.72%	2.63%	347.0	35.4
0.08295	615	998	57.7	0.9	1.18	1.86E-05	3.15	23.1	0.72%	2.62%	353.5	36.1
0.08295	615	998	57.7	0.9	1.18	1.86E-05	3.15	23.2	0.70%	2.54%	354.5	36.2
0.08295	615	998	57.7	0.9	1.18	1.86E-05	3.15	23.2	0.70%	2.56%	350.0	35.8
0.08295	615	998	58.7	0.9	1.15	1.86E-05	3.13	23.0	0.50%	1.87%	366.8	37.5
0.08295	615	998	57.7	0.9	1.18	1.86E-05	3.15	23.1	0.72%	2.63%	347.0	35.4
0.08295	615	998	57.7	0.9	1.18	1.86E-05	3.15	23.1	0.72%	2.62%	353.5	36.1
0.08295	615	998	57.7	0.9	1.18	1.86E-05	3.15	23.2	0.70%	2.54%	354.5	36.2
0.08295	615	998	57.7	0.9	1.18	1.86E-05	3.15	23.2	0.70%	2.56%	350.0	35.8
0.08295	615	998	57.7	0.9	1.18	1.86E-05	3.14	34.4	0.61%	3.31%	359.7	36.7
0.08295	615	998	57.7	0.9	1.18	1.86E-05	3.14	34.4	0.61%	3.30%	360.8	36.9
0.08295	615	998	57.7	0.9	1.18	1.86E-05	3.14	34.5	0.61%	3.33%	360.4	36.8
0.08295	615	998	57.7	0.9	1.18	1.86E-05	3.14	34.5	0.62%	3.34%	361.9	37.0
0.08295	615	998	57.7	0.9	1.18	1.86E-05	3.14	34.5	0.62%	3.34%	354.1	36.2
0.08295	615	998	58.7	0.9	1.15	1.86E-05	3.16	45.9	0.35%	2.60%	377.0	38.5
0.08295	615	998	57.7	0.9	1.18	1.86E-05	3.15	46.1	0.46%	3.30%	339.9	34.7
0.08295	615	998	57.7	0.9	1.18	1.86E-05	3.15	46.2	0.45%	3.29%	346.4	35.4
0.08295	615	998	57.7	0.9	1.18	1.86E-05	3.15	46.2	0.45%	3.27%	343.9	35.1
0.08295	615	998	57.7	0.9	1.18	1.86E-05	3.15	46.2	0.46%	3.37%	343.5	35.1
0.08295	615	998	58.7	0.9	1.15	1.86E-05	3.14	57.5	0.25%	2.36%	327.2	33.4
0.08295	615	998	57.7	0.9	1.18	1.86E-05	3.15	57.7	0.29%	2.63%	317.7	32.4
0.08295	615	998	57.7	0.9	1.18	1.86E-05	3.14	57.7	0.29%	2.62%	316.8	32.4
0.08295	615	998	57.7	0.9	1.18	1.86E-05	3.14	57.7	0.29%	2.67%	316.1	32.3
0.08295	615	998	57.7	0.9	1.18	1.86E-05	3.15	57.8	0.29%	2.61%	316.8	32.4
0.08295	615	998	57.7	0.9	1.18	1.86E-05	3.14	69.5	0.20%	2.19%	346.7	35.4

A_p [m^2]	s [mm]	ρ_L [kg/m_3]	σ [mN/m]	μ_L [mPa.s]	ρ_V [kg/m^3]	μ_g [Pa.s]	U_s [m/s]	Q_L [m^3/(h.m)]	L'/L	L'/G	Holdup [Pa]	Holdup [mm liq]
0.08295	615	998	57.7	0.9	1.18	1.86E-05	3.15	69.6	0.20%	2.19%	345.9	35.3
0.08295	615	998	57.7	0.9	1.18	1.86E-05	3.15	69.6	0.20%	2.20%	344.8	35.2
0.08295	615	998	57.7	0.9	1.18	1.86E-05	3.15	69.7	0.20%	2.20%	345.6	35.3
0.08295	615	998	58.7	0.9	1.15	1.86E-05	3.13	80.3	0.13%	1.64%	345.5	35.3
0.08295	615	998	57.7	0.9	1.18	1.86E-05	3.15	80.6	0.17%	2.10%	379.4	38.7
0.08295	615	998	57.7	0.9	1.18	1.86E-05	3.15	80.6	0.16%	2.06%	377.5	38.6
0.08295	615	998	57.7	0.9	1.18	1.86E-05	3.16	80.7	0.16%	2.05%	378.5	38.7
0.08295	615	998	57.7	0.9	1.18	1.86E-05	3.16	80.7	0.16%	2.06%	376.6	38.5
0.08295	615	998	58.7	0.9	1.15	1.86E-05	3.14	103.0	0.12%	1.93%	301.3	30.8

Table 7. SF_6/water data for 615mm tray spacing.

A_p [m^2]	s [mm]	ρ_L [kg/m_3]	σ [mN/m]	μ_L [mPa.s]	ρ_V [kg/m^3]	μ_g [Pa.s]	U_s [m/s]	Q_L [m^3/(h.m)]	L'/L	L'/G	Holdup [Pa]	Holdup [mm liq]
0.08295	615	997.5	60	1.02	5.81	1.51E-05	1.19	5.7	0.71%	0.34%	338.5	34.6
0.08295	615	997.5	60	1.02	5.80	1.51E-05	1.19	8.6	0.40%	0.29%	372.4	38.1
0.08295	615	997.5	60	1.02	5.80	1.51E-05	1.20	11.4	0.26%	0.25%	397.6	40.6
0.08295	615	997.5	60	1.02	5.82	1.51E-05	1.20	23.1	0.11%	0.22%	468.3	47.9
0.08295	615	997.5	60	1.02	5.81	1.51E-05	1.20	34.2	0.08%	0.22%	527.0	53.9
0.08295	615	997.5	60	1.02	5.80	1.51E-05	1.20	46.4	0.06%	0.22%	567.9	58.0
0.08295	615	997.5	60	1.02	5.78	1.51E-05	1.20	57.3	0.05%	0.23%	587.4	60.0
0.08295	615	997.5	60	1.02	5.79	1.51E-05	1.20	69.0	0.04%	0.23%	590.1	60.3
0.08295	615	997.5	60	1.02	5.78	1.51E-05	1.19	80.5	0.04%	0.25%	576.3	58.9
0.08295	615	997.5	60	1.02	5.79	1.51E-05	1.19	91.8	0.04%	0.30%	544.9	55.7
0.08295	615	997.5	60	1.02	5.81	1.51E-05	1.40	2.9	4.45%	0.93%	267.3	27.3
0.08295	615	997.5	60	1.02	5.80	1.51E-05	1.40	5.8	1.67%	0.69%	320.8	32.8

A_p [m^2]	s [mm]	ρ_L [kg/m_3]	σ [mN/m]	μ_L [mPa.s]	ρ_v [kg/m^3]	μ_g [Pa.s]	U_s [m/s]	Q_L [$m^3/(h.m)$]	L'/L	L'/G	Holdup [Pa]	Holdup [mm liq]
0.08295	615	997.5	60	1.02	5.82	1.51E-05	1.40	8.6	0.87%	0.54%	358.8	36.7
0.08295	615	997.5	60	1.02	5.79	1.51E-05	1.38	11.4	0.50%	0.41%	382.9	39.1
0.08295	615	997.5	60	1.02	5.76	1.51E-05	1.40	22.9	0.21%	0.36%	461.1	47.1
0.08295	615	997.5	60	1.02	5.76	1.51E-05	1.40	22.9	0.21%	0.35%	457.5	46.8
0.08295	615	997.5	60	1.02	5.76	1.51E-05	1.40	34.9	0.14%	0.36%	509.7	52.1
0.08295	615	997.5	60	1.02	5.76	1.51E-05	1.40	45.6	0.11%	0.37%	536.9	54.9
0.08295	615	997.5	60	1.02	5.75	1.51E-05	1.40	57.3	0.10%	0.43%	542.1	55.4
0.08295	615	997.5	60	1.02	5.76	1.51E-05	1.40	68.9	0.09%	0.45%	517.2	52.9
0.08295	615	997.5	60	1.02	5.78	1.51E-05	1.39	79.9	0.08%	0.48%	462.8	47.3
0.08295	615	997.5	60	1.02	5.79	1.51E-05	1.40	92.2	0.06%	0.41%	472.6	48.3
0.08295	615	997.5	60	1.02	5.79	1.51E-05	1.69	2.9	22.91%	4.03%	256.4	26.2
0.08295	615	997.5	60	1.02	5.80	1.51E-05	1.68	2.9	22.88%	4.03%	256.5	26.2
0.08295	615	997.5	60	1.02	5.81	1.51E-05	1.68	2.9	23.15%	4.07%	259.5	26.5
0.08295	615	997.5	60	1.02	5.80	1.51E-05	1.69	3.0	22.52%	3.97%	256.4	26.2
0.08295	615	997.5	60	1.02	5.81	1.51E-05	1.69	5.9	5.49%	1.91%	309.9	31.7
0.08295	615	997.5	60	1.02	5.79	1.51E-05	1.70	5.9	5.35%	1.86%	296.2	30.3
0.08295	615	997.5	60	1.02	5.81	1.51E-05	1.69	5.9	5.45%	1.90%	310.7	31.8
0.08295	615	997.5	60	1.02	5.82	1.51E-05	1.69	8.8	2.53%	1.33%	344.9	35.2
0.08295	615	997.5	60	1.02	5.80	1.51E-05	1.69	11.5	1.45%	1.00%	361.7	37.0
0.08295	615	997.5	60	1.02	5.75	1.51E-05	1.70	23.1	0.58%	0.80%	449.1	45.9
0.08295	615	997.5	60	1.02	5.75	1.51E-05	1.70	23.1	0.58%	0.80%	449.1	45.9
0.08295	615	997.5	60	1.02	5.75	1.51E-05	1.71	35.1	0.50%	1.06%	484.3	49.5
0.08295	615	997.5	60	1.02	5.76	1.51E-05	1.71	35.1	0.52%	1.08%	482.0	49.3
0.08295	615	997.5	60	1.02	5.75	1.51E-05	1.71	35.2	0.51%	1.07%	484.4	49.5
0.08295	615	997.5	60	1.02	5.75	1.51E-05	1.71	35.2	0.51%	1.06%	477.5	48.8
0.08295	615	997.5	60	1.02	5.76	1.51E-05	1.71	45.7	0.46%	1.26%	485.1	49.6

A_p [m^2]	s [mm]	ρ_L [kg/m$_3$]	σ [mN/m]	μ_L [mPa.s]	ρ_v [kg/m^3]	μ_g [Pa.s]	U_s [m/s]	Q_L [m^3/(h.m)]	L'/L	L'/G	Holdup [Pa]	Holdup [mm liq]
0.08295	615	997.5	60	1.02	5.74	1.51E-05	1.70	57.3	0.36%	1.22%	457.2	46.7
0.08295	615	997.5	60	1.02	5.74	1.51E-05	1.70	69.0	0.30%	1.23%	500.6	51.2
0.08295	615	997.5	60	1.02	5.79	1.51E-05	1.69	79.8	0.28%	1.34%	530.9	54.3
0.08295	615	997.5	60	1.02	5.80	1.51E-05	1.70	91.8	0.27%	1.49%	552.8	56.5
0.08295	615	997.5	60	1.02	5.80	1.51E-05	1.98	5.9	20.55%	6.12%	302.1	30.9
0.08295	615	997.5	60	1.02	5.78	1.51E-05	1.99	5.9	20.06%	5.97%	294.9	30.1
0.08295	615	997.5	60	1.02	5.79	1.51E-05	1.97	5.9	19.43%	5.84%	325.7	33.3
0.08295	615	997.5	60	1.02	5.80	1.51E-05	1.98	5.9	20.71%	6.20%	317.3	32.4
0.08295	615	997.5	60	1.02	5.79	1.51E-05	1.98	5.9	19.54%	5.84%	308.7	31.5
0.08295	615	997.5	60	1.02	5.79	1.51E-05	1.98	8.9	7.39%	3.33%	342.1	35.0
0.08295	615	997.5	60	1.02	5.79	1.51E-05	1.99	8.9	7.60%	3.41%	336.4	34.4
0.08295	615	997.5	60	1.02	5.78	1.51E-05	2.00	8.9	7.53%	3.38%	322.1	32.9
0.08295	615	997.5	60	1.02	5.80	1.51E-05	1.99	8.9	7.58%	3.42%	326.4	33.4
0.08295	615	997.5	60	1.02	5.79	1.51E-05	1.98	11.5	4.03%	2.37%	355.0	36.3
0.08295	615	997.5	60	1.02	5.78	1.51E-05	1.98	11.6	3.91%	2.31%	359.9	36.8
0.08295	615	997.5	60	1.02	5.81	1.51E-05	1.98	11.6	4.03%	2.36%	359.4	36.7
0.08295	615	997.5	60	1.02	5.79	1.51E-05	1.98	11.5	4.03%	2.37%	355.0	36.3
0.08295	615	997.5	60	1.02	5.78	1.51E-05	1.98	11.6	3.91%	2.31%	359.9	36.8
0.08295	615	997.5	60	1.02	5.81	1.51E-05	1.98	11.6	4.03%	2.36%	359.4	36.7
0.08295	615	997.5	60	1.02	5.74	1.51E-05	2.00	23.3	3.28%	3.88%	426.1	43.5
0.08295	615	997.5	60	1.02	5.74	1.51E-05	2.00	23.3	2.90%	3.45%	426.0	43.5
0.08295	615	997.5	60	1.02	5.75	1.51E-05	2.01	23.3	3.14%	3.72%	418.3	42.8
0.08295	615	997.5	60	1.02	5.74	1.51E-05	2.01	23.4	3.24%	3.84%	412.7	42.2
0.08295	615	997.5	60	1.02	5.75	1.51E-05	2.00	35.2	3.26%	5.81%	435.6	44.5
0.08295	615	997.5	60	1.02	5.74	1.51E-05	2.00	35.2	2.89%	5.18%	427.3	43.7
0.08295	615	997.5	60	1.02	5.78	1.51E-05	2.01	35.2	3.34%	5.93%	433.5	44.3
0.08295	615	997.5	60	1.02	5.74	1.51E-05	2.01	35.4	3.20%	5.75%	420.6	43.0

Stellenbosch University http://scholar.sun.ac.za

A_p [m^2]	s [mm]	ρ_L [kg/m_3]	σ [mN/m]	μ_L [mPa.s]	ρ_v [kg/m^3]	μ_g [Pa.s]	U_s [m/s]	Q_L [$m^3/(h.m)$]	L'/L	L'/G	Holdup [Pa]	Holdup [mm liq]
0.08295	615	997.5	60	1.02	5.75	1.51E-05	2.00	35.4	3.01%	5.42%	432.0	44.1
0.08295	615	997.5	60	1.02	5.74	1.51E-05	2.01	45.7	2.31%	5.35%	440.7	45.0
0.08295	615	997.5	60	1.02	5.74	1.51E-05	2.01	45.7	2.25%	5.23%	441.9	45.2
0.08295	615	997.5	60	1.02	5.76	1.51E-05	2.00	45.7	2.31%	5.35%	447.0	45.7
0.08295	615	997.5	60	1.02	5.74	1.51E-05	2.01	45.8	2.33%	5.41%	437.5	44.7
0.08295	615	997.5	60	1.02	5.75	1.51E-05	2.01	45.8	2.40%	5.57%	447.6	45.7
0.08295	615	997.5	60	1.02	5.75	1.51E-05	2.00	57.5	2.09%	6.09%	491.2	50.2
0.08295	615	997.5	60	1.02	5.74	1.51E-05	2.00	57.5	2.22%	6.48%	489.6	50.0
0.08295	615	997.5	60	1.02	5.74	1.51E-05	2.01	57.5	2.13%	6.21%	493.9	50.5
0.08295	615	997.5	60	1.02	5.75	1.51E-05	2.01	57.6	2.16%	6.29%	496.2	50.7
0.08295	615	997.5	60	1.02	5.76	1.51E-05	2.00	57.6	2.14%	6.25%	489.3	50.0
0.08295	615	997.5	60	1.02	5.72	1.51E-05	2.00	68.2	2.53%	8.82%	544.8	55.7
0.08295	615	997.5	60	1.02	5.77	1.51E-05	2.01	68.3	2.79%	9.63%	555.9	56.8
0.08295	615	997.5	60	1.02	5.75	1.51E-05	2.01	68.4	2.72%	9.40%	555.6	56.8
0.08295	615	997.5	60	1.02	5.72	1.51E-05	2.01	68.4	2.76%	9.61%	550.8	56.3
0.08295	615	997.5	60	1.02	5.73	1.51E-05	2.00	68.4	2.68%	9.34%	546.6	55.9
0.08295	615	997.5	60	1.02	5.79	1.51E-05	2.00	80.0	4.05%	16.35%	609.8	62.3
0.08295	615	997.5	60	1.02	5.79	1.51E-05	2.00	80.0	3.94%	15.93%	599.7	61.3
0.08295	615	997.5	60	1.02	5.79	1.51E-05	1.99	80.0	3.75%	15.22%	616.6	63.0
0.08295	615	997.5	60	1.02	5.79	1.51E-05	2.00	80.1	3.94%	15.90%	616.2	63.0
0.08295	615	997.5	60	1.02	5.79	1.51E-05	2.00	80.1	4.21%	17.04%	616.3	63.0
0.08295	615	997.5	60	1.02	5.77	1.51E-05	2.00	91.7	5.57%	25.96%	680.8	69.6
0.08295	615	997.5	60	1.02	5.77	1.51E-05	1.99	91.9	5.67%	26.45%	662.2	67.7
0.08295	615	997.5	60	1.02	5.77	1.51E-05	2.00	91.9	5.74%	26.76%	695.0	71.0
0.08295	615	997.5	60	1.02	5.77	1.51E-05	1.99	92.0	5.71%	26.73%	679.5	69.4
0.08295	615	997.5	60	1.02	5.77	1.51E-05	1.99	92.1	5.54%	25.89%	666.0	68.1
0.08295	615	997.5	60	1.02	5.77	1.51E-05	1.99	92.5	5.45%	25.62%	666.8	68.1

Table 8. Air/ethylene glycol data for 315, 415, 515 and 615mm tray spacings.

A_p [m^2]	s [mm]	ρ_L [kg/m^3]	σ [mN/m]	μ_L [mPa.s]	ρ_V [kg/m^3]	μ_g [Pa.s]	U_s [m/s]	Q_L [m^3/(h.m)]	L'/L	L'/G	Holdup [Pa]	Holdup [mm liq]
0.08295	315	1102	37	14.6	1.17	1.86E-05	1.43	3.0	1.46%	1.66%	234.8	21.7
0.08295	315	1102	37	14.6	1.17	1.86E-05	1.44	5.8	0.77%	1.71%	283.5	26.2
0.08295	315	1102	37	14.6	1.17	1.86E-05	1.42	8.6	0.52%	1.71%	317.0	29.3
0.08295	315	1102	37	14.6	1.17	1.86E-05	1.42	11.5	0.40%	1.79%	345.7	32.0
0.08295	315	1102	37	14.6	1.17	1.86E-05	1.43	22.8	0.34%	3.01%	484.8	44.8
0.08295	315	1102	37	14.6	1.17	1.86E-05	1.44	34.1	0.28%	3.68%	526.5	48.7
0.08295	315	1102	37	14.6	1.17	1.86E-05	1.43	46.1	0.24%	4.36%	564.8	52.2
0.08295	315	1102	37	14.6	1.17	1.86E-05	1.45	56.6	0.30%	6.44%	587.6	54.4
0.08295	315	1102	37	14.6	1.17	1.86E-05	1.42	69.2	0.29%	7.89%	608.6	56.3
0.08295	315	1102	37	14.6	1.17	1.86E-05	1.43	79.6	0.36%	11.09%	619.0	57.3
0.08295	315	1102	37	14.6	1.17	1.86E-05	1.42	91.9	0.42%	14.95%	636.7	58.9
0.08295	315	1102	37	14.6	1.17	1.86E-05	1.43	92.3	0.37%	13.10%	630.0	58.3
0.08295	315	1102	37	14.6	1.17	1.86E-05	2.00	3.0	5.55%	4.51%	200.3	18.5
0.08295	315	1102	37	14.6	1.17	1.86E-05	2.00	3.0	5.43%	4.50%	199.7	18.5
0.08295	315	1102	37	14.6	1.17	1.86E-05	1.99	5.8	2.48%	3.93%	245.8	22.7
0.08295	315	1102	37	14.6	1.17	1.86E-05	2.00	8.6	1.57%	3.71%	286.9	26.5
0.08295	315	1102	37	14.6	1.17	1.86E-05	2.00	11.5	1.13%	3.58%	317.0	29.3
0.08295	315	1102	37	14.6	1.17	1.86E-05	2.02	22.7	0.88%	5.49%	413.9	38.3
0.08295	315	1102	37	14.6	1.17	1.86E-05	1.99	34.1	0.79%	7.47%	471.6	43.6
0.08295	315	1102	37	14.6	1.17	1.86E-05	2.01	45.8	0.82%	10.35%	505.3	46.7
0.08295	315	1102	37	14.6	1.17	1.86E-05	2.00	56.7	1.22%	19.08%	532.7	49.3
0.08295	315	1102	37	14.6	1.17	1.86E-05	1.99	68.9	1.38%	26.44%	547.3	50.6
0.08295	315	1102	37	14.6	1.17	1.86E-05	1.99	80.0	1.17%	26.00%	541.7	50.1
0.08295	315	1102	37	14.6	1.17	1.86E-05	2.00	91.9	0.63%	15.93%	488.5	45.2

A_p [m^2]	s [mm]	ρ_L [kg/m_3]	σ [mN/m]	μ_L [mPa.s]	ρ_v [kg/m^3]	μ_g [Pa.s]	U_s [m/s]	Q_L [m^3/(h.m)]	L'/L	L'/G	Holdup [Pa]	Holdup [mm liq]
0.08295	315	1102	37	14.6	1.17	1.86E-05	2.59	2.9	15.44%	9.68%	170.1	15.7
0.08295	315	1102	37	14.6	1.17	1.86E-05	2.59	3.0	15.02%	9.57%	172.9	16.0
0.08295	315	1102	37	14.6	1.17	1.86E-05	2.58	5.8	6.14%	7.56%	222.1	20.5
0.08295	315	1102	37	14.6	1.17	1.86E-05	2.56	8.6	3.67%	6.78%	261.3	24.2
0.08295	315	1102	37	14.6	1.17	1.86E-05	2.56	8.6	3.67%	6.78%	261.3	24.2
0.08295	315	1102	37	14.6	1.17	1.86E-05	2.59	11.4	3.09%	7.57%	286.7	26.5
0.08295	315	1102	37	14.6	1.17	1.86E-05	2.56	23.1	3.20%	15.89%	375.0	34.7
0.08295	315	1102	37	14.6	1.17	1.86E-05	2.56	23.1	3.18%	15.85%	374.5	34.6
0.08295	315	1102	37	14.6	1.17	1.86E-05	2.58	34.1	3.72%	27.10%	428.5	39.6
0.08295	315	1102	37	14.6	1.17	1.86E-05	2.57	34.2	3.58%	26.29%	431.5	39.9
0.08295	315	1102	37	14.6	1.17	1.86E-05	2.58	45.6	3.36%	32.79%	456.2	42.2
0.08295	315	1102	37	14.6	1.17	1.86E-05	2.57	45.8	3.85%	37.98%	476.1	44.0
0.08295	315	1102	37	14.6	1.17	1.86E-05	2.57	56.9	3.64%	44.42%	478.8	44.3
0.08295	315	1102	37	14.6	1.17	1.86E-05	2.56	57.1	3.76%	46.31%	488.5	45.2
0.08295	315	1102	37	14.6	1.17	1.86E-05	2.55	57.2	3.90%	48.37%	480.4	44.4
0.08295	315	1102	37	14.6	1.17	1.86E-05	2.59	68.6	3.15%	45.96%	470.8	43.6
0.08295	315	1102	37	14.6	1.17	1.86E-05	2.56	68.6	3.17%	46.96%	477.4	44.2
0.08295	315	1102	37	14.6	1.17	1.86E-05	2.55	68.7	2.94%	43.65%	493.2	45.6
0.08295	315	1102	37	14.6	1.17	1.86E-05	2.55	79.5	2.22%	38.16%	484.5	44.8
0.08295	315	1102	37	14.6	1.17	1.86E-05	2.56	79.5	2.18%	37.44%	478.4	44.3
0.08295	315	1102	37	14.6	1.17	1.86E-05	3.15	2.9	50.50%	25.93%	166.0	15.4
0.08295	315	1102	37	14.6	1.17	1.86E-05	3.15	3.0	49.68%	26.03%	167.5	15.5
0.08295	315	1102	37	14.6	1.17	1.86E-05	3.15	3.0	49.48%	26.01%	175.7	16.3
0.08295	315	1102	37	14.6	1.17	1.86E-05	3.13	5.8	18.08%	18.33%	206.2	19.1
0.08295	315	1102	37	14.6	1.17	1.86E-05	3.13	5.8	18.01%	18.26%	199.9	18.5
0.08295	315	1102	37	14.6	1.17	1.86E-05	3.13	8.6	11.12%	16.88%	232.1	21.5
0.08295	315	1102	37	14.6	1.17	1.86E-05	3.13	8.6	11.12%	16.95%	243.2	22.5

Stellenbosch University http://scholar.sun.ac.za

A_p [m^2]	s [mm]	ρ_L [kg/m$_3$]	σ [mN/m]	μ_L [mPa.s]	ρ_v [kg/m^3]	μ_g [Pa.s]	U_s [m/s]	Q_L [m^3/(h.m)]	L'/L	L'/G	Holdup [Pa]	Holdup [mm liq]
0.08295	315	1102	37	14.6	1.17	1.86E-05	3.13	8.6	11.12%	16.95%	243.2	22.5
0.08295	315	1102	37	14.6	1.17	1.86E-05	3.13	11.5	9.59%	19.37%	259.9	24.0
0.08295	315	1102	37	14.6	1.17	1.86E-05	3.14	23.1	18.75%	75.81%	389.9	36.1
0.08295	315	1102	37	14.6	1.17	1.86E-05	3.13	23.1	19.69%	80.20%	389.9	36.1
0.08295	315	1102	37	14.6	1.17	1.86E-05	3.13	23.2	18.85%	77.00%	373.0	34.5
0.08295	315	1102	37	14.6	1.17	1.86E-05	3.16	34.5	18.12%	108.8%	434.6	40.2
0.08295	315	1102	37	14.6	1.17	1.86E-05	3.15	34.6	19.66%	119.1%	428.7	39.7
0.08295	315	1102	37	14.6	1.17	1.86E-05	3.15	34.8	19.13%	116.4%	457.6	42.3
0.08295	415	1102	37	14.6	1.17	1.86E-05	1.43	2.9	0.97%	1.08%	237.5	22.0
0.08295	415	1102	37	14.6	1.17	1.86E-05	1.44	5.8	0.48%	1.06%	285.3	26.4
0.08295	415	1102	37	14.6	1.17	1.86E-05	1.43	8.6	0.32%	1.06%	319.1	29.5
0.08295	415	1102	37	14.6	1.17	1.86E-05	1.43	11.6	0.26%	1.16%	351.9	32.6
0.08295	415	1102	37	14.6	1.17	1.86E-05	1.42	34.4	0.11%	1.54%	542.5	50.2
0.08295	415	1102	37	14.6	1.17	1.86E-05	1.44	45.9	0.10%	1.85%	570.3	52.8
0.08295	415	1102	37	14.6	1.16	1.86E-05	1.44	56.7	0.10%	2.22%	593.6	54.9
0.08295	415	1102	37	14.6	1.16	1.86E-05	1.44	68.4	0.10%	2.71%	612.6	56.7
0.08295	415	1102	37	14.6	1.16	1.86E-05	1.40	91.3	0.09%	3.35%	570.8	52.8
0.08295	415	1102	37	14.6	1.17	1.86E-05	1.98	2.9	3.92%	3.10%	202.7	18.8
0.08295	415	1102	37	14.6	1.17	1.86E-05	1.98	2.9	4.13%	3.28%	202.3	18.7
0.08295	415	1102	37	14.6	1.17	1.86E-05	2.00	5.8	1.64%	2.61%	248.5	23.0
0.08295	415	1102	37	14.6	1.17	1.86E-05	2.00	8.6	0.98%	2.33%	288.1	26.6
0.08295	415	1102	37	14.6	1.17	1.86E-05	2.01	11.6	0.69%	2.22%	323.7	29.9
0.08295	415	1102	37	14.6	1.17	1.86E-05	2.01	11.6	0.69%	2.22%	323.7	29.9
0.08295	415	1102	37	14.6	1.17	1.86E-05	1.99	22.9	0.40%	2.53%	418.8	38.7
0.08295	415	1102	37	14.6	1.17	1.86E-05	2.01	34.2	0.32%	3.02%	468.1	43.3
0.08295	415	1102	37	14.6	1.17	1.86E-05	2.01	46.0	0.28%	3.60%	506.5	46.8

A_p [m^2]	s [mm]	ρ_L [kg/m_3]	σ [mN/m]	μ_L [mPa.s]	ρ_v [kg/m^3]	μ_g [Pa.s]	U_s [m/s]	Q_L [m^3/(h.m)]	L'/L	L'/G	Holdup [Pa]	Holdup [mm liq]
0.08295	415	1102	37	14.6	1.16	1.86E-05	1.99	57.3	0.29%	4.56%	530.0	49.0
0.08295	415	1102	37	14.6	1.16	1.86E-05	2.00	57.4	0.30%	4.77%	526.7	48.7
0.08295	415	1102	37	14.6	1.16	1.86E-05	2.02	68.1	0.31%	5.90%	528.4	48.9
0.08295	415	1102	37	14.6	1.16	1.86E-05	2.01	80.1	0.25%	5.52%	474.9	43.9
0.08295	415	1102	37	14.6	1.16	1.86E-05	2.01	91.2	0.15%	3.75%	402.6	37.2
0.08295	415	1102	37	14.6	1.17	1.86E-05	2.57	2.9	10.48%	6.47%	179.4	16.6
0.08295	415	1102	37	14.6	1.17	1.86E-05	2.58	5.8	4.05%	5.04%	222.5	20.6
0.08295	415	1102	37	14.6	1.17	1.86E-05	2.58	8.6	2.26%	4.14%	261.8	24.2
0.08295	415	1102	37	14.6	1.17	1.86E-05	2.59	11.6	1.57%	3.91%	290.1	26.8
0.08295	415	1102	37	14.6	1.17	1.86E-05	2.59	11.6	1.57%	3.91%	290.1	26.8
0.08295	415	1102	37	14.6	1.17	1.86E-05	2.55	23.1	0.97%	4.85%	378.1	35.0
0.08295	415	1102	37	14.6	1.17	1.86E-05	2.58	34.3	0.81%	5.97%	424.9	39.3
0.08295	415	1102	37	14.6	1.17	1.86E-05	2.58	45.9	0.73%	7.15%	455.0	42.1
0.08295	415	1102	37	14.6	1.17	1.86E-05	2.57	57.2	0.65%	8.02%	454.0	42.0
0.08295	415	1102	37	14.6	1.16	1.86E-05	2.59	68.6	0.48%	7.06%	380.6	35.2
0.08295	415	1102	37	14.6	1.16	1.86E-05	2.59	79.9	0.37%	6.33%	351.1	32.5
0.08295	415	1102	37	14.6	1.16	1.86E-05	2.58	91.3	0.28%	5.46%	357.3	33.0
0.08295	415	1102	37	14.6	1.17	1.86E-05	3.12	2.9	39.42%	20.05%	170.2	15.7
0.08295	415	1102	37	14.6	1.17	1.86E-05	3.13	5.8	10.28%	10.60%	204.2	18.9
0.08295	415	1102	37	14.6	1.17	1.86E-05	3.14	8.6	5.45%	8.20%	238.5	22.1
0.08295	415	1102	37	14.6	1.17	1.86E-05	3.15	11.7	3.76%	7.70%	274.6	25.4
0.08295	415	1102	37	14.6	1.17	1.86E-05	3.15	11.7	3.76%	7.70%	274.6	25.4
0.08295	415	1102	37	14.6	1.17	1.86E-05	3.12	23.1	2.73%	11.13%	355.3	32.9
0.08295	415	1102	37	14.6	1.17	1.86E-05	3.15	34.0	2.49%	14.78%	396.1	36.6
0.08295	415	1102	37	14.6	1.17	1.86E-05	3.15	34.2	2.55%	15.26%	384.0	35.5
0.08295	415	1102	37	14.6	1.17	1.86E-05	3.15	45.7	1.55%	12.47%	380.3	35.2

A_p [m^2]	s [mm]	ρ_L [kg/m_3]	σ [mN/m]	μ_L [mPa.s]	ρ_v [kg/m^3]	μ_g [Pa.s]	U_s [m/s]	Q_L [m^3/(h.m)]	L'/L	L'/G	Holdup [Pa]	Holdup [mm liq]
0.08295	415	1102	37	14.6	1.17	1.86E-05	3.16	57.4	1.05%	10.53%	340.1	31.5
0.08295	415	1102	37	14.6	1.17	1.86E-05	3.14	68.8	0.89%	10.84%	351.4	32.5
0.08295	415	1102	37	14.6	1.16	1.86E-05	3.16	80.0	0.89%	12.44%	379.2	35.1
0.08295	415	1102	37	14.6	1.17	1.86E-05	3.15	91.0	0.98%	15.63%	419.8	38.8
0.08295	515	1102	37	14.6	1.18	1.86E-05	2.00	2.9	3.44%	2.69%	196.5	18.2
0.08295	515	1102	37	14.6	1.18	1.86E-05	2.00	6.0	1.29%	2.10%	240.7	22.3
0.08295	515	1102	37	14.6	1.18	1.86E-05	2.00	8.6	0.83%	1.95%	287.4	26.6
0.08295	515	1102	37	14.6	1.18	1.86E-05	2.00	11.5	0.57%	1.80%	322.2	29.8
0.08295	515	1102	37	14.6	1.17	1.86E-05	2.02	11.6	0.57%	1.79%	319.6	29.6
0.08295	515	1102	37	14.6	1.17	1.86E-05	2.02	11.6	0.57%	1.79%	319.6	29.6
0.08295	515	1102	37	14.6	1.17	1.86E-05	2.02	22.9	0.30%	1.87%	405.5	37.5
0.08295	515	1102	37	14.6	1.17	1.86E-05	2.01	34.2	0.20%	1.88%	467.4	43.2
0.08295	515	1102	37	14.6	1.17	1.86E-05	2.00	34.2	0.19%	1.81%	472.9	43.7
0.08295	515	1102	37	14.6	1.17	1.86E-05	2.01	45.5	0.14%	1.80%	509.6	47.1
0.08295	515	1102	37	14.6	1.17	1.86E-05	2.02	45.9	0.16%	2.03%	510.4	47.2
0.08295	515	1102	37	14.6	1.17	1.86E-05	2.02	57.2	0.13%	2.01%	544.7	50.4
0.08295	515	1102	37	14.6	1.17	1.86E-05	2.02	57.2	0.14%	2.22%	541.2	50.1
0.08295	515	1102	37	14.6	1.17	1.86E-05	2.03	68.3	0.15%	2.86%	563.3	52.1
0.08295	515	1102	37	14.6	1.17	1.86E-05	2.01	68.7	0.15%	2.82%	570.2	52.7
0.08295	515	1102	37	14.6	1.17	1.86E-05	2.01	91.7	0.13%	3.15%	535.0	49.5
0.08295	515	1102	37	14.6	1.17	1.86E-05	2.01	92.0	0.13%	3.16%	514.6	47.6
0.08295	515	1102	37	14.6	1.17	1.86E-05	2.02	92.8	0.13%	3.21%	507.8	47.0
0.08295	515	1102	37	14.6	1.18	1.86E-05	2.55	2.9	8.02%	4.99%	182.7	16.9
0.08295	515	1102	37	14.6	1.18	1.86E-05	2.57	2.9	8.63%	5.28%	177.9	16.5
0.08295	515	1102	37	14.6	1.18	1.86E-05	2.58	5.9	3.14%	3.93%	227.1	21.0
0.08295	515	1102	37	14.6	1.18	1.86E-05	2.58	8.6	1.73%	3.16%	258.8	23.9

A_p [m^2]	s [mm]	ρ_L [kg/m_3]	σ [mN/m]	μ_L [mPa.s]	ρ_v [kg/m^3]	μ_g [Pa.s]	U_s [m/s]	Q_L [m^3/(h.m)]	L'/L	L'/G	Holdup [Pa]	Holdup [mm liq]
0.08295	515	1102	37	14.6	1.18	1.86E-05	2.58	11.5	1.17%	2.87%	282.5	26.1
0.08295	515	1102	37	14.6	1.18	1.86E-05	2.58	11.5	1.17%	2.87%	282.5	26.1
0.08295	515	1102	37	14.6	1.18	1.86E-05	2.56	22.8	0.62%	3.05%	371.9	34.4
0.08295	515	1102	37	14.6	1.18	1.86E-05	2.56	34.5	0.42%	3.11%	425.7	39.4
0.08295	515	1102	37	14.6	1.17	1.86E-05	2.61	45.8	0.38%	3.62%	458.9	42.5
0.08295	515	1102	37	14.6	1.17	1.86E-05	2.60	46.2	0.37%	3.63%	459.8	42.5
0.08295	515	1102	37	14.6	1.18	1.86E-05	2.59	57.1	0.32%	3.87%	467.9	43.3
0.08295	515	1102	37	14.6	1.17	1.86E-05	2.58	57.7	0.34%	4.14%	467.9	43.3
0.08295	515	1102	37	14.6	1.17	1.86E-05	2.59	68.8	0.39%	5.72%	461.9	42.7
0.08295	515	1102	37	14.6	1.17	1.86E-05	2.58	68.8	0.37%	5.37%	472.4	43.7
0.08295	515	1102	37	14.6	1.18	1.86E-05	2.60	91.4	0.21%	4.02%	403.8	37.4
0.08295	515	1102	37	14.6	1.17	1.86E-05	2.59	91.7	0.18%	3.55%	381.1	35.3
0.08295	515	1102	37	14.6	1.18	1.86E-05	3.12	2.9	27.72%	13.90%	160.1	14.8
0.08295	515	1102	37	14.6	1.18	1.86E-05	3.13	2.9	26.91%	13.50%	154.7	14.3
0.08295	515	1102	37	14.6	1.18	1.86E-05	3.13	2.9	27.61%	14.04%	160.1	14.8
0.08295	515	1102	37	14.6	1.18	1.86E-05	3.11	5.8	7.39%	7.63%	209.2	19.3
0.08295	515	1102	37	14.6	1.18	1.86E-05	3.12	5.9	7.14%	7.45%	203.6	18.8
0.08295	515	1102	37	14.6	1.18	1.86E-05	3.11	8.5	3.84%	5.74%	236.2	21.8
0.08295	515	1102	37	14.6	1.18	1.86E-05	3.14	11.5	2.56%	5.14%	258.9	23.9
0.08295	515	1102	37	14.6	1.18	1.86E-05	3.14	11.5	2.56%	5.14%	258.9	23.9
0.08295	515	1102	37	14.6	1.18	1.86E-05	3.13	22.7	1.36%	5.40%	353.2	32.7
0.08295	515	1102	37	14.6	1.18	1.86E-05	3.13	34.4	0.94%	5.64%	375.6	34.7
0.08295	515	1102	37	14.6	1.18	1.86E-05	3.15	45.4	0.83%	6.57%	356.6	33.0
0.08295	515	1102	37	14.6	1.18	1.86E-05	3.16	46.0	0.86%	6.87%	359.9	33.3
0.08295	515	1102	37	14.6	1.18	1.86E-05	3.15	57.4	0.58%	5.82%	331.0	30.6
0.08295	515	1102	37	14.6	1.18	1.86E-05	3.16	57.7	0.58%	5.81%	326.3	30.2
0.08295	515	1102	37	14.6	1.17	1.86E-05	3.16	68.0	0.49%	5.75%	346.0	32.0

A_p [m^2]	s [mm]	ρ_L [kg/m$_3$]	σ [mN/m]	μ_L [mPa.s]	ρ_v [kg/m^3]	μ_g [Pa.s]	U_s [m/s]	Q_L [m^3/(h.m)]	L'/L	L'/G	Holdup [Pa]	Holdup [mm liq]
0.08295	515	1102	37	14.6	1.18	1.86E-05	3.16	68.5	0.48%	5.74%	342.2	31.7
0.08295	515	1102	37	14.6	1.18	1.86E-05	3.13	79.9	0.40%	5.55%	382.0	35.3
0.08295	515	1102	37	14.6	1.18	1.86E-05	3.15	91.4	0.34%	5.43%	402.8	37.3
0.08295	515	1102	37	14.6	1.18	1.86E-05	3.14	91.8	0.34%	5.53%	417.2	38.6
0.08295	515	1102	37	14.6	1.18	1.86E-05	3.66	11.6	7.49%	12.96%	267.0	24.7
0.08295	515	1102	37	14.6	1.18	1.86E-05	3.69	22.9	6.92%	23.45%	303.2	28.1
0.08295	515	1102	37	14.6	1.18	1.86E-05	3.68	23.0	6.46%	22.05%	322.0	29.8
0.08295	515	1102	37	14.6	1.18	1.86E-05	3.69	34.4	3.82%	19.50%	267.0	24.7
0.08295	515	1102	37	14.6	1.18	1.86E-05	3.69	34.7	3.74%	19.23%	263.7	24.4
0.08295	515	1102	37	14.6	1.18	1.86E-05	3.70	45.7	2.72%	18.41%	329.6	30.5
0.08295	515	1102	37	14.6	1.18	1.86E-05	3.69	45.7	2.74%	18.60%	330.4	30.6
0.08295	515	1102	37	14.6	1.18	1.86E-05	3.72	45.9	2.94%	19.90%	317.0	29.3
0.08295	515	1102	37	14.6	1.18	1.86E-05	3.72	57.1	2.14%	18.02%	374.9	34.7
0.08295	515	1102	37	14.6	1.18	1.86E-05	3.72	57.3	2.08%	17.61%	375.2	34.7
0.08295	515	1102	37	14.6	1.18	1.86E-05	3.71	57.4	2.10%	17.82%	372.0	34.4
0.08295	515	1102	37	14.6	1.19	1.86E-05	3.67	68.6	1.69%	17.17%	411.7	38.1
0.08295	515	1102	37	14.6	1.18	1.86E-05	3.71	68.8	1.81%	18.44%	413.3	38.2
0.08295	515	1102	37	14.6	1.18	1.86E-05	3.70	68.9	1.78%	18.14%	413.2	38.2
0.08295	515	1102	37	14.6	1.19	1.86E-05	3.66	80.0	1.84%	21.91%	459.5	42.5
0.08295	515	1102	37	14.6	1.19	1.86E-05	3.66	80.0	1.68%	19.98%	470.3	43.5
0.08295	515	1102	37	14.6	1.19	1.86E-05	3.68	80.1	1.80%	21.36%	461.7	42.7
0.08295	515	1102	37	14.6	1.19	1.86E-05	3.67	80.1	1.76%	20.90%	465.7	43.1
0.08295	515	1102	37	14.6	1.18	1.86E-05	3.68	91.2	3.40%	45.97%	556.7	51.5
0.08295	515	1102	37	14.6	1.18	1.86E-05	3.68	91.2	3.19%	43.15%	556.1	51.4
0.08295	515	1102	37	14.6	1.18	1.86E-05	3.67	91.3	3.47%	47.13%	563.3	52.1
0.08295	515	1102	37	14.6	1.18	1.86E-05	3.69	91.4	3.95%	53.59%	572.2	52.9
0.08295	515	1102	37	14.6	1.18	1.86E-05	3.71	91.5	4.43%	59.99%	580.2	53.7

A_p [m^2]	s [mm]	ρ_L [kg/m3]	σ [mN/m]	μ_L [mPa.s]	ρ_V [kg/m^3]	μ_g [Pa.s]	U_s [m/s]	Q_L [m^3/(h.m)]	L'/L	L'/G	Holdup [Pa]	Holdup [mm liq]
0.08295	515	1102	37	14.6	1.18	1.86E-05	3.70	91.7	4.81%	65.35%	582.0	53.8
0.08295	515	1102	37	14.6	1.18	1.86E-05	3.70	91.7	4.30%	58.55%	571.6	52.9
0.08295	515	1102	37	14.6	1.18	1.86E-05	3.69	91.8	4.05%	55.13%	590.9	54.7
0.08295	515	1102	37	14.6	1.18	1.86E-05	3.71	91.8	4.48%	60.68%	572.3	52.9
0.08295	515	1102	37	14.6	1.18	1.86E-05	3.69	91.9	4.35%	59.42%	584.9	54.1
0.08295	615	1102	37	14.6	1.18	1.86E-05	2.28	2.9	4.85%	3.32%		
0.08295	615	1102	37	14.6	1.18	1.86E-05	2.28	2.9	5.00%	3.44%		
0.08295	615	1102	37	14.6	1.19	1.86E-05	2.29	5.9	1.89%	2.65%		
0.08295	615	1102	37	14.6	1.19	1.86E-05	2.27	8.6	1.07%	2.21%		
0.08295	615	1102	37	14.6	1.19	1.86E-05	2.28	11.6	0.75%	2.06%		
0.08295	615	1102	37	14.6	1.18	1.86E-05	2.55	2.9	7.34%	4.58%		
0.08295	615	1102	37	14.6	1.19	1.86E-05	2.54	5.9	2.59%	3.30%		
0.08295	615	1102	37	14.6	1.19	1.86E-05	2.55	8.6	1.53%	2.80%		
0.08295	615	1102	37	14.6	1.19	1.86E-05	2.56	11.5	1.05%	2.57%		
0.08295	615	1102	37	14.6	1.18	1.86E-05	2.57	23.2	0.52%	2.57%	369.5	34.2
0.08295	615	1102	37	14.6	1.18	1.86E-05	2.57	34.2	0.35%	2.53%	425.9	39.4
0.08295	615	1102	37	14.6	1.18	1.86E-05	2.56	45.6	0.26%	2.52%	451.9	41.8
0.08295	615	1102	37	14.6	1.18	1.86E-05	2.56	57.1	0.22%	2.68%	428.2	39.6
0.08295	615	1102	37	14.6	1.18	1.86E-05	2.58	69.0	0.19%	2.73%	359.7	33.3
0.08295	615	1102	37	14.6	1.18	1.86E-05	2.59	92.0	0.14%	2.69%	356.7	33.0
0.08295	615	1102	37	14.6	1.18	1.86E-05	3.12	2.9	22.95%	11.53%		
0.08295	615	1102	37	14.6	1.19	1.86E-05	3.12	5.9	6.54%	6.72%		
0.08295	615	1102	37	14.6	1.19	1.86E-05	3.12	6.0	6.28%	6.52%		
0.08295	615	1102	37	14.6	1.19	1.86E-05	3.11	8.6	3.53%	5.29%		
0.08295	615	1102	37	14.6	1.19	1.86E-05	3.10	11.5	2.17%	4.38%		
0.08295	615	1102	37	14.6	1.19	1.86E-05	3.11	23.2	1.08%	4.36%	359.8	33.3

A_p [m^2]	s [mm]	ρ_L [kg/m$_3$]	σ [mN/m]	μ_L [mPa.s]	ρ_v [kg/m^3]	μ_g [Pa.s]	U_s [m/s]	Q_L [m^3/(h.m)]	L'/L	L'/G	Holdup [Pa]	Holdup [mm liq]
0.08295	615	1102	37	14.6	1.18	1.86E-05	3.12	34.3	0.75%	4.47%	366.2	33.9
0.08295	615	1102	37	14.6	1.19	1.86E-05	3.13	45.7	0.58%	4.59%	305.0	28.2
0.08295	615	1102	37	14.6	1.19	1.86E-05	3.13	45.8	0.58%	4.61%	307.2	28.4
0.08295	615	1102	37	14.6	1.19	1.86E-05	3.13	57.4	0.42%	4.16%	344.0	31.8
0.08295	615	1102	37	14.6	1.19	1.86E-05	3.11	68.9	0.33%	3.94%	388.3	35.9
0.08295	615	1102	37	14.6	1.19	1.86E-05	3.12	69.0	0.33%	3.96%	381.1	35.3
0.08295	615	1102	37	14.6	1.18	1.86E-05	3.13	91.2	0.26%	4.13%	429.0	39.7
0.08295	615	1102	37	14.6	1.17	1.86E-05	3.73	2.9	50.58%	21.56%	-	-
0.08295	615	1102	37	14.6	1.19	1.86E-05	3.68	5.9	16.59%	14.60%	-	-
0.08295	615	1102	37	14.6	1.19	1.86E-05	3.68	8.6	8.58%	10.90%	-	-
0.08295	615	1102	37	14.6	1.19	1.86E-05	3.67	11.5	5.35%	9.14%	-	-
0.08295	615	1102	37	14.6	1.19	1.86E-05	3.66	11.6	5.25%	9.03%	-	-
0.08295	615	1102	37	14.6	1.19	1.86E-05	3.68	23.4	3.87%	13.38%	276.7	25.6
0.08295	615	1102	37	14.6	1.19	1.86E-05	3.68	23.4	3.62%	12.54%	278.4	25.7
0.08295	615	1102	37	14.6	1.19	1.86E-05	3.69	34.5	2.46%	12.50%	276.1	25.5
0.08295	615	1102	37	14.6	1.19	1.86E-05	3.67	46.1	1.33%	9.07%	336.3	31.1
0.08295	615	1102	37	14.6	1.18	1.86E-05	3.68	57.3	0.94%	7.98%	396.0	36.6
0.08295	615	1102	37	14.6	1.19	1.86E-05	3.68	69.0	0.97%	9.87%	486.0	45.0
0.08295	615	1102	37	14.6	1.19	1.86E-05	3.68	91.5	1.14%	15.47%	632.3	58.5
0.08295	615	1102	37	14.6	1.19	1.86E-05	3.69	91.8	1.23%	16.65%	627.3	58.0
0.08295	615	1102	37	14.6	1.19	1.86E-05	3.96	23.5	15.05%	48.61%	288.3	26.7
0.08295	615	1102	37	14.6	1.19	1.86E-05	3.97	23.5	13.54%	43.75%	271.8	25.1
0.08295	615	1102	37	14.6	1.19	1.86E-05	3.96	34.4	7.46%	35.20%	300.0	27.7
0.08295	615	1102	37	14.6	1.19	1.86E-05	3.95	34.4	7.40%	35.03%	300.7	27.8
0.08295	615	1102	37	14.6	1.19	1.86E-05	3.96	34.6	7.86%	37.34%	299.6	27.7
0.08295	615	1102	37	14.6	1.19	1.86E-05	3.95	45.9	2.99%	18.95%	362.0	33.5

A_p [m^2]	s [mm]	ρ_L [kg/m_3]	σ [mN/m]	μ_L [mPa.s]	ρ_v [kg/m^3]	μ_g [Pa.s]	U_s [m/s]	Q_L [$m^3/(h.m)$]	L'/L	L'/G	Holdup [Pa]	Holdup [mm liq]
0.08295	615	1102	37	14.6	1.19	1.86E-05	3.95	46.1	2.92%	18.50%	355.7	32.9
0.08295	615	1102	37	14.6	1.19	1.86E-05	3.96	57.3	1.91%	15.10%	438.8	40.6
0.08295	615	1102	37	14.6	1.19	1.86E-05	3.96	57.3	2.05%	16.12%	433.6	40.1
0.08295	615	1102	37	14.6	1.19	1.86E-05	3.96	68.7	2.38%	22.50%	530.4	49.1
0.08295	615	1102	37	14.6	1.19	1.86E-05	3.97	68.8	2.24%	21.11%	522.9	48.4
0.08295	615	1102	37	14.6	1.19	1.86E-05	3.96	91.5	4.92%	61.81%	678.4	62.8
0.08295	615	1102	37	14.6	1.19	1.86E-05	3.95	91.6	5.90%	74.23%	750.5	69.4
0.08295	615	1102	37	14.6	1.19	1.86E-05	3.95	91.7	5.52%	69.56%	733.3	67.8

Table 9. CO_2/water data for 315, 415, 515 and 615mm tray spacings.

A_p [m^2]	s [mm]	ρ_L [kg/m_3]	σ [mN/m]	μ_L [mPa.s]	ρ_v [kg/m^3]	μ_g [Pa.s]	U_s [m/s]	Q_L [$m^3/(h.m)$]	L'/L	L'/G	Holdup [Pa]	Holdup [mm liq]
0.08295	315	1094.8	35.4	15	1.78	1.493E-05	1.22	2.9	0.72%	0.61%	216.7	20.2
0.08295	315	1094.8	35.4	15	1.78	1.493E-05	1.23	5.8	0.35%	0.60%	275.5	25.6
0.08295	315	1094.8	35.4	15	1.78	1.493E-05	1.23	5.9	0.34%	0.59%	274.9	25.6
0.08295	315	1094.8	35.4	15	1.78	1.493E-05	1.21	8.7	0.24%	0.61%	312.0	29.1
0.08295	315	1094.8	35.4	15	1.78	1.493E-05	1.21	8.7	0.24%	0.61%	312.0	29.1
0.08295	315	1094.8	35.4	15	1.78	1.493E-05	1.21	11.5	0.18%	0.62%	345.5	32.2
0.08295	315	1094.8	35.4	15	1.78	1.493E-05	1.20	22.2	0.17%	1.14%	478.9	44.6
0.08295	315	1094.8	35.4	15	1.77	1.493E-05	1.20	34.1	0.15%	1.56%	533.4	49.7
0.08295	315	1094.8	35.4	15	1.78	1.493E-05	1.22	46.2	0.16%	2.18%	568.1	52.9
0.08295	315	1094.8	35.4	15	1.78	1.493E-05	1.20	57.7	0.19%	3.28%	597.2	55.6
0.08295	315	1094.8	35.4	15	1.78	1.493E-05	1.40	2.9	1.35%	1.01%	213.1	19.8
0.08295	315	1094.8	35.4	15	1.78	1.493E-05	1.42	5.8	0.61%	0.89%	266.5	24.8
0.08295	315	1094.8	35.4	15	1.78	1.493E-05	1.41	8.6	0.40%	0.88%	303.8	28.3

A_p [m^2]	s [mm]	ρ_L [kg/m_3]	σ [mN/m]	μ_L [mPa.s]	ρ_v [kg/m^3]	μ_g [Pa.s]	U_s [m/s]	Q_L [m^3/(h.m)]	L'/L	L'/G	Holdup [Pa]	Holdup [mm liq]
0.08295	315	1094.8	35.4	15	1.78	1.493E-05	1.41	8.6	0.40%	0.88%	303.8	28.3
0.08295	315	1094.8	35.4	15	1.78	1.493E-05	1.40	11.6	0.30%	0.89%	335.3	31.2
0.08295	315	1094.8	35.4	15	1.78	1.493E-05	1.41	22.4	0.28%	1.60%	456.1	42.5
0.08295	315	1094.8	35.4	15	1.78	1.493E-05	1.41	34.1	0.28%	2.46%	508.6	47.4
0.08295	315	1094.8	35.4	15	1.77	1.493E-05	1.40	46.4	0.27%	3.25%	539.7	50.3
0.08295	315	1094.8	35.4	15	1.78	1.493E-05	1.40	57.6	0.36%	5.30%	569.2	53.0
0.08295	315	1100	36	15	1.77	1.493E-05	1.71	2.9	4.01%	2.43%	184.2	17.1
0.08295	315	1100	36	15	1.78	1.493E-05	1.70	5.8	1.52%	1.88%	242.3	22.5
0.08295	315	1100	36	15	1.78	1.493E-05	1.71	8.6	0.99%	1.82%	283.2	26.2
0.08295	315	1100	36	15	1.78	1.493E-05	1.71	11.6	0.72%	1.77%	314.8	29.2
0.08295	315	1100	36	15	1.78	1.493E-05	1.71	22.7	0.64%	3.10%	404.9	37.5
0.08295	315	1100	36	15	1.78	1.493E-05	1.71	34.3	0.66%	4.82%	466.2	43.2
0.08295	315	1100	36	15	1.78	1.493E-05	1.72	46.1	0.70%	6.83%	499.6	46.3
0.08295	315	1100	36	15	1.77	1.493E-05	1.72	57.8	0.89%	10.86%	505.4	46.8
0.08295	315	1100	36	15	1.77	1.493E-05	1.72	58.0	0.86%	10.49%	523.5	48.5
0.08295	315	1100	36	15	1.78	1.493E-05	1.69	68.6	0.84%	12.41%	542.6	50.3
0.08295	315	1100	36	15	1.78	1.493E-05	1.70	68.6	0.94%	13.74%	540.6	50.1
0.08295	315	1100	36	15	1.78	1.493E-05	1.71	68.7	0.92%	13.43%	536.4	49.7
0.08295	315	1100	36	15	1.78	1.493E-05	2.02	2.9	7.85%	4.01%	170.7	15.8
0.08295	315	1100	36	15	1.78	1.493E-05	2.04	6.1	2.76%	2.99%	233.8	21.7
0.08295	315	1100	36	15	1.78	1.493E-05	2.03	8.7	1.77%	2.76%	269.3	25.0
0.08295	315	1100	36	15	1.78	1.493E-05	2.03	11.8	1.33%	2.80%	297.5	27.6
0.08295	315	1100	36	15	1.78	1.493E-05	2.05	22.6	1.76%	7.06%	376.0	34.8
0.08295	315	1100	36	15	1.77	1.493E-05	2.04	34.2	1.68%	10.21%	437.2	40.5
0.08295	315	1100	36	15	1.77	1.493E-05	2.04	45.8	1.97%	16.06%	473.4	43.9
0.08295	315	1100	36	15	1.78	1.493E-05	2.04	45.9	1.98%	16.14%	474.0	43.9

Stellenbosch University http://scholar.sun.ac.za

A_p [m^2]	s [mm]	ρ_L [kg/m$_3$]	σ [mN/m]	μ_L [mPa.s]	ρ_v [kg/m^3]	μ_g [Pa.s]	U_s [m/s]	Q_L [m^3/(h.m)]	L'/L	L'/G	Holdup [Pa]	Holdup [mm liq]
0.08295	315	1100	36	15	1.78	1.493E-05	2.05	57.5	2.04%	20.75%	488.0	45.2
0.08295	315	1100	36	15	1.77	1.493E-05	2.05	57.6	2.00%	20.48%	490.7	45.5
0.08295	415	1094.8	35.4	15	1.78	1.493E-05	1.42	2.9	1.07%	0.80%	195.1	18.2
0.08295	415	1100	36	15	1.78	1.493E-05	1.41	6.0	0.51%	0.78%	250.6	23.2
0.08295	415	1100	36	15	1.78	1.493E-05	1.41	11.5	0.23%	0.66%	322.5	29.9
0.08295	415	1100	36	15	1.78	1.493E-05	1.41	22.8	0.12%	0.68%	434.0	40.2
0.08295	415	1100	36	15	1.78	1.493E-05	1.41	34.3	0.09%	0.77%	495.7	45.9
0.08295	415	1100	36	15	1.78	1.493E-05	1.41	46.0	0.07%	0.85%	528.9	49.0
0.08295	415	1094.8	35.4	15	1.78	1.493E-05	1.42	57.6	0.07%	0.99%	552.7	51.5
0.08295	415	1094.8	35.4	15	1.78	1.493E-05	1.41	69.1	0.07%	1.29%	573.0	53.4
0.08295	415	1094.8	35.4	15	1.78	1.493E-05	1.41	80.1	0.08%	1.59%	585.7	54.5
0.08295	415	1094.8	35.4	15	1.78	1.493E-05	1.72	2.9	2.64%	1.59%	167.4	15.6
0.08295	415	1094.8	35.4	15	1.78	1.493E-05	1.71	5.9	0.91%	1.14%	222.2	20.7
0.08295	415	1100	36	15	1.78	1.493E-05	1.71	11.5	0.39%	0.95%	302.3	28.0
0.08295	415	1100	36	15	1.78	1.493E-05	1.72	22.6	0.24%	1.13%	393.0	36.4
0.08295	415	1100	36	15	1.78	1.493E-05	1.72	34.4	0.17%	1.20%	451.1	41.8
0.08295	415	1100	36	15	1.78	1.493E-05	1.72	45.9	0.15%	1.46%	484.1	44.9
0.08295	415	1094.8	35.4	15	1.78	1.493E-05	1.73	57.7	0.14%	1.71%	506.5	47.2
0.08295	415	1094.8	35.4	15	1.78	1.493E-05	1.72	69.1	0.14%	2.04%	518.9	48.3
0.08295	415	1094.8	35.4	15	1.78	1.493E-05	1.73	80.3	0.14%	2.31%	491.7	45.8
0.08295	415	1094.8	35.4	15	1.77	1.493E-05	2.03	2.9	5.21%	2.66%	156.6	14.6
0.08295	415	1094.8	35.4	15	1.78	1.493E-05	2.04	5.9	1.72%	1.80%	209.1	19.5
0.08295	415	1094.8	35.4	15	1.78	1.493E-05	2.04	8.6	0.93%	1.42%	249.1	23.2
0.08295	415	1094.8	35.4	15	1.78	1.493E-05	2.06	11.4	0.66%	1.32%	275.7	25.7
0.08295	415	1094.8	35.4	15	1.78	1.493E-05	2.06	11.4	0.66%	1.32%	275.7	25.7

A_p [m^2]	s [mm]	ρ_L [kg/m$_3$]	σ [mN/m]	μ_L [mPa.s]	ρ_v [kg/m^3]	μ_g [Pa.s]	U_s [m/s]	Q_L [m^3/(h.m)]	L'/L	L'/G	Holdup [Pa]	Holdup [mm liq]
0.08295	415	1094.8	35.4	15	1.78	1.493E-05	2.05	22.6	0.46%	1.83%	363.3	33.8
0.08295	415	1094.8	35.4	15	1.78	1.493E-05	2.06	34.2	0.36%	2.13%	417.2	38.8
0.08295	415	1094.8	35.4	15	1.78	1.493E-05	2.06	45.9	0.31%	2.48%	448.5	41.8
0.08295	415	1094.8	35.4	15	1.78	1.493E-05	2.03	57.3	0.29%	2.91%	463.2	43.1
0.08295	415	1094.8	35.4	15	1.78	1.493E-05	2.03	69.1	0.23%	2.85%	444.2	41.4
0.08295	415	1094.8	35.4	15	1.78	1.493E-05	2.04	80.1	0.17%	2.44%	365.8	34.1
0.08295	415	1094.8	35.4	15	1.77	1.493E-05	2.34	2.9	10.77%	4.76%	144.5	13.5
0.08295	415	1094.8	35.4	15	1.78	1.493E-05	2.32	5.9	3.03%	2.80%	196.5	18.3
0.08295	415	1094.8	35.4	15	1.78	1.493E-05	2.32	8.6	1.57%	2.11%	234.0	21.8
0.08295	415	1094.8	35.4	15	1.78	1.493E-05	2.31	11.4	1.09%	1.94%	261.7	24.4
0.08295	415	1094.8	35.4	15	1.78	1.493E-05	2.31	11.4	1.09%	1.94%	261.7	24.4
0.08295	415	1094.8	35.4	15	1.78	1.493E-05	2.31	22.7	0.90%	3.20%	352.8	32.9
0.08295	415	1094.8	35.4	15	1.78	1.493E-05	2.31	34.2	0.74%	3.98%	401.9	37.4
0.08295	415	1094.8	35.4	15	1.78	1.493E-05	2.31	45.9	0.59%	4.24%	422.5	39.3
0.08295	415	1094.8	35.4	15	1.77	1.493E-05	2.31	57.2	0.47%	4.17%	407.8	38.0
0.08295	415	1094.8	35.4	15	1.78	1.493E-05	2.31	69.2	0.30%	3.28%	355.3	33.1
0.08295	415	1094.8	35.4	15	1.77	1.493E-05	2.32	80.0	0.23%	2.86%	342.8	31.9
0.08295	515	1094.8	35.4	15	1.77	1.493E-05	1.70	2.9	1.84%	1.13%	182.7	17.0
0.08295	515	1094.8	35.4	15	1.78	1.493E-05	1.71	5.8	0.68%	0.83%	232.3	21.6
0.08295	515	1094.8	35.4	15	1.78	1.493E-05	1.71	8.7	0.37%	0.68%	279.1	26.0
0.08295	515	1094.8	35.4	15	1.78	1.493E-05	1.72	11.4	0.26%	0.62%	310.4	28.9
0.08295	515	1094.8	35.4	15	1.78	1.493E-05	1.72	22.6	0.12%	0.57%	404.5	37.7
0.08295	515	1094.8	35.4	15	1.78	1.493E-05	1.72	22.6	0.12%	0.57%	404.5	37.7
0.08295	515	1094.8	35.4	15	1.78	1.493E-05	1.73	34.6	0.08%	0.58%	463.6	43.2
0.08295	515	1094.8	35.4	15	1.78	1.493E-05	1.72	46.6	0.06%	0.60%	503.7	46.9
0.08295	515	1094.8	35.4	15	1.78	1.493E-05	1.71	55.6	0.06%	0.67%	538.6	50.1

A_p [m^2]	s [mm]	ρ_L [kg/m_3]	σ [mN/m]	μ_L [mPa.s]	ρ_v [kg/m^3]	μ_g [Pa.s]	U_s [m/s]	Q_L [m^3/(h.m)]	L'/L	L'/G	Holdup [Pa]	Holdup [mm liq]
0.08295	515	1094.8	35.4	15	1.78	1.493E-05	1.70	69.3	0.05%	0.80%	565.0	52.6
0.08295	515	1094.8	35.4	15	1.77	1.493E-05	1.73	80.3	0.06%	0.94%	559.1	52.1
0.08295	515	1094.8	35.4	15	1.78	1.493E-05	2.04	2.9	4.03%	2.06%	164.8	15.3
0.08295	515	1094.8	35.4	15	1.78	1.493E-05	2.05	5.8	1.35%	1.38%	215.9	20.1
0.08295	515	1094.8	35.4	15	1.78	1.493E-05	2.04	8.7	0.65%	1.01%	260.2	24.2
0.08295	515	1094.8	35.4	15	1.77	1.493E-05	2.04	11.4	0.45%	0.92%	285.2	26.6
0.08295	515	1094.8	35.4	15	1.77	1.493E-05	2.04	11.4	0.45%	0.92%	285.2	26.6
0.08295	515	1094.8	35.4	15	1.78	1.493E-05	2.03	22.5	0.24%	0.94%	372.7	34.7
0.08295	515	1094.8	35.4	15	1.78	1.493E-05	2.04	34.8	0.16%	0.98%	432.3	40.3
0.08295	515	1094.8	35.4	15	1.78	1.493E-05	2.04	46.6	0.12%	0.97%	470.0	43.8
0.08295	515	1094.8	35.4	15	1.78	1.493E-05	2.04	57.3	0.12%	1.22%	500.1	46.6
0.08295	515	1094.8	35.4	15	1.77	1.493E-05	2.04	69.2	0.12%	1.50%	510.4	47.5
0.08295	515	1094.8	35.4	15	1.78	1.493E-05	2.05	80.3	0.11%	1.51%	477.7	44.5
0.08295	515	1094.8	35.4	15	1.78	1.493E-05	2.33	2.9	7.98%	3.57%	154.4	14.4
0.08295	515	1094.8	35.4	15	1.77	1.493E-05	2.34	5.8	2.40%	2.15%	198.9	18.5
0.08295	515	1094.8	35.4	15	1.78	1.493E-05	2.32	8.7	1.13%	1.53%	241.0	22.4
0.08295	515	1094.8	35.4	15	1.78	1.493E-05	2.33	11.4	0.76%	1.35%	260.2	24.2
0.08295	515	1094.8	35.4	15	1.78	1.493E-05	2.33	11.4	0.76%	1.35%	260.2	24.2
0.08295	515	1094.8	35.4	15	1.78	1.493E-05	2.32	23.1	0.42%	1.52%	356.3	33.2
0.08295	515	1094.8	35.4	15	1.77	1.493E-05	2.33	34.8	0.29%	1.56%	412.2	38.4
0.08295	515	1094.8	35.4	15	1.77	1.493E-05	2.31	46.6	0.22%	1.57%	445.1	41.4
0.08295	515	1094.8	35.4	15	1.78	1.493E-05	2.33	57.4	0.23%	2.03%	452.5	42.1
0.08295	515	1094.8	35.4	15	1.77	1.493E-05	2.33	69.3	0.21%	2.31%	438.1	40.8
0.08295	515	1094.8	35.4	15	1.77	1.493E-05	2.34	80.3	0.13%	1.63%	373.0	34.7
0.08295	515	1094.8	35.4	15	1.77	1.493E-05	2.62	2.9	17.99%	7.17%	146.8	13.7

A_p [m^2]	s [mm]	ρ_L [kg/m_3]	σ [mN/m]	μ_L [mPa.s]	ρ_v [kg/m^3]	μ_g [Pa.s]	U_s [m/s]	Q_L [$m^3/(h.m)$]	L'/L	L'/G	Holdup [Pa]	Holdup [mm liq]
0.08295	515	1094.8	35.4	15	1.78	1.493E-05	2.60	5.8	4.46%	3.58%	191.3	17.8
0.08295	515	1094.8	35.4	15	1.77	1.493E-05	2.61	8.7	2.04%	2.47%	230.5	21.5
0.08295	515	1094.8	35.4	15	1.77	1.493E-05	2.61	11.4	1.29%	2.05%	253.5	23.6
0.08295	515	1094.8	35.4	15	1.77	1.493E-05	2.61	11.4	1.29%	2.05%	253.5	23.6
0.08295	515	1094.8	35.4	15	1.78	1.493E-05	2.61	23.1	0.74%	2.37%	356.0	33.1
0.08295	515	1094.8	35.4	15	1.77	1.493E-05	2.61	35.0	0.58%	2.80%	390.4	36.4
0.08295	515	1094.8	35.4	15	1.78	1.493E-05	2.62	46.6	0.44%	2.81%	386.2	36.0
0.08295	515	1094.8	35.4	15	1.77	1.493E-05	2.63	57.4	0.39%	3.12%	378.7	35.3
0.08295	515	1094.8	35.4	15	1.77	1.493E-05	2.63	69.2	0.26%	2.52%	345.1	32.1
0.08295	515	1094.8	35.4	15	1.77	1.493E-05	2.63	80.4	0.22%	2.40%	377.2	35.1
0.08295	615	1094.8	35.4	15	1.78	1.493E-05	2.02	2.9	3.35%	1.71%	164.2	15.3
0.08295	615	1094.8	35.4	15	1.78	1.493E-05	2.03	5.9	1.09%	1.13%	210.3	19.6
0.08295	615	1094.8	35.4	15	1.78	1.493E-05	2.03	8.6	0.56%	0.86%	254.6	23.7
0.08295	615	1094.8	35.4	15	1.78	1.493E-05	2.03	11.9	0.36%	0.76%	289.8	27.0
0.08295	615	1094.8	35.4	15	1.78	1.493E-05	2.02	23.0	0.18%	0.75%	364.9	34.0
0.08295	615	1094.8	35.4	15	1.78	1.493E-05	2.02	23.0	0.18%	0.75%	364.9	34.0
0.08295	615	1094.8	35.4	15	1.77	1.493E-05	2.03	34.5	0.12%	0.75%	424.6	39.5
0.08295	615	1094.8	35.4	15	1.78	1.493E-05	2.02	46.1	0.09%	0.72%	465.9	43.4
0.08295	615	1094.8	35.4	15	1.77	1.493E-05	2.04	56.2	0.09%	0.94%	493.6	46.0
0.08295	615	1094.8	35.4	15	1.78	1.493E-05	2.03	68.9	0.10%	1.21%	513.1	47.8
0.08295	615	1094.8	35.4	15	1.78	1.493E-05	2.03	80.1	0.11%	1.55%	490.0	45.6
0.08295	615	1094.8	35.4	15	1.78	1.493E-05	2.31	2.9	6.37%	2.88%	153.8	14.3
0.08295	615	1094.8	35.4	15	1.78	1.493E-05	2.33	5.9	1.99%	1.81%	205.7	19.2
0.08295	615	1094.8	35.4	15	1.78	1.493E-05	2.32	5.9	1.96%	1.78%	203.3	18.9
0.08295	615	1094.8	35.4	15	1.78	1.493E-05	2.32	8.6	1.00%	1.34%	242.0	22.5
0.08295	615	1094.8	35.4	15	1.78	1.493E-05	2.31	11.9	0.59%	1.10%	264.4	24.6

Stellenbosch University http://scholar.sun.ac.za

A_p [m²]	s [mm]	ρ_L [kg/m³]	σ [mN/m]	μ_L [mPa.s]	ρ_v [kg/m³]	μ_g [Pa.s]	U_s [m/s]	Q_L [m³/(h.m)]	L'/L	L'/G	Holdup [Pa]	Holdup [mm liq]
0.08295	615	1094.8	35.4	15	1.78	1.493E-05	2.32	23.0	0.31%	1.10%	348.7	32.5
0.08295	615	1094.8	35.4	15	1.78	1.493E-05	2.32	34.6	0.20%	1.07%	409.0	38.1
0.08295	615	1094.8	35.4	15	1.78	1.493E-05	2.32	34.6	0.20%	1.07%	409.0	38.1
0.08295	615	1094.8	35.4	15	1.78	1.493E-05	2.33	46.0	0.16%	1.14%	438.0	40.8
0.08295	615	1094.8	35.4	15	1.77	1.493E-05	2.32	46.1	0.16%	1.16%	445.1	41.4
0.08295	615	1094.8	35.4	15	1.78	1.493E-05	2.32	57.4	0.17%	1.47%	450.4	41.9
0.08295	615	1094.8	35.4	15	1.78	1.493E-05	2.32	57.4	0.16%	1.42%	454.9	42.4
0.08295	615	1094.8	35.4	15	1.78	1.493E-05	2.32	68.9	0.17%	1.81%	443.8	41.3
0.08295	615	1094.8	35.4	15	1.78	1.493E-05	2.35	80.2	0.13%	1.62%	359.9	33.5
0.08295	615	1094.8	35.4	15	1.77	1.493E-05	2.65	2.9	14.34%	5.59%	140.8	13.1
0.08295	615	1094.8	35.4	15	1.78	1.493E-05	2.63	5.9	3.80%	3.07%	185.6	17.3
0.08295	615	1094.8	35.4	15	1.78	1.493E-05	2.62	8.6	1.82%	2.16%	229.8	21.4
0.08295	615	1094.8	35.4	15	1.77	1.493E-05	2.61	11.9	1.00%	1.65%	250.7	23.3
0.08295	615	1094.8	35.4	15	1.78	1.493E-05	2.61	23.1	0.49%	1.56%	345.7	32.2
0.08295	615	1094.8	35.4	15	1.78	1.493E-05	2.61	23.1	0.49%	1.56%	345.7	32.2
0.08295	615	1094.8	35.4	15	1.78	1.493E-05	2.63	34.8	0.35%	1.67%	382.1	35.6
0.08295	615	1094.8	35.4	15	1.78	1.493E-05	2.64	46.1	0.30%	1.91%	383.5	35.7
0.08295	615	1094.8	35.4	15	1.78	1.493E-05	2.63	57.3	0.28%	2.19%	371.6	34.6
0.08295	615	1094.8	35.4	15	1.78	1.493E-05	2.64	68.8	0.22%	2.11%	342.7	31.9
0.08295	615	1094.8	35.4	15	1.78	1.493E-05	2.64	80.2	0.19%	2.11%	377.4	35.1
0.08295	615	1094.8	35.4	15	1.77	1.493E-05	2.92	2.9	28.20%	10.09%	157.9	14.7
0.08295	615	1094.8	35.4	15	1.76	1.493E-05	2.92	2.9	28.05%	10.09%	164.9	15.4
0.08295	615	1094.8	35.4	15	1.77	1.493E-05	2.92	2.9	28.46%	10.28%	165.7	15.4
0.08295	615	1094.8	35.4	15	1.78	1.493E-05	2.91	5.9	6.76%	4.95%	205.6	19.1
0.08295	615	1094.8	35.4	15	1.78	1.493E-05	2.92	8.6	3.32%	3.55%	227.9	21.2
0.08295	615	1094.8	35.4	15	1.77	1.493E-05	2.91	11.9	1.68%	2.48%	261.5	24.4

A_p [m^2]	s [mm]	ρ_L [kg/m$_3$]	σ [mN/m]	μ_L [mPa.s]	ρ_v [kg/m^3]	μ_g [Pa.s]	U_s [m/s]	Q_L [m^3/(h.m)]	L'/L	L'/G	Holdup [Pa]	Holdup [mm liq]
0.08295	615	1094.8	35.4	15	1.77	1.493E-05	2.91	11.9	1.68%	2.48%	261.5	24.4
0.08295	615	1094.8	35.4	15	1.78	1.493E-05	2.92	23.2	0.91%	2.62%	336.9	31.4
0.08295	615	1094.8	35.4	15	1.78	1.493E-05	2.91	34.8	0.74%	3.20%	346.3	32.2
0.08295	615	1094.8	35.4	15	1.77	1.493E-05	2.92	46.0	0.55%	3.13%	284.6	26.5
0.08295	615	1094.8	35.4	15	1.78	1.493E-05	2.91	57.3	0.42%	2.96%	323.3	30.1
0.08295	615	1094.8	35.4	15	1.77	1.493E-05	2.92	68.8	0.37%	3.12%	368.1	34.3
0.08295	615	1094.8	35.4	15	1.78	1.493E-05	2.92	80.2	0.34%	3.36%	421.7	39.3

Table 10. SF_6/ethylene glycol data for 615mm tray spacing.

A_p [m^2]	S [mm]	ρl [kg/m$_3$]	σ [mN/m]	μ_L [mPa.s]	ρ_v [kg/m^3]	μ_g [Pa.s]	U_s [m/s]	Q_L [m^3/(h.m)]	L'/L	L'/G	Holdup [Pa]	Holdup [mm liq]
0.08295	615	1096.5	35	15	5.87	1.51E-05	1.38	2.9	6.61%	1.50%	241.0	22.4
0.08295	615	1096.5	35	15	5.86	1.51E-05	1.37	5.8	2.27%	1.06%	289.2	26.9
0.08295	615	1096.5	35	15	5.84	1.51E-05	1.40	8.8	1.32%	0.91%	321.2	29.9
0.08295	615	1096.5	35	15	5.83	1.51E-05	1.40	11.5	0.87%	0.78%	342.3	31.8
0.08295	615	1096.5	35	15	5.81	1.51E-05	1.38	23.6	0.33%	0.62%	431.6	40.1
0.08295	615	1096.5	35	15	5.81	1.51E-05	1.38	34.6	0.20%	0.56%	496.2	46.1
0.08295	615	1096.5	35	15	5.82	1.51E-05	1.38	45.9	0.15%	0.54%	535.4	49.8
0.08295	615	1096.5	35	15	5.88	1.51E-05	1.70	2.9	22.17%	4.09%	227.7	21.2
0.08295	615	1096.5	35	15	5.85	1.51E-05	1.70	2.9	21.69%	4.02%	227.9	21.2
0.08295	615	1096.5	35	15	5.86	1.51E-05	1.70	6.0	5.79%	2.26%	276.5	25.7
0.08295	615	1096.5	35	15	5.86	1.51E-05	1.70	6.0	5.75%	2.25%	277.7	25.8
0.08295	615	1096.5	35	15	5.85	1.51E-05	1.70	8.6	3.31%	1.83%	301.0	28.0
0.08295	615	1096.5	35	15	5.84	1.51E-05	1.70	8.6	3.29%	1.82%	300.9	28.0
0.08295	615	1096.5	35	15	5.87	1.51E-05	1.69	11.6	1.95%	1.47%	332.6	30.9

Stellenbosch University http://scholar.sun.ac.za

A_p [m^2]	S [mm]	ρl [kg/m_3]	σ [mN/m]	μ_L [mPa.s]	ρ_v [kg/m^3]	μ_g [Pa.s]	U_s [m/s]	Q_L [m^3/(h.m)]	L'/L	L'/G	Holdup [Pa]	Holdup [mm liq]
0.08295	615	1096.5	35	15	5.87	1.51E-05	1.68	23.2	0.62%	0.93%	428.0	39.8
0.08295	615	1096.5	35	15	5.87	1.51E-05	1.68	23.2	0.62%	0.93%	428.0	39.8
0.08295	615	1096.5	35	15	5.86	1.51E-05	1.69	34.8	0.44%	1.00%	471.1	43.8
0.08295	615	1096.5	35	15	5.87	1.51E-05	1.71	46.1	0.40%	1.17%	487.7	45.3
0.08295	615	1096.5	35	15	5.83	1.51E-05	1.72	57.4	0.33%	1.22%	484.8	45.1
0.08295	615	1096.5	35	15	5.84	1.51E-05	1.72	68.1	0.32%	1.39%	548.6	51.0
0.08295	615	1096.5	35	15	5.85	1.51E-05	1.69	80.2	0.32%	1.65%	638.2	59.3
0.08295	615	1096.5	35	15	5.86	1.51E-05	1.99	2.9	63.13%	10.06%	238.1	22.1
0.08295	615	1096.5	35	15	5.85	1.51E-05	1.99	2.9	59.21%	9.49%	246.7	22.9
0.08295	615	1096.5	35	15	5.85	1.51E-05	1.98	2.9	61.85%	9.94%	255.0	23.7
0.08295	615	1096.5	35	15	5.84	1.51E-05	1.99	2.9	60.56%	9.77%	240.1	22.3
0.08295	615	1096.5	35	15	5.85	1.51E-05	1.99	2.9	61.45%	9.90%	238.1	22.1
0.08295	615	1096.5	35	15	5.84	1.51E-05	1.96	6.1	14.38%	4.88%	283.2	26.3
0.08295	615	1096.5	35	15	5.85	1.51E-05	1.97	6.1	14.14%	4.79%	281.6	26.2
0.08295	615	1096.5	35	15	5.86	1.51E-05	1.97	6.1	14.44%	4.88%	293.2	27.3
0.08295	615	1096.5	35	15	5.87	1.51E-05	1.97	6.1	14.59%	4.94%	284.2	26.4
0.08295	615	1096.5	35	15	5.86	1.51E-05	1.97	8.6	6.90%	3.29%	302.7	28.1
0.08295	615	1096.5	35	15	5.85	1.51E-05	1.98	8.6	6.99%	3.33%	287.1	26.7
0.08295	615	1096.5	35	15	5.85	1.51E-05	1.97	8.6	6.86%	3.27%	306.6	28.5
0.08295	615	1096.5	35	15	5.86	1.51E-05	1.97	11.5	3.84%	2.47%	346.6	32.2
0.08295	615	1096.5	35	15	5.86	1.51E-05	1.97	11.5	3.80%	2.45%	333.5	31.0
0.08295	615	1096.5	35	15	5.85	1.51E-05	1.97	11.6	3.71%	2.40%	329.5	30.6
0.08295	615	1096.5	35	15	5.86	1.51E-05	1.97	11.5	3.84%	2.47%	346.6	32.2
0.08295	615	1096.5	35	15	5.86	1.51E-05	1.97	11.5	3.80%	2.45%	333.5	31.0
0.08295	615	1096.5	35	15	5.85	1.51E-05	1.97	11.6	3.71%	2.40%	329.5	30.6
0.08295	615	1096.5	35	15	5.85	1.51E-05	1.97	23.5	2.31%	3.02%	415.6	38.6
0.08295	615	1096.5	35	15	5.86	1.51E-05	1.97	23.5	2.37%	3.10%	403.4	37.5

Stellenbosch University http://scholar.sun.ac.za

A_p [m^2]	S [mm]	ρl [kg/m_3]	σ [mN/m]	μ_L [mPa.s]	ρ_v [kg/m^3]	μ_g [Pa.s]	U_s [m/s]	Q_L [m^3/(h.m)]	L'/L	L'/G	Holdup [Pa]	Holdup [mm liq]
0.08295	615	1096.5	35	15	5.87	1.51E-05	1.97	23.5	2.42%	3.16%	407.8	37.9
0.08295	615	1096.5	35	15	5.88	1.51E-05	1.97	34.9	2.49%	4.82%	439.6	40.9
0.08295	615	1096.5	35	15	5.86	1.51E-05	1.97	34.9	2.55%	4.96%	438.2	40.7
0.08295	615	1096.5	35	15	5.87	1.51E-05	1.97	34.9	2.46%	4.77%	443.7	41.3
0.08295	615	1096.5	35	15	5.85	1.51E-05	1.97	34.9	2.40%	4.67%	431.9	40.1
0.08295	615	1096.5	35	15	5.85	1.51E-05	1.99	46.2	1.98%	5.07%	441.7	41.1
0.08295	615	1096.5	35	15	5.87	1.51E-05	1.99	46.2	2.22%	5.67%	445.5	41.4
0.08295	615	1096.5	35	15	5.86	1.51E-05	1.99	46.2	2.07%	5.28%	440.2	40.9
0.08295	615	1096.5	35	15	5.84	1.51E-05	1.98	46.3	2.02%	5.17%	441.9	41.1
0.08295	615	1096.5	35	15	5.85	1.51E-05	1.99	57.3	2.51%	7.92%	512.6	47.7
0.08295	615	1096.5	35	15	5.84	1.51E-05	1.99	57.3	2.37%	7.51%	511.0	47.5
0.08295	615	1096.5	35	15	5.86	1.51E-05	1.99	57.3	2.53%	7.99%	520.2	48.4
0.08295	615	1096.5	35	15	5.87	1.51E-05	1.99	57.3	2.50%	7.89%	519.6	48.3
0.08295	615	1096.5	35	15	5.85	1.51E-05	1.99	57.4	2.41%	7.61%	510.8	47.5
0.08295	615	1096.5	35	15	5.82	1.51E-05	1.99	68.8	3.50%	13.34%	583.1	54.2
0.08295	615	1096.5	35	15	5.82	1.51E-05	1.99	68.9	3.67%	14.03%	587.0	54.6
0.08295	615	1096.5	35	15	5.81	1.51E-05	1.99	68.9	3.29%	12.61%	593.5	55.2
0.08295	615	1096.5	35	15	5.82	1.51E-05	1.98	68.9	3.43%	13.17%	594.1	55.2
0.08295	615	1096.5	35	15	5.83	1.51E-05	1.99	69.0	3.55%	13.54%	586.9	54.6
0.08295	615	1096.5	35	15	5.83	1.51E-05	1.99	80.5	5.96%	26.59%	673.6	62.6
0.08295	615	1096.5	35	15	5.85	1.51E-05	1.99	80.5	6.32%	28.12%	672.4	62.5
0.08295	615	1096.5	35	15	5.84	1.51E-05	1.99	80.6	6.39%	28.54%	690.8	64.2
0.08295	615	1096.5	35	15	5.84	1.51E-05	1.98	80.6	5.63%	25.13%	676.3	62.9
0.08295	615	1096.5	35	15	5.84	1.51E-05	1.99	80.7	5.80%	25.93%	667.9	62.1

Stellenbosch University http://scholar.sun.ac.za

2. Weeping data

Table 11. Air/water weeping data

A_p [m^2]	ρ_L [kg/m_3]	σ [mN/m]	μ_L [mPa.s]	ρ_V [kg/m^3]	μ_g [Pa.s]	U_s [m/s]	Q_L [m^3/(h.m)]	W'/L	W'/G	Holdup [Pa]	Holdup [mm liq]
0.08295	998.5	54	0.9	1.17	1.86E-05	2.59	2.8	26.3%	14.4%	179.5	18.3
0.08295	998.5	54	0.9	1.17	1.86E-05	2.60	5.8	25.5%	28.2%	224.9	23.0
0.08295	998.5	54	0.9	1.17	1.86E-05	2.61	9.0	21.7%	37.4%	265.4	27.1
0.08295	998.5	54	0.9	1.17	1.86E-05	2.58	11.5	18.0%	40.0%	290.8	29.7
0.08295	998.5	54	0.9	1.17	1.86E-05	2.57	22.6	10.2%	45.0%	374.7	38.2
0.08295	998.5	54	0.9	1.17	1.86E-05	2.58	34.8	7.5%	50.3%	422.4	43.1
0.08295	998.5	54	0.9	1.17	1.86E-05	2.58	45.5	6.4%	56.7%	456.4	46.6
0.08295	998.5	54	0.9	1.17	1.86E-05	2.58	58.6	4.9%	56.0%	487.2	49.7
0.08295	998.5	54	0.9	1.17	1.86E-05	2.57	69.6	3.9%	52.4%	503.6	51.4
0.08295	998.5	54	0.9	1.17	1.86E-05	2.60	80.6	2.5%	38.6%	464.2	47.4
0.08295	998.5	54	0.9	1.17	1.86E-05	3.17	2.9	14.0%	6.3%	127.2	13.0
0.08295	998.5	54	0.9	1.17	1.86E-05	3.12	5.8	19.6%	18.2%	188.2	19.2
0.08295	998.5	54	0.9	1.17	1.86E-05	3.14	9.0	16.6%	23.8%	219.2	22.4
0.08295	998.5	54	0.9	1.18	1.86E-05	3.13	11.5	13.6%	24.9%	249.2	25.4
0.08295	998.5	54	0.9	1.17	1.86E-05	3.15	23.3	6.7%	24.6%	331.2	33.8
0.08295	998.5	54	0.9	1.17	1.86E-05	3.16	34.8	4.6%	25.1%	369.6	37.7
0.08295	998.5	54	0.9	1.17	1.86E-05	3.14	45.0	3.8%	26.9%	389.7	39.8
0.08295	998.5	54	0.9	1.17	1.86E-05	3.16	58.2	2.0%	18.0%	380.8	38.9
0.08295	998.5	54	0.9	1.17	1.86E-05	3.13	70.0	1.0%	10.9%	383.7	39.2
0.08295	998.5	54	0.9	1.17	1.86E-05	3.18	80.5	0.6%	7.6%	356.0	36.3

Table 12. Air/ethylene glycol weeping data.

A_p [m^2]	ρ_L [kg/m^3]	σ [mN/m]	μ_L [mPa.s]	ρ_V [kg/m^3]	μ_g [Pa.s]	U_s [m/s]	Q_L [$m^3/(h.m)$]	W'/L	W'/G	Holdup [Pa]	Holdup [mm liq]
0.08295	1146	37	14.5	1.17	1.86E-05	2.03	5.7	50.0%	81.2%	236.4	21.0
0.08295	1146	37	14.5	1.17	1.86E-05	2.04	8.6	41.6%	101.2%	286.3	25.5
0.08295	1146	37	14.5	1.17	1.86E-05	2.04	8.6	42.7%	103.8%	283.8	25.2
0.08295	1146	37	14.5	1.17	1.86E-05	2.04	11.6	36.5%	119.3%	314.9	28.0
0.08295	1146	37	14.5	1.17	1.86E-05	2.06	22.8	23.3%	148.3%	399.4	35.5
0.08295	1146	37	14.5	1.17	1.86E-05	2.03	34.4	17.7%	172.1%	468.5	41.7
0.08295	1146	37	14.5	1.17	1.86E-05	2.02	34.4	16.3%	158.9%	457.1	40.7
0.08295	1146	37	14.5	1.18	1.86E-05	2.01	45.6	12.3%	158.6%	504.4	44.9
0.08295	1146	37	14.5	1.18	1.86E-05	2.01	57.1	9.1%	147.7%	539.2	48.0
0.08295	1146	37	14.5	1.18	1.86E-05	2.01	68.9	7.4%	144.9%	563.6	50.1
0.08295	1146	37	14.5	1.18	1.86E-05	1.98	91.9	4.6%	120.0%	522.1	46.4
0.08295	1146	37	14.5	1.18	1.86E-05	1.99	92.1	4.7%	123.1%	516.9	46.0
0.08295	1146	37	14.5	1.17	1.86E-05	2.60	5.7	34.8%	43.7%	217.8	19.4
0.08295	1146	37	14.5	1.17	1.86E-05	2.60	5.7	34.6%	43.8%	215.9	19.2
0.08295	1146	37	14.5	1.17	1.86E-05	2.59	8.6	31.1%	59.1%	254.2	22.6
0.08295	1146	37	14.5	1.17	1.86E-05	2.59	11.6	23.8%	61.0%	282.7	25.1
0.08295	1146	37	14.5	1.17	1.86E-05	2.59	22.7	13.4%	67.4%	364.7	32.4
0.08295	1146	37	14.5	1.17	1.86E-05	2.60	34.5	8.9%	68.0%	414.9	36.9
0.08295	1146	37	14.5	1.18	1.86E-05	2.56	45.9	6.6%	67.5%	467.7	41.6
0.08295	1146	37	14.5	1.18	1.86E-05	2.58	57.2	4.9%	62.0%	464.6	41.3
0.08295	1146	37	14.5	1.18	1.86E-05	2.55	68.4	4.1%	62.5%	471.5	41.9
0.08295	1146	37	14.5	1.18	1.86E-05	2.57	91.6	0.8%	15.4%	378.7	33.7
0.08295	1146	37	14.5	1.17	1.86E-05	3.15	5.7	25.5%	26.6%	196.3	17.5
0.08295	1146	37	14.5	1.17	1.86E-05	3.16	5.7	25.8%	26.9%	193.0	17.2

Stellenbosch University http://scholar.sun.ac.za

A_p [m^2]	ρ_L [kg/m$_3$]	σ [mN/m]	μ_L [mPa.s]	ρ_V [kg/m^3]	μ_g [Pa.s]	U_s [m/s]	Q_L [m^3/(h.m)]	W'/L	W'/G	Holdup [Pa]	Holdup [mm liq]
0.08295	1146	37	14.5	1.17	1.86E-05	3.17	8.6	20.3%	31.8%	221.2	19.7
0.08295	1146	37	14.5	1.17	1.86E-05	3.15	11.5	16.4%	34.4%	261.8	23.3
0.08295	1146	37	14.5	1.17	1.86E-05	3.13	22.7	9.9%	41.0%	351.9	31.3
0.08295	1146	37	14.5	1.17	1.86E-05	3.18	34.1	6.5%	39.9%	362.3	32.2
0.08295	1146	37	14.5	1.18	1.86E-05	3.12	45.7	3.8%	31.5%	380.6	33.9
0.08295	1146	37	14.5	1.18	1.86E-05	3.11	56.8	2.8%	29.0%	360.8	32.1
0.08295	1146	37	14.5	1.19	1.86E-05	3.11	68.8	0.5%	6.4%	346.4	30.8
0.08295	1146	37	14.5	1.18	1.86E-05	3.12	91.4	0.6%	9.4%	416.9	37.1
0.08295	1146	37	14.5	1.17	1.86E-05	3.75	5.8	20.0%	17.8%	214.3	19.1
0.08295	1146	37	14.5	1.18	1.86E-05	3.70	8.6	16.6%	22.1%	240.2	21.4
0.08295	1146	37	14.5	1.18	1.86E-05	3.71	11.6	15.0%	26.7%	234.7	20.9
0.08295	1146	37	14.5	1.18	1.86E-05	3.72	22.8	7.8%	27.3%	284.0	25.3
0.08295	1146	37	14.5	1.18	1.86E-05	3.70	34.5	3.3%	17.5%	265.6	23.6
0.08295	1146	37	14.5	1.18	1.86E-05	3.72	34.6	3.2%	17.0%	270.4	24.0
0.08295	1146	37	14.5	1.19	1.86E-05	3.66	45.7	1.4%	9.6%	329.1	29.3
0.08295	1146	37	14.5	1.18	1.86E-05	3.66	56.5	0.1%	1.1%	364.6	32.4

Table 13. Air/silicone oil weeping data.

A_p [m^2]	ρ_L [kg/m$_3$]	σ [mN/m]	μ_L [mPa.s]	ρ_V [kg/m^3]	μ_g [Pa.s]	U_s [m/s]	Q_L [m^3/(h.m)]	W'/L	W'/G	Holdup [Pa]	Holdup [mm liq]
0.08295	984.5	19.9	48.8	1.17	1.86E-05	2.00	5.8	39.28%	56.13%	212.0	22.0
0.08295	984.5	19.9	48.8	1.17	1.86E-05	2.01	8.7	29.33%	62.68%	250.9	26.0
0.08295	984.5	19.9	48.8	1.17	1.86E-05	2.00	11.6	20.98%	60.13%	278.7	28.9
0.08295	984.5	19.9	48.8	1.17	1.86E-05	2.01	22.9	12.64%	71.29%	364.5	37.7
0.08295	984.5	19.9	48.8	1.17	1.86E-05	2.01	33.9	9.11%	76.20%	413.3	42.8

A_p [m^2]	ρ_L [kg/m$_3$]	σ [mN/m]	μ_L [mPa.s]	ρ_V [kg/m^3]	μ_g [Pa.s]	U_s [m/s]	Q_L [m^3/(h.m)]	W'/L	W'/G	Holdup [Pa]	Holdup [mm liq]
0.08295	984.5	19.9	48.8	1.16	1.86E-05	2.01	45.5	6.87%	77.25%	458.9	47.5
0.08295	984.5	19.9	48.8	1.16	1.86E-05	2.01	56.9	5.75%	81.04%	489.4	50.7
0.08295	984.5	19.9	48.8	1.16	1.86E-05	2.02	67.6	4.20%	70.17%	508.2	52.6
0.08295	984.5	19.9	48.8	1.16	1.86E-05	2.02	78.7	3.34%	64.64%	520.0	53.8
0.08295	984.5	19.9	48.8	1.16	1.86E-05	2.58	2.9	28.34%	15.83%	138.7	14.4
0.08295	984.5	19.9	48.8	1.17	1.86E-05	2.57	5.8	22.69%	25.41%	197.2	20.4
0.08295	984.5	19.9	48.8	1.17	1.86E-05	2.58	8.7	18.25%	30.32%	224.1	23.2
0.08295	984.5	19.9	48.8	1.17	1.86E-05	2.59	11.5	13.62%	29.95%	244.1	25.3
0.08295	984.5	19.9	48.8	1.17	1.86E-05	2.56	22.9	6.99%	30.90%	324.1	33.6
0.08295	984.5	19.9	48.8	1.17	1.86E-05	2.57	34.0	5.04%	32.98%	373.0	38.6
0.08295	984.5	19.9	48.8	1.16	1.86E-05	2.57	45.7	3.42%	30.12%	411.1	42.6
0.08295	984.5	19.9	48.8	1.16	1.86E-05	2.58	57.6	2.33%	25.89%	416.8	43.2
0.08295	984.5	19.9	48.8	1.16	1.86E-05	2.60	68.1	1.39%	18.18%	420.9	43.6
0.08295	984.5	19.9	48.8	1.16	1.86E-05	2.60	79.0	1.22%	18.48%	436.5	45.2
0.08295	984.5	19.9	48.8	1.16	1.86E-05	2.59	57.2	2.30%	25.25%	414.4	42.9
0.08295	984.5	19.9	48.8	1.16	1.86E-05	2.58	45.7	3.32%	29.32%	403.2	41.7
0.08295	984.5	19.9	48.8	1.16	1.86E-05	3.17	2.9	12.36%	5.70%	102.3	10.6
0.08295	984.5	19.9	48.8	1.16	1.86E-05	3.15	5.8	16.23%	14.92%	171.2	17.7
0.08295	984.5	19.9	48.8	1.17	1.86E-05	3.14	8.7	14.00%	19.14%	201.1	20.8
0.08295	984.5	19.9	48.8	1.17	1.86E-05	3.14	11.6	10.51%	19.12%	223.4	23.1
0.08295	984.5	19.9	48.8	1.17	1.86E-05	3.13	23.0	6.30%	22.87%	313.8	32.5
0.08295	984.5	19.9	48.8	1.17	1.86E-05	3.15	34.1	3.33%	17.75%	332.0	34.4
0.08295	984.5	19.9	48.8	1.17	1.86E-05	3.15	57.3	0.71%	6.37%	348.1	36.0
0.08295	984.5	19.9	48.8	1.16	1.86E-05	3.16	68.6	0.51%	5.47%	378.9	39.2
0.08295	984.5	19.9	48.8	1.16	1.86E-05	3.16	79.3	0.64%	8.01%	409.4	42.4

Stellenbosch University http://scholar.sun.ac.za

3. Dry tray pressure drop

The dry tray pressure drop was measured with the downcomer apron closed for a range of gas velocities. To determine the liquid hold-up, dry tray pressure drop is subtracted from the total pressure drop across the tray during experiments.

Table 14. Dry tray pressure drop for air.

A_p [m2]	dP [Pa]	P_{abs} [kPa]	T [°C]	R [kJ/(kg.K)]	Gas Flow [kg/h]	ρ_v [kg/m3]	U_s [m/s]	dP est [Pa]
0.08295	39.88	100.45	21.8	287	380.9	1.19	1.07	37.80
0.08295	50.17	100.49	24.4	287	428.0	1.18	1.22	49.49
0.08295	72.60	100.53	24.0	287	518.9	1.18	1.47	74.19
0.08295	95.36	100.57	24.0	287	589.9	1.18	1.67	96.79
0.08295	141.75	100.64	24.2	287	707.7	1.18	2.01	140.86
0.08295	138.13	100.65	26.2	287	703.4	1.17	2.01	141.06
0.08295	181.00	100.71	24.8	287	798.3	1.18	2.27	180.82
0.08295	182.78	100.71	25.9	287	802.8	1.17	2.29	184.29
0.08295	224.50	100.79	25.6	287	881.0	1.18	2.51	221.98
0.08295	235.44	100.81	25.8	287	908.8	1.17	2.59	236.69
0.08295	291.83	100.87	25.9	287	1005.4	1.18	2.86	290.24
0.08295	354.44	100.97	26.0	287	1107.5	1.18	3.15	352.58
0.08295	419.43	101.07	26.1	287	1205.7	1.18	3.43	418.31
0.08295	491.33	101.20	27.1	287	1304.7	1.17	3.72	492.46
0.08295	569.88	101.30	27.6	287	1403.0	1.17	4.00	570.96

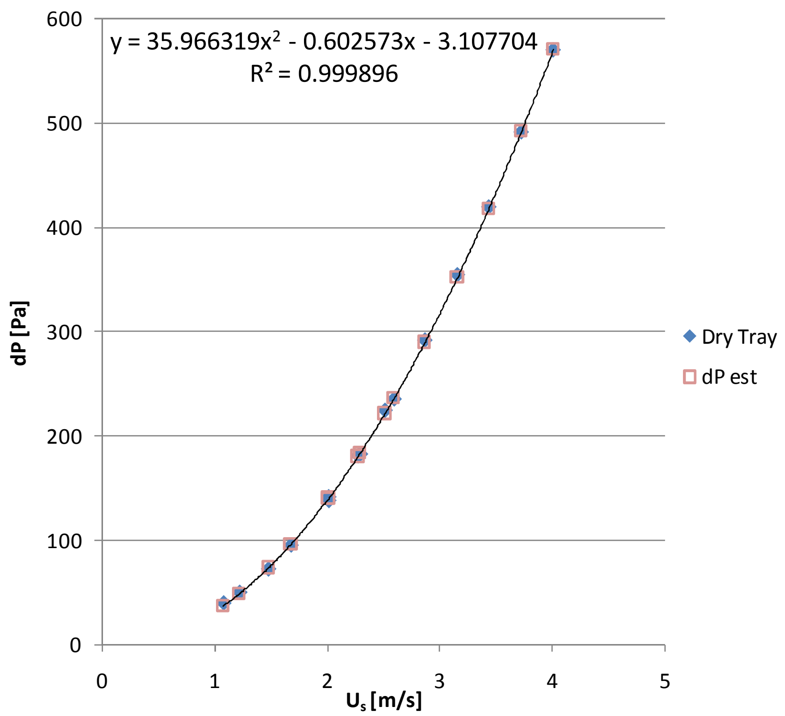

Figure 2. Estimating the dry tray pressure drop for air, using gas superficial velocity.

Table 15. Dry tray pressure drop for CO_2.

A_p [m2]	dP [Pa]	P_{abs} [kPa]	T [°C]	R [kJ/(kg.K)]	Gas Flow [kg/h]	ρ_v [kg/m3]	U_s [m/s]	dP est [Pa]
0.08295	92.82	101.69	23.8	192	620.3	1.78	1.16	92.67
0.08295	164.48	101.68	24.0	192	859.1	1.78	1.61	164.43
0.08295	163.24	101.64	24.0	192	857.0	1.78	1.61	163.89
0.08295	241.38	101.63	24.3	192	1067.2	1.78	2.01	241.04
0.08295	314.75	101.67	24.6	192	1238.4	1.78	2.33	313.46
0.08295	380.09	101.76	25.3	192	1382.2	1.78	2.61	381.72
0.08295	487.70	101.95	26.2	192	1583.2	1.77	2.99	487.25

Stellenbosch University http://scholar.sun.ac.za

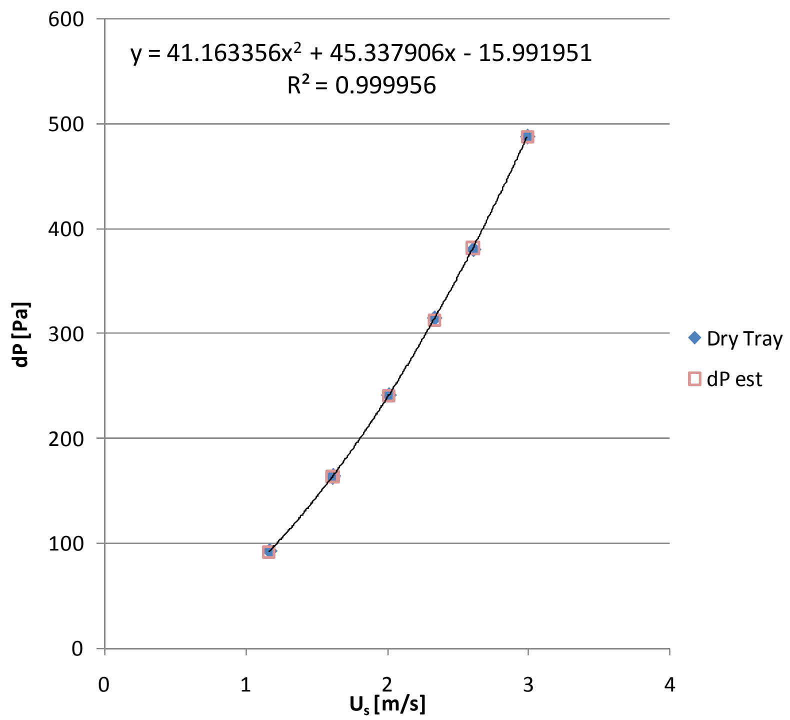

Figure 3. CO_2 dry tray pressure drop estimation as a function of gas velocity.

Table 16. Dry tray pressure drop for SF_6.

A_p [m2]	dP [Pa]	P_{abs} [kPa]	T [°C]	R [kJ/(kg.K)]	Gas Flow [kg/h]	ρ_v [kg/m3]	U_s [m/s]	dP est [Pa]
0.08295	191.96	101.48	24.9	58.6	1657.7	5.81	0.96	191.79
0.08295	392.97	101.03	26.0	58.6	2548.2	5.76	1.48	393.43
0.08295	502.13	101.26	26.3	58.6	2917.9	5.77	1.69	501.87
0.08295	622.44	101.56	26.3	58.6	3288.3	5.79	1.90	623.31
0.08295	762.67	101.83	26.2	58.6	3663.2	5.81	2.11	760.87
0.08295	910.40	101.98	25.8	58.6	4034.0	5.82	2.32	911.28

Stellenbosch University http://scholar.sun.ac.za

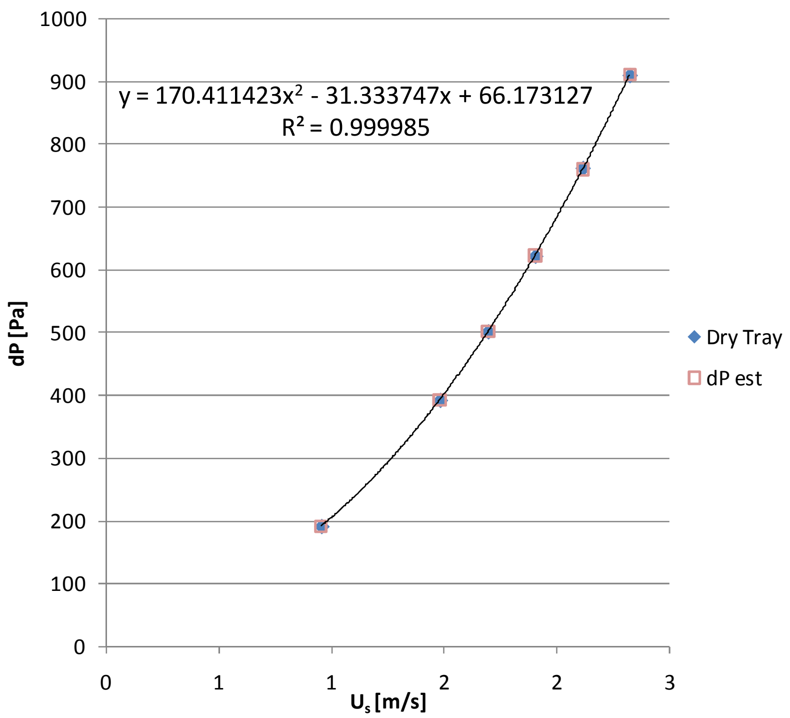

Figure 4. SF_6 dry tray pressure drop estimation as a function of gas velocity.

4. Sample calculations for the different correlations

This table (Table 17) can be used to verify implementation of the different correlations

Table 17. Sample calculation data for the different correlations (Kister and Haas, 1988, Bennett et al., 1995, Uys et al., 2012, Zuiderweg, 1982 and Koziol and Mackowiak, 1990 (K&M)) used in this work, including the new proposed correlation Uys 2012.

Conditions											Kister and Haas 1988			Bennett et al. 1995			Uys 2012			Zuiderweg	K & M
d_H [mm]	A_f [m2]	h_w [mm]	s [mm]	ρ_L [kg/m3]	σ [mN/m]	μ_L [mPa.s]	ρ_g [kg/m3]	U_s [m/s]	Q_L [m3/(h.m)]	μ_g [Pa.s]	L'/Gs	L'/Gf	L'/G	L'/Gs	L'/Gf	L'/G	L'/Gs	L'/Gf	L'/G	L'/Gs	L'/Gs
6.3	0.156	51	609.6	997	73	0.94	1.23	2.77	13.1	1.86E-05	0.79%	0.93%	0.93%	5.33%	3.35%	3.35%	2.10%	1.73%	2.10%	1.91%	0.65%
6.3	0.156	51	609.6	997	73	0.94	1.22	2.65	13.1	1.86E-05	0.63%	0.85%	0.85%	4.64%	2.41%	2.41%	1.81%	1.45%	1.81%	1.44%	0.52%
6.3	0.156	51	609.6	997	73	0.94	1.20	2.47	13.1	1.86E-05	0.44%	0.72%	0.72%	3.81%	1.51%	1.51%	1.44%	1.11%	1.44%	0.92%	0.38%
6.3	0.156	51	609.6	997	73	0.94	1.20	2.16	13.1	1.86E-05	0.24%	0.54%	0.54%	2.80%	0.76%	0.76%	0.94%	0.70%	0.94%	0.43%	0.21%
6.3	0.156	51	609.6	997	73	0.94	1.19	1.86	13.1	1.86E-05	0.12%	0.39%	0.39%	2.08%	0.40%	0.40%	0.58%	0.44%	0.58%	0.17%	0.11%
6.3	0.156	51	609.6	997	73	0.94	1.19	1.62	13.1	1.86E-05	0.06%	0.29%	0.29%	1.68%	0.26%	0.26%	0.37%	0.30%	0.37%	0.08%	0.06%
6.3	0.156	51	609.6	997	73	0.94	1.17	1.28	13.1	1.86E-05	0.02%	0.18%	0.18%	1.31%	0.16%	0.16%	0.17%	0.17%	0.17%	0.02%	0.02%
12.7	0.079	51	609.6	997	73	0.94	1.23	2.77	13.1	1.86E-05	13.74%	4.65%	13.74%	7.63%	43.17%	7.63%	2.10%	1.73%	2.10%	7.44%	7.45%
12.7	0.079	51	609.6	997	73	0.94	1.22	2.65	13.1	1.86E-05	10.97%	3.96%	10.97%	6.96%	28.09%	6.96%	1.81%	1.45%	1.81%	5.60%	6.08%
12.7	0.079	51	609.6	997	73	0.94	1.20	2.47	13.1	1.86E-05	7.73%	3.07%	7.73%	5.94%	15.09%	5.94%	1.44%	1.11%	1.44%	3.61%	4.41%
12.7	0.079	51	609.6	997	73	0.94	1.20	2.16	13.1	1.86E-05	4.17%	1.94%	4.17%	4.39%	5.74%	4.39%	0.94%	0.70%	0.94%	1.66%	2.49%
12.7	0.079	51	609.6	997	73	0.94	1.19	1.86	13.1	1.86E-05	2.02%	1.10%	2.02%	3.10%	2.11%	2.11%	0.58%	0.44%	0.58%	0.67%	1.27%
12.7	0.079	51	609.6	997	73	0.94	1.19	1.62	13.1	1.86E-05	1.04%	0.64%	1.04%	2.35%	1.00%	1.00%	0.37%	0.30%	0.37%	0.30%	0.69%
12.7	0.079	51	609.6	997	73	0.94	1.17	1.28	13.1	1.86E-05	0.35%	0.26%	0.35%	1.64%	0.38%	0.38%	0.17%	0.17%	0.17%	0.08%	0.24%
6.3	0.156	51	615	600	20	0.94	1.00	2.90	26.2	1.86E-05	0.70%	1.20%	1.20%	9.21%	8.77%	8.77%	5.85%	4.57%	5.85%	2.01%	1.53%
6.3	0.156	51	615	700	30	0.94	1.50	2.59	26.2	1.86E-05	0.35%	0.96%	0.96%	8.52%	8.63%	8.63%	3.14%	2.36%	3.14%	1.50%	1.08%
6.3	0.156	51	615	800	40	0.94	2.00	2.41	26.2	1.86E-05	0.28%	0.83%	0.83%	7.99%	8.24%	8.24%	2.09%	1.52%	2.09%	1.22%	0.82%
6.3	0.156	51	615	900	50	0.94	3.00	2.10	26.2	1.86E-05	0.20%	0.64%	0.64%	7.12%	7.62%	7.62%	1.42%	0.84%	1.42%	0.83%	0.54%
6.3	0.156	51	615	1000	73	0.94	4.00	1.83	26.2	1.86E-05	0.21%	0.48%	0.48%	5.53%	4.81%	4.81%	0.82%	0.47%	0.82%	0.47%	0.28%
6.3	0.156	51	615	1000	73	0.94	5.00	1.55	26.2	1.86E-05	0.13%	0.34%	0.34%	4.20%	2.98%	2.98%	0.67%	0.32%	0.67%	0.25%	0.18%
6.3	0.156	51	615	1000	73	0.94	5.00	1.25	26.2	1.86E-05	0.05%	0.21%	0.21%	2.24%	0.78%	0.78%	0.33%	0.23%	0.33%	0.07%	0.09%

5. Enlarged figures for data

Paper 1 figures with experimental data

Figure 3

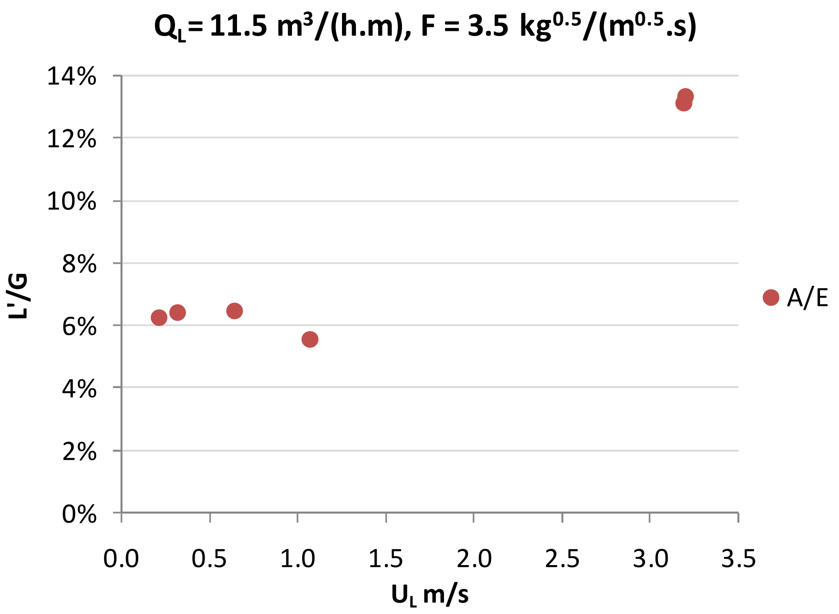

(a)

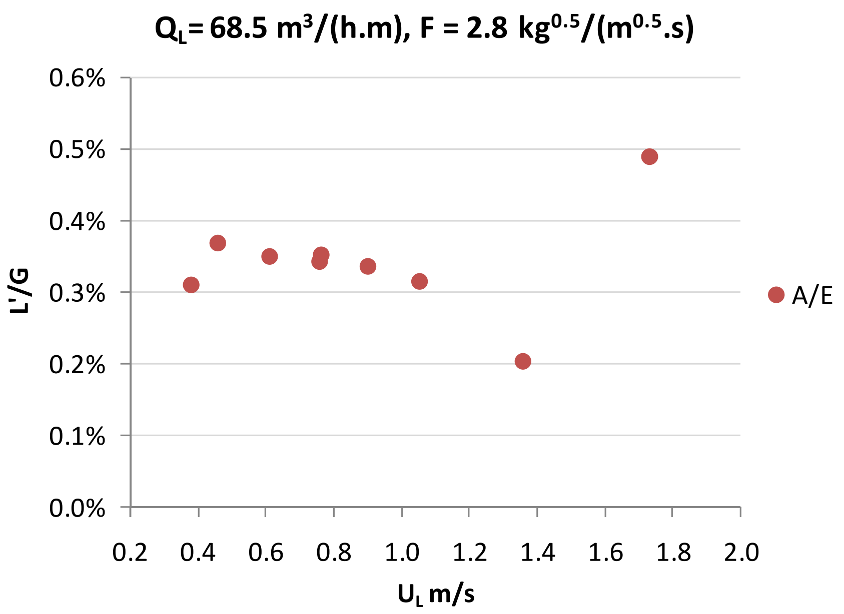

(b)

Figure 4

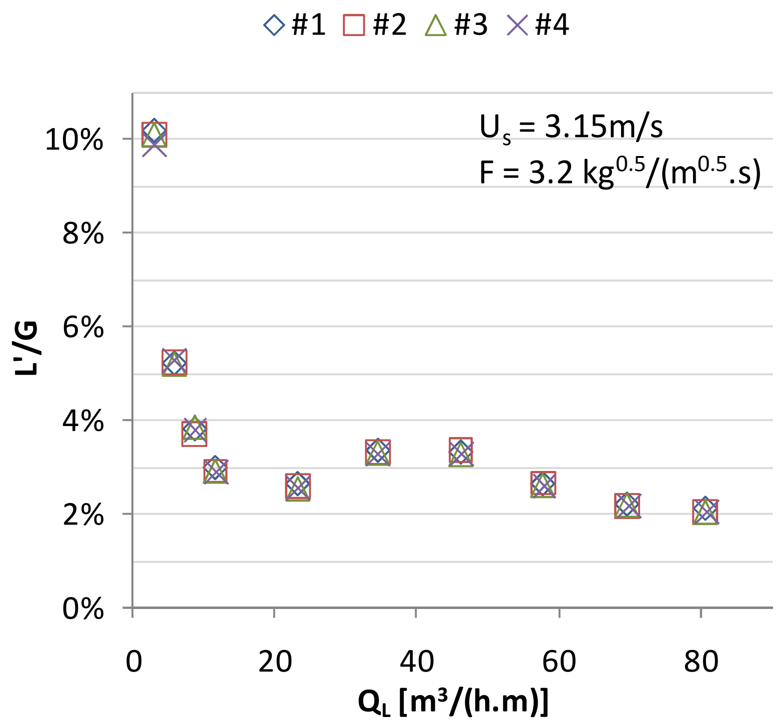
#1 #2 #3 #4
U_s = 3.15m/s
F = 3.2 kg$^{0.5}$/(m$^{0.5}$.s)
10%
8%
6%
4%
2%
0%
L'/G
0
20
40
60
80
Q_L [m³/(h.m)]

(a)

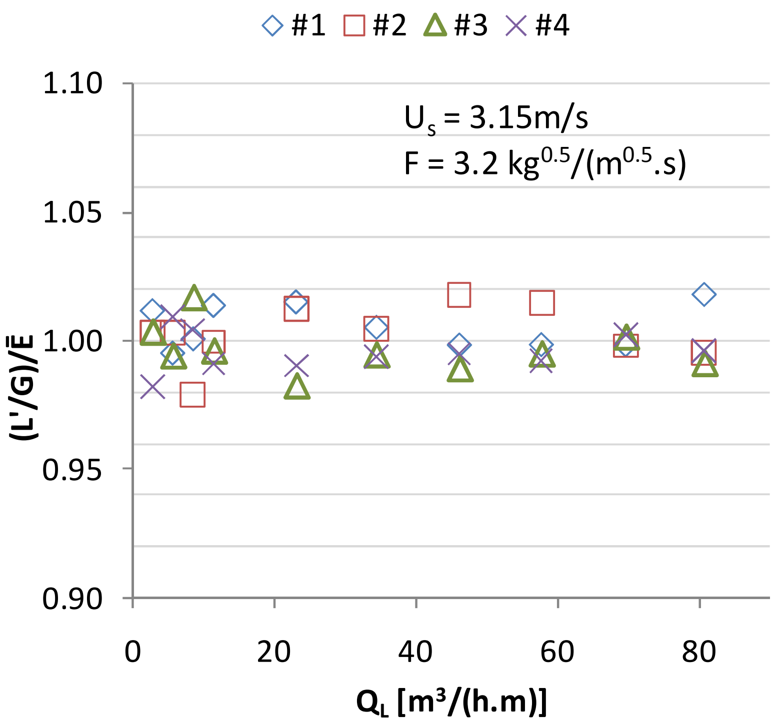
#1 #2 #3 #4
U_s = 3.15m/s
F = 3.2 kg$^{0.5}$/(m$^{0.5}$.s)
1.10
1.05
1.00
0.95
0.90
(L'/G)/Ē
0
20
40
60
80
Q_L [m³/(h.m)]

(b)

Figure 5

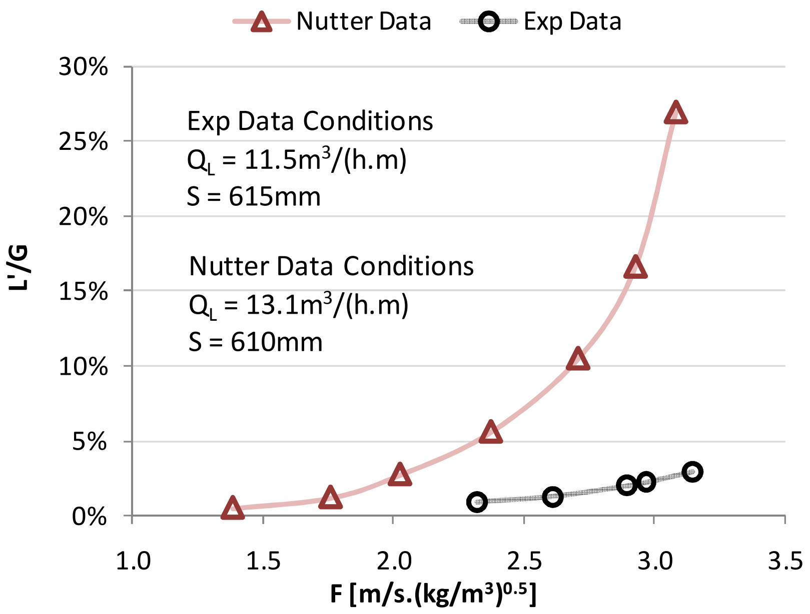
Nutter Data
Exp Data
Exp Data Conditions
Q_L = 11.5m^3/(h.m)
S = 615mm
Nutter Data Conditions
Q_L = 13.1m^3/(h.m)
S = 610mm
L'/G
30%
25%
20%
15%
10%
5%
0%
1.0
1.5
2.0
2.5
3.0
3.5
F [m/s.(kg/m³)$^{0.5}$]

(a)

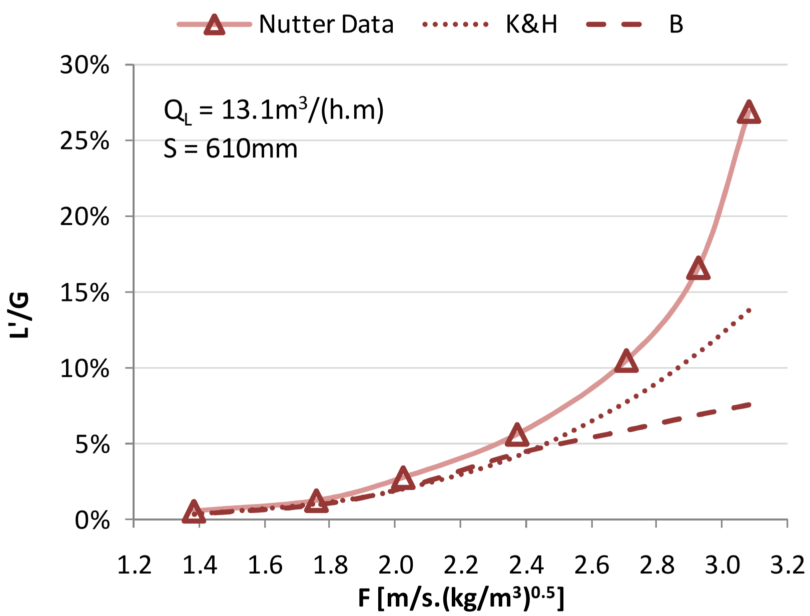
Nutter Data
K&H
B
Q_L = 13.1m^3/(h.m)
S = 610mm
L'/G
30%
25%
20%
15%
10%
5%
0%
1.2
1.4
1.6
1.8
2.0
2.2
2.4
2.6
2.8
3.0
3.2
F [m/s.(kg/m³)$^{0.5}$]

(b)

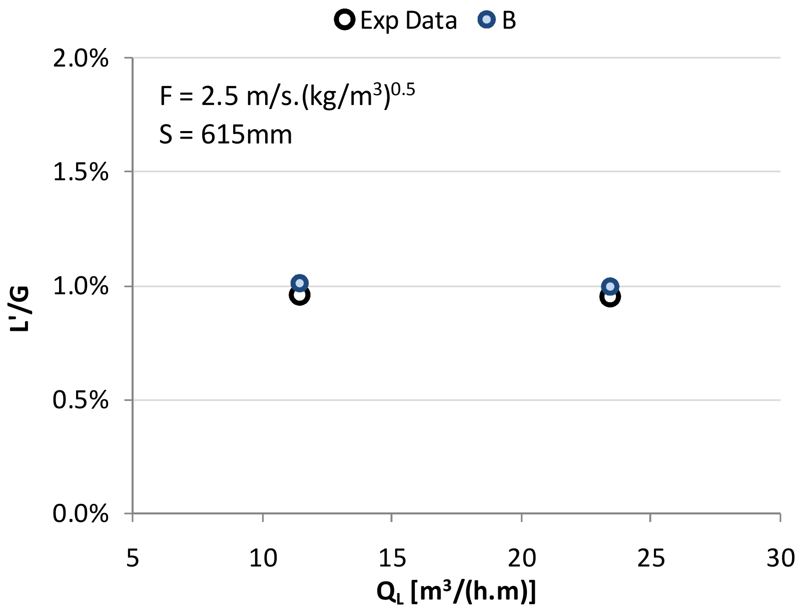

Exp Data
B
F = 2.5 m/s.(kg/m³)^0.5
S = 615mm
2.0%
1.5%
1.0%
0.5%
0.0%
L'/G
5
10
15
20
25
30
Q_L [m³/(h.m)]

(c)

Figure 6

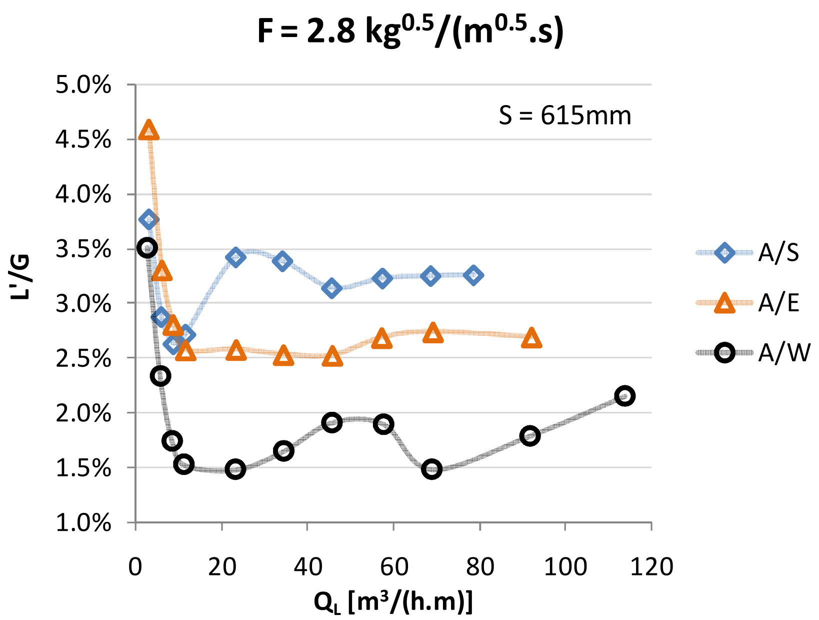

F = 2.8 kg^0.5/(m^0.5.s)
S = 615mm
5.0%
4.5%
4.0%
3.5%
3.0%
2.5%
2.0%
1.5%
1.0%
L'/G
0
20
40
60
80
100
120
Q_L [m³/(h.m)]
A/S
A/E
A/W

(a)

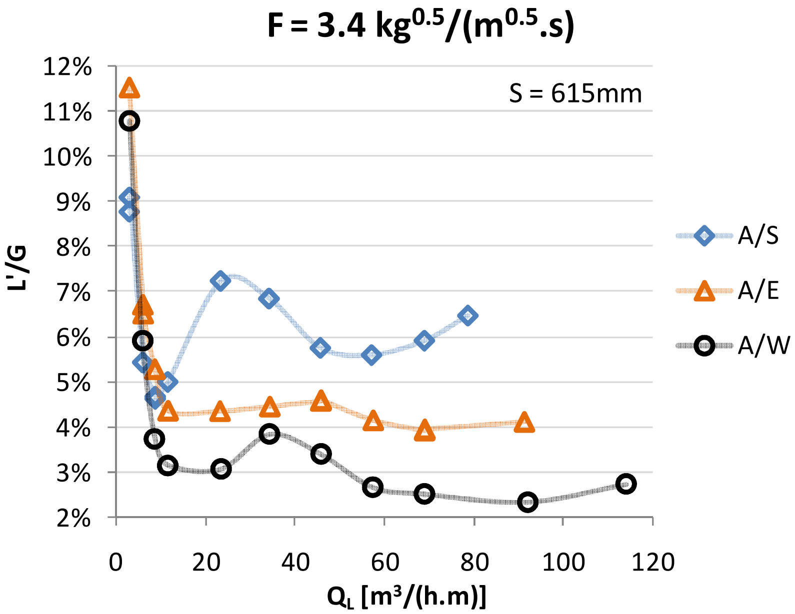
F = 3.4 kg0.5/(m0.5.s)
S = 615mm
L'/G
QL [m³/(h.m)]
A/S
A/E
A/W
12%
11%
10%
9%
8%
7%
6%
5%
4%
3%
2%
0
20
40
60
80
100
120

(b)

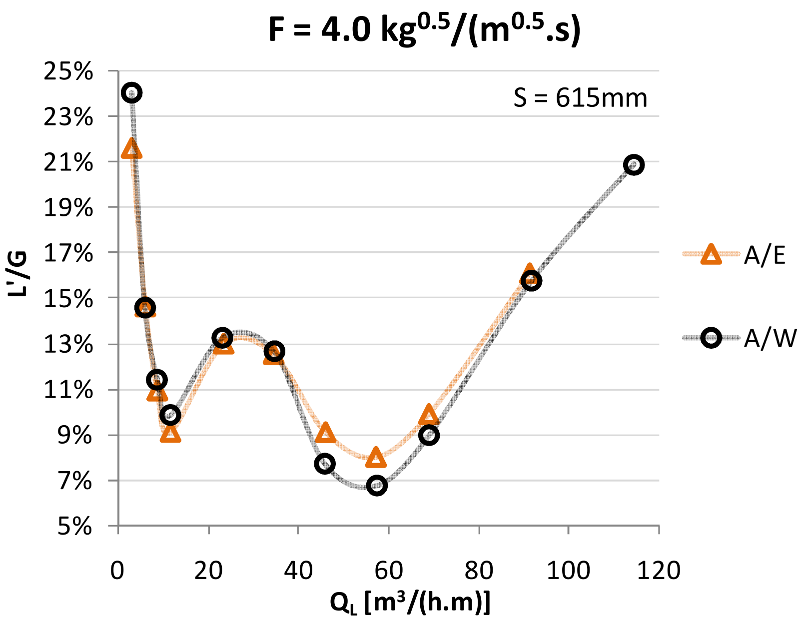
F = 4.0 kg0.5/(m0.5.s)
S = 615mm
L'/G
QL [m³/(h.m)]
A/E
A/W
25%
23%
21%
19%
17%
15%
13%
11%
9%
7%
5%
0
20
40
60
80
100
120

(c)

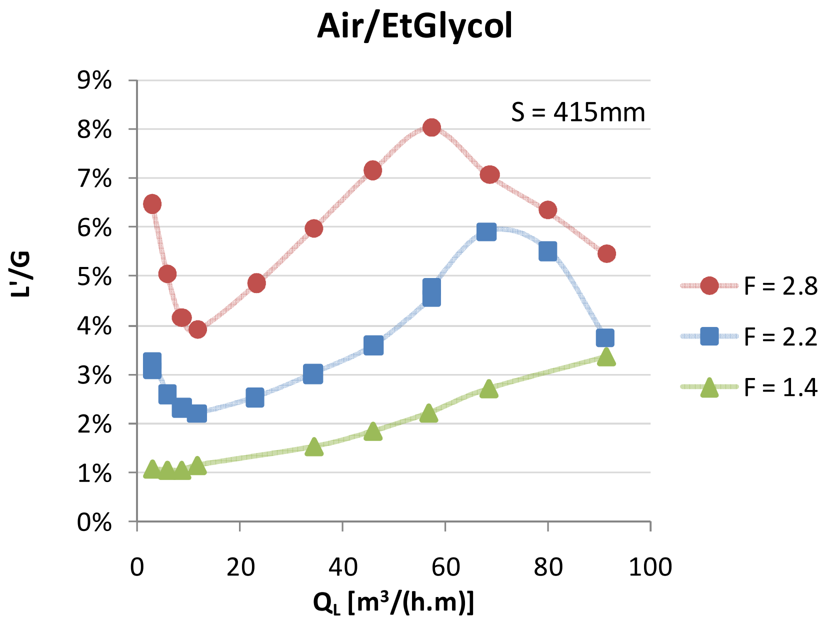
Air/EtGlycol
S = 415mm
L'/G
9%
8%
7%
6%
5%
4%
3%
2%
1%
0%
0
20
40
60
80
100
Q_L [m³/(h.m)]
F = 2.8
F = 2.2
F = 1.4

(d)

Figure 7

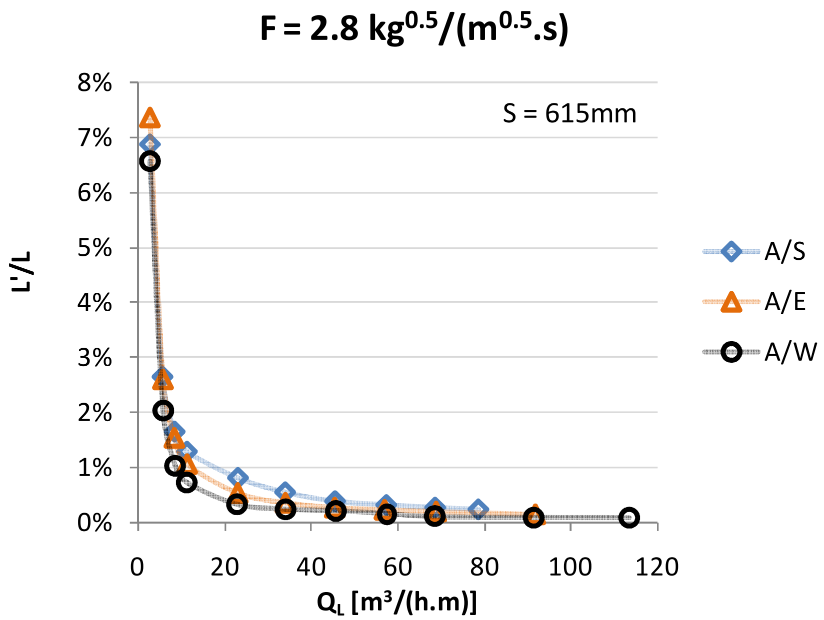
F = 2.8 kg^0.5/(m^0.5.s)
S = 615mm
L'/L
8%
7%
6%
5%
4%
3%
2%
1%
0%
0
20
40
60
80
100
120
Q_L [m³/(h.m)]
A/S
A/E
A/W

(a)

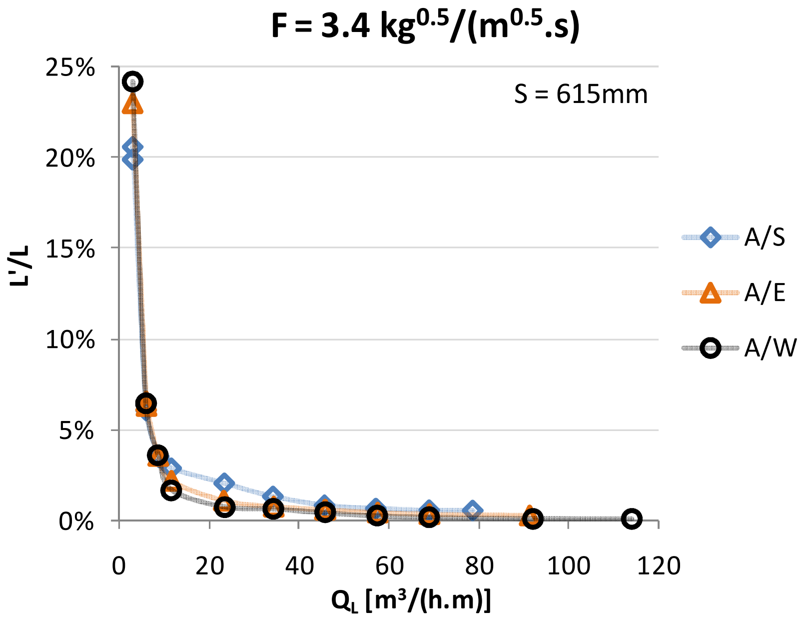
F = 3.4 kg$^{0.5}$/(m$^{0.5}$.s)
S = 615mm
L'/L
25%
20%
15%
10%
5%
0%
0
20
40
60
80
100
120
Q_L [m³/(h.m)]
A/S
A/E
A/W

(b)

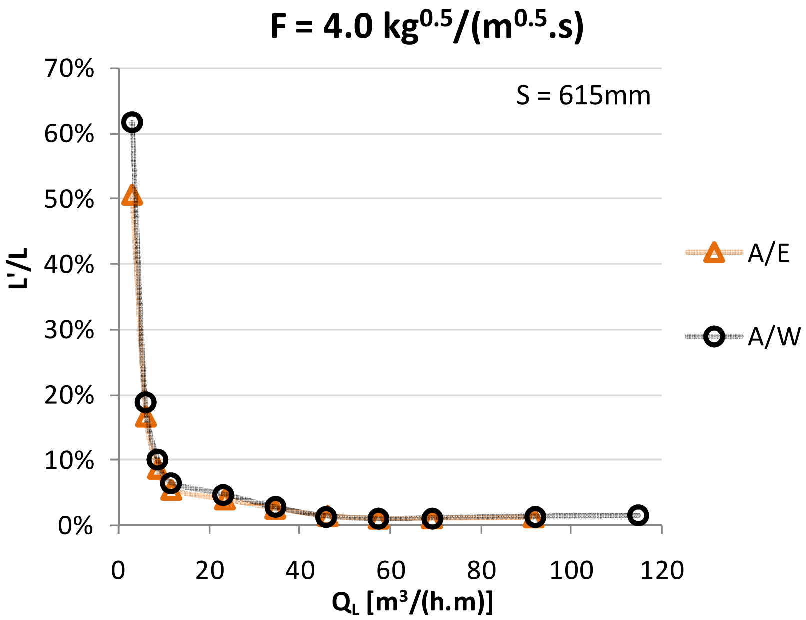
F = 4.0 kg$^{0.5}$/(m$^{0.5}$.s)
S = 615mm
L'/L
70%
60%
50%
40%
30%
20%
10%
0%
0
20
40
60
80
100
120
Q_L [m³/(h.m)]
A/E
A/W

(c)

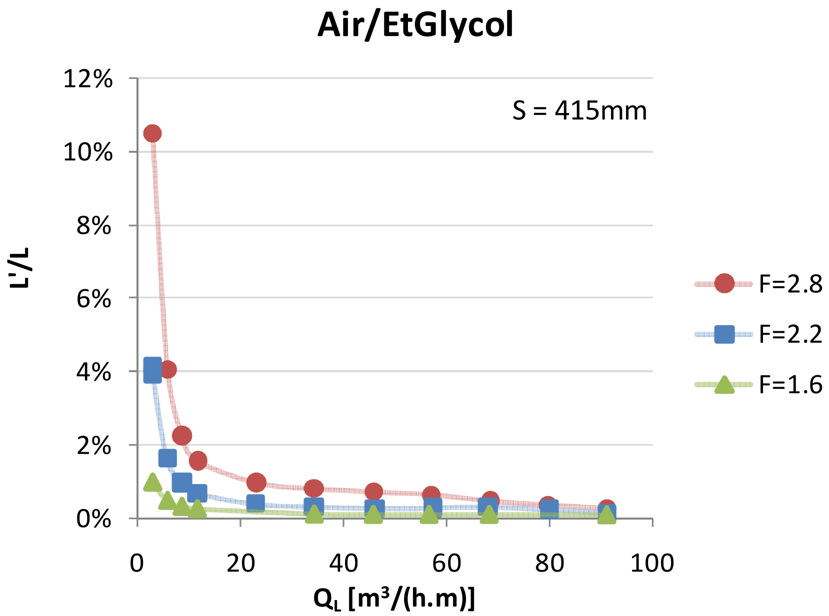
Air/EtGlycol
S = 415mm
12%
10%
8%
6%
4%
2%
0%
L'/L
0
20
40
60
80
100
Q_L [m³/(h.m)]
F=2.8
F=2.2
F=1.6

(d)

Figure 10

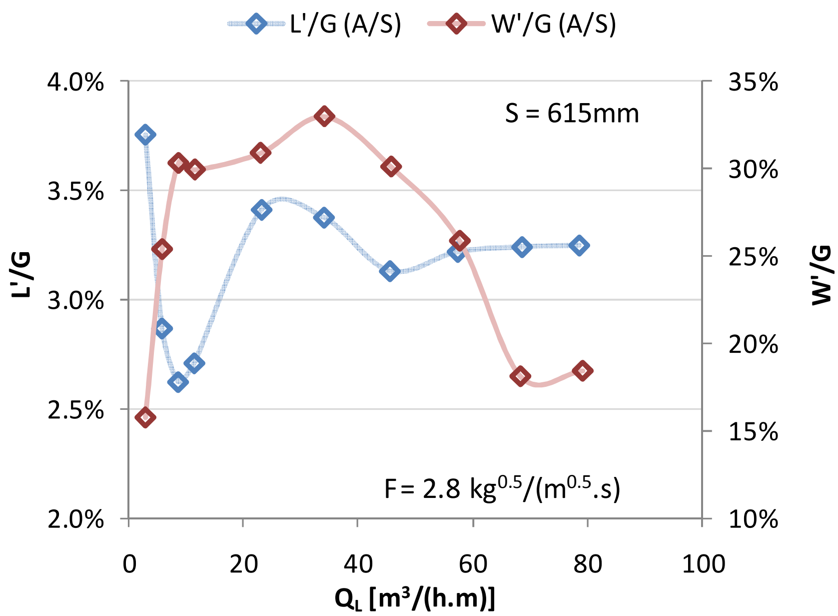
L'/G (A/S)
W'/G (A/S)
S = 615mm
4.0%
3.5%
3.0%
2.5%
2.0%
L'/G
35%
30%
25%
20%
15%
10%
W'/G
F= 2.8 kg^0.5/(m^0.5.s)
0
20
40
60
80
100
Q_L [m³/(h.m)]

(a)

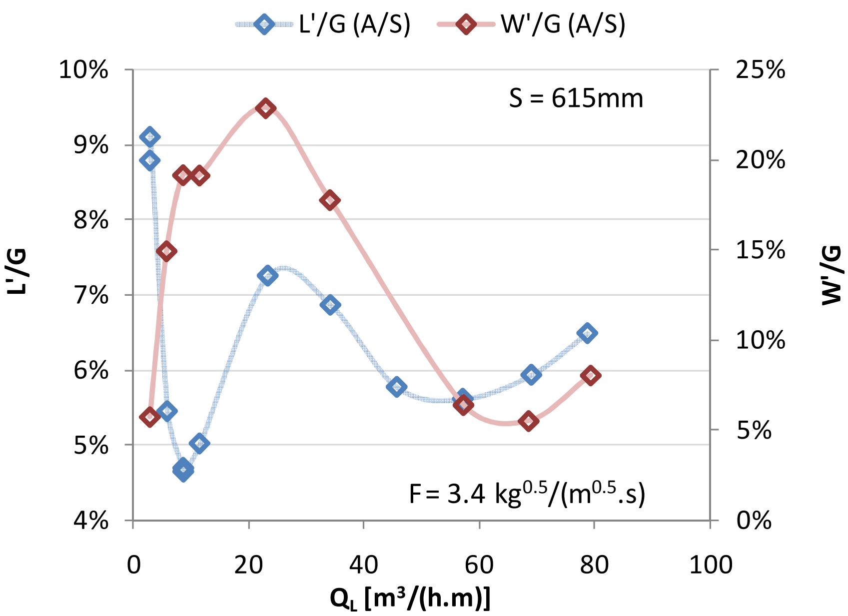
L'/G (A/S)
W'/G (A/S)
S = 615mm
F = 3.4 kg0.5/(m0.5.s)
L'/G
W'/G
10%
9%
8%
7%
6%
5%
4%
25%
20%
15%
10%
5%
0%
0
20
40
60
80
100
QL [m3/(h.m)]

(b)

Figure 11

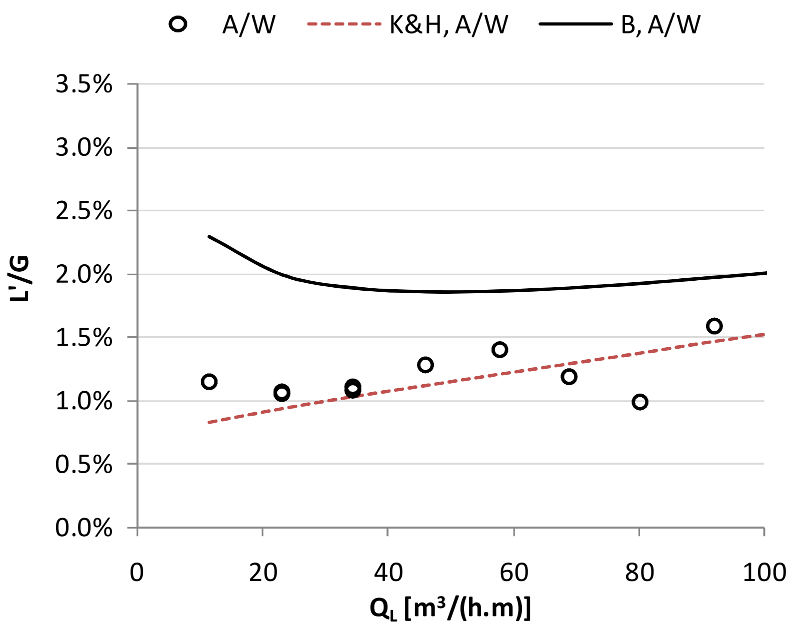
A/W
K&H, A/W
B, A/W
L'/G
3.5%
3.0%
2.5%
2.0%
1.5%
1.0%
0.5%
0.0%
0
20
40
60
80
100
QL [m3/(h.m)]

(b)

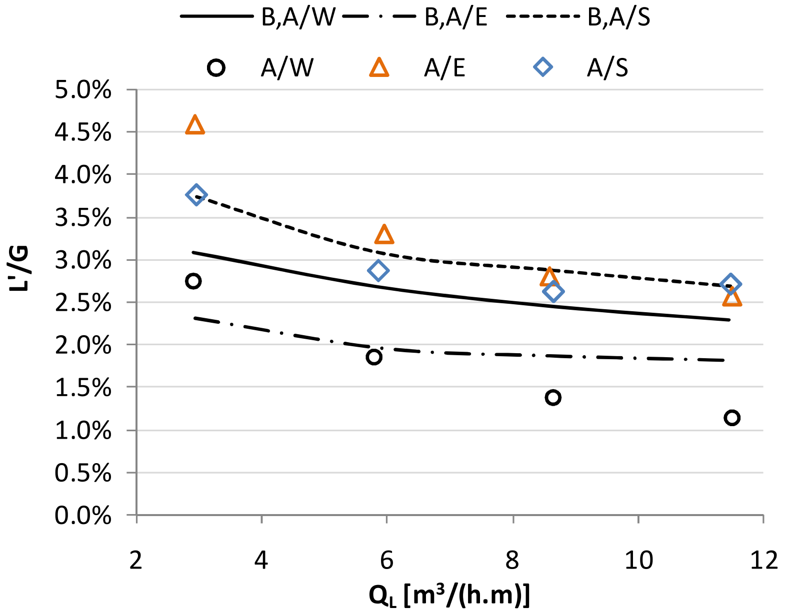
B,A/W
B,A/E
B,A/S
A/W
A/E
A/S
L'/G
5.0%
4.5%
4.0%
3.5%
3.0%
2.5%
2.0%
1.5%
1.0%
0.5%
0.0%
2
4
6
8
10
12
Q_L [m³/(h.m)]

(c)

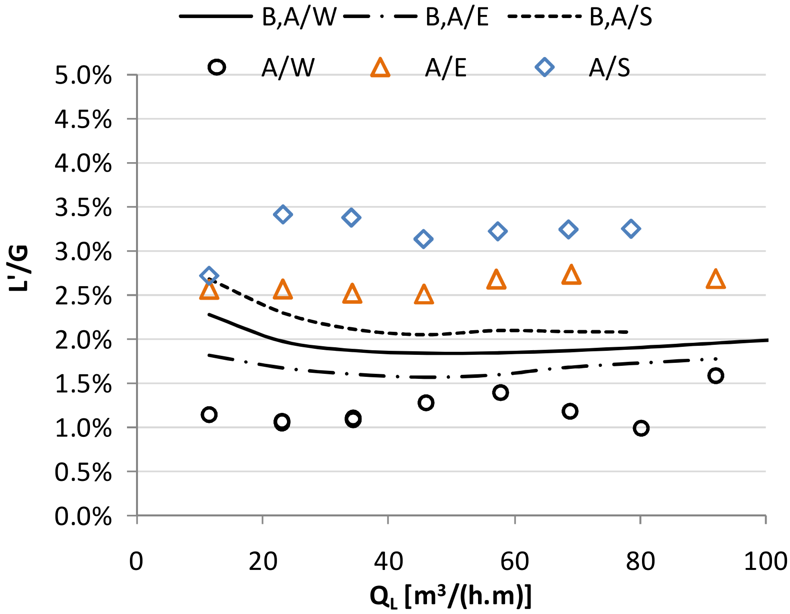
B,A/W
B,A/E
B,A/S
A/W
A/E
A/S
L'/G
5.0%
4.5%
4.0%
3.5%
3.0%
2.5%
2.0%
1.5%
1.0%
0.5%
0.0%
0
20
40
60
80
100
Q_L [m³/(h.m)]

(d)

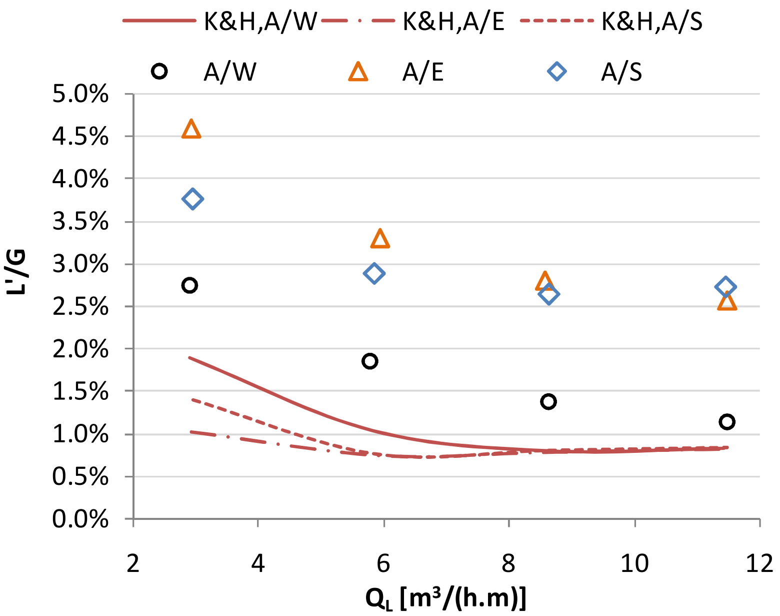
K&H,A/W
K&H,A/E
K&H,A/S
A/W
A/E
A/S
L'/G
5.0%
4.5%
4.0%
3.5%
3.0%
2.5%
2.0%
1.5%
1.0%
0.5%
0.0%
2
4
6
8
10
12
Q_L [m³/(h.m)]

(e)

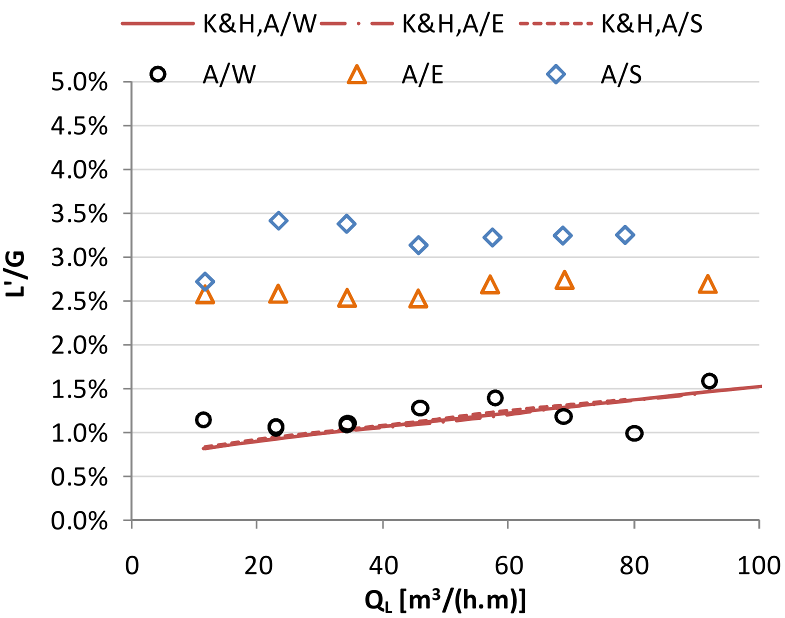
K&H,A/W
K&H,A/E
K&H,A/S
A/W
A/E
A/S
L'/G
5.0%
4.5%
4.0%
3.5%
3.0%
2.5%
2.0%
1.5%
1.0%
0.5%
0.0%
0
20
40
60
80
100
Q_L [m³/(h.m)]

(f)

Manuscript 2 figures with experimental data

Figure 2

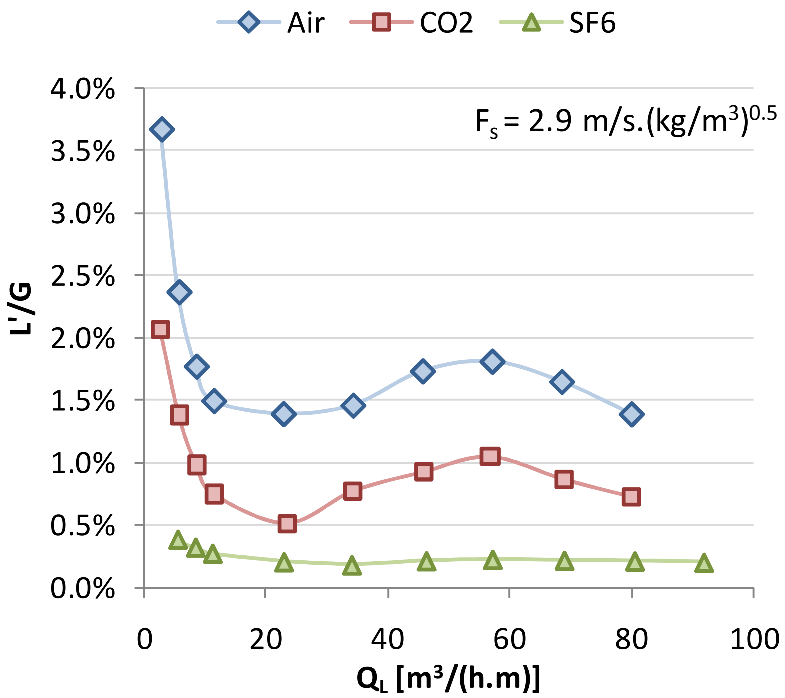

(a)

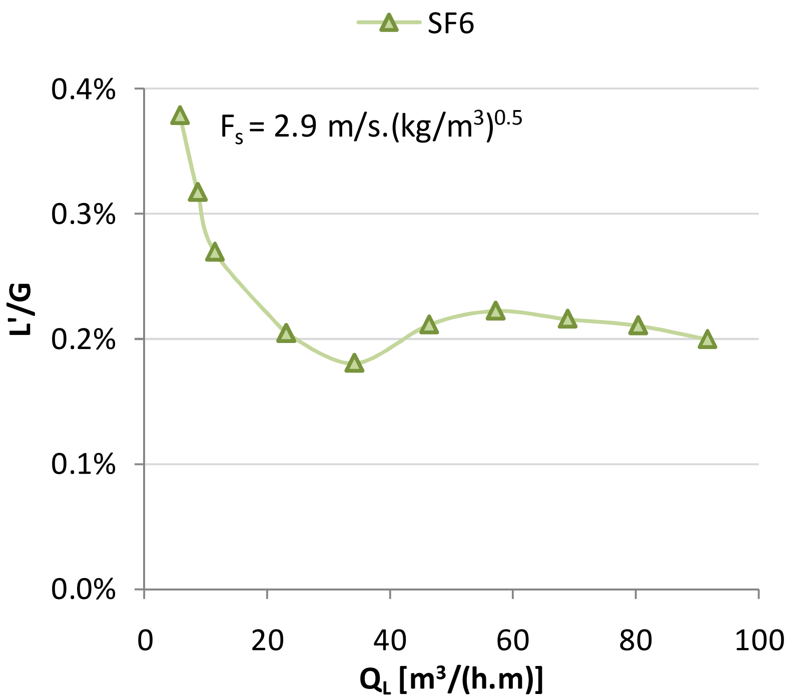
SF6
0.4%
0.3%
0.2%
0.1%
0.0%
L'/G
F_s = 2.9 m/s.(kg/m^3)$^{0.5}$
0
20
40
60
80
100
Q_L [m^3/(h.m)]

(b)

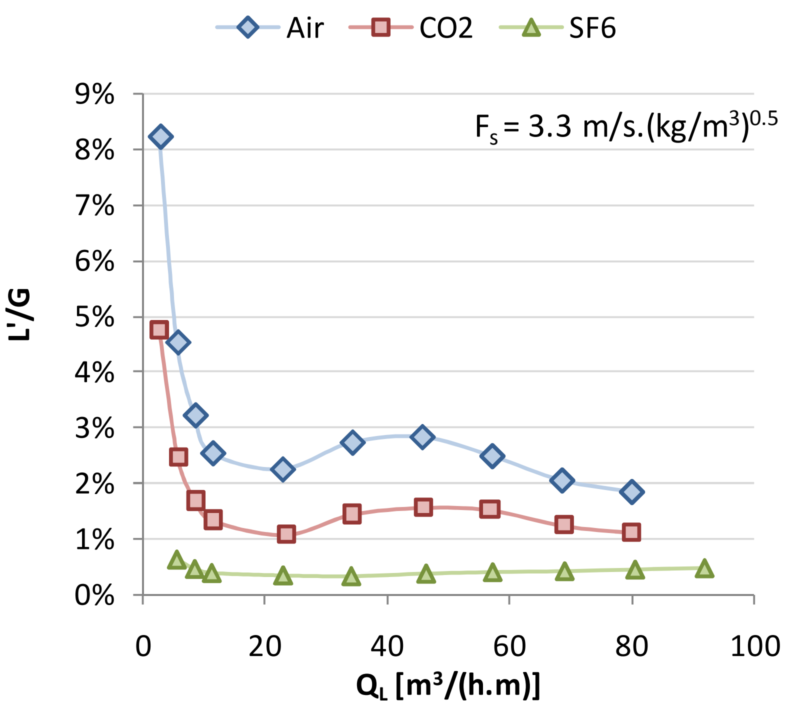
Air
CO2
SF6
9%
8%
7%
6%
5%
4%
3%
2%
1%
0%
L'/G
F_s = 3.3 m/s.(kg/m^3)$^{0.5}$
0
20
40
60
80
100
Q_L [m^3/(h.m)]

(c)

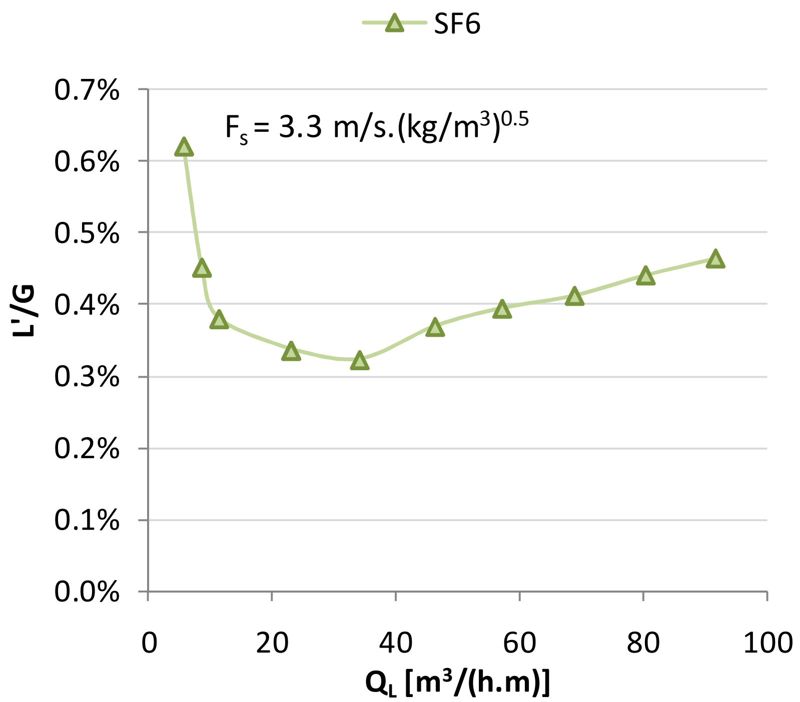
SF6
$F_s = 3.3$ m/s.(kg/m^3)$^{0.5}$
L'/G
0.7%
0.6%
0.5%
0.4%
0.3%
0.2%
0.1%
0.0%
0
20
40
60
80
100
Q_L [m^3/(h.m)]

(d)

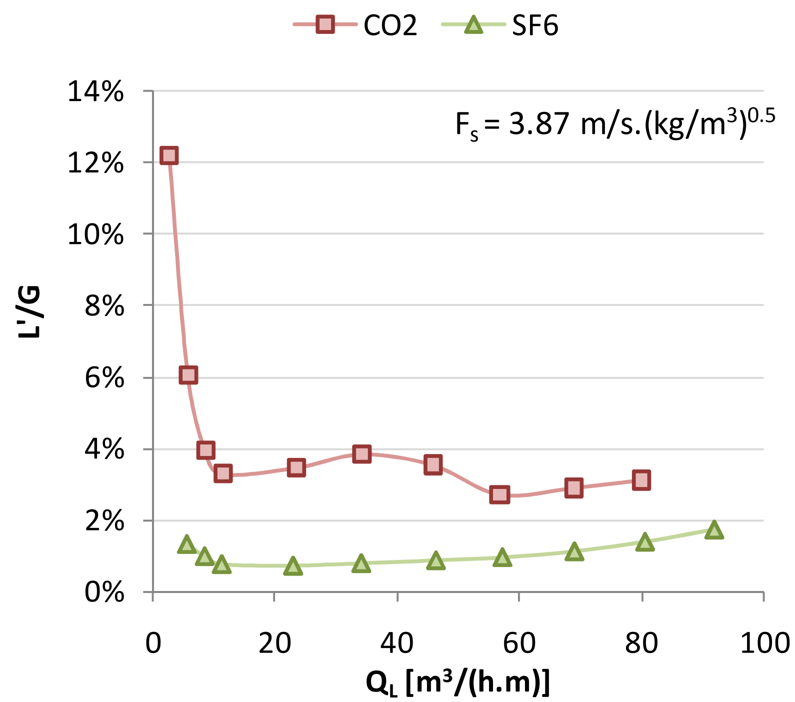
CO2
SF6
$F_s = 3.87$ m/s.(kg/m^3)$^{0.5}$
L'/G
14%
12%
10%
8%
6%
4%
2%
0%
0
20
40
60
80
100
Q_L [m^3/(h.m)]

(e)

Stellenbosch University http://scholar.sun.ac.za

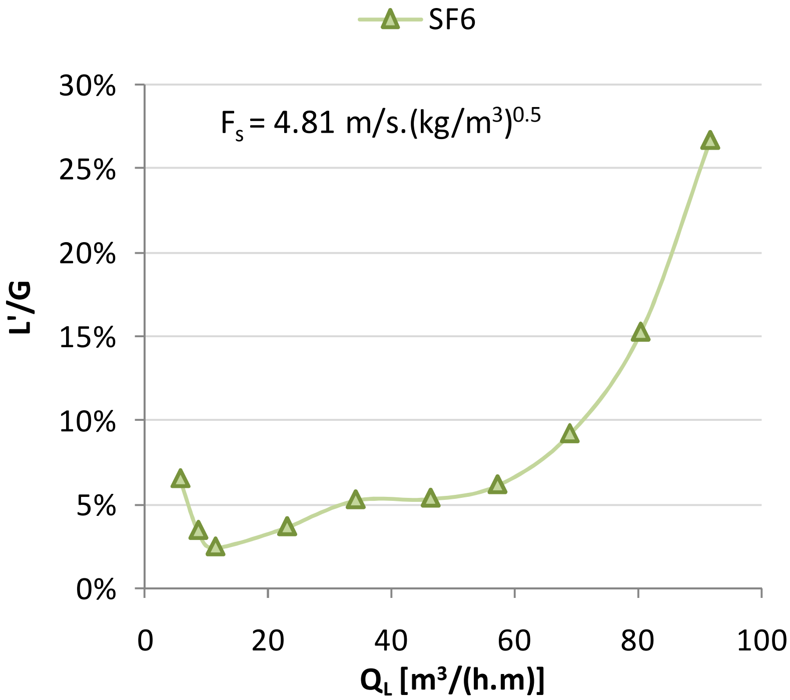

(f)

Figure 3

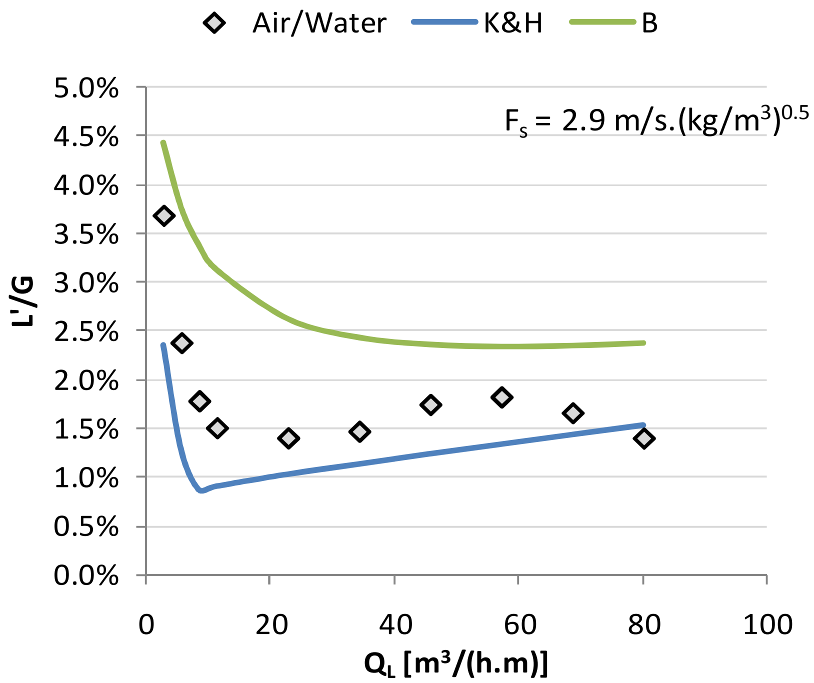
Air/Water
K&H
B
5.0%
4.5%
4.0%
3.5%
3.0%
2.5%
2.0%
1.5%
1.0%
0.5%
0.0%
L'/G
Fs = 2.9 m/s.(kg/m3)0.5
0
20
40
60
80
100
QL [m3/(h.m)]

(a)

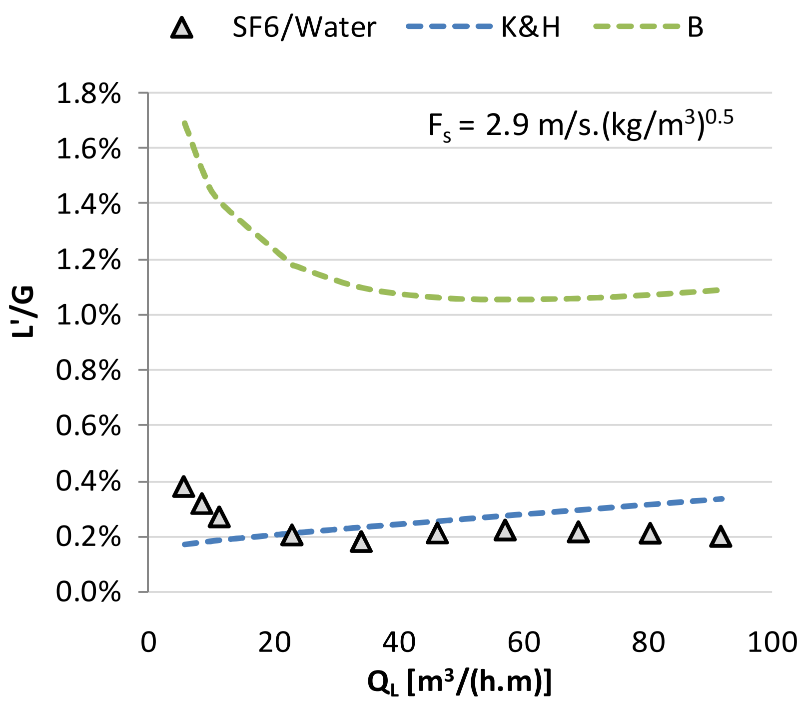
SF6/Water
K&H
B
1.8%
1.6%
1.4%
1.2%
1.0%
0.8%
0.6%
0.4%
0.2%
0.0%
L'/G
Fs = 2.9 m/s.(kg/m3)0.5
0
20
40
60
80
100
QL [m3/(h.m)]

(b)

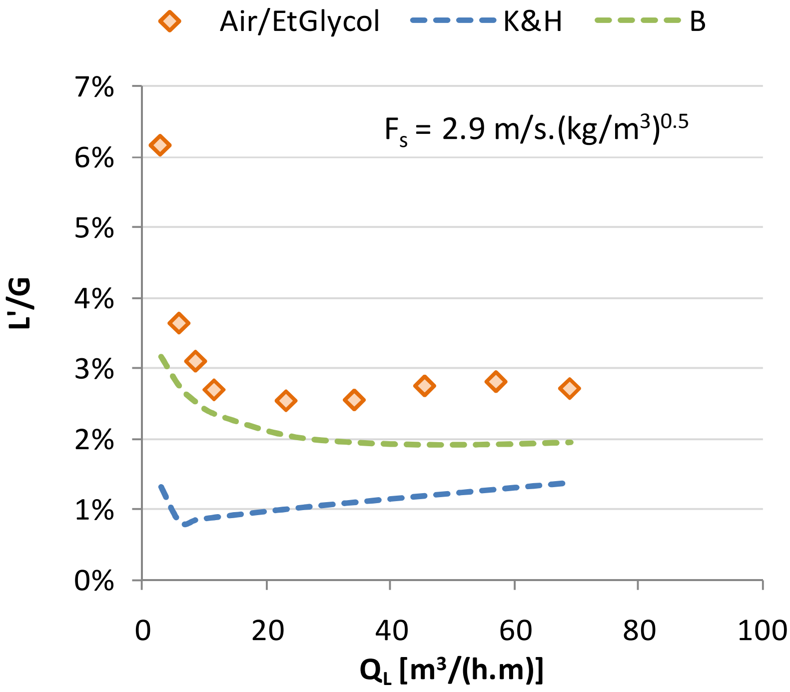
Air/EtGlycol
K&H
B
F_s = 2.9 m/s.(kg/m³)^0.5
7%
6%
5%
4%
3%
2%
1%
0%
L'/G
0
20
40
60
80
100
Q_L [m³/(h.m)]

(c)

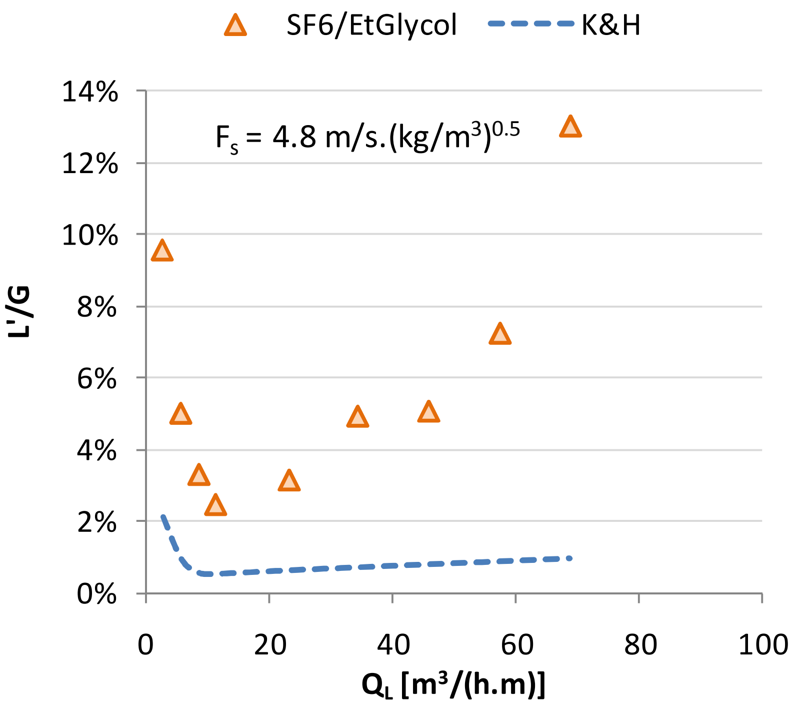
SF6/EtGlycol
K&H
F_s = 4.8 m/s.(kg/m³)^0.5
14%
12%
10%
8%
6%
4%
2%
0%
L'/G
0
20
40
60
80
100
Q_L [m³/(h.m)]

(d)

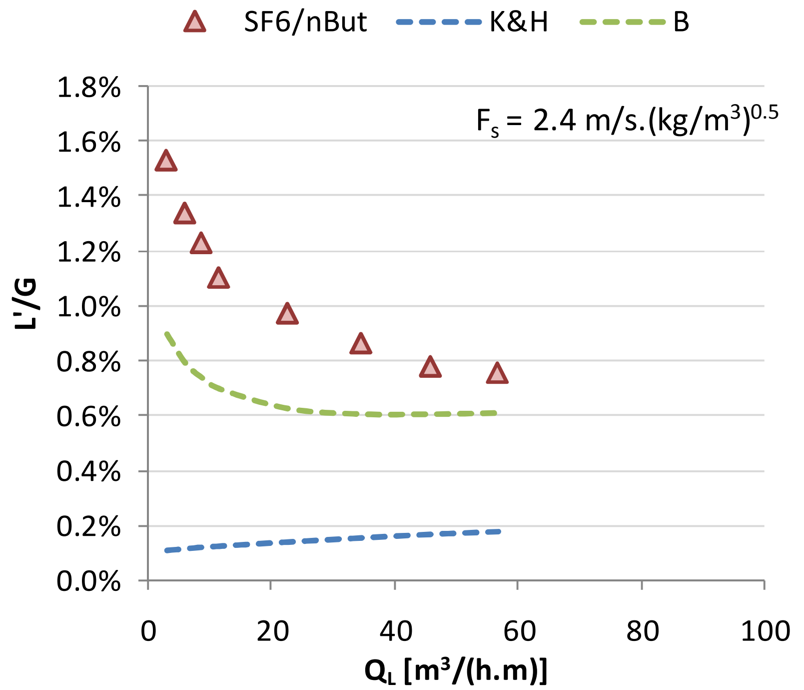
SF6/nBut
K&H
B
F_s = 2.4 m/s.(kg/m³)^0.5
L'/G
1.8%
1.6%
1.4%
1.2%
1.0%
0.8%
0.6%
0.4%
0.2%
0.0%
0
20
40
60
80
100
Q_L [m³/(h.m)]

(e)

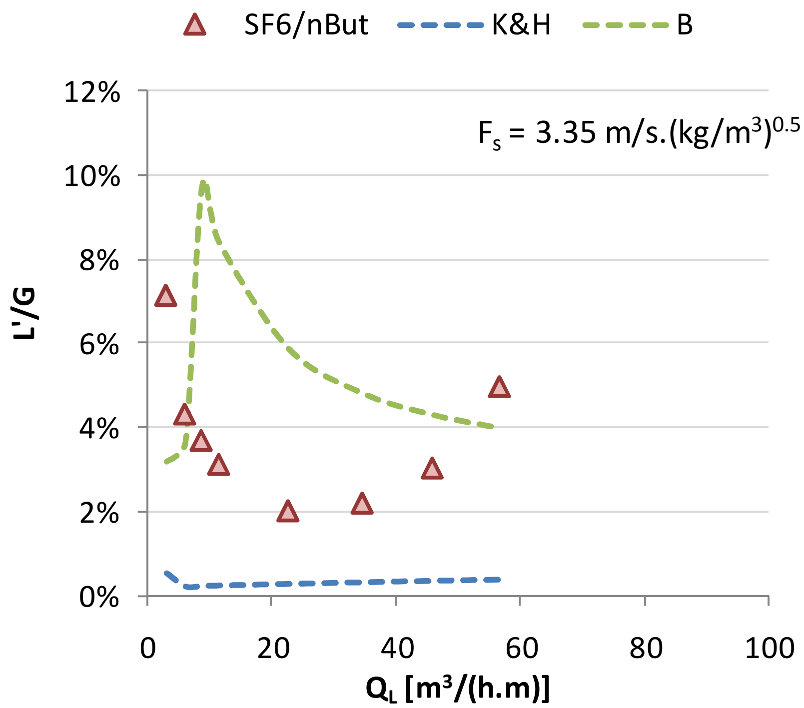
SF6/nBut
K&H
B
F_s = 3.35 m/s.(kg/m³)^0.5
L'/G
12%
10%
8%
6%
4%
2%
0%
0
20
40
60
80
100
Q_L [m³/(h.m)]

(f)

Figure 4

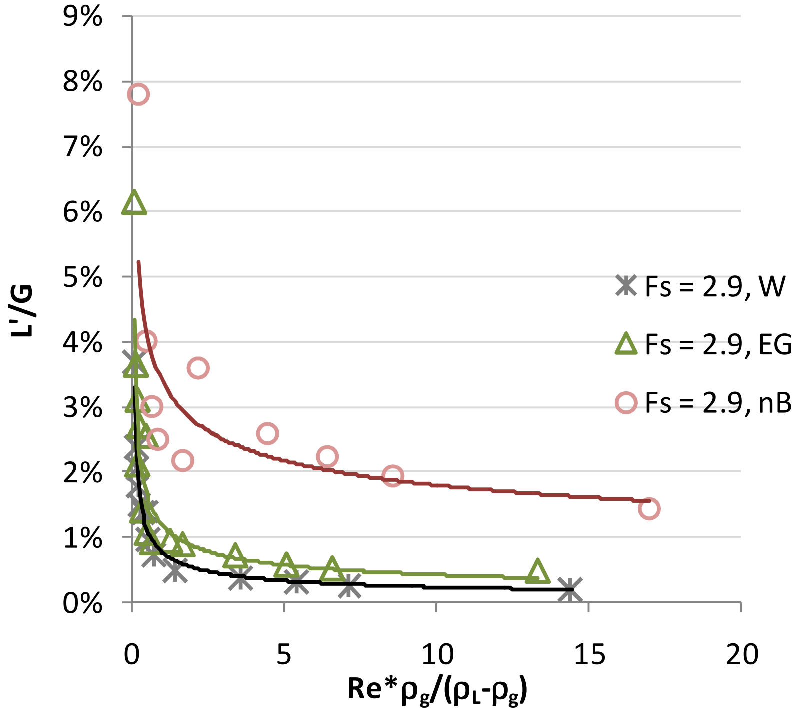
9%
8%
7%
6%
5%
4%
3%
2%
1%
0%
L'/G
0
5
10
15
20
Re*ρg/(ρL-ρg)
Fs = 2.9, W
Fs = 2.9, EG
Fs = 2.9, nB

(a)

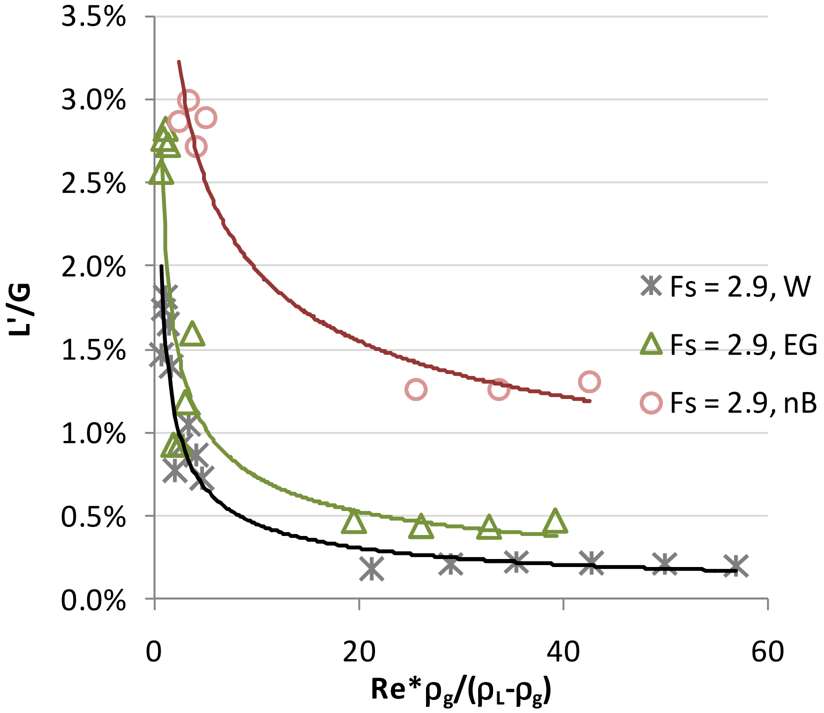
3.5%
3.0%
2.5%
2.0%
1.5%
1.0%
0.5%
0.0%
L'/G
0
20
40
60
Re*ρg/(ρL-ρg)
Fs = 2.9, W
Fs = 2.9, EG
Fs = 2.9, nB

(b)

Stellenbosch University http://scholar.sun.ac.za

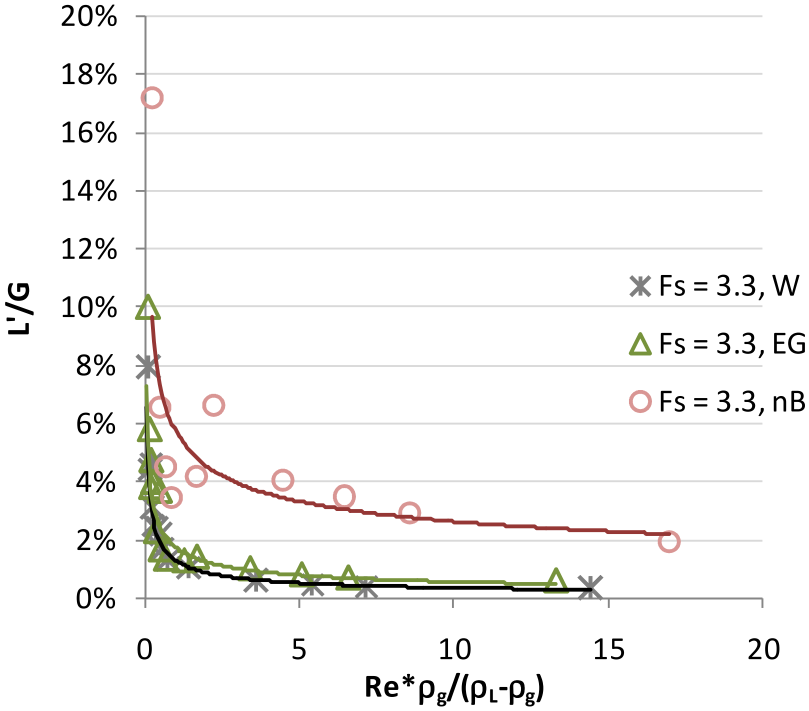

(c)

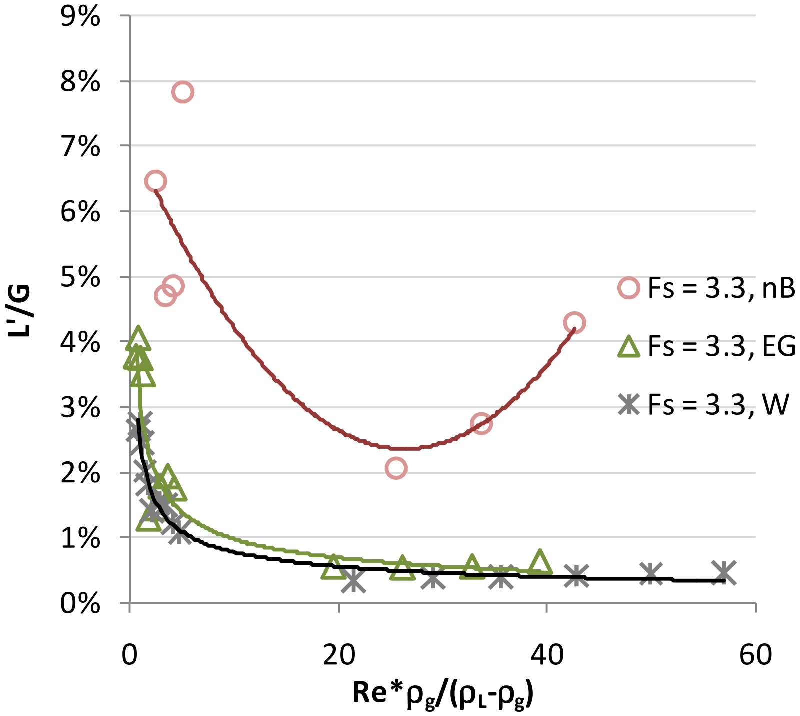

(d)

Stellenbosch University http://scholar.sun.ac.za

Figure 5

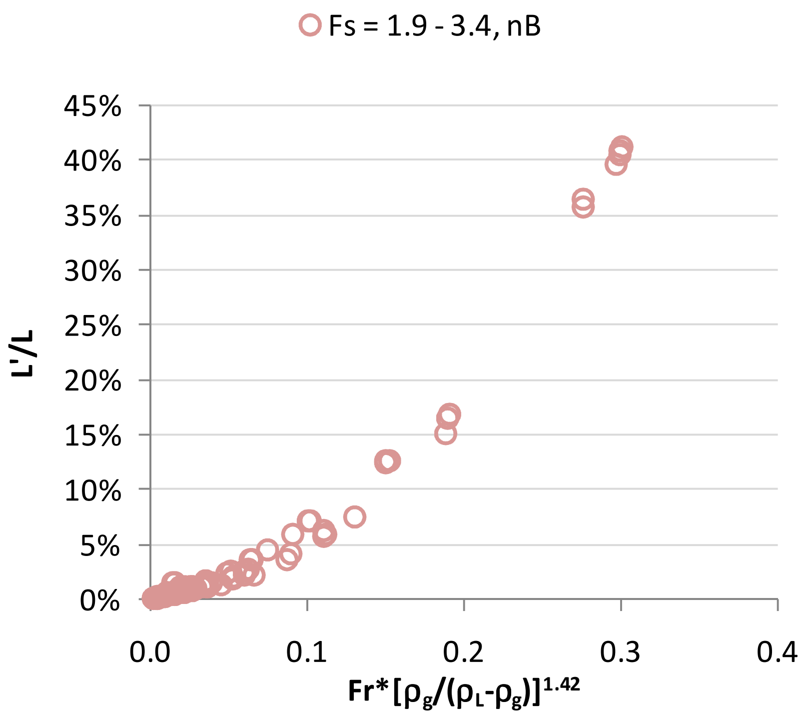

(a)

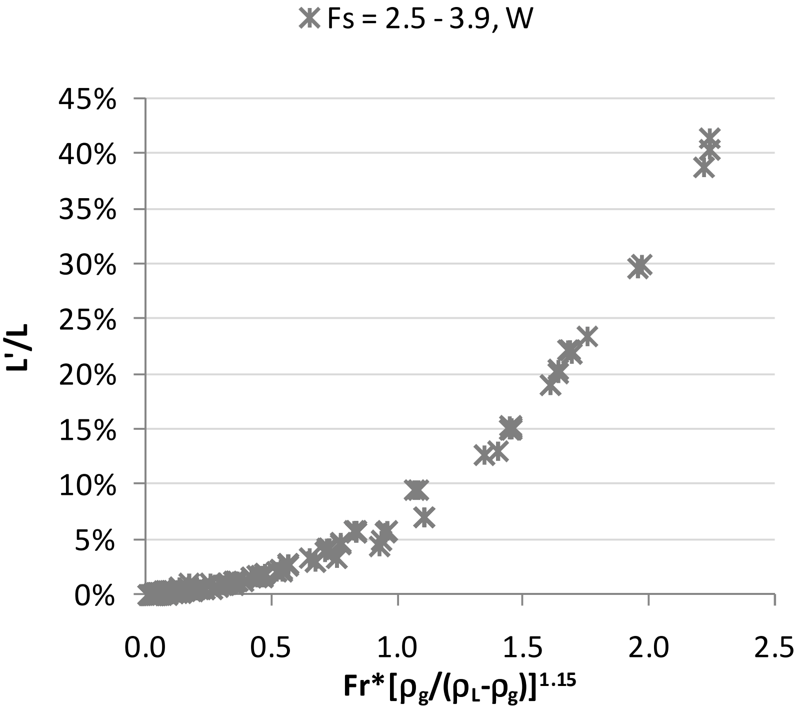
Fs = 2.5 - 3.9, W
45%
40%
35%
30%
25%
20%
15%
10%
5%
0%
L'/L
0.0
0.5
1.0
1.5
2.0
2.5
Fr*[ρg/(ρL-ρg)]1.15

(b)

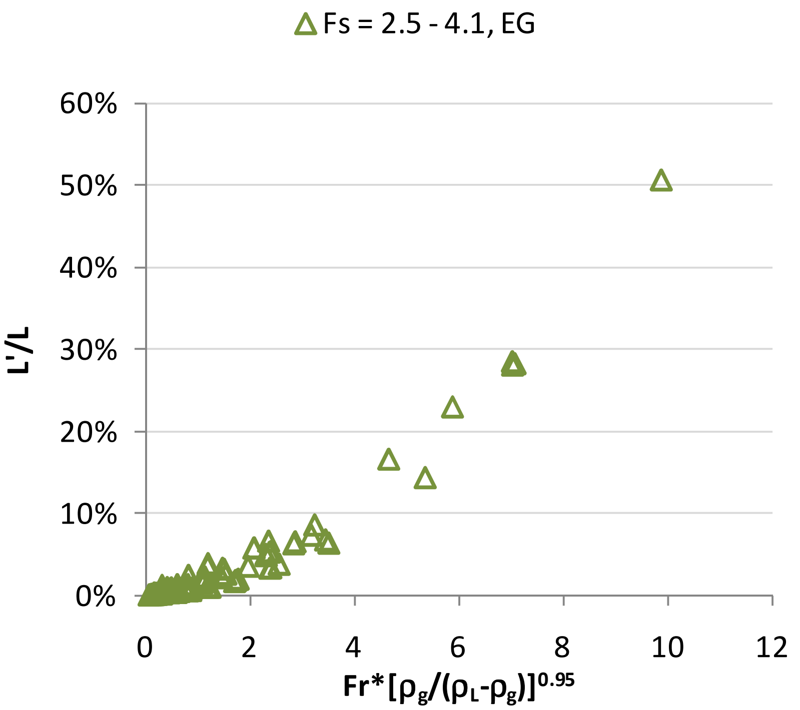
Fs = 2.5 - 4.1, EG
60%
50%
40%
30%
20%
10%
0%
L'/L
0
2
4
6
8
10
12
Fr*[ρg/(ρL-ρg)]0.95

(c)

Stellenbosch University http://scholar.sun.ac.za

Manuscript 3 figures with experimental data

Figure 2

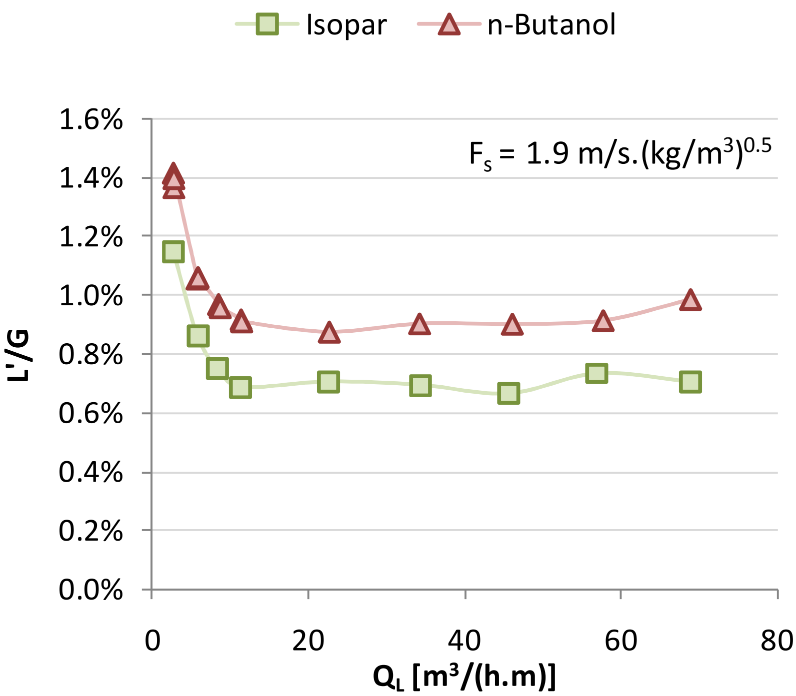

(a)

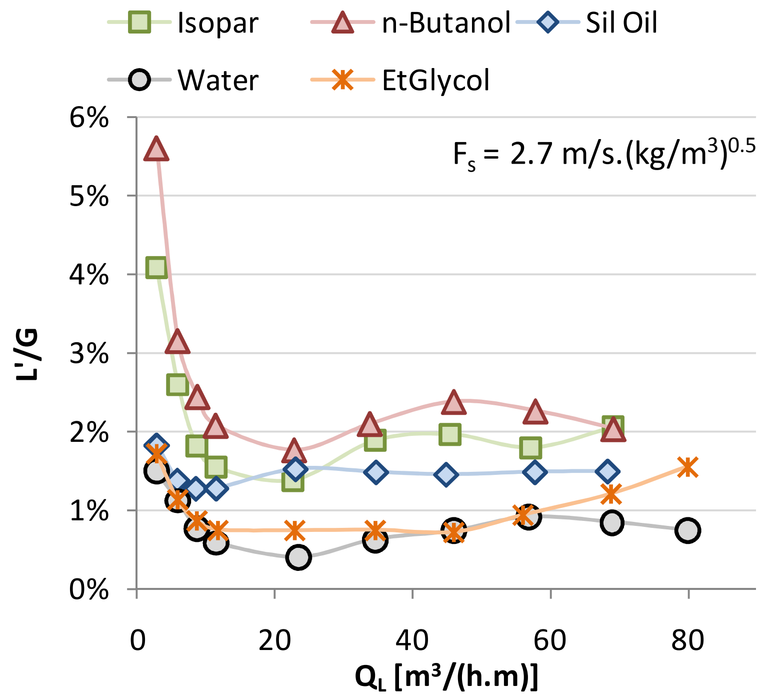
Isopar
n-Butanol
Sil Oil
Water
EtGlycol
F_s = 2.7 m/s.(kg/m³)$^{0.5}$
L'/G
6%
5%
4%
3%
2%
1%
0%
0
20
40
60
80
Q_L [m³/(h.m)]

(b)

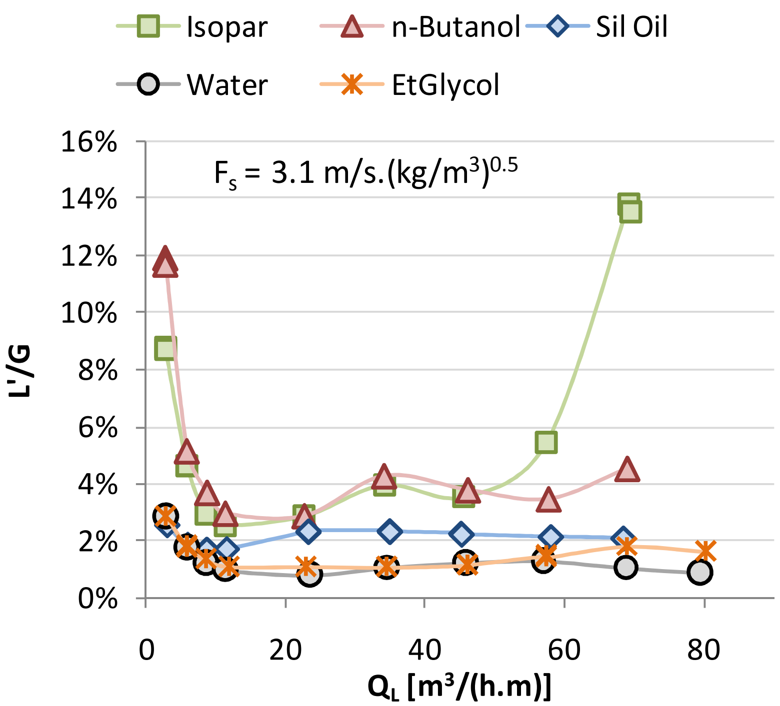
Isopar
n-Butanol
Sil Oil
Water
EtGlycol
F_s = 3.1 m/s.(kg/m³)$^{0.5}$
L'/G
16%
14%
12%
10%
8%
6%
4%
2%
0%
0
20
40
60
80
Q_L [m³/(h.m)]

(c)

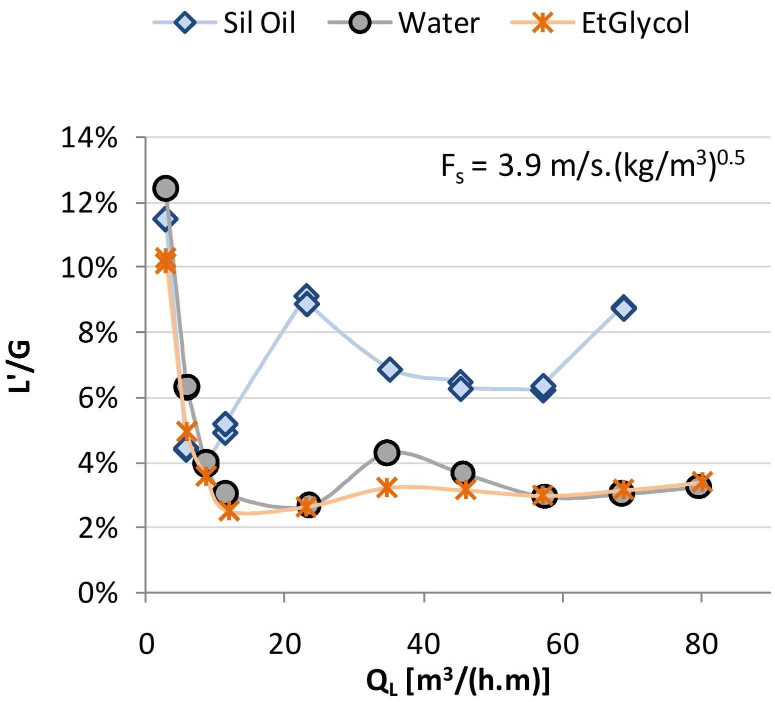
Sil Oil
Water
EtGlycol
14%
12%
10%
8%
6%
4%
2%
0%
L'/G
F_s = 3.9 m/s.(kg/m^3)$^{0.5}$
0
20
40
60
80
Q_L [m³/(h.m)]

(d)

Stellenbosch University http://scholar.sun.ac.za

Figure 3

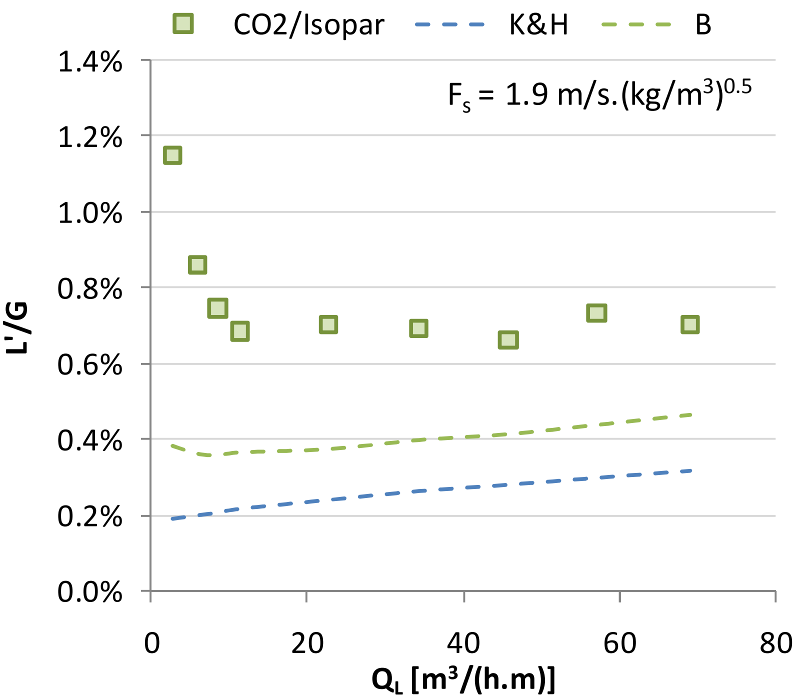

(a)

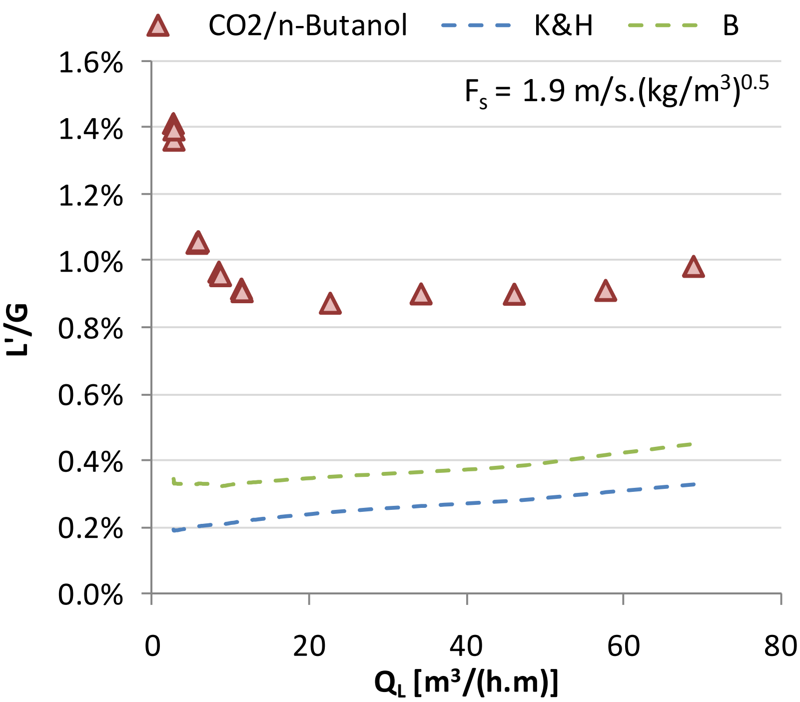

(b)

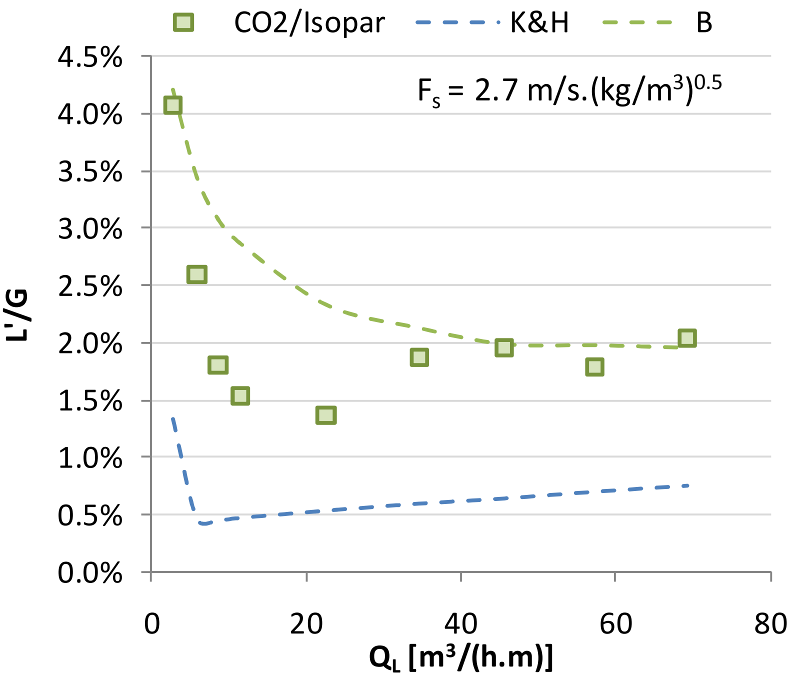
CO2/Isopar
K&H
B
F_s = 2.7 m/s.(kg/m^3)$^{0.5}$
4.5%
4.0%
3.5%
3.0%
2.5%
2.0%
1.5%
1.0%
0.5%
0.0%
L'/G
0
20
40
60
80
Q_L [m^3/(h.m)]

(c)

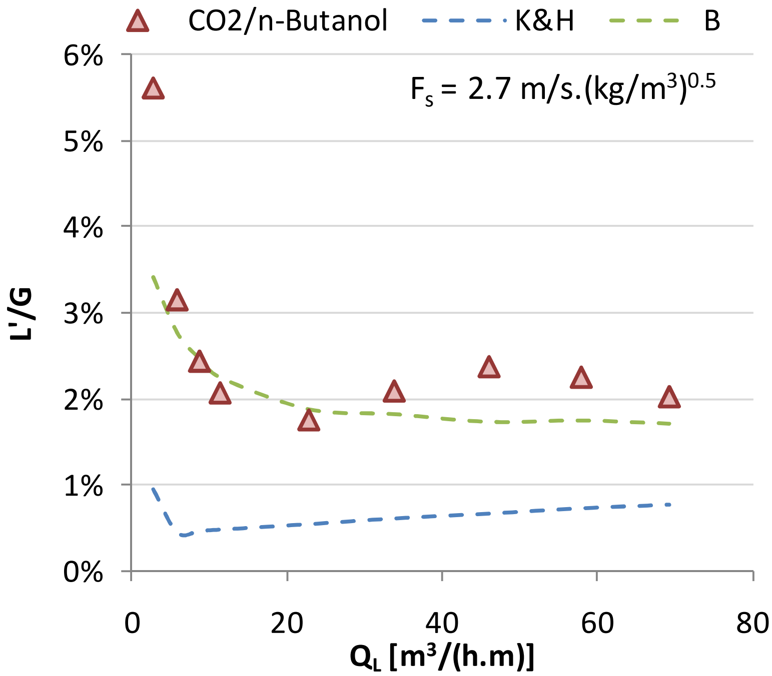
CO2/n-Butanol
K&H
B
F_s = 2.7 m/s.(kg/m^3)$^{0.5}$
6%
5%
4%
3%
2%
1%
0%
L'/G
0
20
40
60
80
Q_L [m^3/(h.m)]

(d)

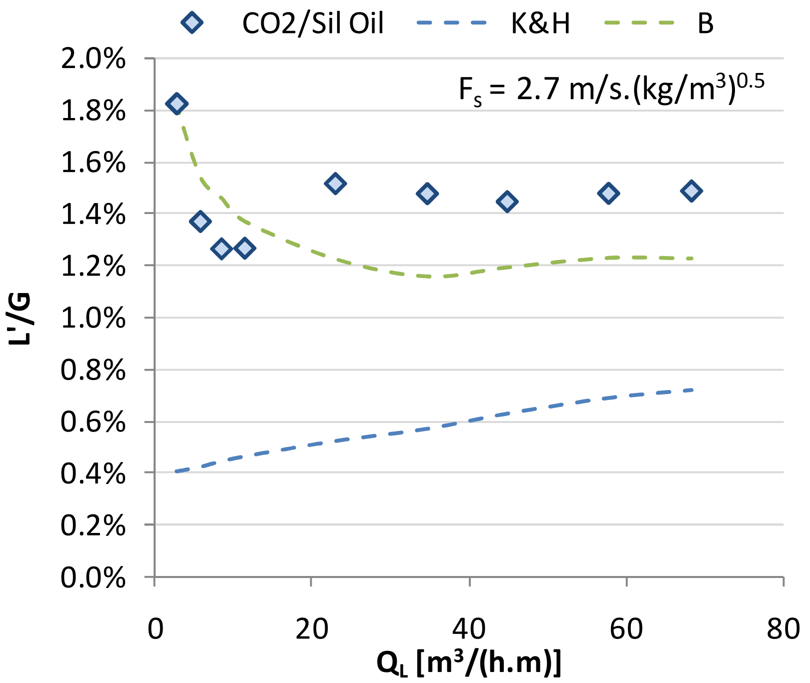
CO2/Sil Oil
K&H
B
F_s = 2.7 m/s.(kg/m³)^0.5
2.0%
1.8%
1.6%
1.4%
1.2%
1.0%
0.8%
0.6%
0.4%
0.2%
0.0%
L'/G
0
20
40
60
80
Q_L [m³/(h.m)]

(e)

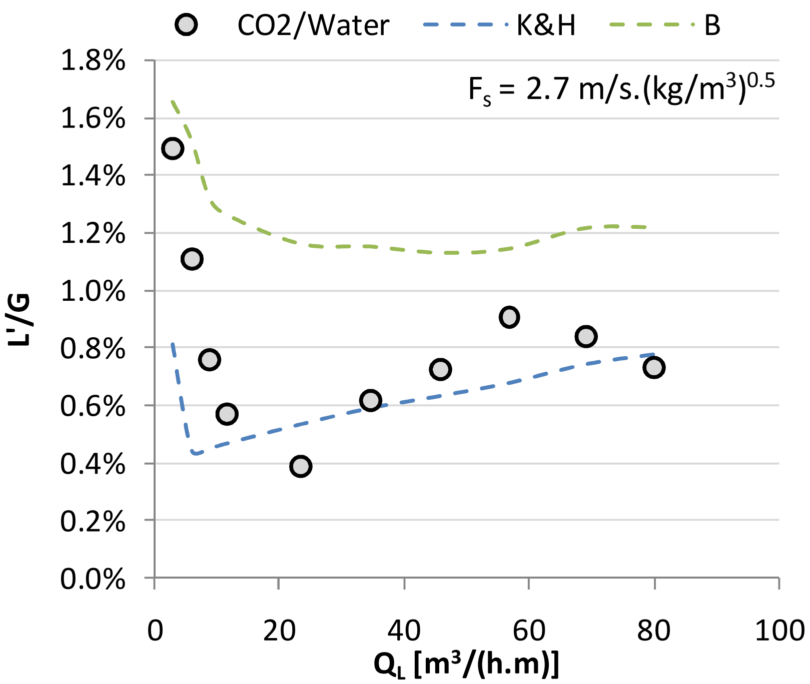
CO2/Water
K&H
B
F_s = 2.7 m/s.(kg/m³)^0.5
1.8%
1.6%
1.4%
1.2%
1.0%
0.8%
0.6%
0.4%
0.2%
0.0%
L'/G
0
20
40
60
80
100
Q_L [m³/(h.m)]

(f)

Figure 4

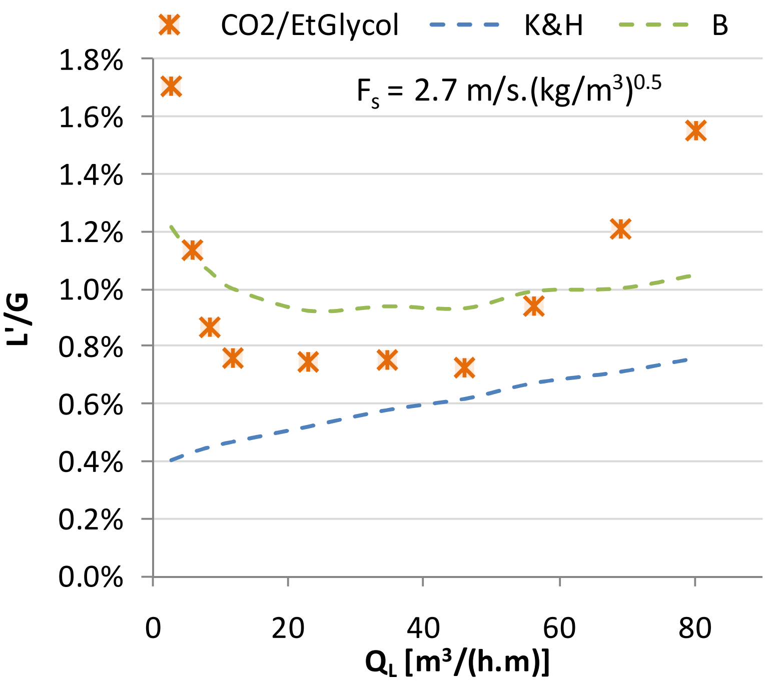
CO2/EtGlycol
K&H
B
F_s = 2.7 m/s.(kg/m³)^0.5
1.8%
1.6%
1.4%
1.2%
1.0%
0.8%
0.6%
0.4%
0.2%
0.0%
L'/G
0
20
40
60
80
Q_L [m³/(h.m)]

(a)

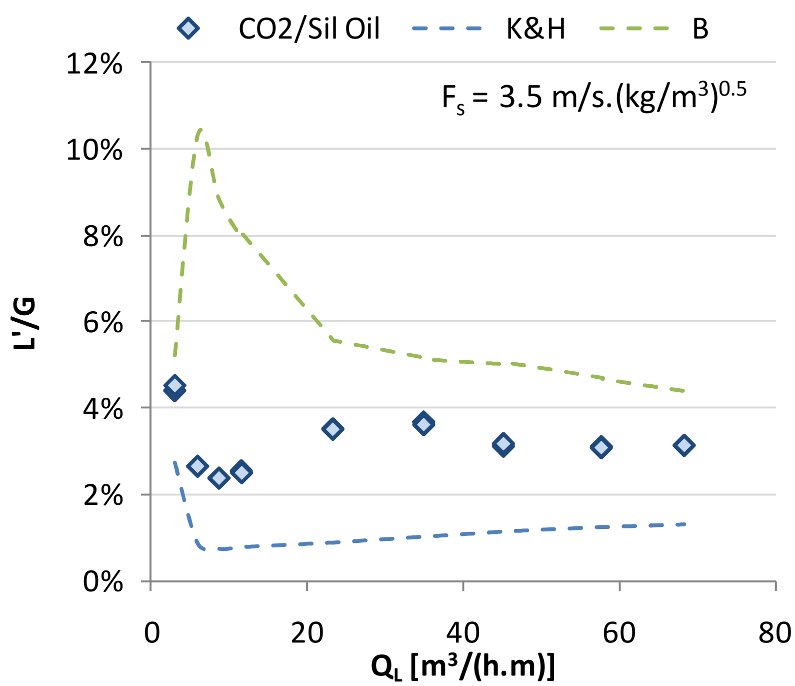
CO2/Sil Oil
K&H
B
F_s = 3.5 m/s.(kg/m³)^0.5
12%
10%
8%
6%
4%
2%
0%
L'/G
0
20
40
60
80
Q_L [m³/(h.m)]

(b)

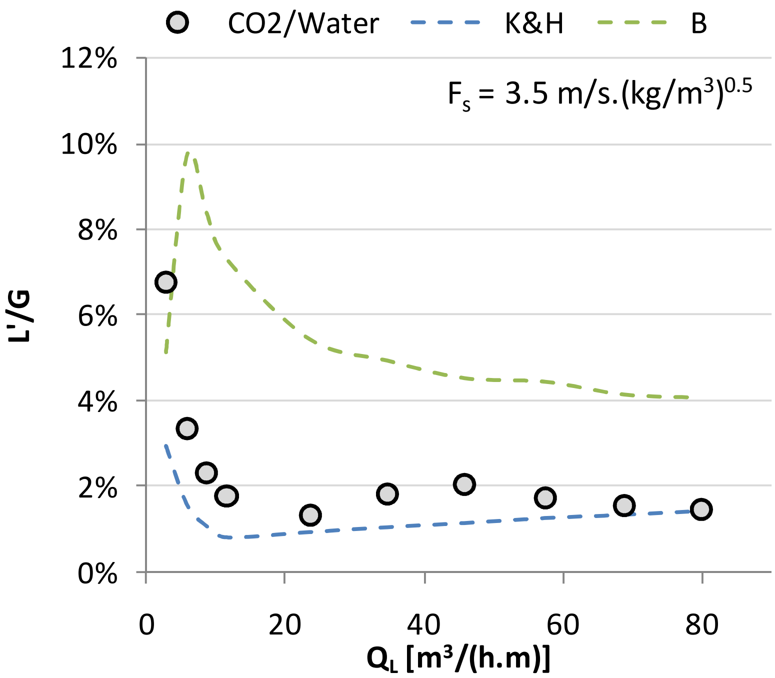
CO2/Water
K&H
B
F_s = 3.5 m/s.(kg/m³)$^{0.5}$
12%
10%
8%
6%
4%
2%
0%
L'/G
0
20
40
60
80
Q_L [m³/(h.m)]

(c)

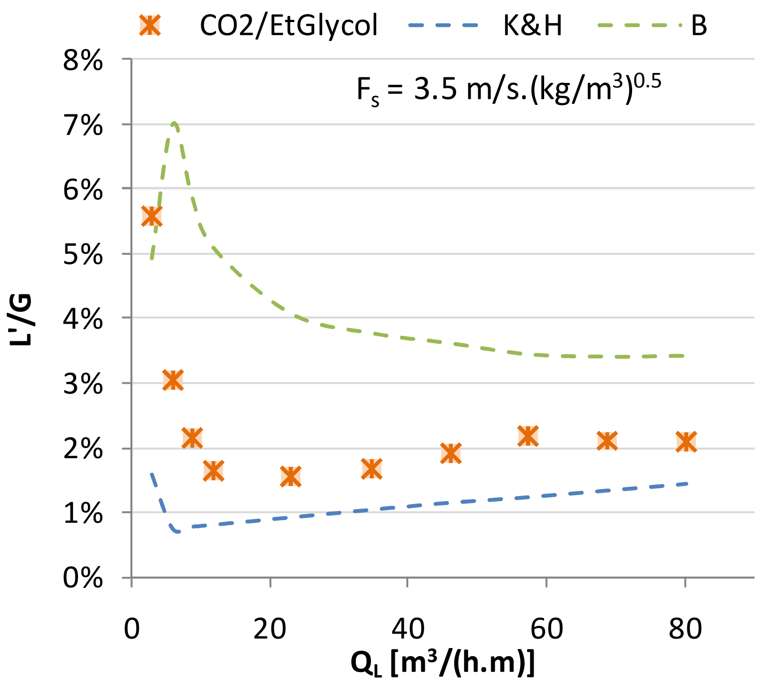
CO2/EtGlycol
K&H
B
F_s = 3.5 m/s.(kg/m³)$^{0.5}$
8%
7%
6%
5%
4%
3%
2%
1%
0%
L'/G
0
20
40
60
80
Q_L [m³/(h.m)]

(d)

Figure 5

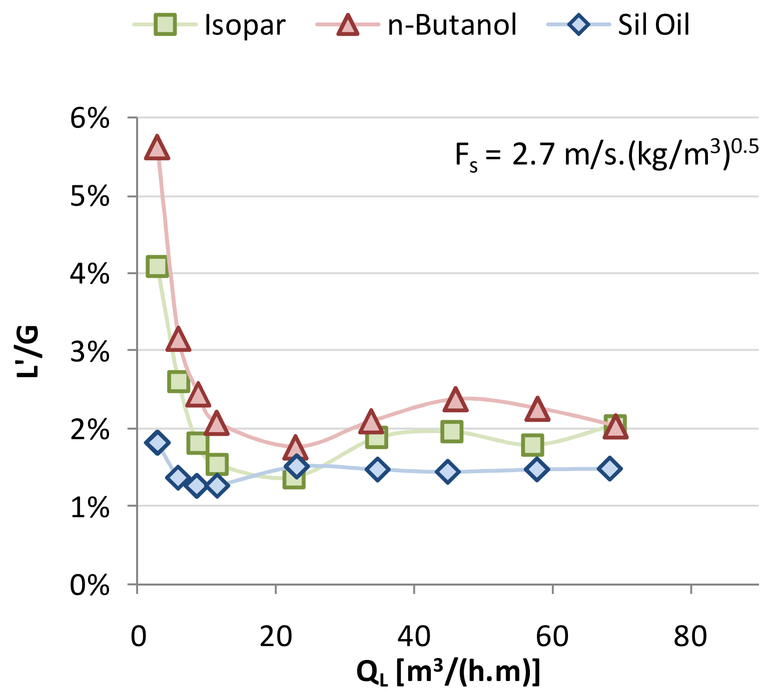
Isopar
n-Butanol
Sil Oil
L'/G
6%
5%
4%
3%
2%
1%
0%
F_s = 2.7 m/s.(kg/m^3)$^{0.5}$
0
20
40
60
80
Q_L [m^3/(h.m)]

(a)

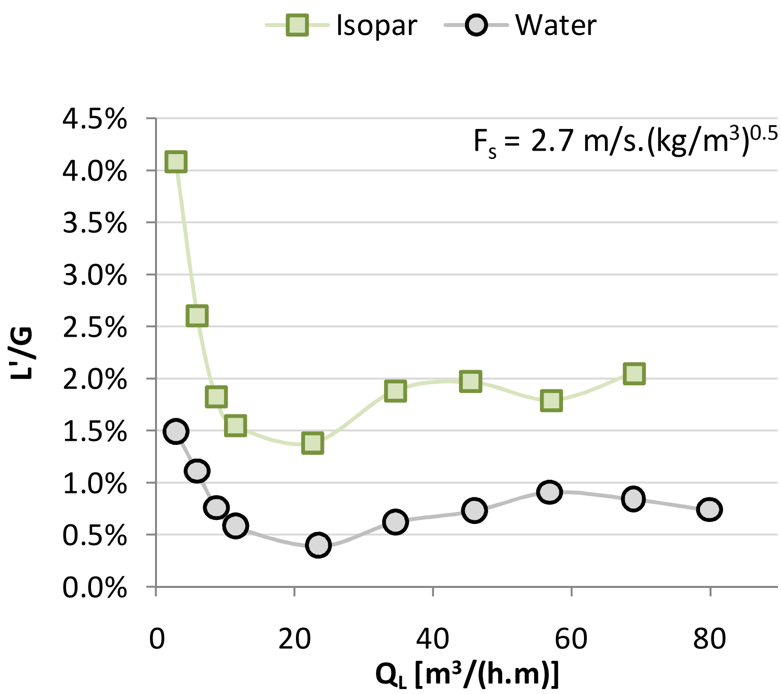
Isopar
Water
L'/G
4.5%
4.0%
3.5%
3.0%
2.5%
2.0%
1.5%
1.0%
0.5%
0.0%
F_s = 2.7 m/s.(kg/m^3)$^{0.5}$
0
20
40
60
80
Q_L [m^3/(h.m)]

(b)

Stellenbosch University http://scholar.sun.ac.za

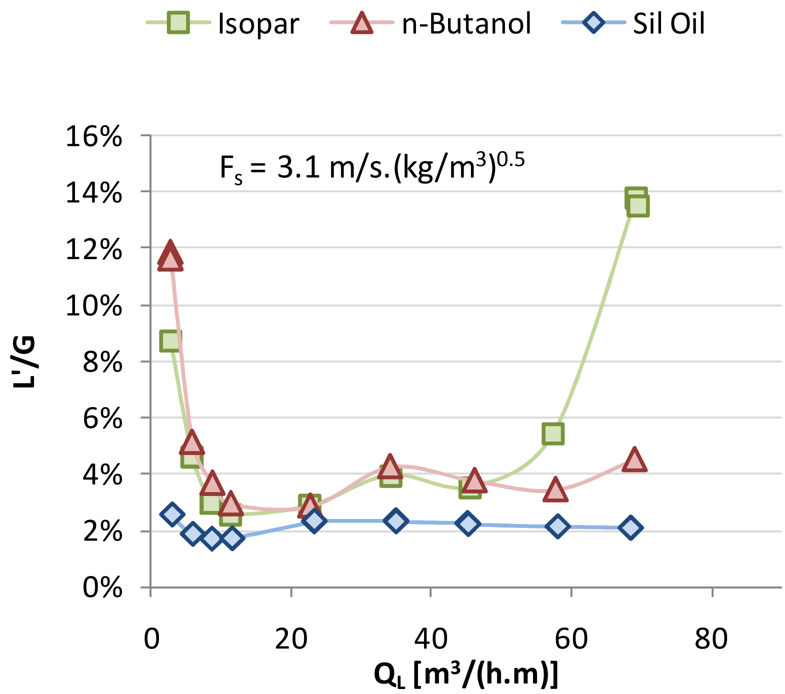

(c)

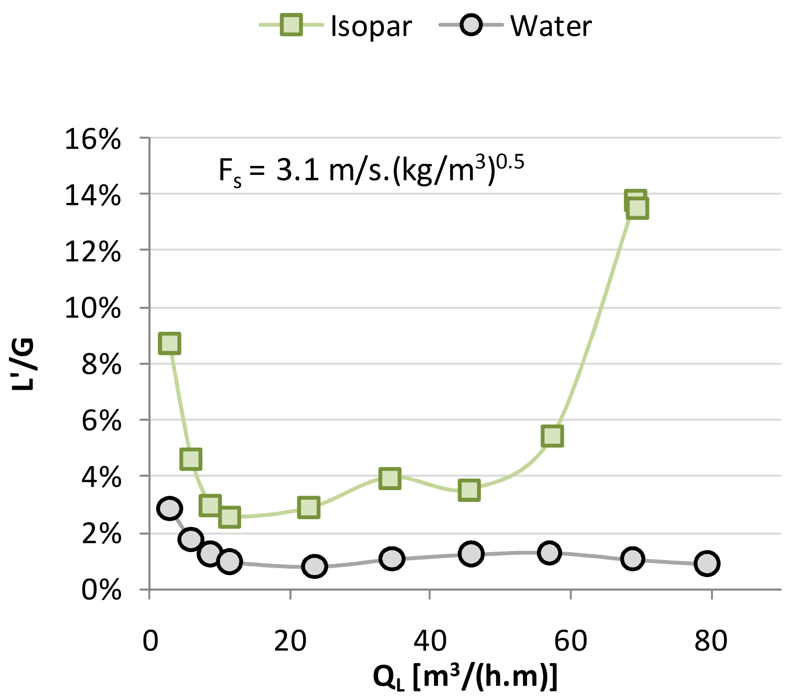

(d)

Figure 7

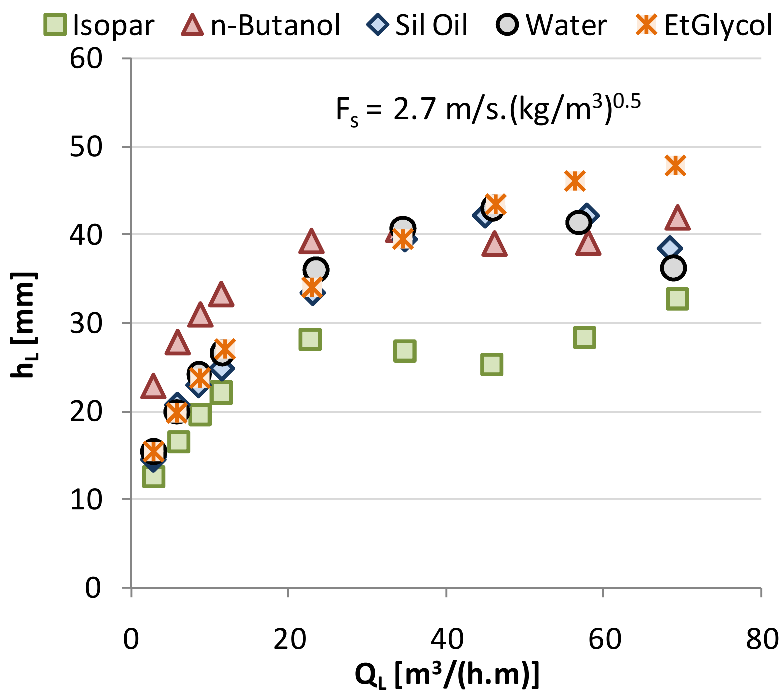

Isopar
n-Butanol
Sil Oil
Water
EtGlycol
F_s = 2.7 m/s.(kg/m^3)$^{0.5}$
h_L [mm]
Q_L [m³/(h.m)]
0
10
20
30
40
50
60
0
20
40
60
80

(a)

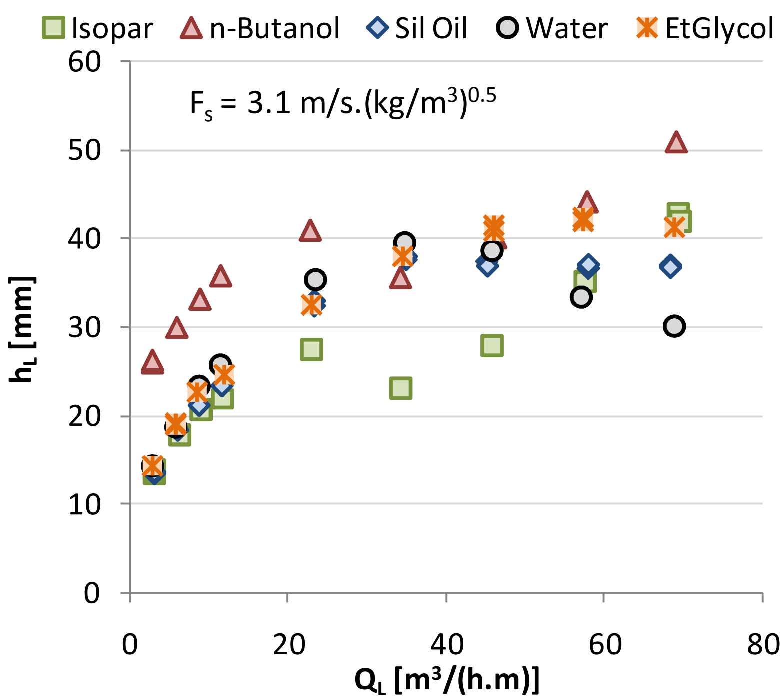

Isopar
n-Butanol
Sil Oil
Water
EtGlycol
F_s = 3.1 m/s.(kg/m^3)$^{0.5}$
h_L [mm]
Q_L [m³/(h.m)]
0
10
20
30
40
50
60
0
20
40
60
80

(b)

Stellenbosch University http://scholar.sun.ac.za

Figure 8

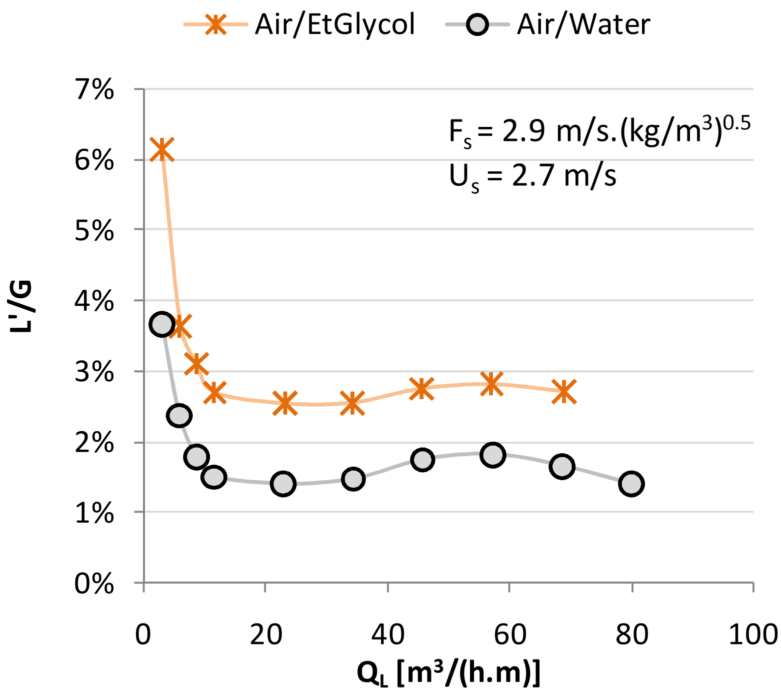

(a)

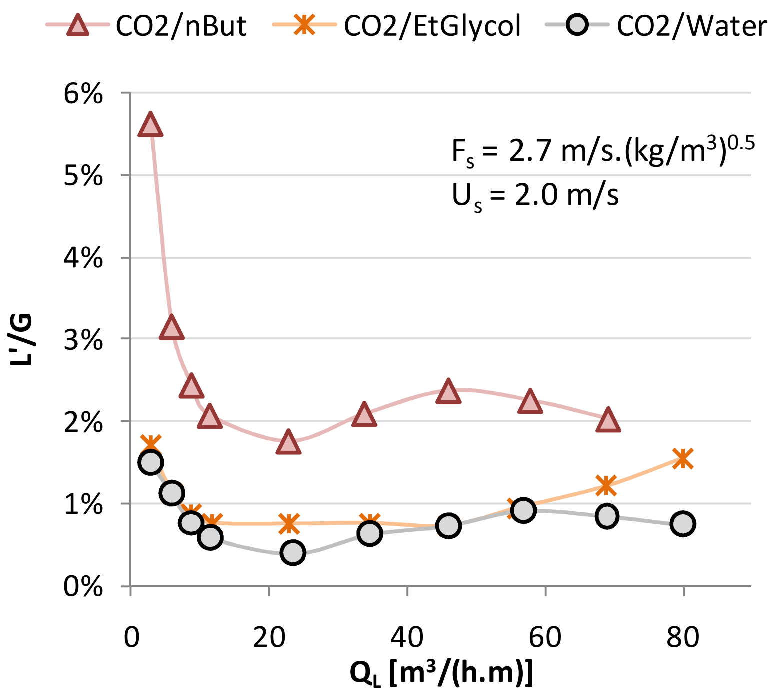

(b)

Stellenbosch University http://scholar.sun.ac.za

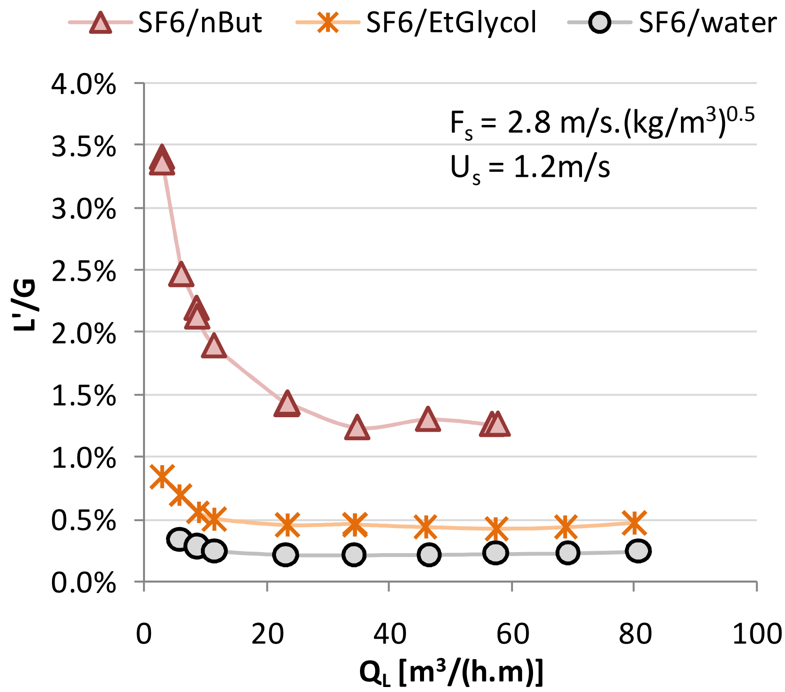

(c)

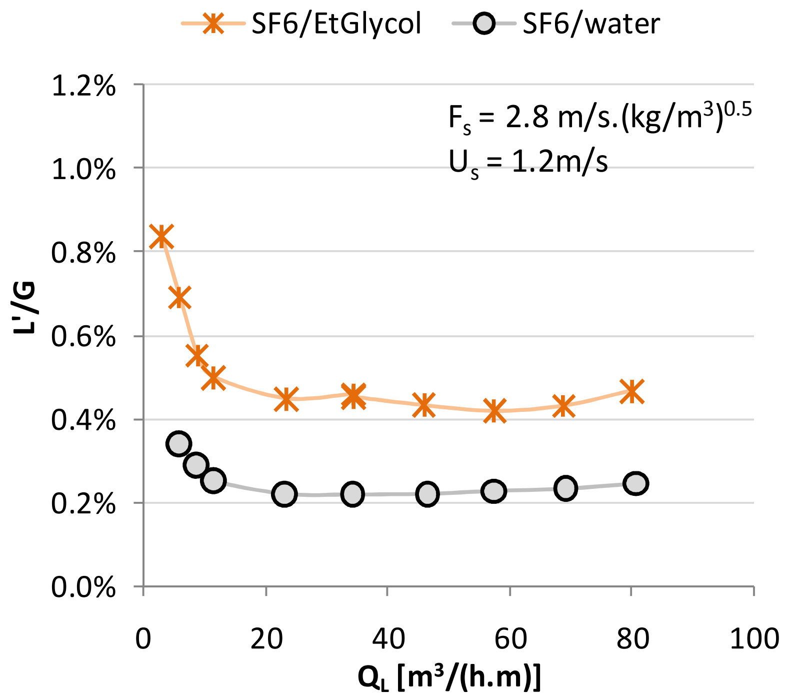

(d)

Stellenbosch University http://scholar.sun.ac.za

Manuscript 4 figures with experimental data

Figure 2

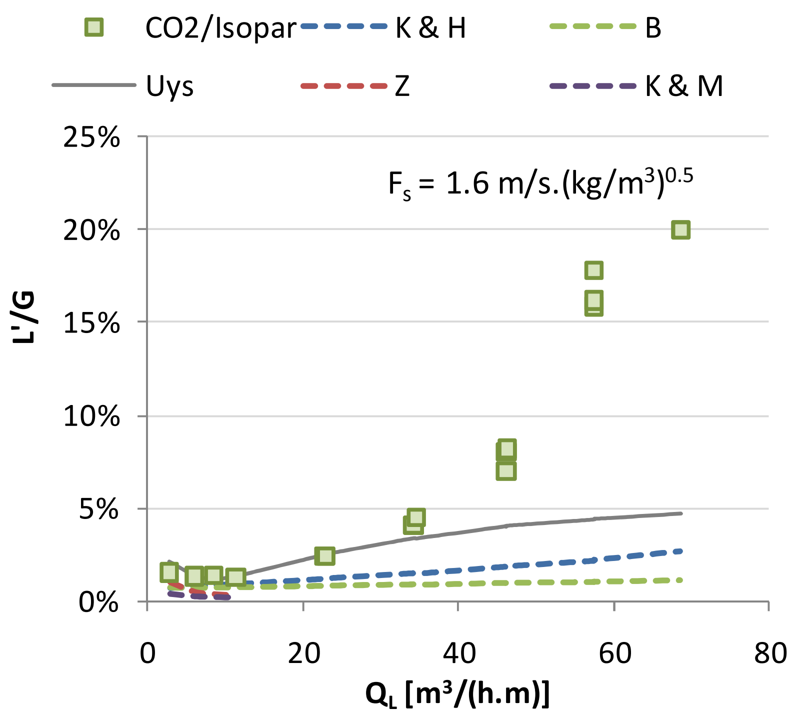

(a)

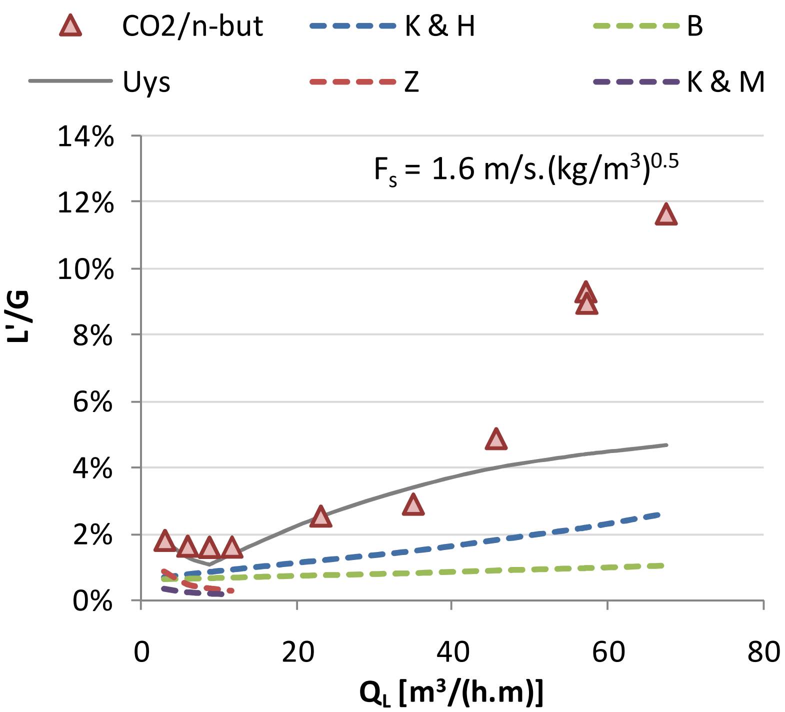
CO2/n-but
K & H
B
Uys
Z
K & M
F_s = 1.6 m/s.(kg/m³)^0.5
14%
12%
10%
8%
6%
4%
2%
0%
L'/G
0
20
40
60
80
Q_L [m³/(h.m)]

(b)

Figure 5

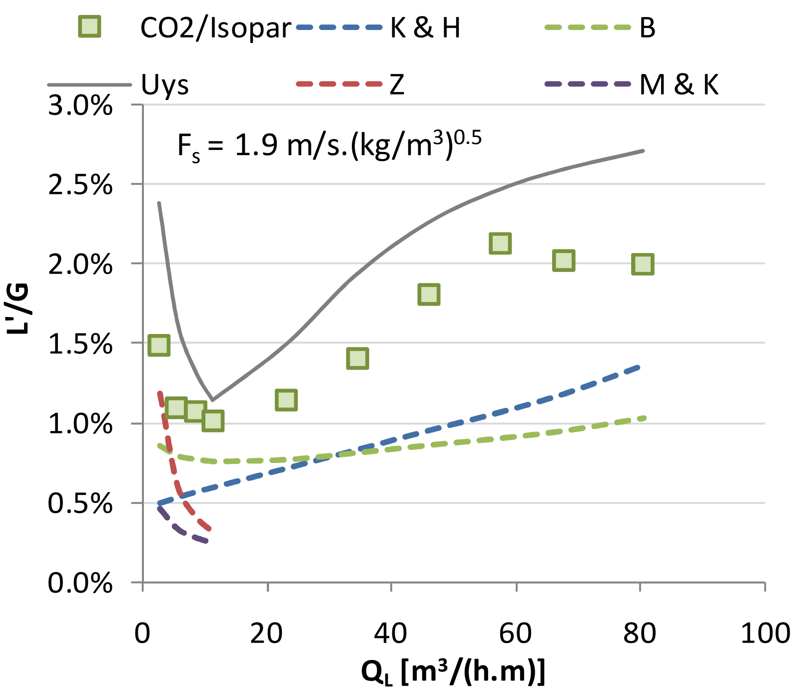
CO2/Isopar
K & H
B
Uys
Z
M & K
F_s = 1.9 m/s.(kg/m³)^0.5
3.0%
2.5%
2.0%
1.5%
1.0%
0.5%
0.0%
L'/G
0
20
40
60
80
100
Q_L [m³/(h.m)]

(a)

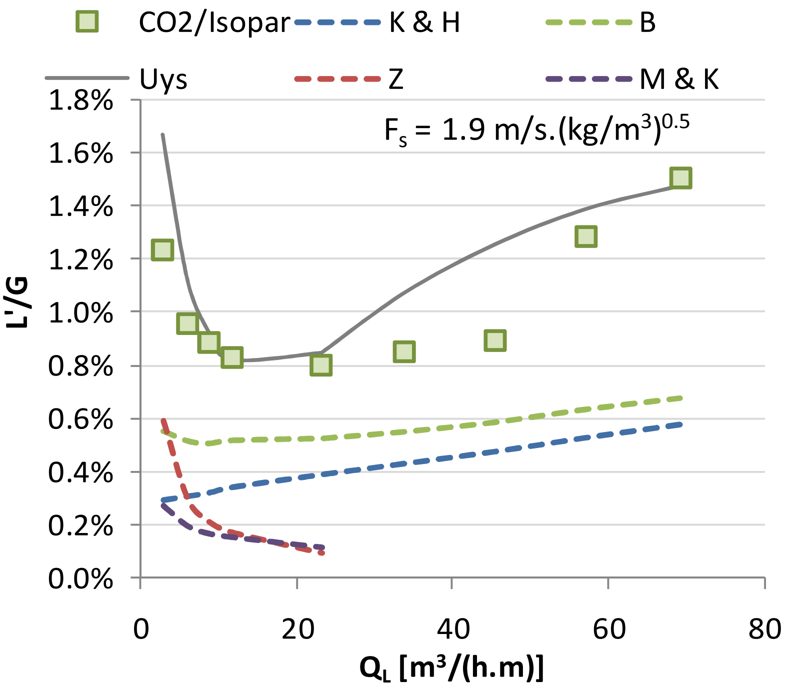
CO2/Isopar
K & H
B
Uys
Z
M & K
F$_s$ = 1.9 m/s.(kg/m^3)$^{0.5}$
1.8%
1.6%
1.4%
1.2%
1.0%
0.8%
0.6%
0.4%
0.2%
0.0%
L'/G
0
20
40
60
80
Q$_L$ [m^3/(h.m)]

(b)

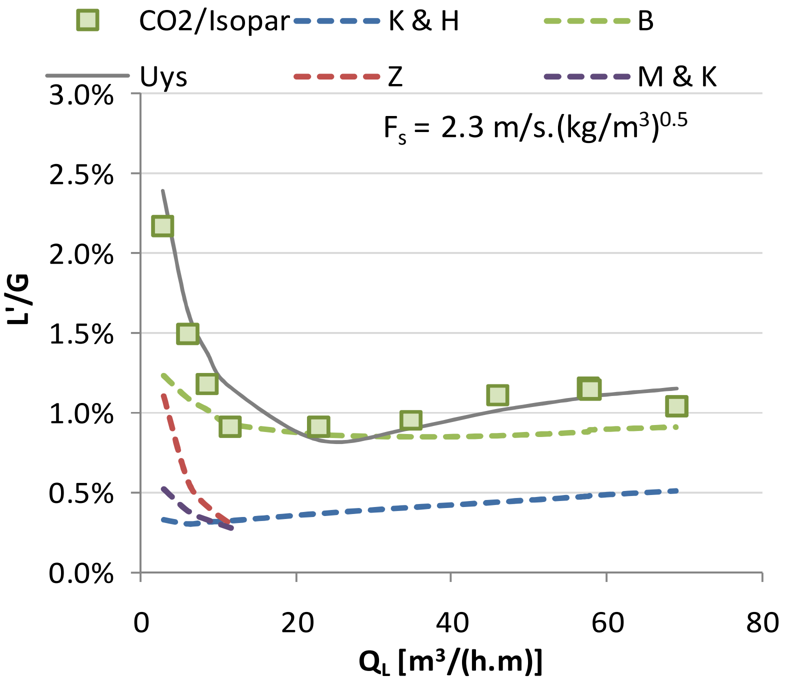
CO2/Isopar
K & H
B
Uys
Z
M & K
F$_s$ = 2.3 m/s.(kg/m^3)$^{0.5}$
3.0%
2.5%
2.0%
1.5%
1.0%
0.5%
0.0%
L'/G
0
20
40
60
80
Q$_L$ [m^3/(h.m)]

(c)

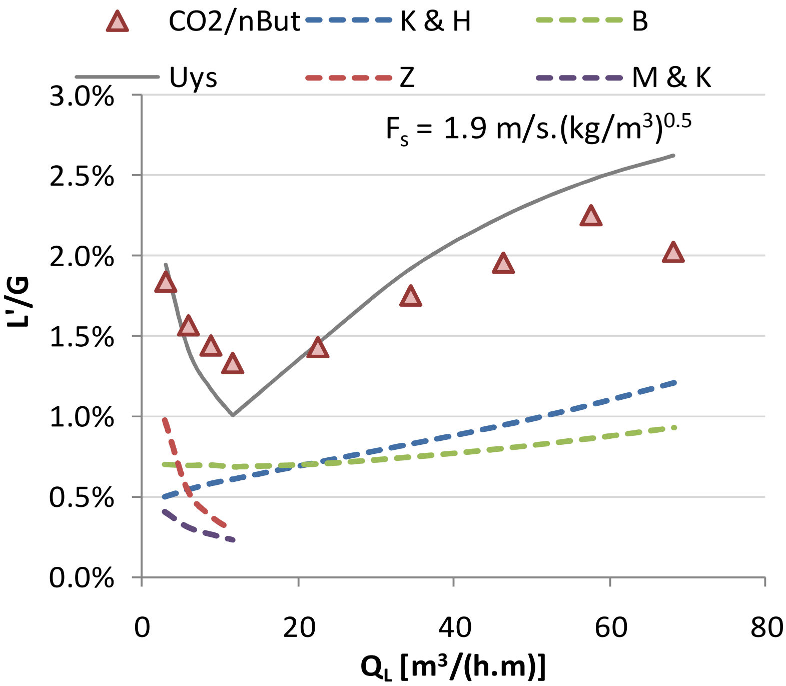
CO2/nBut
K & H
B
Uys
Z
M & K
F_s = 1.9 m/s.(kg/m³)$^{0.5}$
L'/G
3.0%
2.5%
2.0%
1.5%
1.0%
0.5%
0.0%
0
20
40
60
80
Q_L [m³/(h.m)]

(d)

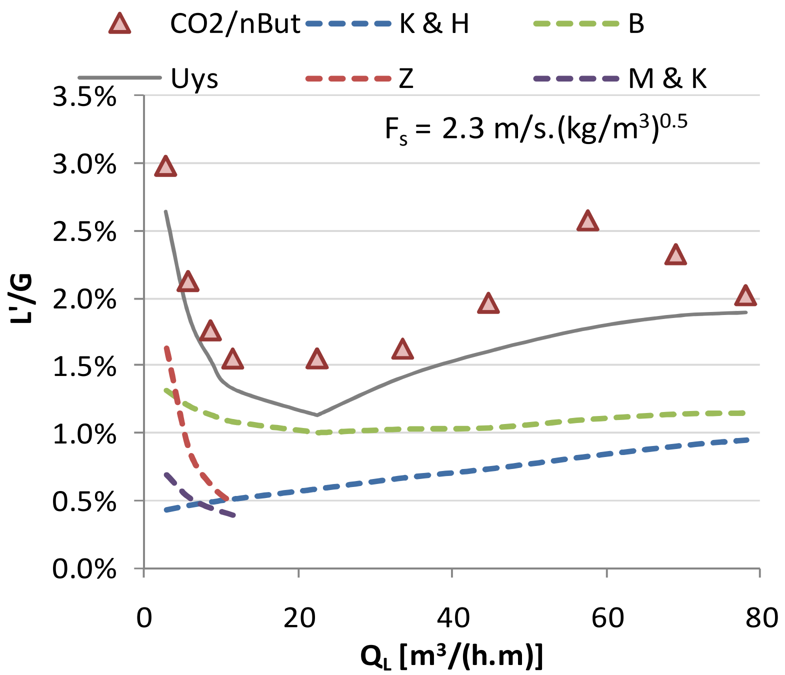
CO2/nBut
K & H
B
Uys
Z
M & K
F_s = 2.3 m/s.(kg/m³)$^{0.5}$
L'/G
3.5%
3.0%
2.5%
2.0%
1.5%
1.0%
0.5%
0.0%
0
20
40
60
80
Q_L [m³/(h.m)]

(e)

Stellenbosch University http://scholar.sun.ac.za

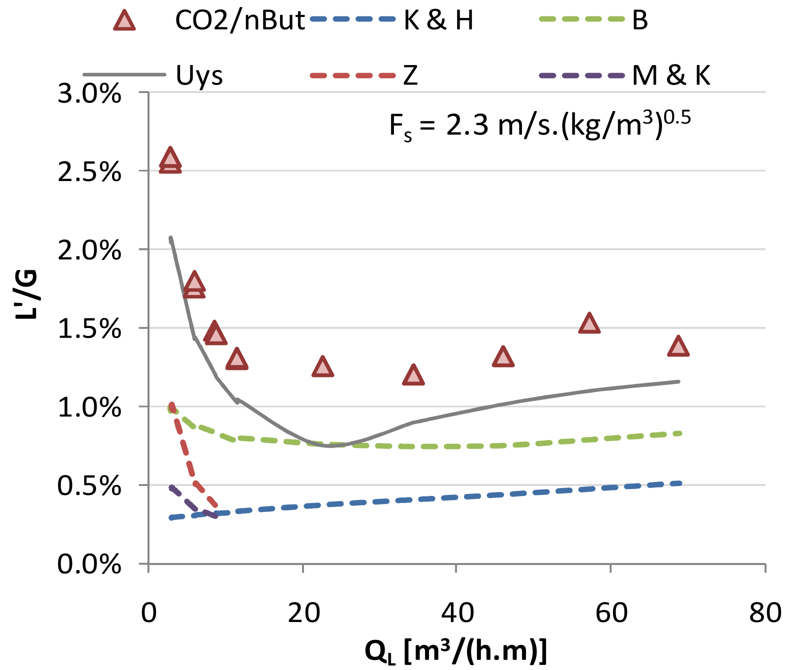

(f)

Figure 6

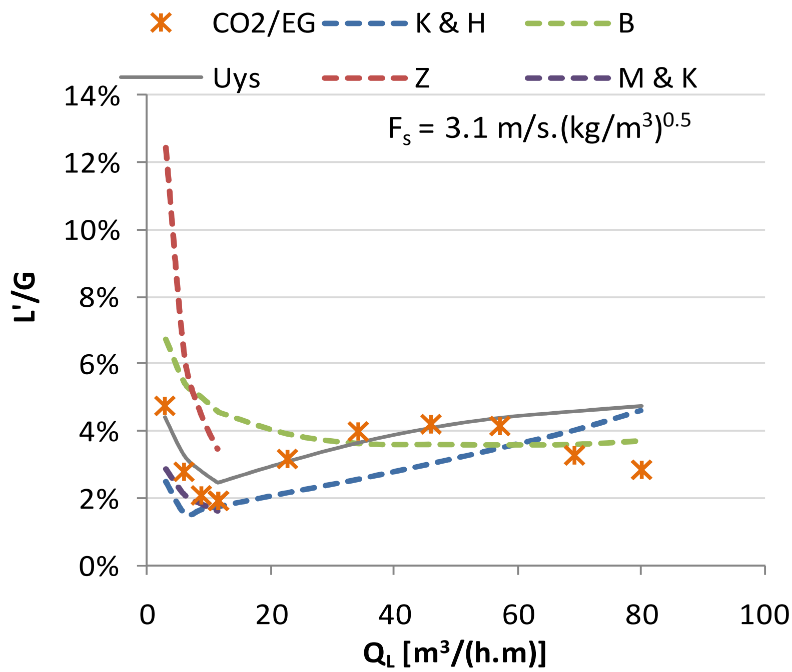

(a)

Stellenbosch University http://scholar.sun.ac.za

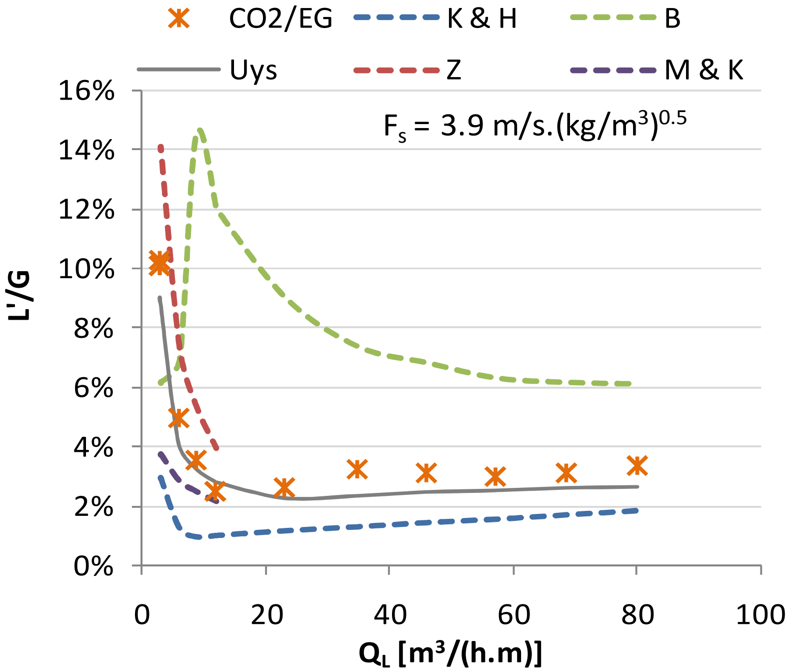

(b)

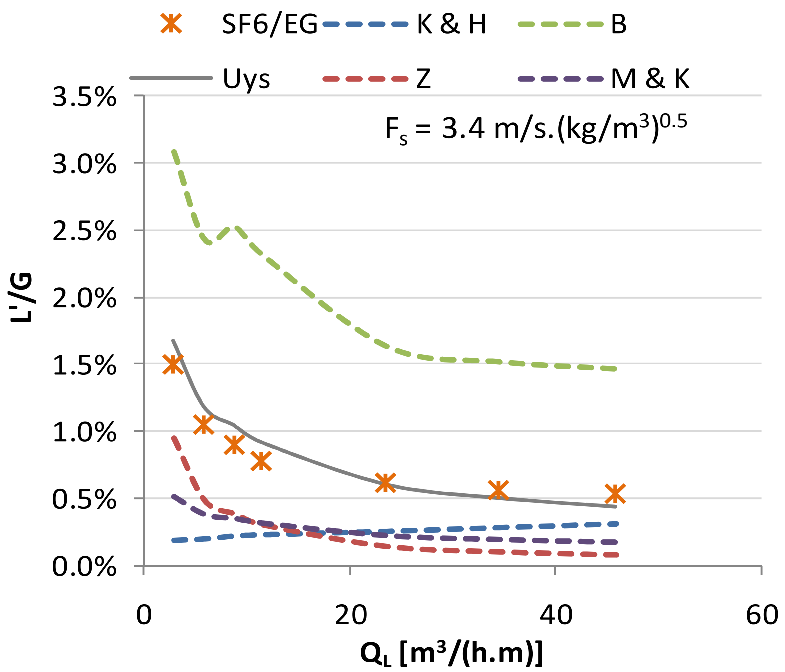

(c)

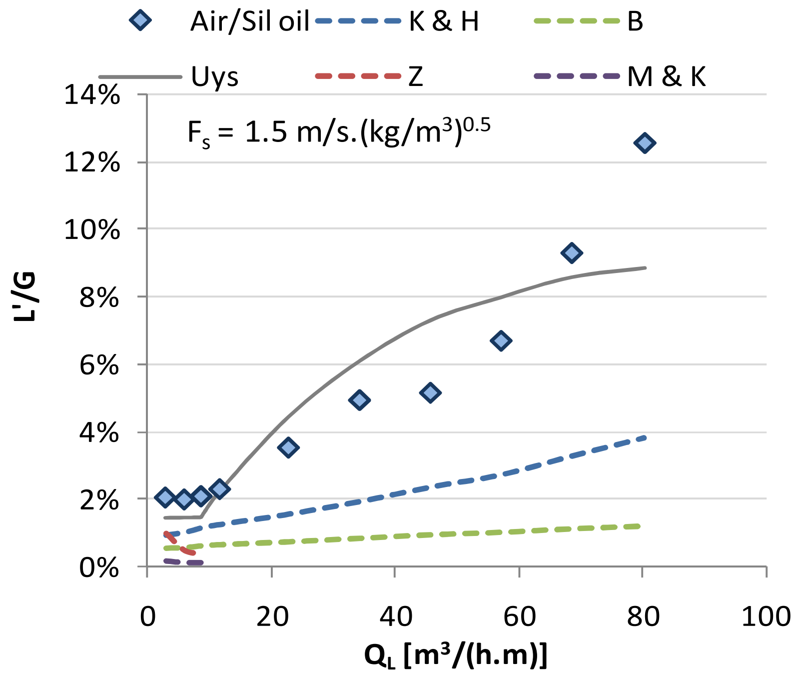
Air/Sil oil
K & H
B
Uys
Z
M & K
F_s = 1.5 m/s.(kg/m^3)^0.5
L'/G
14%
12%
10%
8%
6%
4%
2%
0%
0
20
40
60
80
100
Q_L [m^3/(h.m)]

(d)

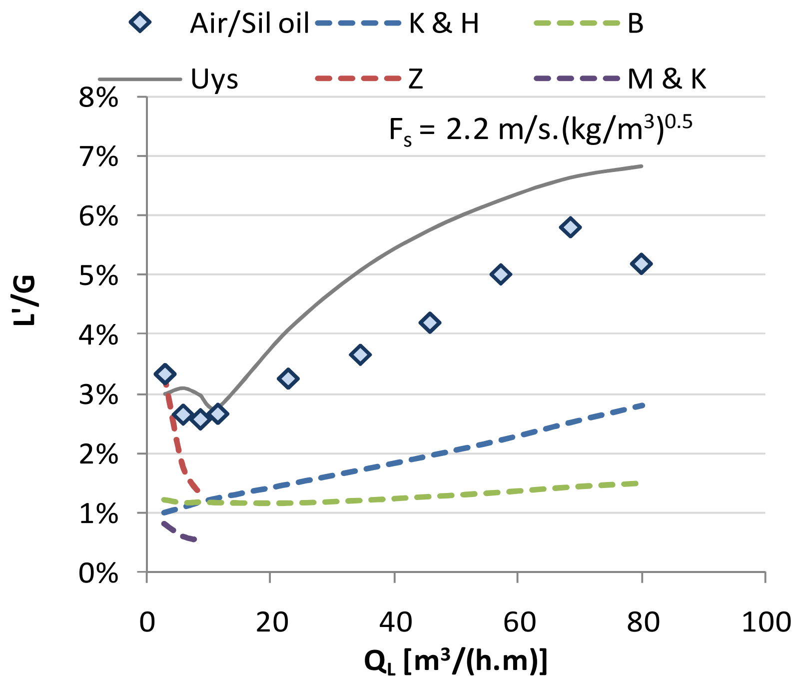
Air/Sil oil
K & H
B
Uys
Z
M & K
F_s = 2.2 m/s.(kg/m^3)^0.5
L'/G
8%
7%
6%
5%
4%
3%
2%
1%
0%
0
20
40
60
80
100
Q_L [m^3/(h.m)]

(e)

Stellenbosch University http://scholar.sun.ac.za

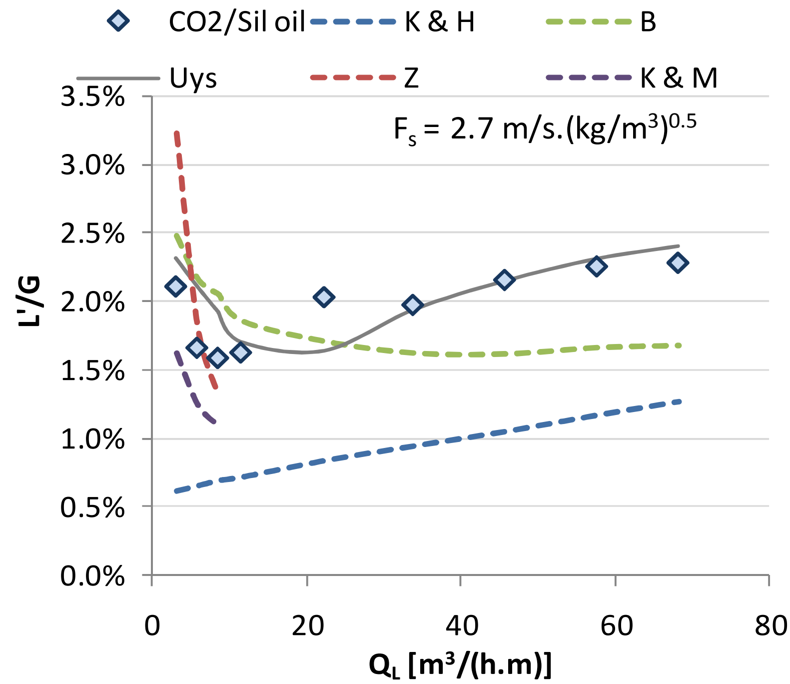

(f)

Figure 10

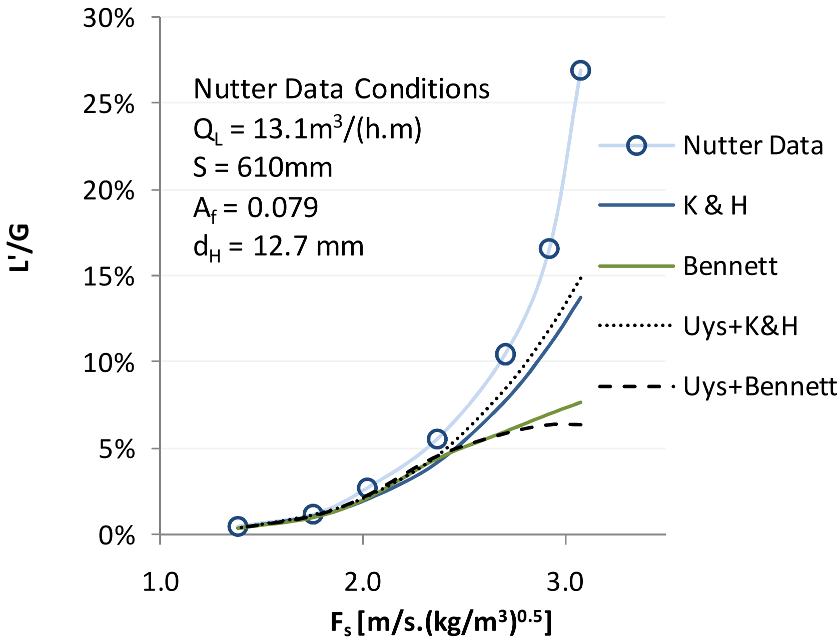

(a)

Stellenbosch University http://scholar.sun.ac.za

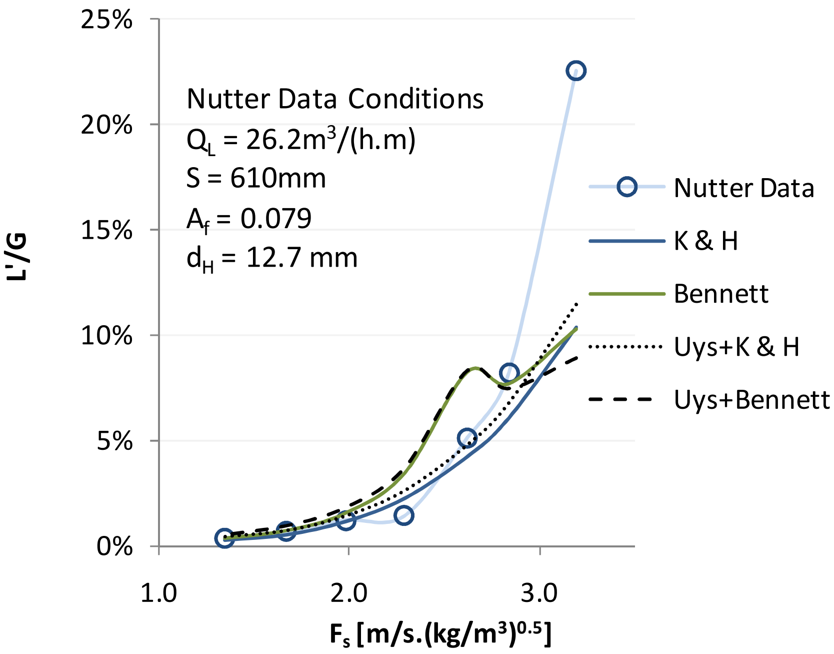

(b)

Stellenbosch University http://scholar.sun.ac.za

6. Determination of dimensionless groups using the Buckingham π-theorem.

Eight variables influenced entrainment based on the scope of this work, combined they should have zero dimension:

$$\frac{L'}{G} = f\left(U_s^{\ a}, \rho_g^{\ b}, Q_L^{\ c}, \rho_l^{\ d}, \sigma^e, \mu_l^{\ f}, g^g, \mu_g^{\ h}, s^i\right) = 0 \quad \textbf{(29)}$$

In terms of physical units

$$\frac{L'}{G} = f\left(\left(\frac{L}{T}\right)^a, \left(\frac{M}{L^3}\right)^b, \left(\frac{L^2}{T}\right)^c, \left(\frac{M}{L^3}\right)^d, \left(\frac{M}{T^2}\right)^e, \left(\frac{M}{LT}\right)^f, \left(\frac{L}{T^2}\right)^g, \left(\frac{M}{LT}\right)^h, (L)^i\right) = 0 \quad \textbf{(29b)}$$

To solve Equation 29a the product of each of the physical variables must equate to zero, therefore:

$$\begin{aligned}&\text{Solving } L: a - 3b + 2c - 3d - f + g - h + i = 0\\&\text{Solving } T: -a - c - 2e - f - 2g - h = 0\\&\text{Solving } M: b + d + e + f + h = 0\end{aligned} \quad \textbf{(29c)}$$

After some trail and error combined with experimental observations gas velocity (U_s), gas density (ρ_g) and liquid flow rate (Q_L) were chosen as the dependent variables. Using Equation 29c they can be solved in terms of the independent variables:

$$\begin{aligned}a &= -e - 3g + i\\b &= -d - e - f - h\\c &= -e - f + g - h - i\end{aligned} \quad \textbf{(29d)}$$

Substituting into Equation 29 gives:

$$\frac{L'}{G} = f\left(U_s^{\ -e-3g+i}, \rho_g^{\ -d-e-f-h}, Q_L^{\ -e-f+g-h-i}, \rho_l^{\ d}, \sigma^e, \mu_l^{\ f}, g^g, \mu_g^{\ h}, s^i\right) \quad \textbf{(29e)}$$

Stellenbosch University http://scholar.sun.ac.za

Rearranging Equation 29e gives the general Equation 30:

$$\frac{L'}{G} = f\left(\left(\frac{\rho_l}{\rho_g}\right)^{a_1}, \left(\frac{\sigma}{\rho_g U_s Q_L}\right)^{a_2}, \left(\frac{\mu_L}{\rho_g Q_L}\right)^{a_3}, \left(\frac{g Q_L}{U_s^{\,3}}\right)^{a_4}, \left(\frac{\mu_G}{\rho_g Q_L}\right)^{a_5}, \left(\frac{U_s s}{Q_L}\right)^{a_6}\right)$$
$$= k\left(\frac{\rho_l}{\rho_g}\right)^{a_1}\left(\frac{\sigma}{\rho_g U_s Q_L}\right)^{a_2}\left(\frac{\mu_L}{\rho_g Q_L}\right)^{a_3}\left(\frac{g Q_L}{U_s^{\,3}}\right)^{a_4}\left(\frac{\mu_G}{\rho_g Q_L}\right)^{a_5}\left(\frac{U_s s}{Q_L}\right)^{a_6} \quad \textbf{(30)}$$

Stellenbosch University http://scholar.sun.ac.za

7. Data acquisition tools, MATLAB.

The data acquisition tools take the data logged as .CSV format file and convert it to entrainment and weeping rate summarised data as .xls files. The raw data (.CSV) is samples obtained every two seconds. This includes the mass entrained, or weeping, liquid in the hold-up tank/s. The script will then convert the flagged data blocks containing the mass (entrainment and/or weeping) measured in the hold-up tank/s to a flow rate. The m-files as specified below should be used with the 'runbatch' command entered in the workspace. From there everything is automated and the .xls sheets is exported to the same directory as the m-files.

runbatch.m script

```
% RUNBATCH runs batch of data processing
% RUNBATCH iterates through a batch of Excel data files in the indicated
working
% directory. Each iteration calls runscript, which performs some data
filtering
% and populates additional worksheets in the Excel data file.
%
% c.2009, jbarnard@sun.ac.za, Stellenbosch University
%===========================================================================
=====

workingdir = '.';
xlsfilefilter = 'DataLog*.csv';

datafile = dir(fullfile(workingdir,xlsfilefilter));

for thisfile=1:numel(datafile)
    runscript('entrainmentsetup',workingdir,datafile(thisfile).name);
    runscript('weepingsetup',workingdir,datafile(thisfile).name);
end
```

runscript.m script

```
% RUNSCRIPT
% [WS2,WS3] = RUNSCRIPT(SETUP,WORKINGDIR,XLSFILE)
%
% c.2009, jbarnard@sun.ac.za, Stellenbosch University
%============================================================
function [worksheet1, worksheet2] = runscript(setup,varargin)

fprintf('\n');
fprintf('Running data processing script\n');
fprintf('------------------------------\n');

assert(nargin>=1,'Please pass in a setup script');
```

Stellenbosch University http://scholar.sun.ac.za


```
%% run setup script
run(setup);

if nargin >= 3
    [workingdir, xlsfile] = varargin{:};
end

%% assert existence of setup variables
if ~exist('workingdir','var')
    workingdir = input('Working directory?','s');
end
if ~exist('xlsfile','var')
    xlsfile = input('Excel file?','s');
end

%% set column selection mask
assert(logical(exist('dataname','var')),'Please define DATANAME');
assert(logical(exist('selectcolumn','var')),'Please define SELECTCOLUMN');
assert(logical(exist('selectscaling','var')),'Please define
SELECTSCALING');
assert(numel(selectscaling)==numel(selectcolumn),'Length(SELECTSCALING)
must equal length(SELECTCOLUMN)');
assert(logical(exist('datacolumn','var')),'Please define DATACOLUMN');
assert(logical(exist('pickflagcolumn','var')),'Please define
PICKFLAGCOLUMN');
assert(logical(exist('displayfigures','var')),'Please define
DISPLAYFIGURES');

%% change to specified working directory
fprintf('Changing directory to %s\n',fullfile(pwd,workingdir));
cd(workingdir);
%% import data file
fprintf('Importing %s\n',fullfile(workingdir,xlsfile));
[data,textdata] = xlsread(xlsfile);

%% precondition data
data(data(:,datacolumn)>65000,datacolumn)=0;

%%
fprintf('Processing data for %s\n',dataname);

begin= 1;
final= 0;
datarangecount = 0;
worksheet1 = {};
worksheet2 = {};

while ~isempty(begin)

    %% pick range boundaries
    begin = final+find(data(final+1:end,pickflagcolumn),1,'first');

    if isempty(begin)
        break;
    else
        datarangecount = datarangecount + 1;
    end
    fprintf('Processing data block %d\n',datarangecount);
    final = begin+find(~data(begin:end,pickflagcolumn),1,'first')-1;
```

```
    %% extract this data range
    thistime = data(begin:final,1);
    thisdata = data(begin:final,datacolumn);

    %% apply linear regression to range
    X = [ones(final-begin+1,1) 24*3600*thistime];
    [b,bconf,residual,resconfidence,stat] = regress(thisdata,X);

    if displayfigures
        %% display fit
        figure
        subplot(2,1,1)
        scatter(X*b,thisdata)
        hold on
        plot(thisdata,thisdata,'g')
        title('Regression fit of original data range')
        xlabel('Measured')
        ylabel('Regression')
        %% display residual
        subplot(2,1,2)
        plot(thistime,residual)
        hold on

plot(thistime,resconfidence(:,1),':',thistime,resconfidence(:,2),':')
        title('Residual of regression on original data range')
        xlabel('Time')
        ylabel('Residual')
    end
    %% define filter for outliers
    exclude = abs(residual)>(mean(residual)+2*std(residual));
    thisfiltrange = begin+find(~exclude)-1;
    Xfilt = [ones(numel(thisfiltrange),1) 24*3600*thistime(~exclude,1)];
    [bfilt,bconffilt,residualfilt,residualconffilt,statfilt] =
regress(thisdata(~exclude,1),Xfilt);

    if displayfigures
    %% display fit of filtered data range
        figure
        subplot(2,1,1)
        scatter(thisdata(~exclude,1),Xfilt*bfilt)
        hold on
        plot(thisdata(~exclude,1),thisdata(~exclude,1))
        title('Regression fit of original data range')
        xlabel('Measured')
        ylabel('Regression')

        %% display residual of regression on filtered data in this range
        subplot(2,1,2)
        plot(thistime(~exclude,1),residualfilt)
        hold on

plot(thistime(~exclude,1),residualconffilt(:,1),':',thistime(~exclude,1),re
sidualconffilt(:,2),':')
        title('Residual of regression on filtered data range')
        xlabel('Time')
        ylabel('Residual')
    end
    %%
    % create temporary estimation output matrix
```

```
    estimation = nan(1,estimationoffset);
    estimation(:,estimationoffset) = bfilt(end);

    % select
    selecteddata = data(thisfiltrange,selectcolumn);
    % rescale
    rescaled = selecteddata.*repmat(selectscaling,size(selecteddata,1),1);
    % merge filter
    mergefilter = ismember(selectcolumn,mergecolumn);
    % Define merge blocks start and stop indices: Assume single, contiguous
    % block to merge.
    mstart = [find(mergefilter(1)),find(diff(mergefilter)==1)+1];
    mstop = [find(diff(mergefilter)==-
1),find(mergefilter(end))*length(mergefilter)];
    % Get median across merge columns
    mergeddata = median(rescaled(:,mergecolumn),2);

    worksheet1{end+1} = [mean([rescaled(:,1:mstart(1)-
1),mergeddata,rescaled(:,mstop(1)+1:end)]),estimation];

    worksheet2{end+1} =
[datarangecount,bfilt(end),bconffilt(end,1),bconffilt(end,2),statfilt(1),..
.
                         numel(thisdata),numel(find(exclude))];

end

%% copy output template to unique output file
xlsoutput = strcat('Output',strcat(strtok(xlsfile,'.'),'.xls'));

%% export worksheet to output workbook

%% export worksheet 1
fprintf('\nFound %d usable data blocks\n\n',datarangecount);
if datarangecount>0
    sheetname = strcat(dataname,'BasicStatistics');
    fprintf('Exporting worksheet %s\n',sheetname);
    worksheet1line1 = textdata(selectcolumn);
    [estimationtitle{1:estimationoffset}] = deal('');
    estimationtitle(estimationoffset) = textdata(datacolumn);
    worksheet1line1 = [worksheet1line1(:,1:mstart(1)-
1),{mergecolname},worksheet1line1(:,mstop(1)+1:end),estimationtitle];
    worksheet1numblock = cat(1,worksheet1{:});
%     worksheet1col2 = repmat({'mean';'median';'std'},datarangecount,1);
%     worksheet1col1 =
regexp(sprintf('%d\n\n\n',1:datarangecount),'\s','split')';
    xlswrite(xlsoutput,worksheet1line1,sheetname,'A1');
%     xlswrite(xlsoutput,worksheet1col1,sheetname,'A2');
%     xlswrite(xlsoutput,worksheet1col2,sheetname,'B2');
    xlswrite(xlsoutput,worksheet1numblock,sheetname,'A2');
    %% export worksheet 2
    sheetname = strcat(dataname,'FlowRate');
    fprintf('Exporting worksheet %s\n',sheetname);
    worksheet2line1 = {'Flow rate and regression statistics'};
    worksheet2line2 = {'Range','Flowrate','Lower Conf','Upper
Conf','R^2','NumOfPoints','NumOfOutliers'};
    worksheet2numblock = cat(1,worksheet2{:});
    xlswrite(xlsoutput,worksheet2line1,sheetname,'A1');
    xlswrite(xlsoutput,worksheet2line2,sheetname,'A2');
    xlswrite(xlsoutput,worksheet2numblock,sheetname,'A3');
```

```
end
fprintf('\nDone with workbook %s\n\n',fullfile(workingdir,xlsoutput));
%%%%%%%%%%%%%%%%%%%%%%%%%%%%%%%%%%%%%%%%%%%%%%%%%%%%%%%%%%%%%%%%%%%%%%%%%%%
%%
function assert(boolean, errormsg)

if boolean == true
    % do nothing
else
    error(errormsg);
end
```

entrainmentsetup.m script

```
%% Get user input


%% set data name
dataname = 'Entrainment';
%% set column selection mask
selectcolumn = 2:15;

%% set scaling vector (must length of selectcolumn)
selectscaling = [1,1,1,0.1,0.1,0.1,1,0.01,0.1,0.1,0.1,0.1,0.001,1];

%% set columns to merge by taking mean over all elements, rowwise augmented
mergecolumn = [10,11,12];
mergecolname = 'T';

%% set data column
datacolumn = 16;

%% set dependent data scaling factor
dependentscaling = 0.1;

%% set use range flag column
pickflagcolumn = 18;

%% set display of figures
displayfigures = false;

%% Set estimated output offset in basic statistics sheet
estimationoffset = 1;
```

weepingsetup.m script

```
%% Get user input


%% set data name
dataname = 'Weeping';

%% set column selection mask
selectcolumn = 2:15;
```

```
%% set scaling vector (must length of selectcolumn)
selectscaling = [1,1,1,0.1,0.1,0.1,1,0.01,0.1,0.1,0.1,0.1,0.001,1];

%% set columns to merge by taking mean over all elements, rowwise augmented
mergecolumn = [10,11,12];
mergecolname = 'T';
%% set data column
datacolumn = 17;

%% set dependent data scaling factor
dependentscaling = 0.1;

%% set use range flag column
pickflagcolumn = 19;

%% set display of figures
displayfigures = false;

%% Set estimated output offset in basic statistics sheet
estimationoffset = 2;
```

8. Data fitting, an optimising MATLAB tool

The script developed to fit the developed correlation to the data is displayed in this section. After the .xlsx file has been imported and the 'b' matrix (data) has been defined the fitfroudemodel can be entered into the workspace.

fitfroudemode.m script

```
%FITFROUDEMODEL Fit Froude model to entrainment data

function s = fitfroudemodel(X,yentrn,c0)

% set options for nonlinear fit
% defaultOptions = statset('nlinfit');
% options        =
statset(defaultOptions,'Display','final','Robust','off','MaxIter',1000);
%
% do nonlinear model fitting
% [b,resid,J,~,mse] = nlinfit(X,yentrn,@froudemodel,b0,options);

% calculate confidence intervals of coefficients
% ci = nlparci(b,resid,'jacobian',J);

% s.BetaNames    = {'k1','k2','k3','a1','a2','a3','a4'};
% s.Beta         = b;
% s.ConfInterval = ci;
% s.Residuals    = resid;
% s.MSE          = mse;

defaultOptions = optimset;
```

Stellenbosch University http://scholar.sun.ac.za


```
options         = optimset(defaultOptions,'Algorithm','active-
set','Diagnostics','off','MaxFunEvals',4000,'MaxIter',4000);
%('TolFun',1*eps,'TolX',1*eps);
numRestarts     = 1000;
% lower bound
lb               = repmat(-6,size(c0));
% lb(1) = -inf;
lb([2,3,4,5,6,7,8]) = 0.001;


% upper bound
ub              = repmat(6,size(c0));
ub([2,3,4,5,6,7,8])= 6;
% ub(12)            = 8;
ub(1)           = 1000;

gs = MultiStart; % create GlobalSearch object

gs.StartPointsToRun = 'bounds';
gs.Display          = 'iter';

problem =
createOptimProblem('fmincon','objective',@(bb)froudemodelsse(@froudemodel,b
b,yentrn,X),'x0',c0,'lb',lb,'ub',ub,'options',options);

%problem =
createOptimProblem('fmincon','objective',@(bb)froudemodelrelnorm(@froudemod
el,bb,yentrn,X),'x0',c0,'lb',lb,'ub',ub,'options',options);

[c,sse,exitflag,output,solutions] = gs.run(problem,numRestarts);

[~,yerr] = froudemodelsse(@froudemodel,c,yentrn,X);

s.Beta = c;
s.Ypred= froudemodel(c,X);
s.MSE       = sse/numel(yentrn);
s.R2        = rsquare(yentrn,s.Ypred);
s.Residuals = yerr;
s.ExitFlag      = exitflag;
s.FminconOutput = output;
s.Solutions     = solutions;
```

froudemodel.m script

```
%FROUDMODEL Froude model for entrainment, here the model structure is
defined

function yentrn = froudemodel(b,x)

k0 = b(1);
k1 = b(2);
k2 = b(3);
k3 = b(4);
k4 = b(5);
k5 = b(6);
k6 = b(7);
```

Stellenbosch University http://scholar.sun.ac.za


```
k7 = b(8);
a1 = b(9);
a2 = b(10);
a3 = b(11);
a4 = b(12);
a5 = b(13);
a6 = b(14);
a7 = b(15);
b1 = b(16);
b2 = b(17);
b3 = b(18);
b4 = b(19);
b5 = b(20);
b6 = b(21);
b7 = b(22);


A1 = x(:,1);
A2 = x(:,2);
A3 = x(:,3);
A4 = x(:,4);
A5 = x(:,5);
A6 = x(:,6);
A7 = x(:,7);


yentrn = k0*((A1.^b1 + k1).^a1) .* ((A2.^b2 + k2).^a2) .* ((A3.^b3 +
k3).^a3) .* ((A4.^b4 + k4).^a4) .* ((A5.^b5 + k5).^a5) .* ((A6.^b6 +
k6).^a6).*((A7.^b7 + k7).^a7);
```

rsquare.m script

```
% rsquare: calculates R^2 statistic of two time series
% [r2] = rsquare(target,predicted);
% Input:
%   target = vector of observed values
%   predicted = vector of predicted values
%
% Output:
%   r2 = R^2 value
%
% c.1997, G Schmitz
% mod.1998, JP Barnard
% *** added comments
%%%%%%%%%%%%%%%%%%%%%%%%%%%%%%%%%%%%%%%%%%%%%%%%%%%%%%%%%%%%%%%%%%%%%%%%%%%%%%
%%%%
function [r2] = rsquare(target,predicted)
%%%%%%%%%%%%%%%%%%%%%%%%%%%%%%%%%%%%%%%%%%%%%%%%%%%%%%%%%%%%%%%%%%%%%%%%%%%%%%
%%%%
% calculates error
e=target-predicted;
n=length(target);

% calculate Pearson's R^2
%r2 = rsquarep(target,predicted);
%return
```

```
%calculates Greg's R^2
r2 = 1 - (norm(e)^2)/(n-1)/std(target)^2;

% set range limits
if r2 < 0,
    r2 = 0;
elseif r2 > 1.0
    r2 = 1.0;
end

%%%%%%%%%%%%%%%%%%%%%%%%%%%%%%%%%%%%%%%%%%%%%%%%%%%%%%%%%%%%%%%%%%%%%%%%%%%
%%%%
return
```

froudemodelrelnorm.m script

```
%FROUDMODELERROR  Froud model for entrainment

function [yrelnorm,yerr] = froudemodelrelnorm(modelFcn,b,yentrn,x)

yentrnHat = modelFcn(b,x);
Err       = yentrn - yentrnHat;
yerr      = abs(Err)./yentrn;
%yerr      = yentrnHat - yentrn;
yrelnorm  = abs(yerr)./yentrn;
```

froudemodelsse.m script

```
%FROUDMODELERROR  Froud model for entrainment

function [ysse,yerr] = froudemodelsse(modelFcn,b,yentrn,x)

yentrnHat = modelFcn(b,x);
Err       = yentrn - yentrnHat;
yerr      = abs(Err)./yentrn;
ysse      = sum(yerr.*yerr);
```

froudemodelinfnorm.m script

```
%FROUDMODELERROR  Froud model for entrainment

function [yinfnorm,yerr] = froudemodelinfnorm(modelFcn,b,yentrn,x)

yentrnHat = modelFcn(b,x);
yerr      = yentrn - yentrnHat;
yinfnorm  = norm(yerr,Inf);
```

froudemodelneginfnorm.m script

```
%FROUDMODELERROR  Froud model for entrainment
```

Stellenbosch University http://scholar.sun.ac.za


```
function [yinfnorm,yerr] = froudemodelneginfnorm(modelFcn,b,yentrn,x)

yentrnHat = modelFcn(b,x);
yerr      = yentrn - yentrnHat;
yinfnorm  = norm(yerr,-Inf);
```